UNIVERSITÀ
DEGLI STUDI
FIRENZE

PhD in
Industrial Engineering

CYCLE XXXIII

COORDINATOR Prof. Manfrida Giampaolo

Environmental impact assessment of energy storage technologies in photovoltaic systems

Academic Discipline (SSD) ING-IND/09

Doctoral Candidate
Dr. Rossi Federico

Supervisor
Prof. Sinicropi Adalgisa

Coordinator
Prof. Manfrida Giampaolo

Years 2017/2020

Ph.D. Pegaso Regione Toscana

UNIVERSITÀ DEGLI STUDI FIRENZE

UNIVERSITÀ DI SIENA 1240

UNIVERSITÀ DI PISA

Environmental impact assessment of energy storage technologies in photovoltaic systems

A dissertation submitted in partial fulfilment of the requirements for the degree of

Doctor of Philosophy in Industrial Engineering

Curricula: Energy and Innovative Industrial and Environmental Technologies

Scientific Area: ING–IND/09

Ph.D. Candidate: Ing. Federico Rossi

Tutor: Prof. Adalgisa Sinicropi

Ph.D. School Coordinator: Prof. Giampaolo Manfrida

Ph.D. School Cycle: XXXIII (2017–2020)

RES LABORATORY

Acknowledgments

This thesis results from three years of study and work during which lots of professors, researchers and friends contributed to my personal growth and scientific enrichment. Firstly, I would like to acknowledge prof. Adalgisa Sinicropi for being such a great supervisor who supported and trusted me all the time. Indeed, I believe that prof. Sinicropi is a valuable researcher, teacher, and manager of the group because she is very good at understating people thus enhancing their qualities. I am glad to keep working with her because she motivates me to do my best, which is fundamental to turn the passion for my job to concrete results and satisfactions. I really appreciate the human side of prof. Sinicropi who has always been kind and caring with me since the very beginning of my PhD.

The second person I would like to acknowledge is prof. Riccardo Basosi, a senior professor who, although his retirement, always shares his wide knowledge and experience with the group. Since the first time we met, when he introduced me to the group, I have been impressed by his capacity to catch the attention and transmit passion with his words. He told me to consider him as a grandfather who is always there for advice, but I can say that he is much more than that. Our talks along the Firenze-Siena road were really inspiring; he taught me to be always optimistic and to see the big picture of things and he showed the importance of creating a friendship network with other professors and researchers. I see a lot of similarities between prof. Sinicropi and him and I still have much to learn from them, so I hope I will have the pleasant opportunity to ask for their advice for a very long time.

Moreover, I would like to acknowledge all the other members of my research group, the R^2ES Laboratory of the University of Siena, including prof. Maria Laura Parisi who gave a great contribution to my research during my PhD, and she keeps doing that during my research fellow.

I am also glad to acknowledge prof. Giampaolo Manfrida, my PhD coordinator and a good friend and co-worker who introduced me to prof. Basosi and Sinicropi through the "*Progetto Pegaso*". I have to acknowledge Regione Toscana for this program which gave me the opportunity to carry out my PhD and to live a fantastic experience in Berkeley (USA) at the Lawrence Berkeley National Laboratory. In Berkeley I had the opportunity to create a fruitful collaboration with Dr. Miguel Heleno that I really want to thank for his support and his friendship during that period.

A special acknowledgment goes to my family because my dad Tiziano, my mom Luciana, my sister Francesca, my grandma Lietta and, obviously, my cat Pepe have been fundamental to get such a great achievement as a PhD. Making them proud of me has always been the best satisfaction for me and I hope that I will be able to keep doing that over all my career.

Moreover, I would like to thank all my friends who always give me a great support. Particularly, I acknowledge Niccolò Albasini, who is like a brother to me, all my other friends from my hometown and surroundings that luckily are too many to be listed, and my former university mates Giordano, Francesco, Lorenzo, and Marco.

During my PhD I had the opportunity to extend my horizons to Siena; although I actually never lived there, the personal relations that I created in this period became really important, much more than I would have ever expected. A special acknowledgement goes to Laura because our chemistry and connection turned out to be more than just a friendship. Moreover, I really want to thank Mayra, Carmen, Jessica, Lorenzo, Giuseppe, and Simone for the special moments we lived so far. Special thanks also go to Giulia, Wahwah, Luciana, Antonio, Alexandre, David, and Andrea because they made me feel home even when I was on the other side of the World. The long-lasting friendship that we created in Berkeley in just a few months went well beyond my expectations.

Abstract

This thesis addresses the issue of the environmental impact assessment of residential energy systems named Solar Home Systems and Renewable Energy Communities that produce electricity using photovoltaic modules and store it in energy storage systems. These installations are playing a key role in the energy transition and decarbonization because they do not imply direct emissions to the environment and do not directly consume fossil fuels. Nevertheless, these technologies have some environmental impacts during their life cycle. For instance, several rare critical raw materials are necessary for their manufacturing and greenhouse gases are emitted during their production and end of life. Life Cycle Assessment represents the most suitable methodology to evaluate environmental indicators like the natural resources' depletion. In order to replace traditional power plants, renewable energy and storage technologies should become competitive from the techno-economic point of view. For such reason, it is fundamental to integrate Life Cycle Assessment with auxiliary methodologies like mathematical modelling, optimization tools and Life Cycle Costing. The results of this thesis are collected in five papers where an *integrated* Life Cycle Assessment approach, combining environmental and techno-economic analyses, is performed. The goal of these works is the evaluation of the most sustainable Solar Home Systems and Renewable Energy Communities configurations. The combination of different methodologies allows to consider all the variables of the problem, such as the spatial and temporal variability of solar radiation and the techno-economic properties and maturity of different energy storage technologies. Among the mature technologies, nickel cobalt manganese and nickel cobalt aluminium lithium-ion batteries are assessed as the most sustainable solutions in all the considered European installation sites (Denmark, France, Spain, Italy, Portugal, Romania, Hungary, and Greece). Nevertheless, an environmental and economic cross evaluation highlights the importance of reducing their costs. Some innovative batteries like solid state lithium-ion batteries, sodium-ion batteries, and vanadium redox flow batteries, already show a great potential being competitive with mature technologies, although some characteristics still need to be improved. Finally, system-level results show that Solar Home Systems and Renewable Energy Communities can provide relevant advantages to the national energy systems, especially when they are connected to the grid and specific economic incentives for their members are considered.

Tables of contents

List of Figures

List of Tables

Nomenclature

ADP	Abiotic Depletion Potential
AIB	Aluminium-ion Battery
AP	Acidification Potential
BESS	Battery Energy Storage System
BMS	Battery Management System
CAES	Compressed Air Energy Storage
CED	Cumulative Energy Demand
CHS	Compressed Hydrogen Storage
CIS	Commonwealth of Independent States
C-rate	Charge Rate
DoD	Depth of Discharge
D-rate	Discharge Rate
EES	Engineering Equation Solver
ESS	Energy Storage System
FDP	Fossil Depletion Potential
GHG	Greenhouse Gases
GWP	Global Warming Potential
HTP	Human Toxicity Potential
IEA	International Energy Agency
IPCC	Intergovernmental Panel on Climate Change
ISO	International Organisation for Standardization
LCA	Life Cycle Assessment
LCC	Life Cycle Costing
LCI	Life Cycle Inventory
LCIA	Life Cycle Impact Assessment
LCO	Lithium Cobalt Oxide
LCP	Lithium Cobalt Phosphate
LFP	Lithium Iron Phosphate
LIB	Lithium-ion battery
LiPON	Lithium Phosphorous Oxynitride
LiSB	Lithium Sulphur Battery

LMO	Lithium Manganese Oxide
LTO	Lithium Titanate Oxide
MDP	Metal Depletion Potential
MILP	Mixed Integer Linear Programming
NaS	Sodium Sulphur
NCA	Nickel Cobalt Aluminium
NCM	Nickel Cobalt Manganese
NiMH	Nickel Metal Hydride
PbA	Lead Acid
PEF	Product Environmental Footprint
PEFCR	Product Environmental Footprint Category Rules
PHS	Pumped Hydro Storage
PMF	Particulate Matters Formation
PNIEC	National Integrated Plan for Energy and Climate
Pt	Eco-points
PV	Photovoltaic
REC	Renewable Energy Community
RES	Renewable Energy Source
SET-Plan	European Strategic Technology Plan
SHS	Solar Home System
SIB	Sodium-ion battery
SOC	State of Charge
SOH	State of Health
SSLIB	Solid State lithium-ion battery
TEES	Thermo Electric Energy Storage
UNFCCC	United Nations Framework Convention on Climate Change
VPP	Virtual Power Plant
VRFB	Vanadium Redox Flow Battery
ZEBRA	Zero Emission Battery Research Activities

1. Introductory remarks

The two pillars of a sustainable energy policy are energy efficiency and renewable energies. The former implies to minimize energy wastes, the latter to use resources which are naturally replenished on a human timescale. Unfortunately, some renewable energy sources (RESs) are variable in time and space and their availability is directly connected with weather conditions. Therefore, a mismatch between the energy production and demand occurs over time. In this context, energy storage systems can accumulate the energy surplus and use it in case of lack of RESs thus contributing to the increase of energy efficiency and renewable energies penetration. For such reasons, storage plays a key role in the energy transition and decarbonization. Moreover, the installation of storage and renewable energy systems, supported by adequate automation and control digital technologies, allows traditional grids to become "Smart".

According to the concept of "Smart Grids", the future grids will be multi-layer energy systems, integrating traditional centralized power plants with distributed installations including thermal and electric energy production and storage systems. In this context, solar home systems (SHSs) [1] and renewable energy communities (RECs) [2] represent some of the main actors of the energy transition. These systems are respectively single-user and multi-users installations mainly composed of photovoltaic (PV) modules, energy storage systems (ESSs) and other auxiliary components including cables, electric converters, and a backup generator in case the installation is disconnected from the grid.

Although renewable energy technologies are thought to produce sustainable energy and some of them do not imply direct emissions to the environment, they are responsible for an environmental impact at least during the production and waste management. Therefore, a reliable environmental impact analysis should consider the whole life cycle of the analysed system. In this perspective Life Cycle Assessment (LCA) represents one of the best approaches recognized by the European Union and regulated by the International Organisation for Standardization (ISO) [3,4].

Combined to environmental impact evaluations, techno-economic analyses of the performances of renewable energy technologies could contribute to the prediction of their possible competitiveness in the perspective of a large-scale diffusion.

In light of this, in this thesis, technical, economic, and environmental issues are addressed using an "Integrated LCA" to estimate the overall sustainability of SHSs and RECs. For this purpose, LCA is combined to Life Cycle Costing (LCC) [5], mathematical modelling and optimization tools. A wide range of storage technologies differing for technical properties, materials, cost, and maturity exists. All these factors contribute to determine the eco-profile of such technologies and of the overall system where they are employed. Several issues, dealing with ESSs efficiency, energy density, lifespan, and raw materials sustainability, still need to be faced. Therefore, an "Integrated LCA" analysis evaluating the relation among all these factors is of great research interest.

Moreover, energy systems sustainability represents a central topic of many national and international programs like the European Green Deal [6], a set of policy initiatives proposed by the European Union aiming to the climate neutrality in 2050. In this context, energy storage research and development activities are addressed by the European Strategic Technology Plan (SET Plan) as one

of the 10 key actions towards a decarbonized society. Notably, the targets defined by the SET Plan for energy storage technologies concern environmental, economic, and technical challenges. Therefore, the "Integrated LCA" analysis of SHSs and RECs presented in this thesis is a contribution to energy research field.

1.1. Objectives and Structure

1.1.1. Goal of the thesis

The object of this research thesis is the environmental and techno-economic assessment of residential PV and storage systems. Such evaluation aims to point out the most sustainable SHSs and RECs configurations depending on the characteristics of different energy storage technologies.

1.1.2. Structure

This thesis is composed of 5 Sections, including the Introductory remarks, and two Appendix sections:

- Section 2 is dedicated to the State of the Art: first the World Energy Scenario and energy storage technologies are overviewed, then a literature review of the existing LCA studies about batteries and PV installations are proposed.
- Section 3 is devoted to the Methods: LCA is carefully described as well as its integration with other approaches like LCC, mathematical modelling and mixed integer linear programming (MILP) optimization tools.
- Section 4 contains the results and collects 5 papers introduced by a brief preface describing the role of the study within the overall research project.
- Section 5 is dedicated to the conclusions of this research work.
- Appendix A includes a paper addressing the environmental sustainability of a water disinfection system based on solar energy that could be fruitfully integrated in remote SHSs and RECs to face energy poverty issues.
- Appendix B collects the supporting information files related to the above-mentioned papers.

2. State of the Art

2.1. World Energy Scenario

The World energy sector is radically changing because the global energy demand is increasing very fast; electricity production is significantly growing because this energy vector, unlike heat, can flow through long distances without relevant losses. Figure 1 shows that the electricity demand in 2019 was more than double compared to the value measured in 1990 and it is expected to further increase in the future. Such trend is mainly due to the exponential industrial growth of some Asian countries, like China and India, as consequence of their recent development [7].

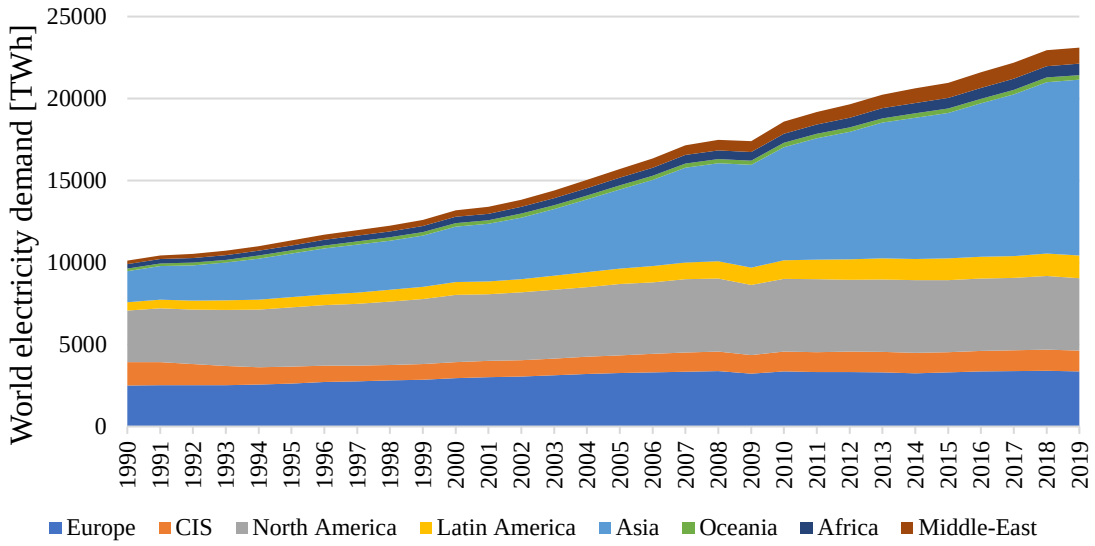

Figure 1: World electricity demand since 1990 by geographical area; including Europe, Commonwealth of Independent States (CIS), North America, Latin America, Asia, Oceania, Africa and Middle East [8].

Such an increasing electricity demand requires the massive consumption of fossil resources. At the current depletion rate, the temporal horizon of exploitable fossil resources availability is quite short: coal is expected to be over in 114 years whereas natural gas and oil in 52.8 and 50.7 years respectively [9].

Furthermore, the combustion of fossil fuels is responsible for the release of carbon dioxide to the atmosphere thus increasing its concentration. Therefore, similarly to the global energy demand, also the worldwide carbon dioxide emissions due to the combustion of fossils is growing very fast since 1990 as illustrated by Figure 2.

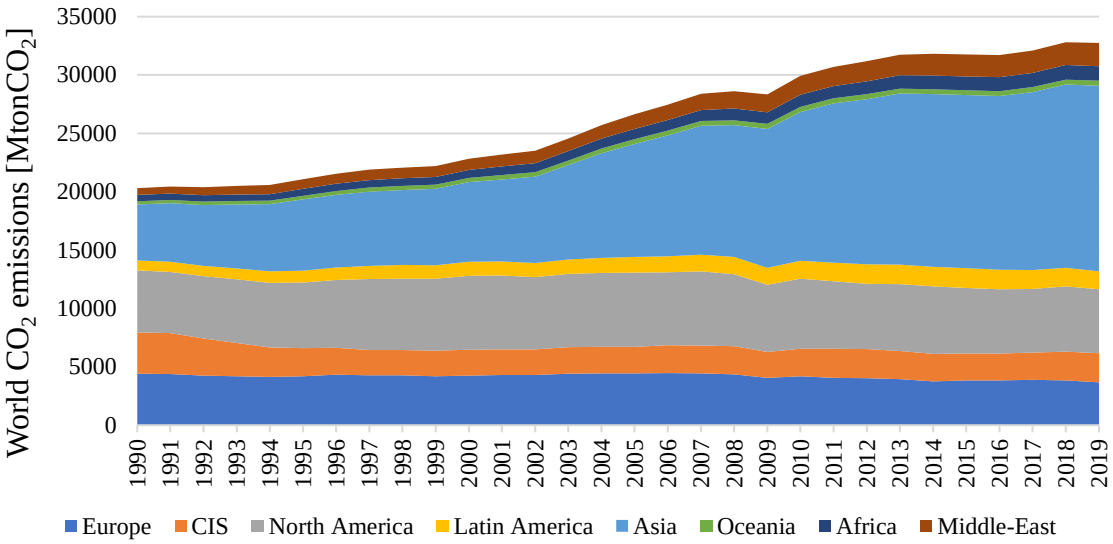

Figure 2: World carbon dioxide emissions since 1990 by geographical area; including Europe, Commonwealth of Independent States (CIS), North America, Latin America, Asia, Oceania, Africa and Middle East [8].

Carbon dioxide absorbs the solar radiation reflected by Earth surface and causes a growth of the average temperature on the planet. The Kyoto Protocol [10], an international agreement signed in 1992, indicates other five gases (methane, nitrous oxide, hydrofluorocarbons, perfluorocarbons, and sulphur hexafluoride) that, similarly to carbon dioxide, are responsible for Global Warming and for such reason they are all addressed as greenhouse gases (GHGs). According to the Intergovernmental Panel on Climate Change (IPCC), a United Nations body for assessing the science related to climate change, the consequences of Global Warming could become dramatic and irremediable [11]. Climate Change effects include the desertification of wide areas of the planet, the ice melting, the increase of seas level, frequent extreme meteorological events, wars, and massive migrations. These risks pushed 190 states (including European Union members) to sign a fundamental agreement in 2015 during the 21st Conference of the Parties of the United Nations Framework Convention on Climate Change (UNFCCC) [12]. Notably, the Paris agreement aims to keep the increase of the average Earth temperature well below 2°C compared to the pre-industrial levels. Moreover, all the countries that signed the agreement declared their commitment to keep such temperature increase below 1.5°C, since this would significantly reduce the risks and the impacts of Climate Change [12]. Nevertheless, their efforts currently seem insufficient because carbon dioxide concentration in the atmosphere is still growing (Figure 3a) and, according to the IPCC projections (Figure 3b), an average Earth temperature increase of 1.5°C could be reached in 2040 [13].

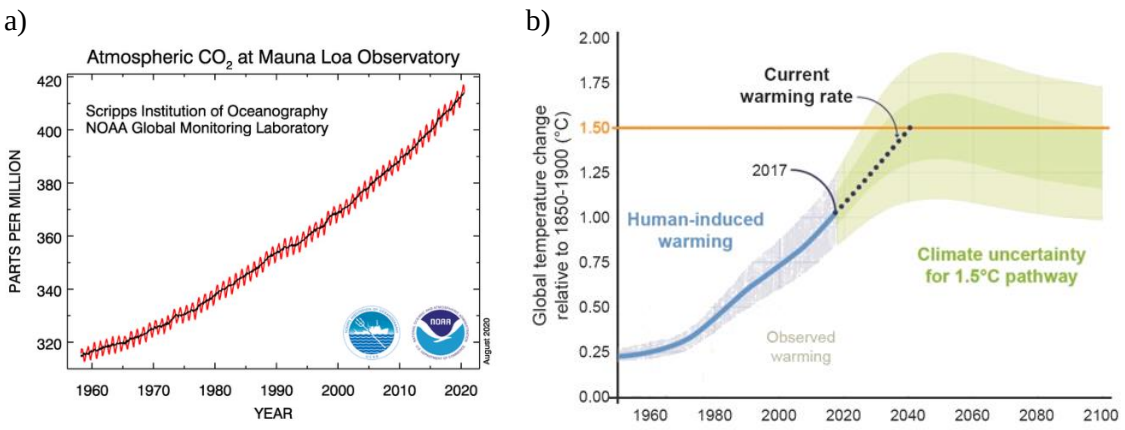

Figure 3: a) Atmospheric carbon dioxide concentration and b) average temperature increase compared since 1960 [13].

An explanation for these trends could be provided by analysing the International Energy Agency [7] data illustrated in Figure 4; this chart shows that the share of RESs still needs to be strongly enhanced to pursue the goals of the Paris agreement. Notably, among renewable energy systems only hydro, historically the most consolidated one, currently has a relevant share in the World electricity mix (16%) whereas all the other RESs represent together a very low percentage (10%).

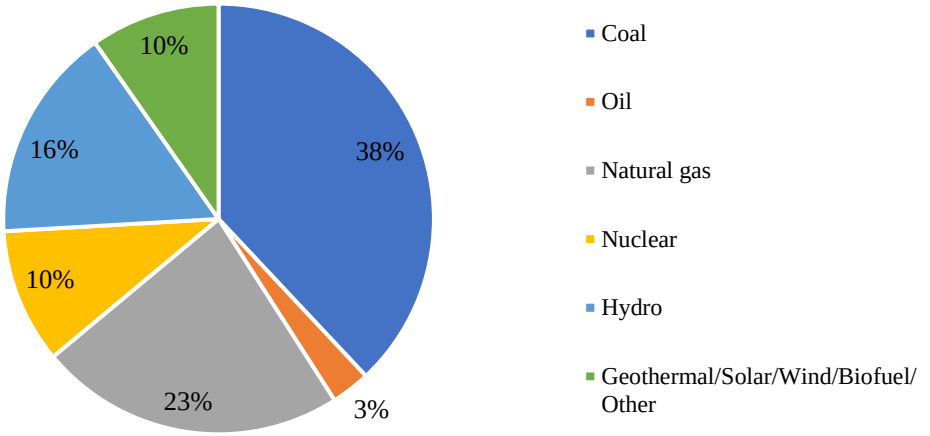

Figure 4: Share of fossil and renewable sources to the World gross electricity production, 2018 [7].

Therefore, it is fundamental to accelerate the energy transition investing in low carbon technologies; in this perspective, the International Energy Agency (IEA) expects that renewables will supply two-thirds of all capacity additions to 2040; PV will become the first electricity source by 2035 and wind generators installed power will triple thanks to off-shore plants [14].

At European level, the targets set by the European Commission 2030 climate and energy framework are the following [15]:

- A reduction of 40% of greenhouse gas emissions from 1990 levels.
- Enhancing the share of renewable energies to 32% of the total primary energy supply.
- An improvement of 32.5% in energy efficiency.

In Italy, according to the National Integrated Plan for Energy and Climate (PNIEC) [16], the contribution of renewables to the total primary energy supply is expected to grow from 18.3% in 2017 to 30% in 2030, whereas in the electricity sector, RESs share will grow from 34.1% to 55.0%. These goals will be hopefully achieved mostly thanks to PV and wind energy whose installed power will be respectively three and two times the current values.

Even though the perspective of a World fuelled by RESs is encouraging, this scenario is not free of challenges. Indeed, pushing the contribution of RESs to such high-level requires a renovation of electric grids to "Smart Grids". Over the technical and the economic issues implied by this transition, also its environmental sustainability should be considered. Indeed, all technologies, including renewable energy systems, have an environmental impact during their life cycle (i.e., during the production and waste management). Moreover, the environmental burdens of energy systems do not involve only natural resources depletion and Global Warming, but also other environmental indicators like particulate matter formation, ozone depletion, eco-toxicity, acidification, and eutrophication. For such reason, the evaluation of all these indicators is fundamental to assess the environmental effectiveness of electric grids.

2.2. Smart Grids

The Smart Grid concept was born in 2006 when the European Smart Grids Technology Platform report [17] was published to face the transition from centralized to distributed power generation. In Smart Grids, consumers start playing an active role in the energy network thus becoming "prosumers" because they can dispatch and store electricity as well as they consume it [18]. For these reasons, new generation electric grids should become flexible enough to manage fluctuating bi-directional energy flows; moreover, they should provide a reliable and low-cost energy supply to all the users [17]. These goals can be achieved through the smart integration of the following large-scale sub-systems to the main grid:

- Microgrids are low voltage networks connecting energy users, producers, and prosumers; microgrids are normally connected to the main grid but they can also turn to islanded mode in case of grid failures.

- Virtual Power Plants (VPPs) aggregate energy users, producers, and prosumers upgrading part of the existing grid. Therefore, differently from Microgrids, VPPs are not able to work as virtual islands [19].

Such systems are still mostly at research stage because of their complexity that implies several technological problems to overcome [20]. Different considerations can be done for small scale systems involving single users or small groups of users:

- Nano-grids are single users installations equipped with renewable energy technologies and storage systems [21]. SHSs are particular nano-grids composed of PV modules, a battery energy storage system (BESS) and further electric equipment (such as electric converters and cables) [1]. These installations can be connected to the grid or work in isolated mode in case they have a backup energy source.

- RECs are regulated by the European Union Renewable Energy Directive [22] as an aggregation of users (reaching a demand of few hundreds of kW) sharing the costs of technologies to get environmental and economic benefits from the deployment of renewable energy technologies and storage. Most of the RECs are owned by citizens but they can also be promoted by private companies and local authorities or municipalities [22].

Among renewable energy technologies, PV modules particularly fit with small behind-the-meter installations like SHSs and RECs whereas other generators (like hydro, wind, or geothermal systems) are more suitable for large power plants directly connected with the transmission or distribution grid. Using storage devices, SHSs and RECs can store the electricity they produce thus extending the self-consumption and the energy injection to the grid over time (Figure 5). In other words, ESSs allow to enhance RESs contribution to the national energy system [23].

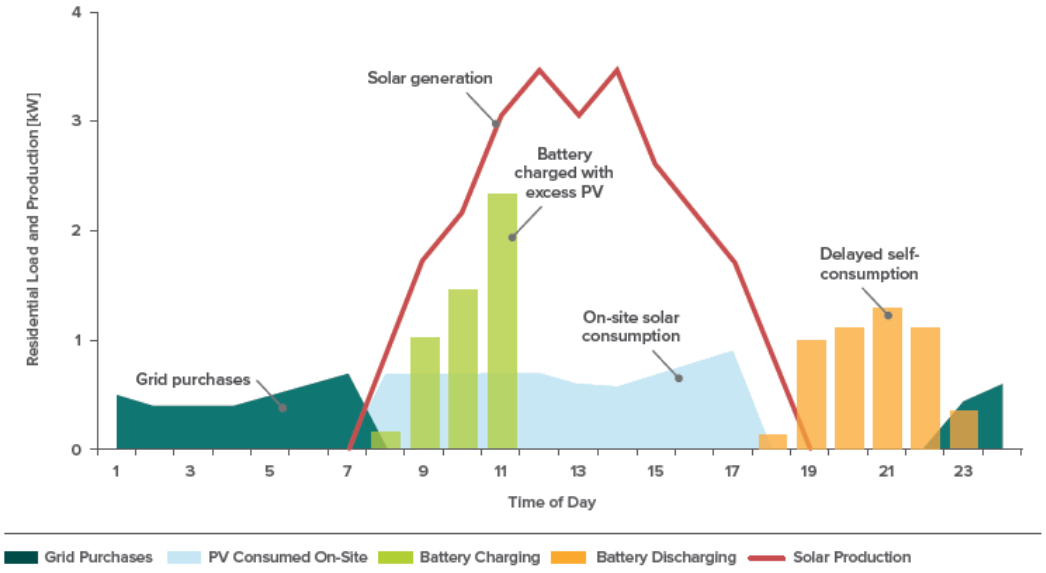

Figure 5: Representation of the energy flows in a residential PV system during applying a Demand Charge Reduction and Increased PV Self-Consumption strategies [23].

Moreover, by storing electricity, SHSs and RECs can prevent the overload of the grid during peaks of solar radiation; such service is known as energy curtailment. Indeed, without adequate storage systems, RESs variable electricity throughput may overload the limited capacity of a grid branch and change its electrical characteristics. Furthermore, energy storage can provide other additional services to the utility like smoothing the variations of voltage and frequency induced by the variable contribution of RESs. ESSs can also contribute to decongest the network and to guarantee continuous and safe electricity supply to the users [23].

ESSs can be deployed by the utility at grid level through centralized installations or by energy prosumers as distributed behind-the-meter systems. The storage capacity of SHSs and RECs can provide relevant advantages both to their own users and to the downstream transmission and distribution network [23]. Differently, centralized storage systems can be used by the utility, but they do not allow prosumers to manage their electricity production. Therefore, the deployment of distributed systems by prosumers is preferred to centralized ones [23]. Solar energy technologies like

SHSs and RECs also represent a fundamental tool to fight energy poverty: many people in the World have no access to primary needs like water and energy [24,25]; this problem can be addressed by the installation of SHSs and RECs both in underdeveloped and advanced countries [26].

Once energy is stored, prosumers can adopt different strategies to manage it. For instance, a simple energy management consists of supplying their load using their PV energy production and accumulating the surplus in storage systems thus extending the self-consumption. Therefore, by adopting this strategy, prosumers purchase electricity only in case ESSs are empty and inject the electricity surplus to the grid only when they are full. More advanced energy management strategies could be defined by prosumers: decisions could be taken using an optimization algorithm minimizing the costs or the environmental impact of the system, depending on the priorities of the prosumer. In case prosumers adopt economic rationality, incentives like feed-in tariffs play a key role in their decisions. Therefore, the utility could use feed-in tariffs to drive SHSs and RECs to enhance their environmental benefits to the grid.

2.3.Energy Storage

The previous subsection highlights the importance of storage in energy systems applications. Several types of ESSs having very different characteristics exist. For such reason, in order to describe and classify ESSs, it is necessary to define their operative parameters [27]:

- Nominal Voltage: a representative voltage value (V) typically defined in technical datasheets.
- Nominal Capacity and Energy: a representative charge (Ah) and energy (Wh) value accumulable by the device.
- Energy Density: the nominal energy stored by the ESSs per unit of mass - gravimetric energy density (Wh/kg) - or volume (Wh/l) - volumetric energy density.
- Power Density: the power delivered by the ESSs per unit of mass (W/kg) - gravimetric energy density - or volume (W/l) - volumetric energy density.
- C-rate and D-rate: the charge and discharge velocity (h^{-1}) of the ESS; each technology is limited by a maximum allowed charge and discharge rate.
- State of Charge (SOC): the residual ESS charge as percentage of its nominal capacity.
- Depth of Discharge (DoD): the consumed ESS charge as percentage of its nominal capacity; this value is complementary to SOC.
- Lifespan: the lifespan of an ESS depends on the operative conditions (like temperature, current rate, and DoD) and is determined by the sum of two ageing processes. The cyclic ageing is the ESS degradation due to the charge-discharge stress; the calendar ageing is the ESS degradation process naturally occurring regardless of its operation. The effects of ageing mechanisms are a loss of capacity and of rated power.
- State of Health (SOH): the nominal capacity of an ESS after degradation as percentage of the initial one.
- Roundtrip efficiency: the energy delivered by the ESS during the discharge as percentage of the energy used to charge it.

ESSs can be classified in five large families [27] as summarized by Figure 6.

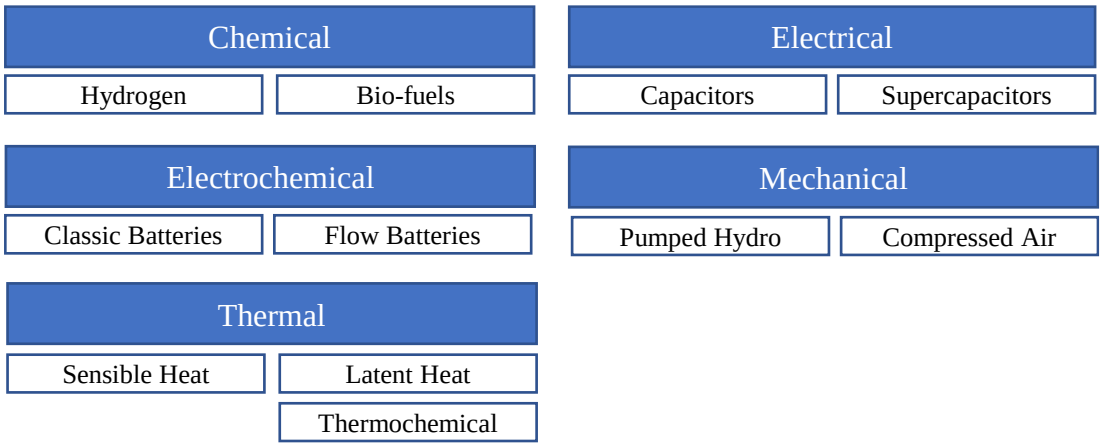

Figure 6: Overview of the main of energy storage technologies, adapted from [28].

Chemical storage consists of accumulating energy as the chemical energy of a fuel. Among all the chemical storage solutions, compressed hydrogen storage (CHS) is considered as one of the most promising ones. Indeed, even though most of hydrogen is currently produced by natural gas reforming, new sustainable production pathways based on RESs are emerging. One of them is electrolysis, namely a chemical reaction occurring inside an electrolyzer that splits water to gaseous hydrogen and oxygen by consuming electricity (that could be provided by a PV system). Then the gas is compressed and stored inside specific tanks until it is re-converted to electricity using fuel cells, electrochemical devices producing electricity by recombining oxygen and hydrogen. Hydrogen shows a great potential because it is a very light gas with a high gravimetric and volumetric energy density compared to other storage families (around 30 kWh/kg and 2 kWh/l) [29]. The conversion electricity-hydrogen-electricity in CHS systems is made of several steps that negatively affect the overall roundtrip efficiency (maximum 40%) [30]. Another way to store chemical energy is using biofuels that can be produced by chemical or photochemical treatment of biomasses [31].

Electrochemical storage devices convert electricity to chemical energy and vice-versa through batteries. Depending on their chemistry, such electrochemical cells have a certain voltage and capacity that determine the amount of storable energy. To achieve the desired overall voltage and capacity, multiple cells are connected in series and parallel and they are wrapped in a case to create a BESS. The gravimetric and volumetric energy density achievable by battery cells are variable depending on the chemistry (90-235 Wh/kg and 200-630 Wh/l) and they decrease moving from single cells to the overall battery systems. In any case such energy density values are much lower than those reached by CHS, but they have the advantage of being much simpler and more efficient. Indeed, the roundtrip efficiency is generally higher than 90%, but it depends on the battery type [30]. Electrochemical storage devices can be classified as classic and flow batteries; a more careful characterization of these technologies is detailed in the following subsection [30].

Electric storage devices convert electricity to an electromagnetic field; capacitors and supercapacitors are the most common devices belonging to this category. Despite of their low energy density, reaching maximum 5 Wh/kg, the power density of supercapacitors is very high and approximately equal to 20 kW/kg (versus 0.5 kW/kg of BESSs) [28]. Similarly to batteries, the low complexity of capacitors and supercapacitors guarantees very high efficiency values (around 90%) [30].

Mechanical storage is the most consolidated technology because, since many years, hydro power plants have been used as pumping stations to push water back to reservoirs and enhance the exploitable volume of water during the peaks of demand. This process determines some energy losses affecting the pumped hydro storage (PHS) efficiency (around 70-85%) [30]. Compressed air energy storage (CAES) technologies use the RESs energy surplus to compress and store air in underground caverns; then, the high-pressure fluid expands in turbines to produce electricity. Several components are necessary to install a CAES, and each step is responsible for some energy losses; therefore, the overall efficiency drops to 70% [30]. Both CHS and PHS require some very specific geomorphological conditions which limit the possibility to deploy them in several contexts [30]. This description highlights that mechanical storage systems can be large plants composed of heavy machines; therefore, they are not designed to have good energy and power density values, but to reach high power rates and capacity values.

Thermal storage allows to accumulate thermal energy by increasing the temperature of a fluid (sensible heat) or inducing a transition phase of a body (latent heat), typically from liquid to solid and vice-versa. Heat can also be used to trigger an endothermal reversible reaction and such energy can be released afterwards by the reverse chemical reaction (thermochemical storage) [28].

The above mentioned ESSs can be collected in a chart, known as Ragone plot, based on the gravimetric energy and power density of storage technologies. The Ragone plot illustrated in Figure 7 collects capacitors, supercapacitors, different types of batteries, and CHS. PHS and CAES are not included because, as previously mentioned, they are not precisely classifiable using their energy and power density. This chart shows that some technologies are particularly suitable when a high-power density is required (power storage applications), and other technologies are useful to store a large amount of energy (energy storage applications). This plot also contains the combustion engines and gas turbines and underlines that, although they are known to be impactful for the environment, their power and energy density are very competitive compared to other storage families [32].

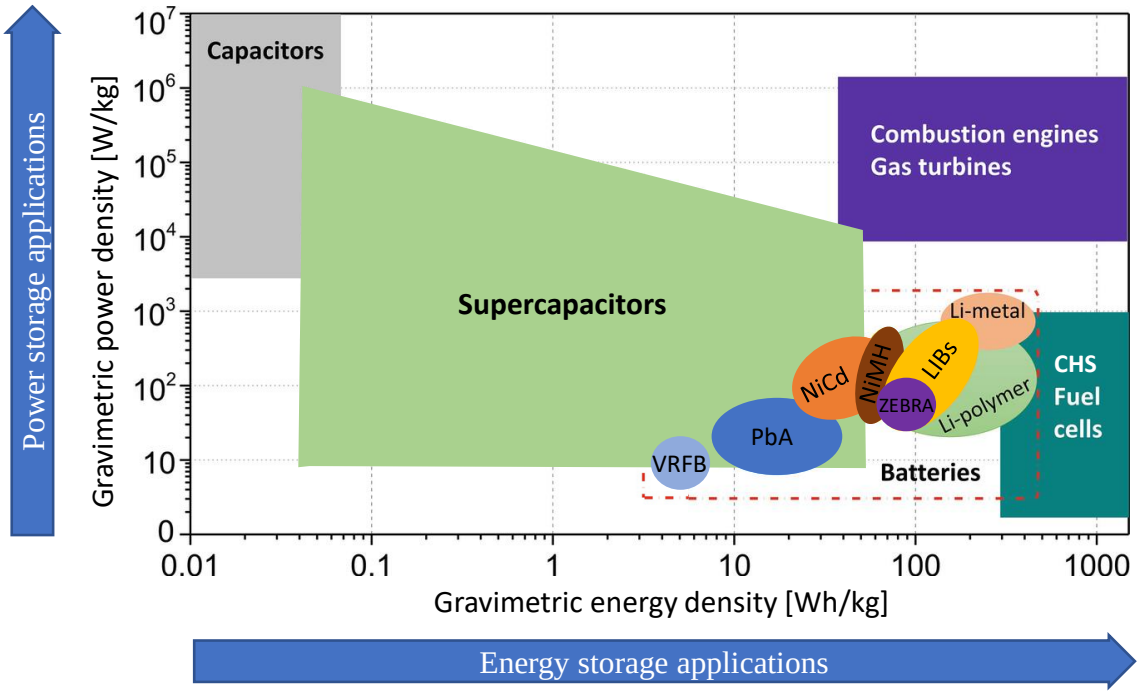

Figure 7: Ragone Plot for the classification of ESSs systems. Adapted from [32].

- Capacitors and supercapacitors are not suitable to store a high quantity of energy because of their low energy density but, differently from other technologies, they have a high specific power density that allows them to release much power in a very short time in power storage applications.

- Batteries are a heterogeneous family of devices; most of them have a good energy density which allows to guarantee a daily autonomy to the users. Nevertheless, such energy density values are not sufficiently high to guarantee larger autonomies because this would require an excessively high number of cells. The specific properties of different battery types are detailed in the following sub-section.

- CHS can be applied for long-term storage thanks to their high energy density values due to the possibility to compress hydrogen and accumulate it in relatively small volumes.

Considered that all storage technologies have a quite specific application, hybridization allows to design heterogeneous ESSs suitable for several tasks. For instance, a hybrid system could guarantee power storage using supercapacitors, daily storage thanks to a BESS, seasonal storage thanks to CHS.

The above mentioned families do not include another innovative system named thermoelectric energy storage (TEES) [33], that is a combination of thermal (sensible heat) and mechanical systems. Indeed, such an installation is composed of three subsystems (Figure 8):

- A refrigeration cycle powered by PV recharges a cold sensible heat storage.

- A heat pump powered by PV recharges a hot sensible heat storage.

- A power cycle (typically an Organic Rankine Cycle) subtracts heat from the hot storage, converts it to electricity with a turbine and releases waste heat to the cold storage during the discharge phase.

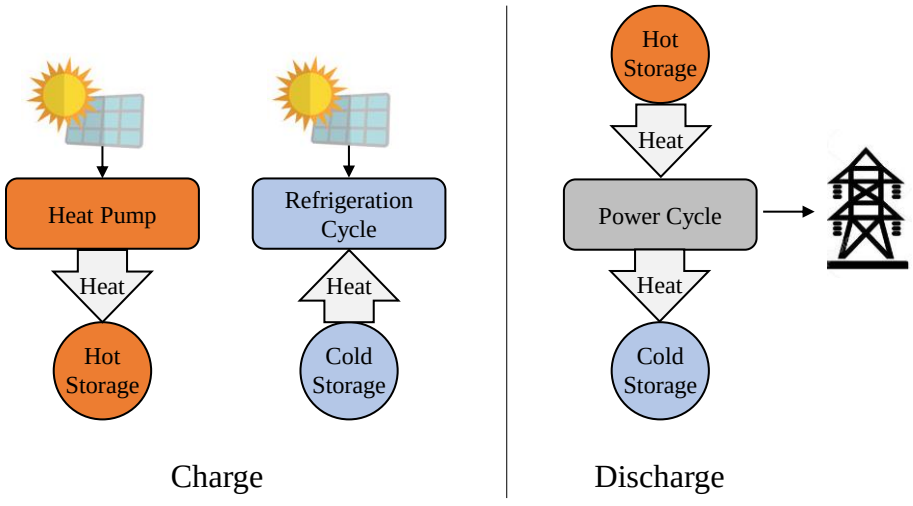

Figure 8: Simplified flowchart of TEES charge and discharge.

Differently from other ESSs, the thermodynamic irreversibility of thermal processes occurring in TEES are responsible for a relevant loss of energy quality, namely exergy. Energy quality is not addressed by traditional environmental assessments based on a quantitative energy evaluation, but this difference should be considered addressing thermal energy technologies.

2.3.1. Batteries

Among energy storage technologies, electrochemical storage represents one of most promising choices [28] because their characteristics are suitable for many applications. One of the main batteries advantages is their scalability that allows to obtain the desired capacity and voltage just connecting cells together; this makes them suitable for most of residential stationary applications. Moreover, batteries are efficient and simple technologies that do not contain moving parts and that do not require much maintenance and particular geological conditions [28].

As underlined in Figure 6, these devices are classified as classic and flow batteries. The working principle of classic batteries is known since 1799 when Alessandro Volta invented the first electrochemical cell (Figure 9); this cell was a "primary battery" because the recharge of the device was not possible [27] whereas those batteries that can be recharged are named "secondary batteries".

Figure 9: One of the first battery examples invented by Alessandro Volta shown in the museum "Tempio Voltiano" [27].

The basic principle of a secondary cell is the following: two electrodes, a negative one named anode and a positive one named cathode, are externally connected by an electric circuit and are divided by an electrolyte inside the cell. A polymer microporous separator is present to avoid short-circuits potentially caused by the contact between the electrodes [34]. During the charge and discharge processes, the voltage of secondary batteries varies between a cut-off and a maximum value during the charge and discharge cycles [35]. The profiles representing the battery voltage as function of the residual capacity are named charge and discharge curves that, together, create a hysteresis (Figure 10). The red area inside the hysteresis represents the energy losses of the battery and thus it is related to its roundtrip efficiency [35]. Different profiles can be drawn depending on the current rates and the cells temperature.

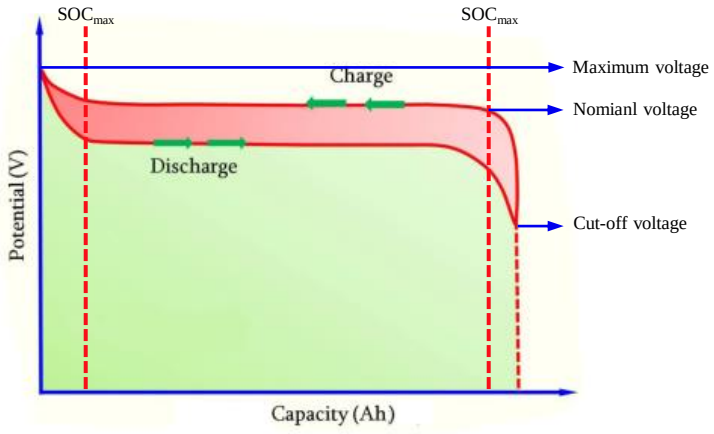

Figure 10: Typical Charge and Discharge curves of an ESS; the red area represents the energy losses and the green on represents the discharged energy. Adapted from [35].

The earliest secondary cell was a lead-acid (PbA) battery invented in 1859 by a French physicist named Gaston Planté and it has been largely used for stationary applications until the last years [28]. In PbA batteries the anode and cathode are respectively made of lead dioxide (PbO_2) and spongy lead (Pb) whereas the electrolyte is aqueous sulphuric acid [30].

Then, nickel metal hydride (NiMH) and nickel cadmium (NiCd) devices were invented but they didn't find as much space as PbA systems in the market [30]. Although most of the currently operative stationary installations are equipped with PbA batteries [30], another technology named lithium-ion batteries (LIBs) is gradually taking over them [28], indeed Stanley Whittingham, John Goodenough and Akira Yoshino won the Nobel Prize for Chemistry in 2019 for their invention [30]. These batteries can have different electrode materials, but their common characteristic is to contain some lithium-ions Li^+ inside the electrodes where they permeate with a mechanism named "intercalation". While electrons flow though the external circuit, lithium ions cross the electrolyte, usually made up of lithium salts (such as $LiPF_6$) dissolved in organic liquids. The cathode can be composed of several metals: the most common devices have a lithium cobalt oxide (LCO) cathode because it enhances the energy density of the device. Nevertheless, cobalt scarcity is becoming a major issue [36] that is drastically affecting the costs of LIBs and their environmental sustainability as well. Indeed cobalt and lithium are classified by the European Commissions as critical raw materials [37]. Therefore, research is pushing towards the development of LIBs having a low-cobalt content, such as nickel cobalt aluminium (NCA) and manganese (NCM) devices; moreover, also cobalt-free LIBs exist, such as lithium-iron-phosphates (LFP) and lithium manganese oxide (LMO). Over the materials availability, another strength of cobalt-free batteries is the possibility to perform more cycles during their life and to exchange higher current rates. Typical LIBs cells have a graphite anode but in novel lithium iron titanate (LTO) batteries, this material is replaced by titanium dioxide [38]. Other innovative types of LIBs are lithium cobalt phosphates (LCP) devices [39], mixed LMO-NCM batteries [40] and molybdenum disulphide NCM batteries (NCM- MoS_2) [41]. Even though manganese and nickel are more abundant than lithium and cobalt, they are anyway listed among the 25 rarest materials on the Earth [37]. Therefore, the metal depletion indicator is a major problem to address regardless of the battery type. A scheme of the very first LIB proposed by their inventors in 1985, namely a LCO battery with a petroleum coke anode, is illustrated in Figure 11 [30].

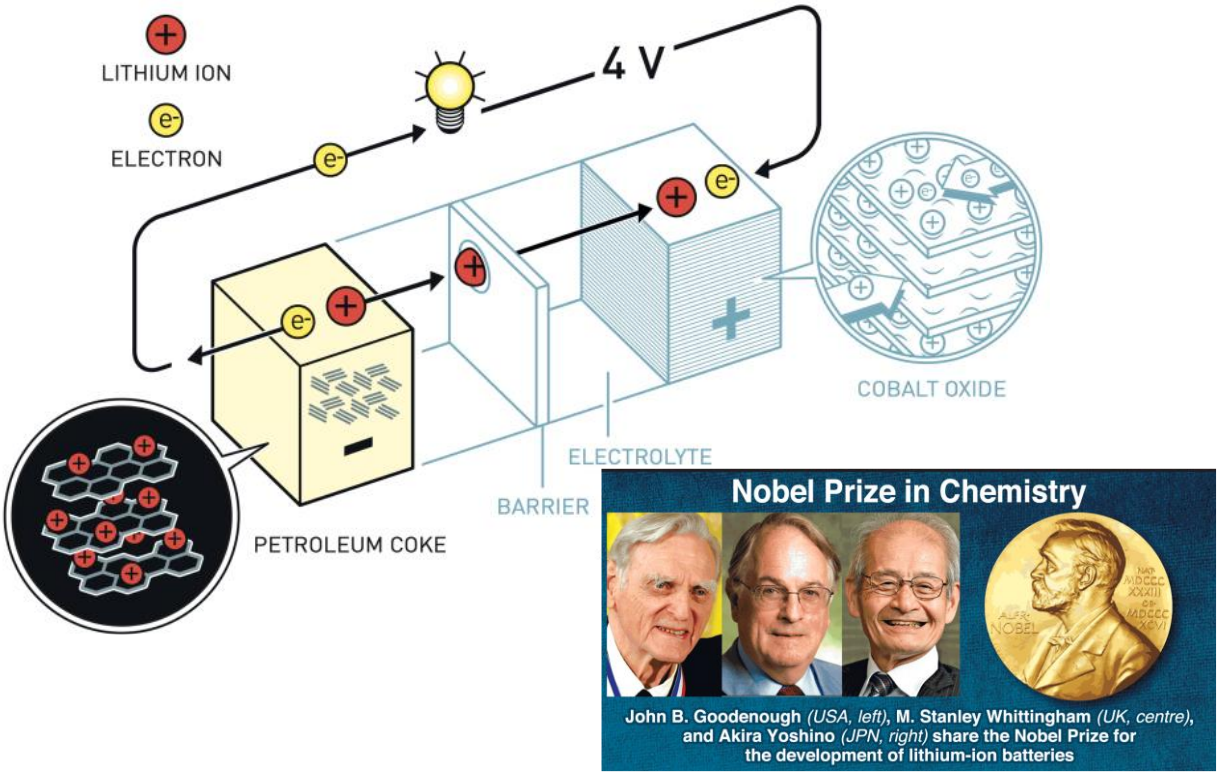

Figure 11: Illustration of the first LIBs prototype and of its inventors [30].

One of the research priorities for LIBs, especially in stationary applications, is extending their lifespan. The cyclic degradation of these devices is due to several types of stressing processes [42]: the flow of lithium ions across the electrodes surface determines continuous expansions and contractions of the materials resulting in a mechanic degradation and a loss of capacity. The electrodes degradation is also induced by high cells temperatures [43] that also accelerates the undesired reactions determining the battery natural ageing [34]. Furthermore, another major problem in LIBs is the "lithium planting" [44], namely the formation of metal lithium dendrites on the anode surface potentially creating short circuits by penetrating through the separator. Such metal lithium spikes can grow as consequence of high current rates affecting lithium ions intercalations; moreover, in low temperature environmental conditions, the battery reaction rate slows down thus inducing lithium planting. From the safety point of view instead, high temperatures can be dangerous because they can trigger a degenerative process, named thermal runaway, leading to the explosion of the battery [45].

To prevent fire risks and to increase the energy density of the battery, the liquid electrolyte can be replaced by a solid one in solid state lithium-ion batteries (SSLIBs). One of the main materials to replace liquid electrolytes is a crystalline solid named lithium phosphorous oxynitride (LiPON). The positive effects of the electrolyte replacement is the increase of the energy density whose value approximately doubles [46]. Another valuable alternative to LiPON is a polymer named polyacrylonitrile that is commonly used in lithium-polymer batteries.

Lithium-metal batteries represent another group of electrochemical devices: these cells are precursors of LIBs because the battery prototype proposed by Stanley Whittingham contained a metal lithium anode. These devices are negatively affected by lithium planting: dendrites rapidly grow on the lithium metal anode surface and, after reaching the cathode, they induce the explosion of the device [30]. Nevertheless, research never gave up on solving such safety and durability issues because

lithium-metal batteries, compared to LIBs, can take advantage of a great energy density. In the last years, this problem has been mitigated but lithium-metal batteries are still not competitive with LIBs from this point of view. Depending on the cathode materials, several battery chemistries are included in this family: among these batteries, much research is focused on lithium-sulphur batteries (LiSBs) [47] and lithium-air batteries [48]. In order to replace lithium with a more common metal, Zinc-air batteries represent another interesting field of research [49].

Indeed, some literature studies show that cobalt scarcity is not the only problem from the materials availability perspective: lithium is also addressed as a critical raw material and about 40% of its extraction is devoted to the production of batteries [50]. Therefore, research is also focusing on alternative materials. For instance, LIBs are part of a wider family named metal-ion devices, including sodium-ion batteries (SIBs) [51] and aluminium-ion batteries (AIBs) [52]. Among these cells, SIBs are the most mature devices but none of them have reached a diffused commercialization. Notably SIBs have a problem related to the sodium ions size, bigger than lithium, which impedes their intercalation in graphite layers. To face this issue researchers are working on graphene as anode material; furthermore they are trying to enhance SIBs lifespan and their energy density [53].

Other electrochemical cells that do not contain lithium are addressed as molten-salt batteries because they have a molten-salts based electrolyte; for such reason, they require higher operative temperature levels than other batteries. Among these devices sodium-nickel chloride batteries, also addressed as ZEBRA (Zero Emission Battery Research Activities) [54], are the most consolidated devices. The cathode is composed of nickel chloride, sodium chloride and sodium aluminium chloride whereas the anode is made of sodium and are both at liquid phase. For these reasons, these cells operate in a temperature range between 270 and 320°C. Another promising battery belonging to the category of molten-salts devices is the sodium-sulphur (NaS) battery [55] that also have liquid electrodes.

The above-mentioned electrochemical devices are all addressed as classic batteries; flow batteries differ from them because their electrolyte is stored inside two tanks and is pumped inside the electrochemical cells. Among them, vanadium redox flow batteries (VRFBs) are the most consolidated technologies (Figure 12): two semi-cells respectively contain an anolyte (an electrolyte with a negative charge) and a catholyte (having a positive charge). Both electrolytes contain vanadium compounds dissolved in a sulphuric acid (H_2SO_4) aqueous solution that can be completely recovered and regenerated [56]. This is very important because of vanadium scarcity; indeed this material is considered by the European Commission as a critical raw material and it is even rarer than lithium [37]. To avoid the mixing of catholyte and anolyte, an ion exchange membrane is put between the two semi-cells.

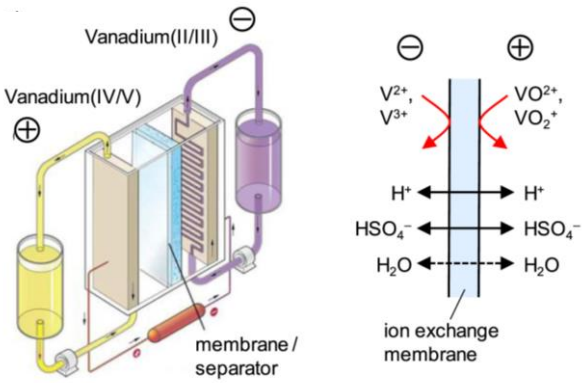

$$VO^{2+} + H_2O \underset{discharge}{\overset{charge}{\rightleftharpoons}} VO_2^+ + 2H^+ + e^-$$

$$V^{3+} + e^- \underset{discharge}{\overset{charge}{\rightleftharpoons}} V^{2+}$$

Figure 12: Description of a VRFB components and reactions, adapted from [57].

The main drawback of this technology is its very low energy density whereas the main advantage is the design flexibility of the storage system: the volume of storage tanks determines the battery capacity whereas the membrane surface determines the nominal power. Moreover, they can perform a very long number of cycles and are slightly affected by natural ageing [56].

Among the previous batteries, the most mature and commercialized technologies are classified in terms of energy and power density by the Ragone plot illustrated in Figure 7.

One of the main issues of BESSs is currently the possibility to recycle their materials as some metals contained by the cells are rare and expensive. Some traditional batteries like PbA or NiMH technologies can already be recycled at industrial level. Contrarily LIBs recycling is not implemented at industrial scale because of the very high costs [58]. Indeed, some metallurgical processes could be suitable for LIBs recycling, but they need to be optimized for this scope. The first steps are the physical treatments of the battery, namely the disassembly, the separation of the components and the liquid electrolyte evaporation to prevent explosions. Then, the batteries are subject to a pyrometallurgical process that melts the cells metals to produce an alloy; a valuable alternative is an hydrometallurgical process where metals are recovered by leaching [59].

Energy storage represents one of the 10 key Actions (namely Action 7) defined by the SET Plan to develop low carbon technologies, an important research Program at European level coordinating and financing national and international research projects. Notably, batteries research is organized according to five flagships (Figure 13a) and three focus areas (Figure 13b) [60].

a)

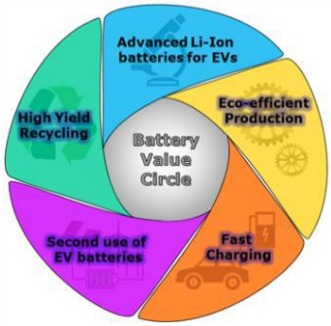

b)

Focus Area 1: Material/Chemistry/Design+ Recycling	
1.1 Advanced Lithium-Ion batteries for e-mobility	*Part of Materials Flagship*
1.2 Influence of Fast/Hyper charging of Li ion batteries on materials and battery degradation	*Fast-charge Flagship*
1.3 Advancement of batteries for stationary energy storage (ESS)	*Part of Materials Flagship*
1.4 Beyond Li ion / Li based batteries for e-mobility	*Part of Materials Flagship*
1.5 Develop circular economy and de-bottleneck availability of critical raw materials	*Recycling Flagship*
1.6 Lithium recovery from European geothermal brines and sustainable beneficiation processes for indigenous hard rock occurrences of lithium	
Focus Area 2: Manufacturing	
2.1 Foster development of materials processing techniques and components for fast industrialization compatible with present mass production lines	*Manufacturing Flagship*
2.2 Foster development of cell and battery manufacturing equipment	*Manufacturing Flagship*
Application and Integration	
3.1 Hybridisation of battery systems for stationary energy storage (ESS)	

Figure 13: a) Research flagships b) focus areas for SET-Plan Action 7 [60].

Figure 13 mentions most of the batteries issues addressed in this section such as the raw materials scarcity, the battery ageing, the hybridization and the waste management [60]. Furthermore, the SET Plan defines the main research priorities for stationary applications: the main goal at component level is enhancing the lifespan and the energy density and reducing batteries costs. At system level instead, research should focus on the smart management of batteries grid integration and the hybridization of ESSs [60].

According to the SET-Plan roadmap, classic and advanced LIBs are expected to be the leader technology until 2025; after that year SSLIBs and post-LIBs are likely going to take over them in the market. China currently has a relevant industrial advantage in batteries manufacturing, but Europe decided to invest in the development of these technologies to become competitive with Asian market in the next future. In this perspective, the European Battery Alliance was born in 2017 to facilitate the cooperation between all the stakeholders and to capture a market of up to €250 billion a year from 2025 onwards in the batteries manufacturing industry [61]. Moreover, the SET-Plan determines some specific targets for batteries research that concern both technical, economic and recycling challenges as illustrated in Table 1.

Table 1: Main target for batteries research proposed by the SET-Plan. Adapted from [61]

		(2014-2015)	2020	2030
Performance targets				
1	Gravimetric energy density [Wh/kg]			
	Pack level	85-135	235	>250
	Cell level	90-235	350	>400
2	Volumetric energy density [Wh/l]			
	Pack level	95-220	500	>500
	Cell level	200-630	750	>750
3	Gravimetric power density [W/kg]			
	Pack level	330-400	470	>470
	Cell level		700	>700
4	Volumetric power density [W/l]			
	Pack level	350-550	1000	>1000
	Cell level		1500	>1500
5	Fast recharge time [min]	30	22	12
6	Battery lifespan (at normal ambient temperature)			
	Cycle life for automotive – 80% DoD [cycles]		1000	2000
	Cycle life for stationary – 80% DoD [cycles]	1000-3000	3000-5000	10000
	Calendar life [years]	8-10	15	20
Cost target				
7	Battery pack cost for automotive [€/kWh]	180-285	90	75
	Battery pack cost for stationary [€/kWh/cycle]		0.1	0.05
Recycling target				
8	Recycling efficiency	50%	50%	50%
	Economy of recycling	Not economically viable	Break even	Economically viable
	Second Life	Not developed	Developed	Fully established

2.3.2. Literature Review

According to the SET Plan, batteries research should follow a life cycle approach, indeed the flagships and the focus areas depicted in Figure 13 involve raw materials, manufacturing, applications, and end of life. Such life cycle approach is particularly relevant when assessing the eco-profile of batteries and PV systems since they are not responsible for direct emissions of GHGs.

A standardized approach to perform a LCA of batteries is provided by specific Product Environmental Footprint Category Rules (PEFCR) [62]. Such guidelines are mandatory to perform a Product Environmental Footprint (PEF), but they provide useful insights to perform all types of environmental assessments.

Concerning the construction phase, a review of 79 LCA studies of LIBs is proposed by Peters et al. [63]. Among them, Peters and Weil [64] selected those studies proposing an extensive, reproducible and reliable inventory based on primary data about batteries construction. Relevant differences exist between these studies in terms of methodological assumptions; therefore, the authors modified the original inventories to create a harmonized database where every battery is modelled grounding on a common approach. This database is provided as a downloadable file which can be imported in openLCA, an open source software to perform LCA analyses [65]. The studies analyzed by Peters and Weil are the following [64]:

- Ellingsen et al. [66] performed the environmental assessment of a NCM battery production.
- Majeau Bettez et al. [67] compared NCM and LFP batteries production.
- Notter et al. [68] assessed the environmental performances of LMO batteries production.
- Zackrisson et al. [69] performed a LCA of LFP batteries production.
- Bauer et al. [70] analyzed the environmental performances of NCA batteries production.

The above-mentioned batteries inventories are widely used and mentioned along all this thesis. Concerning the other LCA studies about batteries available in literature, several differences exist between them. For instance, when the study is focused on the production of battery systems, the environmental impacts are usually expressed per unit of mass or per unit of storable energy. It is possible to switch between these expressions multiplying by the gravimetric energy density. Some papers address the use phase and express the results per unit of delivered energy during the life cycle. A few literature papers carefully evaluate batteries end of life because of the lack of literature data and of their very high uncertainty [71]. Table 2 collects 27 literature studies that propose the LCA of battery systems. As underlined by this table, some of these papers also include PV modules in the system boundaries whereas others only include the battery system. Among all the papers collected in Table 2, only a small number (underlined in Table 2) provide a full and reproducible inventory. Most of the studies collected in Table 2 are about PbA, NiCd, NiMH and LIBs, but a few examples of post-LIBs assessments are also available. Those papers considering electric vehicles LCA without focusing on the batteries at component level are excluded from the review because they are out of the scope of the thesis.

Table 2: Summary of literature studies about batteries LCA available in literature.

Paper	Battery chemistry	Paper	Battery chemistry
Batteries LCA studies			
Ellingsen et al., 2103 [66]	NCM	Dunn et al., 2015 [72]	LMO
Ambrose and Kendall, 2016 [73]	LFP	McManus, 2012 [74]	PbA
	NCA		LIB generic
	LTO		NiCd
	NCA		NiMH
	NCM		NaS
Hammond and Hazeldine, 2015 [75]	LIB	Hiremath et al., 2015 [76]	VRFB
	ZEBRA		NaS
	NiCd		PbA
Majeau Bettez et al., 2011 [67]	NiMH		LIB
	NCM	Raugei and Windfield, 2019 [39]	LCP
	LFP	Cusenza et al., 2019 [40]	LMO-NCM
Zackrisson et al., 2010 [69]	LFP	Troy et al., 2016 [77]	SSLCO
Richa et al., 2017 [78]	LMO	Peters et al., 2016 [79]	SIB
Kim et al.,2016 [80]	LMO-NMC	Longo et al., 2014 [54]	ZEBRA
Faria et al., 2014 [81]	LMO	Delgado et al., 2019 [82]	AIB
Larcher and Tarascon, 2015 [83]	LIB generic	Santos et al., 2020 [84]	Zinc-Air
Weber et al., 2018 [85]	VRFB	Zackrisson et al., 2016 [48]	Lithium-Air
Deng et al., 2017 [41]	NCM-MoS_2	Lastoskie and Dai, 2015 [46]	LIBs
Notter et al., 2010 [68]	LMO		SSLIBs
Deng et al., 2017 [47]	LiSB	Bauer et al., 2010 [70]	NCA
Batteries + PV			
Krebs et al., 2020 [86]	NCM	Kabakian et al. , 2015 [87]	PbA
	LFP		PbA
Stolz et al., 2018 [88]	NCM	Dufo Lopez et al., 2011 [89]	LFP
Belmonte et al. [90]	Generic LIB	Jones et al., 2017 [91]	PbA

The results of the analyses collected in Table 2 vary within a very wide range of values because they are affected by different methodological approaches and assumptions concerning the system boundaries and the geographical reference of production processes. The main environmental indicators addressed by studies in Table 2 are:

- 100% of the proposed analyses calculate the Global Warming Potential (GWP). This indicator is expressed as the amount of equivalent carbon dioxide ($kgCO_2eq$) emissions, including all the GHGs released over batteries life cycle.
- 33% of the proposed analyses calculate the Human Toxicity Potential (HTP). This indicator is expressed by most of the impact assessment methods as the amount of equivalent 1,4-Dichlorobenzene (kg1,4 DCBeq) emissions.
- 37% of the proposed analyses calculate the Acidification potential (AP). This indicator is expressed as the amount of equivalent sulphur dioxide ($kgSO_2eq$) released over batteries life cycle.
- 37% of the proposed analyses calculate the Abiotic Depletion Potential (ADP). This indicator expresses the consumption of non-living resources as equivalent antimony ($kgSb_{eq}$). Some

impact assessment methods distinguish between metal depletion potential (MDP) and fossil depletion potential (FDP), respectively measured as equivalent mass of iron ($kgFe_{eq}$) and oil ($kgoil_{eq}$) consumed.

- 19% of the proposed analyses calculate the Particulate matter formation (PMF). This indicator is expressed as the mass of solid particles having a diameter lower than 10 μm (kgPM10) emitted to the atmosphere over batteries life cycle.
- 22% of the proposed analyses calculate the Cumulative Energy Demand (CED). This indicator is expressed as the amount of energy embedded in batteries as it is consumed during all their life cycle stages.
- Only one of the proposed analyses [84] calculate a single score environmental impact through normalization and weighting to summarize multiple impact indicators. This environmental impact value is expressed as eco-point (Pts).

The main outcomes resulting from such literature review are the following

- There is an extensive literature about batteries production LCA analyses, but only a few studies publish full and reproducible datasets.
- The environmental impact indicators range should be extended; moreover, normalization and weighting should be more extensively applied to evaluate single scores useful to compare different systems.
- There is a wide literature about currently commercial batteries like LIBs, but there is lack of LCA studies addressing advanced post-LIBs.
- LCA models are weakly integrated by a techno-economic evaluations of batteries performances.
- Batteries end of life represents a big literature gap due to the scarcity of reliable data [71].

2.4. Contribution of the research project

As underlined in the Introductory remarks section, the goal of the paper is performing and "Integrated LCA" to assess the sustainability SHSs and RECs focusing on the role of the storage system. The previous subsections underline the importance of SHSs and RECs in the energy transition and decarbonization and describe the characterization of storage technologies. Notably, this chapter highlights the problems and the challenges that these energy systems should face and that affect their techno-economic and environmental performances. In other words, this general overview points out the variables of the "Integrated LCA" proposed in this project, highlighted as following:

- Spatial variability: depending on the environmental conditions of the site, the performances of solar energy systems can drastically change. A particular attention is posed to Italy as reference country of the analysis, but also other European countries are considered.
- Temporal variability: in all installation site, the working conditions of SHSs and RECs change over time, depending on solar radiation seasonal and daily variations.
- Scale: results could be different considering single users and multi-users prosumers or assessing their effects on the national energy system.

- System Configurations: results could be strongly different if the proposed installations are connected to the grid or work in islanded mode. Moreover, ESSs can be simple (i.e., only made of batteries) or hybrid.
- Technologies maturity: some of the energy storage technologies are already consolidated and diffused whereas others show a great potential but still need to be further developed.
- Costs: economic considerations are very important when addressing consumers decisions about technologies investments and energy management strategies.
- Energy quality: when thermal storage and TEES is analysed, the effects of exergy losses should be considered.

All these variables are addressed by the "Integrated LCA" proposed in this thesis grounding on the life cycle inventory and the techno-economic data available in literature.

3. Methods

In this section, the methods adopted in this research project are described. LCA represents the main methodology because it allows to evaluate the environmental performances of SHSs and RECs during their life cycle. Nevertheless, LCA is not sufficient to address all the variables of the problem, for such reason it is integrated with some auxiliary approaches. The overall methodology obtained by combining different methodologies is named "Integrated LCA".

3.1. Life Cycle Assessment

LCA is regulated by the International Organization for Standardization ISO 14040 [3] and ISO 14044 [4] since 2006, but the earliest environmental analysis that can be considered a LCA was named "Resource and Environmental Profile Analysis" and it was performed by Coca Cola in 1969 [92]. Then the Society of Environmental Toxicology and Chemistry gave the first formal definition of the LCA methodology in 1993 [93], schematized by Figure 14:

"*An Assessment that includes the entire life cycle of a product, process or activity, encompassing, extracting and processing raw materials; manufacturing, transportation and distribution; use, re-use, maintenance; recycling, and final disposal"*

Figure 14: Sketch of Life Cycle Assessment methodology.

Therefore, after many years of conceptualization, standardization, and methodological elaboration, LCA analyses are now largely used both in industry and in research [94]. According to ISO 14040 [3], an LCA analysis is composed of four phases as illustrated in Figure 15: Goal and Scope Definition, Life Cycle Inventory (LCI), Life Cycle Impact Assessment (LCIA) and Interpretation.

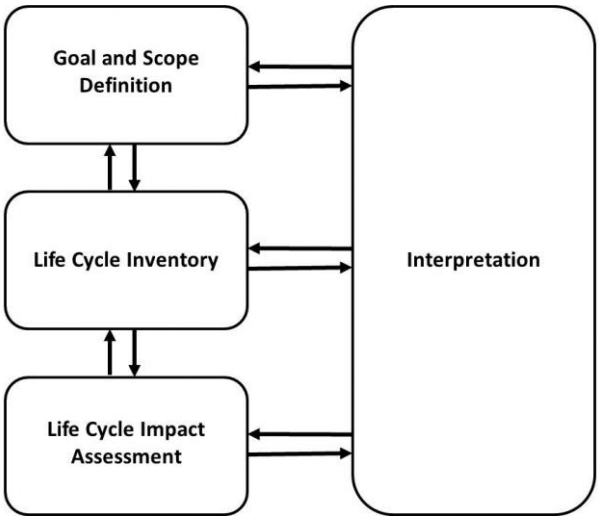

Figure 15: Definition of the four phases of life cycle assessment according to ISO 14040 [3].

3.1.1. Goal and scope definition

The first phase of an LCA study, namely the Goal and Scope definition, is fundamental to define the following aspects of the analysis:

- Intended application of the results.
- Assumptions and limitations of the LCA model.
- The function, the functional unit, and the reference flow of the analysed system.
- The system boundaries and the cut-off rules, where all the processes excluded and included in the product system are indicated.
- Selection of the LCIA method and of the impact categories.
- The data and information sources.

According to ISO 14040 [3], the function of the system represents the performance characteristics of the product system whereas the functional unit quantifies the function and creates a correlation between inputs and outputs of the product system. A reference flow is a quantified amount of the product(s), including product parts, necessary for a specific product system to deliver the performance described by the functional unit.

According to the goal and scope of the analysis, three different approaches can be defined:

- Cradle to Grave analysis: environmental impacts are calculated considering the whole life cycle of the product system, from raw materials extraction to their end of life.
- Cradle to gate: environmental impacts are calculated considering part of the life cycle of the product system which starts from raw materials extraction and stops before the end of life, evaluation (for instance at the production level or the use phase).
- Gate to gate: environmental impacts are calculated considering and intermediate part of the life cycle of the product system (for instance focusing on the use phase).

3.1.2. Life Cycle Inventory

The LCI is the collection and the quantification of the input and output flows included in the system boundaries. The source of these data is defined in the Goal and Scope definition: primary data are preferred because they specifically apply for the analysed system. Whether primary data are not

available, secondary data can be obtained from previous literature studies or life cycle databases like Ecoinvent [95]. To perform a correct analysis, the LCI should have a spatial and temporal resolution and should be reproducible.

3.1.3. Life Cycle Impact Assessment

According to ISO 14040 [3], the fourth phase of the analysis is the LCIA; an LCIA method converts the LCI results to environmental impact values following 4 steps: Classification, Characterization, Normalization and Weighting. As underlined by Figure 16, the first two steps are mandatory whereas the last two are optional.

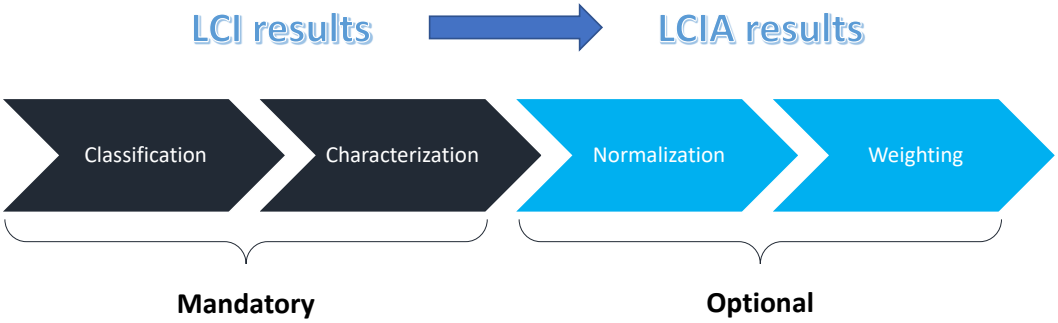

Figure 16: Steps of the LCIA phase.

During the classification, the LCI results are associated to environmental impact categories proposed by the LCIA method. During the Characterization, the LCI results are multiplied by some characterization factors. Results can be expressed by Midpoint indicators, representing the potential burden of the system for a certain category before damage occurs, or by Endpoint indicators, representing the potential damage to the Ecosystems, Human Health and Resources. The Normalization process consists of applying to the characterized results a normalization factor represented by a reference impact. Then, the Weighting step allows to convert the normalized results to a single score; this is particularly useful to compare different product systems.

3.1.4. Interpretation

According to ISO standards, the Interpretation of the first three steps of the analysis is important to make the following main checks:

- The consistency with Goal and Scope should be evaluated.
- A contribution analysis of the most relevant processes should be done.
- The appropriateness of the LCIA method should be analysed.
- The coherency and validity of assumptions should be verified.
- Uncertainty should be assessed.

3.2. Auxiliary approaches

As underlined in the Introductory remarks, this project proposes an “Integrated LCA” where the following auxiliary methodologies are combined.

3.2.1. Life Cycle Costing

LCC is a methodology standardized by ISO 15686 [5] and grounds on the same principles of LCA: the economic costs of SHSs and RECs should be evaluated over their life cycle as well as their environmental impact. Indeed, for many long living goods, the purchase price represents only a small share of the overall costs "of ownership" whereas the operation and disposal can relevantly contribute to the overall costs. Among the variables of the "Integrated LCA" analysis proposed in this thesis (defined in Section 2.4), LCC allows to assess the life cycle economic impact of the analysed systems.

3.2.2. Design Equations

As described in Section 3.1, LCA is an input-output methodology which requires, as far as possible, primary data from direct measurements. Nevertheless, this research project is not focused on a specific case study, but it concerns a general evaluation of SHSs and RECs environmental performances. Therefore, for several installation sites, the design equations are used to size SHSs and RECs components using representative data as inputs (i.e., the average values of energy demand and solar radiation). Among the variables of the "Integrated LCA" analysis, the design equations allow to address the spatial variability of the problem, the comparison of different system configurations, and the technical properties of ESSs having different maturity levels.

3.2.3. Mathematical Modelling

After SHSs and RECs are designed, dynamic simulations allow to evaluate their performances in time. Notably, simulations are performed running mathematical models composed of a set of equations that express energy balances and the degradation of ESSs. Therefore, Mathematical Modelling considers the spatial and temporal resolution of the analysis highlighting the differences between different configurations and between mature and research-level technologies.

3.2.4. Mixed Integer Linear Programming optimization

Mixed Integer Linear Programming (MILP) is an optimization approach that minimizes a linear cost function constrained by the modelling equations. Several mathematical solvers have been developed to solve this mathematical problem, one of them is CPLEX [96]. LCC and LCA can be used to define the objective functions minimized by an optimal design algorithm of SHSs and RECs. Therefore, this auxiliary approach can be used to combine economic and environmental assessments.

3.2.5. Exergo-environmental and Exergo-economic analysis

As underlined in Section 2.3, when evaluating the economic and environmental performances of TEES, it is important to consider both the energy quantity and the energy quality. Exergo-economic and exergo-environmental [97] analyses represent a valuable tool already used in literature to address this issue.

3.3. Software used

1. OpenLCA: an open source software to perform life cycle evaluations [65].

2. Matlab/Simulink: a programming software to write codes and perform simulations [98].

3. TRaNsient SYstems Simulation Program 16 (TRNSYS16): a dynamic simulation software to model energy systems [99].

4. Engineering Equation Solver (EES): a programming software thought for engineering applications to write codes and perform simulations [100].

5. Python 3.7: programming software used to perform the MILP optimization with CPLEX [101]

4. Results and discussion

The results of the Project are collected in 6 papers: 5 of them are already published in International Journals and one is submitted. These papers are not presented in chronological order, but following the path illustrated in Figure 17. This figure highlights in bullet points the variables of the "Integrated LCA" analysis addressed by each one of the following papers:

1. Fiaschi, D., Manfrida, G., Petela, K., Rossi, F., Sinicropi, A., Talluri, L., 2020. Exergo-Economic and Environmental Analysis of a Solar Integrated Thermo-Electric Storage. Energies 13, 3484. https://doi.org/10.3390/en13133484 [105].

2. Rossi, F., Parisi, M.L., Maranghi, S., Basosi, R., Sinicropi, A., 2020. Environmental analysis of a nano-grid: A Life Cycle Assessment. Sci. Total Environ. 700, 134814. https://doi.org/10.1016/j.scitotenv.2019.134814 [102].
   Associated to *Data in Brief*:
   Rossi, F., Parisi, M.L., Maranghi, S., Basosi, R., Sinicropi, A., 2020. Data in brief Life Cycle Inventory datasets for nano-grid configurations. Data Br. 28, 104895. https://doi.org/10.1016/j.dib.2019.104895 [103].

3. Rossi, F., Parisi, M.L., Greven, S., Basosi, R., Sinicropi, A., 2020. Life Cycle Assessment of Classic and Innovative Batteries for Solar Home Systems in Europe. Energies 13, 3454. https://doi.org/10.3390/en13133454 [104].

4. Rossi, F., Heleno, M., Basosi, R., Sinicropi, A., 2020. Environmental and economic optima of solar home systems design: A combined LCA and LCC approach. Sci. Total Environ. 744, 140569. https://doi.org/10.1016/j.scitotenv.2020.140569 [106].

5. Rossi, F., Heleno, M., Basosi, R., Sinicropi, A., 2021. LCA driven solar compensation mechanism for Renewable Energy Communities: the Italian case. *Submitted to Energy*.

6. Rossi, F., Parisi, M.L., Maranghi, S., Manfrida, G., Basosi, R., Sinicropi, A., 2019. Environmental impact analysis applied to solar pasteurization systems. J. Clean. Prod. 212, 1368–1380. https://doi.org/10.1016/j.jclepro.2018.12.020 [107].

According to Figure 17, Paper 1 proposes a general environmental assessment where several ESSs are compared including batteries; in this preliminary paper, TEES assessment is particularly detailed compared to the other ESSs. Then, the project takes a more specific direction focusing on batteries for SHSs applications. In Paper 2, LIBs are considered as reference technology because they represent the most mature one in the market; in this case, batteries LCA is much more detailed than that proposed by Paper 1. Paper 3 instead expands the analysis to SSLIBs and other post-LIBs such as SIBs. After that, Paper 4 introduces the problem of energy tariffs and PV and ESSs costs. Notably, a LCA and LCC cross-analysis is presented considering LIBs as reference storage technology as their cost can be more precisely than other devices. Paper 5 proposes an upscaling of the analysis as the environmental effects of RECs to the national grid is analysed using novel specific incentives. Paper 6 proposes a further application of solar energy technologies that could integrate SHSs and RECs.

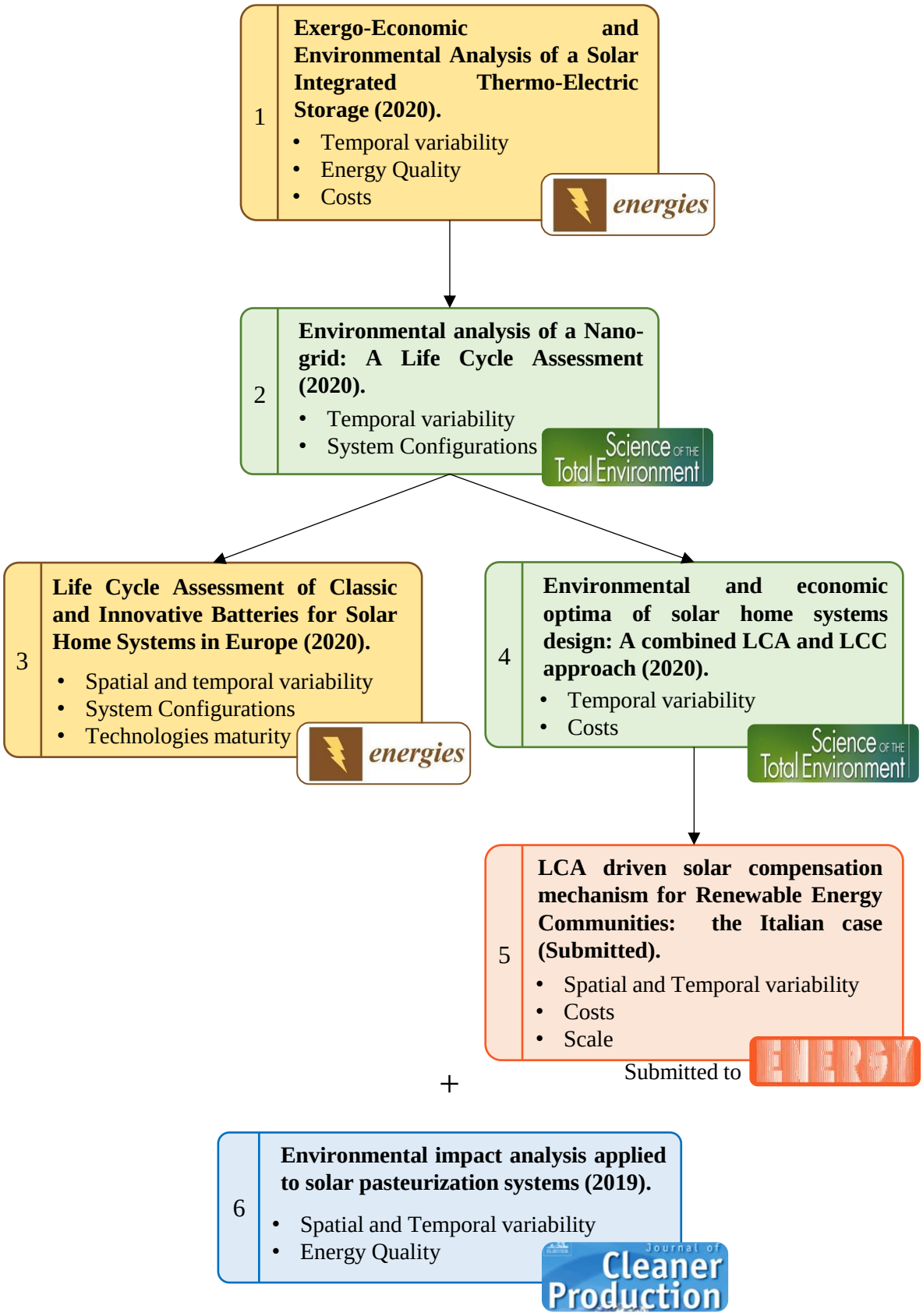

Figure 17: Path of the publications collected in the research project and variables addressed by the paper.

In the following subsections, a brief introduction to the manuscripts along with a comment to specify candidate's contribution is presented.

4.1.1. Paper 1: Exergo-Economic and Environmental Analysis of a Solar Integrated Thermo Electric Storage

Paper 1 is published in *Energies* and provides a preliminary comparison of the environmental performances of several energy storage technologies through LCA: TEES, LIBs, and CHS. These are supposed to perform daily cycles, charged by a PV system installed in Italy (Crotone); furthermore, a PHS representative for Italy is also considered for comparison.

In addition to the LCA analysis of these ESSs, the paper also proposes a careful evaluation of the economic and environmental impacts due to the loss of energy quality occurring in TEES, expressed by the variable "exergy". For this purpose, a dynamic simulation model is developed to perform the exergo-economic and exergo-environmental analyses. The main outcomes of the paper are:

- The evaluation of the life cycle environmental impact of the analysed systems as Midpoint and Endpoint indicators.
- The levelized cost of electricity stored by TEES.
- The total environmental impact of TEES evaluated as the sum of LCA single score and of the exergy destructions burden.
- A contribution analysis of TEES components.

Authors names are listed in alphabetic order; the Ph.D. candidate contributed to perform the LCA and exergo-environmental analyses.

energies

MDPI

Article

Exergo-Economic and Environmental Analysis of a Solar Integrated Thermo-Electric Storage

Daniele Fiaschi [1], Giampaolo Manfrida [1], Karolina Petela [2,*], Federico Rossi [1,3], Adalgisa Sinicropi [3,4,5] and Lorenzo Talluri [1,*]

[1] Department of Industrial Engineering, University of Florence, 50134 Florence, Italy; daniele.fiaschi@unifi.it (D.F.); giampaolo.manfrida@unifi.it (G.M.); fe.rossi@unifi.it (F.R.)
[2] Department of Thermal Technology, Silesian University of Technology; Konarskiego 22, 44-100 Gliwice, Poland
[3] Department of Biotechnology, R2ES Lab, Chemistry and Pharmacy, University of Siena, Via A. Moro, 2, 53100 Siena, Italy; adalgisa.sinicropi@unisi.it
[4] CSGI, Center for colloid and surface science, via della Lastruccia 3, 50019 Sesto Fiorentino, Italy
[5] Institute of Chemistry of Organometallic Compounds (CNR-ICCOM), Via Madonna del Piano 10, 50019 Sesto Fiorentino, Italy; adalgisa.sinicropi@unisi.it
* Correspondence: karolina.petela@polsl.pl (K.P.); lorenzo.talluri@unifi.it (L.T.)

Received: 30 April 2020; Accepted: 28 June 2020; Published: 6 July 2020

Abstract: Renewable energies are often subject to stochastic resources and daily cycles. Energy storage systems are consequently applied to provide a solution for the mismatch between power production possibility and its utilization period. In this study, a solar integrated thermo-electric energy storage (S-TEES) is analyzed both from an economic and environmental point of view. The analyzed power plant with energy storage includes three main cycles, a supercritical CO_2 power cycle, a heat pump and a refrigeration cycle, indirectly connected by sensible heat storages. The hot reservoir is pressurized water at 120/160 °C, while the cold reservoir is a mixture of water and ethylene glycol, maintained at −10/−20 °C. Additionally, the power cycle's evaporator section rests on a solar-heated intermediate temperature (95/40 °C) heat reservoir. Exergo-economic and exergo-environmental analyses are performed to identify the most critical components of the system and to obtain the levelized cost of electricity (LCOE), as well as the environmental indicators of the system. Both economic and environmental analyses revealed that solar energy converting devices are burdened with the highest impact indicators. According to the results of exergo-economic analysis, it turned out that average annual LCOE of S-TEES can be more than two times higher than the regular electricity prices. However, the true features of the S-TEES system should be only fully assessed if the economic results are balanced with environmental analysis. Life cycle assessment (LCA) revealed that the proposed S-TEES system has about two times lower environmental impact than referential hydrogen storage systems compared in the study.

Keywords: energy storage; exergo-economic; exergo-environmental; solar energy; TEES; LCA

1. Introduction

The correct management of electric grids is being challenged by the widespread utilization of renewable energy sources (RES) [1]. This is due to the unsteady behavior of the variable renewable energies (VREs), which have the characteristic of being highly stochastic (wind), or dependent on daily cycles (solar). At present, the problem is approached with several measures, and among the others, energy storage represents an option that will certainly need to be used to support high market penetration of RES. Several energy storage systems are present in the market, from pumped-storage

hydroelectricity to flywheel storage (FS), batteries, compressed or liquid air energy storage (CAES/LAES), or chemical storage [2]. Each solution holds specific performance characteristics, which favors or hinders the selection of one technology over the other. Specifically, the most important selection criteria are the cost of the system, the total efficiency, the energy density, and the power rating. Table 1 presents the state of the art of the current studied storage technologies compared to the proposed solution of thermo-electric energy storage.

Table 1. Technological characteristics of energy storage systems [3–11].

Technology	Total Efficiency	Power Rating	Energy Density	Capital Cost (€/kWh)	Lifetime	Maturity
PHS	70–85%	200 MW—2 GW	Moderate	500–1500	>40 yr.	Mature
CAES/LAES	60–70%	10–300 MW	Medium	400–1200	>30 yr.	Early Commercial
CHS	35%	10 MW—1 GWh	Very High	900	>10 yr.	Demo
Flywheel	≥90%	1–20 MW	Medium-High	500–2000	20,000–100,000 cycles	Early Commercial
Li-ion batteries	85–95%	<10 MW	Very High	1000–3000	1000–10,000 cycles	Early Commercial
Lead—acid batteries	70–80%	<10 MW	High	500–1500	500–10,000 cycles	Mature
Super conductors	>90%	100 kW—5 MW	Medium-High	100–500	500,000 cycles	Demo
TEES	55–70%	100 kW—300 MW	Medium-High	500–2000	>25 yr.	Demo

Pumped storage technology is the most widespread one, and it has already been fully exploited, particularly in Europe [3]. The power range which it covers is quite wide and ranges from a few hundred MWs to a few GWs with total round-trip efficiencies in the span of 70–80%. The energy density of this technology is not very high, as it requires very big reservoirs, even if the capital cost is relatively low. Compressed air energy storage is one the preferred solution in short term scenario, as it guarantees a flexible configuration, and allows efficiency up to 70%. The power range is one order of magnitude below the pumped hydro storage (PHS), and it spans between 10 to 300 MWs. Liquid air energy storage can be examined as a CAES system with increased energy density. CAES and LAES systems have much higher energy density compared to PHS. [4] The main advantage of the flywheel storage system is the high storage density and the high response to charge and discharge cycles. Another main feature is the very high efficiencies that can be reached, over 90%, while the main issues are the relatively low lifetime (<100,000 cycles) and the high cost per kW installed. The power range of this technology is between 1 and 20 MW [5]. Several types of batteries are utilized as energy storages, but the most common ones are lead-acid and lithium-ion ones. The main trait of batteries is the very high energy intensity, coupled with a high roundtrip efficiency. The main drawbacks of batteries are the low lifetime, the high cost and the very high environmental impact [6]. In the last years, superconducting magnetic energy storage has been studied, as it guarantees very high conversion efficiency (>90%), with relatively high-power density. The Power range for this technology is between 10 kW and 5 MW. The capital cost of this technology is moderate [3,7].

Among the other technologies, thermo-electric energy storage (TEES) allows being utilized in a wide range of operation, giving, therefore, a suitable solution to the dispatch ability issue [12], without incurring in the intrinsic drawbacks of pumped-storage hydroelectricity [13], which is bound to geographical constraints, or batteries, having a limited lifetime [14] and raising problems in the end-of-life management.

The basic configuration of a TEES system is the one including a power cycle, which works between two temperature levels, fixed through the utilization of storage tanks, a heat pump and a

refrigeration cycle, which maintain the temperature levels of the storages. The power cycle may be either a trans-critical CO_2 cycle [15,16] or a Brayton cycle [17,18]. Supercritical CO_2 cycles have recently found a widespread interest both in the research and the industrial world. Particularly, in [19], an extensive review of the architecture, the components, and the optimal cycle condition is carried out. The TEES solution has been mainly proposed for large electrical energy storage, using sensible heat hot rocks for the high-temperature heat storage; this can indeed be an attractive solution for large utilities and grid operators, as a substitute or in support of pumped hydro.

In [4] it was shown that multi-MW TEES could achieve roundtrip efficiency close to 70%, for complex investigated configuration of the cycles, while utilizing the simplest solution only a 50% efficiency was reached. Furthermore, they presented a valuable model for the dimensioning of ground heat exchangers, which are often used in TEES applications as hot storage tanks. Furthermore, in [5] a thermo-economic optimization of the TEES system with transcritical CO_2 cycles was carried out. The main result was the complex optimization which provided, for the assessed case a roundtrip efficiency of about 65% for the system to be economically viable. Another exergo-economic analysis was carried out in [20], where a marginal round trip efficiency of 72% was found, and LCOE of 0.49 €/kWh was obtained for a hundred kW TEES configuration.

Therefore, when comparing TEES storage systems, to other technologies, it emerges that it is not the most outstanding one regarding cost and efficiency, however, it has several assets, such as its flexible configuration, no geographical constraints, relatively long lifetime and, when compared to other storage technologies (e.g., batteries), also a lower environmental impact.

Thermo-electric energy storage (TEES) systems utilizing solar energy to increase the storage roundtrip efficiency are scarcely studied in the literature [21], especially from an environmental point of view. Therefore, the exergy, exergo-economic and exergo-environmental analyses of a solar-assisted TEES system are proposed in the present study to investigate the possibility of developing a multi-functional energy storage system, capable to provide electricity, heat and/or cold at a reasonable cost and with attractive environmental performance. The current proposal addresses much lower power ranges (100–200 kWe peak) compared to the literature and energy storages in the range from 100 to 300 kWh, capable to serve the daily needs of small communities largely relying on photovoltaics (20–50 kWe peak) for their energy supply (typical southern Europe or African countries climate conditions), with a special focus on environmental performance. This is because—in recent years—environmental issues are becoming increasingly pressing, and an economic analysis alone can no longer provide sufficient indications to guarantee the attractiveness and feasibility of a plant.

Several types of environmental impact assessment methods are commonly applied to energy storage systems as these technologies aim to improve the environmental sustainability of energy and electric systems. Among these, life cycle assessment (LCA) is one of the most commonly used as it allows to analyze all the phases of the lifecycle of a technology. An interesting overview of studies focusing on the application of LCA to energy storage systems is provided in [22], where the eco-profile of photovoltaic systems assisted by lithium-ion batteries (LIBs) and compressed hydrogen storage (CHS) is evaluated. The work presented in [22] grounds on the harmonization of LIBs LCA analyses provided by [23], but it is possible to find in literature other case studies where this methodology is applied to alternative types of batteries [24–28], power to gas hydrogen production [29] and capacitors [30]. Connected to the LCA analysis is the exergo-environmental analysis (EEnvA), which is an advanced environmental impact assessment tool. The EEnvA enables to evaluate how the loss of energy quality affects the environmental impacts, through the weighting of exergy, and it is especially useful when applied to solar thermal systems [31].

Therefore, in the present study, alongside an exergo-economic analysis, an exergo-environmental analysis of a solar integrated thermo-electric energy storage system is carried out. The analysis has been performed for a selected reference study of a specific site (Crotone, southern Italy). The coupling of exergo-economic and exergo-environmental analyses allow drawing more in-depth considerations on the management of the system, enabling to evaluate the correct seasoning functioning of the TEES systems, not only from an economic point of view, as highlighted in [32], but

also from an environmental impact perspective. Economic analysis has been here enriched by a sensitivity analysis, while the discussion on environmental aspects appears for the first time.

In Section 2, the system design and the methodology applied to evaluate TEES economic and environmental impact is carefully described. Section 3 contains the discussion and interpretation of the results. Finally, Section 4 contains the conclusions of the study.

2. TEES Description and Methods of Analysis

2.1. Description of Thermo-Electric Energy Storage System

The proposed TEES configuration has been introduced in a previous work [32], which dealt with the exergo-economic analysis of the proposed system. The storage system uses sensible heat liquid reservoirs, both for the cold and hot storage. The reason for this choice arose by the need for easy and fast control of the mass flow rate, aimed at correctly coupling the heat capacities in the heat exchangers both in the charging and discharging times. The proposed solar integrated TEES consists of three main sections: a trans-critical CO_2 power cycle (PC), a supercritical CO_2 heat pump (HP) and a subcritical R134a refrigeration cycle (RC). The inverse cycles (HP and RC) recharge the storage reservoirs (hot water cold reservoir, HWCR and hot water hot reservoir, HWHR and cold medium cold reservoir, CMCR and cold medium hot reservoir, CMHR) and make use of the solar energy during the daylight, both through thermal and electric energy conversion. A large fraction of the PV output is directed to satisfying the consumer's electric loads (the system is thought in support of a local micro or mini-grid), but, as frequently happens in good climates, there is at noon a surplus production of PV electricity, which is directed to store heat in the HWHR (through the HP) and cold in the CMCR (through the RC). The main power cycle PC works between the two average temperature levels of the HW and CM reservoirs during the discharging time, producing the power output. At present, the model just operates the PC at full power without any modulation (which would imply an off-design model of the PC). The efficiency of the system is enhanced by introducing a pre-heating of the main cycle working fluid through the utilization of an intermediate temperature reservoir (intermediate hot reservoir—IHR and intermediate cold reservoir—ICR), which is heated directly through solar thermal energy.

Figures 1 and 2 show the schematic of the heat pump and power cycles. A supercritical CO_2 cycle is proposed for the heat pump, because of the opportunity to recharge the hot reservoir at a relatively high temperature (145 °C). The heat pump configuration includes an expander, which replaces the commonly used throttling valve, aimed at improving the coefficient of performance (COP) [33]. The compressor is powered by the excess electricity available in the daytime from the photovoltaic (PV) solar field, while the evaporator temperature is kept at an intermediate level (95/40 °C) through the utilization of thermal solar collectors, which are connected by a three-way valve to an IHR. It is also utilized for the pre-heating of the power cycle working fluid.

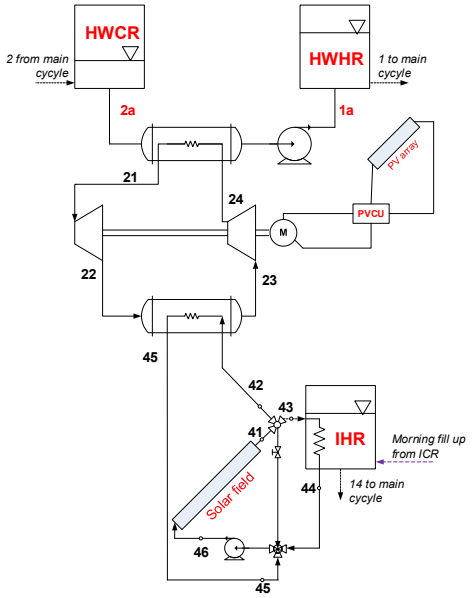

Figure 1. Scheme of the solar-assisted heat pump cycle.

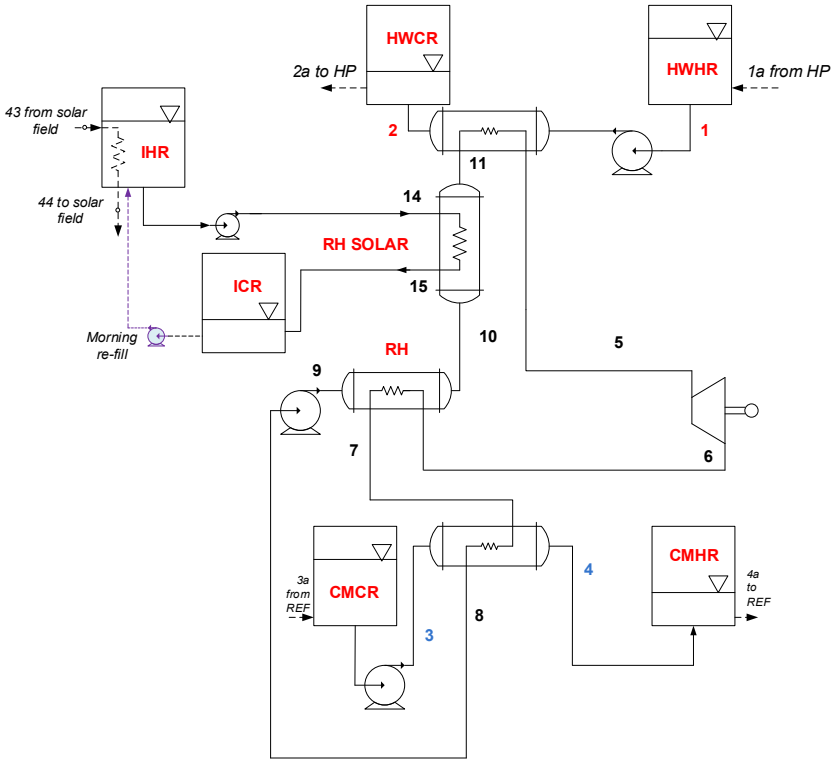

Figure 2. Scheme of the power cycle.

The proposed power cycle implements a trans-critical CO_2 configuration, which is a favorable solution considered the temperature range of both the hot and cold sinks (HW and CM reservoirs). The IHR allows the time de-coupling from the availability of the solar resource during the discharging time, which usually does not take place during the daytime.

The considered refrigeration cycle is a standard configuration arrangement using R134a as working fluid (which is suitable considering the limited cold conditions in the CM reservoirs, −10 to −20 °C). The objective of this inverse cycle is recharging the cold storage reservoirs (which are filled with water mixtures with appropriate anti-freeze additives, such as NaCl, $CaCl_2$ or Ethylene Glycol).

The utilization of cold storage reservoirs allows increasing the pressure ratio of the turbine and, therefore, the increase of power output and efficiency of the cycle. The presence of low-temperature cold storage is of paramount importance if suitable roundtrip efficiency is coveted. The working parameters of the whole system can be found in [32].

The sizing of the solar fields refers to the specific location (Crotone, southern Italy), utilizing a single-reference-day (in May, for instance) quasi-dynamic model approach. It was agreed that analysis of system behavior during a single hour on a given day cannot represent the design point simulation of the system. By relying on an energy source of intermittent nature, authors have decided to use the term of a representative day instead. It became then a reference case for design day analysis. A single-reference-day of the month is created by using the source meteorological data from the Meteonorm database. The relevant data (direct, diffuse solar radiation and ambient temperature) are extracted every 60 min over one year. These data are processed to generate 12 average days statistically representative for each month of the year. The radiation and ambient temperature profiles were imported as Lookup Tables inside the dynamic simulation code, which was programmed using Engineering Equation Solver (EES). The quasi-dynamic approach rests on performing a simulation using a marching-forward procedure if meteorological data are considered, neglecting however more complex inertia phenomena during design analysis.

Commercially available flat plate solar collectors were assumed for the solar thermal field (η_0 = 0.719, a_1 = 1.45 W/(m^{2}K), a_2 = 0.0051W/(m^{2}K^2)). The number of solar collectors was determined by the heat demand from the heat pump evaporator, and the required temperature of the IHR reservoir; while the number of PV panels was obtained knowing the required power by the compressors of the inverse cycles. Commercially available polycrystalline modules were considered [34].

An off-design approach was then applied to assess the behavior of the whole system throughout the year and its dependence on the outer conditions. For off-design simulation, it is assumed that the size of all components within the system are already known, as specified in [32], and their performance can only be affected by independent external energy inputs or by involving some control procedure. The off-design analysis was solved numerically in EES through a time-forward simulation, assuming a length-adaptive time step, defined as the required time for the volume of heat transfer fluid (HTF) to close the loop in the solar field. The off-design analysis allows for the investigation of the capability of the charging cycles to load the reservoirs under the assumptions of variable meteorological conditions. Variable meteorological conditions are affecting solar thermal collectors and PV array output. Moreover, changing load conditions are also reflected by a performance curve applied to the turbine model. Table 2 summarizes the main design parameters of the thermo-electric storage system, which are fully described in [32].

Table 2. TEES design operating parameters.

Variable	Value
Power cycle	
T_1, T_2 (HWR)	95/145 °C
p_{HWR}, p_{IHR}, p_{CMR}	1800/100/100 kPa
$\dot{m}_{HW}$	1 kg/s
T_{14}, T_{15} (RH SOLAR)	95/40 °C
p_5	12,000 kPa
$\Delta T_{HOT} = T_1 - T_5 = \Delta T_{SOLAR} = T_{14} - T_{11}$	5 °C
$\Delta T_{COLD} = T_8 - T_3$	10 °C
T_3, T_4 (CWR)	−20/−10 °C
ε_{RH}	0.8
η_t, η_p	0.9/0.8
Operation Time (Power Cycle)	h
Heat Pump Cycle	
$\Delta T_{CO2\text{-}HW} = T_{21} - T_{2a}$	5 °C
$p_{min,HP}$	13,500 kPa
$\Delta T_{solar\text{-}CO2} = T_{42} - T_{23}$	5 °C
Refrigeration Cycle	
$\Delta T_{COLD} = T_{31} - T_0$	10 °C
$\Delta T_{EVA} = T_{3a} - T_{32}$	5 °C
Solar thermal collector fields	
Location	Crotone, Italy
Month for reference day	May
The slope of solar collector	45° towards South
η_0	0.719
a_1	1.45 W/(m^{2}K)
a_2	0.0051 W/(m^{2}K^2)
A_{sc}	1.6 m^2
$T_{41} = T_{42} = T_{43}$	95 °C
$\Delta T_{HTF} = T_{42} - T_{45} = T_{43} - T_{44}$	10 K
Collectors arrangement	Parallel in 10 rows

2.2. Exergo-Economic Models

It is assumed that to rationally assess the cost-effectiveness of a given plant, the economic costs should be rather assigned to exergy than to energy. This approach can be accepted if one remembers that exergy is seen as the indeed useful part of energy. The exergo-economic analysis combines the exergy analysis and the economic models, to provide the user with a clear and efficient evaluation of the cost-effectiveness of each component of the power plant, introducing the costs per exergy unit [35]. The exergy analysis is useful to assess not only the efficiency of energy systems but also the irreversibilities of each component [36]. It is done by application of the First and Second laws of thermodynamics. In the present work, the exergy is calculated at each point (j-th stream) of the system by simply applying its definition, which is the maximum work achievable from the interaction between the analyzed process and the environment (1):

$$\dot{E}x_j = \dot{m}_j[(h_j - h_o) - T_o(s_j - s_o)] \quad (1)$$

Knowing the exergy rate assigned to each stream, an exergy balance is provided for each component remembering about exergy destruction and loss occurring within.

The developed economic model determines the daily costs of each component. The annual investment cost is calculated from (2):

$$Z_k^{an} = \frac{IR \cdot (1 + IR)^n}{(1 + IR)^n - 1} \dot{Z}_k \quad (2)$$

where:

- IR is the interest rate, which was assumed at 8%.
- n is the year lifetime, here assumed at 20 years.
- $\dot{Z}_k$ is the sum of cost rates associated with investments for the k-th component.

While estimating the purchase costs of each component of the systems, the authors decided to take advantage of findings presented by Henchoz et al. in [31] and compared them with cost functions given in the thermo-economic literature [37]. Since a storage-power cycle of similar principle was investigated in [31], with results consistent with those present in literature, it is expected that the applied cost functions are reliable. The cost functions applicable to the system components are presented in Table 3. Costs were updated to 2018 values, by using the CEPCI (Chemical Engineering Plant Cost Index) indexes [38] and by applying a proper €/$ currency exchange rate. Solar collectors cost was assumed as a function of the surface area, at 210 $/m^2 [39]. The PV modules' investment cost was assumed at 250 $/module [40]. The applied currency exchange rate was 0.877 €/$.

Table 3. Cost functions for the equipment [29,34].

Component	Function [10^3 $, 2009]
Turbine	$1.5 \cdot \dot{W}_T^{0.6} + 10$
Compressor	$6 \cdot \dot{W}_C^{0.6} + 10$
Pump	$44 \cdot \dot{V}_{wf}^{0.75} + 20$
Heat Exchanger	$0.3 \cdot A_{HE}^{0.82} + 1$
Reservoir (HWHR/HWCR, CMHR/CMCR, IHR/ICR)	$0.2 \cdot V_k^{0.785} + 2$

The exergo-economic approach outlined in [35,36] was then adopted by defining, for each component k, a cost balance equation, as shown in (3).

$$\dot{C}_{P,k} = \dot{C}_{F,k} + \dot{Z}_k$$
$$c_{P,k}\dot{E}x_{P,k} = c_{F,k}\dot{E}x_{F,k} + \dot{Z}_k \quad (3)$$

where:

- $\dot{C}_{P,k}$ and $\dot{C}_{F,k}$ are the cost rates associated respectively with exergy products and fuels.
- $c_{P,k}$ and $c_{F,k}$ are the costs per unit of exergy of product or fuel

Coupled to the cost balances, auxiliary equations were required to solve the system of equations, therefore the model suggested in [35,41] was applied. The solar radiation was assumed as costless.

The exergy destruction cost rate was calculated through (4):

$$\dot{C}_{D,k} = c_{F,k} \cdot \dot{E}x_{D,k} \quad (4)$$

Finally, an exergo-economic factor, which associates the investment cost of the component to the sum of the investment cost and the cost of exergy destruction, was calculated through (5):

$$f_k = \frac{\dot{Z}_k}{\dot{Z}_k + \dot{C}_{D,k}} \quad (5)$$

All calculations were integrated over the day, considering the average reference day of each month. The yearly investment cost of the overall system also includes installation and maintenance costs, which were assumed at 20% of the total investment cost of the system [35].

The exergo-economic analysis was supplemented by a sensitivity analysis. It was performed in order to assess the susceptibility of levelized cost of electricity to change. The independent variable is the length of operational season.

2.3. LCA Model

LCA is one of the most widespread methods for the evaluation of the environmental impact and, according to the ISO 14040 and ISO 14044 regulations [42] it's defined as a four steps methodology including goal and scope definition; life cycle inventory (LCI); life cycle impact assessment (LCIA) and life cycle interpretation.

In the context of this article, the goal of the LCA is the estimation of the environmental impacts of a TEES system. An open-source software, named openLCA [43] and the database Ecoinvent 3.4 [44] was used for the environmental assessment of PV assisted TEES during daily charge and discharge cycles. The TEES eco-profile was compared to LIBs and CHS working in the same conditions. Furthermore, a pumped hydro storage system was considered. The functional unit of the LCA was set to 1 MWh of output electricity. Concerning the definition of the system boundaries, a 1% cut-off was set, excluding all those flows whose contribution to the overall emissions, raw materials and energy consumption is lower than that percentage. This allows fast calculations and can be done with a simple command in openLCA that was enabled for all the analyzed systems (TEES, PHS, LIBs, CHS) to guarantee the same cut-off conditions. Furthermore, coherently with the exergo-economic analysis, the TEES piping was not considered in the analysis and, consequently, also the amount of fluid inside it. On the other hand, the amounts of water and antifreeze liquid (calcium chloride) were evaluated based on the CWR and HWR volumes and temperatures.

As no primary data are available, Ecoinvent represents a reliable source of information. Thanks to the processes contained in the database, the materials depletion and all the emissions to the environment were estimated considering the construction, operation and maintenance, and disposal phases. The inventory data are collected in Table 4; although the system is supposed to be installed in Crotone, none of the Ecoinvent processes used in the LCI has Italy as a geographical reference, therefore Switzerland (CH) has been used as a proxy. To estimate how the choice of the reference location affects the results, global (GLO) processes valid for every location will be also considered.

Considering the size of the solar plant, the land occupation represents a non-negligible part of the inventory and it has been modeled assuming that the system is installed in an industrial area.

Table 4. Life Cycle Inventory of the TEES system.

Flow	Amount	Unit	Process
Pump PC	696	Items	pump production, 40 W—CH
Turbine PC	1.73	Items	micro gas turbine production, 100 kW electrical—CH
Compressor HP	7.85	Items	air compressor production, screw-type compressor, 4 kW—RER (Europe)
Turbine HP	1.22	Items	air compressor production, screw-type compressor, 4 kW—RER
Throttle Valve RC	500	g	average for metal product manufacturing—RER
Compressor RC	3.55	Items	air compressor production, screw-type compressor, 4 kW—RER
Sol. collectors	320	m^2	evacuated tube collector production—GB
	6400	m^2·yr	Occupation, industrial area
IHR tank	4.59	Items	heat storage production, 2000 L—CH
HWR reservoir	3.74	Items	heat storage production, 2000 L—CH
CMR reservoir	0.05	Items	water storage construction—CH
PV panels	291.2	m^2	photovoltaic panel production, multi-Si—RER
	5824	m^2·yr	Occupation, industrial area
Plane HE	20	m^2	market for tin plated chromium steel sheet, 2 mm—GLO stone wool production—CH
Shell and tube HE	197	m^2	market for chromium steel pipe—GLO average for chromium steel product manufacturing—RER stone wool production—CH
Water	55,284	kg	market for water, deionised, from tap water—Europe without Switzerland
Calcium Chloride	32,750	kg	market for calcium chloride—GLO

Maintenance	3	Items	heat and power co-generation unit, 160 kW electrical | maintenance—RER market for maintenance, refrigeration machine—GLO

The electricity output over the TEES lifespan T (20 years) depends on its actual operation time. Five possible scenarios were proposed because, depending on the solar radiation, maintaining the plant operative might not be, in principle, economically convenient.

Some further information about LIBs is necessary to perform the analysis: the battery energy density, the efficiency, and the lifespan are respectively set to 116.1 Wh/kg, 90% and 1000 cycles [17,45]. Concerning the CHS, the storage system is composed of solid oxide fuel cells, solid oxide electrolyzers and a storage tank for the compressed gas accumulation. The inventory of Type III (350 bar) and Type IV (700 bar) hydrogen tanks and their expected lifespan (10 yrs) is provided by literature [46]. The fuel cells' environmental performances were modeled thanks to an Ecoinvent process, that can be also used as a proxy for the electrolyzer. Literature provides values for CHS roundtrip efficiency (67%) [47] and fuel cells lifespan, set to 48,000 h [44].

The LCI of the systems which, in this study, are compared to the TEES is described in Table 5.

Table 5. Life Cycle Inventory of the PHS, LIBs and CHS.

Flow	Amount	Unit	Process
PHS			
Electricity	1	MWh	electricity production, hydro, pumped storage—IT
LIBs			
Inputs			
PV panels	291.2	m^2	photovoltaic panel production, multi-Si—RER
	5824	m^2·yr	Occupation, industrial area
Inverter	2	Items	inverter production, 500 kW—RER
Battery charger	56.5	kg	charger production, for electric scooter—GLO
Batteries	30,967	kg	battery production, Li-ion, rechargeable, prismatic—GLO
Outputs			
Electricity	1862	MWh	Reference Flow
CHS			
Inputs			
PV panels	291.2	m^2	photovoltaic panel production, multi-Si—RER
	5824	m^2·yr	Occupation, industrial area
Electrolyser	0.4	Items	fuel cell production, solid oxide, 125 kW electrical—CH
Fuel Cell	1.83	Items	fuel cell production, solid oxide, 125 kW electrical—CH
Inverter	2	Items	inverter production, 500 kW—RER
Storage Tank	98.5	Items	Type II and Type IV Tank production, adapted from [26]
Outputs			
Electricity	1058.9	MWh	In case of pressurization up to 350 bar
	1011.4	MWh	In case of pressurization up to 700 bar

Both the LIBs and CHS storage systems are designed to be charged by the PV system during the day and discharged during the night, similarly to the TEES. For this reason, they are supposed to perform one full cycle per day for a period of T (20 yrs). Another consequence is that the design value of stored energy is set to the maximum daily PV productivity E (394 Wh). Based on these assumptions, the amount of necessary batteries is:

$$m = \frac{E}{DoD \cdot d} \cdot \frac{T \cdot 365}{N} \quad (6)$$

where DoD, d, and N are respectively the depth of discharge (%), the energy density (Wh/kg) and the lifespan (cycles).

Concerning the CHS storage, a 172 kW solid oxide fuel cell and a 37 kW electrolyzer have been chosen because their power is respectively equal to the turbine and the PV plant of TEES. The mass of Type III and Type IV storage tanks is obtained scaling an 8 kWh tank whose LCI is analyzed by [46]. The output electricity must be evaluated considering the roundtrip efficiency of the storage system, the efficiency of common inverters (set to 90%) and charge controllers (set to 98%) and of the electric connections (set to 90%). In the case of CHS, the energy used to compress the gas must also be subtracted [47].

In the LCIA, some calculation methods convert the LCI to environmental impacts, classifying them in categories. The classification and characterization don't allow the calculation of a single score impact value, which can be obtained thanks to a normalization and weighting set. This is very important, as it allows comparing easily two different systems and to perform the related exergo-environmental analysis. The main drawback of a single score impact calculation is that normalization and weighting operations add uncertainty to the LCA model. For such reason, results should always be discussed also at the midpoint level, which means using a problem-oriented approach to analyze the environmental issues of the product system without evaluating their effects. Seventeen midpoint environmental impact categories are proposed by ReCiPe (version 2016) but some of them are largely more consolidated than others. For instance, global warming potential (GWP) represents the most widely analyzed category, but also acidification potential (AP), human toxicity potential (HTP), particulate matter formation (PMF) and photochemical ozone formation (POF) are usually considered as the most relevant for energy storage studies [17]. Furthermore, the evaluation of single score results summarizing all the impact categories was carried out thanks to a European normalization and weighting set (ReCiPe Europe H/A), as the selected location is Crotone. The unit of measurement commonly used for single score environmental impact is the eco-point, abbreviated as Pts, introduced by Eco-indicator 99 and then adopted by other LCIA methods like ReCiPe [48].

2.4. Exergo-Environmental Model

An integral exergo-environmental analysis was carried out over the representative day of each month of the year, coherently with the thermo-economic analysis [49]. The environmental cost rates related to each j-stream $\dot{B}_j$ (Pts/s) were allocated to their exergy content $\dot{E}x_j$ (kWh/s) to evaluate the specific environmental impacts b_j (Pts/kWh) through (7):

$$b_j = \frac{\dot{B}_j}{\dot{E}x_j} \quad (7)$$

This methodology is based on the solution of impact balances performed for every k-component, using (8):

$$\sum \dot{B}_{j,k,in} + \dot{Y}_k = \sum \dot{B}_{j,k,out} \quad (8)$$

where $\dot{Y}_k$ (Pts/s) is the environmental impact rate associated with the construction, operation and maintenance, and disposal phases. This parameter is connected with the LCA results, expressed considering 1 MWh as a functional unit (Pts/MWh). So, the single score impact was multiplied by the

yearly productivity; after that, an impact rate $\dot{Y}_k$ was achieved by the ratio with the charge and discharge time.

The environmental costs per unit of exergy (Pts/kWh) of product $b_{P,k}$ and fuel $b_{F,k}$ were defined according to the exergo-economics. This allowed the evaluation of an environmental cost rate $\dot{B}_{D,k}$ (mPts/s) associated with the exergy destructions occurring inside each component through (9):

$$\dot{B}_{D,k} = b_{F,k} \cdot \dot{E}x_{D,k} \quad (9)$$

Based on these definitions, an exergo-environmental factor $f_{d,k}$ representing the percentage contribution of $\dot{Y}_k$ compared to the total $\dot{B}_{D,k} + \dot{Y}_k$, was calculated using (10):

$$f_{d,k} = \frac{\dot{Y}_k}{\dot{B}_{D,k} + \dot{Y}_k} \quad (10)$$

3. Results

As mentioned above, detailed energy, exergy and exergo-economic analysis results of the seasonal simulation have already been published by the authors in [32]. The seasonal off-design simulation was performed using as input fixed geometry of the system found for design day analysis (May in Crotone). The main important design sizes are the volumes of the tanks (V_{HWR} = 3.74 m^3, V_{IHR} = 9.175 m^3. V_{CMR} = 65.5 m^3), the number of solar collectors installed (200), number of PV modules installed (224). For the design day simulation, during which the charging lasted 7 h and the discharge time was 1 h, it was possible to generate 172,6 kW in the turbine. The marginal round-trip efficiency was then 51%. If the simulation was repeated in the off-design mode for reference days of other months (April–September), the input simulation data included meteorological conditions, size of solar fields, maximum volumes of reservoirs. Variable outer conditions affected i.a. the duration of charging, discharging, power output, round-trip marginal efficiency. Quantitative results of off-design analysis are available in [32].

The analysis in here presented research was firstly extended by an exergo-economic sensitivity analysis with operational season length being the sensitivity factor. The system performance was then assessed in terms of LCA and exergo-environmental analysis. To maintain the originality of the research and to avoid duplication of results presentation, only the new findings are here cited.

3.1. Exergo-Economics

Table 6 introduces a summary of the exergo-economic sensitivity analysis results. The sensitivity analysis indicates how the change of operation periods (from summer months only to the whole year) would affect the levelized cost of the produced electricity. It is clear, as expected, that the yearly working period significantly affects LCOE. Anyhow, it is interesting to notice how the decrease of LCOE with the yearly working period is not linear and the gradient is more relevant in the short periods: for example, being able to extend the exploitation of the TEES from 3 to 5 months per year in spring-summer months reduces the LCOE of about 40%. On the other hand, further extensions of TEES yearly operational time towards seasons with less insulation leads to a progressive marginalization of LCOE reduction.

Table 6. Annual operational details for TEES systems operated in Crotone (39.08 °N, 17.11 °E), considering different possible working periods.

	June–August	May–September	April–October	January–December
Total operation time of TEES (h/year)	734	1234	1744	2800
Productivity (MWh/year)	15.1	24.9	34.1	49.0
Annual average LCOE (€/kWh)	2.76	1.67	1.22	0.85

Levelized cost of electricity is treated as a break-even economic indicator, showing the minimum sale price at which the plant generates enough revenue during lifetime (here 20 years with assumed discount rate) to pay back all of the associated costs. If a simple payback period were calculated and no discounted cash flows were analyzed, it would happen already after 10 years.

3.2. LCA

The midpoint results of LCA are presented in Figure 3. Considering the GWP (Figure 3a) and AP (Figure 3b) impact categories, TEES is assessed as the second less impactful storage system after LIBs, mainly because of the carbon dioxide and the sulfur dioxide emissions dealing with the industrial heat required by the production of the components. Particularly, considering the GWP category the PV plant (24.1%), the CMR (16.5%) and the solar thermal system (13.9%) are the most impactful components. Similarly, the thermal solar system (25.9%), the CMR (16.7%) and the PV plant (15.1%), represent the main contributors to the TEES burden for the AP category too. The results calculated for HTP (Figure 3c) are slightly different as TEES is assessed as more impactful than PHS but less than LIBs, whose copper content (mainly present in the current collector) affects its environmental performances for this category. Solar collectors are largely the most impactful TEES components for AP because of the big amount of copper used in the absorber. Concerning the PMF category, TEES is assessed as a less sustainable solution than both PHS and LIBs (Figure 3d): PM_{10} and $PM_{2.5}$ are mainly produced during the industrial manufacturing of solar thermal (20.7%) and PV (16.3%) panels. The results obtained for the POF impact category (Figure 3d) are similar to those of GWP and HTP because TEES is the second most sustainable system after LIBs. In this case, the nitrogen oxides emitted during the manufacturing of the thermal solar plant (20.8%), the PV plant (16.3%) and the HEs (14.1%) are the main responsible for the impact. For every impact category, it is possible to appreciate that both CHS solutions represent the most impactful storage system and the storage tanks represent the major contributor to this impact (from 40% to 56%, depending on the category). Figure 3 also shows that, depending on the operation time of the system, the TEES could become more impactful than the competitors for all the impact categories.

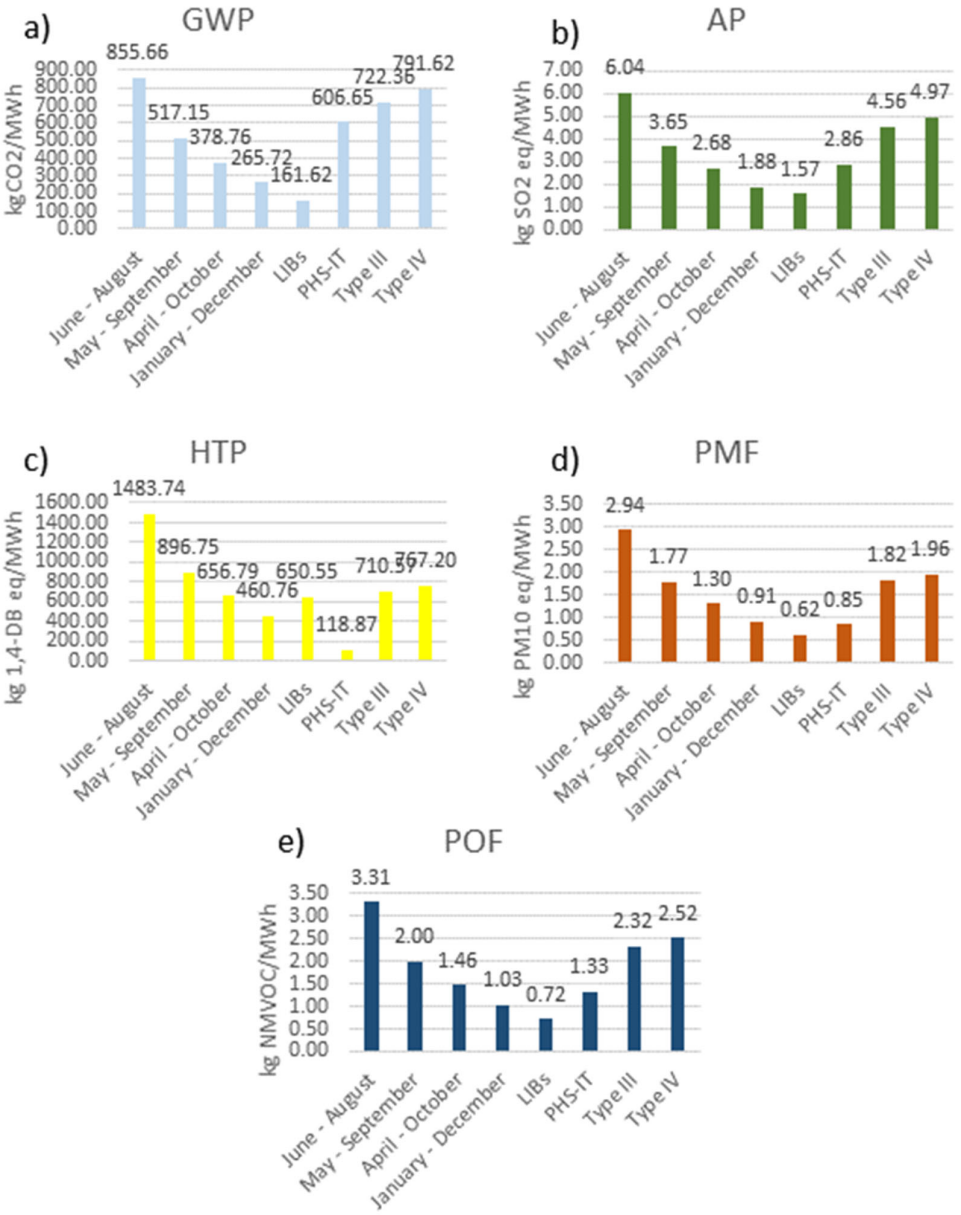

Figure 3. Midpoint environmental impacts of the analyzed systems for the impact categories: (**a**) GWP; (**b**) AP; (**c**) HTP; (**d**) PMF and (**e**) POF.

The single score environmental impacts of the TEES are shown in Figure 4, where they are represented per unit of output electricity, coherently with the choice of the functional unit. The environmental performances of TEES have been assessed varying the operation time whereas the other storage systems are supposed to be always operative. This affects the resulting eco-profiles because, coherently with the functional unit definition, the environmental impacts are divided by the productivity of the solar integrated TEES. Therefore, enlarging the operation time guarantees an environmental benefit as an effect of higher energy output. As TEES is powered by PV, this benefit is higher whether it works in months of high solar. For instance, in case the system is operative only in the summer months (June–August), the environmental impact is 202.84 Pts/MWh but if May and September, when radiation is powerful, are also considered the impact falls to 122.59 Pts/MWh. Extending the working time, the environmental advantage is progressively reduced because the system works in low radiation periods. Indeed, the burden decreases to 89.79 Pts/MWh when including April and October and to 62.99 Pts/MWh in case the full-year operation. Changing

geographical reference to the processes in Table 3 and Table 5 the results are slightly different as TEES environmental impact is about 5% higher.

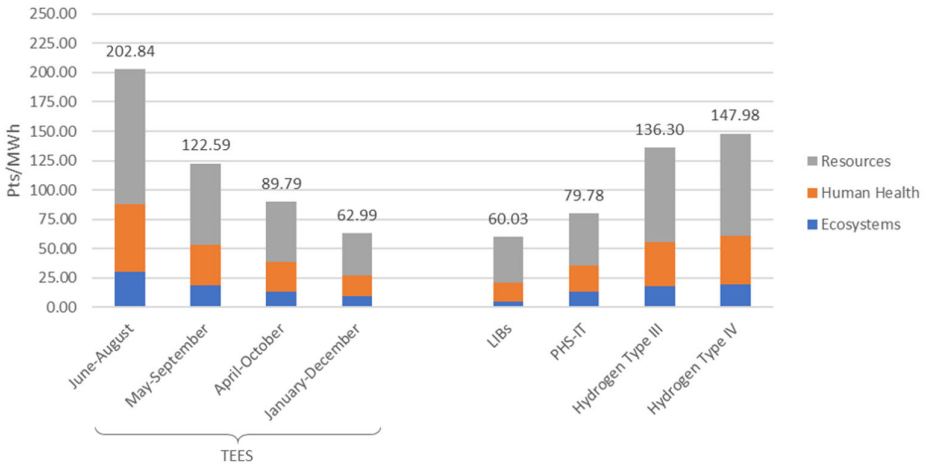

Figure 4. Single score environmental impacts of the analyzed systems.

The assessment of the TEES single components contribution represents an input for the exergo-environmental analysis: both the thermal solar and PV give the highest contribution to the single score impact, at 21% level. They are followed by the concrete CMR (18%), whose high volume determines a relevant burden connected with the consumption of raw materials and calcium chloride, used as antifreeze.

The single score impacts illustrated in Figure 4 are obtained weighting all the 17 midpoint categories proposed by ReCiPe. These indicators contribute to the total impact in different measures: particularly, GWP represents 14% of the single score and affects both human health and ecosystems damage categories; the depletion of fossil and metal resources contributes together to about 60% of the single score as underlined by the size of the grey column in Figure 4. The other indicators have minor relevance in the TEES eco-profile.

Another impactful component is the turbine in the TEES PC, whose burden represents 12% of the total. Concerning the comparison with other storage systems, a $LiMn_2O_4$ LIB bank was designed to store the PV output energy in the average day of the most productive month (394 kWh). Its environmental impact (60.03 Pts/MWh) is comparable with the TEES: even though these batteries are more efficient (90% roundtrip efficiency [17]), their lifespan is much shorter than TEES. Indeed, assuming a discharge time of 1 h (similarly to TEES) and an 80% depth of discharge, this type of batteries can perform 1000 cycles [38], responding to about three years. Batteries are often installed for household applications, whereas pumped hydro storage represents the most diffused high-power competitor to produce and store dispatchable energy on a large scale. The environmental impact of a representative PHS system installed in Italy was evaluated using an Ecoinvent process [44] per MWh of output electricity and its single score damage results to be higher than that of TEES (+27%) and LIBs (+33%). Concerning the hydrogen storage systems, two scenarios differing for the operative pressure, and consequently for the type of storage tank (type III and type IV), were proposed. In both cases, their environmental impact is much higher than that of the other competitors (about two times higher than TEES) because of the low roundtrip efficiency (61%) and the use of rare construction materials in electrolyzers and fuel cells manufacturing (platinate materials). The above results are evaluated using a classic LCA but a novel approach named prospective LCA also exists and may bring to different findings. This methodology is commonly used to compare systems having different maturity levels: the future characteristics of emerging technologies can be forecasted to valorize their future potential [50].

3.3. Exergo-Environmental Analysis

The results of the exergo-environmental analysis are collected in Table 7, using a reference day of May to visualize the results collecting the following parameters:

- $\dot{Y}_k$ is the life cycle environmental impact of the TEES components, that is calculated from the LCA: first a contribution analysis is done to evaluate the burden of every TEES component as Pts/MWh; then this result is converted to Pts/day multiplying it by the solar TEES productivity in the reference day.
- $\dot{B}_{D,k}$ is the environmental impact of the exergy destructions that estimates the environmental drawback of losing energy quality due to thermodynamic irreversibility.
- $\dot{Y}_k$+$\dot{B}_{D,k}$ is the total environmental impact considering the above contributions.
- $b_{F,k}$ is the specific environmental impact of the inlet exergy flows to the components.
- $b_{P,k}$ is the specific environmental impact of the output exergy flows from the components.
- $f_{b,k}$ represents the percentage contribution of $\dot{Y}_k$ to the total environmental impact.

Concerning the total environmental impact ($\dot{Y}_k$+$\dot{B}_{D,k}$), which includes both the burdens related to the components life cycle and the exergy destructions, the CMR resulted as the most impactful component, representing the 20% of the total score. 29% of the CMR impact value is related to the specific cost of the component ($\dot{Y}_k$), whereas 71% is attributable to the exergy destructions ($\dot{B}_{D,k}$). Indeed, the thermodynamic irreversibility occurring inside the CMR contributes to 22% of the total impact of exergy destructions.

Table 7. Results of the exergo-environmental analysis on a reference day of May.

k	Component	$\dot{Y}_k$ (Pts/day)		$\dot{B}_{D,k}$ (Pts/day)		$\dot{Y}_k$+$\dot{B}_{D,k}$ (Pts/day)		$b_{F,k}$ (Pts/kWh)	$b_{P,k}$ (Pts/kWh)	$f_{b,k}$ (%)
1	Condenser PC	0.09	1%	0.74	3%	0.83	2%	0.05	0.06	11%
2	Pump PC	0.45	4%	0.51	2%	0.96	3%	0.09	0.13	47%
3	RH—int PC	0.17	1%	0.15	1%	0.32	1%	0.07	0.28	52%
4	RH—solar PC	0.50	4%	0.88	4%	1.37	4%	0.03	0.06	36%
5	HTHE PC	0.28	2%	0.13	1%	0.42	1%	0.04	0.05	68%
6	Turbine PC	1.34	12%	1.85	8%	3.19	9%	0.07	0.09	42%
7	Evaporator HP	0.02	0%	0.09	0%	0.11	0%	0.02	0.02	17%
8	Compressor HP	0.38	3%	0.39	2%	0.77	2%	0.02	0.03	49%
9	Condenser HP	0.07	1%	3.00	13%	3.07	9%	0.03	0.03	2%
10	Turbine HP	0.06	1%	0.32	1%	0.38	1%	0.03	0.04	16%
11	Condenser RC	0.18	2%	1.26	6%	1.44	4%	0.09	0.20	12%
12	Throttle Valve RC	0.00	0%	0.54	2%	0.54	2%	0.02	0.02	0%
13	Evaporator RC	0.09	1%	3.78	17%	3.87	11%	0.02	0.03	2%
14	Compressor RC	0.17	2%	0.36	2%	0.53	2%	0.01	0.01	33%
15	Sol. collectors	2.44	21%	0.00	0%	2.44	7%	0.00	0.02	100%
17	IHR tank	0.40	4%	0.57	3%	0.97	3%	0.02	0.03	41%
21	HWR reservoir	0.33	3%	3.11	14%	3.43	10%	0.03	0.04	9%
22	CMR reservoir	2.05	18%	4.93	22%	6.97	20%	0.03	0.05	29%
23	PV panels	2.40	21%	0.00	0%	2.40	7%	0.00	0.01	100%

The solar thermal and PV systems were estimated as the most impactful components in LCA, but since they just use sustainable solar energy, the environmental cost of the exergetic fuel is assumed to be zero as well as the impact of exergy destructions. Consequently, the contribution of thermal solar plants to $\dot{Y}_k + \dot{B}_{D,k}$ is reduced to 7%. Although their limited contribution to the LCA results, other impactful components are the evaporator in the refrigeration cycle and the HWR, because of their relevant exergy destructions. The low exergo-environmental factor ($f_{b,k}$) evaluated for some components, like reservoirs and heat exchangers, is due to a high contribution of thermodynamic irreversibility and exergy destructions to the total environmental impact. The same findings can be obtained for the representative day of all the other months as well (Figure 5). Figure

5 is useful to understand that, in each month, the impact of the exergy destructions is higher than that of the components' life cycle, and that the total environmental impact varies in a range between 14.0 and 24.5 Pts/day. Energy systems fueled by fossils are typically characterized by high-impact exergy destructions because of the specific environmental burden of the fuel [50]. Contrarily, in this case, the contribution of life cycle impacts (in blue) is lower but not negligible compared to the exergy destructions impacts (in orange). This can happen when technologies like solar collectors or photovoltaic modules are involved in the system because they don't contribute to $\dot{B}_{D,k}$ but only to $\dot{Y}_k$ [21,51,52] as the specific impact of their fuel (solar energy) is zero. This consideration is valid for the typical day of each month.

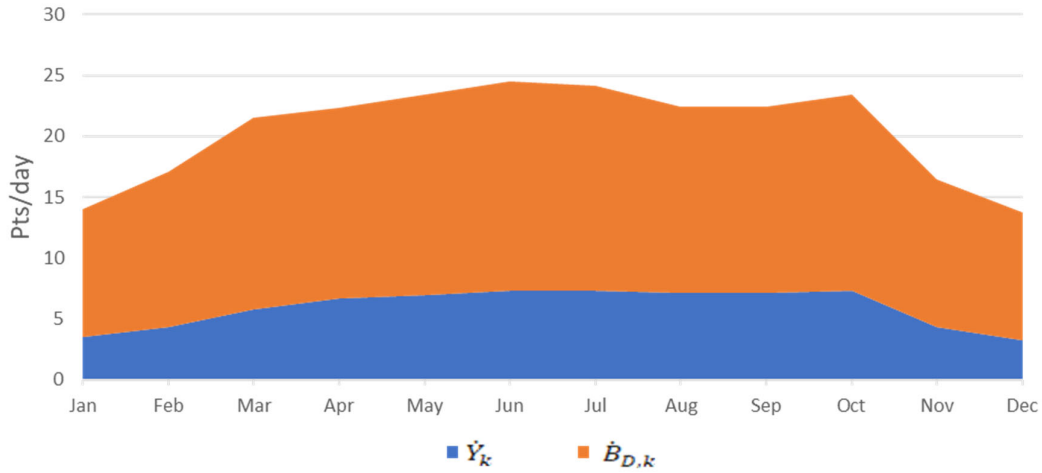

Figure 5. Total environmental impact of TEES as the sum of the burdens dealing with components and exergy destructions during the year.

4. Conclusions

The manuscript deals with the impact assessment of a solar TEES system by the means of exergo-economic and exergo-environmental analysis. The exergo-economic analysis does not reveal market-competitive results. The average annual levelized cost of electricity from the system is at least 2.5 times higher than currently binding electricity costs. However, it still might be considered attractive considering other standalone RES systems.

LCA results are first discussed at the midpoint level, to analyze the environmental problems of TEES for several categories (GWP, AP, HTP, PMF, and POF). These results show that in case of full working time, TEES eco-profile can be compared with LIBs and PHS, whereas CHS is the less sustainable energy storage system. If the yearly working time is reduced for economic reasons, TEES becomes less competitive from the environmental point of view. PV and solar thermal panels represent the main contribution to the impact for most of the selected categories. Furthermore, LCA provided the single score environmental impacts of the TEES components, which were inputs to the exergo-environmental procedure. These results do not substantially differ from midpoint results. Indeed, concerning both types of results visualization approaches, the Thermal Solar and PV panels give the highest contribution (21% of the single score), followed by concrete CMR (18% of the single score). The comparison with the environmental impact of competitive storage systems for dispatchable energy production like PHS and LIBs revealed single-score damage at the same level of TEES if the latter is operative in the range of half year. On the other hand, hydrogen storage systems, under two possible different scenarios, showed a much higher environmental impact level over TEES (about two times higher). Referring to the total exergo-environmental impact of single components, CMR was the most critical (20% of the total score), mainly due to exergy destructions.

Finally, despite the highest contribution of solar thermal and PV to overall LCA impacts, their exergo-environmental score is reduced to 7%, following the assumption of zero environmental costs

per unit of exergy of incoming solar radiation. As a concluding remark, the exergo-environmental analysis acts as an added value to the LCA results, because the environmental impact of some components, like heat exchangers or solar panels, are significantly different considering the effect of exergy destructions, as expressed by low exergo-environmental factors. For these reasons, the application of this methodology is recommended to better address the comparison of different energy storage systems.

This paper is very extensive and innovative because energy, exergy, exergoeconomic, and exergo-environmental analyses have been applied to TEES for the first time in the synergic approach. Nevertheless, some further work may be added in the future: TEES performances could be evaluated considering the productivity profile of a power plant, like a PV system, and a realistic load profile of a residential or industrial user. The system can dispatch energy to the grid depending on the economic convenience of time-variable tariffs and feed-in remuneration. These boundary conditions would affect affecting the size, the performances of the storage system, and consequently the results of the exergoeconomic and exergo-environmental analyses. Moreover the LCA approach adopted in this paper could be furtherly improved using prospective LCA.

Author Contributions: Conceptualization, D.F. and G.M.; Investigation, K.P., F.R. and L.T.; Methodology, D.F., G.M., K.P., A.S., F.R. and L.T.; Software, F.R.; Supervision, D.F., G.M. and A.S.; Writing—original draft, F.R. and L.T.; Writing—review and editing, D.F., G.M., K.P. and A.S. All authors have read and agreed to the published version of the manuscript.

Funding: This research received no external funding.

Conflicts of Interest: The authors declare no conflict of interest.

Nomenclature:

Symbols and acronyms

A	area, m^2
AP	Acidification Potential
$\dot{C}$	Cost rate associated with exergy transfer, €/day
$\dot{B}$	Impact rate associated with exergy transfer, €/day
CAES	Compressed air energy storage
CHS	Compressed hydrogen storage
CMR	Cold medium reservoir (common name for CMHR and CMCR assembly)
CMHR	Cold medium-hot reservoir
CMCR	Cold medium-cold reservoir
COP	Coefficient of performance
d	Energy density, Wh/kg
DoD	Depth of discharge, %
ES	Energy storage
Ex	Total exergy, kw
F	Exergo-economic factor, %
FS	Flywheel storage
GWP	Global Warming Potential
HP	Heat Pump
LIB	Lithium-Ion Battery
HWR	Hot water reservoir (common name for HWHR and HWCR assembly)
HWHR	Hot water hot reservoir
HWCR	Hot water cold reservoir
HTP	Human Toxicity Potential
ICR	Intermediate-heat cold reservoir
IHR	Intermediate-heat hot reservoir
IR	Interest rate
HTF	Heat transfer fluid
LAES	Liquid air energy storage
LCOE	Levelized cost of electricity (stored), €/kWh
m	Mass of the batteries, kg

N	Batteries lifespan, cycles
n	Operation year
PC	Power cycle
PHS	Pumped hydro storage
PMF	Particulate Matter Formation
POF	Photochemical Ozone Formation
PT	Eco-points
PV	Photovoltaic
PVCU	PV conversion unit
RC	Refrigeration cycle
RES	Renewable energy sources
RH	Reheater
S-TEES	Solar integrated thermoelectric energy storage
T	Reference time of the analysis, yrs
TEES	Thermoelectric energy storage
V	Volume, m^3
VRE	Variable renewables
$\dot{V}$	Volumetric flow rate, m^3/s
$\dot{W}$	Power, kw
Z	Cost rate associated with capital investment and O&M costs, €/day

Subscripts and superscripts

C	Compressor
f	Fuel
he	Heat exchanger
k	Plant component
P	Product
p	Pump
t	Turbine
tank	Tank
wf	Working fluid (CO_2 in the main power cycle)

References

1. McPherson, M.; Tahseen, S. Deploying storage assets to facilitate variable renewable energy integration: The impacts of grid flexibility, renewable penetration, and market structure. *Energy* **2018**, *145*, 856–870.
2. *Renewable Energy Policies in a Time of Transition*; IRENA, OECD/IEA, and REN21: 2018; ISBN 978-92-9260-061-7. Available online: https://www.irena.org/-/media/Files/IRENA/Agency/Publication/2018/Apr/IRENA_IEA_REN21_Policies_2018.pdf (accessed on 2 July 2020)
3. ENEA Consulting. *Facts & Figures: Le Stockage d'Energie*; ENEA Consulting: Paris, France, 2012.
4. Ayachi, F.; Tauveron, N.; Tartière, T.; Colasson, S.; Nguyen, D. Thermo-Electric Energy Storage involving CO_2 transcritical cycles and ground heat storage. *Appl. Therm. Eng.* **2016**, *108*, 1418–1428.
5. Morandin, M.; Mercangozz, M.; Hemrle, J.; Marechal, F.; Favrat, D. Thermoeconomic design optimization of a thermo-electric energy storage system based on transcritical CO_2 cycles. *Energy* **2013**, *58*, 571–587.
6. Ren, J.; Ren, X. Sustainability ranking of energy storage technologies under uncertainties. *J. Clean. Prod.* **2018**, *170*, 1387–1398.
7. Hadjipaschalis, I.; Poulikkas, A.; Efthimiou, V. Overview of current and future energy storage technology for electric power applications. *Renew. Sustain. Energy Rev.* **2009**, *13*, 1513–1522.
8. Wang, J.; Lu, K.; Ma, L.; Wange, J.; Dooner, M.; Miao, S.; Li, J.; Wang, D. Overview of compressed air energy storage and technology development. *Energies* **2017**, *10*, 991.
9. Abdi, H.; Mohammadi-ivatloo, B.; Javadi, S.; Khodaei, A.R.; Dehnavi, E. Energy Storage Systems. In *Distributed Generation Systems, Design, Operation and Grid Integration*; Butterworth-Heinemann: Oxford, UK, 2017.
10. International Energy Agency. Technology Roadmap Hydrogen and Fuel Cells [WWW Document]. 2015. Available online: http://ieahydrogen.org/pdfs/TechnologyRoadmapHydrogenandFuelCells-(1).aspx (accessed on 20 March 2020).

11. NREL. Energy Storage [WWW Document]. 2019. Available online: https://www.nrel.gov/docs/fy19osti/73520.pdf (accessed on 21 March 2020).
12. Luo, X.; Wange, J.; Dooner, M.; Clarke, J. Overview of current development in electrical energy storage technologies and the application potential in power system operation. *Appl. Energy* **2015**, *137*, 511–536.
13. Tauveron, N.; Macchi, E.; Nguyen, D.; Tartière, T. Experimental study of supercritical CO_2 heat transfer in a Thermo-Electric Energy Storage based on Rankine and heat pump cycles. *Energy Procedia* **2017**, *129*, 939–946.
14. Benato, A.; Stoppato, A. Pumped thermal electricity storage: A technology overview. *Therm. Sci. Eng. Prog.* **2018**, *6*, 301–315.
15. Morandin, M.; Maréchal, F.; Mercangoz, M. Butcher, Conceptual design of a thermo-electrical energy storage system based on heat integration of thermodynamic cycles-Part A: Methodology and base case. *Energy* **2012**, *45*, 375–385.
16. Morandin, M.; Maréchal, F.; Mercangoz, M. Butcher, Conceptual design of a thermo-electrical energy storage system based on heat integration of thermodynamic cycles-Part B: Alternative system configurations. *Energy* **2012**, *45*, 386–396.
17. White, A.; Parks, G.; Markides, C.N. Thermodynamic analysis of pumped thermal electricity storage. *Appl. Therm. Eng.* **2013**, *53*, 291–298.
18. McTigue, J.D.; White, A.J.; Markides, C.N. Parametric studies and optimization of pumped thermal electricity storage. *Appl. Energy* **2015**, *137*, 800–811.
19. Liu, Y.; Wang, Y.; Huang, D. Supercritical CO_2 Brayton cycle: A state of the art review. *Energy* **2019**, *189*, 115900.
20. Talluri, L.; Manfrida, G.; Fiaschi, D. Thermoelectric energy storage with geothermal heat integration–Exergy and exergo-economic analysis. *Energy Convers. Manag.* **2019**, *199*, 111883.
21. Henchoz, S.; Buchter, F.; Favrat, D.; Morandin, M.; Mercangoz, M. Thermoeconomic analysis of a solar enhanced energy storage concept based on thermodynamic cycles. *Energy* **2012**, *45*, 358–365.
22. Rossi, F.; Parisi, M.L.; Maranghi, S.; Basosi, R.; Sinicropi, A. Science of the Total Environment Environmental analysis of a nano-grid : A Life Cycle Assessment. *Sci. Total Environ.* **2020**, *700*, 134814, doi:10.1016/j.scitotenv.2019.134814.
23. Peters, J.F.; Weil, M. Providing a common base for life cycle assessments of Li-Ion batteries. *J. Clean. Prod.* **2018**, *171*, 704–713, doi:10.1016/j.jclepro.2017.10.016.
24. Weber, S.; Peters, J.F.; Baumann, M.; Weil, M. Life Cycle Assessment of a Vanadium Redox Flow Battery. *Environ. Sci. Technol.* **2018**, *52*, 10864–10873, doi:10.1021/acs.est.8b02073.
25. Troy, S.; Schreiber, A.; Reppert, T.; Gehrke, H.G.; Finsterbusch, M.; Uhlenbruck, S.; Stenzel, P. Life Cycle Assessment and resource analysis of all-solid-state batteries. *Appl. Energy* **2016**, *169*, 757–767, doi:10.1016/j.apenergy.2016.02.064.
26. Zackrisson, M.; Fransson, K.; Hildenbrand, J.; Lampic, G.; O'Dwyer, C. Life cycle assessment of lithium-air battery cells. *J. Clean. Prod.* **2016**, *135*, 299–311, doi:10.1016/j.jclepro.2016.06.104.
27. Peters, J.; Buchholz, D.; Passerini, S.; Weil, M. Life cycle assessment of sodium-ion batteries. *Energy Environ. Sci.* **2016**, *9*, 1744–1751, doi:10.1039/c6ee00640j.
28. Deng, Y.; Li, J.; Li, T.; Gao, X.; Yuan, C. Life cycle assessment of lithium-sulfur battery for electric vehicles. *J. Power Sources.* **2017**, *343*, 284–295, doi:10.1016/j.jpowsour.2017.01.036.
29. Parra, D.; Zhang, X.; Bauer, C.; Patel, M.K. An integrated techno-economic and life cycle environmental assessment of power-to-gas systems. *Appl. Energy* **2017**, *193*, 440–454, doi:10.1016/j.apenergy.2017.02.063.
30. Smith, L.; Ibn-Mohammed, T.; Koh, S.C.L.; Reaney, I.M. Life cycle assessment and environmental profile evaluations of high volumetric efficiency capacitors. *Appl. Energy* **2018**, *220*, 496–513, doi:10.1016/j.apenergy.2018.03.067.
31. Rossi, F.; Parisi, M.L.; Maranghi, S.; Manfrida, G.; Basosi, R.; Sinicropi, A. Environmental impact analysis applied to solar pasteurization systems. *J. Clean. Prod.* **2019**, *212*, 1368–1380, doi:10.1016/j.jclepro.2018.12.020.
32. Fiaschi, D.; Manfrida, G.; Petela, K.; Talluri, L. Thermo-Electric Energy Storage with Solar Heat Integration: Exergy and Exergo-Economic Analysis. *Energies* **2019**, *12*, 648.
33. Ferrara, G.; Ferrari, L.; Fiaschi, D.; Galoppi, G.; Karellas, S.; Secchi, R.; Tempesti, D. Energy Recovery By Means Of A Radial Piston Expander In A CO2 Refrigeration System. *Int. J. Refrig.* **2016**, *72*, 147–155.

34. Schott Applied Power Corporation, High Efficiency Multi-Crystal Photovoltaic Module. Available online: http://abcsolar.com/pdf/schott165.pdf/ (accessed on 27 February 2019).
35. Bejan, A.; Tsatsaronis, G.; Moran, M. *Thermal Design and Optimization*; John Wiley & Sons, Inc.: New York, NY, USA, 1996.
36. Kotas, T.J. *The Exergy Method of Thermal Plant Analysis*; Butterworth-Heinemann: Oxford, UK, 1985.
37. Turton, R.; Bailie, R.; Whiting, W.; Shaeiwitz, J. *Analysis, Synthesis and Design of Chemical Processes*; Prentice Hall: Upper Saddle River, NJ, USA, 2003.
38. Chemical Engineering, Economic Indicators. Available online: https://www.chemengonline.com/site/plant-cost-index/ (accessed on 28 February 2019).
39. Kalogirou, S.A. *Solar Energy Engineering, Processes and Systems*, 2nd ed.; Academic Press: Cambridge, MA, USA, 2013.
40. Freecleansolar, 165W Module Schott SAPC-165 Poly. Available online: https://www.freecleansolar.com/165W-module-Schott-SAPC-165-poly-p/sapc-165.htm (accessed on 28 February 2018).
41. Lazzaretto, A.; Tsatsaronis, G. SPECO: A systematic and general methodology for calculating efficiencies and costs in thermal systems. *Energy* **2006**, *31*, 1257–1289.
42. International Standards Organization. EN ISO 14040:2006-Valutazione del Ciclo di Vita. Principi e Quadro di riferimento. *Environ. Manag.* **2010**, 14040. Available online: http://www.eliosingegneria.it/i-nostri-servizi/tutela-dellambiente/75-valutazione-del-ciclo-di-vita-uni-en-iso-140402006 (accessed on 2 July 2020)
43. Greendelta. OpenLCA 2018. Available online: https://www.greendelta.com/ (accessed on 2 July 2020).
44. Moreno Ruiz, E.; Valsasina, L.; Fitzgerald, D.; Brunner, F.; Vadenbo, C.; Bauer, C.; Wernet, G. Documentation of changes implemented in the Eco-invent database v3.4. *Ecoinvent V3* **2017**, *4*, 1–97.
45. Peters, J.F.; Baumann, M.; Zimmermann, B.; Braun, J.; Weil, M. The environmental impact of Li-Ion batteries and the role of key parameters–A review. *Renew. Sustain. Energy Rev.* **2017**, *67*, 491–506, doi:10.1016/j.rser.2016.08.039.
46. Agostini, A.; Belmonte, N.; Masala, A.; Hu, J.; Rizzi, P.; Fichtner, M.; Baricco, M. Role of hydrogen tanks in the life cycle assessment of fuel cell-based auxiliary power units. *Appl. Energy* **2018**, *215*, 1–12, doi:10.1016/j.apenergy.2018.01.095.
47. Hansen, J.B. Solid oxide electrolysis–a key enabling technology for sustainable energy scenarios. *Early Dev.* **2015**, 9–48, doi:10.1039/c5fd90071a.
48. PRé Sustainability. Eco-Indicator 99 Manual for Designers. Available online: https://www.pre-sustainability.com/download/EI99_Manual.pdf (accessed on 2 July 2020).
49. Meyer, L.; Tsatsaronis, G.; Buchgeister, J.; Schebek, L. Exergoenvironmental Analysis for Evaluation of the Environmental Impact of Energy Conversion Systems. *Energy* **2009**, *1*, 75–89.
50. Mousavi, S.A.; Mehrpooya, M. A comprehensive exergy-based evaluation on cascade absorption-compression refrigeration system for low-temperature applications-exergy, exergoeconomic, and exergoenvironmental assessments. *J. Clean. Prod.* **2020**, *246*, 119005, doi:10.1016/j.jclepro.2019.119005.
51. Bonforte, G.; Buchgeister, J.; Manfrida, G.; Petela, K. Exergoeconomic and exergoenvironmental analysis of an integrated solar gas turbine/combined cycle power plant. *Energy* **2018**, *156*, 352–359, doi:10.1016/j.energy.2018.05.080.
52. José, E.; Cavalcanti, C. Exergoeconomic and exergoenvironmental analyses of an integrated solar combined cycle system. *Renew. Sustain. Energy Rev.* **2017**, *67*, 507–519, doi:10.1016/j.rser.2016.09.017.

4.1.2. Paper 2: Environmental analysis of a nano-grid: A Life Cycle Assessment.

While in Paper 1 several storage technologies are encompassed, Paper 2 focuses on a SHS application of electrochemical storage technologies which, as described in Section 2, represent the most promising ESSs. More specifically, Paper 2, published in *Science of the Total Environment*, aims to compare seven different types of LIBs differing for electrodes materials. Through a comparative assessment, Paper 2 aims to point out a trade-off between the advantages and the drawbacks of different LIBs and of hybrid storage for a single-user application considering Siena (Italy) as reference installation site. Furthermore, several nano-grids configurations are compared including off-grid and on-grid SHSs and an off-grid hybrid nano-grid that integrates CHS and LIBs. The LCI is based on an Ecoinvent 3.2 version and is collected in an associated *Data in Brief* paper. The main outcomes of the paper are:

- The comparative evaluation of the LIBs and of the hybrid ESS in terms of single score environmental impacts.
- The contribution analysis of each part of the product system.
- A comparison of nano-grids environmental performances with those of national electricity mix.

The Ph.D. is the first author of the paper and contributed to the conceptualization, the development of the methodology, the results evaluation, and the writing of the paper.

Science of the Total Environment 700 (2020) 134814

Contents lists available at ScienceDirect

Science of the Total Environment

journal homepage: www.elsevier.com/locate/scitotenv

Environmental analysis of a nano-grid: A Life Cycle Assessment

Federico Rossi [a,b], Maria Laura Parisi [a,c,d], Simone Maranghi [a,c], Riccardo Basosi [a,c,d,*], Adalgisa Sinicropi [a,c,d]

[a] University of Siena, R²ES Lab, Department of Biotechnology, Chemistry and Pharmacy, Via A. Moro, 2, Siena, Italy
[b] University of Florence, Department of Industrial Engineering, Via Santa Marta, 3, Florence, Italy
[c] CSGI, Center for Colloid and Surface Science, via della Lastruccia 3, 50019 Sesto Fiorentino, Italy
[d] Institute of Chemistry of Organometallic Compounds (CNR-ICCOM), Via Madonna del Piano 10, 50019 Sesto Fiorentino, Italy

HIGHLIGHTS

- Among the analysed LIBs, NCA batteries are the most suitable for SHSs applications.
- The main responsible for the SHSs impacts is the backup energy from the generator.
- Combining batteries and hydrogen storage is a promising way to lower the NG impacts.
- The connection of a SHS to a large-scale SG is the most sustainable configuration.

GRAPHICAL ABSTRACT

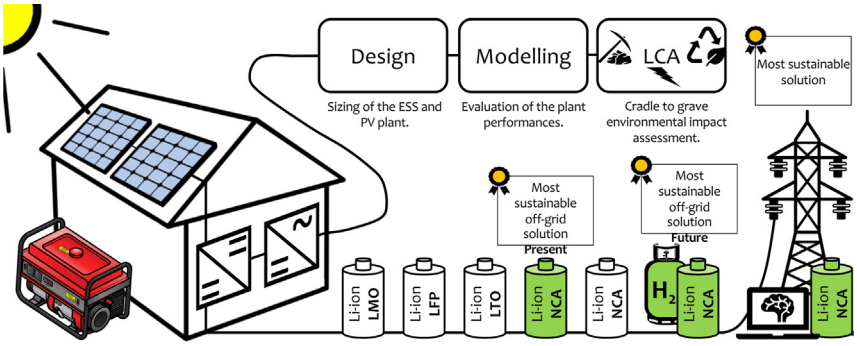

ARTICLE INFO

Article history:
Received 29 July 2019
Received in revised form 4 September 2019
Accepted 2 October 2019
Available online 21 October 2019

Editor: Yifeng Zhang

ABSTRACT

Renewable energy sources are fundamental to face the problem of climate changes. Unfortunately, some resources, such as wind and solar radiation, have fluctuations affecting the electrical grids stability. Energy storage systems can be used for a smart energy management to accumulate power from renewable sources. For such reason, these devices play a key role to achieve a sustainable electric system. On the other hand, they are affected by some environmental drawbacks mainly connected with the depletion of rare and expensive materials. Based on these considerations, in this study a nano-grid composed by a photovoltaic plant, a backup generator and an energy storage system is analysed by an environmental Life Cycle Assessment approach. A Solar Home System is designed, and its environmental profile is evaluated considering several Lithium-ion batteries. Among them, nickel-cobalt aluminium oxide cells resulted to be the most suitable solution for a Solar Home System (46.66 Pts/MWh). Moreover, a sensitivity analysis of the Solar Home System is performed and a hybrid energy storage plant integrating hydrogen and batteries is proposed to face the problem of seasonal solar radiation variability. Four scenarios having different gas pressure levels and lifespan of the devices are considered. Results show that currently the most sustainable configuration is represented by the Solar Home System, but in the future a hybrid nano-grid equipped with 700 bar hydrogen storage might be the best off-grid configuration for minimizing the impact on the environment (37.77 Pts/MWh). Extending the perspective of our analysis to future on-grid potential configurations, an efficient connection of the Solar Home System with a smart-grid is assessed as it looks more sustainable than other off-grid solutions (22.81 Pts/MWh).

* Corresponding author at: University of Siena, R²ES Lab, Department of Biotechnology, Chemistry and Pharmacy, Via A. Moro, 2, Siena, Italy.
E-mail address: riccardo.basosi@unisi.it (R. Basosi).

https://doi.org/10.1016/j.scitotenv.2019.134814
0048-9697/

Nomenclature

BMS	Battery Management System
C	Battery bank capacity, Ah
c_p	Hydrogen specific heat capacity at constant pressure, kJ/(kg*K)
CC	Charge Controller
CO	Construction
C-rate	Batteries charge and discharge rates, 1/h
DoD	Depth of Discharge, %
E	Electrolyser
E_{LIB}	Energy stored by the battery, kJ
$E_{load,day}$	Daily energy consumption design value, kWh
E_{PV}	Photovoltaic energy production over 25 years, MWh
E_{load}	Energy delivered to the load over 25 years, MWh
E_{Exc}	Exceeding energy production over 25 years, MWh
E_{Loss}	Energy losses over 25 years, MWh
ECM	Equivalent Circuit Model
EoL	End of Life
ESS	Energy Storage System
ETP	European Technology Platform
F	Amplification factor, adimensional
FC	Fuel Cell
h_{eq}	Equivalent full power operating time, h
HNG	Hybrid Nano-grid
I	Inverter
LCA	Life Cycle Assessment
LCI	Life Cycle Inventory
LCIA	Life Cycle Impact Assessment
LCP	Lithium Cobalt Phosphate
LFP	Lithium Iron Phosphates
LIB	Lithium-ion Battery
LMO	Lithium Manganese Oxide
LTO	Lithium Titanate
m_{H_2}	Hydrogen stored by the tanks, kg
$\dot{m}_{PEME,H_2}$	Hydrogen production mass flow rate, kg/s
$\dot{m}_{PEMFC,H_2}$	Hydrogen consumption mass flow rate, kg/s
NCA	Nickel Cobalt Aluminium Oxide
NCM	Nickel Cobalt Manganese Oxide
NG	Nano-grid
NREL	National Renewable Energy Laboratory
OP	Operation
P_{load}	Power required by the load, kW
P_{loss}	Power losses, kW
P_{min}	Minimum power required to the photovoltaic plant, kW
P_{PV}	Effective maximum power of the photovoltaic plant, kW
PEME	Proton Exchange Membrane Electrolyser
PEMFC	Proton Exchange Membrane Fuel Cell
PV	Photovoltaic
PVGIS	Photovoltaic Geographical Information System
Q_{loss}	Percentage capacity reduction due to batteries natural ageing, %
RPC	Reciprocating Piston Compressor
SG	Smart Grid
SHS	Solar Home System
SoC	State of Charge, %
ST	Storage Tank
T_{in,H_2}	Hydrogen inlet temperature to the compressor, K
t	Simulation time, days
V	Voltage, V
VI	Virtual Island
VRFB	Vanadium-redox flow battery
P_{Comp}	Compressor power absorption, kW
β	Compression ratio, adimensional
γ	Hydrogen heat capacity ratio, adimensional
ΔC	Percentage difference of battery bank capacity, %
ΔI	Percentage difference of environmental impact, %
ΔP	Percentage difference of photovoltaic power, %
η_{NG}	Nano-grid overall efficiency, %
η_{el}	Electric efficiency, %
η_{is}	Iso-entropic efficiency of the compressor, %

1. Introduction

Electricity is a very important energy vector because, unlike heat, it can be transmitted and distributed over long distances with minimum losses. Currently electricity is mainly produced by centralized power plants burning fossil fuels, but the contribution of renewable energy sources is growing, and a large increase is expected in the future. Today fossil fuels provide most of the electricity worldwide but, thanks to the efforts to reduce global warming, the share of renewable energies is expected to increase from 25% to 40% by 2040 with a significant contribution of photovoltaics (PV) (International Energy Agency – IEA, 2018).

PV is a technology able to convert the solar radiation to electricity and it shows an intrinsic daily and seasonal variability. Hence, using PV, the electricity output is characterized by fluctuations affecting the performances of the electrical grid, designed to operate in quasi-constant conditions. The same fluctuations apply to other renewable energy sources like wind. Thus, traditional electricity networks are not ready for the expected sudden expansion of discontinuous renewable energies and it is therefore urgent and necessary to develop Smart Grids (SGs). They actually were introduced in 2005 when an initiative named European Technology Platform (ETP) Smart Grids was founded to encourage the development of Europe's electrical grids (European Commission, 2006). SGs have been described by the ETP as a fundamental tool to increase the level of sustainability in the energy field and to create industrial and economic opportunities. Energy Storage Systems (ESSs) are one of the core issues of SGs. In fact, the storage of the exceeding energy from renewable sources is necessary to solve the issue of their variable production. Indeed, ESSs allow a disconnection between the energy production and consumption and provide the solution to manage electricity in a smart and sustainable way. For these reasons ESSs are indicated in one of the 10 key Actions of the European Strategic Technology Plan (SET Plan), an important research Program at European level to develop low carbon technologies and to reduce their costs by coordinating and financing national and international R&D programs (European Commission – SET Plan, 2018).

One of the prerogatives of a SG is to connect centralized and distributed power plants thanks to a layered structure. The smallest unit of a SG is called nano-grid (NG) and it can be connected with the rest of the grid or it can work independently as a Virtual Island (VI) (Nordman, 2010). A NG is defined as a small-scale electric grid involving a maximum power of 100 kW and distributing energy to a single user or a limited number of loads (Asmus and Wilson, 2017). Several types of storage systems can be applied in NGs and the choice strongly depends on the storage timescale. For instance, batteries are generally employed to overcome the problem of daily variability of solar radiation, whereas hydrogen is the appropriate solution for seasonal storage applications (International Energy Agency, 2015). Batteries are electrochemical devices composed of two electrodes, an electrolyte and a polymeric separator avoiding the contact between the electrodes. Among the most commercialized technologies (Ease and EERA, 2017) lithium-

ion batteries (LIBs) are considered as the nearest-future leader devices for both mobility and stationary applications thanks to their high energy density and long lifecycle. However, they have not reached their technological maturity yet (Steen et al., 2017). Even if LIBs represent an essential component to implement a sustainable electric network, there are some environmental drawbacks associated to their diffusion in the market. In fact, the use of rare materials, such as lithium or cobalt, represents both an environmental and economic problem for batteries. In the world, electrochemical storage industry represents the first consumer of lithium and cobalt, as it is responsible for the 39% and 30% of their depletion, respectively (Monge and Gil-alana, 2019). In the past, lithium availability was considered as the major limiting factor for the development of batteries, but according to the US Geological Survey (U.S. Department of the Interior and U.S. Geological Survey, 2018), the availability of this material has increased after the discovery of new reservoirs in the last years. Different considerations must be done for cobalt that is mainly mined in Congo (58% of the global extraction worldwide) and consumed in China, where the 80% of this material is used for the manufacturing of rechargeable cells (U.S. Department of the Interior and U.S. Geological Survey, 2018). These problems could cause a great harm to the environment and consequently advanced cobalt free LIBs represent a very important research topic, provided that their performances are demonstrated to be technically competitive. Moreover, the burdens connected with LIBs manufacturing and disposal must be considered to assess their environmental effectiveness. Based on these considerations, the analysis of ESSs and NGs must be inclusive of all the aspects of their sustainability and for such reason Life Cycle Assessment (LCA) has been selected as the best methodology for the environmental impact estimation because the whole life cycle of the devices is considered. Several LCA studies can be found in literature about ESSs, especially concerning LIBs. Peters et al. (2017) proposed a very interesting review of these studies whereas Peters and Weil (2018) selected the most detailed ones to provide a harmonized dataset (Peters and Weil, 2018). This is particularly relevant because one of the main obstacles for a coherent comparison of LIBs is the heterogeneity of data sources. New promising types of LIBs are growing recently, for instance Raugei and Winfield (2019) performed for the first time a LCA analysis of a new type of LIB named lithium cobalt phosphate (LCP) concluding that, compared to other LIBs, it represents a promising alternative to mitigate the global warming. LCA has also been applied to mixed lithium manganese oxide (LMO) and nickel cobalt manganese oxide (NCM) batteries by Cusenza et al. (2019) and to NCM-MoS_2 batteries by Deng et al. (2017a,b), who concluded that NCM devices are currently more sustainable than NCM-MoS_2. Moreover, Sanfélix et al. (2015) evaluated the environmental performances of a hybrid battery pack for mobility applications. Vanadium Redox Flow Batteries (VRFBs) and sodium/nickel chloride batteries currently represent valuable alternatives to LIBs for stationary applications. Weber et al. (2018) used LCA to compare VRFBs to LIBs providing a detailed description of their EoL whereas Dassisti et al. (2016) benchmarked VRFBs sustainability focusing on the electrolyte synthesis. VRFBs environmental and economic assessment has also been studied by Arbabzadeh et al. (2015) depending on a wind power plant working conditions. One of the expected developments for LIBs is the replacement of liquid with solid electrolytes in solid state batteries, whose environmental impact has been calculated by Troy et al. (2016). Furthermore post-LIBs will be developed in the future; for instance lithium-sulfur batteries have been assessed, using a LCA analysis, to become more sustainable than LIBs in the future (Deng et al., 2017a,b). Zackrisson et al. (2016) estimated the environmental impact of lithium-air batteries affirming that in the long-term, their effect on climate change will be at least 4 times lower than today's LIBs. Another solution to increase batteries sustainability is the replacement of lithium with sodium, that is more abundant in the planet. In this perspective Peters et al. (2016) performed an environmental assessment of sodium-ion devices. LCA methodology has been applied to other ESSs: for instance a power-to-gas hydrogen production plant (Parra et al., 2017) and high efficiency capacitors (Smith et al., 2018).

Grounding on the SET Plan strategies and the study of Peters and Weil (2018), we performed a LCA for the technical and environmental analysis of a NG virtually located in one of the most developed countries for PV plants installations, such as Italy. Although the LCA performed by Peters and Weil is fundamental for our analysis, as it represents the basis for the study, it does not allow to point out which is the most sustainable type of LIB. Furthermore, their LCA focused on the construction phase of the devices (CO) left out of the system boundaries the operation (OP) and End of Life (EoL) phases. The aim of our paper is to develop Peters and Weil study integrating the LIBs in a NG during their OP phase and considering their EoL management.

In a first step the NG is designed as an off-grid Solar Home System (SHS), which is a particular type of NG where a PV system powers a residential load equipped with LIBs and a diesel backup generator (Good Solar Initiative, 2015). In a following step, a sensitivity analysis is described and several solutions and scenarios to improve the NG eco-profile are evaluated. For instance, integrating LIBs and hydrogen storage in a hybrid nano-grid (HNG) could mitigate the environmental impact. Nowadays SHSs are mainly installed in rural centres of under-developed and developing Countries or in small islands where the electrical grid is not accessible. Indeed, solar energy is a fundamental resource in isolated conditions as it allows to satisfy some primary needs of the population such as drinking pasteurized water (Dainelli et al., 2017; Manfrida et al., 2017; Rossi et al., 2019) and electricity (Bravi et al., 2010; Parisi et al., 2019, 2013; Maranghi et al., 2019). For instance, Azimoh et al. (2014) remarked the importance of SHS applications in several African and Asian countries. Their paper is focused on a case study in South Africa to stress how off-design working conditions affect the performances and the costs of these systems. Another economic analysis of a SHS has been performed considering Honolulu as reference location using an optimization software provided by the U.S National Renewable Energy Laboratory (NREL) (O'Shaughnessy et al., 2018). Other studies considered developed countries as suitable installation sites for a SHS. For instance, a grid-connected SHS has been recently analysed in Italy comparing several approaches to assess the effects of weather forecast errors on the self-consumption rate (Petrollese et al., 2018). Furthermore, an economic analysis showed that a cost reduction of batteries is strongly required to make SHSs profitable in short-terms scenarios. Quoilin et al. (2016) obtained similar results analysing the self-consumption rate of SHSs in various European countries using statistical and economic methods. Their paper underlines the strategic role of ESSs to increase the percentage of self-sufficiency. Improving the expected lifetime of electrochemical devices is very important to mitigate the economic and environmental impacts of LIBs in SHSs. Indeed, Narayan et al. (2018) approached this topic using an innovative cycle-counting method. In this specific application LIBs devices expected lifespan is very long (16.7 years) compared to lead-acid (usually between 5.1 and 5.6 years) and nickel-cadmium batteries (2.9 years). Other authors combined environmental and economic considerations about renewable energy technologies and ESSs. For instance, Dufo-López et al. (2011) proposed an optimization analysis of a PV and a wind power system equipped with a diesel generator and battery storage system minimizing the cost of electricity and the carbon dioxide emissions. Another multi-objective approach has been proposed by Terlouw et al. (2019) who analysed the environmental

and economic impact related to the application of different battery chemistries in a flexible Community Energy Storage. Kabakian et al. (2015) focused their analysis only on the environmental performances of a small PV plant equipped with batteries compared to fossil fuels. Enlarging the perspective to other ESSs, hydrogen represents one of the main solutions to integrate batteries in PV plants. Jacob et al. (2018) proposed a design procedure of hybrid ESSs based on pinch analysis and made a general overview of other design methods in literature. Singh and Baredar (2016) performed an economic assessment of a hybrid renewable energy system composed by a biomass gasifier, a solar PV plant and a fuel cells (FCs) and electrolysers (Es) system to evaluate the cost of energy production. Contextually, the authors discuss how fuzzy logic programming can be useful to design and optimize the performances of hybrid renewable energy systems concluding that hydrogen FCs and batteries play a strategic role to meet load demand (Singh et al., 2017; Singh and Baredar, 2017). Nagapurkar and Smith (2018) instead applied economic optimization and LCA to a hybrid electrical grid connecting dozens of energy users in United States. LCA has been used by Belmonte et al. (2016) for a comparison between two PV plants respectively equipped with hydrogen storage and batteries. Their results show that, in both cases, the PV panels are responsible for the major contribution to the overall environmental impact. The environmental burden of hybrid micro-cogeneration has also been analysed by Balcombe et al. (2015) proposing the assessment of a PV power plant assisted by a Stirling Motor and batteries.

This literature overview highlights the need for a detailed environmental impact analysis of a NG based on a harmonized dataset of batteries and overarching all their lifecycle stages. Indeed, technical and economic analyses are widely available in the literature whereas the environmental assessment studies of NGs are less abundant and none of them is based on a common harmonized inventory. Another shortcoming of the available NGs LCA studies is the lack of a detailed evaluation of the use phase. Notably, in this work, a detailed design and modelling step, particularly for the LIBs, has been used to generate data supporting the LCA of the OP phase of NGs. More in details, this paper describes the eco-design of many NGs starting from the design phase, followed by the dynamic simulation and using the LCA as decisional tool for the individuation of the most sustainable ESS configuration for this application. The wide range of storage devices, including hybrid ESSs, considered for the comparison represents another novelty of this study. Although the results obtained in this paper are referred to a specific case study, the methodological framework presented here can be considered as a very general approach to be usefully implemented for other case studies.

This makes this study likely to be further developed considering other installation sites, other storage systems or other backup sources.

2. Material and methods

This study presents an eco-design procedure based on technical and environmental analysis of a NG powered by a PV plant and equipped with EESs. The goal is the identification of the most sustainable NG configuration. As the results strictly depend on the climatic conditions of the installation site, Siena, a small town in the centre of Tuscany region (Italy), has been selected as a case study location. A three-steps methodology is applied for the assessment of the system eco-profile (Fig. 1). The first phase is the design of a SHS composed of a PV plant, a LIBs storage system and a backup generator. The second step is the evaluation of the plant performances: as no experimental prototypes are available, a mathematical model has been employed to estimate the energy flows of the NG and the lifespan of the LIBs. The third step is the application of LCA that is used as decisional tool to assess the most sustainable NG configuration. Such eco-design approach was applied first to a SHS in order to indicate the LIBs chemistry which minimizes the global environmental impact. The interpretation of the SHS analysis suggested the integration of LIBs with a hydrogen ESS. Thus, the same three-steps methodology has been employed to study a HNG equipped with the most sustainable type of LIB and a hydrogen ESS. LCA has also been applied to an on-grid configuration, supposing to connect the SHS to a large-scale SG capable to accept all the PV energy exceeding the maximum LIBs capacity.

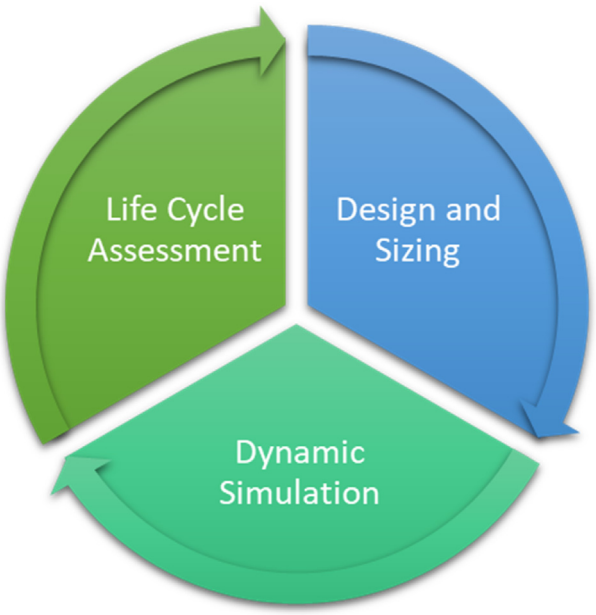

Fig. 1. Sketch of the multi-step approach applied for the eco-design of the NG.

2.1. Description of the components

The definition of the components and of their operative parameters is necessary for the eco-design of the NG. A PV plant produces all the electricity required by the user over one day; an ESS guarantees electricity supply even when the solar radiation is not available and a backup generator burning fossil fuels is employed as safe backup system. The Inverters (Is) and Charge Controllers (CCs) are electric converters necessary to adequately connect all these components. Two different ESSs have been investigated in this paper: LIBs and hydrogen. Batteries are electrochemical devices whose classification is based on the electrode materials. Currently, the most used types of LIBs are composed of a graphite anode and a lithium cobalt oxide (LCO) cathode. The shortage of cobalt represents an economic and environmental concern; for such reason much research effort has been done in order to limit its depletion. For instance, Peters and Weil (2018) analysed the eco-profiles of the post-LCO batteries listed in Table 1. More specifically, cobalt-free cathodes are used in Lithium iron phosphates (LFP) and Lithium Manganese Oxide (LMO) batteries; on the other hand, in Nickel Cobalt Aluminium Oxide (NCA) and Nickel Cobalt Manganese Oxide (NCM) batteries the content of cobalt is sensibly lower compared to LCO. In Lithium Titanate (LTO) batteries the graphite anode is replaced by $Li_4Ti_5O_{12}$ whereas the cathode is made of Lithium iron phosphates. Each of these batteries have different performances which can be suitably described by their operative parameters (MIT Team Electric Vehicle Team, 2008):

- Energy density: amount of energy which can be stored by the device per unit of mass;

Table 1
Technical characterization of LIBs.

	M-B (LFP)	Zack (LFP)	Bauer (LTO)	Notter (LMO)	Bauer (NCA)	Ell (NCM)	M-B (NCM)	Ref
Original Source	(Majeau-bettez et al., 2011)	(Zackrisson et al., 2010)	(Bauer, 2010)	(Notter et al., 2010)	(Bauer, 2010)	(Ellingsen et al., 2014)	(Majeau-bettez et al., 2011)	
Cathode	$LiFePO_4$	$LiFePO_4$	$LiFePO_4$	$LiMn_2O_4$	$LiNiCoAlO_2$	$LiNiMnCoO_2$	$LiNiMnCoO_2$	
Anode	Graphite	Graphite	$Li_4Ti_5O_{12}$	Graphite	Graphite	Graphite	Graphite	
Energy Density [Wh/kg]	109.3	82.9	52.4	116.1	133.1	130.3	139.1	(Peters and Weil, 2018)
Nominal Charge/Discharge Rate [h^{-1}]	1/1	1/1	1/1	0.7/1	0.7/1	0.7/1	0.7/1	(Buchamann, 2016)
Maximum Charge/Discharge Rate [h^{-1}]	10/10	10/10	5/10	3/5	4/4	1/5	1/5	(NEI Corporation, 2018)
Reference Discharge Curve	(Sony Energy Devices Corporation, 2011)	(Sony Energy Devices Corporation, 2011)	(Toshiba Corporation, 2017)	(GRST, 2017)	(Panasonic Corporation, 2017)	(GRST, 2017)	(GRST, 2017)	
Lifespan [Cycles]	6000	3000	10,000	1000	5000	2000	3000	(Peters et al., 2017)
DoD	80%	80%	80%	80%	80%	80%	80%	(Peters et al., 2017)
Coulombic Efficiency*	90%	90%	–	85%	–	95%	90%	(Peters et al., 2017)

* When defined by the reference author.

- Depth of Discharge (DoD): discharged energy expressed as a percentage of its maximum capacity, which is complementary to the state of charge (SoC).
- Nominal charge and discharge rate (C-rate): ratio between the nominal electricity flowing though the battery and its capacity;
- Maximum charge and discharge rate (C-rate): ratio between the maximum electricity flowing though the battery and its capacity;
- Discharge curve: battery voltage as a function of the SoC during the discharge phase;
- Battery lifespan: number of cycles which can be performed in standard conditions (temperature of 20 °C, nominal C-rates and DoD of 80%);
- Battery charge–discharge efficiency: rated energy during the discharge phase as percentage of the inlet energy during the charge phase.

From a rapid inspection of Table 1 we can observe that the use of cobalt as cathode material in NCA and NCM batteries gives a higher energy density than the others. Contrarily LFP and LTO batteries allow the highest nominal and maximum charge and discharge rates for the longest number of performed charge and discharge cycles. The real LIBs lifespan values depend on operative conditions and on natural degradation processes; for such reason they will be evaluated through mathematical modelling. Hydrogen represents the main solution for a long-term storage as it is possible to reduce the volume occupied by the gas by compression. Nowadays, the technology for the hydrogen conversion to and from electricity consists of FCs and Es (Sharaf and Orhan, 2014). These electrochemical devices are built using the same materials and are based on a reversed chemical reaction. Typically, for stationary applications at residential scale, FCs have an electric efficiency from 30% to 60% and a useful life of 12,000 h, but the technologically achievable target for the future can be 60,000 h (Sanson and Giuffrida, 2017). Proton Exchange Membrane Fuel Cells (PEMFCs) and Electrolysers (PEMEs) are the most commercialized technologies and for such reason they have been selected for this case study (Sanson and Giuffrida, 2017). Concerning the other components, non-lubricated reciprocating piston compressors (RPCs), widely used in refineries, are a suitable technology for hydrogen compression. Specific STs for hydrogen are available in the market: Type III and Type IV tanks are able to store pressurized hydrogen at 350 bar and 700 bar respectively (Agostini et al., 2018).

In this analysis we wish to compare several types of ESSs for a specific stationary application; for such reason the rest of the equipment, whose characteristics are listed in Table 2, is fixed in any configuration. PV panels, CCs and Is in Table 2 have been selected as they have an average efficiency representative of other commercial products in the market (Baumgartner, 2017; Jestin, 2012).

Despite the storage system is designed to provide autonomy to the NG, a safe source of backup energy is however necessary because of the unpredictability of weather conditions. The main sources of energy fuelling backup generators are gasoline, diesel and natural gas: nevertheless the gaseous fuels application for backup energy supply is increasing, diesel is traditionally the most common solution as it guarantees several technical and practical advantages (Kirchner, 2012) and for such reason it has been chosen as reference fuel for the backup generator in this study.

2.2. Design phase

As described in the previous sections, Siena (Italy) has been set as the reference location for this analysis; in this city, the equivalent full-power working time of the PV plant (h_{eq}), expressed as number of hours, has been evaluated using the Photovoltaic Geo-

Table 2
Technical characteristics of PV panels, CCs and Is.

Component	Power [W]	Voltage [V]	Efficiency	Model	Ref
PV panels	330	38	17%	Tenka Solar – 330W-72M	(Tenka Solar, 2015)
CCs	3600 DC (input)	52.8–115 DC (input) 48 DC (output)	98%	Mastervolt – SCM60 MPPT-MB	(Mastervolt, 2018)
Is	3500 AC (output)	38–62 DC (input) 180–260 AC (output)	92%	Mastervolt – Mass Combi Ultra 48/3500–50 (230 V)	(Mastervolt, 2018)

graphical Information System (PVGIS), a free tool available online developed by the Joint Research Centre (JRC) (JRC, 2019) of EU. The total Italian residential electricity consumption over the year 2017 was 64,491 GWh (Terna S.p.A., 2017); considering a population of 60.6 million people (The World Bank Group, 2018) and assuming that the user is a family composed of three people, the daily energy consumption of the users ($E_{load,day}$) has been estimated to 8.75 kWh. An adequate number of PV panels are supposed to be connected in series to make arrays whose voltage must be compatible with the input requirements of the CCs. Indeed, PV arrays are directly connected with DC/DC converters, whose role is to adapt the voltage of the PV generator and of the battery bank. The CCs also have some supplementary functions, for instance a Maximum Power Point Tracking (MPPT) system is implemented to allow the PV plant to work in optimum power conditions. The CCs are connected to the Is, which turns the DC to AC as required by the load. The Battery Management System (BMS) is a supplementary electronic device managing the energy flows in the system to guarantee its electrical safety and maximum LIBs performances. The energy required by the user directly goes from the PV plant to the load. If the energy consumption is higher than the production, their difference is provided by the storage system, otherwise the batteries are charged (Fig. 2).

Batteries are electrochemical devices composed of one or more cells; several batteries are connected in series and parallel to prepare a LIBs bank. Commercially, the capacity and the voltage of these electrochemical devices are very variable. As the goal of this part of the study is the definition of the most sustainable cell chemistry for this application, the capacity and voltage of the ESS is assumed to be the same for every analysed case. Otherwise the analysis would not be coherent and would be affected by the choice of the battery manufacturer. Concerning the design of the HNG, a hydrogen conversion system composed of PEMEs and PEMFCs has been designed to overcome the problem of solar radiation seasonal variability. Furthermore, the plant must be integrated by a RPC and pressurized hydrogen STs. This hydrogen ESS has been designed to work in parallel with the LIBs as the electricity that cannot be stored in batteries is converted to a gaseous fuel.

2.3. Modelling phase

Once the size of the PV plant and of the LIBs bank has been defined, modelling the system is required to simulate its performances in dynamic off-design conditions. The simulation is supposed to start on January 1st and to finish when the LIBs maximum capacity is equal to 80% of the starting value because, in that moment, their lifespan is considered over. Based on the simulation, the number of LIBs banks and the energy flows involved in the SHS are estimated over a period of 25 years. As starting conditions for the simulation, batteries are supposed to be fully charged. LIBs are assumed to be installed in a close environment with a controlled temperature. The electricity consumption profile of a user cannot be precisely predicted because it depends on people behaviour. Literature provides an example of electricity absorption profile in Italy in 2004 (Danese and Di Franco, 2004); these data have been taken as a basis and adapted to more updated measurements (Terna S.p.A., 2017). Furthermore, a stochastic noise has been added to consider the casual variability of the load and the temporary peaks occurring when some electric loads are turned on. Dynamic solar radiation data are hard to be predicted, but many years of recording have brought to development of a reliable weather datasets. The simulation software TRNSYS16 (The University of Wisconsin Madison, 2006) contains a detailed library including ambient conditions for many locations (Meteonorm, 2006) and the model of a Single-crystal PV plant for the assessment of its productivity (TRNSYS 16, 2006). The dynamic simulation of the battery storage system has been performed using Matlab/Simulink (Mathworks, 2018) whose library contains a battery block implementing an Equivalent Circuit Model (ECM) (Tremblay and Dessaint, 2009). A wide range of LIBs models is available in literature and the choice mainly depends on the intended application. Empirical models show low accuracy, but allow for very fast calculations; contrarily, physical models are very detailed, but their computational cost is higher. ECMs simulate a circuit, containing electric components, whose performances fit well those of batteries. As ECMs do not really describe a LIB, they cannot be considered physical models, but they are more detailed

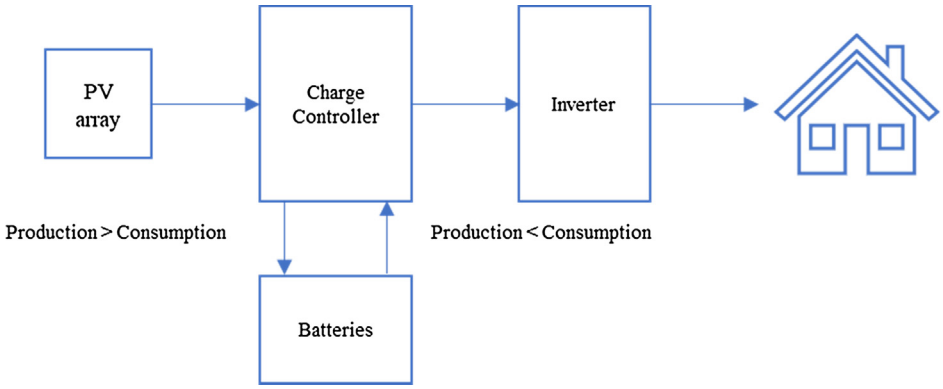

Fig. 2. Energy flows diagram of the SHS.

than empirical models and have a good computational efficiency. This is very important because the simulation time is in the order of years for this application; consequently, ECMs have been chosen as the best trade-off between accuracy and computational cost (Northrop and Crow, 2014). Unfortunately, natural ageing models of LIBs are not implemented in the battery block. This is a quite complex and unexplored field of research, and only a few detailed studies can be found so far in the literature. Among those, a paper describing a simplified method developed by Grolleau et al. (2016) has been selected. ECMs can also be applied to hydrogen conversion systems such as PEMFCs and PEMEs. Indeed, the simulation of the HNG has been performed using the Matlab/Simulink (Mathworks, 2018) software whose library contains a block implementing an ECM for the PEMFCs. The ECM of PEMEs instead has been built based on the equations used in another paper by Atlam and Kolhe (2011). Furthermore, a thermodynamic model for the RPC and a mass balance of the STs have been developed using Matlab/Simulink (Mathworks, 2018), considering two scenarios differing only for the level of pressure (350 and 700 bar).

2.4. Life Cycle Assessment

Life Cycle Assessment (LCA) is a four phases methodology to evaluate the environmental impacts of a product, process or a service. LCA study is standardized by to the ISO 14040 and 14044 regulations (International Standards Organization, 2006). The steps of a LCA analysis are:

- The goal and scope definition: the description of the system model and its boundaries;
- Life Cycle Inventory (LCI): all the inlet and outlet flows of energy and raw materials and the releases into the environment are listed and quantified;
- Life Cycle Impact Assessment (LCIA): the impacts generated by the system are evaluated through a calculation method translating all the emissions, resources and energy uses into environmental indicators;
- Life Cycle Interpretation: all the findings and the critical points identified through the LCA are evaluated to outline proposals and improvements for the eco-profile of the system and to point out the best available alternative.

Table 3
Expected lifespan of the components.

Component	Time		Unit	Ref
PV panels	25		yr	(Latunussa et al., 2016)
LIBs	Estimated by the model		yr	
Is	15		yr	(Belmonte et al., 2016)
CCs	15		yr	(Belmonte et al., 2016)
Wiring	25		yr	(Bekkelund, 2013)
STs	10		yr	(Agostini et al., 2018)
RPCs	10		yr	(Purchasing.com, 2015)
PEMFCs	12,000	60,000	h	(Sanson and Giuffrida, 2017)
PEMEs	12,000	60,000	h	(Sanson and Giuffrida, 2017)

Calculations have been performed with the open source software OpenLCA version 1.8 (Greendelta, 2018).

2.4.1. Goal and scope definition

A cradle-to-grave approach was employed for the assessment of the useful electricity provided to the load and 1 MWh of electricity was chosen as the functional unit. The boundaries of the system are defined according to the sketch illustrated in Fig. 3: the environmental impacts of all the components have been considered during the CO, OP and EoL phases. The expected lifespan of the components is summarized in Table 3; two scenarios have been considered for the hydrogen conversion system lifecycle duration. PEMEs and PEMFCs lifespan values are assumed to be approximately the same as they are made of the same materials and are based on the same operating principles (Schmidt et al., 2017). The connection cables are supposed to have the same lifespan of the PV panels (Bekkelund, 2013).

Some further assumptions are necessary:

- The impact related to the installation and maintenance of the SHS have been neglected as their contribution can be considered negligible compared to the lifetime of the SHS;
- As the PV plant is rooftop installed for household consumption and batteries are supposed to be placed in an indoor room of the building, no burden related to the direct land occupation and transformation occurs;
- The impact of some supplementary equipment of the SHS, such as switches and safety devices, has not been considered as it accounts for a very small amount of the total mass of the system.

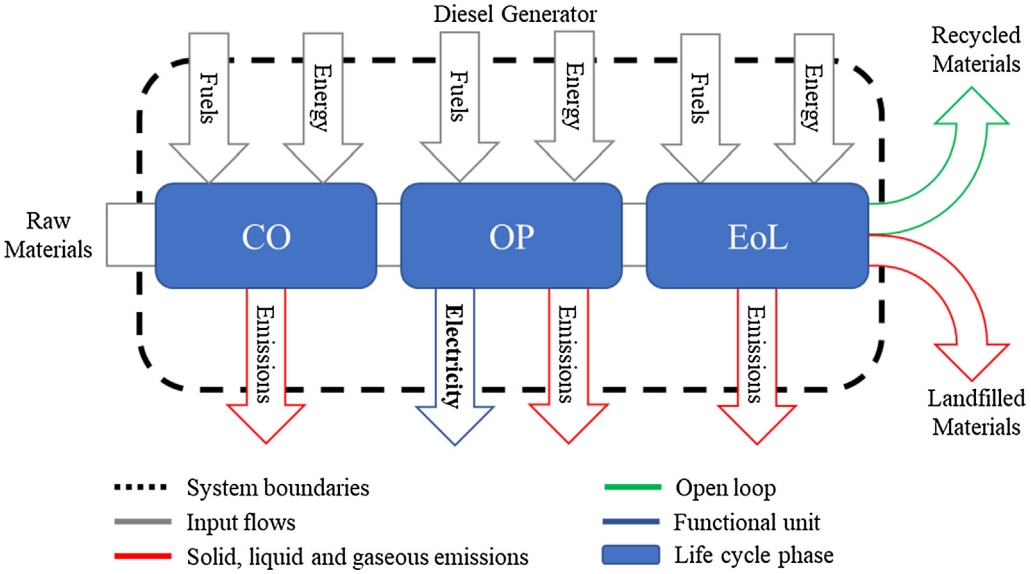

Fig. 3. Sketch of the system boundaries of the SHS.

2.4.2. Life Cycle inventory (LCI)

All the energy and matter input and output flows of the plant have been collected using the database Ecoinvent 3.2 (Moreno Ruiz et al., 2014). Market processes including materials transportations have been used. The entire LIBs production inventory, including also the BMS, has been directly extracted by Peters and Weil (2018) thanks to a downloadable openLCA file provided as supplementary materials and importable in the software. Quantitative data about the wiring of the PV plant are estimated as a function of the PV surface (Bekkelund, 2013). The LCI of the hydrogen STs manufacturing was built using literature data (Elgowainy et al., 2012). Recycling processes have been considered to mitigate the environmental impact associated to the EoL phase of the components, especially batteries (Weber et al., 2018) and the PEMFCs and PEMEs (Duclos et al., 2017; Stropnik et al., 2018), as they contain rare metals that have to be recovered. Furthermore also the EoL phase of the PV panels, the electric converters have been modelled assuming a recycling rate as described in the reference papers (Latunussa et al., 2016; Tschümperlin et al., 2016). A specific inventory for STs recycling is not available in the literature, but as carbon fibre represents the main construction material, a specific recovery process of this material has been considered in the model (Rosa et al., 2016). As the exceeding hydrogen represents a very useful fuel, it has been considered as a by-product of the NG in the LCA analysis.

2.4.3. Life cycle impact assessment

The *ReCiPe* 1.11 (2014) calculation method has been chosen for the calculation of the eco-profile as it provides a wide range of different impact categories and the environmental burdens can be expressed as mid-point and end-point values. For the assessment, a *Hierarchist (H)* model has been selected as it is generally the default choice as it is considered a trade-off between the most optimistic and precautionary scenarios (Goedkoop et al., 2013). As the installation site is supposed to be in Europe, the normalization and weighting set *Europe (H/A)* was generally chosen as the default for energy systems studies to obtain single score results and compare SHSs equipped with different LIBs (Goedkoop et al., 2013). In this way, all the environmental impact values are evaluated using a common measurement unit (eco-points, Pts).

2.4.4. Sensitivity analysis

Sensitivity analysis is employed to analyse the effect of a parameter variation on the results (Saltelli, 2002) and it is very important to verify the reliability of the LCA analysis. To this aim, the most influencing parameters must be individuated, and their value must be variated inside a limited range. The maximum percentage deviation from the nominal result is an indicator of the LCA model sensitivity. This procedure has been applied to the SHS design parameters: the PV plant power (P_{PV}) and the LIBs capacity (C).

3. Theory and calculations

3.1. SHs

The three-steps approach described in the previous section has been firstly applied to a standard SHS to identify the most sustainable LIB solution. All the configurations have been compared with each other and with the Italian electricity mix in terms of environmental performances.

3.1.1. SHS design phase

Concerning the design of the SHS, $E_{load,day}$ (expressed as kWh) and h_{eq} (expressed as h) represent the inputs for the sizing equations. Furthermore, we must consider that when electricity is supplied to electronic devices, part of its energy content is lost, and this affects the components efficiency (Table 2). Other undesired losses are related to thermal, resistive and optical phenomena occurring inside the plant; it's hard to predict in detail these quantities, but their contribution has been prudently estimated to 20% of the total productivity (Massimo Montopoli, 2012). Excluding the efficiency of the panels (whose value has been considered in the calculation of h_{eq}) the global electric efficiency of the plant (η_{el}) has been evaluated to 72%. Thus, the minimum power of the PV system (P_{min}, expressed as kW) has been calculated using Eq. (1):

$$P_{min} = \frac{E_{loadday}}{\eta_{el} \cdot h_{eq}} \tag{1}$$

Commercial PV panels are characterized by a nominal rated power which is usually defined in the technical sheet provided by the producer. The connection of several panels allows to increase the nominal power of the PV plant (P_{PV}): thanks to the calculation of P_{min}, we can evaluate the minimum number of panels so that P_{PV} becomes major thanP_{min}. Furthermore, the panels have been connected in series to make arrays whose voltage must be compatible with the input requirements of the CCs.

Concerning the design of the storage system, the definition of the DoD (80%) and an amplification factor F (1.15) allows the calculation of the capacity (C, expressed as Ah) of the battery bank, which is the amount of charge contained in the devices, using Eq. (2):

$$C = \frac{E_{load,day} \cdot 1000}{DoD \cdot V} \cdot F \tag{2}$$

where V is the nominal voltage of the battery system, set to 48 V.

Concerning the electrical equipment, the number of CCs is calculated in order to accept the maximum power of the PV plant; the number of Is, instead, only depends on the output power required by the load.

3.1.2. SHS modelling phase

As described in the methodological section, the design phase is followed by the dynamic simulation of the SHS which is necessary to evaluate the performances of the plant considering time-variable absorption and meteorological profiles. The productivity profile of the PV plant has been evaluated based on dynamic weather conditions using TRNSYS16 and is illustrated in Fig. 4a, whereas the average energy absorption profile is illustrated in Fig. 4b. This consumption profile has been obtained adapting direct measurements (Danese and Di Franco, 2004) to the design value $E_{loadday}$. Furthermore, a stochastic variability has been applied to the load profile in order to consider occasional peak loads.

These profiles represent inputs to model the ESSs which disconnect the energy production and consumption according to a power balance expressed by Eq. (3):

$$\frac{d}{dt}E_{LIB} = P_{PV} - P_{loss} - P_{load} \tag{3}$$

when the power produced by the PV arrays (P_{PV}), net of the NG losses (P_{loss}), is higher than the user absorption (P_{load}) the LIBs are charged and their energy content increases because $dE_{LIB}/dt > 0$; contrarily the SoC decreases when $dE_{LIB}/dt < 0$. When the batteries are discharged over the maximum DoD (80%), a backup generator provides energy supply to the load while the PV arrays charge the LIBs; when the SOC reaches the 100%, the exceeding energy is dissipated. A simple energy balance is not enough to describe how LIBs really work and the ageing mechanisms affecting their performances (Barré et al., 2013): indeed, the electrochemical phenomena occurring inside the storage system must be considered. As men-

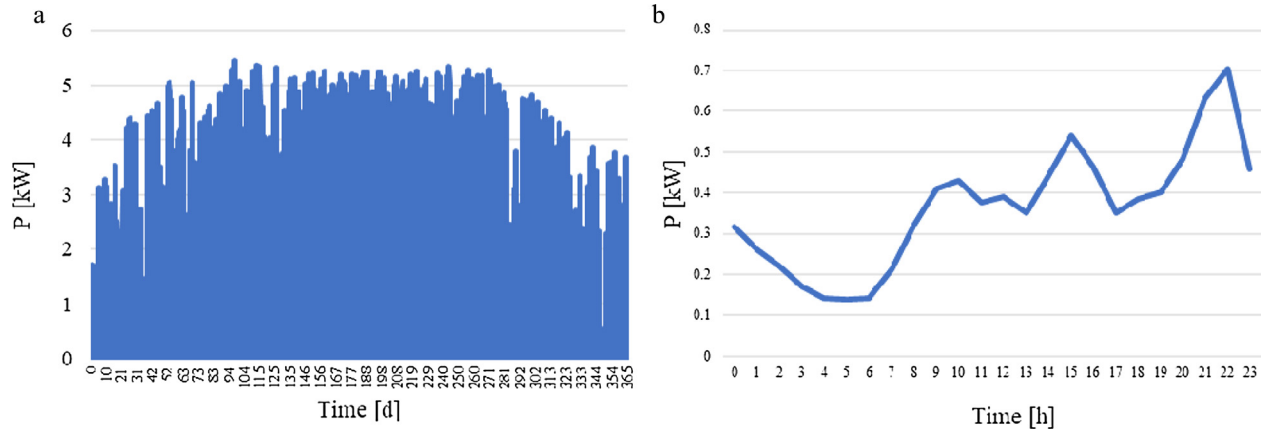

Fig. 4. a) Productivity profile of the PV plant b) Average energy absorption profile.

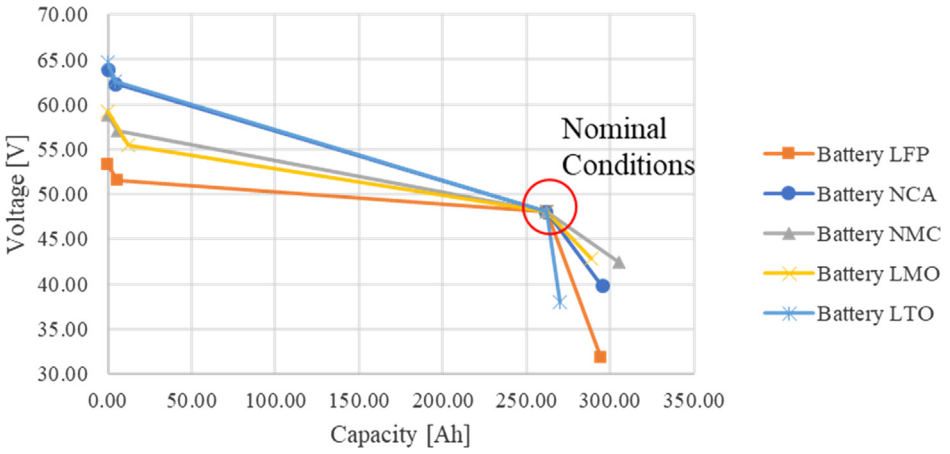

Fig. 5. Discharge curves of the LIBs bank in standard conditions.

tioned in the methodological section, a Simulink battery block implementing an ECM has been used (Mathworks, 2018; Tremblay and Dessaint, 2009). The model requires as input the discharge curve of the batteries, which are usually provided by the manufacturers (Table 1). The LIBs bank discharge voltage profiles (Fig. 5) have been obtained scaling the curves provided by the manufacturers to obtain the nominal design values of voltage and capacity. This is equivalent to connecting the batteries in series and parallel.

Even if the discharge voltage depends on the cell temperature, not all the manufacturers provide temperature-dependent curves. As few data are available for all the cell chemistries, the effects of the discharge temperature have been evaluated based on a literature study: Feng et al. (2014) illustrate how the discharge curve changes from 20 °C to 40 °C. Thus, the profiles illustrated in Fig. 5 have been modified proportionally to their results to achieve the LIBs discharge curves at 40 °C (Fig. 6). In this way it is possible to use them as inputs for a LIBs thermal model implemented in the Simulink battery block (Saw et al., 2014; Zhu et al., 2013).

Based on these discharge curves, the battery block automatically evaluates the charge curve and consequently the Coulombic efficiency. The block also allows the estimation of LIBs lifetime (Omar et al., 2014) affected by complex ageing mechanisms (Barré et al., 2013). Avoiding the rapid over-charge and over-discharge of the battery would be very useful to limit ageing effects. The study of Xu et al. (2018) provides a curve, valid for generic LIBs in standard conditions, representing the number of cycles as function of the DoD. As each battery has a different expected lifespan, the Xu et al. (2018) curve has been adapted to match with the lifetime duration values reported in Table 1 obtaining the profiles illustrated in Fig. 7.

The degradation processes are influenced by operating conditions. Temperature and C-rates dependent charts have been taken from the literature concerning the lifespan variation in non-standard conditions (Wu et al., 2017). Thus, using the same procedure of the discharge curves, the profiles illustrated in Fig. 7a have been modified proportionally to literature results (Fig. 7b and c) and used as battery block inputs.

Concerning the natural ageing estimation, Grolleau et al. (2016) developed a simple model for the estimation of the percentage capacity loss related to the natural degradation of devices. In case the cell temperature is approximated to 25°, this value is calculated according to Eq. (4):

$$Q_{loss}\left(25^{\circ}C, t\right) = 0.333 \cdot \sqrt{t} \tag{4}$$

where Q_{loss} is expressed as percentage and t is the simulation time expressed as days.

The outputs of the system are the batteries lifespan and the integral values of SHS energy flows:

- the productivity of the PV plant (E_{PV});
- the energy delivered to the load (E_{load});
- the missing energy required to the backup system ($E_{missing}$);

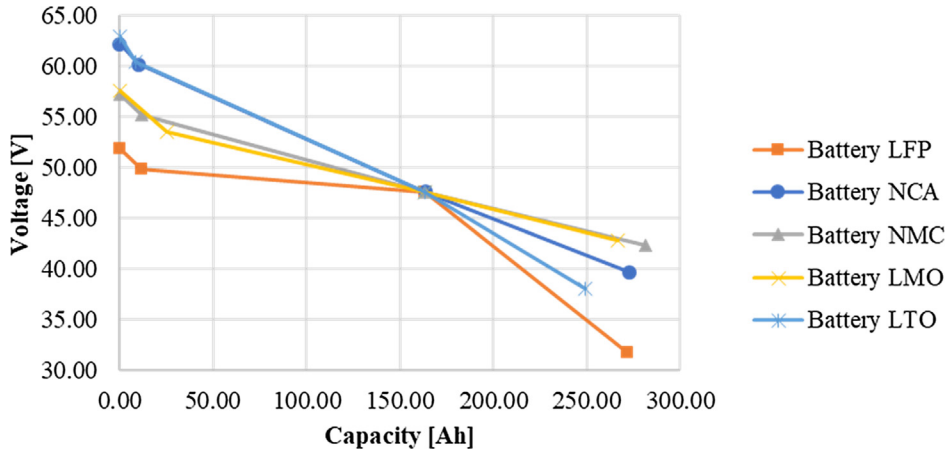

Fig. 6. Discharge curves of the LIBs bank at 40 °C.

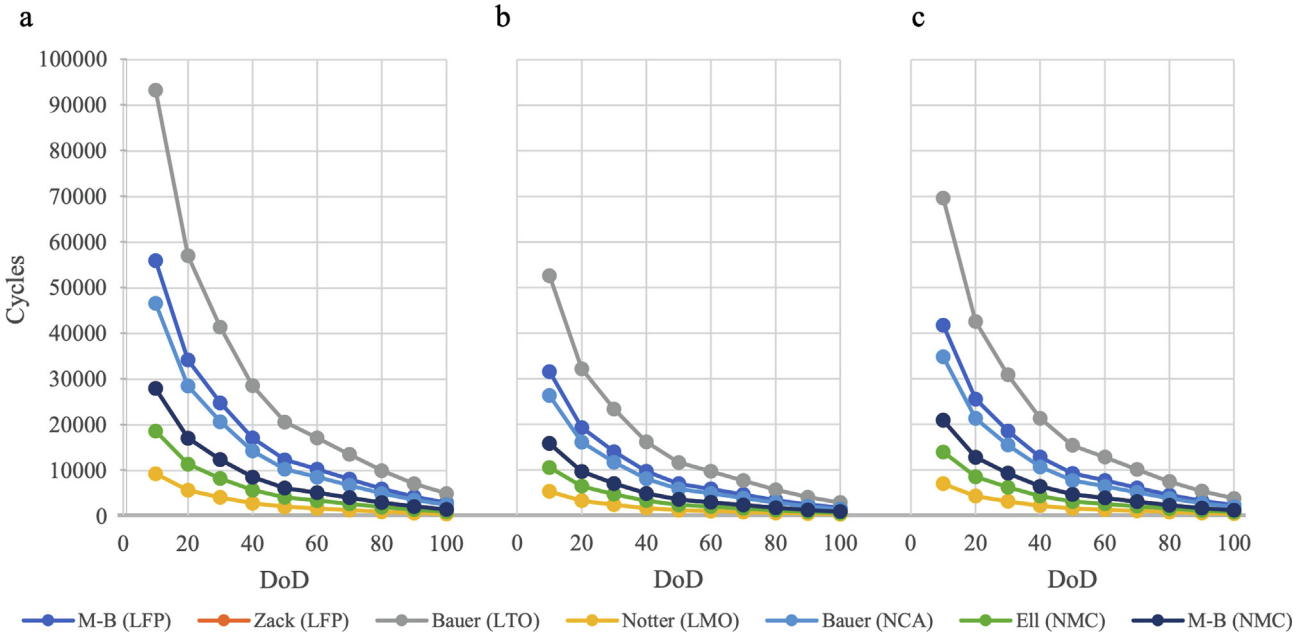

Fig. 7. Number of cycles as function of the DoD for all the battery chemistries a) in standard conditions; b) at 40 °C c) at their maximum C-rate.

- the exceeding energy that must be dissipated (E_{Exc});
- the SHS energy losses (E_{Loss});

In such way, it is also possible to calculate the overall SHS efficiency (Eq. (5)):

$$\eta_{NG} = 1 - \frac{E_{Loss} + E_{Exc}}{E_{PV} + E_{missing}} \quad (5)$$

3.1.3. SHS Life Cycle Assessment and sensitivity analysis

The results of the design and modelling phases represent inputs for the LCA as the inventory must contain quantitative data about all the energy and materials flows involved in the system boundaries. As described in the methodological section, the *ReCiPe* 1.11 (2014) allows an automatic evaluation of a Single Score environmental impact of the analysed system.

As described in the methodological section, the goal of the sensitivity analysis is to assess how small perturbations of the design parameters affect the results. Thus, small percentage variations (ΔP and ΔC) with steps of 5% have been applied to P_{PV} and C in a range of ±20%. The responding percentage alteration of the environmental impact (ΔI) has been evaluated.

3.2. HNG

A HNG configuration has been considered in order to improve the eco-profile of the SHS. Four scenarios are proposed and compared with the most sustainable SHS and with an on-grid arrangement.

3.2.1. HNG design phase

The design of the HNG has been focused on the definition of the hydrogen storage and conversion systems while the other parts of the plants are maintained the same of the SHS. Coherently with the LIBs system, the nominal voltage of the hydrogen conversion plant is set to 48 V. A PEME is designed to accept an electricity flow equal to the difference between the nominal PV power and the user maximum absorption. A PEMFC is designed to provide an adequate power of 3 kW to the user. The estimation of the RPCs absorption and of the STs volume is based on the dynamic simulation results

for both pressure levels. As underlined by the description of the ESS described in this study, hydrogen storage is much more complex than a battery storage as several different components are required. This is a drawback which affects the roundtrip efficiency of the system. Indeed, a reference value for LIBs coulombic efficiency is assessed between 85% and 90%. Contrarily, PEMEs maximum efficiency can be 82% (Schmidt et al., 2017) whereas PEMFCs have a nominal efficiency of about 55% (Souleman et al., 2009). Furthermore, as the isentropic efficiency is 80% (Çengel, 2009), the overall roundtrip efficiency of the ESS is estimated to 36%.

3.2.2. HNG modelling phase

Concerning the modelling phase, the PEME working equations (Atlam and Kolhe, 2011) have been implemented using Simulink (Mathworks, 2018) to evaluate the hydrogen temperature, pressure and mass flow rate ($\dot{m}_{PEME,H_2}$). These values represent an input for the compressor, whose absorbed power (P_{Comp}) is evaluated by Eq. (6):

$$P_{Comp} = \frac{\dot{m}_{PEME,H_2} T_{in,H_2} c_p \left(1 - \beta^{\frac{\gamma-1}{\gamma}}\right)}{\eta_{is}} \quad (6)$$

where T_{in,H_2} is the electrolysis temperature, c_p is the specific heat capacity of the gas, β is the compression ratio (the ratio between outlet and inlet pressures), γ is the hydrogen heat capacity ratio and η_{is} is the isentropic efficiency of the compressor (80%) (Çengel, 2009). The PEMFC is modelled by a block, available in the Simulink library, implementing an ECM (Njoya et al., 2009). The outputs are the hydrogen consumption rate ($\dot{m}_{PEMFC,H_2}$) and the electricity production that are necessary to define the hydrogen mass balance in the storage tank (Eq. (7)):

$$\frac{d}{dt} m_{H_2} = \dot{m}_{PEME,H_2} - \dot{m}_{PEMFC,H_2} \quad (7)$$

Table 4
Description of the hydrogen energy storage scenarios.

	Hydrogen pressure [bar]	PEMFCs and PEMEs lifespan [hours]
HNG-A	350	12,000
HNG-B	700	12,000
HNG-C	350	60,000
HNG-D	700	60,000

During the simulation, the working hours of PEMFCs and PEMEs have been accounted for; these will be useful to evaluate the number of components over 25 years. The simulation starts in January when the hydrogen ST is supposed to be empty. The efficiency of the HNGs is calculated according to Eq. (5).

3.2.3. HNG Life Cycle Assessment

The LCA of the HNGs has been performed following the same criteria of the SHS, but in this case the hydrogen storage system environmental footprint has been analysed considering four different scenarios as summarized in Table 4. The exceeding hydrogen produced at the end of the 25 years HNG lifespan is considered as a by-product: a physical allocation has been applied to evaluate the environmental impacts related to every reference flow of the system.

4. Results and discussion

In this section, the results obtained by the application of the three-steps methodological approach described before are illustrated, explained and interpreted. As previously mentioned, the outputs of the intermediate steps of the methodology represent inputs for the following ones.

The first finding of the analysis is the evaluation of the HNG and SHS configuration, including the number of the components, in order to provide safe energy supply as required by the user. These results are summarized in Table 5:

Based on these results, a dynamic simulation of the SHS has been performed for every type of LIB considered by Peters and Weil (2018). The energy flows involved in the SHS over the system lifespan are summarized in Table 6. Furthermore, the batteries lifespan (*Age*) is another fundamental result of the simulation. Regardless of the battery type, some general considerations can be done. Even if the storage system is designed to guarantee an autonomy of one day, in dynamic off-design conditions a small part of energy must be integrated by the backup generator during the winter season. Contrarily, during summer, when the solar radiation is maximum, the accumulators cannot contain all the exceeding electricity generated by the PV and a big part of it must be dissipated. Clearly the integral value of productivity and electricity consumption are independent from the choice of the LIB. Contrarily, the missing and exceeding energy and the energy losses are variable depending on the type of battery. Indeed, LIBs effective capacity and efficiency depends on their specific operating parameters compared to the working conditions and this

Table 5
Results of the design phases of the HNG and SHS.

Component	n°	Characteristics
PV panels	18	Eq. (1) gives as result that a 5.94 kW PV plant is required. The plant is made of 9 parallel arrays, composed of 2 panels in series; its maximum power voltage, 76 V, falls in the range of acceptability for the CCs.
CCs	2	The CCs peak input power is 3.6 kW, and together they can accept 5.94 kW at 76 V from the PV plant.
Is	1	The I has a peak output power of 3.5 kW, enough to provide energy supply to the household loads whose maximum absorption is typically 3 kW.
LIBs banks	1	Eq. (2) gives as result that a 262 Ah at 48 V battery bank is required. Cells and batteries are connected to build one battery bank storing an amount of energy of 12.576 kWh.
Backup Systems	1	A 4 kW diesel generator provides safe energy supply to the user.
PEMEs	1	A 3 kW PEME is required to accept the exceeding energy of the plant. This design value is evaluated as the difference between the nominal PV power (5.94 kW) and the maximum absorption (3 kW).
PEMFCs	1	A 3 kW PEMFC is required to provide an adequate power to the user.
RPCs	1	A 600 W compressor is required to pressurize hydrogen up to 350 bar and an 800 W compressor to pressurize it to 700 bar (assessed by the dynamic simulation).
Type III STs	14	A total amount of 3.6 m^3 of pressurized hydrogen (350 bar) must be stored because, according to the dynamic simulation, it is the user's yearly consumption. Each Type III ST has a volume of 258 l (Elgowainy et al., 2012).
Type IV STs	12	A total amount of 1.8 m^3 of pressurized hydrogen (700 bar) should be stored because, according to the dynamic simulation, it is the user's yearly consumption. Each Type IV ST has a volume of 149 l (Elgowainy et al., 2012).

Table 6
Results of the SHSs dynamic simulation.

	E_{PV} MWh	E_{load} MWh	$E_{missing}$ MWh	E_{Exc} MWh	E_{Loss} MWh	*Age* yr.
M-B (LFP)	195.39	100.42	15.09	58.73	51.33	6.55
Zack (LFP)	195.39	100.42	15.47	59.15	51.29	5.03
Bauer (LTO)	195.39	100.42	14.91	58.41	51.47	8.17
Notter (LMO)	195.39	100.42	13.96	56.61	52.32	3.54
Bauer (NCA)	195.39	100.42	13.92	54.08	54.81	9.12
Ell (NMC)	195.39	100.42	13.22	55.45	52.74	7.85
M-B (NMC)	195.39	100.42	13.87	53.64	55.20	8.40

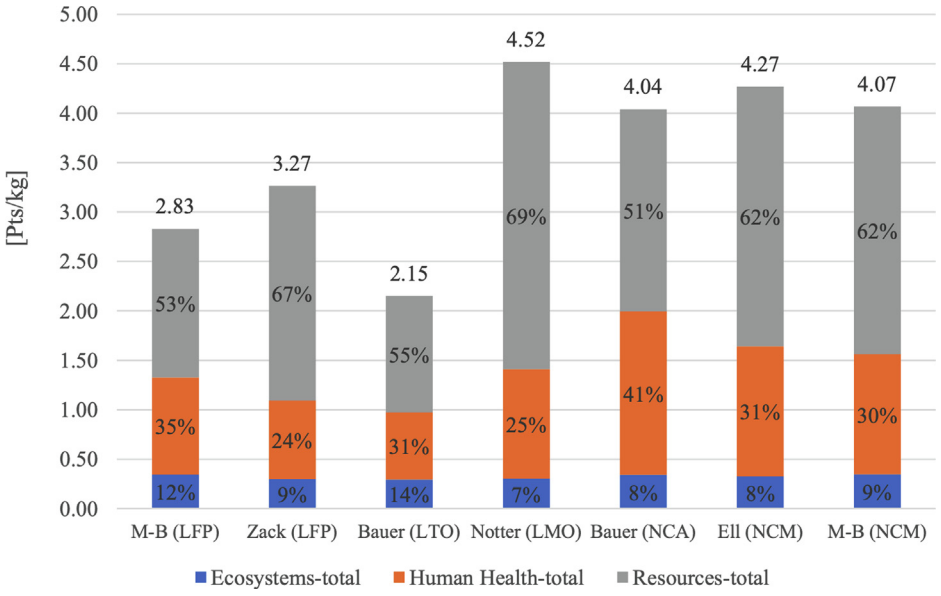

Fig. 8. Recipe Single Score results of several LIBs.

influences the LIBs energy balance. Concerning the charge and discharge rates, the dynamic simulation shows that the electricity flow rate in the batteries are very low, around 0.1 h^{-1}, coherently with the results of Narayan et al. (2018). This is typical of SHSs applications as the ESSs must guarantee a daily autonomy to the user. Consequently, the cell temperature does not increase sensibly (because of the Joule effect), and its value is almost constant and equal to 25 °C. Thus, the assumption made to simplify the natural LIBs ageing is verified. Table 6 summarizes also the duration of LIBs lifespan as combination of cyclic and natural degradation. The results are coherent with the rankings expected by Peters et al. (2017), except for LFP and LTO batteries whose life is shorter than NCA as they are working farther from nominal conditions. Narayan et al. (2018), studying SHSs applications, overestimated the lifespan of LFP batteries because their natural ageing has been neglected. The efficiency calculated using Eq. (5) is approximately the same for every SHS and very close to 48%; this value is strongly affected by the amount of exceeding energy that is dissipated. A connection of the SHS to a large-scale SG would avoid this energy dissipation and bring the efficiency over 70%.

The following phase is the SHS environmental impact evaluation. In order to correctly understand the LCA of the SHS, a focus on the sustainability of the batteries studied by Peters and Weil is required. Peters and Weil (2018) performed LCA for seven types of LIBs analysing five different impact categories. A wider overview of the eco-profile of LIBs during the CO phase is possible by calculating the environmental burdens as single scores [1]per unit of mass. The histograms in Fig. 8 clearly show that cobalt free LFP and LTO batteries are much more sustainable than the others. LMO batteries instead, despite the absence of cobalt, are the most impactful because of the manganese depletion and the groundwater contamination due to this metal.

Concerning the results of the SHS environmental analysis, illustrated in Fig. 9, some observations can be done. All the SHSs have a lower environmental impact than the Italian electricity mix (69.46 Pts/MWh), excluding the system equipped with LMO batteries. The main finding is that NCA batteries are the most sustainable solution for the SHS configuration modelled in this case study. The reason is that the combination of cobalt and other cathode materials represents the best trade-off between high energy density, materials consumption and lifecycle duration. For the same reason, in this ranking the second battery chemistry is NCM whose burden is a little bit higher than NCA.

Although LFP and LTO devices show the best level of sustainability per unit of mass (Fig. 8), the environmental performances of a SHS equipped with these batteries are not satisfactory mainly

[1] Single scores are environmental impact values calculated through the normalisation and weighting operations of LCA methodology. Indeed, weighted results have all the same unit and can be summed up to evaluate a single score environmental impact. This facilitates the comparison of the eco-profiles of different product systems and the decision making, since it is immediately clear whether a product's impact is higher or lower than the alternatives.

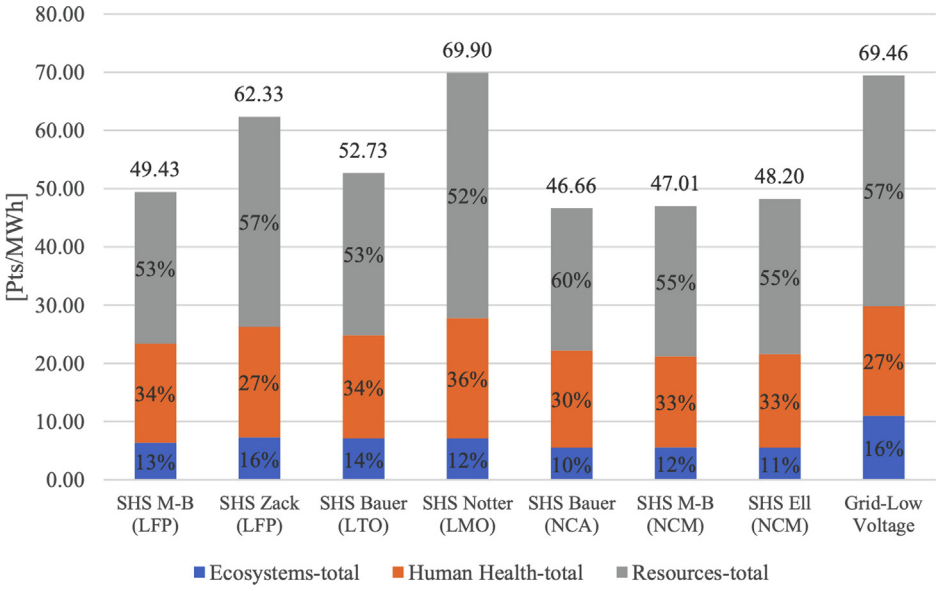

Fig. 9. Recipe Single Score results of several SHSs configured with a variety of LIBs chemistry.

Table 7
Contribution analysis of the SHS components.

	M-B (LFP)	Zack (LFP)	Bauer (LTO)	Notter (LMO)	Bauer (NCA)	Ell (NCM)	M-B (NCM)
PV	29%	23%	25%	21%	30%	29%	30%
LIBs	24%	38%	28%	46%	21%	26%	22%
Diesel Generator	46%	38%	43%	31%	46%	42%	45%
Electronics and wiring	1%	2%	5%	2%	3%	3%	3%

because of the low energy density. One advantage of LFP batteries is the possibility to exchange elevated current flows (Table 1), but in this case, the C-rate is in the order of 0.1 h^{-1} and consequently there is no need for charging and discharging LIBs very fast. The SHS equipped with LMO batteries is estimated, as expected, to be the worst solution because of their low energy density, the shortest lifespan and the highest specific environmental impact per unit of mass (Fig. 8). A detailed contribution analysis of the components of the system (Table 7) shows that LMO batteries represent the main responsible for the burden of the related SHS (46%); in the other cases the contributions associated to LIBs are in a range between 21% and 38%. Generally, the depletion of materials such as lithium and, in some cases, manganese and cobalt is responsible for most of LIBs environmental burden. Increasing the energy density would be very important to mitigate this problem as a lower amount of materials would be necessary. Also, the environmental burden of the PV plant gives a significative contribution, assessing between 21% and 30% of the total score. Anyway, the most impactful component is the diesel backup generator whose contribution is between 31% and 46%. This is particularly true for the *Ecosystem* and for the *Human Health* categories because of the emissions of CO_2 and NO_X with the combustion of diesel. The *Resources* category is also negatively influenced by the diesel generator as it affects the fossil fuels depletion category. The damage related to the diesel generator for backup energy supply represents a big environmental inefficiency considering that a bigger amount of sustainable energy is wasted when solar radiation is high. For such reason, accumulating the exceeding energy with a seasonal ESS might compensate the missing energy and would be important to mitigate the NG environmental impact.

As much as the sensitivity is concerned, the results analysis shows that varying the PV power from −20% to +20%, the environmental impact decreases because less energy is required from the diesel generator. The resulting percentage environmental (ΔI) impact variations are low and assessed between −5% and +10% (Fig. 10a). Concerning the perturbation of the LIBs capacity (Fig. 10b), the variation of this parameter from −20% to +20% makes the environmental impact profile to assume a convex profile with a minimum. The reason is that, when the battery capacity decreases, less materials are consumed but a higher amount of backup energy is required. On the other hand, if the battery capacity increases, more materials are required, but the backup energy does not decrease significantly as the PV power doesn't change. For these reasons the environmental impact increases. However, ΔI is always under 3%, which means that, in both cases, small input perturbations correspond to small variations of the results.

Based on the design values of the hydrogen storage plant (Table 5), the HNG has been modelled as described in the methodological section. The results of the dynamic simulation are summarized in Table 8 considering two scenarios of different hydrogen operating pressure levels (350 and 700 bar).

The first observation is that a very small amount of energy must be produced by the backup system at the beginning of the simulation as the starting condition has been set with the hydrogen ST empty. The energy losses are higher compared to the simulation of the SHS case, as the roundtrip efficiency of the hydrogen conversion system must be considered. As stressed by the results of the SHS simulation, the exceeding energy dumped during high radiation periods is higher than the missing electricity that must be integrated by the FC (Table 6). Consequently, the hydrogen production from the exceeding electricity, net of the compressor absorption, is higher than the consumption. Therefore, the HNGs can produce some exceeding hydrogen whose quantity depends on the electricity absorption of the compressors as it is subtracted from the gas production. As the exceeding electricity is converted to hydrogen and it is not dissipated, the result is an enhancement of the efficiency of the system; nevertheless, this parameter does not increase so much because it is affected by the energy losses

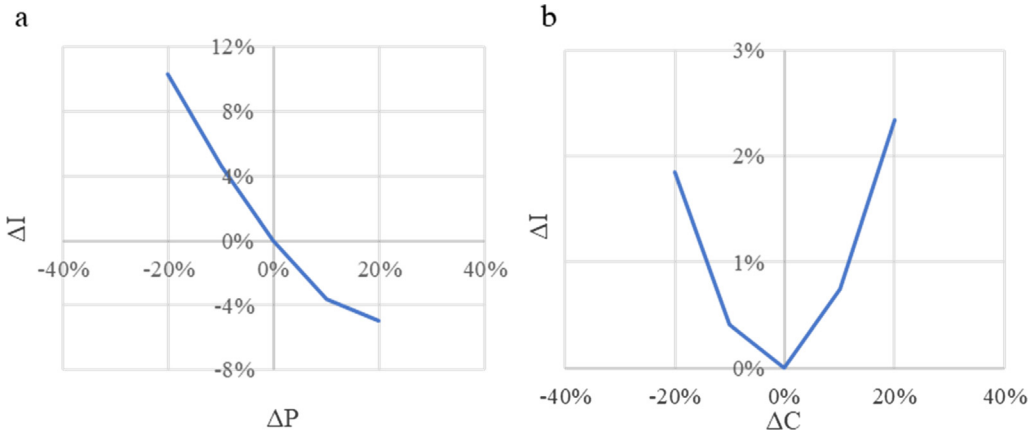

Fig. 10. a) Sensitivity analysis of the PV power. b) Sensitivity analysis of the LIBs capacity.

Table 8
Results of the hybrid NG simulation for two pressure levels scenarios.

	E_{PV}	E_{load}	$E_{missing}$	E_{Exc}	E_{Loss}	m_{H_2}	Age	Working hours	
	MWh	MWh	MWh	MWh	MWh	kg	yr.	PEMFC	PEME
350 bar	195.39	100.42	0.47	0	81.49	507.86	9.12	30,205	33,175
700 bar					80.89	470.45	9.12	30,205	33,175

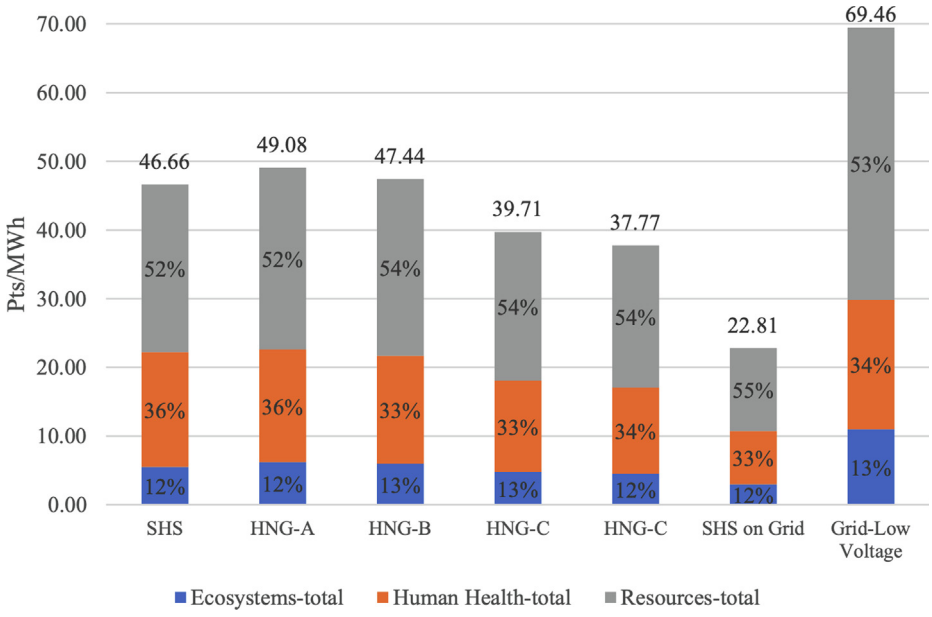

Fig. 11. Single Score results of the advanced NG configurations.

Table 9
Contribution analysis of the advanced NGs components.

	SHS	HNG-A	HNG-B	HNG-C	HNG-D	SHS on Grid
PV	30%	24%	26%	28%	30%	40%
LIBs	21%	17%	18%	20%	22%	29%
Diesel generator	46%	1%	1%	1%	1%	0%
Grid	0%	0%	0%	0%	0%	27%
PEMFCs/PEMEs	0%	22%	23%	5%	6%	0%
STs	0%	30%	25%	37%	32%	0%
RPC	0%	2%	4%	3%	5%	0%
Electronics and wiring	3%	4%	3%	6%	4%	4%

in the hydrogen conversion system and it is estimated to about 58% using Eq. (5).

These results allow us to perform a complete LCA of the four HNGs scenarios, accordingly to the scheme reported in Table 4. The eco-profiles of these advanced NG configurations are discussed in terms of single score damages (Fig. 11) and have been compared with the SHS eco-profile and the connection with a large-scale SG. The components contribution analysis is described in Table 9 for all the considered arrangements. The histograms show that all the proposed NG configurations are more sustainable than the current Italian electricity mix (69.46 Pts/MWh) because fossil fuels represent currently the main source of electricity in Italy. On the other hand, all the arrangements are more impactful than a SG-connected configuration (22.81 Pts/MWh). The reason is that if a NG is integrated in a larger smart electric system which can accept efficiently the fluctuating electricity without failures, no sustainable energy will be wasted. Unfortunately, as stressed in the introduction, most of the electrical grids are not smart yet and renewable energies can be responsible for failures and black outs. For such reason the transformation of the Italian electric network to a SG would be important to solve many environmental issues. In the HNG-A scenario the impact of the system (49.08 Pts/MWh) is higher than the SHS because the burden of the hydrogen ESS is not balanced by the gains connected with low diesel consumption. Indeed, the STs are responsible for the 30% of the impact whereas PEMFCs and PEMEs together give a contribution of 22%. Even if the exceeding hydrogen can be considered a by-product of the system, which mitigates the environmental impact allocated to electricity, this advantage is limited by the inefficiencies occurring in hydrogen ESS. Because of the gas volume reduction in HNG-B, where the pressure is 700 bar, the contribution of the STs is partially lowered to the 25% of the single score value (47.44 Pts/MWh). In this scenario the damage of the RPCs increases; this value is still quite limited (4%) but increasing the hydrogen pressure determines a minor hydrogen production and thus an indirect environmental drawback. Anyway, the expected growth of PEMFCs and PEMEs lifespan would be very important to mitigate the damage of hybrid ESSs. In the HNG-C scenario, the contribution of PEMFCs and PEMEs represents only the 5% of the total impact (39.71 Pts/MWh). Furthermore, concerning the HNG-C scenario, the installation of 700 bar STs makes the HNG even more sustainable as the single score value is 37.77 Pts/MWh. These values are lower than the burdens evaluated for the SHS. A standard SHS equipped with NCA batteries has a sustainable eco-profile compared to the Italian electricity mix. Concerning the HNGs, the contributions of the hydrogen ESS affect their environmental effectiveness making them very similar to the SHS. Increasing the lifespan of hydrogen conversion devices would be a decisive environmental advantage. Summarizing, currently a SHS with NCA batteries results to be the most sustainable off-grid solution, but in the future the HNGs will be probably the best off-grid configuration for the environment. In the future, the national electric system will be hopefully smart enough to accept fluctuating energy safely and, thanks to a high-efficient communication with a SHS, the environmental performances will be more sustainable than any off-grid configuration.

5. Conclusions

In this paper the eco-design of several NGs has been proposed on the goals of the SET-plan EU Action 7 research program and the available literature data on the LIBs environmental sustainability (Peters and Weil, 2018). The main idea of the study is to point out the most sustainable ESS configuration for a specific stationary application. Such goal has been achieved through the implementation of a three-steps methodological approach encompassing the design of the systems, dynamic simulation and LCA for the calculation of its eco-profile. The environmental analysis has been used as decisional tool for the choice of the most sustainable NG configuration. Its results have been interpreted to get some suggestions about possible improvements of the NG eco-profile. First, a SHS, has been analysed to define the most sustainable battery type. The plant is composed of LIBs, PV modules, electronic equipment and a diesel backup generator. The aim of the first phase of the study was the identification of the most sustainable LIB chemistry for SHS off-grid applications: indeed, the use of different materials implies that batteries have different technical characteristics and, consequently, different performances depending on the operating conditions. For this purpose, several cell chemistries have been considered, but NCA batteries resulted the most sustainable solution thanks to a good matching between performances and environmental impact. The SHS single score environmental impact value (46.66 Pts/MWh) is lower than that of the Italian electricity mix (69.46 Pts/MWh), and the use of a diesel backup system represents its main environmental drawback. This problem can be mitigated integrating LIBs with a hydrogen seasonal ESS. After a sensitivity analysis, some advanced HNG configurations have been analysed using the same methodological approach. The goal of this phase of the study was to assess the effectiveness of the integration of hydrogen and batteries in order to mitigate the NG environmental impact. Four scenarios have been proposed: hydrogen is supposed to be stored and compressed at 350 bar (HNG-A) and 700 bar (HNG-B) considering a lifespan of 12,000 h for PEMEs and PEMFCs. A future lifetime expansion has also been considered for both systems (HNG-C and HNG-D). The SHS was assessed as the most sustainable off-grid solution because it is characterized by a lower environmental damage than that of HNG-A (49.08 Pts/MWh) and of HNG-B (47.44 Pts/MWh). The main reason is that PEMFCs, PEMEs and ST use up a big amount of rare materials. The environmental benefit connected to the very low backup energy consumption from diesel combustion is not enough to compensate the HNG drawbacks, unless an increase of PEMFCs, PEMEs lifespan is obtained. Indeed, HNG-C and HNG-D were assessed as the most promising off-grid solution for the environment as their impact values are 39.71 Pts/MWh and 37.77 Pts/MWh, respectively. Although a large connection of distributed PV plants and ESSs to the grid is currently quite problematic, this solution is expected to become much diffused in the future. For such reason, in the last phase of the analysis, the previous off-grid systems were compared to an on-grid configuration of the SHS with NCA batteries. The conclusion is that, in the future, the connection to a large-scale SG would be probably the most efficient and sustainable configuration (22.81 Pts/MWh). For such reason the development of a large-scale SG integrating NG should be strongly encouraged. The installation of advanced LIBs and post-LIBs may represent a further development of this study as ESSs features are changing and improving very fast. Furthermore, as the environmental performances of NGs powered by PV plants strictly depend on weather conditions, their assessment in different countries could be further investigated.

Declaration of Competing Interest

The authors declare that they have no known competing financial interests or personal relationships that could have appeared to influence the work reported in this paper.

Acknowledgments

Authors acknowledge MIUR Grant – Department of Excellence 2018–2022. FR is grateful for the Ph.D. grant within the "Progetto Pegaso" funded by Regione Toscana.

Careful reading and revising of the manuscript by Professor Emeritus Michael Rodgers, Bowling Green State University, is gratefully acknowledged.

References

Agostini, A., Belmonte, N., Masala, A., Hu, J., Rizzi, P., Fichtner, M., Moretto, P., Luetto, C., Sgroi, M., Baricco, M., 2018. Role of hydrogen tanks in the life cycle assessment of fuel cell-based auxiliary power units. Appl. Energy 215, 1–12. https://doi.org/10.1016/j.apenergy.2018.01.095.

Arbabzadeh, M., Johnson, J.X., De Kleine, R., Keoleian, G.A., 2015. Vanadium redox flow batteries to reach greenhouse gas emissions targets in an off-grid configuration. Appl. Energy 146, 397–408. https://doi.org/10.1016/j.apenergy.2015.02.005.

Asmus, P., Wilson, A., 2017. Microgrids, Mini-grids, and Nanogrids: An Emerging Energy Access Solution Ecosystem [WWW Document]. URL http://energyaccess.org/news/recent-news/microgrids-mini-grids-and-nanogrids-an-emerging-energy-access-solution-ecosystem/ (accessed 7.19.19).

Atlam, O., Kolhe, M., 2011. Equivalent electrical model for a proton exchange membrane (PEM) electrolyser. Energy Convers. Manage. 52, 2952–2957. https://doi.org/10.1016/j.enconman.2011.04.007.

Azimoh, C.L., Wallin, F., Klintenberg, P., Karlsson, B., 2014. An assessment of unforeseen losses resulting from inappropriate use of solar home systems in South Africa. Appl. Energy 136, 336–346. https://doi.org/10.1016/j.apenergy.2014.09.044.

Balcombe, P., Rigby, D., Azapagic, A., 2015. Environmental impacts of microgeneration: Integrating solar PV, Stirling engine CHP and battery storage. Appl. Energy 139, 245–259. https://doi.org/10.1016/j.apenergy.2014.11.034.

Barré, A., Deguilhem, B., Grolleau, S., Gérard, M., Suard, F., Riu, D., 2013. A review on lithium-ion battery ageing mechanisms and estimations for automotive applications. J. Power Sources 241, 680–689. https://doi.org/10.1016/j.jpowsour.2013.05.040.

Bauer, C., 2010. Okobilanz von Lithium-Ionen Batterien.

Baumgartner, F., 2017. The Performance of Photovoltaic (PV) Systems. https://doi.org/10.1016/C2014-0-02701-3.

Bekkelund, K., 2013. A Comparative Life Cycle Assessment of PV Solar Systems, Master thesis in Energy and Environmental Engineering, Norwegian University of Science and Technology (NTNU), Department of Energy and Process Engineering. [WWW Document]. URL https://ntnuopen.ntnu.no/ntnu-xmlui/handle/11250/235329 (accessed 7.17.19).

Belmonte, N., Girgenti, V., Florian, P., Peano, C., Luetto, C., Rizzi, P., Baricco, M., 2016. A comparison of energy storage from renewable sources through batteries and fuel cells: a case study in Turin. Italy. Int. J. Hydrogen Energy 41, 21427–21438. https://doi.org/10.1016/j.ijhydene.2016.07.260.

Bravi, M., Parisi, M.L., Tiezzi, E., Basosi, R., 2010. Life cycle assessment of advanced technologies for photovoltaic panels production. Int. J. Heat Technol. 28, 129–135.

Buchamann, I., 2016. Batteries in a Portable World. Cadex Electronics Inc..

Çengel, Y., 2009. Introduction to Thermodynamics and Heat Transfer. Paolo Roncoroni.

Cusenza, M.A., Bobba, S., Ardente, F., Cellura, M., Di Persio, F., 2019. Energy and environmental assessment of a traction lithium-ion battery pack for plug-in hybrid electric vehicles. J. Clean. Prod. 215, 634–649. https://doi.org/10.1016/j.jclepro.2019.01.056.

Dainelli, N., Manfrida, G., Petela, K., Rossi, F., 2017. Exergo-economic evaluation of the cost for solar thermal depuration of water. Energies, 1–19. https://doi.org/10.3390/en10091395.

Danese, A., Di Franco, A., 2004. Progetto Micene: Misure dei consumi di energia elettrica nel settore domestico [WWW Document]. eERG, end-use Effic. Res. Gr. URL http://www.eerg.it/resource/pages/it/Progetti_-_MICENE/compendio_misure_consumi_elettrici.pdf (accessed 5.11.19).

Dassisti, M., Cozzolino, G., Chimienti, M., Rizzuti, A., Mastrorilli, P., L'Abbate, P., 2016. Sustainability of vanadium redox-flow batteries: benchmarking electrolyte synthesis procedures. Int. J. Hydrogen Energy 41, 16477–16488. https://doi.org/10.1016/j.ijhydene.2016.05.197.

Deng, Y., Li, J., Li, T., Zhang, J., Yang, F., Yuan, C., 2017b. Life cycle assessment of high capacity molybdenum disulfide lithium-ion battery for electric vehicles. Energy 123, 77–88. https://doi.org/10.1016/j.energy.2017.01.096.

Deng, Y., Li, J., Li, T., Gao, X., Yuan, C., 2017a. Life cycle assessment of lithium sulfur battery for electric vehicles. J. Power Sources 343, 284–295. https://doi.org/10.1016/j.jpowsour.2017.01.036.

Duclos, L., Lupsea, M., Mandil, G., Svecova, L., Thivel, P.-X., Laforest, V., 2017. Environmental assessment of proton exchange membrane fuel cell platinum catalyst recycling. J. Clean. Prod. 142, 2618–2628. https://doi.org/10.1016/j.jclepro.2016.10.197.

Dufo-López, R., Bernal-Agustín, J.L., Yusta-Loyo, J.M., Domínguez-Navarro, J.A., Ramírez-Rosado, I.J., Lujano, J., Aso, I., 2011. Multi-objective optimization minimizing cost and life cycle emissions of stand-alone PV-wind-diesel systems with batteries storage. Appl. Energy 88, 4033–4041. https://doi.org/10.1016/j.apenergy.2011.04.019.

Ease, EERA, 2017. European Energy Storage Technology Development [WWW Document]. URL https://www.eera-set.eu/wp-content/uploads/148885-EASE-recommendations-Roadmap-04.pdf (accessed 7.17.19).

Elgowainy, A., Reddi, K., Wang, M., 2012. Life-Cycle Analysis of Hydrogen On-Board Storage Options, in: The 2013 DOE Fuel Cell Technologies Program Annual Merit Review and Peer Evaluation Meeting. Arlington, VA.

Ellingsen, L.A., Majeau-Bettez, G., Singh, B., Srivastava, A.K., Valøen, L.O., Strømman, A.H., 2014. Life cycle assessment of a lithium-ion battery vehicle pack. J. Ind. Ecol. 18, 113–124. https://doi.org/10.1111/jiec.12072.

European Commission – SET Plan, 2018. Integrated SET - Plan Action 7 "Become competitive in the global battery sector to drive e – mobility and stationary storage forward" [WWW Document]. URL https://setis.ec.europa.eu/sites/default/files/set_plan_batteries_implementation_plan.pdf (accessed 7.17.19).

European Commission, 2006. European SmartGrids Technology Platform - Vision and Strategy for Europe's Electricity Networks of the Future [WWW Document]. URL https://ec.europa.eu/research/energy/pdf/smartgrids_en.pdf (accessed 9.17.19).

Feng, F., Lu, R., Zhu, C., 2014. A Combined State of Charge Estimation Method for Lithium-Ion Batteries Used in a Wide Ambient Temperature Range [WWW Document]. https://doi.org/10.3390/en7053004.

Goedkoop, M.J., Heijungs, R., Huijbregts, M., De Schryver, A., Struijs, J., R, V.Z., 2013. ReCiPe 2008, A life cycle impact assessment method which comprises harmonised category indicators at the midpoint and the endpoint level; First edition Report I: Characterisation; 6 January 2009 133. https://doi.org/http://www.lcia-recipe.net.

Good Solar Initiative, 2015. Quality Charter Technical & Service Quality Standards for Accredited Solar Suppliers.

Greendelta, 2018. OpenLCA V 1.8.

Grolleau, S., Baghdadi, I., Gyan, P., Marzouk, M. Ben, Duclaud, F., 2016. Capacity fade of lithium-ion batteries upon mixed calendar/cycling aging protocol [WWW Document]. URL https://hal.archives-ouvertes.fr/hal-01363521.

GRST, 2017. GRST batteries datasheet [WWW Document]. URL http://www.grstenergy.com/Cells.html (accessed 7.17.17).

International Energy Agency – IEA, 2018. World Energy Outlook.

International Energy Agency, 2015. Technology Roadmap - Hydrogen and Fuel Cells.

International Standards Organization, 2006. EN ISO 14040: 2006 – valutazione del ciclo di vita Principi e quadro di riferimento. Environ. Manage. 14040.

Jacob, A.S., Banerjee, R., Ghosh, P.C., 2018. Sizing of hybrid energy storage system for a PV based microgrid through design space approach. Appl. Energy 212, 640–653. https://doi.org/10.1016/j.apenergy.2017.12.040.

Jestin, Y., 2012. Comprehensive Renewable Energy [WWW Document]. URL https://www.sciencedirect.com/topics/engineering/monocrystalline-silicon-cell (accessed 7.17.19).

Joint Research Center (JRC), 2019. Photovoltaic Geographical Information System (PVGIS) [WWW Document]. Jt. Res. Cent. URL http://re.jrc.ec.europa.eu/pvgis/ (accessed 1.2.19).

Kabakian, V., McManus, M.C., Harajli, H., 2015. Attributional life cycle assessment of mounted 1.8kWp monocrystalline photovoltaic system with batteries and comparison with fossil energy production system. Appl. Energy 154, 428–437. https://doi.org/10.1016/j.apenergy.2015.04.125.

Kirchner, M., 2012. Understanding backup power system fuel choices [WWW Document]. Consult. Specif. Eng. Mag. URL https://www.csemag.com/articles/understanding-backup-power-system-fuel-choices/.

La Rosa, A.D., Banatao, D.R., Pastine, S.J., Latteri, A., Cicala, G., 2016. Recycling treatment of carbon fibre/epoxy composites: materials recovery and characterization and environmental impacts through life cycle assessment. Compos. Part B 104, 17–25. https://doi.org/10.1016/j.compositesb.2016.08.015.

Latunussa, C.E.L., Ardente, F., Blengini, G.A., Mancini, L., 2016. Life Cycle Assessment of an innovative recycling process for crystalline silicon photovoltaic panels. Sol. Energy Mater. Sol. Cells 156, 101–111. https://doi.org/10.1016/j.solmat.2016.03.020.

Majeau-bettez, G., Hawkins, T.R., Strømman, A.H., 2011. Life Cycle Environmental Assessment of Lithium-Ion and Nickel Metal Hydride Batteries for Plug-In Hybrid and Battery Electric Vehicles 4548–4554. https://doi.org/10.1021/es103607c.

Maranghi, S., Parisi, M.L., Basosi, R., Sinicropi, A., 2019. Environmental Profile of the Manufacturing Process of Perovskite Photovoltaics: Harmonization of Life Cycle Assessment Studies. Energies 12, 3746. https://doi.org/10.3390/en12193746.

Manfrida, G., Petela, K., Rossi, F., 2017. Natural circulation solar thermal system for water disinfection. Energy 141, 1204–1214. https://doi.org/10.1016/j.energy.2017.09.132.

Mastervolt, 2018. Mastervolt products datasheet [WWW Document]. URL https://www.mastervolt.it/prodotti/regolatori-di-carica-solari/scm60-mppt-mb/ (accessed 12.29.18).

Mathworks, 2018. Matlab/Simulink program – R2018a.

Meteonorm, 2006. Meteonorm global meteorological database [WWW Document]. URL https://meteonorm.com/ (accessed 2.7.19).

MIT Team Electric Vehicle Team, 2008. A Guide to Understanding Battery Specifications [WWW Document]. URL http://web.mit.edu/evt/summary_battery_specifications.pdf (accessed 7.17.19).

Monge, M., Gil-alana, L.A., 2019. Automobile components: lithium and cobalt. Evidence of persistence. Energy 169, 489–495. https://doi.org/10.1016/j.energy.2018.12.068.

Massimo Montopoli, 2012. Impianti Fotovoltaici: Guida Pratica. CEI - Comitato Elettrotecnico Italiano.

Moreno Ruiz, E., Lévová, T., Bourgault, G., Wernet, G., 2014. Ecoinvent 3.2 Report of Changes [WWW Document]. URL https://www.ecoinvent.org/files/20140630_report_of_changes_ecoinvent_3.01_to_3.1.pdf (accessed 7.17.19).

Nagapurkar, P., Smith, J.D., 2018. Techno-economic optimization and environmental life cycle assessment (LCA) of microgrids located in the US using genetic algorithm. Energy Convers. Manage. 181, 272–291. https://doi.org/10.1016/j.enconman.2018.11.072.

Narayan, N., Papakosta, T., Vega-Garita, V., Qin, Z., Popovic-Gerber, J., Bauer, P., Zeman, M., 2018. Estimating battery lifetimes in Solar Home System design using a practical modelling methodology. Appl. Energy 228, 1629–1639. https://doi.org/10.1016/j.apenergy.2018.06.152.

NEI Corporation, 2018. Nanomyte products Specification Sheet [WWW Document]. URL https://www.neicorporation.com/media/product-specs/#tab-id-2 (accessed 7.17.19).

Njoya, S.M., Tremblay, O., Dessaint, L.-A., 2009. A generic fuel cell model for the simulation of fuel cell vehicles. 2009 IEEE Vehicle Power and Propulsion Conference. IEEE, 1722–1729. https://doi.org/10.1109/VPPC.2009.5289692.

Nordman, B., 2010. Nanogrids evolving our electricity systems from the bottom up [WWW Document]. URL http://assets.fiercemarkets.net/public/smartgridnews/Smart_Grid_News_-_LBNL_Nanogrid_Report.pdf (accessed 7.12.19).

Northrop, P.W.C., Crow, M.L., 2014. Battery Energy Storage System (BESS) and Battery Management System (BMS) for Grid-Scale Applications. https://doi.org/10.1109/JPROC.2014.2317451.

Notter, D.A., Gauch, M., Widmer, R., Patrick, W.A., Stamp, A., Zah, R., Althaus, R.G., 2010. Contribution of Li-ion batteries to the environmental impact of electric vehicles. Environ. Sci. Technol. 44, 6550–6556. https://doi.org/10.1021/es1029156.

O'Shaughnessy, E., Cutler, D., Ardani, K., Margolis, R., 2018. Solar plus: A review of the end-user economics of solar PV integration with storage and load control in residential buildings. Appl. Energy 228, 2165–2175. https://doi.org/10.1016/j.apenergy.2018.07.048.

Omar, N., Abdel, M., Firouz, Y., Salminen, J., Smekens, J., Hegazy, O., Gaulous, H., Mulder, G., Van Den Bossche, P., Coosemans, T., 2014. Lithium iron phosphate based battery – assessment of the aging parameters and development of cycle life model. Appl. Energy 113, 1575–1585. https://doi.org/10.1016/j.apenergy.2013.09.003.

Panasonic Corporation, 2017. Datasheet : Specifications Powercell NCR18650B [WWW Document]. URL https://industrial.panasonic.com/ww/products/batteries/secondary-batteries/lithium-ion (accessed 6.6.19).

Parisi, M.L., Maranghi, S., Sinicropi, A., Basosi, R., 2013. Development of dye sensitized solar cells: A life cycle perspective for the environmental and market potential assessment of a renewable energy technology. Int. J Heat Technol., 31

Parisi, M.L., Ferrara, N., Torsello, L., Basosi, R., 2019. Life cycle assessment of atmospheric emission profiles of the Italian geothermal power plants. J. Clean. Prod. 234, 881–894. https://doi.org/10.1016/j.jclepro.2019.06.222.

Parra, D., Zhang, X., Bauer, C., Patel, M.K., 2017. An integrated techno-economic and life cycle environmental assessment of power-to-gas systems. Appl. Energy 193, 440–454. https://doi.org/10.1016/j.apenergy.2017.02.063.

Peters, J.F., Baumann, M., Zimmermann, B., Braun, J., Weil, M., 2017. The environmental impact of Li-Ion batteries and the role of key parameters – a review. Renew. Sustain. Energy Rev. 67, 491–506. https://doi.org/10.1016/j.rser.2016.08.039.

Peters, J., Buchholz, D., Passerini, S., Weil, M., 2016. Life cycle assessment of sodium-ion batteries. Energy Environ. Sci. 9, 1744–1751. https://doi.org/10.1039/c6ee00640j.

Peters, J.F., Weil, M., 2018. Providing a common base for life cycle assessments of Li-Ion batteries. J. Clean. Prod. 171, 704–713. https://doi.org/10.1016/j.jclepro.2017.10.016.

Petrollese, M., Cau, G., Cocco, D., 2018. Use of weather forecast for increasing the self-consumption rate of home solar systems: an Italian case study. Appl. Energy 212, 746–758. https://doi.org/10.1016/j.apenergy.2017.12.075.

Purchasing.com, 2015. Air Compressor Purchasing Guide Introduction to the Air Compressor Buying Process [WWW Document]. URL http://www.purchasing.com/construction-equipment/air-compressors/purchasing-guide/ (accessed 7.1.19).

Quoilin, S., Kavvadias, K., Mercier, A., Pappone, I., Zucker, A., 2016. Quantifying self-consumption linked to solar home battery systems: statistical analysis and economic assessment. Appl. Energy 182, 58–67. https://doi.org/10.1016/j.apenergy.2016.08.077.

Raugei, M., Winfield, P., 2019. Prospective LCA of the production and EoL recycling of a novel type of Li-ion battery for electric vehicles. J. Clean. Prod. 213, 926–932. https://doi.org/10.1016/j.jclepro.2018.12.237.

Rossi, F., Parisi, M.L., Maranghi, S., Manfrida, G., Basosi, R., Sinicropi, A., 2019. Environmental impact analysis applied to solar pasteurization systems. J. Clean. Prod. 212, 1368–1380. https://doi.org/10.1016/j.jclepro.2018.12.020.

Saltelli, A., 2002. Sensitivity Analysis for Importance Assessment 22. https://doi.org/10.1111/0272-4332.00040.

Sanfélix, J., Messagie, M., Omar, N., Van Mierlo, J., Hennige, V., 2015. Environmental performance of advanced hybrid energy storage systems for electric vehicle applications. Appl. Energy 137, 925–930. https://doi.org/10.1016/j.apenergy.2014.07.012.

Sanson, A., Giuffrida, L.G., 2017. Decarbonizzazione dell'economia italiana [WWW Document]. URL http://www.dsctm.cnr.it/images/Eventi_img/de_carbonizzazione_3_ottobre_2017/RSE Decarbonizzazione_WEB.PDF (accessed 5.17.19).

Saw, L.H., Somasundaram, K., Ye, Y., Tay, A.A.O., 2014. Electro-thermal analysis of lithium iron phosphate battery for electric vehicles. J. Power Sources 249, 231–238. https://doi.org/10.1016/j.jpowsour.2013.10.052.

Schmidt, O., Gambhir, A., Staffell, I., Hawkes, A., Nelson, J., Few, S., 2017. Future cost and performance of water electrolysis: an expert elicitation study. Int. J. Hydrogen Energy 42, 30470–30492. https://doi.org/10.1016/j.ijhydene.2017.10.045.

Sharaf, O.Z., Orhan, M.F., 2014. An overview of fuel cell technology: fundamentals and applications. Renew. Sustain. Energy Rev. 32, 810–853. https://doi.org/10.1016/j.rser.2014.01.012.

Singh, A., Baredar, P., 2016. Techno-economic assessment of a solar PV, fuel cell, and biomass gasifier hybrid energy system. Energy Rep. 2, 254–260. https://doi.org/10.1016/j.egyr.2016.10.001.

Singh, A., Baredar, P., Gupta, B., 2017. Techno-economic feasibility analysis of hydrogen fuel cell and solar photovoltaic hybrid renewable energy system for academic research building. Energy Convers. Manag. 145, 398–414. https://doi.org/10.1016/j.enconman.2017.05.014.

Singh, A., Baredar, P., 2017. Power sharing and cost optimization of hybrid renewable energy system for academic research building. J. Electr. Eng. Technol. 12, 1511–1518. https://doi.org/10.5370/JEET.2017.12.4.1511.

Smith, L., Ibn-Mohammed, T., Koh, S.C.L., Reaney, I.M., 2018. Life cycle assessment and environmental profile evaluations of high volumetric efficiency capacitors. Appl. Energy 220, 496–513. https://doi.org/10.1016/j.apenergy.2018.03.067.

Sony Energy Devices Corporation, 2011. Sony FortelionIJ1001M [WWW Document]. URL https://www.sonyenergy-devices.co.jp/en/ (accessed 7.17.19).

Souleman, N.M., Tremblay, O., Dessaint, L.A., 2009. A generic fuel cell model for the simulation of fuel cell vehicles. 5th. IEEE Veh. Power Propuls. Conf. VPPC '09, 1722–1729. https://doi.org/10.1109/VPPC.2009.5289692.

Steen, M., Lebedeva, N., Di Persio, F., Boon-Brett, L., 2017. JRC Science for policy report- EU Competitiveness in Advanced Li-ion Batteries for E-Mobility and Stationary Storage Applications – Opportunities and Actions. https://doi.org/10.2760/75757.

Stropnik, R., Sekavčnik, M., Ferriz, A.M., Mori, M., 2018. Reducing environmental impacts of the ups system based on PEM fuel cell with circular economy. Energy 165, 824–835. https://doi.org/10.1016/j.energy.2018.09.201.

Tenka Solar, 2015. Mono Crystalline Module [WWW Document]. URL http://www.tenkasolar.com/prodotti/ (accessed 1.5.19).

Terlouw, T., AlSkaif, T., Bauer, C., van Sark, W., 2019. Multi-objective optimization of energy arbitrage in community energy storage systems using different battery technologies. Appl. Energy 239, 356–372. https://doi.org/10.1016/j.apenergy.2019.01.227.

Terna S.p.A., 2017. Statistic Data [WWW Document]. Off. website. URL http://www.terna.it/SistemaElettrico/StatisticheePrevisioni/DatiStatistici.aspx (accessed 12.29.18).

The University of Wisconsin Madison, 2006. TRaNsient SYstems Simulation Program-TRNSYS16 [WWW Document]. URL https://sel.me.wisc.edu/trnsys/features/ (accessed 1.2.18).

The World Bank Group, 2018. World Population Prospects [WWW Document]. URL https://data.worldbank.org/indicator/SP.POP.TOTL?locations=IT (accessed 7.19.19).

Toshiba Corporation, 2017. Toshiba Rechargeable Battery SCiB [WWW Document]. URL https://www.scib.jp/en/product/module.htm (accessed 5.11.19).

Tremblay, O., Dessaint, L., 2009. Experimental validation of a battery dynamic model for EV applications. World Electr. Veh. J. 3, 289–298.

TRNSYS 16, 2006. Mathematical Reference 4, 1–486.

Troy, S., Schreiber, A., Reppert, T., Gehrke, H.G., Finsterbusch, M., Uhlenbruck, S., Stenzel, P., 2016. Life Cycle Assessment and resource analysis of all-solid-state batteries. Appl. Energy 169, 757–767. https://doi.org/10.1016/j.apenergy.2016.02.064.

Tschümperlin, L., Stolz, P., Frischknecht, R., 2016. Life cycle assessment of low power solar inverters (2.5 to 20 kW) Swiss Federal Office of. Energy SFOE 3.

U.S. Department of the Interior, U.S. Geological Survey, 2018. Mineral Commodity Summaries 2018 [WWW Document]. URL https://pubs.er.usgs.gov/publication/70194932 (accessed 5.3.19).

Weber, S., Peters, J.F., Baumann, M., Weil, M., 2018. Life cycle assessment of a vanadium redox flow battery. Environ. Sci. Technol. 52, 10864–10873. https://doi.org/10.1021/acs.est.8b02073.

Wu, Y., Keil, P., Schuster, S.F., Jossen, A., 2017. Impact of temperature and discharge rate on the aging of a LiCoO2/LiNi0.8Co0.15Al0.05O2 lithium-ion pouch cell. J. Electrochem. Soc. 164, A1438–A1445. https://doi.org/10.1149/2.0401707jes.

Xu, B., Member, S., Oudalov, A., Ulbig, A., Andersson, G., Kirschen, D.S., 2018. Modeling of lithium-ion battery degradation for cell life assessment. IEEE Trans. Smart Grid 9, 1131–1140. https://doi.org/10.1109/TSG.2016.2578950.

Zackrisson, M., Avellán, L., Orlenius, J., 2010. Life cycle assessment of lithium-ion batteries for plug-in hybrid electric vehicles e Critical issues. J. Clean. Prod. 18, 1519–1529. https://doi.org/10.1016/j.jclepro.2010.06.004.

Zackrisson, M., Fransson, K., Hildenbrand, J., Lampic, G., O'Dwyer, C., 2016. Life cycle assessment of lithium-air battery cells. J. Clean. Prod. 135, 299–311. https://doi.org/10.1016/j.jclepro.2016.06.104.

Zhu, C., Li, X., Song, L., Xiang, L., 2013. Development of a theoretically based thermal model for lithium ion battery pack. J. Power Sources 223, 155–164. https://doi.org/10.1016/j.jpowsour.2012.09.035.

4.1.3. Paper 3: Life Cycle Assessment of Classic and Innovative Batteries for Solar Home Systems in Europe.

Following the environmental assessment performed in Paper 2, the range of batteries and installation sites of SHSs is extended in Paper 3, published in *Energies*. Indeed, the same kind of analysis is performed in Denmark, Spain, France, Greece, Hungary, Italy, Portugal, and Romania. For all these installation sites, SSLIBs and post-LIBs devices are compared to classic LIBs.

The LCI is based on an Ecoinvent 3.4 and is collected in an associated *Data* paper together with a more extensive description of the results. The main outcomes of the paper are:

- The evaluation of the most sustainable SHSs as function of the installation sites in terms of midpoint indicators and single score environmental impacts.
- The contribution analysis of each part of the product system.
- A comparison with the national electricity mixes.

The Ph.D. is the first author of the paper and mainly contributed to the conceptualization, the development of the methodology, the results evaluation, and the writing of the paper.

energies

MDPI

Article

Life Cycle Assessment of Classic and Innovative Batteries for Solar Home Systems in Europe

Federico Rossi [1,2], Maria Laura Parisi [1,3,4], Sarah Greven [5], Riccardo Basosi [1,3,4] and Adalgisa Sinicropi [1,3,4,*]

[1] R²ES Lab, Department of Biotechnology, Chemistry and Pharmacy, University of Siena, 53100 Siena, Italy; fe.rossi@unifi.it (F.R.); marialaura.parisi@unisi.it (M.L.P.); riccardo.basosi@unisi.it (R.B.)
[2] Department of Industrial Engineering, University of Florence, Via Santa Marta 3, 50139 Florence, Italy
[3] CSGI—Consortium for Colloid and Surface Science, via della Lastruccia 3, Sesto Fiorentino, 50019 Florence, Italy
[4] CNR-ICCOM, National Research Council—Institute for the Chemistry of OrganoMetallic Compounds, Sesto Fiorentino, 50019 Florence, Italy
[5] ENSICAEN, Chimie Materiaux, 6 bd Maréchal Juin—CS 45053, CEDEX 4, F-14050 Caen, France; sarah.graven2@gmail.com
* Correspondence: adalgisa.sinicropi@unisi.it

Received: 8 June 2020; Accepted: 30 June 2020; Published: 3 July 2020

Abstract: This paper presents an environmental sustainability assessment of residential user-scale energy systems, named solar home systems, encompassing their construction, operation, and end of life. The methodology adopted is composed of three steps, namely a design phase, a simulation of the solar home systems' performance and a life cycle assessment. The analysis aims to point out the main advantages, features, and challenges of lithium-ion batteries, considered as a benchmark, compared with other innovative devices. As the environmental sustainability of these systems is affected by the solar radiation intensity during the year, a sensitivity analysis is performed varying the latitude of the installation site in Europe. For each site, both isolated and grid-connected solar home systems have been compared considering also the national electricity mix. A general overview of the results shows that, regardless of the installation site, solid state nickel cobalt manganese and nickel cobalt aluminium lithium-ion batteries are the most suitable choices in terms of sustainability. Remarkably, other novel devices, like sodium-ion batteries, are already competitive with them and have great potential. With these batteries, the solar home systems' eco-profile is generally advantageous compared to the energy mix, especially in on-grid configurations, with some exceptions.

Keywords: energy storage; LCA; batteries; solar energy; photovoltaic; smart grids

1. Introduction

This work addresses the issue concerning the choice of the most suitable in terms of sustainability battery energy storage systems (BESSs) for specific applications, namely the so-called solar home systems (SHSs). These systems belong to a larger category of residential installations that allow energy users to produce and exchange energy with the grid, thus becoming prosumers [1], and share their management to create grid-connected or isolated communities and microgrids [2–4].

SHSs are composed of a PV system, a converter named charge controller (CC), an inverter (In) and a BESS. The choice of the battery is particularly complex because many factors are involved simultaneously and contribute to the environmental and energy performance: manufacturing processes, raw materials consumption, operative parameters, working conditions, and waste management are those that mainly affect the overall performance. Furthermore, the most sustainable

solution is intrinsically dependent on the geographical site, as one installation might not be the best one in a different context, or it could have a different effectiveness. For all these reasons, designing SHSs to be competitive with the national electricity mix can be challenging, especially if innovative technologies are considered. The aim of this work is to approach such an issue from a broader perspective that could support in the definition of the best BESSs for SHSs by evaluating their environmental performances and including a sensitivity analysis of the installation site.

Life cycle assessment (LCA) has a crucial role in the methodological approach presented in this paper because it allows to consider the whole life cycle of the SHS, from cradle to grave. LCA, standardized by the ISO family of rules [5,6], is one of the most recognized methods for environmental impact evaluation. The life cycle perspective of LCA allows to consider the raw material consumption and the emissions to the environment occurring during the whole life cycle of a product, process, or service. LCA has been widely used in the field of renewable energies whose greenhouse gases direct emissions might be null or, at least, be much more limited than for fossil fuels-based power systems. On the other hand, they may have remarkable environmental impacts due to their production and end of life disposal. For instance, the scientific literature provides examples of LCA applied to solar energy-based systems such as collectors [7] or traditional and novel PV systems [8–10].

Currently lithium-ion batteries (LIBs) represent the most mature storage devices on the market [11], but they still have some technical, environmental and economic drawbacks pushing scientific research to find alternative types of BESSs. Many LCA studies are available in the literature, most of them collected and harmonized in the work of Peters and Weil [11]. In this paper, the following batteries are considered: nickel cobalt aluminium (NCA) [12] nickel cobalt manganese (NCM) [13,14]; lithium manganese oxide (LMO) [15], lithium iron phosphate (LFP) [14,16] and lithium iron titanate (LTO) [12]. Recently, new types of LIBs have been designed like lithium manganese nickel oxide (LMNO), molybdenum-disulfide NCM (NCM-MoS_2) and lithium cobalt phosphate (LCP). The eco-profile of such LIBs has been assessed by Cusenza et al. [17], Deng et al. [18] and Raugei and Winfield [19], respectively. Another interesting development in LIBs is the replacement of the liquid electrolyte with a solid one [20], thus moving towards solid state lithium-ion batteries (SSLIBs). Troy et al. [21] and Lastoskie and Dai [22] proposed an interesting environmental assessment of SSLIBs that showed them to be competitive with classic LIBs. Regardless of the electrode materials, LIBs are intrinsically affected by the availability of lithium that is quite limited [19]; moreover cobalt, used in the cathodes of most of LIBs to increase the energy density, is even more rare and expensive than lithium [23]. Indeed, lithium-cobalt oxide (LCO) batteries, whose LCA is performed by Grimsmo et al. [24], are the most widely used devices, but the impact of cobalt extraction in the Congo represents a major contribution to the overall environmental burden. For these reasons, research is focusing on the study of novel cobalt-free batteries working with the same principle of LIBs but replacing lithium-ions with sodium, magnesium or aluminium. The environmental assessment of sodium-ion batteries (SIBs) and aluminium-ion batteries (AIBs) has been performed by Peters et al. [25] and Delgado et al. [26], respectively. According to these studies SIBs already display good performance whereas AIBs are still at a laboratory level and far from industrial scale up. From the same perspective, other solutions to obtain lithium- and cobalt-free BESSs are sodium-nickel chloride batteries, named ZEBRA [27], and vanadium redox flow batteries (VRFBs). Some LCA studies [28,29] have demonstrated that these batteries have a very interesting potential to improve the environmental performance of stationary installations. Scientific and industrial research is focusing on high energy density batteries to make BESSs smaller and lighter: some of them have lithium metal as anodic material, like lithium-sulfur batteries (LiSBs) or lithium-air batteries. Environmental assessments of these devices have already been performed by Deng et al. [30] and Zackrisson et al. [31], who concluded that their potential is remarkable, but the fast degradation due to several ageing mechanisms at the moment hinders their diffusion in the market. The same kind of conclusions have been drawn by LCA studies of sodium sulphur [32], magnesium-sulphur [33] and zinc-air [34] batteries aiming to replace lithium.

The literature analysis shows that the environmental impact of batteries represents a very interesting research topic many authors have addressed. Nevertheless, all the abovementioned

studies are performed at the components level and are focused on the production phase and, only in some cases, on the end of life stage of BESSs. The operation phase is usually neglected or modelled in a simplified way which does not really allow one to determine the effect of the BESS operative parameters on the results. Some detailed environmental analyses of BESSs applications do however exist and were reviewed by Tian et al. [35]. For instance, grid-connected SHSs economic and environmental feasibility, including LCA, have been assessed by Nagapurkar and Smith [36]. On the other hand, Wang et al. [37] analyzed a standalone battery system for an electric grid installed in Hong Kong. Solar systems assisted by batteries are also discussed by Longo et al. [38] who developed a new tool, based on LCA, to estimate the eco-profile of these systems. Kabakian et al. [39] compared a 1.8 kW PV system assisted by a BESS with the Lebanese electricity grid eco-profile underlining the substantive environmental merits of PV. All these studies at the system level are valuable but lack in analyzing how the different batteries can change the eco-profile of the system depending on the installation site.

Thus, it is possible to assert that there is a gap in the scientific literature concerning studies giving insights on how to choose the best battery to improve the environmental performance of SHSs. Ultimately, in the context highlighted by such a scientific study overview, comparative LCA studies about the effects of the components, in particular the batteries, on the overall system performances and eco-profiles are, to the best of our knowledge, not found in the literature. Indeed, this kind of analysis requires one to merge a detailed environmental assessment of batteries at the component level and a careful evaluation of the performances of SHSs depending on the batteries' operative parameters. In order to do this, we proposed a three-steps methodology in our previous papers [40,41] including the design, the operative parameter simulation and the LCA of SHSs equipped with LIBs in Italy. In this work, our approach is employed for its application to a larger number of case studies in several European countries. Moreover, a larger group of batteries is analyzed including LIBs and novel BESSs. Much effort has been done to extend the methodology, initially valid for LIBs, to be applicable to every BESS and thus investigate the differences among them. Remarkably, the improvement of the three-steps methodology [40,41] allowed us to perform the comparison of different batteries and installation sites for SHSs eco-profiles evaluation.

The remainder of this paper is organized as follows: in Section 2, we describe the methodology, in Section 3, we present the analyzed case studies. Finally, we discuss the results and our conclusions in Sections 4 and 5, respectively.

2. Methodology

As described in the Introduction, SHSs are composed of a PV plant, a BESS, an In and a CC. When SHSs are configured as isolated installations, a generator provides backup energy to the user whereas grid-connected SHSs can exchange energy with the electric utility [40]. The methodology used to evaluate the eco-profile of both types of SHSs is composed of three steps:

- The design phase, in which the calculation of the components' capacity is addressed.
- The modelling phase, which provides the dynamic simulation of the SHSs performances.
- The LCA for the SHSs environmental impact calculation.

A summary of BESSs is presented before the description of the abovementioned methodology steps and a flowchart illustrating such an approach is depicted in Figure 1.

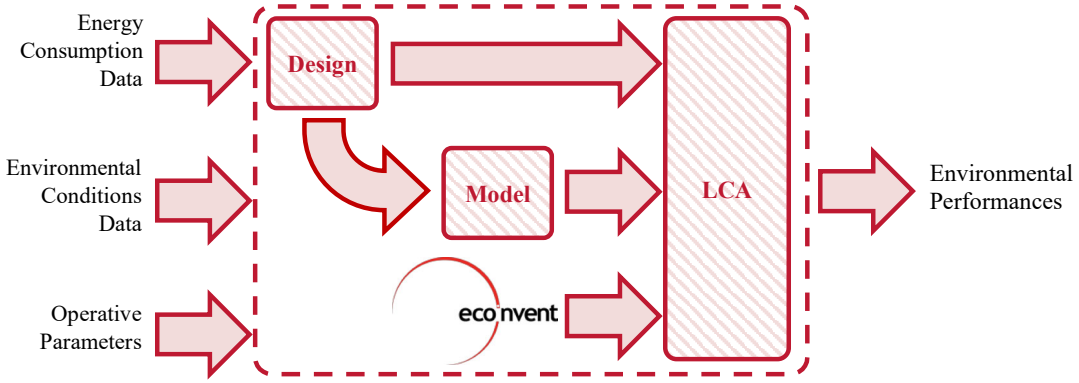

Figure 1. Flowchart of the three-steps methodology implemented in this work.

2.1. Batteries Description

The operative parameters of the examined batteries are summarized in Table 1 which collects their construction materials, the energy density, the lifespan, the depth of discharge (DoD) and the efficiency.

LIBs are electrochemical devices where lithium-ions move from the anode to the cathode during discharge, and back when charging. Traditional LIBs include an organic liquid electrolyte (like ethylene carbonate or ethylene glycol dimethyl ether [42]) where lithium salts are dissolved. SSLIBs represent a development of classic LIBs where the liquid electrolyte is replaced by a solid crystalline one, namely LiPON, allowing one to double the energy density [22]. Thus, the energy density of the SSLIBs has been estimated multiplying with a factor of two the values of the corresponding LIBs. Several types of LIBs are available nowadays, differing in the electrode materials and consequently their energy density, efficiency and lifespan values [40].

Even though LIBs are the most diffused BESSs, several other batteries with different levels of maturity are available on the market. Based on the data availability in the literature, some alternative BESSs (aBESSs) have been selected to perform their environmental assessment in this work.

Peters' devices (SIBs) [25] work similarly to LIBs because sodium-ions are exchanged by the electrodes with the same mechanism of lithium-ions in LIBs; indeed they belong to the same category named metal-ion batteries [43]. Sodium ions move from a sodium nickel manganese magnesium titanium oxide (NMMT) cathode to a hard carbon anode through a liquid electrolyte where sodium hexafluorophosphate ($NaPF_6$) is dissolved [25]. These batteries are studied in the perspective of replacing lithium with sodium, much more abundant on the Earth. Nevertheless, according to a recent scientific report published by Yusoff et al. [43], the effects of the different size of sodium-ions are a lower cyclability, a lower capacity (and consequently energy density) and a lower power rate. Indeed Table 1 shows that SIBs energy density and cyclic lifespan are respectively 102 Wh/kg and 2000 cycles whereas in LIBs they can be significantly higher. In the literature there is lack of information about SIBs' natural lifespan but, as Yusoff et al. [43] do not stress any difference for this parameter, the same value assumed by LIBs has been assumed.

Deng batteries (LiSBs) have metal lithium as anodic material whereas sulphur is present in the cathode mixed with a graphene structure [30]. They can reach a high energy density although the electrolyte is liquid and composed of a solution of lithium bistrifluoromethanesulfonimidate (LiTFSI), dimethyl glycol (DME), dioxolane (DOL) and lithium nitrate ($LiNO_3$). The main drawback of this battery chemistry is the very fast cyclic degradation due to several chemical and physical ageing mechanisms [30,44]. Few data are available about their natural lifespan because research is meanly focused on studying the cyclic degradation that is the dominant effect. Deng et al. [30] estimate that, similarly to LIBs, LiSBs lifespan can reach 10 years that is set as reference value for the natural lifespan.

Table 1. Batteries operative parameters [a].

	LIBs/SSLIBs							aBESS			
	M-B (LFP) [1]	**Zack (LFP) [2]**	**Bauer (LTO) [3]**	**Notter (LMO) [4]**	**Bauer (NCA) [5]**	**Ell (NCM) [6]**	**M-B (NCM) [7]**	**Peters (SIBs) [8]**	**Deng (LiSBs) [9]**	**Eco. (ZEBRA) [10]**	**Weber (VRFBs) [11]**
Cathode	$LiFePO_4$ [b]	$LiFePO_4$	$LiFePO_4$	$LiMn_2O_4$ [c]	$LiNiCoAlO_2$ [d]	$LiNiMnCoO_2$ [e]	$LiNiMnCoO_2$ [e]	NMMT	Graphene-sulfur composite	Nickel chloride	PAN
Anode	Graphite	Graphite	$Li_4Ti_5O_{12}$ [f]	Graphite	Graphite	Graphite	Graphite	Hard carbon	Lithium metal	Sodium chloride	PAN
Electrolyte	$LiPF_6$ [g] LiPON [j] (SS)	LiCl [h] LiPON [j] (SS)	$NaBF_4$ [i] LiPON [j] (SS)	$LiPF_6$ [g] LiPON (SS)	$NaBF_4$ [i] LiPON (SS)	$LiPF_6$ [g] LiPON (SS)	$LiPF_6$ [g] LiPON (SS)	$NaPF_6$	LiTFSI, DOL, DME, $LiNO_3$	Sodium aluminium chloride	Vanadium, sulfuric acid, phosphoric acid, water
Energy Density [Wh/kg]	109.3 218.6 (SS)	82.9 165.8 (SS)	52.4 104.8 (SS)	116.1 232.2 (SS)	133.1 266.2 (SS)	130.3 260.6 (SS)	139.1 278.2 (SS)	102	220	116	28
Lifespan [Cycles]	6000	3000	10,000	1000	5000	2000	3000	2000	400	4500	-
Lifespan [years]	10	10	10	10	10	10	10	10	-	15	20
DoD	80%	80%	80%	80%	80%	80%	80%	80%	85%	80%	95%
Efficiency	90%	90%	90%	85%	90%	95%	90%	90%	85%	90%	75%

(a) Parameters taken from [11,25,26,29,30,45]; (b) lithium-iron phosphate; (c) lithium manganese oxide; (d) lithium nickel cobalt aluminum oxide; (e) lithium nickel cobalt manganese oxide; (f) lithium titanate oxide; (g) lithium hexafluorophosphate; (h) lithium chloride; (i) sodium tetrafluoroborate; (j) lithium phosphorous oxynitride; (1) LFP battery proposed by Majeau-Bettez et al. [14], (2) LFP battery proposed by Zackrisson et al. [16]; (3) LTO battery proposed by Bauer et al. [12]; (4) LMO battery proposed by Notter et al. [15]; (5) NCA battery proposed by Bauer et al. [12]; (6) NCM battery proposed by Ellingsen et al. [13]; (7) NCM battery proposed by Majeau-Bettez et al. [14]; (8) SIB proposed by Peters et al. [25]; (9) LiSB proposed by Deng et al. [30]; (10) ZEBRA battery proposed by Ecoinvent 3.4 [46]; (11) VRFB proposed by Weber et al. [29].

Eco (ZEBRA) [46] batteries contain sodium composites in the electrolyte and in the anode, whereas nickel represents the main cathodic material [38]. Differently from the others, these devices operate at high temperatures, over 270 °C [28], and therefore they require a heating system to be constantly in operation [45]. The cyclic lifespan and the energy density is comparable to some types of LIBs but the natural lifespan is longer [45]. Among the alternative batteries analyzed in this study, ZEBRA batteries present the highest maturity level.

Weber systems (VRFBs) [29] are significantly different from the other devices: they are flow batteries where two vanadium-based liquid electrolytes are stored in two storage tanks which determine the capacity of the battery. The liquids are pumped through a piping system to a stack where they are separated by a proton exchange membrane that, together with polyacrylonitrile (PAN) carbon felt electrodes, allows the development of the reaction; the surface of the membrane determines the power of the battery [29]. Therefore, the strength of VRFBs is the possibility to design separately the storage tanks (devoted to store energy) and the stack (devote to exchange power) according with the needs of the user. Moreover, it is possible to recycle the electrolyte completely and to achieve a very long lifespan. Indeed, the natural lifespan of the electrolyte is 20 years, that of the stack is 10 years whereas the cyclic ageing is negligible [29]. The main drawback of VRFBs is the very low energy density which might be solved finding new types of electrolytes in the future.

2.2. SHS Design

The design equations [40] applied to evaluate the PV power (P_{PV}) and the BESSs nominal capacity (E_{BESS}) for a daily energy storage are defined as follows (1) and (2):

$$P_{PV} = \frac{E_{Load,day}}{\eta_{el} \cdot h_{eq}} \quad (1)$$

$$E_{BESS} = \frac{E_{Load,day}}{\mathrm{DoD}} \quad (2)$$

where $E_{Load,day}$ is the daily energy consumption, η_{el} is the electric efficiency of the SHS set to 72% [40], h_{eq} is the minimum equivalent daily full power operation time (expressed as hours) of the PV system (estimated using the online tool PV-GIS [47]) and DoD is the depth of discharge (80%) [40]. The nominal voltage of the BESS (V) is set to 48 V [40].

The role of the CC is to connect the PV system and the BESS guaranteeing a match among their electrical characteristics; the In has to provide to the user the maximum power required by the load (P_{load}^{max}), evaluated analyzing the users demand profile in time [48]. To this scope, the size of the CC (P_{CC}) and of the In (P_{In}) can be defined (3) and (4). Considering the design of the VRFB, its power is not physically correlated to its capacity, thus the BESS is designed to work with a power rate of 0.5 h^{-1}, typical of stationary applications [49] (5):

$$P_{CC} = P_{PV} \quad (3)$$

$$P_{In} = P_{load}^{max} \quad (4)$$

$$P_{VRFB} = 0.5\ E_{BESS} \quad (5)$$

2.3. SHS Modelling

After the SHS is designed, its performances are estimated by a dynamic simulation model. A discretization of the time variable (t) is necessary to perform the simulation, and a time step Δt = 1 h is defined. The outputs of the simulation are the amounts of missing (E_{miss}) and exceeding (E_{exc}) energy during the BESS lifespan (L_{BESS}). The SHS model is composed of three parts:

- The PV productivity profiles ($P_{PV,t}$), calculated with PV-GIS [47].
- The power demand profiles ($P_{load,t}$), provided by Quoilin et al. [48].

- The BESS model that uses $P_{PV,t}$ and $P_{load,t}$ as inputs to evaluate the missing (P_{miss}) and exceeding (P_{exc}) power of the SHSs. E_{miss} and E_{exc} are calculated integrating P_{miss} and P_{exc} in time and an ageing model allows to estimate L_{BESS}.

In our previous work [40] the BESS operation has been modelled using a Matlab/Simulink block only valid for LIBs [50]. Therefore, this model is not adequate to describe all the batteries considered in this study and, thus, a flexible BESS model has been implemented here using the parameters collected in Table 1.

The power flowing through the BESS during the charge ($P^c_{BESS,t}$) and discharge ($P^d_{BESS,t}$) phases is assessed by the following balances (6) and (7):

$$P^c_{BESS,t} = (\eta_{el}\, P_{PV,t} - P_{load,t}) \cdot \eta_{BESS,c} \quad (6)$$

$$P^d_{BESS,t} = \frac{(\eta_{el}\, P_{PV,t} - P_{load,t})}{\eta_{BESS,d}} \quad (7)$$

where $\eta_{BESS,c}$ and $\eta_{BESS,d}$ are the BESS charge and discharge efficiency values, both equal to the squared root of the overall Coulombic efficiency (Table 1). The actual power flowing through the BESS ($P_{BESS,t}$) is equal to $P^c_{BESS,t}$ during the charge phase ($P^c_{BESS,t} > 0$) and to $P^d_{BESS,t}$ during the discharge phase ($P^d_{BESS,t} < 0$). Additionally, some constraints are necessary:

- if the battery capacity is totally full (SOC_{t-1} = 1), the BESS cannot be furtherly charged and the exceeding power is exported to the grid or, in off-grid SHSs, it is dumped.
- if the battery capacity has reached the minimum level (SOC_{t-1}= 1 − DoD), the BESS cannot be furtherly discharged and, in that case, the backup source intervenes.

The power rate (r_t), representing the charge and discharge velocity [51], is defined as (8):

$$r_t = \frac{P_{BESS,t}}{E_{BESS}} \quad (8)$$

Every type of BESS has a maximum power rate allowed, but it will be demonstrated that it doesn't represent a limiting factor as usual in stationary applications [21,40,49]. At this point, the current BESS state of charge (SOC_t) can be calculated using (9):

$$SOC_t = SOC_{t-1} + \frac{P_{BESS,t} \cdot \Delta t}{E_{BESS} \cdot SOH_t} \quad (9)$$

where the BESS state of health (SOH_t) is assessed using an ageing model. Cardoso et al. [49] proposed a capacity fade model for the assessment of a generic battery using (10), evaluating the BESS capacity loss (Q_t) as the sum of the cyclic ageing and the natural degradation.

$$Q_t = \frac{E^{ref}_{BESS}}{E_{BESS}}(\alpha\, T^2 + \beta\, T + \gamma) e^{(\delta T + \varepsilon) r_t} \sum_t \frac{P^d_{BESS,t}}{V^{ref}_{BESS}} + \theta e^{-\frac{E_a}{RT}} \sqrt{t} \quad (10)$$

where:

- r_t is the solution of (8).
- E^{ref}_{BESS} is the capacity of a reference battery (712.9 Wh).
- V^{ref}_{BESS} is the voltage of the reference battery (5 V).
- E_a is the activation energy of the reaction of the reference battery (24,500 J · mol^{-1}).
- T is the cell temperature that, in SHSs application, can be set to a constant value (298 K for all the batteries [49] except for ZEBRA whose temperature is 543 K [46]).
- R is the constant of gases.
- $\alpha, \beta, \gamma, \delta, \varepsilon, \theta$ are the ageing coefficients, calibrated to match with the values in Table 1 in nominal conditions (T = 298 K and r_t = 1 h^{-1}).

The ageing parameters, calibrated grounding on the data provided by Cardoso et al. [49], are collected in Table 2.

Table 2. Ageing parameters of BESSs.

BESS	α	β	γ	δ	ε	θ
	[$Ah^{-1} \cdot K^{-2}$]	[$Ah^{-1} \cdot K^{-1}$]	[Ah^{-1}]	[$h\ K^{-1}$]	[h]	[$s^{-0.5}$]
Bauer (LTO, SSLTO)	2.95×10^{-7}	-1.76×10^{-4}	2.61×10^{-2}	-6.70×10^{-3}	2.35×10^{0}	1.93×10^{1}
Bauer (NCA, SSNCA)	5.91×10^{-7}	-3.51×10^{-4}	5.23×10^{-2}	-6.70×10^{-3}	2.35×10^{0}	1.93×10^{1}
Ell (NCM, SSNCM)	1.48×10^{-6}	-8.78×10^{-4}	1.31×10^{-1}	-6.70×10^{-3}	2.35×10^{0}	1.93×10^{1}
M-B (LFP, SSLFP)	4.92×10^{-7}	-2.93×10^{-4}	4.35×10^{-2}	-6.70×10^{-3}	2.35×10^{0}	1.93×10^{1}
M-B (NCM, SSNCM)	9.84×10^{-7}	-5.85×10^{-4}	8.71×10^{-2}	-6.70×10^{-3}	2.35×10^{0}	1.93×10^{1}
Notter (LMO, SSLMO)	2.95×10^{-6}	-1.76×10^{-3}	2.61×10^{-1}	-6.70×10^{-3}	2.35×10^{0}	1.93×10^{1}
Zack (LFP, SSLFP)	9.84×10^{-7}	-5.85×10^{-4}	8.71×10^{-2}	-6.70×10^{-3}	2.35×10^{0}	1.93×10^{1}
Peters (SIB)	7.38×10^{-6}	-4.39×10^{-3}	6.53×10^{-1}	-6.70×10^{-3}	2.35×10^{0}	1.93×10^{1}
Deng (LiSB)	3.04×10^{-7}	-1.81×10^{-4}	5.81×10^{-2}	-3.11×10^{-3}	2.35×10^{0}	1.57×10^{1}
Eco. (ZEBRA)	1.48×10^{-6}	-8.78×10^{-4}	1.31×10^{-1}	-6.70×10^{-3}	2.35×10^{0}	1.93×10^{1}
Weber (VRFB)	0.00×10^{0}	0.00×10^{0}	0.00×10^{0}	0.00×10^{0}	0.00×10^{0}	1.36×10^{1}

Concluding, SOH_t is calculated using Equation (11):

$$SOH_t = 1 - \frac{Q_t}{100} \tag{11}$$

All these equations are implemented in Matlab/Simulink [52] and when the SOH_t is equal to 0.8, the simulation is stopped and L_{BESS} is calculated.

A further consideration must be done for VRFBs. Like every flow battery, the VRFBs electrolyte is pumped inside the cell consuming energy that is provided by the backup source. The power absorbed by the pump ($P_{p,t}$), is calculated by (12) to overcome the pressure losses in the system ($\Delta p_{tot,t}$) [53]:

$$P_{p,t} = \frac{q_t \cdot \Delta p_{tot,t}}{\eta_p} \tag{12}$$

where η_p is the efficiency of the pump (90%), $\Delta p_{tot,t}$ can be calculated using well known fluid-dynamics equations and the electrolyte flow rate (q_t) is calculated using Equation (13) [53].

$$q_t = f \frac{P_{BESS,t}}{V\ n\ F\ c} \tag{13}$$

where the oversizing factor f is set to 7.5, n is the number of electrons involved in the reaction (1 electron), F is the Faraday constant and c is the vanadium concentration (1.6 mg/L) [53].

2.4. LCA

The last phase of the three-steps methodology is the implementation of the LCA. According to the ISO standards [5,6] four steps are necessary to perform correctly this analysis:

- Goal and scope definition: the objectives of the study are defined, thus the reference flow (RF) and the functional unit (FU) of the product system are set accordingly. Moreover, the system boundaries are drawn to choose which processes are included in the analysis and which ones are left outside.
- Life cycle inventory (LCI): all the input and output flows of matter and energy involved in the system boundaries are collected and quantified.
- Life cycle impact assessment (LCIA): in this step all the flows collected in the LCI are classified and multiplied for characterization factors to calculate the environmental impact indicators value.
- Interpretation: the results obtained should be carefully evaluated to point out possible improvements of the product system in accordance with the scope and goal of the assessment and, eventually, to modify and implement the LCA system model.

2.4.1. Goal and Scope Definition

The goal of the study is estimating and comparing the environmental performances of several SHSs equipped with different types of BESSs to identify the most sustainable one. In this perspective, the effects of the installation site variation on the results are assessed through a sensitivity analysis. The comparison with the national electricity mixes allows us to estimate the SHSs environmental effectiveness in every country. The function of SHSs is producing useful electricity, therefore in off-grid systems the RF is equal to the user energy demand whereas in on-grid configurations it is the sum of the load and the electricity dispatched to the grid. In both cases the FU is 1 MWh. A cradle to grave approach encompassing the construction (CO), operation (OP) and end of life (EoL) of SHSs is implemented. The impact of the components' transportations to the installation sites have not been included to focus the attention only on the SHS site-specific performances.

2.4.2. Life Cycle Inventory (LCI)

The LCI has been built using the Ecoinvent database v3.4 [46]. First of all, all the inventories have been modelled at a component level. Reproducible data for the CO of all the batteries are available in the scientific literature [11,25,29,30,44] except for SSLIBs. Therefore, it is necessary to convert LIBs to SSLIBs replacing the same amount of liquid electrolyte with LiPON, whose LCI is reported in Table 3.

Table 3. LCI for the LiPON electrolyte production.

Figure	Process	Amount	Unit
	Inputs		
Heat	market for heat, district or industrial, natural gas—Europe without Switzerland	0.23	kWh
Hydrogen peroxide	market for hydrogen peroxide, without water, in 50% solution—GLO	2.28	kg
Lithium hydroxide	market for lithium hydroxide–GLO	1.60	kg
	Outputs		
Lithium oxide	Lithium oxide production	1.00	kg
	Inputs		
Ammonia	market for ammonia, liquid—RoW	0.52	kg
Phosphorus pentachloride	market for phosphorus pentachloride—GLO	3.84	kg
	Outputs		
Triphosphorous pentanitride	triphosphorous pentanitride production	1.00	kg
	Inputs		
Lithium oxide	Lithium oxide production	0.67	kg
Phosphorous pentoxide	market for phosphoric acid, industrial grade, without water, in 85% solution APOS, S—GLO	0.13	kg
Triphosphorous pentanitride	triphosphorous pentanitride production	0.20	kg
Heat	market for heat, district or industrial, natural gas—Europe without CH	2.96	kWh
	Outputs		
LiPON	LiPON production	1	kg

According to Senevirathne et al. [20], LiPON precursors are lithium oxide, phosphorous pentoxide and triphosphorous pentanitride with a mass ratio 1 : 0.2 : 0.3.

- Lithium oxide is prepared by thermal decomposition of lithium peroxide that, on its turn, is produced with the reaction of hydrogen peroxide and lithium hydroxide [54] consuming 25.8 kJ/mol [54].
- Phosphorous pentoxide inventory has been approximated to phosphoric acid having a similar structure.

- Triphosphorous pentanitride is prepared from ammonia and phosphorus pentachloride [54].

Furthermore, LiPON powder is heated for 10 h with a temperature rate of 5 °C/min [20]; the energy consumption for the production of 1 kg of LiPON is estimated considering lithium powder specific heat as a proxy (0.85 cal/g/K) [55].

The inventories of SIBs, VRFBs and LiSBs have been faithfully reproduced using detailed LCIs available in the literature [25,29,30] whereas a complete LCI for ZEBRA batteries is available in Ecoinvent v 3.4 (market for battery, NaCl—GLO) [46].

Deng et al. [30] and Weber et al. [29] describe the EoL inventory for LiSBs and VRFBs as well as the CO. Contrarily, LIBs waste treatment is not considered by Peters and Weil [11], but Huang et al. [56] clearly describes that each part of these BESSs can be recycled with an efficiency of about 90%. During the EoL, the battery pack is disassembled and then, after a thermal treatment for the evaporation of the liquid electrolyte, the main CO materials can be recovered: a pyrometallurgical process is necessary if cobalt is present in the battery, otherwise a hydrometallurgical process is preferred. On the other hand, plastic materials and LiPON are supposed to be incinerated. Therefore, after the evaluation of the mass contribution of each part of the battery pack, the inventory for LIBs and SSLIBs waste treatment has been modeled (Table 4) including the recovered materials. The same approach has been used also for Peters (SIB) EoL.

Table 4. LIBs, SSLIBs and Peters (SIB) inventory for EoL.

	Bauer (LTO)	**Bauer (NCA)**	**Ell (NCM)**	**M-B (LFP)**	**M-B (NCM)**	**Notter (LMO)**	**Zack (LFP)**	**Peters (SIBs)**	
Inputs									
Waste BESS	1								kg
Treatment of used Li-ion battery, hydrometallurgical GLO	0.49	0.00	0.00	0.5	0.00	0.61	0.53	0.47	kg
Treatment of used Li-ion battery, pyrometallurgical GLO	0.00	0.52	0.6	0.00	0.5	0.00	0.00	0.00	kg
Market for hazardous waste, for incineration Europe without CH	0.44	0.4	0.35	0.41	0.41	0.39	0.39	0.14	kg
Market for waste electric and electronic equipment GLO	0.05	0.05	0.05	0.05	0.05	0.05	0.05	0.06	kg
Market for scrap steel—Europe without CH	0.02	0.02	0.02	0.02	0.02	0.02	0.02	0.35	kg
Market for inert waste, for final disposal RoW	0.23	0.14	0.14	0.26	0.15	0.16	0.30	0.14	kg
Market for diesel, burned in building machine GLO	0.1								MJ
Market for electricity, medium voltage Europe without CH	0.01								kWh
Outputs (Avoided Products)									
Market for lithium hexafluorophosphate GLO	19 (l) 0 (s)	15 (l) 0 (s)	13 (s) 0 (s)	16 (l) 0 (s)	16 (l) 0 (s)	15 (l) 0 (s)	16 (l) 0 (s)	0	mg

Table 4. *Cont.*

Sodium hexafluorophosphate production	0	0	0	0	0	0	0	12	mg
Market for lithium GLO	10	8	9	12	8	6	15	20	mg
Market for sodium GLO	0	0	0	0	0	0	0	3	mg
Market for cobalt GLO	0	67	75	0	70	0	0	0	mg
Market for copper GLO	9	125	179	116	116	185	49	0	mg
Market for aluminium scrap, new RER	107	94	46	55	55	115	25	54	mg
Market for nickel, 99.5% GLO	0	67	75	0	70	0	0	8	mg
Market for manganese GLO	0	0	70	0	65	101	0	76	mg
Market for steel, unalloyed GLO	0	0	0	0	0	0	0	308	mg
Market for iron ore, beneficiated, 65% Fe GLO	79	0	0	95	0	0	119	0	mg
Market for titanium, primary GLO	167	0	0	0	0	0	0	7	mg
Market for graphite GLO	0	148	121	94	111	162	134	210	mg

Moving to the system level, a complete LCI of the SHS valid for all the installation sites is collected in Table 5. The PV system and the wires are supposed to be recycled (with efficiency 90%), whereas the plastic materials are incinerated; the EoL of converters and electronics (like the In and CC) are modeled using a specific Ecoinvent [46] process.

Table 5. LCI of the SHS.

Process	Amount	Unit	Description
	Inputs		
Market for photovoltaic slanted-roof installation, 3 kWp, single-Si, panel, mounted, on roof—GLO (inverter considered separately)	$\frac{P_{PV}}{3}\frac{L_{SHS}}{L_{PV}}$	items	CO of the PV system, mounting system; the In has been excluded.
Market for cable, unspecified cable, unspecified —GLO	$0.1\ \frac{P_{PV}}{0.17}\ \frac{L_{SHS}}{L_w}$	kg	CO of cables for a 0.17 kW/m² PV system [57].
Market for tube insulation, elastomere—GLO	$0.06\ \frac{P_{PV}}{0.17}\ \frac{L_{SHS}}{L_w}$	kg	CO of plastic wires coating for a 0.17 kW/m² PV system [57].
Market for inverter, 2.5kW—GLO	$\frac{P_{In}}{2.5}\frac{L_{SHS}}{L_{In}}$	items	-
Market for charger, electric passenger car—GLO	$1.53\ P_{CC}\frac{L_{SHS}}{L_{CC}}$	kg	CO of a DC/DC converter weighting 1.53 kg/kW [58].
BESS	$E_{BESS}\frac{L_{SHS}}{L_{BESS}}$	kWh	CO of the BESS [25,29,30,42,44].
VRFB stack	$10.02\ P_{VRFB}\ \frac{L_{PV}}{L_s}$	kg	In case of VRFB [29].
VRFB periphery	$5.13\ P_{VRFB}\ \frac{L_{SHS}}{L_p}$	kg	In case of VRFB [29].
Market for electricity, low voltage	$E_{miss}\frac{L_{SHS}}{L_{BESS}}$	MWh	In case of grid-connected SHSs.
Market for diesel, burned in diesel-electric generating set, 18.5kW—GLO	$E_{miss}\frac{L_{SHS}}{L_{BESS}}$	MWh	In case of off-grid SHSs.

Table 5. *Cont.*

Market for waste electric wiring—GLO	$-0.1\ \frac{P_{PV}}{0.17}\ \frac{L_{SHS}}{L_w}\cdot 10\%$	kg	EoL of cables for a 0.17 kW/m² PV system supposing 90% recycling efficiency [57].
Market for used cable—GLO	$-0.1\ \frac{P_{PV}}{0.17}\ \frac{L_{SHS}}{L_w}\cdot 90\%$	kg	EoL of cables for a 0.17 kW/m² PV system supposing 90% recycling efficiency [57].
Market for waste wire plastic—GLO	$-0.06\ \frac{P_{PV}}{0.17}\ \frac{L_{SHS}}{L_w}$	kg	EoL of plastic wires coating for a 0.17 kW/m² PV system [57].
Market for waste electric and electronic equipment—GLO	$-1.53\ P_{CC}\ \frac{L_{SHS}}{L_{cc}}$	kg	EoL of a DC/DC converter weighting 1.53 kg/kW [40,58].
Market for waste electric and electronic equipment—GLO	$-4.37\ P_{In}\ \frac{L_{SHS}}{L_{In}}$	kg	CO of a DC/AC converter weighting 4.37 kg/kW [40,59].
Market for auxiliary heating unit, electric, 5kW—GLO	$0.001\ E_{ZEBRA}\ \frac{L_{SHS}}{L_h}$	items	Number of electric heaters considering an energy supply of 6.67W per kWh of capacity [46]
	Outputs		
Electricity (RF)	$(E_{load} + E_{exc})\ \frac{L_{SHS}}{L_{BESS}}$	MWh	In case of grid-connected SHS.
	$E_{load}\ \frac{L_{SHS}}{L_{BESS}}$	MWh	In case of off-grid SHS.
Exhausted BESS, waste treatment	$E_{BESS}\ \frac{L_{SHS}}{L_{BESS}}$	kWh	CO of a DC/AC converter weighting 4.37 kg/kW [40,59].
Exhausted PV, waste treatment	$4.29\ P_{PV}\ \frac{L_{SHS}}{L_{PV}}$	kg	EoL of PV modules weighting 4.29 kg/kW [40,60,61].
Market for cable, unspecified—GLO	$0.1\ \frac{P_{PV}}{0.17}\ \frac{L_{SHS}}{L_{SHS}}\cdot 90\%$	kg	Avoided product, from cables recycling.

A complete LCI is provided as Supplementary Materials. The lifespan of the SHS (L_{SHS}) is set to 25 years and responds to that of the most long-living component (the PV plant) of the system. All the components lifespan values are collected in Table 6.

Table 6. Expected lifespan of the components.

Component		Lifespan	Unit	
PV	L_{PV}	25	yr	[62]
BESS	L_{BESS}	-	yr	[62]
In	L_{In}	10	yr	[62]
CC	L_{CC}	11	yr	[62]
Wiring	L_w	10	yr	[62]
VRFB stack	L_s	10	yr	[29]
VRFB periphery	L_p	10	yr	[29]
ZEBRA battery heater	L_h	10	yr	[45]

2.4.3. Life Cycle Impact Assessment (LCIA)

In this work the ReCiPe Endpoint (H) 2016 method, considering 17 impact categories with weighting set Europe H/A person/year specifically calibrated for the European context, is employed. LCIA results have been characterized both at the midpoint and endpoint level. The further aggregation of the endpoint results in single scores, measured as eco-points per MWh (Pts/MWh) allows an effective overview of the global environmental performances of the SHSs and a more concise discussion. For instance, fossil fuels based power systems may be concerned mostly about global warming potential and fossil resources depletion whereas PV or BESSs metals depletion may be more reasonable [62].

3. Case Studies

In this section, the above described three-steps methodology will be applied to some case studies. Different from our previous work [40], where a SHS was presumed to be installed in Siena (central Italy), this work is focused on the assessment of the SHSs eco-profile working at different installation sites [62]. This allows to evaluate how the SHS environmental performances respond to different operative conditions and to estimate its effectiveness with respect to the national electricity mixes. Eight different European countries, already considered by Quoilin et al. [48] for a statistic analysis of SHS energy consumption, have been selected for the analysis. To assess the environmental conditions of the installation sites, each country is represented by the respective capital city. The installation sites are the following: Denmark (DK)—Copenhagen, Spain (ES)—Madrid, France (FR)—Paris, Greece (GR)—Athens, Hungary (HU)—Budapest, Italy (IT)—Rome, Portugal (PT)—Lisbon and Romania (RO)—Bucharest.

According to the procedure described in Section 2, the design parameters need to be defined. DoD and η_{el} have already been specified in Section 2 and they don't depend on the installation site; contrarily, $E_{Load,day}$ and h_{eq} are different and their values are collected in Table 7. Their estimate is based on the daily average energy consumption of a family composed of three people [63] and PV-GIS [47].

Table 7. Input data for the design of the SHSs in several countries.

Parameter	DK	ES	FR	GR	HU	IT	PT	RO
$E_{Load,day}$	5.4	4.5	7.2	5.6	3.3	3.2	3.8	1.8
h_{eq}	0.7	3.3	1.2	2.9	1.0	2.8	3.3	1.6

Concerning the modelling phase, the productivity profile of the PV plant, whose configuration is defined in the design phase, has been assessed using PV-GIS [47]. Furthermore, among the power demand profiles proposed by Quoilin et al. [48], the one whose integral is the closest to average energy consumption value over one year [63] has been chosen and scaled proportionally to match exactly with that value. At the beginning of the simulation, the BESS is supposed to be totally charged and to be installed in a controlled environment having a temperature of 25 °C.

4. Results and Discussion

4.1. Design Phase Results

The outputs of the design phase are the SHSs components capacity values, namely P_{PV}, P_{In}, P_{CC} and E_{BESS}, that are collected in Table 8 for every installation site.

Table 8. Results of the design phase.

	P_{PV} [kW]	P_{In} [kW]	P_{CC} [kW]	E_{BESS} [kWh]		
				LIBs, SSLIBs, SIBs, ZEBRA	LiSBs	VRFBs
DK	32.03	4.53	32.03	18.53	17.44	17.61
ES	4.33	2.55	4.33	15.41	14.51	12.98
FR	16.86	17.44	16.86	24.54	23.10	20.67
GR	6.52	5.64	6.52	19.05	17.93	16.04
HU	8.22	2.21	8.22	11.45	10.77	9.64
IT	3.82	3.56	3.82	10.89	10.25	9.17
PT	4.27	4.43	4.27	13.00	12.24	10.95
RO	4.01	1.55	4.01	6.27	5.90	5.28

Analyzing the results in Table 8, it is possible to observe that large PV systems are required in DK and FR, as results of the combination of low solar radiation and high energy consumption (Table 7). Contrarily, smaller installations are required where the solar irradiance is elevated (IT, ES, PT) or the energy consumption is low (RO). As a consequence of the high peak power, in FR and DK the use

of a large size In is required. Concerning the BESS, the size depends on the battery type and particularly on the DoD (Table 1): a big difference among the installation sites exists in relation to the different energy demand.

4.2. Modelling Phase Results

In this subsection the results of the modelling phase are described and discussed: the SHSs designed in the first step of the analysis are modelled and their performances are simulated in order to calculate L_{BESS}, E_{miss} and E_{exc}. These results have been evaluated for each battery type and every installation site. Table 9 summarizes the results collecting the maximum and minimum values assumed by the model outputs. The lifespan of the VRFB is not present in Table 9 because, according to the assumptions used to model the ageing, it is equal to 20 years in any case. A full summary of the modelling phase results is provided as Supplementary Materials.

Table 9. Results of the modelling phase, minimum and maximum values, excluding the lifespan of VRFB.

	L_{BESS} [yr]				E_{miss} [MWh]				E_{exc} [MWh]			
	Min		**Max**		**Min**		**Max**		**Min**		**Max**	
DK	1.63	Deng (LiSB)	8.31	Eco. (ZEBRA)	11.31	Ell (NCM)	13.93	Weber (VRFB)	337.73	Deng (LiSBs)	361.76	Peters (SIB)
ES	1.89	Deng (LiSB)	8.95	Eco. (ZEBRA)	7.30	Ell (NCM)	13.02	Deng (LiSBs)	6.21	Weber (VRFB)	19.28	Deng (LiSBs)
FR	1.59	Deng (LiSB)	8.13	Eco. (ZEBRA)	8.30	Ell (NCM)	11.67	Notter (LMO)	66.55	Notter (LMO)	103.48	M-B (NCM)
GR	1.86	Deng (LiSB)	8.86	Eco. (ZEBRA)	10.16	Ell (NCM)	13.54	Weber (VRFB)	26.74	Weber (VRFB)	36.24	Ell (NCM)
HU	1.72	Deng (LiSB)	8.52	Eco. (ZEBRA)	3.64	Ell (NCM)	4.90	Weber (VRFB)	62.16	Weber (VRFB)	75.35	Ell (NCM)
IT	1.97	Deng (LiSB)	9.06	Eco. (ZEBRA)	5.75	Ell (NCM)	8.31	Weber (VRFB)	9.60	Weber (VRFB)	13.64	Ell (NCM)
PT	1.71	Deng (LiSB)	8.52	Eco. (ZEBRA)	4.45	Ell (NCM)	6.31	Weber (VRFB)	11.23	Weber (VRFB)	16.57	Ell (NCM)
RO	1.86	Deng (LiSB)	8.88	Eco. (ZEBRA)	2.93	Ell (NCM)	3.67	Weber (VRFB)	29.86	Weber (VRFB)	34.14	Ell (NCM)

As expected, Deng batteries (LiSBs) have the shortest lifespan among the considered BESSs because of the low number of cycles that can be performed; contrarily, ZEBRA batteries result to have the longest lifespan thanks to their long calendar life. For these reasons, the most and the less long-living batteries are the same regardless of the installation site. Nevertheless, their lifetime values can be slightly different; indeed, the different operative power rates, determined by the combination of the PV productivity and load profiles, can stress the BESS differently in each country.

Focusing on the energy flows evaluation, generally the use of Weber devices (VRFB) requires more backup energy than the others and have the lowest amount of surplus energy. This is due to the low efficiency of this BESS (Table 1) and to the power demand of the pumps. Contrarily Ell batteries (NCM), thanks to their high efficiency, require less backup energy than the others, whereas the surplus energy is the most elevated. Nevertheless, there are some exceptions; indeed, certain combinations of power production, demand, and state of health of the battery can change the ranking (like in DK, ES and FR).

Comparing the installation sites, remarkable variations in terms of imported and exported energy exist as effect of the different sizes of the SHSs components and of the seasonal distribution of the solar radiation. Indeed, in southern installation sites, the solar radiation is more constant than in northern Europe, where variability is higher. Therefore, in FR and DK there is a remarkable difference between the summer and the winter in terms of PV productivity and, as the systems are designed for winter conditions, the missing and surplus energy are in respect to an optimum balance, higher than in the other sites.

Another piece of information provided by the simulation model is the operative BESS power rate that, as assumed preliminarily, is not a limiting factor as the maximum values are about 0.35 h^{-1}. Indeed, all the BESSs can reach maximum rates of at least 0.7 h^{-1} [64] whereas VRFBs are designed to reach 0.5 h^{-1}.

4.3. LCA Results

In this section the results of the environmental assessment are illustrated: first the results will be depicted using midpoint indicators and then as single score impact values summarizing all the 17 impact categories proposed by ReCiPe for every SHSs and every installation site.

To provide a synthetic description of SHSs midpoint environmental performances, their eco-profiles will be focusing on a single installation site and three midpoint indicators. Similarly to our previous paper [40], Italy has been selected as reference location for SHSs whereas those indicators representing the highest contributions to the total environmental impact have been chosen: climate change, human toxicity and fossil fuel depletion.

The climate change indicator represents the amount of greenhouse gases emitted during SHSs' life cycles expressed as carbon dioxide equivalents ($kgCO_2eq/MWh$) and is illustrated in Figure 2.

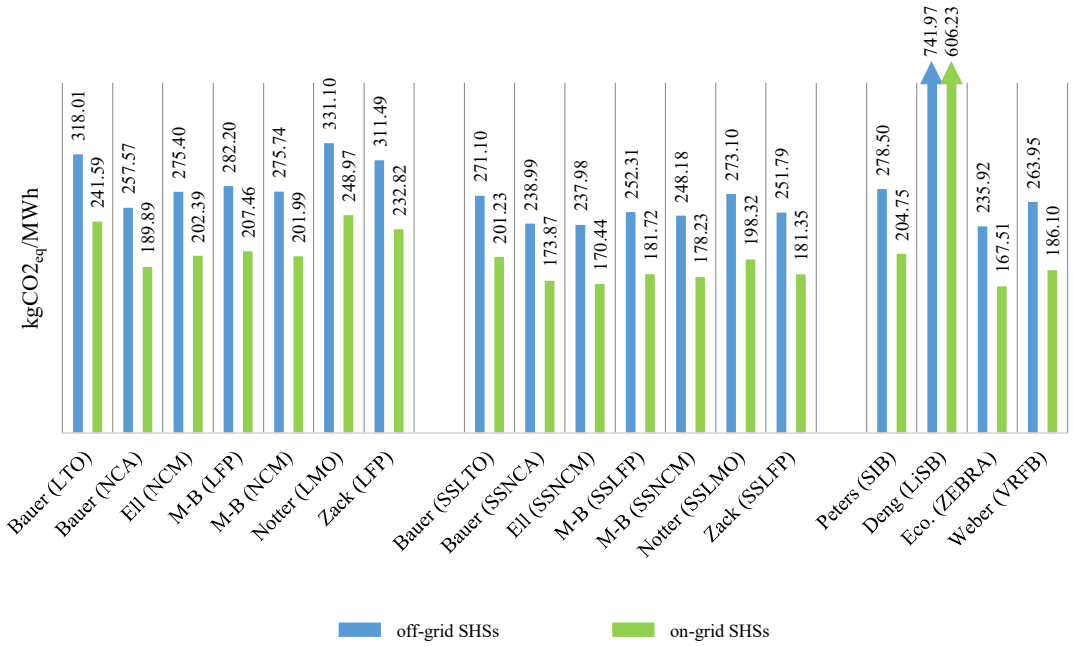

Figure 2. LCA impact values of SHSs in Italy for the climate change indicator.

The results underline that installing Ell (SSNCM) batteries allows one to minimize the climate changes burden: in on-grid systems, 61% of this burden is due to the energy embedded in the PV panels production, whereas the BESS accounts for 15% of the total. The impact of off-grid systems is clearly higher than grid-connected ones because of the contribution of the backup energy that increases from 15% to 30% whether the grid is replaced by a diesel generator. Contrarily Deng batteries (LiSBs) are by far the most impactful BESS because of their very short lifespan, indeed in both configurations it represents more than 70% of the total contribution.

Concerning the human toxicity, measured as equivalent 1,4-dichlorobenzene (kg 1,4-DB/MWh), similar considerations can be made: Figure 3 shows that M-B (SSNCM) are the most sustainable choice for this category. Like in the discussion of climate change indicator, the PV system is the main factor responsible for this burden accounting for about 50% of the total in both SHS configurations. Recycling copper and other metals is fundamental to lower the BESS from 30% to 10% of the total human toxicity impact. Also concerning this indicator, Deng batteries (LiSBs) have the worst eco-profile and their contribution to the SHS impact is higher than 60%.

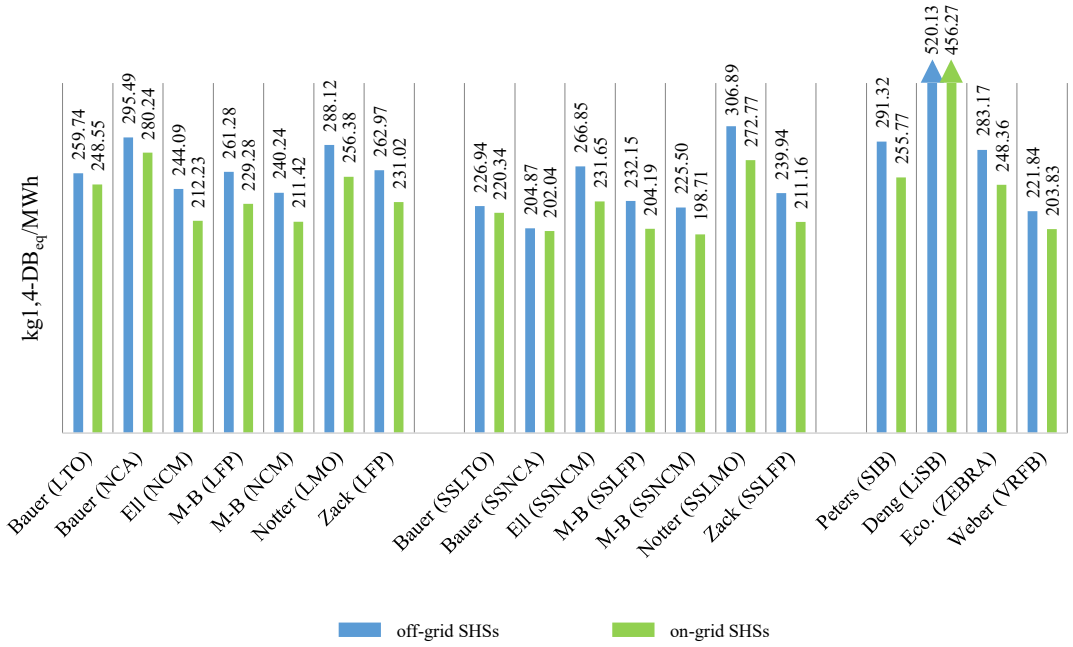

Figure 3. LCA impact values of SHSs in Italy for Human Toxicity indicator.

The last considered midpoint indicator is the fossil-fuel depletion: it is important to stress that SHSs' impact on fossil resources is more than on the metal because of the positive effects of BESS recycling. This impact category is evaluated as the equivalent amount of oil consumed over the product system life cycle (kgOileq/MWh) and the results are illustrated in Figure 4.

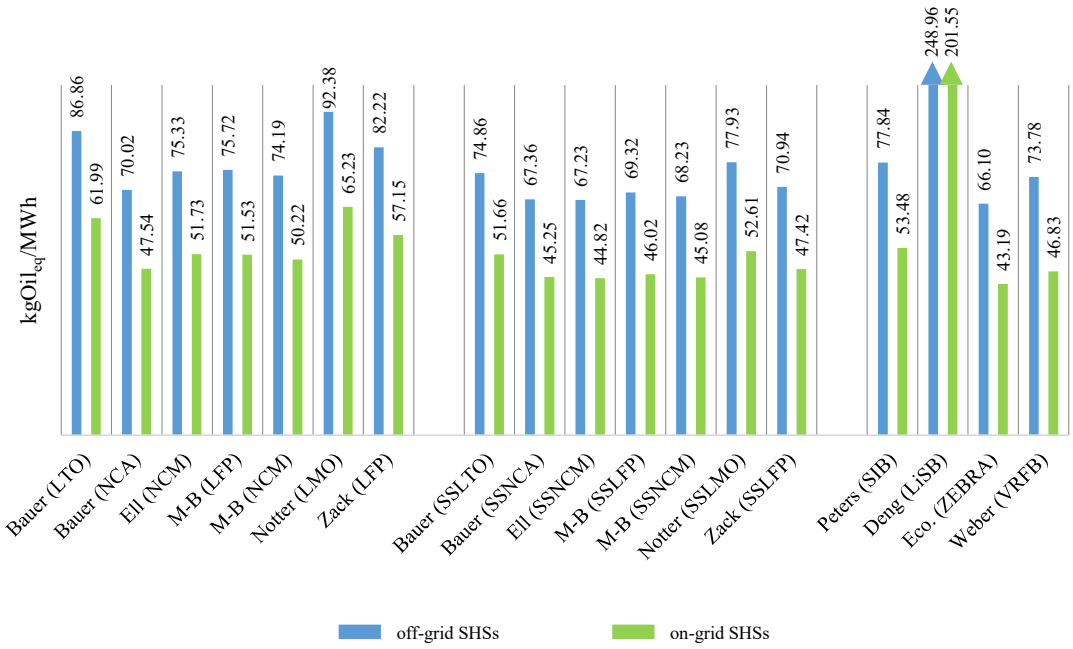

Figure 4. LCA impact values of SHSs in Italy for the fossil depletion indicator.

The most sustainable battery type is, in this case, Eco. (ZEBRA): its percentage contribution is 8% in off-grid systems and 10% in on-grid ones. In both configurations the PV system production represents the main feature responsible for this indicator as the percentage burden is 47% in off-grid and 60% in on-grid SHSs. The remarkable impact difference between these arrangements is due to

the backup energy, representing 37% of the total impact whether provided by diesel and 18% in case on off-grid systems. The same considerations concerning Deng devices' (LiSBs) effects on climate changes and human toxicity are valid for fossil-fuel depletion as good and the BESS percentage burden is over 70% of the SHS one. The above midpoint indicators evaluated for all the other installation sites are provided as Supplementary Materials.

Differently from midpoint indicators, single score results allow a global comparison of all the SHSs. Table 10 collects the most sustainable SHSs for each battery group (LIBs, SSLIBs and aBESSs), Table 11 shows the contribution analysis of the components and Figures 5–12 provide further details about all the SHSs. Indeed, the environmental impact of all the batteries has been depicted together with the corresponding national electricity mix for an easy and immediate comparison. Both on-grid and off-grid configurations are reported. The red columns represent the environmental impacts of the national electricity mixes.

Table 10. LCIA results of the most sustainable batteries by categories and by installation sites.

	Best SHS, with LIBs [Pts/MWh]			**Best SHS, with SSLIBs [Pts/MWh]**			**Best SHS, with aBESS [Pts/MWh]**			**Mix**
	On-Grid	**Off-Grid**	**On-Grid**	**On-Grid**	**Off-Grid**	**BESS**	**On-Grid**	**On-Grid**	**BESS**	**[Pts/MWh]**
DK	24.00	93.02		23.18	90.05		22.75	89.62	Peters (SIB)	42.43
ES	19.24	26.39		16.76	23.63		18.78	27.90	Weber (VRFB)	37.45
FR	26.82	47.25		24.87	44.18		26.31	45.84	Weber (VRFB)	7.58
GR	24.59	31.10	Ell	22.40	28.34	Ell	25.99	31.13	Weber (VRFB)	112.96
HU	21.55	43.56	(NCM)	20.04	40.68	(SSNCM)	22.15	44.11	Peters (SIB)	55.36
IT	22.40	31.51		20.11	28.83		22.28	32.59	Weber (VRFB)	41.56
PT	20.95	28.12		18.50	25.23		20.02	27.36	Weber (VRFB)	39.53
RO	22.32	42.65		20.75	39.91		22.67	46.36	Weber (VRFB)	56.83

Table 11. Components contribution analysis of the most sustainable SHSs by categories and by installation sites.

	PV		**BESS**		**In**		**CC**		E_{exc}	
	On-Grid	**Off-Grid**	**On-Grid**	**Off-Grid**	**On-Grid**	**Off-Grid**	**On-Grid**	**Off-Grid**	**On-Grid**	**Off-Grid**
DK	83.24%	77.63%	9.76%	9.11%	2.46%	2.30%	0.29%	0.27%	4.25%	10.69%
ES	60.70%	47.86%	13.39%	10.57%	7.49%	5.90%	5.37%	4.24%	13.05%	31.43%
FR	70.50%	45.14%	7.11%	6.31%	15.25%	13.54%	6.24%	5.54%	0.90%	29.47%
GR	48.79%	48.61%	8.86%	8.83%	8.82%	8.79%	4.32%	4.30%	29.21%	29.47%
HU	75.85%	71.06%	6.85%	6.41%	4.26%	3.99%	6.71%	6.29%	6.33%	12.25%
IT	59.93%	48.99%	10.33%	8.44%	11.69%	9.55%	5.30%	4.34%	12.75%	28.68%
PT	60.84%	52.38%	12.04%	10.37%	13.21%	11.38%	5.39%	4.64%	8.52%	21.23%
RO	71.04%	64.43%	6.83%	6.20%	5.77%	5.24%	6.29%	5.73%	10.07%	18.40%

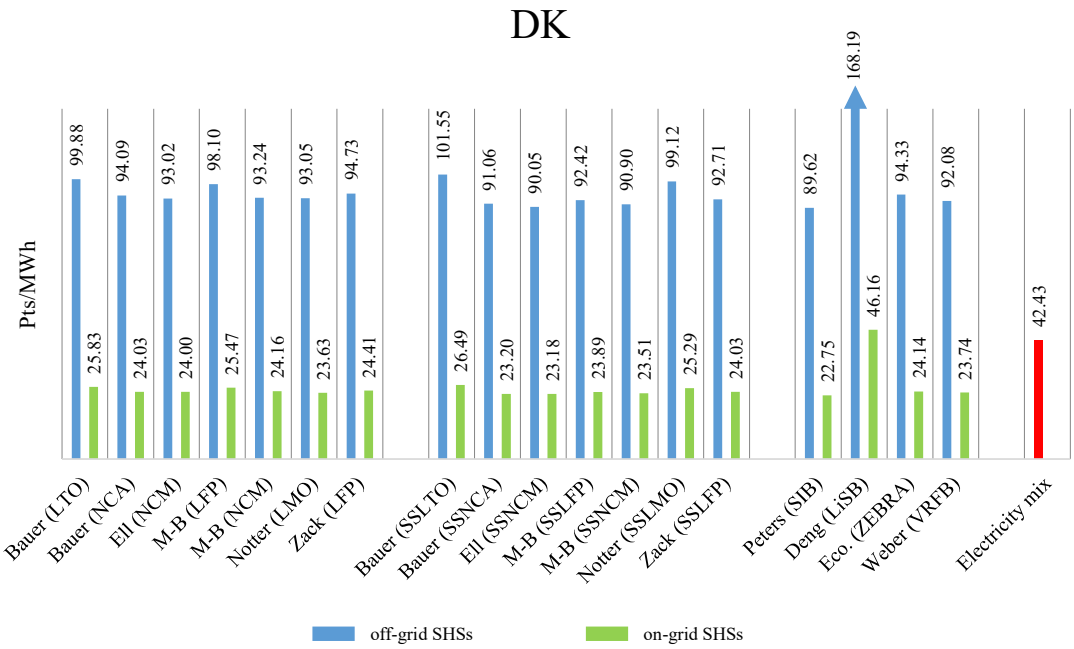

Figure 5. LCA impact values of SHSs in Denmark as single scores.

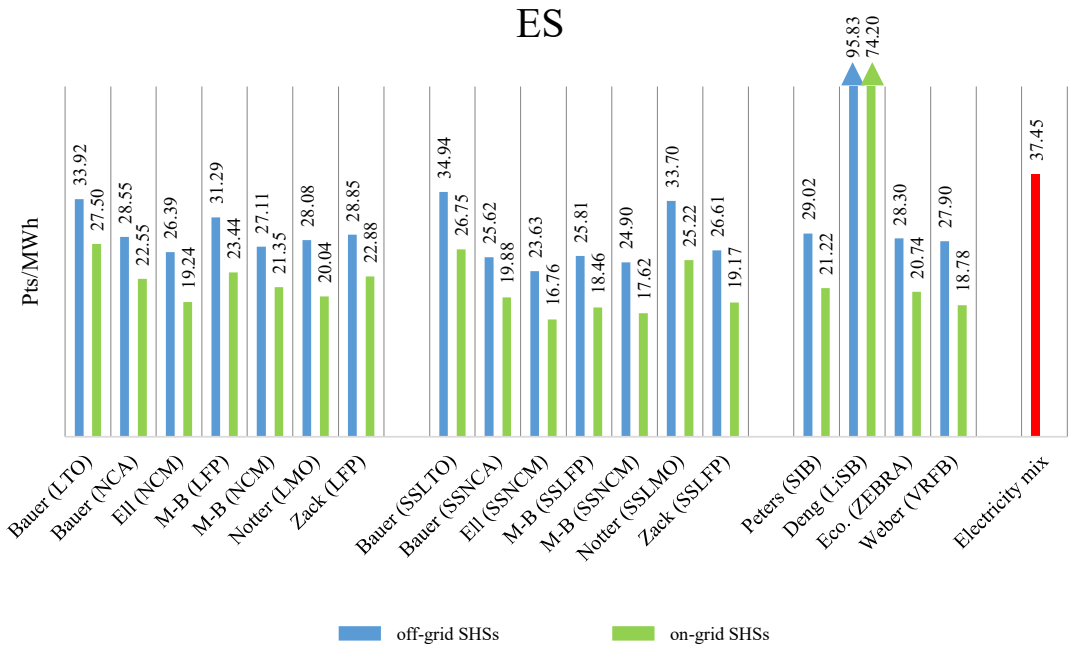

Figure 6. LCA impact values of SHSs in Spain as single scores.

Figure 7. LCA impact values of SHSs in France as single scores.

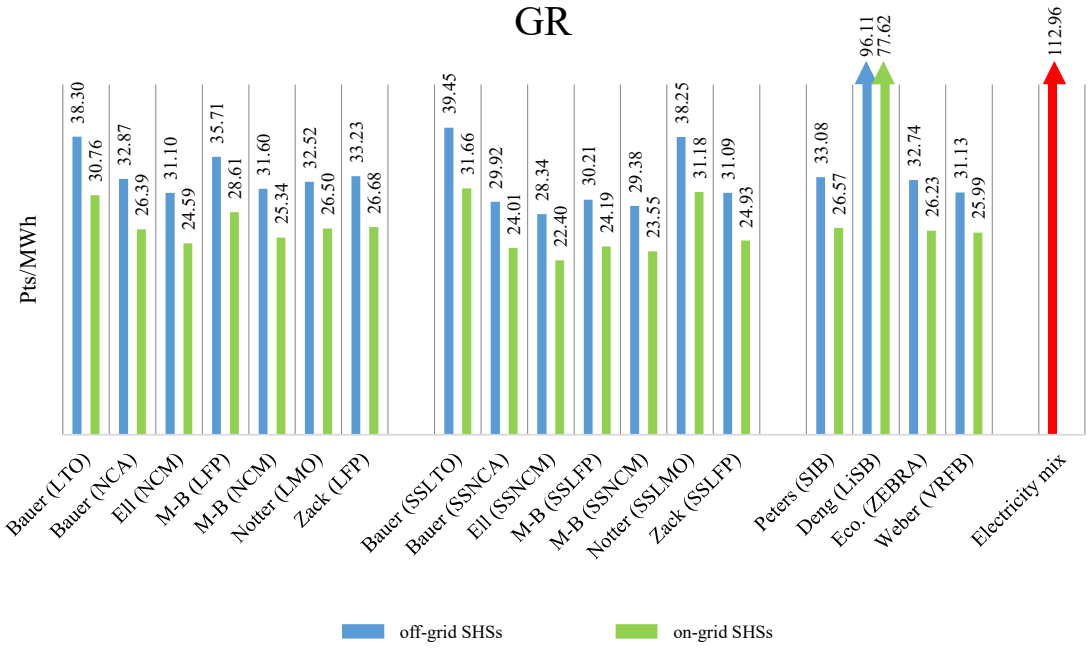

Figure 8. LCA impact values of SHSs in Greece as single scores.

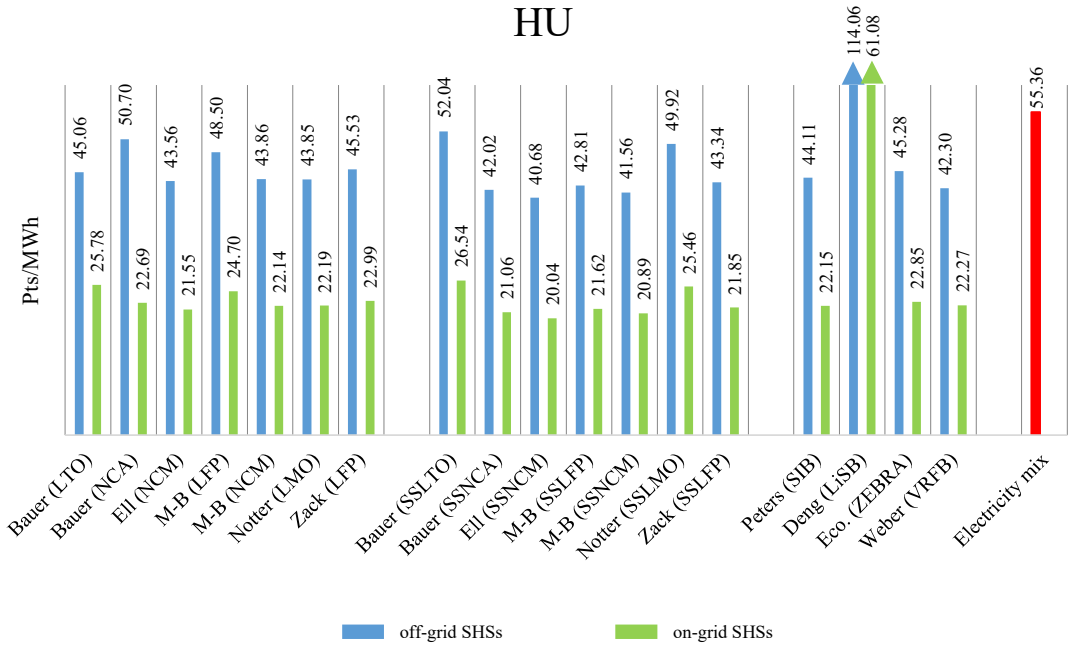

Figure 9. LCA impact values of SHSs in Hungary as single scores.

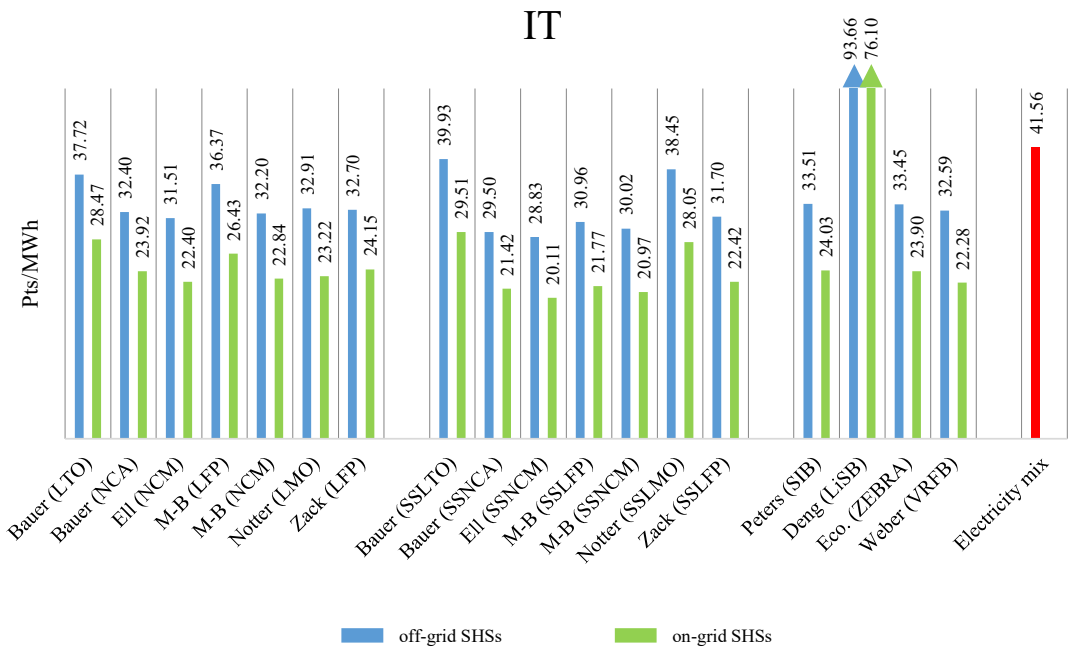

Figure 10. LCA impact values of SHSs in Italy as single scores.

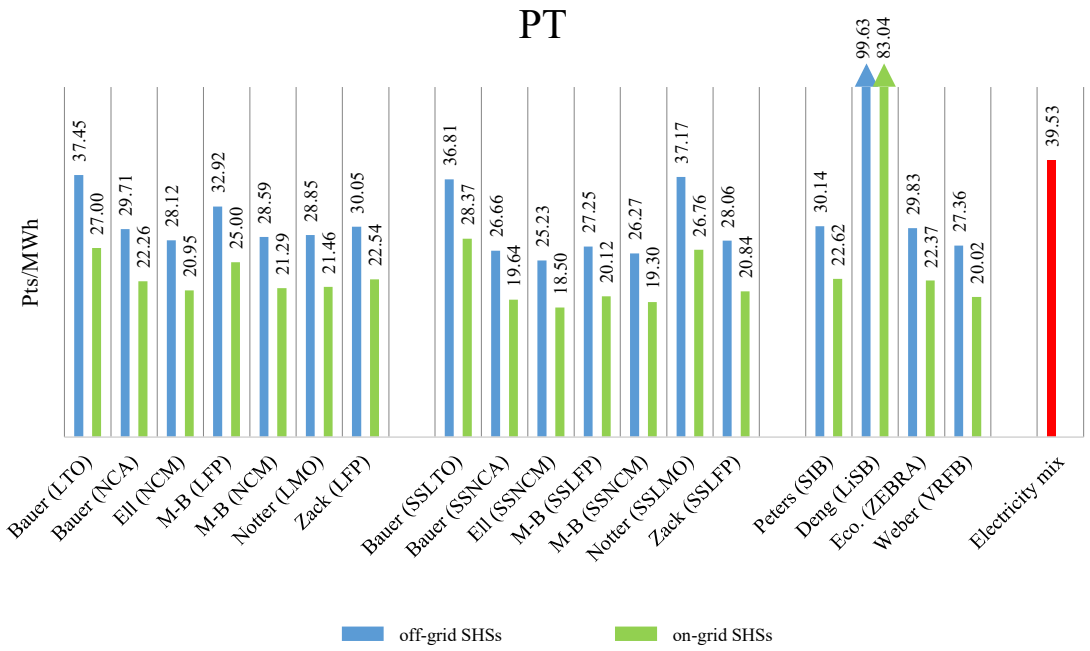

Figure 11. LCA impact values of SHSs in Portugal as single scores.

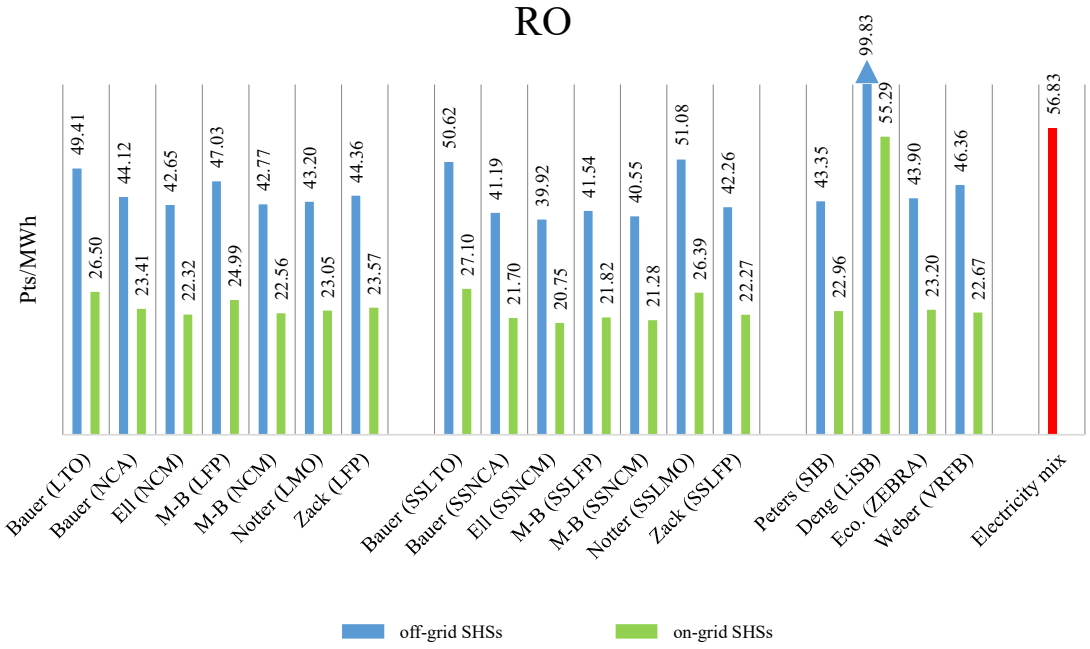

Figure 12. LCA impact values of SHSs in Romania as single scores.

From the results presented in Table 10, it is possible to observe that among LIBs, Ell (NCM) batteries allow us to minimize the SHS environmental impact values thanks to a good combination of efficiency, energy density, materials availability, and lifespan. For the same reasons, Ell (SSNCM) represents the most sustainable choice among SSLIBs. The best aBESS varies with the installation site as Peters (SIB) represents the best solution in DK and HU whereas Weber (VRFB) is assessed as the best in the other countries. A general comparison including all the BESSs categories shows that SHSs equipped with Ell (SSNCM) have the most sustainable environmental performance in every installation site, except for DK, where Peters (SIBs) results to be the best configuration. These results underline that solid electrolytes have an environmental benefit because their impact is comparable

to the liquid ones, but a double energy density allows to halve the weight of the battery as well as their contribution to the total SHS impact. Particularly, moving from Ell (NCM) to Ell (SSNCM) the SHS environmental burden is reduced of a remarkable percentage.

Concerning the environmental impact values, different considerations can be done for on-grid and off-grid SHSs. The burdens of grid-connected systems are included in a quite narrow range (16.76 Pts/MWh–24.87 Pts/MWh in case of Ell (SSNCM) installation) depending on the installation site. In northern countries a low solar radiation value imposes the use of large power plant thus representing a major contribution to the overall impact (Table 11). Nevertheless, in these conditions, the amount of energy exceeding the batteries' capacity is relevant and the possibility to inject it to the grid (Table 9) mitigates the environmental impact per MWh. On the contrary, in off-grid SHSs this possibility does not exist, and the surplus energy must be dissipated. For such reason, the environmental impact per MWh increases, especially in northern installation sites, and the range of values assumed by the SHSs impact is much larger (23.63 Pts/MWh–90.05 Pts/MWh in case of Ell (SSNCM) installation). Therefore off-grid SHSs are more impactful than on-grid configurations and the diesel generator contribution, higher than that of the electricity imported from the grid, strengthens this difference. The only exception is GR, where most of the electricity is produced by coal and its burden is comparable with that of SHSs.

Concerning the national electricity mixes eco-profiles, that of FR is particularly low because of the high nuclear energy contribution to the electricity mix. However, a detailed discussion about the FR electricity mix sustainability is beyond the scope of this paper. This value will be just used as a reference for comparison. In this context, on-grid systems are more sustainable than the electricity mix in all the installation sites except for FR whereas off-grid systems are not competitive with the grid in DK and FR. The batteries recycling phase has an important role in the SHS environmental impact mitigation: indeed, the best BESSs have a percentage contribution in the order of 10%, but without an adequate recycling of the raw materials this percentage could be over 25%.

The previous considerations have been done analyzing the best BESSs for every battery group. Histograms reported in Figures 4–11 are used to provide a more general overview about all the others SHSs. These figures show that many SHSs, although not the best, are effective to produce more sustainable electricity than the energy mix thanks to their BESS. Among LIBs, Bauer (NCA), M-B (NCM), Ell (NCM) have similar environmental performances; the same considerations can be done for Bauer (SSNCA), M-B (SSNCM), Ell (NCM) and Zack (LFP). The worse batteries are the Notter (LMO), Zack (LFP), Bauer (LTO) and the respective SSLIBs, whose low energy density compromise their environmental performances. The obtained results are coherent with those of our previous work [40] where Bauer (NCA) was assessed as the best solution. Indeed, in both cases Bauer (NCA) and Ell (NCM) environmental performances are very close to each other. This means that, although the simulation model and some input data have been slightly changed and a BESS recycling model has been improved, the best solutions can be obtained mixing cobalt with other more common metals.

In the perspective of replacing LIBs with alternative BESS, Deng (LiSB) is currently very far from the performances of the other batteries because, despite its high energy density, its lifespan is too low to be competitive with the others. Contrarily the Peters (SIBs), Eco. (ZEBRA) and Weber (VRFB) proposals all have good environmental performances; their impact is similar to that of Ell (SSNCM) ones. Considering the operative parameters in Table 1, these devices can improve in terms of energy density. Particularly, Peters batteries (SIB) are still at a research level and the number of cycles which can be performed will probably increase as well as the energy density and, considering that they are already competitive with LIBs stationary batteries, the potential is very large. It's important to stress that LiSBs, despite currently presenting a high environmental impact, should not be under-evaluated because they have some very good characteristics like their energy density, but it's very important to improve strongly their lifespan and the recycling processes in order to be competitive with the other devices.

5. Conclusions

In this paper the environmental sustainability assessment of SHSs equipped with different types of batteries is performed through a three-steps methodology including design, modelling and LCA. Some of these batteries, namely LIBs, currently represent a benchmark in the market whereas others have a lower maturity. A sensitivity analysis of the installation site is proposed considering different European countries, at different latitude, represented by their capital city.

From the results it is possible to draw conclusions concerning three major points:

- Geographical dependencies on the variation of battery types: the choice of the most sustainable BESSs does not change significantly with the installation site. Regardless of the solar radiation profile and energy demand curves, Ell (SSNCM) batteries are assessed as the best in almost every country (16.76–24.87 Pts/MWh). M-B (SSNCM) (17.62–23.41 Pts/MWh), M-B (SSLFP) (18.46–26.13 Pts/MWh), Peters (SIB) (21.22–27.51 Pts/MWh) and Weber (VRFB) (18.38–26.31 Pts/MWh) environmental performances are all close to Ell (SSNCM).
- Structural properties and operative characteristics of batteries: the main strength of the mentioned SSLIBs is in having a high energy density. Peters (SIB) devices instead take great advantage of the low impact on natural resources consumption as sodium is more abundant on the Earth's surface whereas Weber (VRFB) batteries have a very long lifespan. Even though SSLIBs guarantee an important improvement compared to simple LIBs and currently they have the most sustainable eco-profile, Peters systems (SIBs) probably have the lowest maturity level among the cited BESSs, therefore the highest potential for the future. Deng batteries (LiSBs), penalized by their short lifespan, are by far the most impactful battery whereas all the others have an intermediate environmental impact.
- SHSs' environmental advantages and batteries contributions to their eco-profiles in the various European countries: extending the overview to the overall SHS, it is possible to conclude that the choice of the batteries affects the results in southern Europe countries where the percentage contribution is the most relevant, whereas in northern Europe they have a minor contribution. Considering the best batteries, their impact is usually of the order of 10% of the total thanks to the materials recovery in the EoL, while without this percentage it could be more than double. Grid-connected SHSs are always more profitable compared to the off-grid ones, especially in northern countries, thanks to the possibility to inject more electricity to the grid avoiding the use of a diesel generator. Both types of SHSs are generally more sustainable than the national electricity mix, except for FR where the grid electricity is estimated to have a very low impact, and DK where off-grid configuration is more impactful.

Supplementary Materials: Supplementary Materials: The following are available online at https://www.mdpi.com/xxxxxxxx/s1, Pdf file S1: energies-845703-supplementary.pdf.

Author Contributions: Conceptualization, F.R., M.L.P., R.B. and A.S.; Investigation, F.R.:, M.L.P. and S.G.; Supervision, R.B. and A.S.; Writing – original draft, F.R., R.B. and A.S.; Writing – review & editing, F.R., M.L.P., S.G., R.B. and A. S. All authors have read and agreed to the published version of the manuscript.

Funding: This research received no external funding.

Acknowledgments: F.R., M.L.P., R.B. and A.S. acknowledge MIUR Grant—Department of Excellence 2018-2022. FR is grateful for the Ph.D. grant within the "Progetto Pegaso" funded by Regione Toscana.

Conflicts of Interest: The authors declare no conflict of interest.

Abbreviations

aBESS	Alternative Battery Energy Storage System
AIB	Aluminium-ion Battery
BESS	Battery Energy Storage System
CC	Charge Controller
CO	Construction
DK	Denmark

DME	Dimethyl Glycol
DoD	Depth of Discharge
DOL	Dioxolane
EoL	End of Life
ES	Spain
FU	Functional Unit
FR	France
GR	Greece
HU	Hungary
In	Inverter
IT	Italy
ISO	International Organization for Standardization
LCA	Life Cycle Assessment
LCI	Life Cycle Inventory
LCIA	Life Cycle Impact Assessment
LCO	Lithium Cobalt Oxide
LCP	Lithium Cobalt Phosphate
LFP	Lithium Iron Phosphate
LIB	Lithium-ion battery
LiPON	Lithium Phosphorous Oxy-Nitride
LiSB	Lithium-sulphur Battery
LiTFSI	Lithium Bistrifluoromethanesulfonimidate
LMNO	Lithium Manganese Nickel Oxide
LMO	Lithium Manganese Oxide
LTO	Lithium Iron Titanate
NCA	Nickel Cobalt Aluminium
NCM	Nickel Cobalt Manganese
NMMT	Nickel Manganese Magnesium Titanium Oxide
OP	Operation
PON	Polyacrylonitrile
PT	Portugal
PV	Photovoltaic
PV-GIS	Photovoltaic Geographical Information System
RF	Reference Flow
RO	Romania
SHS	Solar Home System
SIB	Sodium-ion Battery
SOC	State of Charge
SOH	State of Health
SSLFP	Solid State Lithium Iron Phosphate
SSLIB	Solid State Lithium-ion Battery
SSLMO	Solid State Lithium Manganese Oxide
SSLTO	Solid State Lithium Iron Titanate
SSNCA	Solid State Nickel Cobalt Aluminium
SSNCM	Solid State Nickel Cobalt Manganese
VRFB	Vanadium Redox Flow Battery
ZEBRA	Zero Emissions Batteries Research Activity

References

1. Liu, N.; Cheng, M.; Yu, X.; Zhong, J.; Lei, J. Energy-Sharing Provider for PV Prosumer Clusters: A Hybrid Approach Using Stochastic Programming and Stackelberg Game. *IEEE Trans. Ind. Electron.* **2018**, *65*, 6740–6750, doi:10.1109/TIE.2018.2793181.
2. Bashir, A.A.; Pourakbari-Kasmaei, M.; Contreras, J.; Lehtonen, M. A novel energy scheduling framework for reliable and economic operation of islanded and grid-connected microgrids. *Electr. Power Syst. Res.* **2019**, *171*, 85–96, doi:10.1016/j.epsr.2019.02.010.

3. Pourakbari-Kasmaei, M.; Asensio, M.; Lehtonen, M.; Contreras, J. Trilateral Planning Model for Integrated Community Energy Systems and PV-Based Prosumers—A Bilevel Stochastic Programming Approach. *IEEE Trans. Power Syst.* **2020**, *35*, 346–361, doi:10.1109/TPWRS.2019.2935840.
4. Mohammadi, S.; Soleymani, S.; Mozafari, B. Scenario-based stochastic operation management of MicroGrid including Wind, Photovoltaic, Micro-Turbine, Fuel Cell and Energy Storage Devices. *Int. J. Electr. Power Energy Syst.* **2014**, *54*, 525–535, doi:10.1016/j.ijepes.2013.08.004.
5. International Standards Organization. *EN ISO 14040:2006—Valutazione del ciclo di vita Principi e Quadro di Riferimento*; International Standards Organization: Geneva, Switzerland, 2010; p. 14040.
6. International Standards Organization. *UNI EN ISO 14044:2006—Gestione Ambientale—Valutazione del ciclo di vita—Requisiti e Linee Guida*; International Standards Organization: Geneva, Switzerland, 2006.
7. Rossi, F.; Parisi, M.L.; Maranghi, S.; Manfrida, G.; Basosi, R.; Sinicropi, A. Environmental impact analysis applied to solar pasteurization systems. *J. Clean. Prod.* **2019**, *212*, 1368–1380, doi:10.1016/j.jclepro.2018.12.020.
8. Bravi, M.; Parisi, M.L.; Tiezzi, E.; Basosi, R. Life Cycle Assessment of advanced technologies for photovoltaic panels production. *Int. J. HEAT Technol.* **2010**, *28*, 133–140, doi: 10.18280/ijht.28021710.18280/ijht.280217.
9. Maranghi, S.; Parisi, M.L.; Basosi, R.; Sinicropi, A. Environmental Profile of the Manufacturing Process of Perovskite Photovoltaics: Harmonization of Life Cycle Assessment Studies. *Energies* **2019**, *12*, 3746, doi:10.3390/en12193746.
10. Parisi, M.L.; Maranghi, S.; Sinicropi, A.; Basosi, R. Development of dye sensitized solar cells: A life cycle perspective for the environmental and market potential assessment of a renewable energy technology. *Int. J. Heat Technol.* **2013**, *31*, 143–148, doi:10.18280/ijht.310219.
11. Peters, J.F.; Weil, M. Providing a common base for life cycle assessments of Li-Ion batteries. *J. Clean. Prod.* **2018**, *171*, 704–713, doi:10.1016/j.jclepro.2017.10.016.
12. Bauer, C. *Okobilanz Von Lithium-Ionen Batterien*; Paul Scherrer Institut, Labor für Energiesystem-Analysen (LEA): Villingen, Switzerland, 2010.
13. Ellingsen, L.A.; Majeau-Bettez, G.; Singh, B.; Srivastava, A.K.; Valøen, L.O.; Strømman, A.H. Life Cycle Assessment of a Lithium-Ion Battery Vehicle Pack. *J. Ind. Ecol.* **2014**, *18*, 113–124, doi:10.1111/jiec.12072.
14. Majeau-bettez, G.; Hawkins, T.R.; Strømman, A.H. Life Cycle Environmental Assessment of Lithium-Ion and Nickel Metal Hydride Batteries for Plug-In Hybrid and Battery Electric Vehicles. *Environ. Sci. Technol.* **2011**, *45*, 4548–4554, doi:10.1021/es103607c.
15. Notter, D.A.; Gauch, M.; Widmer, R.; Patrick, W.A.; Stamp, A.; Zah, R.; Althaus, R.G. Contribution of Li-Ion Batteries to the Environmental Impact of Electric Vehicles. *Environ. Sci. Technol.* **2010**, *44*, 6550–6556, doi:10.1021/es903729a.
16. Zackrisson, M.; Avellán, L.; Orlenius, J. Life cycle assessment of lithium-ion batteries for plug-in hybrid electric vehicles e Critical issues. *J. Clean. Prod.* **2010**, *18*, 1519–1529, doi:10.1016/j.jclepro.2010.06.004.
17. Cusenza, M.A.; Bobba, S.; Ardente, F.; Cellura, M.; di Persio, F. Energy and environmental assessment of a traction lithium-ion battery pack for plug-in hybrid electric vehicles. *J. Clean. Prod.* **2019**, *215*, 634–649, doi:10.1016/j.jclepro.2019.01.056.
18. Deng, Y.; Li, J.; Li, T; Zhang, J.; Yang, F.; Yuan, C. Life cycle assessment of high capacity molybdenum disulfide lithium-ion battery for electric vehicles. *Energy* **2017**, *123*, 77–88, doi:10.1016/j.energy.2017.01.096.
19. Raugei, M.; Winfield, P. Prospective LCA of the production and EoL recycling of a novel type of Li-ion battery for electric vehicles. *J. Clean. Prod.* **2019**, *213*, 926–932, doi:10.1016/j.jclepro.2018.12.237.
20. Senevirathne, K.; Day, C.S.; Gross, M.D.; Lachgar, A.; Holzwarth, N.A.W. A new crystalline LiPON electrolyte : Synthesis , properties , and electronic structure. *Solid State Ionics* **2013**, *233*, 95–101, doi:10.1016/j.ssi.2012.12.013.
21. Troy, S.; Schreiber, A.; Reppert, T.; Gehrke, H.G.; Finsterbusch, M.; Uhlenbruck, S.; Stenzel, P. Life Cycle Assessment and resource analysis of all-solid-state batteries. *Appl. Energy* **2016**, *169*, 757–767, doi:10.1016/j.apenergy.2016.02.064.
22. Lastoskie, C.M.; Dai, Q. Comparative life cycle assessment of laminated and vacuum vapor-deposited thin fi lm solid-state batteries. *J. Clean. Prod.* **2015**, *91*, 158–169, doi:10.1016/j.jclepro.2014.12.003.
23. U.S. Department of the Interior, U.S. Geological Survey. *Mineral Commodity Summaries 2018*; U.S. Geological Survey: Washington, DC, USA, 2018.

24. Grimsmo, B.; Strømman, A.H.; Ellingsen, L. Life Cycle Assessment LCA of Li-Ion batteries for electric vehicles. Available online: https://ntnuopen.ntnu.no/ntnu-xmlui/handle/11250/2400819 (accessed on 18 February 2020).
25. Peters, J.; Buchholz, D.; Passerini, S.; Weil, M. Life cycle assessment of sodium-ion batteries. *Energy Environ. Sci.* **2016**, *9*, 1744–1751, doi:10.1039/c6ee00640j.
26. Delgado, M.A.S.; Usai, L.; Ellingsen, L.A.W.; Pan, Q.; Strømman, A.H. Correction: Comparative Life Cycle Assessment of a Novel Al-Ion and a Li-Ion Battery for Stationary Applications. *Materials* **2019**, *12*, 3270, doi:10.3390/ma12193270.
27. Hosseinifar, M.; Petric, A. High temperature versus low temperature Zebra (Na/NiCl 2) cell performance. *J. Power Sources* **2012**, *206*, 402–408, doi:10.1016/j.jpowsour.2012.01.125.
28. Longo, S.; Antonucci, V.; Cellura, M.; Ferraro, M. Life cycle assessment of storage systems: The case study of a sodium/nickel chloride battery. *J. Clean. Prod.* **2014**, *85*, 337–346, doi:10.1016/j.jclepro.2013.10.004.
29. Weber, S.; Peters, J.F.; Baumann, M.; Weil, M. Life Cycle Assessment of a Vanadium Redox Flow Battery. *Environ. Sci. Technol.* **2018**, *52*, 10864–10873, doi:10.1021/acs.est.8b02073.
30. Deng, Y.; Li, J.; Li, T.; Gao, X.; Yuan, C. Life cycle assessment of lithium sulfur battery for electric vehicles. *J. Power Sources* **2017**, *343*, 284–295, doi:10.1016/j.jpowsour.2017.01.036.
31. Zackrisson, M.; Fransson, K.; Hildenbrand, J.; Lampic, G.; O'Dwyer, C. Life cycle assessment of lithium-air battery cells. *J. Clean. Prod.* **2016**, *135*, 299–311, doi:10.1016/j.jclepro.2016.06.104.
32. Hiremath, M.; Derendorf, K.; Vogt, T. Comparative life cycle assessment of battery storage systems for stationary applications. *Environ. Sci. Technol.* **2015**, *49*, 4825–4833, doi:10.1021/es504572q.
33. Montenegro, C.T.; Peters, J.F.; Zhao-Karger, Z.; Wolter, C.; Weil, M. CHAPTER 13 Life Cycle Analysis of a Magnesium–Sulfur Battery. In *Magnesium Batteries*; The Royal Society of Chemistry: London, UK, 2020; pp. 309–330, doi:10.1039/9781788016407-00309.
34. Santos, F.; Urbina, A.; Abad, J.; López, R.; Toledo, C.; Romero, A.J.F. Environmental and economical assessment for a sustainable Zn/air battery. *Chemosphere* **2020**, *250*, 126273, doi:10.1016/j.chemosphere.2020.126273.
35. Tian, J.; Xiong, R.; Shen, W. A review on state of health estimation for lithium ion batteries in photovoltaic systems. *eTransportation* **2019**, *2*, 100028, doi:10.1016/j.etran.2019.100028.
36. Nagapurkar, P.; Joseph; Smith, D. Techno-Economic Optimization and Environmental Life Cycle Assessment (LCA) of Microgrids located in the US using Genetic Algorithm. *Energy Convers. Manag.* **2018**, *181*, 272–291, doi:10.1016/j.enconman.2018.11.072.
37. Wang, R.; Lam, C.; Hsu, S.; Chen, J.; Engineering, E.; Hong, T.; Polytechnic, K.; Kong, H. Life cycle assessment and energy payback time of a standalone hybrid renewable energy commercial microgrid : A case study of Town Island in Hong Kong. *Appl. Energy* **2019**, *250*, 760–775, doi:10.1016/j.apenergy.2019.04.183.
38. Longo, S.; Beccali, M.; Cellura, M.; Guarino, F. Energy and environmental life-cycle impacts of solar-assisted systems : The application of the tool "ELISA". *Renew. Energy* **2020**, *145*, 29–40, doi:10.1016/j.renene.2019.06.021.
39. Kabakian, V.; McManus, M.C.; Harajli, H. Attributional life cycle assessment of mounted 1.8kWp monocrystalline photovoltaic system with batteries and comparison with fossil energy production system. *Appl. Energy* **2015**, *154*, 428–437, doi:10.1016/j.apenergy.2015.04.125.
40. Rossi, F.; Parisi, M.L.; Maranghi, S.; Basosi, R.; Sinicropi, A. Environmental analysis of a Nano-Grid: A Life Cycle Assessment. *Sci. Total Environ.* **2019**, *700*, 134814, doi:doi.org/10.1016/j.scitotenv.2019.134814.
41. Rossi, F.; Parisi, M.L.; Maranghi, S.; Basosi, R.; Sinicropi, A. Life Cycle Inventory datasets for nano-grid configurations. *Data Br.* **2020**, *28*, 104895, doi:10.1016/j.dib.2019.104895.
42. *Ease, EERA, European Energy Storage Technology Development*; European Association for Storage of Energy (EASE): Brussels, Belgium, 2017.
43. Yusoff, N.F.M.; Idris, N.H.; Din, M.F.M.; Majid, S.R.; Harun, N.A.; Rahman, M.M. Investigation on the Electrochemical Performances of Mn2O3 as a Potential Anode for Na-Ion Batteries. *Sci. Rep.* **2020**, *10*, 9207, doi:10.1038/s41598-020-66148-w.
44. Wolff, D.; Casals, L.C.; Benveniste, G.; Corchero, C.; Trilla, L. The effects of lithium sulfur battery ageing on second-life possibilities and environmental life cycle assessment studies. *Energies* **2019**, *12*, 2440, doi:10.3390/en12122440.

45. Bignucolo, F.; Coppo, M.; Crugnola, G.; Savio, A. Application of a simplified thermal-electric model of a sodium-nickel chloride battery energy storage system to a real case residential prosumer. *Energies* **2017**, *10*, 1497, doi:10.3390/en10101497.
46. Ruiz, E.M.; Valsasina, L.; Brunner, F.; Symeonidis, A.; Fitzgerald, D.; Treyer, K.; Bourgault, G.; Wernet, G. Documentation of Changes Implemented in the Ecoinvent Database v3.4 (2018.08.23). Available online: https://www.ecoinvent.org/files/change_report_v3_4_20171004_1.pdf (accessed on 20 March 2020).
47. Joint Research Center (JRC). Photovoltaic Geographical Information System (PVGIS), Jt. Res. Cent. (n.d.). Available online: http://re.jrc.ec.europa.eu/pvgis/ (accessed on 5 May 2019).
48. Quoilin, S.; Kavvadias, K.; Mercier, A.; Pappone, I.; Zucker, A. Quantifying self-consumption linked to solar home battery systems: Statistical analysis and economic assessment. *Appl. Energy* **2016**, *182*, 58–67, doi:10.1016/j.apenergy.2016.08.077.
49. Cardoso, G.; Brouhard, T.; DeForest, N.; Wang, D.; Heleno, M.; Kotzur, L. Battery aging in multi-energy microgrid design using mixed integer linear programming. *Appl. Energy* **2018**, *231*, 1059–1069, doi:10.1016/j.apenergy.2018.09.185.
50. Tremblay, O.; Dessaint, L. Experimental Validation of a Battery Dynamic Model for EV Applications. *World Electr. Veh. J.* **2009**, *3*, 289–298.
51. MIT Team Electric Vehicle Team. *A Guide to Understanding Battery Specifications*; MIT: Cambridge, MA, USA, 2008.
52. Mathworks. Matlab/Simulink 2019b Software, 2018. Available online: https://it.mathworks.com/ (accessed on 20 March 2019).
53. Tang, A.; Bao, J.; Skyllas-kazacos, M. Studies on pressure losses and fl ow rate optimization in vanadium redox fl ow battery. *J. Power Sources* **2014**, *248*, 154–162, doi:10.1016/j.jpowsour.2013.09.071.
54. Tanifuji, T.; Nasu, S. Heat capacity and thermal decomposition of lithium peroxide. *J. Nucl. Mater.* **1979**, *87*, 189–195, doi:10.1016/0022-3115(79)90138-7.
55. Amrical Elements. *Lithium Powder Properties*; Amrical Elements: Los Angeles, CA, USA, 2020.
56. Huang, B. Recycling of lithium-ion batteries: Recent advances and perspectives. *J. Power Sources* **2018**, *399*, 274–286, doi:10.1016/j.jpowsour.2018.07.116.
57. Bekkelund, K. A Comparative Life Cycle Assessment of PV Solar Systems. Master's Thesis, Norwegian University of Science and Technology (NTNU), Trondheim, Noruega, 2013; 243p. Available online: https://ntnuopen.ntnu.no/ntnu-xmlui/bitstream/handle/11250/235329/654872_FULLTEXT01.pdf?sequence=1 (accessed on 11 February 2020).
58. Mastervolt. SCM60 MPPT-MB Datasheet, (n.d.). Available online: https://www.mastervolt.it/conversione/ (accessed on 5 May 2019).
59. Mastervolt. Mass Combi Ultra 48/3500-50 (230 V) Datasheet, (n.d.). Available online: https://www.mastervolt.it/conversione/ (accessed on 5 May 2019).
60. Tenka Solar. MONO CRYSTALLINE MODULE 300–330 Watt Technical Datasheet. 2017. Available online: http://www.tenkasolar.com/ (accessed on 20 March 2019).
61. Latunussa, C.E.L.; Ardente, F.; Blengini, G.A.; Mancini, L. Life Cycle Assessment of an innovative recycling process for crystalline silicon photovoltaic panels. *Sol. Energy Mater. Sol. Cells* **2016**, *156*, 101–111, doi:10.1016/j.solmat.2016.03.020.
62. Rossi, F.; Parisi, M.L.; Maranghi, S.; Basosi, R.; Sinicropi, A. Environmental effectiveness of the Solar Home Systems based on LCA. In Proceedings of the Atti Del XIII Convegno Della Rete Italiana LCA-VIII Convegno Dell'Associazione Rete Italiana LCA Roma, Rome, Italy, 13–14 June 2019; pp. 132–139. Available online: https://www.enea.it/it/seguici/pubblicazioni/pdf-volumi/2019/atti_lca_roma-2019.pdf (accessed on 10 March 2020).
63. European Commission. Eurostat. 2017. Available online: https://ec.europa.eu/eurostat/web/gisco/geodata/reference-data (accessed on 1 February 2020).
64. Buchamann, I. *Batteries in a Portable World*, 4th ed.; Cadex Electronics Inc.: Richmond, BC, Canada, 2016.

4.1.4. Paper 4: Environmental and economic optima of solar home systems design: A combined LCA and LCC approach.

After focusing on the environmental analyses of SHSs, Paper 4, published in *Science of the Total Environment*, proposes a combined economic and environmental evaluation of SHSs; LIBs are considered for this purpose because they represent the most widely commercialized devices. More specifically, this work is a cross-analysis of economic and environmental optima evaluated using MILP optimization. An algorithm that allows to use LCA and LCC results as inputs to minimize an objective function is applied. This function can be represented by the cost or by the environmental impact of SHSs and allows to point out their optimal design and the optimal energy management. A sensitivity analysis of technologies costs and energy tariffs is also performed to consider their uncertainty. This innovative methodology is applied to the same case study proposed in Paper 2. The main outcomes of the paper are:

- The comparison of the economic and of the environmental optima in terms of costs and single score environmental impacts.
- The results variations as function of technology costs and energy tariffs.

The Ph.D. is the first and corresponding author of the paper and contributed to the conceptualization, the development of the methodology, the results evaluation, and the writing of the paper.

Science of the Total Environment 744 (2020) 140569

Contents lists available at ScienceDirect

Science of the Total Environment

journal homepage: www.elsevier.com/locate/scitotenv

Environmental and economic optima of solar home systems design: A combined LCA and LCC approach

Federico Rossi [a,b,*], Miguel Heleno [c], Riccardo Basosi [b,d,e], Adalgisa Sinicropi [b,d,e]

[a] University of Florence, Department of Industrial Engineering, Via Santa Marta, 3, Florence, Italy
[b] University of Siena, R²ES Lab, Department of Biotechnology, Chemistry and Pharmacy, Via A. Moro, 2, Siena, Italy
[c] Grid Integration Group, Lawrence Berkeley National Laboratory, Berkeley, Cyclotron Road, 1, CA 94720, USA
[d] CSGI, Center for Colloid and Surface Science, Via della Lastruccia 3, 50019 Sesto Fiorentino, Italy
[e] Institute of Chemistry of Organometallic Compounds (CNR-ICCOM), Via Madonna del Piano 10, 50019 Sesto Fiorentino, Italy

HIGHLIGHTS

- Life cycle analyses and optimization allow to compare the SHS costs and impacts.
- The environmental optimum has a low impact, but a high cost compared to the grid.
- The economic optimum has low impacts and costs compared to the grid.
- Improving the SHS eco-profile with batteries is at the moment expensive.
- A decrease of technology costs can enhance the economic optimum sustainability.

GRAPHICAL ABSTRACT

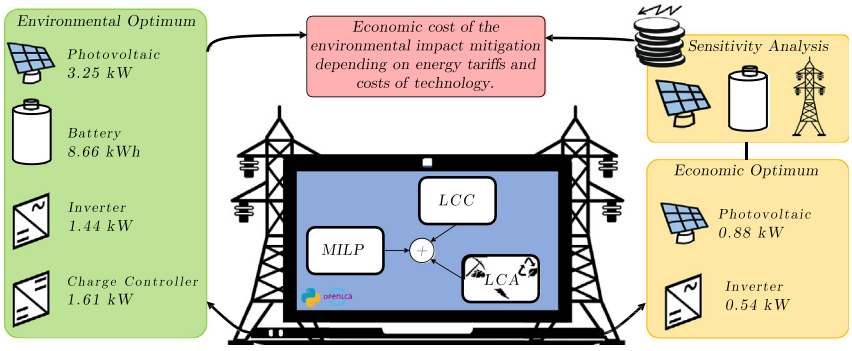

ARTICLE INFO

Article history:
Received 7 March 2020
Received in revised form 31 May 2020
Accepted 26 June 2020
Available online 11 July 2020

Editor: Deyi Hou

Keywords:
LCA
LCC
Optimization
Batteries
Solar energy

ABSTRACT

This paper compares the economic and environmental optimal design of Solar Home Systems (SHSs) and explores the role of economic incentives (such as tariffs and technology costs) in approximating the two optima. To achieve that, we present a methodology for the environmental and economic evaluation of grid-connected SHSs: user-scale electric systems involving a photovoltaic (PV) power system and a battery energy storage system. The proposed methodology is based on a mixed integer linear programming (MILP) optimization, life cycle assessment and life cycle costing. This methodological framework is applied to a case study involving a typical SHS installation in Italy. The results of the environmental optimal design brought to the evaluation of a 3.25 kW PV assisted by 8.66 kWh of nickel cobalt manganese batteries, whereas the costs of the SHS are minimized by a small PV system (less than 1 kW). Results underline that the environmental optimal configurations rely on battery technologies, which entails a significant cost compared to the grid connection. In contrast, the economic optimal design solutions is less impactful than the grid mix both from an environmental and economic points of view. Thanks to a reduction of batteries and PV costs, the environmental impact of the economic optimal design is expected to decrease in the future.

1. Introduction

This paper is focused on the evaluation of a user-scale electric system, named Solar Home System (SHS), composed of a photovoltaic (PV) system, a battery energy storage system (BESS), a charge controller

* Corresponding author at: University of Florence, Department of Industrial Engineering, Via Santa Marta, 3, Florence, Italy.
E-mail address: fe.rossi@unifi.it (F. Rossi).

https://doi.org/10.1016/j.scitotenv.2020.140569
0048-9697/

(CC), an inverter (In) and a backup power source (the grid or a backup generator) (Narayan et al., 2018). The installation of SHSs are motivated by different objectives, typically the electrification of remote rural areas (Sovacool, 2018; Khan, 2020; Khan et al., 2019; Kennedy et al., 2019) or the economic gains (self-consumption and feed-in remuneration) in grid connected installations (O'Shaughnessy et al., 2018a; Jacob et al., 2018). Besides the economic viability of such installations, the increasing concerns about the environmental problems dealing with the traditional power systems, fueled by fossil fuels, has brought environmental sustainability analyses to be as important as the economic ones (Nagapurkar and Smith, 2019). Therefore two SHS optimal configurations are designed in this paper: one minimizing the costs and the other minimizing the environmental impact. This choice comes from the need of comparing the two approaches to evaluate the distance between their results in terms of costs and environmental impacts and to assess which is the economic cost of improving the SHS eco-profile. This comparison is key to support SHS related policies that can generate economic incentives in the direction of environmental optimum. Therefore, this paper explores some of the potentials of theses economic incentives, in particular how the SHS impact results are affected by technologies costs and energy tariffs.

The literature on SHS systems planning and impact is extensive and involves different economic and environmental perspectives. On the economic side, O'Shaughnessy (O'Shaughnessy et al., 2018a) published an interesting review summarizing the results of seventeen SHS economic analyses available in literature, and later proposed their own economic optimal design to size a SHS (O'Shaughnessy et al., 2018b). Petrollese et al. (2018) proposed an Italian case study where optimization is used to maximize the SHS economic benefits associated with self-consumption. Zubi et al. (2019) estimated the cost of the energy produced by a SHS, focusing on the contribution of the BESS, whereas Diouf et al. (Diouf and Avis, 2019) had a broader perspective on the economic benefits related to the adoption of SHSs in some African states. SHSs economic issues have also been addressed by Azimoh et al. (2014) with a particular emphasis on role of the installation and use of those systems in mitigating life cycle costs. Ndwali et al. (2019) optimized the design of a batteries assisted PV system considering the overall costs of energy and technologies; NREL performed a very detailed analysis on these costs and released a benchmark study (NREL, 2016). According to this evaluation, batteries have a very important impact on the SHS cost; indeed, NREL estimates the cost of a 5.6 kW PV installation to about 14,000 EUR whereas adding a 6kWh BESS, typical of residential systems, it is about 25,000 EUR (NREL, 2016). Still in the context of SHS economic analysis, the paper of Cardoso et al. (2018) is particularly relevant as the optimal economic configuration of a SHS is defined using mixed integer linear programming (MILP). MILP represents the most widely used approach for power systems optimization because, contrarily to mixed integer non-linear programming (MINLP), its convergence and optimality are guaranteed (Cardoso et al., 2018). Differently from simulation-based optimization, MILP is a mathematical minimization of a cost function that does not involve intermediate results. Other studies, although less abundant, propose the SHS environmental impact estimation. For instance Martinopoulos (2020) presents a broad overview of economic and environmental impact analyses of electricity production from PV in European context. Nagapurkar and Smith (2019) used LCA to evaluate the carbon dioxide emissions of a cost-optimized Microgrid whereas Zhang et al. (2015) analyzed the environmental impacts of a combined heat and power (CHP) based off-grid system. Recent papers published by Rossi et al. (2020a, 2020b) show how the design, modeling and environmental impact assessment of some user scale electric systems based on PV generation, including SHSs, can be connected with each other in a three-steps methodology. The authors concluded that a grid-connected SHS represents the best configuration for the environment.

On the side of the environmental impacts, life cycle assessment (LCA) is particularly useful because it allows to consider all the direct and indirect burdens connected with all the phases of the life cycle of a technology. Indeed it is possible to evaluate the negative and positive effects on the environment of the natural resources consumption and of the direct and indirect emissions occurring during the raw materials extraction, transports, manufacturing, operation and the disposal (Goglio et al., 2020). Moreover, several environmental impact categories can be investigated including global warming potential, resources depletion, acidification and eutrophication potential and other types of impacts (Rossi et al., 2019). This represents a remarkable difference with other environmental assessment methods which include only direct carbon dioxide emissions to the environment (Jung and Villaran, 2017). This is particularly relevant in the evaluation of technologies, such as PV and BESS, that are not responsible for pollutant emissions in their operation, but have a significant impact during other phases of their life (Maranghi et al., 2019). For all these reasons, the International Organization for Standardization (ISO) decided to define a standard procedure to perform a LCA analysis in ISO 14040 and ISO 14044 regulations (International Organization for Standardization, 2016a, 2016b). The life cycle approach became so important that it has been extended from the environmental analyses to the economic and social evaluations with Life Cycle Costing (LCC) and social LCA (Toniolo et al., 2020). The tools necessary to perform a LCA analysis are a database, provided by Ecoinvent (2016) to collect the information for the model definition, and a computational software, in this case openLCA (GreenDelta GmbH, 2019).

In the field of LCA, a particular attention is devoted to the energy storage system (ESS) due to the variety of battery chemistries, materials and technical properties. For instance cobalt is a metal providing high energy density to the battery, but at the same time it is becoming rare and expensive (Monge and Gil-Alana, 2019). In order to perform LCA of batteries, the input data have been recovered from Peters et al. (Peters et al., 2017; Peters and Weil, 2018). In these papers the main LCA studies based on primary data of the main Lithium-ion batteries (LIBs) commercially available have been gathered and modified to provide a single harmonized database. The same nomenclature adopted by Peters and Weil (2018) has been used to address these LIBs: particularly nickel cobalt manganese (NCM), lithium iron phosphates (LFP) (Majeau-Bettez et al., 2011; Ellingsen et al., 2014; Zackrisson et al., 2016), nickel cobalt aluminium (NCA), lithium iron titanate (LTO) (Bauer, 2010) and lithium manganese oxide (LMO) (Notter et al., 2010) batteries have been compared. Concerning the costs of these devices, some very detailed and reliable analyses are available in literature (NREL, 2016; Xu et al., 2017) and are considered as a reference in this study. Additionally, it was demonstrated that the ageing of ESSs strongly affects the results of optimization during the design and management phases (Cardoso et al., 2018) and represents a major concern for economic and environmental problems. For such reason, batteries degradation models (Severson et al., 2019) are often applied in investments decisions tools (Cardoso et al., 2018; He et al., 2018). Some of these models are also very specific for SHS applications (Narayan et al., 2018; Rossi et al., 2020a) but usually they aren't involved in SHS design optimization (Cardoso et al., 2018). MILP is a very powerful instrument because it allows, using appropriate assumptions, to include both cyclic and calendar ageing expressions in SHSs optimal design (Cardoso et al., 2018).

Despite the rich literature on SHSs, there is a lack of attention to the cross-analysis between economic and environmental optimal designs in different contexts. The methodology presented in this paper is built on Rossi et al. (2020a, 2020b) and Cardoso et al. (2018) papers. The contributions are threefold:

- An optimization model for optimal environmental design, based on LCA. This model mimics the economic model.
- A comparative cross-analysis between economic and environmental solutions in a realistic case study. This involves evaluating the environmental impacts of the economic optimum and vice-versa; the

comparison of the results allows to discuss the costs related to the mitigation of the SHS environmental impact.
- A sensitivity analysis around the cost of technologies and energy tariffs.

The rest of the paper is divided as follows: in Section 2 the innovative approach applied in this paper will be explained and in Section 3 it will be applied to a case study; in Section 4 the results will be illustrated and in Section 5 the conclusions will be presented.

2. Methodology

In this methodological section, the economic and environmental optimization models will be illustrated. First, the cost functions of the problem will be defined, then the mathematical constraints coming from the physical limits of the SHS will be described. Finally, a methodological framework for the comparison of the results provided by the economic and environmental optimization problems will be proposed in order to discuss the economic costs of improving the SHS environmental performances. This evaluation can be very useful to support decisions during the design of a SHS. A high level of detail is used to design this methodology because, although it is based on well known approaches, their integration is proposed for the first time and therefore it can be considered as part of the results of the study as well. A sketch of the methodological framework is illustrated in Fig. 1.

2.1. Economic optimal design

In this section, the economic optimal design of a SHS will be discussed to minimize the costs of private consumers investing for the adoption of a SHS. Consumers decisions will be assumed to be driven only by rationality in the acquisition and utilization of DER technologies. In this section, this rationality is presented as an economic optimal design, where individual consumers size their SHS and dispatch energy to minimize the costs. The economic optimal design model proposed by Cardoso et al. (2018) and included in the overall modeling framework of the Distributed Energy Resources Customer Adoption Model (DER-CAM) tool (Lawrence Berkeley National Laboratory (LBNL), 2019), has been adopted as a reference for this study. This model considers all the annualized expenses that a user should afford in case its energy consumption is guaranteed by a grid-connected SHS. According to ISO 15686 (International Organization for Standardization, 2017) standard for LCC, these expenses are distributed over the SHS lifespan: the cost of technologies includes several contributions like the construction, the supply chain, the marketing and the disposal. Furthermore, during the operation of the SHS, the user might import and export energy from the grid, which implies costs and revenues for the user. In other terms, an optimized LCC is performed grounding on Cardoso et al. (2018) model. As common practice in LCA and LCC, the results are referred to a Reference Flow (RF). As the function of the SHS is providing electricity to the user, the RF is defined as the amount of electricity provided to the load (Eq. (1)).

$$RF = \sum_{t \in \tau_{yr}} \left(\frac{Ld_t}{1000} \right) \tag{1}$$

where, Ld_t is the power absorption of the user hour by hour, whereas τ_{yr} is the set of hourly time points over one year. The cost function (Eq. (2)) takes into account the costs of technologies (defined by the subscript k). These costs are classified as fixed ($CFix_k$), that don't depend on the components capacity (cap_k), and variable ($CVar_k$) that depend on the capacity. Furthermore, the tariffs are also taken into account: the hourly costs (EC_t) of the electricity withdrawn from the grid (ui_t) and the remuneration paid by the utility (FI_t) for the energy injected into the grid (ue_t) are required. All these costs must be annualized and represent input parameters of the economic optimal design. The variable i_k is a binary variable discriminating the technologies which are adopted and those that are not. The overall SHS life cycle cost per MWh of energy supplied to the user (C) is calculated by the economic cost function (Eq. (2)):

$$C = \frac{\sum_{k \in \{SHS\}} (CFix_k \cdot i_k + CVar_k \cdot cap_k) Ann_k + \sum_{t \in \tau_{yr}} (ui_t \cdot EC_t - ue_t \cdot FI_t)}{RF} \tag{2}$$

where τ_{yr} is the set of hourly time points over a year and the factor Ann_k is calculated defining an interest rate (ir) of 3% using Eq. (3) (Dainelli et al., 2017) and setting the lifespan of the components (L_k):

$$Ann_k = \frac{ir}{1 - (1 + ir)^{L_k}} \tag{3}$$

2.2. Environmental optimal design

Economic analyses of renewable energy technologies aim to improve their economic competitiveness compared to traditional energy systems using fossil fuels. Several environmental problems, such as climate changes and desertification, are attributable to greenhouse gases emissions due to the combustion of fossils. For such reason some consumers are also starting to follow a rationality driven by the environmental sustainability. Indeed, in this section we propose an optimization model equivalent to the one described in the previous section where the environmentalist rationality is considered as the only criterion for the SHS design and management. An environmental cost

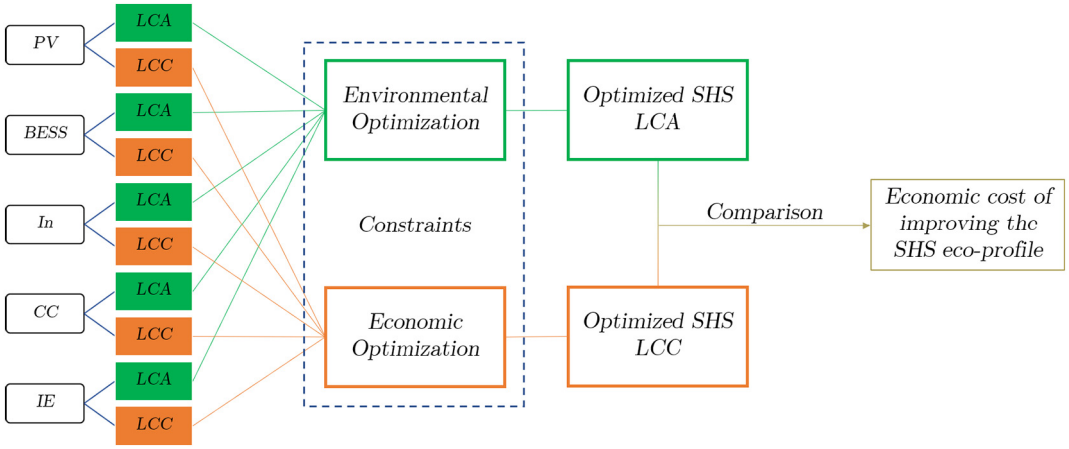

Fig. 1. Sketch of the applied methodology.

function, derived from the economic optimization, minimizing the environmental impact of SHSs is defined. Differently from the economic side, an optimized LCA based on a MILP does not exist so far and is developed in this study. Indeed the big novelty compared to DER-CAM environmental optimization (Jung and Villaran, 2017), which is based on direct carbon dioxide emissions, is that LCA allows to evaluate more environmental impact categories: all the direct and indirect environmental burdens, including raw materials consumption, over the SHS life cycle can be accounted for. The parameters involved in the environmental optimization problem are calculated through a LCA. According to ISO 14040 and ISO 14044 standards, LCA is composed of 4 steps (International Organization for Standardization, 2016a):

- *Goal and Scope definition*: the aim of the analysis is described including the definition of the system boundaries, the function of the system, the RF and the functional unit (FU).
- *Life Cycle Inventory (LCI)*: all the input and output flows of matter and energy involved in the system boundaries during the system lifespan are considered and quantified;
- *Life Cycle Impact Assessment (LCIA)*: the environmental impacts are calculated using standard assessment methods converting the amounts of energy and matter defined in the LCI phase to impact values;
- *Interpretation*: the LCA analyst should evaluate the results of the LCIA and all the previous steps of the analysis in order to adapt and modify the LCA model if necessary.

From a methodological point of view, LCA is equivalent to LCC as it is useful to assess the environmental impacts of a product, a system or an industrial process during their life cycle.

The function of the SHS is to provide electricity to the load and thus the RF, defined as the main output, is the amount of energy supplied to the user (Eq. (1)). The FU, set to 1 MWh, must be coherent with the RF but it doesn't depend on its amount; indeed it is a quantity used to make the SHS comparable with other product systems having the same function: for instance expressing the SHS environmental impacts per MWh of energy provided to the user allows the comparison with 1 MWh of energy from the electricity mix. The LCA analysis is performed using the software openLCA (GreenDelta GmbH, 2019) and the database Ecoinvent 3.4 (Ecoinvent, 2016) that allows to define the inputs and the outputs of a SHS, named Flows, represented in this case by the SHS components and energy flows. The production, the installation, the disposal and all the other operations involved in the Flows life cycle are named Processes and are also contained in the database. As any LCA software, openLCA evaluates the LCI of the SHS summarizing all the Elementary Flows (the liquid, gaseous or solid emissions to the environment and the raw materials) involved in the SHS life cycle. LCIA calculation methods multiply the Elementary Flows by impact factors and then sum the results to get an environmental impact value. As 1 MWh of energy to the load is set as FU of the study, the results must be divided by the RF.

The same result evaluated with this classical approach, could be obtained changing the order of the LCIA steps as following. For each Flow of the SHS, the unitary environmental impacts of the components and of energy are calculated, which means evaluating the burden of a 1 kW In, 1 kW CC, 1kWh BESS, 1 kW PV system and 1 kWh of electricity imported from the grid. After that, all the unitary impacts are multiplied by the respective Flow Quantity. In the end, the sum of these products is divided by the RF to respect the functional unit of the system. If the Quantities (cap_k) are not considered as inputs but as variables of this problem, this formulation of the LCIA can be seen as a cost function whose minimization provides the minimum SHS environmental impact and the optimal capacity of the PV system (cap_{pv}), of the BESS (cap_s), of the CC (cap_{cc}) and of the In (cap_{in}). The unitary environmental impacts are the optimization problem parameters. Nevertheless some adaptations are necessary to make these two equations equivalent and consequently comparable.

First, the unitary environmental impacts must be classified as variable impacts ($IVar_k$), which depend on the Quantity, and fixed impacts ($IFix_k$), which don't depend on the Quantity.

Moreover, in order to be coherent with Eq. (2), the life cycle impacts of the SHS Flows must be annualized. Whereas the economic costs of technologies are annualized by Eq. (3) considering an interest rate, to obtain annualized environmental costs of technologies it is enough to divide the impacts by the components lifespan (L_k). In this way, the longer is the components lifespan, the lower is their annualized impact.

As the SHS is supposed to be connected to the grid, the system can inject exported energy (EE) and use imported energy (IE) from it. The economic optimization problem includes the evaluation of some revenues coming from the electricity exportation to the grid. In LCA, the evaluation of the by-products is not always necessary, but two different methods exist: system expansion and allocation (Cederberg and Stadig, 2003) which are of difficult use in our case. Indeed using the system expansion is equivalent to set some environmental revenues because the exported electricity can be defined as an output flow that allows to avoid the production of the same amount of electricity from the mix, whose impact is consequently subtracted to the total. Nevertheless in this case the system expansion would lead to unrealistic results because the size of the PV system would be out of the range of residential applications and the SHS would lead to a very big negative environmental impact. For such reason allocation has been preferred by Rossi et al. (2020a, 2020b) to describe this multi-output process: using this approach, part of the impacts are allocated on the RF, and part of them on the by-product. Physical allocation is one of the most widely used allocation methods and consists on multiplying the impacts for an allocation factor, calculated as $RF/(RF + EE)$. The allocation factor has in the denominator the exported electricity which is an optimization variable: consequently the cost function would become non-linear. Non-linear problems are more complex to be solved than linear and their convergence is not guaranteed. The same issue exists if other types of allocation are chosen; for instance the economic allocation could be suitable for an environmental and economic cross analysis. In that case the allocation factor is similar, but *RF* and *EE* are multiplied by the respective costs without changing the non-linearity of the equation. For such reason, in order to preserve the problem linearity, no allocation will be done, which means that all the impacts will be allocated on the RF. According to these considerations, the environmental cost function (Eq. (4)), minimizing the SHS life cycle impact (I) can be defined using the same nomenclature adopted for the economic cost function (Eq. (2)).

$$I = \frac{\sum_{k\in\{SHS\}}(IFix_k \cdot i_k + IVar_k \cdot cap_k)EAnn_k + \sum_{t\in\tau_{yr}}(ui_t \cdot EI_t - ue_t \cdot EFI_t)}{RF} \tag{4}$$

where $EAnn_k$ is equal to $1/L_k$ and EI_t and EFI_t are the electricity mix environmental impact and the environmental revenues coming from the electricity injection to the grid. It's very important to stress that this approach is valid assuming that the components impacts ($IFix_k$ and $IVar_k$) are constant with the size of the system. This assumption is realistic if we limit our analysis to a residential SHS, whose power is typically in a range between 0 and 10 kW (Solar Power Europe, 2018).

2.3. System description and constraints

As underlined in the introduction, the system is composed of the In, the CC, the BESS and the PV system. Fig. 2 demonstrates that the PV system and the BESS are connected to a DC bus. The BESS requires a CC (a DC/DC converter) to interface with the PV system because they have a different voltage. The DC bus is connected through the In (a DC/AC converter) to an AC bus exchanging electricity with the load and the grid. Fig. 2 also demonstrates that some energy flows are bidirectional:

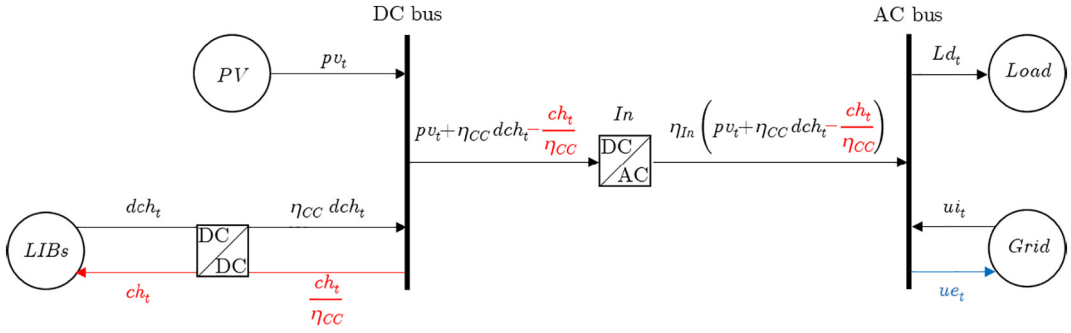

Fig. 2. Graphical description of a grid-connected SHS.

batteries can be charged and discharged depending on the SHS energy balance. Furthermore, the electricity can be exported to the grid or imported from it. Fig. 2 also provides quantitative information about the energy flows in the system, which allow to determine the problem constraints.

As *n* different types of LIBs are evaluated, each one of them is considered as a different BESSs having the following constraints. The battery energy flows must respect the storage energy balance (Eq. (5)); this reservoir model is also constrained by the maximum storage capacity (Eq. (6)) and the maximum power allowed by the batteries (Eq. (7)), as well as inequalities precluding simultaneous charging and discharging (Eqs. (8)–(9)). Indeed α is a binary variable assuming the value 0 during the discharge phase and 1 during the charge phase and *M* can be set to an indefinitely large value.

for j=1:n

$$soc_{t,j} = soc_{t-1,j} + ch_{t,j}\cdot\eta_{s,c} - \frac{dch_{t,j}}{\eta_{s,d}} \tag{5}$$

$$MiSoc\cdot cap_{s,j} \le soc_{t,j} \le cap_{s,j} \tag{6}$$

$$ch_{t,j}, dch_{t,j} \le cap_{s,j}\cdot PCr \tag{7}$$

$$ch_{t,j} \le \alpha\cdot M \tag{8}$$

$$dch_{t,j} \le (1-\alpha)\cdot M \tag{9}$$

where soc_t is the battery state of charge, $ch_{t,j}$ and $dch_{t,j}$ are the charge and discharge power of the battery *j*, $\eta_{s,c}$ and $\eta_{s,d}$ are the batteries charge and discharge efficiency and *MiSoc* and *PCr* are the minimum allowed battery state of charge and the maximum batteries rated power.

The total charge (ch_t) and discharge (dch_t) power flows exchanged by the ESS is given by the sum of the power flows exchanged with the single BESSs (Eqs. (10), (11)):

$$dch_t = \sum_{j=1}^{n} dch_{t,j} \tag{10}$$

$$ch_t = \sum_{j=1}^{n} ch_{t,j} \tag{11}$$

In this environmental optimization the impacts of the components are annualized dividing by their lifespan and for such reason these parameters are fundamental to determine the solution. Nevertheless, the batteries degradation depends on their operational conditions and can be calculated as function of the optimization variables, which makes the problem non-linear. In order to guarantee the linearity, and consequently the convergence of the problem, the batteries lifespan has to be fixed in a target value. This modeling technique is applied by Cardoso et al. (Cardoso et al., 2018) and adds an new constraint to their problem (Eq. (12)):

$$\sum_{t\in\tau_{yr}} dch_t \le \frac{cap_s}{cap_s^r}\frac{\overline{T}}{L_s}\cdot\frac{\left(\overline{Q}-\theta_s e^{\frac{E_a}{RK}}\sqrt{L_s}\right)V}{\left(\alpha_s K^2+\beta_s K+\gamma_s\right)e^{(\delta_s K+\varepsilon_s)PCr}} \tag{12}$$

where cap_s^r is the reference battery capacity, $\overline{T}$ is the reference time of the analysis, $\overline{Q}$ is the maximum acceptable degradation level and *V* is the reference voltage of the battery. The parameters θ_s, ε_s, α_s, β_s, γ_s, ε_s and δ_s are the natural and ageing parameters of LIBs whereas E_a, *K* and *R* are the activation energy, the cell temperature and the gas constant.

Then the variable N^0 is set. It represents the maximum number of cycles per year depending on the target life and the maximum capacity fade (Eq. (13)):

$$N^0 = \frac{1}{cap_s^r}\frac{\overline{T}}{L_s}\cdot\frac{\left(\overline{Q}-\theta_s e^{\frac{E_a}{RK}}\sqrt{L_s}\right)V}{\left(\alpha_s K^2+\beta_s K+\gamma_s\right)e^{(\delta_s K+\varepsilon_s)PCr}} \tag{13}$$

By the combination of Eqs. (12) and (13), the constraint (12) can be simplified to Eq. (14):

$$\sum_{t\in\tau_{yr}} dch_t \le cap_s\cdot N^0 \tag{14}$$

The ageing parameters are defined by Cardoso et al. (2018) for generic LIBs considering both the cyclic and calendar degradation of the devices. Nevertheless several materials can be used for the electrodes production and relevant differences can be noted concerning the cyclic battery ageing, whereas the natural degradation is approximately the same for every LIB (Rossi et al., 2020a, 2020b). Rossi et al. (2020a, 2020b) provide information about the number of cycles which can be performed in standard operative conditions by the main types of LIBs on the market (temperature of 298 K, $MiSoc = 20\%$ and $PCr = 1\ h^{-1}$). Consequently, a correction factor k_j representative of the selected battery chemistry is defined as the ratio between the generic LIBs cycle life in standard conditions, evaluated using Eq. (13), and the reference values adopted by Rossi et al. (2020a, 2020b). Therefore, the number of cycles performed by each battery type for generic operative conditions is calculated (Eq. (15)):

for $j = i : n$

$$N_j^0 = \frac{1}{cap_s^r}\frac{\overline{T}}{L_s}\cdot\frac{\left(\overline{Q}-\theta_s e^{\frac{E_a}{RK}}\sqrt{L_s}\right)V}{k_j\left(\alpha_s K^2+\beta_s K+\gamma_s\right)e^{(\delta_s K+\varepsilon_s)PCr}} \tag{15}$$

Concluding, the constraint used to consider the battery ageing in our optimization problem (Eq. (16)) is obtained replacing N^0 with N_j^0 in Eq. (14):

for $j = i : n$

$$\sum_{t \in \tau_{yr}} dch_{t,j} \leq cap_{s,j} \cdot N_j^0 \tag{16}$$

After having set the constraints of the BESS, a constraint for the power of the CC is necessary: according to Eq. (17), the CC capacity must be always greater than or equal to the inlet power: as the CC can be crossed by a bi-directional flow, the input power is equal to dch_t during the discharge phase, and to ch_t/η_{cc} during the battery charge (Fig. 2):

$$dch_t + \frac{ch_t}{\eta_{cc}} \leq cap_{cc} \tag{17}$$

where η_{cc} is the efficiency of the CC.

Concerning the energy generation, the PV productivity profile (pv_t) is constrained by the environmental conditions as it is calculated as the product of the capacity and the productivity of a 1 kW system (SR_t), which is typical of the installation site (Eq. (18)).

$$pv_t \leq cap_{pv} \cdot SR_t \tag{18}$$

Moreover, the In capacity must be constrained to be greater than or equal to the input power (Eq. (19)) whereas the energy balance of the AC bus (Eq. (20)) constrains the SHS to provide to the user the power absorbed by the load:

$$pv_t + \eta_{cc} \cdot dch_t - \frac{ch_t}{\eta_{cc}} \leq cap_{in} \tag{19}$$

$$Ld_t = ui_t - ue_t + \eta_{\text{in}} \cdot \left(pv_t + \eta_{cc} \cdot dch_t - \frac{ch_t}{\eta_{\text{cc}}} \right) \tag{20}$$

where η_{in} is the efficiency of the In.

Concluding, a last constraint (21) is necessary to set the capacity cap_k to 0 when, according to the value assumed by i_k, the component is not purchased.

$$cap_k \leq i_k \cdot M \tag{21}$$

2.4. Economic and environmental optima comparison

The result of the economic and environmental optimization models is the definition of the most sustainable and cost-effective configurations of the SHS. Particularly, the following outputs can be pointed out:

- the SHS configuration corresponding to the minimum environmental impact (Environmental Optimum);
- the life cycle impact and cost of the Environmental Optimum per MWh of energy provided to the load;
- the SHS configuration corresponding to the minimum economic cost (Economic Optimum);
- the life cycle impact and cost of the Economic Optimum per MWh of energy provided to the load.

In order to provide a general evaluation of the SHS, including both environmental and economic issues, the results calculated by the optimization models are represented in a Cartesian diagram having environmental impacts and costs as x and y axes: the Environmental Optimum will be addressed as P_1 and the Economic Optimum as P_2. Furthermore the SHSs are compared to the Grid whose representative point, addressed as P_g, is defined by the electricity mix average environmental impact and tariffs. This representation is very effective to assess how the SHS cost changes depending on its environmental impact.

Then, the effect of the variation of the costs of technologies and of the energy tariffs on the results will be assessed. Three LIBs future cost profiles have been proposed by NREL (National Renewable Energy Laboratory (NREL), 2019) supposing that, in long term scenarios, the LIBs costs could be about 80%, 40% and 20% of the current value. Furthermore, NREL also estimates that the costs of crystalline PV, which decreased fast in the last years, could become 65% of the current value in long term (National Renewable Energy Laboratory (NREL), 2018).

Two strategies have been adopted to simulate tariffs variations: first the electricity consumption costs and the revenues coming from the injection to the grid have been varied proportionally, then the revenues have been gradually lowered up to zero keeping the tariffs constant (Comello and Reichelstein, 2017). According to these assumptions, the following scenarios have been defined in Table 1 applying the multiplication factors a_1, a_2, a_3 and a_4 respectively to the tariffs, the revenues, the LIBs and the PV costs.

From the Economic and Environmental cost functions (Eqs. (2), (4)) it is clear that only the economic optimal design is affected by the variations of costs and tariffs; as consequence, economic optimal design has been performed for all the previous scenarios and the distance from the minimum possible environmental impact, represented by the Environmental Optimum, is estimated.

3. Case study

After the general methodology is explained, a case study has been identified in order to test it in a realistic optimization design problem. As underlined in the Introduction, this paper grounds on the environmental assessment proposed by Rossi et al. (2020a, 2020b) where a grid-connected SHS equipped with NCA batteries has been evaluated as the most sustainable Nano-grid configuration in case the user is represented by a family of three people in Siena (Italy). Rossi et al. (2020a, 2020b) obtained their results using a methodology involving the system design, modeling and LCA. In the perspective of using optimization to improve the SHS eco-profile compared to other design methods, the innovative methodology described in the previous section has been applied to the same case study of Rossi et al. (2020a, 2020b). Nevertheless, a more accurate load profile, obtained through a detailed statistical analysis and direct measurements of SHSs, has been used (Quoilin et al., 2016). Quoilin et al. (2016) provide for Italy several load profiles with hourly power absorption data: among them, one profile whose integral over the year is equal to the average yearly energy consumption (European Commission, 2018) of a user composed of three people has been selected. In this optimization problem, the productivity profile of a 1 kW PV system is required as input (Eq. (17)) and is calculated using TRNSYS16 (University of Wisconsin-Madison, 2007), whose library contains Meteonorm (2006) meteorological data and models for PV performances estimation. Concerning the BESS, all the LIBs analyzed by Peters and Weil (2018) and used by Rossi et al. (2020a, 2020b), are evaluated as candidates for this SHS application

Table 1
Multiplication factors adopted for the sensitivity analysis.

Scenario	a_1	a_2	a_3	a_4	Description
A	1.25	1.25	1.00	1.00	Moderate increase of tariffs.
B	1.50	1.50	1.00	1.00	Strong increase of tariffs.
C	1.00	0.60	1.00	1.00	Moderate reduction of feed-in remunerations.
D	1.00	0.30	1.00	1.00	Strong reduction of feed-in remunerations.
E	1.00	0.00	1.00	1.00	Cancellation of feed-in remunerations.
F	1.00	1.00	0.80	0.65	Pessimistic decrease of technologies cost.
G	1.00	1.00	0.40	0.65	Realistic decrease of technologies cost.
H	1.00	1.00	0.20	0.65	Optimistic decrease of technologies cost.

and the same nomenclature adopted by these authors has been maintained.

3.1. LCA goal and scope definition

The goal and scope of the cradle to grave optimized LCA analysis performed in this study is calculating the minimum environmental impact assumed by a SHS in the described conditions and the respective configuration. In order to do this, the environmental burden of the PV system, the In and the CC must be evaluated per kW of rated power whereas the BESS and the electricity mix impact must be assessed per kWh. These impact have been assessed using a classic cradle to grave LCA approach and represent inputs for the optimized LCA. In other words, this optimized LCA whose functional unit is 1 MWh of electricity provided to the load, is based on five separated LCA studies. Most of the impacts related to the construction (CO), the operation (OP) and end of life (EoL) of the SHS are considered as variable. In the range of residential PV systems, the impacts related to the installation, the transportation to the site and the maintenance are the only considered as independent from the size of the system. Nevertheless, because of their high uncertainty and minor relevance compared to the other impacts, they have been neglected in LCA similarly to Rossi et al. (2020a, 2020b).

3.2. Life cycle inventory

The LCI of this environmental assessment is based on that one published by Rossi et al. (2020a, 2020b) about the whole SHS; this inventory has been disassembled in order to get a different LCI for every element of the analyzed system. Furthermore, an updated version of the database (Ecoinvent 3.4 (Ecoinvent, 2016)) has been used to model the SHS environmental performances. Particularly, the CO of LIBs has been modelled thanks to the database file provided by Peters and Weil (2018) and imported in openLCA (GreenDelta GmbH, 2019); their OP don't imply any environmental impact whereas the EoL processes have been carefully evaluated grounding on Huang et al. (2018) and Weber et al. (2018) studies. Concerning the PV system, the In and the CC, their CO was modelled directly using Ecoinvent 3.4 (Ecoinvent, 2016) processes; similarly to the BEES no burdens occur during the OP whereas the references for EoL are respectively Latunussa et al. (2016) and Tschümperlin et al. (2016). The only impact occurring during the SHS operation deals with the electricity consumption from the grid. Ecoinvent 3.4 provides a detailed inventory to evaluate the impact of electricity mixes, including the Italian one that was used for this purpose. As Ecoinvent market processes are used, the embedded transports involved in the CO, OP and EoL phases is already included in the inventory.

3.3. Life cycle impact assessment

Similarly to Rossi et al. (2020a, 2020b), the ReCiPe Endpoint (Pre-sustainability, ReCIPE 2017, 2017) calculation method has been applied with a Europe H/A normalization and weighting set, aiming to evaluate results as single scores (Stranddorf et al., 2005). This choice is particularly useful to compare in a clearer way two Product Systems including all the impact categories proposed by the LCIA method, at the price of increasing the uncertainty of the LCA model. In this study, an updated version of ReCiPe (2016) (Pre-sustainability, ReCIPE 2017, 2017) compared to that used by Rossi et al. (2020a, 2020b) has been used. Indeed, this choice is necessary to compare coherently the environmental impacts of SHSs designed using a classic and an optimized approach. Furthermore ReCiPe has been used because it includes the evaluation of seventeen impact categories, being the most complete among all the LCIA methods (Pre-sustainability, ReCIPE 2017, 2017).

3.4. Life cycle costing

Concerning the economic optimization parameters, the costs of the SHS are set grounding on a NREL (NREL, 2016) benchmark LCC study of a PV system. In this NREL analysis, several types of costs are accounted to calculate the total. Particularly in this paper the cost of technologies have been considered as variable and include the manufacturing expenses afforded by the producers, the profits they wants to get by selling their products and the total amount of taxes that burden on the product (including a fee for the components disposal). Contrarily the costs related to the supply chain, the installation, the marketing and permitting processes costs are supposed to be fixed. NREL provides information about the costs of two different PV systems; the first one doesn't include the BESS whereas the second one does: the LIBs costs are estimated by the difference. Nevertheless NREL considers generic LIBs cells in its benchmark analysis; Xu et al. (2017) instead published a very interesting study where LIBs costs are estimated depending on the battery chemistry. Since many types of LIBs are evaluated, the costs of the cells proposed by NREL have been replaced by the costs proposed by Xu et al. (2017). Concerning the CC, as its cost is not explicitly defined in the NREL analysis but it's included in the electrical balance of system, a market component pointed out by Rossi et al. (2020a, 2020b) as a representative converter has been selected for the cost estimation (Mastervolt, 2019). Concerning the tariffs, the Italian Energy Manager (Gestore Mercati Energetici, 2019) provides historical data about the market value of energy. The remuneration coming from the electricity exportation to the grid is equal to the energy market value, whereas taxes must be added in case of electricity withdrawal (Gestore dei servizi energetici spa, 2007). All the costs and impacts are summarized in Table 2 whereas Table 3 collects all the LIBs ageing parameters, the components lifespan and efficiency values.

4. Results and discussion

The previous sections provide a detailed description of LCA, LCC and MILP which are usually performed separately. The integration of these methodologies in a cross-evaluation of the economic and environmental optimal designs is proposed for the first time and therefore its detailed definition represents itself one of the results of the study. Furthermore, applying this methodology to a case study, some interesting findings and results have been evaluated.

Table 2
Environmental impact and cost parameters.

Costs			Impacts		
Parameter	Value	Unit	Parameter	Value	Unit
$CFix_s$	5766.3	EUR	$IFix_s$	0	Pts
$CVar_{s,1}$	610.4	EUR/kWh	$IVar_{s,1}$	20.1	Pts/kWh
$CVar_{s,2)}$	610.4	EUR/kWh	$IVar_{s,2}$	24.1	Pts/kWh
$CVar_{s,3}$	898.4	EUR/kWh	$IVar_{s,3}$	32.1	Pts/kWh
$CVar_{s,4}$	529.4	EUR/kWh	$IVar_{s,4}$	23.2	Pts/kWh
$CVar_{s,5}$	583.4	EUR/kWh	$IVar_{s,5}$	18.2	Pts/kWh
$CVar_{s,6}$	592.4	EUR/kWh	$IVar_{s,6}$	15.5	Pts/kWh
$CVar_{s,7}$	592.4	EUR/kWh	$IVar_{s,7}$	14.0	Pts/kWh
$CFix_{pv}$	4128.6	EUR	$IFix_{pv}$	0.0	Pts
$CVar_{pv}$	1216.6	EUR/kW	$IVar_{pv}$	210.8	Pts/kW
$CFix_{in}$	1830.5	EUR	$IFix_{in}$	0.00	Pts
$CVar_{in}$	539.4	EUR/kW	$IVar_{in}$	24.6	Pts/kW
$CFix_{cc}$	479.5	EUR	$IFix_{cc}$	0.0	Pts
$CVar_{cc}$	141.3	EUR/kW	$IVar_{cc}$	9.6	Pts/kW
EC_t	Gestore Mercati Energetici, 2019	EUR/kWh	EI_t	4.2e-02	Pts/kWh
FI_t	Gestore Mercati Energetici, 2019	EUR/kWh	EFI_t	0.0	Pts/kWh

Table 3
Other operative parameters.

Parameter	Value	Unit	Reference
V	5	V	Cardoso et al., 2018
$\overline{Q}$	20	%	Cardoso et al., 2018
α	5.04e−06	$Ah^{-1}K^{-2}$	Cardoso et al., 2018
β	−2.998e−03	$Ah^{-1}K^{-1}$	Cardoso et al., 2018
γ	0.446	Ah^{-1}	Cardoso et al., 2018
δ	−6.7e−03	$K^{-1}h$	Cardoso et al., 2018
ε	2.35	h	Cardoso et al., 2018
θ	17,127	$yr^{-1/2}$	Cardoso et al., 2018
k, 1	0.125	–	–
k, 2	0.250	–	–
k, 3	0.075	–	–
k, 4	0.750	–	–
k, 5	0.150	–	–
k, 6	0.375	–	–
k, 7	0.250	–	–
E_a	24,500	$Jmol^{-1}$	Cardoso et al., 2018
cap_s^r	712.9	Wh	Cardoso et al., 2018
PCr	0.3	h^{-1}	Cardoso et al., 2018
K	298	K	Cardoso et al., 2018
$\overline{T}$	1	yr	Cardoso et al., 2018
L_{pv}	25	yrs	Rossi et al., 2020a, 2020b
L_s	10	yrs	Cardoso et al., 2018
L_{in}	10	yrs	Rossi et al., 2020a, 2020b
L_{cc}	10	yrs	Rossi et al., 2020a, 2020b
η_{cc}	0.95	–	Rossi et al., 2020a, 2020b
η_{in}	0.90	–	Rossi et al., 2020a, 2020b
$\eta_{s,\,c}$	0.90	–	Rossi et al., 2020a, 2020b
$\eta_{s,\,d}$	0.90	–	Rossi et al., 2020a, 2020b
MiSoc	0.20	–	Cardoso et al., 2018

4.1. Reference case

In this subsection, the economic and the environmental optimal designs are compared considering a reference case where the input parameters assume the values listed in Tables 2 and 3. First of all the optimal configurations designed with the optimization program are illustrated in Table 4.

These results underline that, as assumed in the methodological section, both the Environmental and Economic Optima can be classified as residential installations because the PV power is in a range between 0 and 10 kW. In this phase of the discussion, these two configurations will be analyzed separately. Concerning the Environmental Optimum, a 3.25 kW PV system is installed; this value is about 50% lower than the size of the PV system designed with the method used by Rossi et al. (2020a, 2020b) (5.94 kW). Also the BESS installed capacity (8.66 kWh) is lower compared to the system designed by Rossi et al. (2020a, 2020b) for daily storage (12.58 kWh). According to the optimization results, M-B (NCM) batteries are identified by the model as the most sustainable LIBs for this SHS. This result partially confirms the conclusions of Rossi et al. (2020a, 2020b): indeed, although they assessed Bauer (NCA) batteries as the most sustainable technology, they stress the point that mixing cobalt and other less rare materials represents the best trade off between the batteries LCA parameters. Concerning the Economic Optimum, a battery-free PV system, whose power is 0.88 kW, is the configuration which minimizes the SHS costs. From an economic point of view, exchanging energy with the grid is more convenient than having a high self-consumption rate, which is assessed to 79% for the Environmental Optimum and 28% for the Economic one.

Table 4
Economic and environmental optima configurations.

Flow	Environmental optimum	Economic optimum	Unit
	Quantity	Quantity	
M-B (NCM)	8.66	0.00	kWh
PV	3.25	0.88	kW
In	1.44	0.54	kW
CC	1.61	0.00	kW

A cross-evaluation of the environmental and economic performances of the system allowing for the identification of the best solution was made on the basis of the results reported in Fig. 3. Indeed, the impacts and the costs of the SHSs and the Italian electricity mix, they are expressed as three points in the Cartesian diagram represented in Fig. 3. The results collected in Table 4, although very interesting, just represent the capacity of the SHSs components.

In their study, Rossi et al. (2020a, 2020b) calculated an environmental impact of 22.81 Pts/MWh that is slightly higher than the minimum environmental impact calculated in this study; nevertheless Rossi et al. (2020a, 2020b) considered a physical allocation to evaluate the environmental benefits coming from the exportation of electricity to the grid. As underlined in the methodological section, the use of allocation in the optimization problem would lead to a non-linear cost function, but an allocation can be done afterwards to compare the results with those evaluated by Rossi et al. (2020a, 2020b). Indeed, multiplying the results by the allocation factor $A = RF/(EE + RF)$, a minimum environmental impact of 16.52 Pts/MWh is calculated (about 30% lower than Rossi et al., 2020a, 2020b). Fig. 3 also allows to compare the Environmental and the Economic Optima with a benchmark case, where the user is supplied by the utility. According to the results, the burden of the Environmental Optimum is lower than the impact of the electricity mix (53%), whereas its cost is much higher (7.16 times the energy costs). Concerning the Economic Optimum, the environmental impact and the cost of the SHS are evaluated as about 78% and 88% of the average energy tariff. The costs of these optimal configurations can be compared with those of a reference SHS described in an annual report focused on levelized cost of energy sources (LAZARD Inc, 2019): even though specific data for Italy are not available in literature, this report proposes a range of values that a battery assisted PV installation can present. These costs vary from 412 to 736 EUR/MWh and are between those of the economic and the environmental optima. For all these reasons, it is possible to conclude that the Economic Optimum is in general more sustainable than the grid whereas the economic impact represents a very critical value for the Environmental Optimum. The interpretation of these results leads to the conclusion that mitigating the environmental impact of a SHS moving from the Economic to the Environmental Optimum by the use of ESSs is quite expensive from an economic point of view. For such reason, in the next section we'll try to mitigate the environmental impact of the Economic Optimum by the variation of cost parameters.

4.2. Sensitivity analysis

The results evaluation brought to the conclusion that optimized LCA is effective to minimize the SHS impact as the Environmental Optimum is more sustainable than the Economic Optimum and than the grid, but its costs are much higher. Both the Economic Optimum costs and impacts instead are lower compared to the grid. Consequently we can conclude that the two optimal designs are very far from them but in the future the costs of technologies and the energy tariffs may change significantly and the results might be affected by this change. Applying economic optimal design to the scenarios proposed in Table 1, the resulting SHS configurations are illustrated in Table 5.

Analysing the SHS economic optimal designs it's possible to point out that a breakdown of the costs of technologies is the only case where BEES becomes economically profitable; indeed, in Scenario H an ESS with relevant capacity is included in the economic optimal design. Another observation is that, because of the lower cost of the materials, the battery type minimizing the SHS cost in this scenario is Bauer (LTO), differently from the environmental optimal design where M-B (NCM) is assessed as the most sustainable LIB. Thus the

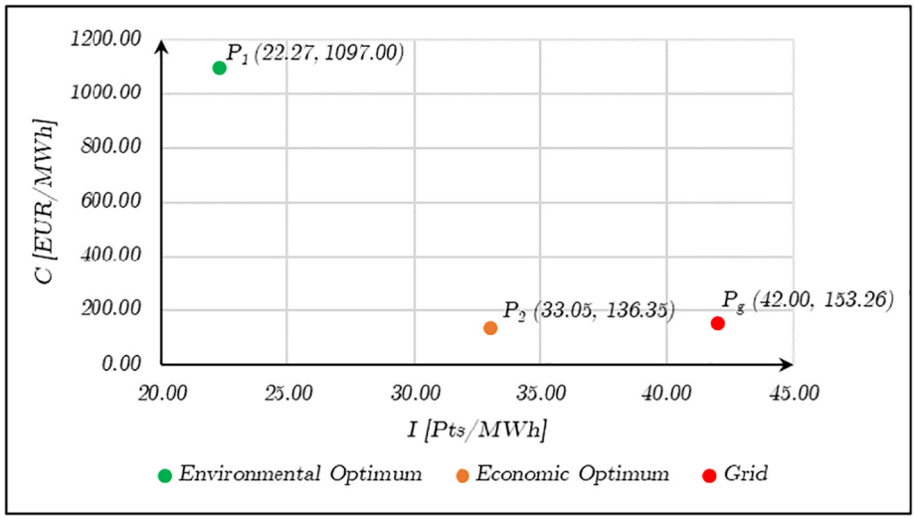

Fig. 3. Graphical representation of economic and environmental optima impacts and costs compared to the Italian electricity mix.

Table 5
Economic optimum configurations in the considered scenarios: A) Moderate increase of tariffs; B) Strong increase of tariffs; C) Moderate reduction of feed-in remunerations; D) Strong reduction of feed-in remunerations; E) Cancellation of feed-in remunerations; F) Pessimistic decrease of technologies cost; G) Realistic decrease of technologies cost; H) Optimistic decrease of technologies cost.

Flow	A	B	C	D	E	F	G	H	Unit
Bauer (LTO)	0.00	0.00	0.00	0.00	0.00	0.00	0.21	5.04	kWh
PV	1.16	1.46	0.84	0.81	0.79	1.33	1.36	2.27	kW
In	0.71	0.90	0.51	0.49	0.48	0.70	0.70	0.78	kW
CC	0.00	0.00	0.49	0.00	0.00	0.00	0.07	0.82	kW

SHSs cross-analysis allows to conclude that, in this scenario, the choice of the BESS depends on the rationality adopted designing the SHS.

Fig. 4 graphically demonstrates that the environmental impact calculated for the SHS economic optimal configuration in Scenario H is the closest to the minimum, which results from the environmental optimal design and is represented by a green line in Fig. 4. Indeed, its environmental impact is 25.72 Pts/MWh, about 20% less than the Reference case, whereas the Environmental Optimum and the grid have an impact of 22.27 PTs/MWh and 42.00 Pts/MWh respectively. Concerning the economic considerations, the Economic Optimum in scenario H has a cost of 117.95 EUR/MWh, lower than the Reference case (136.35 EUR/MWh) and the grid electricity (153.26 EUR/MWh). This is due to the positive effect of producing and storing energy with very low cost PV modules and LIBs. Contrarily, other less optimistic scenarios do not allow a significant environmental impact mitigation. Increasing the energy tariffs and revenues is slightly effective to lower the SHS environmental impact, whereas decreasing the revenues from the injection to the grid is assessed to increase the environmental impact.

5. Conclusions

In this paper, a new methodological framework for the optimal design of a SHS is proposed, where a MILP approach is used to minimize the life cycle environmental impacts and the economic costs of a SHS. Moreover an innovative approach for the comparison of

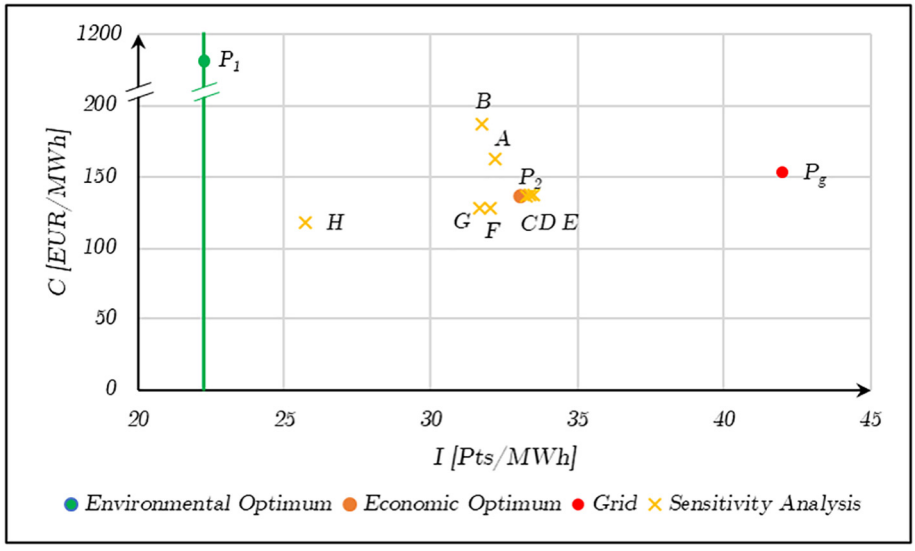

Fig. 4. Graphical representation of the sensitivity analysis results compared to the reference case. The analyzed scenarios are: A) Moderate increase of tariffs; B) Strong increase of tariffs; C) Moderate reduction of feed-in remunerations; D) Strong reduction of feed-in remunerations; E) Cancellation of feed-in remunerations; F) Pessimistic decrease of technologies cost; G) Realistic decrease of technologies cost; H) Optimistic decrease of technologies cost.

the optimal configurations is also included. The environmental and economic optimal designs were applied to a case study comprising a SHS serving a 3 users building in Siena (Italy). According to the cross-evaluation analysis, lowering the environmental impact moving from the grid to the economic optimum is possible using a simple PV system that would bring an economic benefit as well. A further impact mitigation is possible moving from the economic optimum to the environmental optimum thanks to the installation of a more powerful PV system and a BESS, but the cost of this environmental improvement is very high. Therefore other strategies have been adopted to mitigate the economic optimum environmental impact: reducing the costs of technologies and varying the energy tariffs. Changing the tariffs and the revenues allows, in some cases, to enhance the PV power; nevertheless, without a relevant decrease of technologies costs, this operation is not very effective for the environment. Indeed, a cost reduction of batteries and of PV allows the economic optimum environmental impact to get much closer to the minimum also having an economic advantage. One possible extension of the study would be using this methodology to investigate the role of SHSs and ESSs in energy communities, analysing the interaction between several producers, consumers and ESSs.

Declaration of competing interest

None.

Acknowledgements

F.R., A.S. and R.B. acknowledge MIUR Grant - Department of Excellence 2018–2022. F.R. is grateful for the Ph.D. grant within the “Progetto Pegaso” funded by Regione Toscana.

CRediT author statement

Federico Rossi: Conceptualization, Methodology, Writing - Original Draft. **Miguel Heleno:** Software, Supervision, Resources. **Riccardo Basosi:** Writing - Review & Editing, Supervision. **Adalgisa Sinicropi:** Writing - Review & Editing, Supervision.

Appendix A. Supplementary data

The Nomenclature used in this paper is collected in a Supporting Information file to facilitate the readers in the comprehension of the text. Supplementary data to this article can be found online at https://doi.org/10.1016/j.scitotenv.2020.140569.

References

Azimoh, Chukwuma Leonard, et al., 2014. An assessment of unforeseen losses resulting from inappropriate use of solar home systems in South Africa. Appl. Energy 136, 336–346. https://doi.org/10.1016/j.apenergy.2014.09.044 URL. http://www.sciencedirect.com/science/article/pii/S0306261914009921 (ISSN: 0306-1619).

Bauer, Christian, 2010. ökobilanz von lithium-ionen batterien. URL. http://www.thelma-emobility.net/pdf/Vergleich_LCA_ElektroPW_EKZ_PSI_Empa.pdf (visited on 03/20/2019).

Cardoso, Gonçalo, et al., 2018. Battery aging in multi-energy microgrid design using mixed integer linear programming. Appl. Energy 231, 1059–1069. https://doi.org/10.1016/j.apenergy.2018.09.185 URL. http://www.sciencedirect.com/science/article/pii/S0306261918315058 (ISSN: 0306-2619).

Cederberg, Christel, Stadig, Magnus, 2003. System expansion and allocation in life cycle assessment of milk and beef production. Int. J. Life Cycle Assess. 6, 350–356. https://doi.org/10.1007/BF02978508 URL. https://link.springer.com/article/10.1007/BF02978508#citeas (ISSN: 1614-7502).

Comello, Stephen, Reichelstein, Stefan, 2017. Cost competitiveness of residential solar pv: the impact of net metering restrictions. Renew. Sust. Energ. Rev. 75, 46–57. https://doi.org/10.1016/j.rser.2016.10.050 URL. http://www.sciencedirect.com/science/article/pii/S136403211630702X (ISSN: 1364-0321).

Dainelli, N., et al., 2017. Exergo-economic evaluation of the cost for solar thermal depuration of water. Energies 10 (9). https://doi.org/10.3390/en10091395 (ISSN: 19961073).

Diouf, Boucar, Avis, Christophe, 2019. The potential of li-ion batteries in ecowas solar home systems. J. Energy Storage 22, 295–301. https://doi.org/10.1016/j.est.2019.02.021 URL. http://www.sciencedirect.com/science/article/pii/S2352152X18307369 (ISSN: 2352-152X).

Ecoinvent, 2016. Ecoinvent 3.4 report of changes. URL. https://www.ecoinvent.org/database/older-versions/ecoinvent-34/report-of-changes-ecoinvent-34/report-of-changes-ecoinvent-34.html.

Ellingsen, Linda Ager-Wick, et al., 2014. Life cycle assessment of a Lithium-Ion Battery Vehicle Pack. Journal of Industrial Ecology 18 (1), 113–124. https://doi.org/10.1111/jiec.12072 eprint. https://onlinelibrary.wiley.com/doi/pdf/10.1111/jiec.12072 URL. https://onlinelibrary.wiley.com/doi/abs/10.1111/jiec.12072.

European Commission, 2018. Eurstat. URL. https://ec.europa.eu/eurostat (visited on 683 03/20/2019).

Gestore dei servizi energetici spa, 2007. GSE – Ritiro Dedicato, Manuale Utente. URL. https://www.gse.it/servizi-per-te/fotovoltaico/ritiro-dedicato (visited on 3/20/2019).

Gestore Mercati Energetici, 2019. Statistiche. URL. https://www.mercatoelettrico.org/It/download/DownloadStatYY.aspx (visited on 03/20/2019).

Goglio, P., et al., 2020. Advances and challenges of life cycle assessment (lca) of greenhouse gas removal technologies to fight climate changes. J. Clean. Prod. 244, 118896. https://doi.org/10.1016/j.jclepro.2019.118896 URL. http://www.sciencedirect.com/science/article/pii/S0959652619337667 (ISSN: 0959-6526).

GreenDelta GmbH, 2019. openLCA comprehensive user manual. URL. http://www.openlca.org/wp-content/uploads/2019/07/openLCA-1-9_User-Manual.pdf.

He, Guannan, et al., 2018. Electrochemical energy storage management. Nat. Energy 3 (May). https://doi.org/10.1038/s41560-018-0129-9 (ISSN: 2058-7546).

Huang, Bin, et al., 2018. Recycling of lithium-ion batteries: recent advances and perspectives. J. Power Sources 399, 274–286. https://doi.org/10.1016/j.jpowsour.2018.07.116 URL. http://www.sciencedirect.com/science/article/pii/S0378775318308498 (ISSN: 0378-7753).

International Organization for Standardization, 2016a. ISO 14040:2006 Environmental management - Life cycle assessment - Principles and framework. URL. https://www.iso.org/standard/37456.html (visited on 12/05/2019).

International Organization for Standardization, 2016b. Environmental management – life cycle assessment – requirements and guidelines. URL. https://www.iso.org/standard/38498.html (visited on 12/05/2019).

International Organization for Standardization, 2017. Buildings and constructed assets – service life planning – part 5: life-cycle costing. URL. https://www.iso.org/standard/38498.html.

Jacob, Ammu Susanna, Banerjee, Rangan, Ghosh, Prakash C., 2018. Sizing of hybrid energy storage system for a pv based microgrid through design space approach. Applied Energy. vol. 212 , pp. 640–653. https://doi.org/10.1016/j.apenergy.2017.12.040 URL. http://www.sciencedirect.com/science/article/pii/S0306261917317543 (ISSN: 0306-2619).

Jung, Jaesung, Villaran, Michael, 2017. Optimal planning and design of hybrid renewable energy systems for microgrids. Renew. Sust. Energ. Rev. 75, 180–191. https://doi.org/10.1016/j.rser.2016.10.061 URL. http://www.sciencedirect.com/science/article/pii/S1364032116307316 (ISSN: 1364-0321).

Kennedy, Ryan, et al., 2019. Multilevel customer segmentation for off-grid solar in developing countries: Evidence from solar home systems in Rwanda and Kenya. Energy. vol. 186 , p. 115728. https://doi.org/10.1016/j.energy.2019.07.058 URL. http://www.sciencedirect.com/science/article/pii/S0360544219313854 (ISSN: 0360-5442).

Khan, Imran, 2020. Impacts of energy decentralization viewed through the lens of the energy cultures framework: solar home systems in the developing economies. Renewable and Sustainable Energy Reviews. vol. 119 , p. 109576. https://doi.org/10.1016/j.rser.2019.109576 URL. http://www.sciencedirect.com/science/article/pii/S1364032119307841 (ISSN: 1364-0321).

Khan, Tahsina, et al., 2019. Determinants of microfinance facility for installing solar home system (shs) in rural Bangladesh. Energy Policy. vol. 132 , pp. 299–308. https://doi.org/10.1016/j.enpol.2019.05.047 URL. http://www.sciencedirect.com/science/article/pii/S0301421519303519 (ISSN: 0301-4215).

Latunussa, Cynthia E.L., et al., 2016. Life Cycle Assessment of an innovative recycling process for crystalline silicon photovoltaic panels. Sol. Energy Mater. Sol. Cells 156, 101–111. https://doi.org/10.1016/j.solmat.2016.03.020 (ISSN: 09270248).

Lawrence Berkeley National Laboratory (LBNL), 2019. Distributed energy resources - customer adoption model (DER-CAM). URL. https://building-microgrid.lbl.gov/projects/der-cam.

LAZARD Inc, 2019. Levelized cost of energy and levelized cost of storage 2019. URL. https://www.lazard.com/perspective/lcoe2019.

Majeau-Bettez, Guillaume, Hawkins, Troy R., Strømman, Anders Hammer, 2011. Life cycle environmental assessment of lithium-ion and nickel metal hydride batteries for plug-in hybrid and battery electric vehicles. Environ. Sci. Technol. 45 (10), 4548–4554. https://doi.org/10.1021/es103607c.

Maranghi, Simone, et al., 2019. Environmental profile of the manufacturing process of perovskite photovoltaics: harmonization of life cycle assessment studies. Energies 12 (19). https://doi.org/10.3390/en12193746 URL. https://www.mdpi.com/1996-1073/12/19/3746 (ISSN: 1996-1073).

Martinopoulos, Georgios, 2020. Are rooftop photovoltaic systems a sustainable solution for europe? A life cycle impact assessment and cost analysis. Appl. Energy 257, 114035. https://doi.org/10.1016/j.apenergy.2019.114035 URL. http://www.sciencedirect.com/science/article/pii/S0306261919317222 (ISSN: 0306-2619).

Mastervolt, 2019. Mastervolt charge regulator SCM 60 MPPT MB. URL. https://www.mastervolt.it/prodotti/regolatori-di-carica-solari/scm60-mppt-mb/.

Meteonorm, 2006. Meteonorm information. URL. https://meteonorm.com/ (visited on 03/20/2019).

Monge, Manuel, Gil-Alana, Luis A., 2019. Automobile components: Lithium and cobalt. Evidence of persistence. Energy 169, 489–495 ISSN: 0360-5442. https://doi.org/

10.1016/j.energy.2018.12.068 URL. http://www.sciencedirect.com/science/article/pii/S0360544218324344.
Nagapurkar, Prashant, Smith, Joseph D., 2019. Techno-economic optimization and environmental life cycle assessment (lca) of microgrids located in the us using genetic algorithm. Energy Conversion and Management. vol. 181 , pp. 272–291. https://doi.org/10.1016/j.enconman.2018.11.072 URL. http://www.sciencedirect.com/science/article/pii/S0196890418313244 (ISSN: 0196-8904).
Narayan, Nishant, et al., 2018. Estimating battery lifetimes in solar home system design using a practical modelling methodology. Applied Energy. vol. 228 , pp. 1629–1639. https://doi.org/10.1016/j.apenergy.2018.06.152 URL. http://www.sciencedirect.com/science/article/pii/S0306261918310225 (ISSN: 0306-2619).
National Renewable Energy Laboratory (NREL), 2018. Crystalline silicon photovoltaic module manufacturing costs and sustainable pricing: 1H 2018 benchmark and cost reduction road map. URL. https://www.nrel.gov/docs/fy19osti/72134.pdf.
National Renewable Energy Laboratory (NREL), 2019. Annual technology baseline: electricity. URL. https://atb.nrel.gov/electricity/2019/index.html?t=st (visited on 03/20/2019).
Ndwali, Kasereka, Njiri, Jackson G., Wanjiru, Evan M., 2019. Mu lti-objective optimal sizing of grid connected photovoltaic batteryless system minimizing the total life cycle cost and the grid energy. Renew. Energy https://doi.org/10.1016/j.renene.2019.10.065 URL. http://www.sciencedirect.com/science/article/pii/S0960148119315563 (ISSN: 0960-1481).
Notter, Dominic A., et al., 2010. Contribution of Li-Ion Batteries to the Environmental Impact of Electric Vehicles. Environ. Sci. Technol. 44 (19), 6550–6556. https://doi.org/10.1021/es903729a eprint:. https://doi.org/10.1021/es1029156 URL. https://doi.org/10.1021/es1029156.
NREL, 2016. Installed cost benchmarks and deployment barriers for residential solar photovoltaics with energy storage. URL. https://www.nrel.gov/docs/fy17osti/67474.pdf (visited on 03/20/2019).
O'Shaughnessy, Eric, et al., 2018a. Solar plus: Optimization of distributed solar pv through battery storage and dispatchable load in residential buildings. Applied Energy. vol. 213 , pp. 11–21. https://doi.org/10.1016/j.apenergy.2017.12.118 URL. http://www.sciencedirect.com/science/article/pii/S0306261917318421 ISSN: 0306-2619.
O'Shaughnessy, Eric, et al., 2018b. Solar plus: A review of the end-user economics of solar pv integration with storage and load control in residential buildings. Applied Energy. vol. 228 , pp. 2165–2175. https://doi.org/10.1016/j.apenergy.2018.07.048 URL. http://www.sciencedirect.com/science/article/pii/S0306261918310766 ISSN: 0306-2619.
Peters, Jens F., Weil, Marcel, 2018. Providing a common base for life cycle assessments of Li-Ion batteries. J. Clean. Prod. 171, 704–713. https://doi.org/10.1016/j.jclepro.2017.10.016 URL. http://www.sciencedirect.com/science/article/pii/S0959652617323077 (ISSN: 0959-6526).
Peters, Jens F., et al., 2017. The environmental impact of Li-Ion batteries and the role of key parameters – a review. Renew. Sust. Energ. Rev. 67, 491–506. https://doi.org/10.1016/j.rser.2016.08.039 URL. http://www.sciencedirect.com/science/article/pii/S1364032116304713 (ISSN: 1364-0321).
Petrollese, Mario, Cau, Giorgio, Cocco, Daniele, 2018. Use of weather forecast for increasing the self-consumption rate of home solar systems: an italian case study. Applied Energy. vol. 212 , pp. 746–758. https://doi.org/10.1016/j.apenergy.2017.12.075 URL. http://www.sciencedirect.com/science/article/pii/S0306261917317907 (ISSN: 0306-2619).
Pre-sustainability, ReCIPE 2017, 2017. A harmonized life cycle impact assessment method at midpoint and endpoint level. URL. https://www.pre-sustainability.com/download/Report_ReCiPe_2017.pdf (visited on 01/03/2020).
Quoilin, Sylvain, et al., 2016. Quantifying self-consumption linked to solar home battery systems: statistical analysis and economic assessment. Appl. Energy 182, 58–67. https://doi.org/10.1016/j.apenergy.2016.08.077 URL. http://www.sciencedirect.com/science/article/pii/S0306261916311643 (ISSN: 0306-2619).
Rossi, F., et al., 2019. Environmental impact analysis applied to solar pasteurization systems. J. Clean. Prod. 212. https://doi.org/10.1016/j.jclepro.2018.12.020 (ISSN: 09596526).
Rossi, Federico, et al., 2020a. Environmental analysis of a nano-grid: a life cycle assessment. Sci. Total Environ. 700, 134814. https://doi.org/10.1016/j.scitotenv.2019.134814 URL. http://www.sciencedirect.com/science/article/pii/S0048969719348053 (ISSN: 0048-9697).
Rossi, Federico, et al., 2020b. Life cycle inventory datasets for nano-grid configurations. Data Brief 28, 104895. https://doi.org/10.1016/j.dib.2019.104895 URL. http://www.sciencedirect.com/science/article/pii/S2352340919312508 (ISSN: 2352-3409).
Severson, Kristen A., et al., 2019. Data-driven prediction of battery cycle life before capacity degradation. Nat. Energy 4 (May), 383–391. https://doi.org/10.1038/s41560-019-0356-8 (ISSN: 2058-7546).
Solar Power Europe, 2018. Global market outlook for solar power 2018–2022. URL. https://www.solarpowereurope.org/wp-content/uploads/2018/09/Global-Market-Outlook-2018-2022.pdf.
Sovacool, Benjamin K., 2018. Success and failure in the political economy of solar electrification: Lessons from world bank solar home system (shs) projects in Sri Lanka and Indonesia. Energy Policy. vol. 123 , pp. 482–493. https://doi.org/10.1016/j.enpol.2018.09.024 URL. http://www.sciencedirect.com/science/article/pii/S0301421518306293 (ISSN: 0301-4215).
Stranddorf, Heidi K., Ho_mann, Leif, Schmidt, Andres, 2005. Impact categories, normalisation and weighting in LCA. URL. https://www2.mst.dk/udgiv/publications/2005/87-7614-574-3/pdf/87-7614-575-1.pdf (visited on 01/03/2020).
Toniolo, Sara, et al., 2020. In: Ren, Jingzheng, Toniolo, Sara (Eds.), Chapter 3 - Life Cycle Thinking Tools: Life Cycle Assessment, Life Cycle Costing and Social Life Cycle Assessment , pp. 39–56 https://doi.org/10.1016/B978-0-12-818355-7.00003-8 URL. http://www.sciencedirect.com/science/article/pii/B9780128183557000038.
Tschümperlin, Laura, Stolz, Philippe, Frischknecht, Rolf, 2016. Life Cycle Assessment of Low Power Solar Inverters (2.5 to 20 kW) Swiss Federal Office of Energy SFOE. (3.October). .
University of Wisconsin-Madison, 2007. TRaNsient SYstems simulation program. URL. http://sel.me.wisc.edu/trnsys/user-resources/index.html.
Weber, Selina, et al., 2018. Life cycle assessment of a vanadium redox flow battery. Environ. Sci. Technol. 52 (18), 10864–10873. https://doi.org/10.1021/acs.est.8b02073 (ISSN: 15205851).
Xu, Gaojie, et al., 2017. Li4Ti5O12-based energy conversion and storage systems: status and prospects. Coord. Chem. Rev. 343, 139–184. https://doi.org/10.1016/j.ccr.2017.05.006 URL. http://www.sciencedirect.com/science/article/pii/S0010854517301121 (ISSN: 0010-8545).
Zackrisson, Mats, et al., 2016. Life cycle assessment of lithium-air battery cells. J. Clean. Prod. 135, 299–311. https://doi.org/10.1016/j.jclepro.2016.06.104 (ISSN: 0959-6526).
Zhang, Di, et al., 2015. Optimal design of chp-based microgrids: multiobjective optimisation and life cycle assessment. Energy 85, 181–193. https://doi.org/10.1016/j.energy.2015.03.036 URL. http://www.sciencedirect.com/science/article/pii/S0360544215003308 (ISSN: 0360-5442).
Zubi, Ghassan, et al., 2019. The unlocked potential of solar home systems; an effective way to overcome domestic energy poverty in developing regions. Renewable Energy. vol. 132 , pp. 1425–1435. https://doi.org/10.1016/j.renene.2018.08.093 URL. http://www.sciencedirect.com/science/article/pii/S0960148118310437 (ISSN: 0960-1481).

4.1.4. Paper 5: LCA driven solar compensation mechanism for Renewable Energy Communities: the Italian case.

After the environmental and economic cross-evaluation of single-user installations, Paper 5, submitted to *Energy* journal, considers RECs and their effects at national level. Particularly, this study assumes that RECs members optimize the design and energy management to minimize their costs. The LCI is based on an Ecoinvent 3.6 and the environmental performances of RECs in Italy are assessed in terms of Global Warming Potential; different eco-profiles are calculated depending on the size and on the installation site. Since RECs members follow an economic rationality, RECs performances depend on the economic incentives proposed by the utility. The environmental benefits deriving from a large-scale diffusion of RECs are assessed first considering the current feed-in tariffs and then proposing a new feed-in tariffs framework. The main outcomes of the paper are:

- The environmental impact of RECs in terms of Global Warming Potential.
- The evaluation of RECs environmental benefits to the national energy system considering the current and the proposed feed-in tariffs.
- The evaluation of novel feed-in tariffs.

The Ph.D. is the first and corresponding author of the paper and contributed to the conceptualization, the development of the methodology, the results evaluation, and the writing of the paper.

LCA driven solar compensation mechanism for Renewable Energy Communities: the Italian case

Federico Rossi[a,c,d,*], Miguel Heleno[b], Riccardo Basosi[a,c,e], Adalgisa Sinicropi[a,c,e]

[a] *University of Siena, R^2ES lab, Department of Biotechnology, Chemistry and Pharmacy, Via A. Moro,2, Siena, Italy.*
[b] *Grid Integration Group, Lawrence Berkeley National Laboratory, Berkeley, Cyclotron Road, 1, CA 94720, USA.*
[c] *CSGI, Center for colloid and surface science, via della Lastruccia 3, 50019, Sesto Fiorentino, Italy.*
[d] *University of Florence, Department of Industrial Engineering, Via Santa Marta,3, Florence, Italy.*
[e] *Institute of Chemistry of Organometallic Compounds (CNR-ICCOM), Via Madonna del Piano 10, 50019 Sesto Fiorentino, Italy.*

Abstract

Renewable energy communities are multi-users energy systems that are expected to become popular in all countries, including Italy. This paper discusses environmental-driven solar compensation mechanisms, specifically designed for energy communities. Such mechanisms consider the adoption of Distributed Energy Resources by the communities and reflect their overall life cycle environmental benefit. Notably, an innovative three-steps iterative methodology is adopted to design new feed-in tariffs including: (i) the optimal economic sizing of solar technologies, (ii) the life cycle assessment and (iii) the evaluation of a solar compensation mechanism. In the last step, the emissions avoided by communities are converted into economic solar compensation mechanisms (via feed-in tariffs) using the current value of carbon taxes. After the general methodology description, the proposed approach is applied to a specific Italian case study. In case carbon taxes are set to the current value, namely 15.4 EUR/tonCO_2eq, the yearly national emissions are mitigated by the adoption of the proposed solar compensation from 121.1 MtonCO_2eq/yr to 108.2 MtonCO_2eq/yr. Differently, if taxes are increased to 20 EUR/tonCO_2eq, the emissions are reduced to 84.3 MtonCO_2eq/yr; in case carbon taxes are extended over this value, the grid gets saturated by communities electricity and the additional environmental advantages are negligible.

Keywords: Renewable Energy Communities, Photovoltaic Systems, Batteries, Life Cycle Assessment, Incentives.

Declarations of interest: none

1. Introduction

This paper addresses the problem of designing a sustainable policy to promote photovoltaic (PV) and energy storage systems installed in Renewable Energy Communities (RECs) by proposing a novel approach for solar compensation applied to an Italian case study. RECs are defined by the European Union Renewable

*Corresponding author
Email address: federico.rossi3@unisi.it (Federico Rossi)

Energy Directive (RED II) [1], which is part of the European Commission's Clean Energy Package [2], as non-commercial entities whose purpose is providing environmental, economic and social benefits. They are composed of a group of users investing in energy production technologies from renewable sources and storage systems, whose costs are shared among the community members; this is particularly useful because such technologies can have high investment costs [3]. Moreover, RECs allow to face energy poverty issues [2] affecting many areas of the World, including some parts of Italy [4, 5]. Some of the most commonly deployed technologies in RECs are PV modules for the energy production and battery energy storage systems (BESSs) to store the PV energy surplus. For instance, a REC has been recently installed in Crevillent (Spain) where about 70 households deployed 125 kW of PV and a 200 kWh BESS [6].

RECs belong to the category of behind the meter installations and several types of economic benefits, named incentives, can be used to promote their deployment. Some European countries like Germany and Denmark have already designed an energy policy framework for RECs [2]; differently, in Italy a specific policy is still under evaluation [7]. Notably, coherently with the RED II principles [1], the Italian Energy Authority [8] is working on the development of a bonus (that could be formalized soon) promoting the self-consumption (SC) of the energy shared by RECs members [8]. Nevertheless the following incentives for PV systems are already available [9]:

- Net metering: users can get a reimbursement calculated as the product between the exchanged energy (namely the lower value between the electricity imports and exports) and a reference remuneration; moreover electricity can be sold to the utility at market value. In Italy this mechanism is known as "scambio sul posto" and the reference remuneration is approximately equal to 70% of the energy cost [10]. Currently, this incentive applies for PV installations whose size is lower than 500 kW [9].

- Feed-in tariffs (FITs): the electricity exported to the grid can be sold by providing a guaranteed, above-market price for producers [11]. Currently in Italy, according to a mechanism known as "ritiro dedicato", the minimum price guaranteed is generally lower than the price set by the market, and therefore electricity is commonly sold at market value [9].

- Tax deductions: users can get a reimbursement for the cost of PV installations or other residential interventions increasing the energy efficiency of a building. In Italy such incentive reimburses a percentage between 50% and 110% of installation costs depending on the type of intervention [12].

Different economic tools like bidding systems [13], Green Certificates [14, 15] and Renewable Portfolio Standards [16] are instead applied to power plants, but they are out of the scopes of this paper.

Another way to indirectly promote renewable energy systems is adopting carbon taxes that penalize the massive consumption of fossil resources. Carbon taxes obligate energy producers from fossil resources to pay a fee for the amount of carbon dioxide released to the atmosphere. The mechanism of carbon taxes is carefully described in a report published by the Organisation for Economic Co-operation and Development (OECD) [17]. Nevertheless, this report underlines that most of the OECD countries have not adopted

an adequate carbon taxes policy, especially in some strategic sectors like electricity production; indeed, in Italy carbon dioxide emissions are taxed at 15.4 EUR/tonCO_2, whereas in USA it is not taxed at all [17]. Differently, Northern European countries have taxed carbon dioxide emissions at a higher rate; some examples are Denmark (104.57 EUR/tonCO_2), Sweden (193.08 EUR/tonCO_2), Norway (1344.38 EUR/tonCO_2) and Iceland (4168.18 EUR/tonCO_2). Moreover, carbon taxes only affect the carbon dioxide direct emissions from electricity production through fossil resources, whereas the life cycle greenhouse gases (GHGs) emission of renewable energy technologies is not considered as a negative externality.

All these incentives and economic tools are thought to promote rapid adoption of renewable energy technologies because they are generally considered as sustainable for the environment. Nevertheless, excessive incentives may lead to over-investments in PV as demonstrated by Poponi et al. [18] analyzing Italian FITs in the last decade. Furthermore, all energy systems, including RECs, determine some environmental impacts over their life cycle. Therefore, if incentives or tariffs do not consider the full environmental performances of RECs, they might provide wrong economic signals and lead to an inadequate deployment of PV from an environmental perspective [19]. For these reasons, the current incentives have some limitations dealing with their environmental compatibility. In order to address such an issue, this paper aims to achieve three targets regarding incentives for PV adoption by RECs:

- Incentives should be directly correlated with RECs sustainability: most of policy strategies aim to push as more users as possible to purchase PV systems assuming that the more is the renewable capacity, the lower are the environmental impacts.
- Incentives should be defined through a granular evaluation: as PV energy production is variable as well as the energy mix sustainability, policymakers should define incentives on hourly basis as function of PV environmental benefits to the grid in time.
- Incentives should be adaptive to the changes that new installations apply to the grid energy mix sustainability.

In other words, it is important to design a new energy policy framework whose aim is not increasing renewable energies installed power but pursuing the sustainability of the national energy systems. In this perspective, as RECs are expected to reach a large diffusion in all countries, promoting them with adequate incentives represents a great opportunity towards a sustainable energy transition. More specifically, the problem addressed in this paper consists on including environmental impact analyses in a FITs design model through a mathematical correlation with a life cycle assessment (LCA). This problem is solved by defining a three-steps methodology that includes RECs economic Optimal Design, LCA and the FITs cost allocation. As the economic Optimal Design, that is the first step, requires as an input the FITs, that are assessed in the last step, the approach has to be iterative.

This paper is structured as following: Section 2 contains the literature background of the proposed study; in Section 3 the methodology is detailed; in Section 4 the readers can find the case study description; Section

5 contains the results description and discussion and Section 6 contains the conclusions and suggestions for future works.

2. Literature review

This section summarizes the background literature that contributed to this study and it underlines the substantial differences between the proposed model and the models discussed by previous scholars.

This study grounds on an existing algorithm, named Distributed Energy Resources Customer Adoption Model (DER-CAM) [20], that allows to design PV systems by minimizing the costs for their energy users. DER-CAM has been used in literature to forecast the deployment of behind the meter PV and storage installations, given some tariffs [21, 22]. Moreover, Cardoso et al. [23] used DER-CAM to evaluate the components size and the energy management of a system composed of PV modules and storage, also named Solar Home System [24]; batteries degradation is also included in the optimization. The model proposed by Cardoso et al. [23] has been adapted in our previous paper [25] to evaluate the economic and the environmental optimal configurations of Solar Home Systems. According to the cross-analysis of costs and impacts, economic optimization is assessed as the best methodology to design these energy systems. The same economic Optimal Design method is also suitable for RECs, that could be considered as large Solar Home System shared by multiple users. Therefore, economic Optimal Design is adopted within the proposed methodology to evaluate RECs portfolio of investments and the energy management of the communities. Similarly, the LCA analysis included in the proposed methodology is based on the environmental analysis defined in our previous paper [25] and on the LCA data-sets published by Peters and Weil [26] and previous LCA studies [27, 28, 29]. Differently from the above-mentioned studies, aimed to the design of the Solar Home Systems, this paper grounds on the models and the equations proposed by these scholars to evaluate new incentives for RECs.

Among the incentives for renewable energies over-viewed in Section 1, FITs became an issue of massive interest in scientific literature. Indeed FITs, compelling the utilities by law to purchase the renewable energy surplus produced by the users, led to a higher renewable energy deployment than other types of incentives [30, 31, 32]. For instance, Candelise and Ruggieri [33] underlined that 17 PV and wind based RECs have been installed in Italy since 2010 thanks to FITs but only 3 of them survived to the reduction of such incentives in 2013 and are currently operative. Similarly to Italy [11], FITs played a key role in RECs development also in other countries like Canada [34], United Kindom and Germany [35, 36]. Considered the importance given to FITs by literature, this type of incentive is selected to promote RECs in this analysis. Moreover, the temporal granularity of FITs, that are variable on hourly basis, is defined in Section 1 as one of the targets for the proposed design approach.

All the FITs design approaches available in literature are based only on techno-economic criteria whereas environmental analyses are never directly considered. For instance, Kim and Lee [37] developed an algorithm that allows policymakers to optimize the contribution of renewable energies to the grid; Ayompe and Duffy

[38] instead designed incentives in order to improve PV domestic installations cost-efficiency. Mpholo et al. [39] defined an innovative FITs mechanism for Leshoto (Southern Africa) to face the high poverty rate of its population. In contrast, Devine et al. [40] and Barbosa et al. [41] based their FITs evaluation on the analysis of the uncertainty affecting the investments in PV; the latter also provided a tool for policymakers to design new FITs in such uncertain conditions. Martin and Rice [42] addressed the problem of FITs design and adopted an approach named Concept Analysis and Mapping using historical data to point out the main design parameters. Among these parameters, life cycle environmental impacts evaluations are not directly included.

This literature review underlines that environmental impact assessment methods are not considered in common FITs design approaches. Nevertheless, as underlined in Section 1, RECs are responsible for some life cycle GHGs emissions over their life cycle and the adoption of inadequate incentives could lead to an excessive and not sustainable deployment of PV systems [43]. For such reason, the environmental performances of renewable energy technologies should be accounted when evaluating environmental friendly FITs for RECs. LCA is the main methodology to assess the environmental impact of products and processes [44, 45] and it is frequently used in literature to describe future scenarios of the energy mix eco-profile [46, 47]; nevertheless, it has never been directly used to design incentives.

According to the above literature review, FITs are an important tool to promote the diffusion of RECs and of renewable energy systems in all countries. Previous scholars proposed valuable FITs design models that could be suitable for all countries, including Italy, but they only involve some techno-economic variables of the problem. Differently, the model proposed aims to fill such literature gap by combining a techno-economic assessment based on DER-CAM [20] with an environmental analysis for the calculation of new LCA-driven solar compensations. The proposed methodology can be easily extended to other countries, but in this paper we limited ourselves to Italy as a case study. Moreover, a sensitivity analysis is performed to assess the results variations depending on the main parameters of the problem.

3. Methodology

In this section, the methodology used to evaluate new FITs for RECs is described. This approach assumes economic rationality in RECs' adoption of technologies: the size and utilization of PV and storage devices are determined in order to minimize the annualized costs of energy from the RECs perspective. We define their PV and storage investments based on an economic rational model [25], which calculates the optimal investments taking into account technology costs as well as specific RECs data, such as load and solar radiation. We assume that many communities will spread throughout the Italian territory, thus providing positive environmental effects to the national energy system. The novel FITs design approach proposed in this paper grounds on the following three-steps iterative methodology.

In Step 1, RECs are designed using an economic optimization model that allows to evaluate the optimal portfolio of investments and the optimal energy management: the electricity produced by RECs can be

self-consumed or injected to the grid depending on the economic convenience. Producing electricity with their PV systems, RECs allow to reduce the energy injected to the grid by other producers.

In Step 2, the environmental performances of RECs are calculated. RECs electricity production from renewable sources allows, in principle, to reduce the amount of GHGs emitted. Nevertheless all energy systems, including PV and storage, have a carbon footprint over their life cycle. Therefore the GHGs emissions avoided by RECs are calculated, net of their own impact, using LCA.

In Step 3, the emissions avoided by RECs electricity injection to the grid are converted into additional solar compensations and added to the current FITs. Indeed, the GHGs avoided by RECs also represent an economic advantage because carbon dioxide emissions are subject to taxation. For such reason an economic surplus resulting from RECs avoided emissions exists and it is used to reward their members. Differently from the policy currently adopted in OECD countries, in this work carbon taxes application is extended to all life cycle GHGs. Therefore, hereinafter carbon taxes will be expressed per ton of equivalent carbon dioxide (EUR/tonCO_2eq instead of EUR/tonCO_2).

If the analysis stops at this level, it is possible to calculate RECs environmental performances using the current FITs. Nevertheless, communities could take advantage of the additional incentives evaluated in Step 3 and change the optimal size of components and the optimal energy management accordingly. Therefore, in the proposed approach, the FITs calculated through Step 3 are used as inputs for Step 1 in the second iteration. Nevertheless, the emissions avoided at the second iteration are lower because the energy mix has already been improved at the first one; therefore additional FITs are lower as well. In other words, this adaptive methodology iteratively leads to an equilibrium condition where RECs cannot provide further environmental benefits to the grid. A sketch of this methodology is illustrated in Figure 1. This scheme highlights that the model is constructed in a general and objective way and that the case study just provides some representative inputs for Italian communities to the model; therefore, the approach proposed can be considered as valid for all countries.

The input data required to apply such methodology are the current FITs, the carbon taxes, the energy demand and production mix, and some meaningful load profiles for RECs. Therefore, the proposed FITs design approach could be applied to all countries just using specific values for the previous inputs. For such reason the innovative methodology detailed in this section has a general value that goes beyond the choice of the country.

According to this methodological overview, the equations presented in this section contain variables depending on time (t), on the iteration number (i) and on the community type (j). Notably, 72 representative community types (Nt) with a prototypical load are considered. Furthermore, in order to reach the required penetration level, each type of REC should reach a certain number of installations (Nc). Further details about the definition of RECs representative communities and their number are provided in the following section.

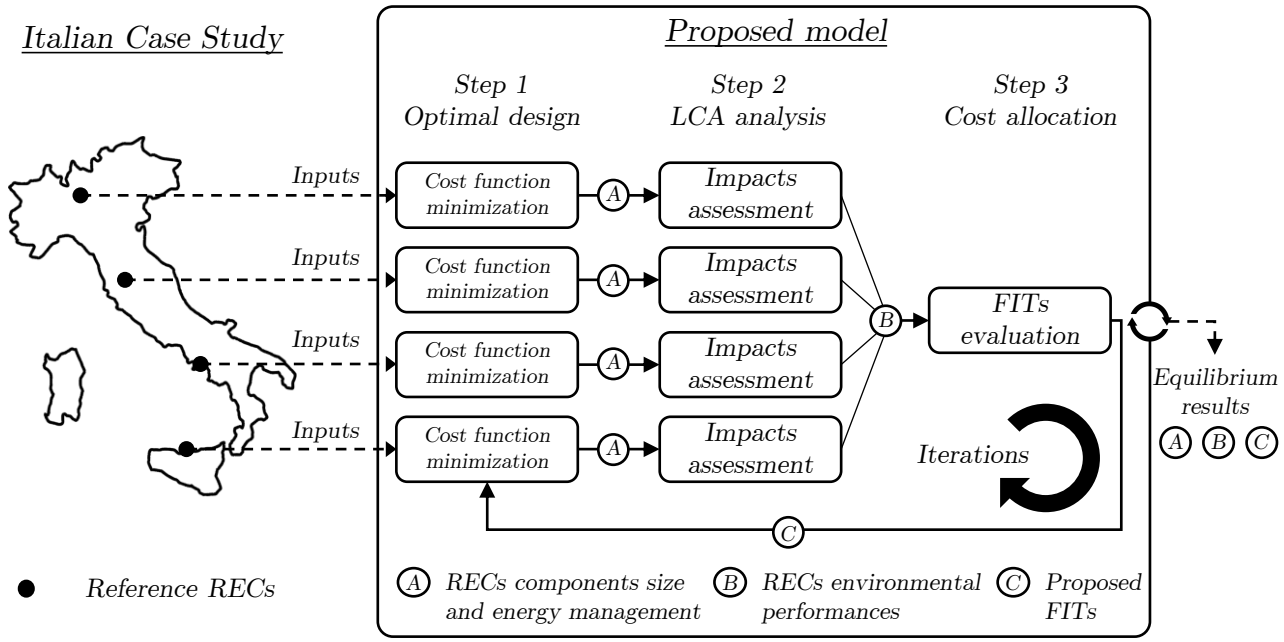

Figure 1: Sketch of the applied methodology.

3.1. Optimal Design

An economic Optimal Design model has been developed in our previous paper [25] to evaluate the best portfolio of solar and battery investments. Such model is based on a mixed integer linear programming (MILP) optimization algorithm and requires the following inputs:

- the energy costs (EC_t) for the users;
- the feed-in tariffs at the previous iteration ($FIT_{t,i-1}$);
- the fixed costs of the k-technology ($CFix_k$) which do not depend on its capacity;
- the variable costs of the k-technology ($CVar_k$) which depend on its capacity.

In order to stress the generality of the approach, it is underlined that these inputs are PV and storage investement and operation costs that in principle could be related to any country. Using these data, the optimization model allows for the evaluation of the following outcomes:

- the choice of the adoption of the k-technology through a binary decision variable ($i_{k,i,j}$);
- the capacity of the k-technology ($cap_{k,i,j}$);
- the electricity imported from the grid ($ui_{t,i,j}$);
- the electricity exported to the grid ($ue_{t,i,j}$);

The variables of the model are evaluated through the minimization of an objective function, represented by the costs for energy users (investment costs are annualized using a discount rate ir of 3%). As shown in [25], this model is constrained by the energy balance of the BESS, of the charge controller (CC), of the inverter (In) and of the overall system. Moreover constraints include the maximum PV productivity, the maximum power exchanged by the storage, its maximum capacity and the ageing of storage devices. Notably, thanks to an ageing model valid for different lithium-ion batteries, economic optimization allows to minimize the costs guaranteeing that the BESS lifespan reaches a target value set by the user (10 years). Depending on batteries characteristics, the Optimal Design model can select the most suitable battery to minimize costs.

According to the above description of the problem, the objective function minimized by the optimization algorithm is set to the annualized costs of energy communities ($C_{i,j}$) (1). The first term of the equation contains the fixed ($CFix_k$) and variable ($CVar_k$) costs of components whereas the second term contains the costs due to energy imports and the revenues from energy exports. This MILP optimization model is solved using CPLEX [48], via a python (Pyomo) implementation [49]. All values for input costs and revenues are defined in Section 4 whereas the outputs of the minimization are listed in the previous bullet points.

$$C_{i,j} = \sum_{k=1}^{Nk} \Big(CFix_k \cdot i_{k,i,j} + CVar_k \cdot cap_{k,i,j} \Big) Ann_k + \sum_{t=1}^{\bar{T}} (ui_{t,i,j} \cdot EC_t - ue_{t,i,j} \cdot FIT_{t,i-1}) \tag{1}$$

Where Nk is the number of components installed by the communities and Ann_k is an annualization factor of costs (2):

$$Ann_k = \frac{ir}{1 - \big(1 + ir\big)^{-L_k}} \tag{2}$$

In this equation, L_k is the k-component lifespan.

Another result that will be useful in the following of the methodology is the communities SC ($sc_{t,i,j}$) calculated as the difference between the community load ($load_{t,j}$) and the energy imported from the grid (3):

$$sc_{t,i,j} = load_{t,j} - ui_{t,i,j} \tag{3}$$

The full model, including the techo-economic constraints, is detailed in [25].

3.2. LCA analysis

Concerning the environmental performances of energy communities, LCA is one of the best approaches to estimate them. In this study the analysed technologies are not responsible for direct GHGs emissions, but some burdens occur anyway during their construction and end of life. According to ISO standards [44, 45], LCA analyses should follow four different phases: Goal and Scope definition, Life Cycle Inventory (LCI), Life Cycle Impact Assessment (LCIA) and Interpretation.

3.2.1. Goal and Scope definition

The first phase of LCA is the Goal and Scope definition. The environmental analysis performed in this study aims to calculate energy communities GHGs emissions from cradle to grave to estimate the net environmental benefits of the electricity injection and SC. In this phase, the following information about the LCA study is also provided:

- RECs function is to guarantee the energy supply to their members but they can also export electricity to the grid.
- The reference flow of the product system is the load supply whereas the electricity injection to the grid is considered as a by-product; a physical allocation of impacts is done to address this issue.
- The functional unit of the analysis is set to 1 kWh.
- The system boundaries include the energy imports from the grid and the production and end of life of components. Concerning batteries waste management, the system is supposed to be disassembled to recover the cells housing and other external materials; then hydro-metallurgical and pyro-metallurgical processes are used to recover the electrodes metals [28, 29, 27].
- Coherently with the scope of the analysis, the environmental indicator Global Warming Potential (GWP) is adopted to summarize all the GHGs emissions; indeed, results are expressed as equivalent carbon dioxide emissions ($kgCO_2eq$).

3.2.2. Life Cycle Inventory

The second phase is creating a LCI; this operation is done using openLCA [50] and the database Ecoinvent 3.6 [51]. A LCI represents a data collection of all the energy flows and materials consumption and of the emissions occurring during the communities life cycle. Similarly to the model defined in our previous work [25], the proposed algorithm requires as inputs the environmental impact of a 1 kW PV system, a 1 kWh BESS, a 1 kW In, a 1 kW CC and a 1 kWh of energy imported from the grid. In light of these considerations, the LCI is detailed in Table 1. This table collects as inputs all the processes occurring during the components life cycle, namely the production and waste treatment, and the Italian electricity production mix. In case some of these processes are not directly provided by Ecoinvent [51], the data source is cited. The input quantities are expressed as a mass or as number of items depending on the data source. All the outputs are converted to the aforementioned functional units (1 kWh or 1 kWh) according to the components' characteristics declared by the data source. Since every community can purchase their components from the market, the LCI grounds on Ecoinvent market processes.

Inputs			
market for photovoltaic slanted-roof installation, 3kWp, single-Si, panel, mounted, on roof	0.33	pieces	PV system production, In excluded [51]

photovoltaic system waste treatment	102.33	kg	Reproduced from [52]
Outputs			
PV system	1	kW	LCI of a 1 kW PV
Inputs			
lithium-ion batteries production	1.00	kWh	Reproduced from [26]
lithium-ion batteries waste treatment	1.00	kWh	Reproduced from [53]
Outputs			
BESS system	1	kWh	LCI of a 1 kWh BESS
Inputs			
market for inverter, 2.5kW	0.40	pieces	In production [51]
market for waste electric and electronic equipment	7.40	kg	In waste treatment [51]
Outputs			
In	1	kW	LCI of a 1 kW In
Inputs			
market for charger, electric passenger car	1.71	kg	CC production [51]
market for waste electric and electronic equipment	1.71	kg	CC waste treatment [51]
Outputs			
CC	1	kW	LCI of a 1 kW CC
Inputs			
market for electricity, low voltage IT	1	kWh	Italian energy production mix [51]
Outputs			
Energy Imports	1	kWh	LCI of 1 kWh energy imports

Table 1: LCI of RECs components and imported energy.

3.2.3. Life Cycle Impact Assessment

The third phase of LCA analyses is the LCIA, namely the evaluation of the environmental impact of the product system thanks to a standard LCIA method. Particularly, the European Commission is engaged in the construction of a reliable method, named ILCD [54], providing results for several impact categories including GWP. Therefore in this study, ILCD is adopted to evaluate this midpoint indicator, expressed as the amount of equivalent carbon dioxide emissions. Calculations are run using openLCA [50].

Environmental impacts can be classified as fixed ($kgCO_2eq$) or variable ($kgCO_2eq/kW$ or $kgCO_2eq/kWh$) according to their relation with the size of the components [25]. In order to calculate the GHGs emissions of the overall RECs ($kgCO_2eq$), the fixed ($IFix_k$) and the variable ($IVar_k$) environmental impacts are respectively multiplied by the binary decision variable $i_{k,i,j}$ and the components capacity $cap_{k,i,j}$, namely

the outputs of the Optimal Design model. Such emissions are physically allocated to the energy injection ($Eue_{t,i,j}$) (4) and SC ($Esc_{t,i,j}$) (5), that are the two energy outputs of the PV system electricity production model. All the impact values related to components and energy are collected in Section 4.

$$Eue_{t,i,j} = \frac{\sum_{k=1}^{Nk} \left(IFix_k \cdot i_{k,i,j} + IVar_k \cdot cap_{k,i,j}\right) EAnn_k}{OT_{i,j}} \cdot \frac{ue_{t,i,j}}{ue_{t,i,j} + sc_{t,i,j}} \tag{4}$$

$$Esc_{t,i,j} = \frac{\sum_{k=1}^{Nk} \left(IFix_k \cdot i_{k,i,j} + IVar_k \cdot cap_{k,i,j}\right) EAnn_k}{OT_{i,j}} \cdot \frac{sc_{t,i,j}}{ue_{t,i,j} + sc_{t,i,j}} \tag{5}$$

In these equations $EAnn_k$ is an annualization factor of the k-component environmental impact calculated as the reciprocal of its lifespan value [25] and $OT_{i,j}$ is the operative time of RECs. Coherently with our previous study [25] and with the LCI in Table 1, all the impacts of components can be considered as variable because they depend on their capacity.

During the operation RECs import electricity from the grid: the load supply is partially covered by the SC and partially by the grid; therefore, the impact of RECs electricity imports is totally allocated to the load. Accordingly, the equivalent carbon dioxide released for the load supply ($Eload_{t,i,j}$) is expressed by Eq. (6)

$$Eload_{t,i,j} = ui_{t,i,j} \cdot Imix_{t,i} + Esc_{t,i,j} \tag{6}$$

According to the functional unit definition, the RECs impacts must be expressed as $kgCO_2eq/kWh$. Therefore the load and the energy injection impact values are calculated as the ratio between the equivalent carbon dioxide emissions ($Eload_{t,i,j}$, $Eue_{t,i,j}$) and the corresponding energy flows ($load_{t,j}$, $ue_{t,i,j}$).

The electricity mix environmental impact changes because RECs injected energy avoids some carbon dioxide emissions whereas SC reduces the electricity needs from the main grid. The energy mix impact in time ($Imix_{t,i}$), expressed as equivalent carbon dioxide per kWh of energy in the network ($kgCO_2eq/kWh$), is assessed by the following balance (7):

$$Imix_{t,i} = Imix_{t,i-1} - \frac{Nc \cdot \sum_{j=1}^{Nt} \left((ue_{t,i,j} - ue_{t,i-1,j}) \cdot Imix_{t,i-1} - (Eue_{t,i,j} - Eue_{t,i-1,j})\right)}{D_t - Nc \cdot \sum_{j=1}^{Nt} sc_{t,i,j}} \tag{7}$$

In this equation, D_t is the national electricity demand profile supplied by the grid before RECs deployment. Similarly to the economic data, also the energy and environmental inputs like the national energy demand and energy mix impact could be referred, in principle, to all countries.

3.2.4. Interpretation

The fourth phase of LCA analyses is the Interpretation. All the previous steps are suitable to interpretation because both the LCI and LCIA results should match with the goal and scope of the analysis. The overall LCA analysis adopted in this study is schematized in Figure 2.

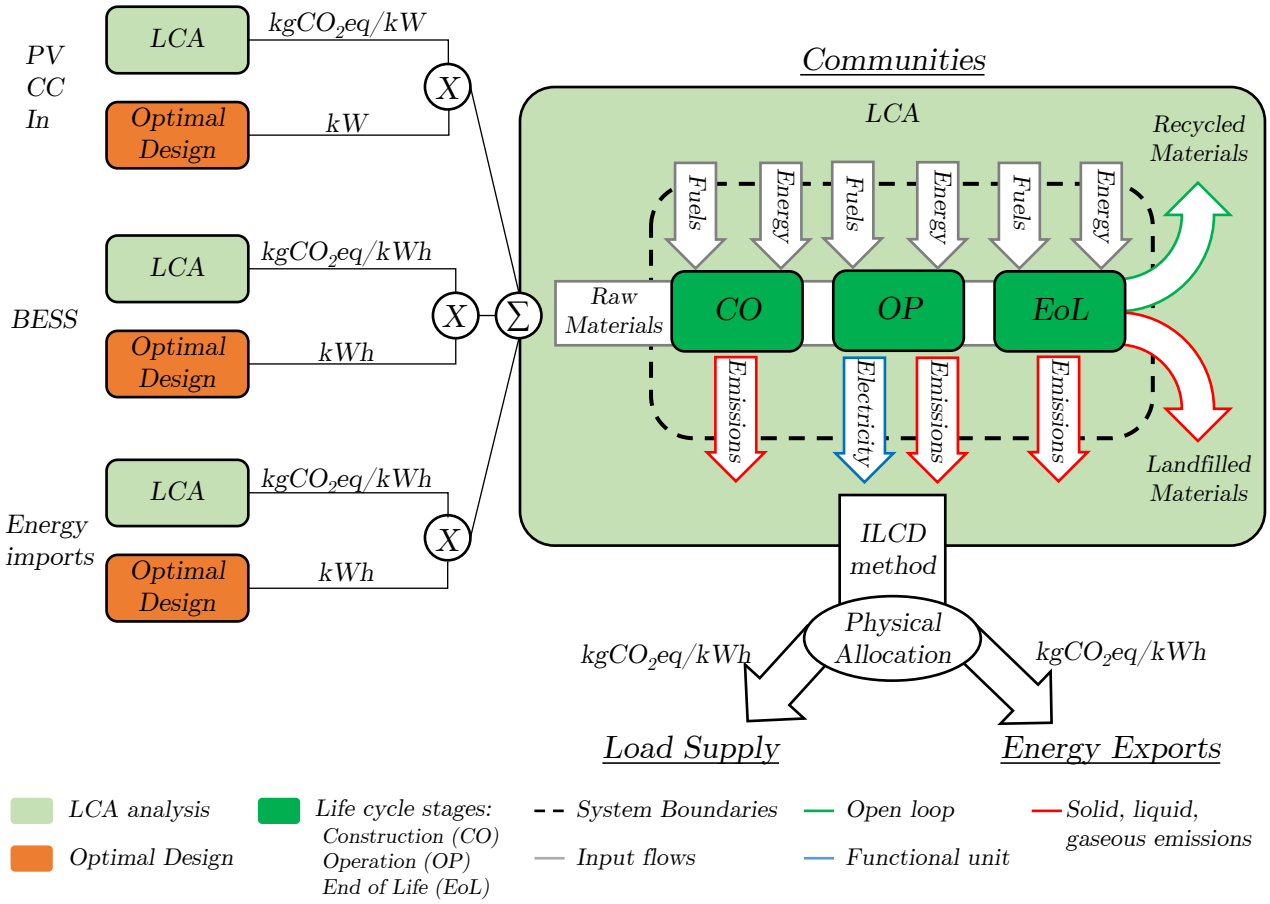

Figure 2: Sketch of the LCA analysis.

3.3. Cost allocation

During the Step 3, at every iteration the environmental benefits of RECs are converted to additional economic incentives. The environmental benefits due to the additional emissions avoided by RECs exports are calculated and converted to economic savings through the product with carbon taxes. These GHGs savings are divided by the energy exports to the grid to evaluate the additional FITs to the previous step (8). All these operations that bring to the evaluation of the new FITs are included in Eq. (8).

$$FIT_{t,i} = FIT_{t,i-1} + \frac{Nc \cdot \sum_{j=1}^{Nt}((ue_{t,i,j} - ue_{t,i-1,j}) \cdot Imix_{t,i-1} - (Eue_{t,i,j} - Eue_{t,i-1,j})) \cdot CT}{Nc \cdot \sum_{j=1}^{Nt} ue_{t,i,j}} \tag{8}$$

In this equation, CT represents carbon taxes and the terms addressed as ue and Eue are respectively the energy exports assessed by the Optimal Design and the emissions evaluated during the LCA analysis.

4. Case study

This section describes the characterization of RECs and collects all the data necessary to apply the methodology. As demonstrated by the equations in the previous section, the proposed model is constructed in a general and objective way. Nevertheless, to guarantee the results reliability, the Case Study must be tailored for the Italian conditions. For instance, Italy has an elongated territory that covers a wide range of latitudes and thus of solar radiation values and load profiles. Therefore, the diversification of several representative RECs, differing for PV productivity and load profiles, is fundamental to make the model applicable to Italy.

The PV productivity profiles are evaluated by dividing the Italian territory in 4 regions according to the latitude: North, Centre-North, Centre-South and South. For each region, a representative city is selected: Milan for North, Florence for Centre-North, Naples for Centre-South and Palermo for South. In all these locations, the electricity production profile of a 1 kW PV installation is calculated using the online tool photovoltaic geographical information system (PV-GIS) [55].

Concerning the electric load of communities, Quoilin et al. [56] published a data-set containing several profiles obtained through a statistical analysis of direct measurements in micro-grids. 154 profiles are related to Italy and for each one of them an average daily load profile is evaluated. This operation allows to simplify the classification: those profiles having a peak during the morning, the afternoon and the evening are selected and grouped by category. Then the profiles can be classified in two groups, depending whether the peak load occurs in the summer or in the winter. Communities are formed by aggregating these profiles into different sizes: small, medium and big communities respectively have an average demand of 100 kW, 200 kW and 300 kW.

When combining 4 different PV productivity geographic profiles with 18 load profiles, we obtain 72 representative communities at the national level (Nt). Assuming that all communities are uniformly distributed in the Italian territory, it is possible to evaluate the number of communities by type Nc to reach the penetration level P as following (9):

$$Nc = P \cdot \frac{\bar{NL}}{\bar{CL} \cdot Nt} \tag{9}$$

Where $\bar{NL}$ and $\bar{CL}$ are respectively the average national load and communities load.

Technology costs are classified as fixed and variable costs and are adapted from [25] whereas the environmental impacts are calculated using Ecoinvent 3.6 [51] database and ILCD impact assessment method [54]. All the fixed environmental impacts are null [25] whereas the variable impacts are the carbon footprint of the energy imports, the PV, the In, the CC (respectively addressed with the subscripts pv, in and cc) and the BESS considering seven battery types (addressed using the subscripts $s1$,...,$s7$ according to the nomenclature adopted in [25]). All the economic and environmental cost parameters are collected in Table 2.

Costs			**Impacts**		
Parameter	Value	Unit	Parameter	Value	Unit
$CFix_s$	200	EUR	$IFix_s$	0	$kgCO_2eq$
$CVar_{s,1}$	305.2	EUR/kWh	$IVar_{s,1}$	156.6	$kgCO_2eq/kWh$
$CVar_{s,2}$	305.2	EUR/kWh	$IVar_{s,2}$	181.6	$kgCO_2eq/kWh$
$CVar_{s,3}$	449.2	EUR/kWh	$IVar_{s,3}$	274.7	$kgCO_2eq/kWh$
$CVar_{s,4}$	265.2	EUR/kWh	$IVar_{s,4}$	120.9	$kgCO_2eq/kWh$
$CVar_{s,5}$	291.7	EUR/kWh	$IVar_{s,5}$	104.1	$kgCO_2eq/kWh$
$CVar_{s,6}$	296.2	EUR/kWh	$IVar_{s,6}$	105.1	$kgCO_2eq/kWh$
$CVar_{s,7}$	296.2	EUR/kWh	$IVar_{s,7}$	116.4	$kgCO_2eq/kWh$
$CFix_{pv}$	400.6	EUR	$IFix_{pv}$	0.0	$kgCO_2eq$
$CVar_{pv}$	1216.6	EUR/kW	$IVar_{pv}$	156.6	$kgCO_2eq/kW$
$CFix_{in}$	50	EUR	$IFix_{in}$	0.00	$kgCO_2$
$CVar_{in}$	539.4	EUR/kW	$IVar_{in}$	99.5	$kgCO_2eq/kW$
$CFix_{cc}$	500	EUR	$IFix_{cc}$	0.0	$kgCO_2eq$
$CVar_{cc}$	141.3	EUR/kW	$IVar_{cc}$	99.5	$kgCO_2eq/kW$

Table 2: Environmental impact and cost parameters.

Concerning the electricity mix, hourly data about the energy flowing through the national grid are available in a database provided by the Italian transmission system operator (Terna S.p.a.) [57] for all energy sources: the total power is the sum of the electricity produced by thermal plants, from renewable sources (PV, wind, hydro, geothermal) and the energy imported from other countries. Ecoinvent 3.6 [51] contains LCA models for all the energy production pathways contributing to the Italian mix (such as natural gas combined cycles, different types of PV, hydro and wind installations and many other power plants). Keeping constant the Ecoinvent 3.6 [51] proportions among all the production pathways based on the same energy source, the impact of the electricity produced from geothermal (0.071 $kgCO_2eq/kWh$), from PV (0.075 $kgCO_2eq/kWh$), from thermal power plants (0.656 $kgCO_2eq/kWh$), wind (0.020 $kgCO_2eq/kWh$), hydro (0.032 $kgCO_2eq/kWh$) and of the electricity imported from other countries (0.267 $kgCO_2eq/kWh$) can be assessed. From the economic point of view, a reference database containing the current FITs [58] and the energy costs [8] are provided by the national authorities. All the other parameters required to run the model (like the ageing and operational parameters of the batteries) are set as in [25].

This section demonstrates that all the data necessary to perform the analysis are valid and reliable for Italy because they are obtained by processing primary data provided by National Energy Authorities [8, 58], transmission system operators [57] and reliable international databases for LCA [51]. Differently, CT

is uncertain because policymakers may change taxes to improve the effectiveness of the adopted policy [17] and the communities penetration P is still unknown and it is arbitrarily estimated to 25%.

5. Results and discussion

In this section, the main outcomes of the analysis are collected and discussed. Although the results are calculated and presented sequentially in this section, they are all interdependent and comprise an equilibrium between three aspects:

- RECs components size and energy management.
- RECs environmental performances.
- Proposed FITs that allocate the environmental benefits to costs.

In order to highlight the effectiveness of the proposed incentives, results are also calculated using the current FITs as terms of comparison; furthermore the situation before RECs deployment is also considered for comparison. Two parameters must be set before running the calculations: the penetration of RECs inside the territory (P), determining the number of communities, and the carbon taxes (CT). First, a Base Case Scenario where P is set to 25% and CT to 15.4 EUR/tonCO_2eq (the current value of carbon taxes in Italy) will be considered, and then a sensitivity analysis will be performed.

5.1. Base Case Scenario

This section illustrates the main results evaluated in the Base Case Scenario. Figure 3a and Figure 3b respectively represent the optimal size of the PV system and of the BESS providing the geographical resolution of the results. Analyzing the similarities between the communities designs, 12 representative RECs can be pointed out: these communities differ for their installation site and size. Particularly, moving from the north to the south of the country, the components capacity values increase, especially the BESSs. Indeed, southern RECs members can take advantage of a larger solar energy surplus to be stored in batteries. Comparing the existing FITs with the incentives proposed in this paper (which reflect RECs environmental performances), the average size of PV systems increases with the new FITs; contrarily storage capacity is still about the same. The main reason is that the FITs proposed in this paper reward RECs for the net environmental benefits of the electricity injected. This creates a slightly higher incentive for PV injection and does not produce any value for storage. As expected, the higher the REC electricity consumption, the larger the PV and storage installed capacities. Furthermore the Optimal Design model evaluates that, among the batteries considered by Peters and Weil [26], the lithium manganese oxide (LMO) devices analysed by Notter et al. [59] allow to minimize the cost. This outcome results from the cross evaluation of the costs and the ageing parameters of all the considered batteries in RECs operative conditions.

The dispatch of technologies, including the exports and imports to/from the main grid, is determined using an optimization algorithm [25]. Each REC can decide hour by hour to import electricity from the grid

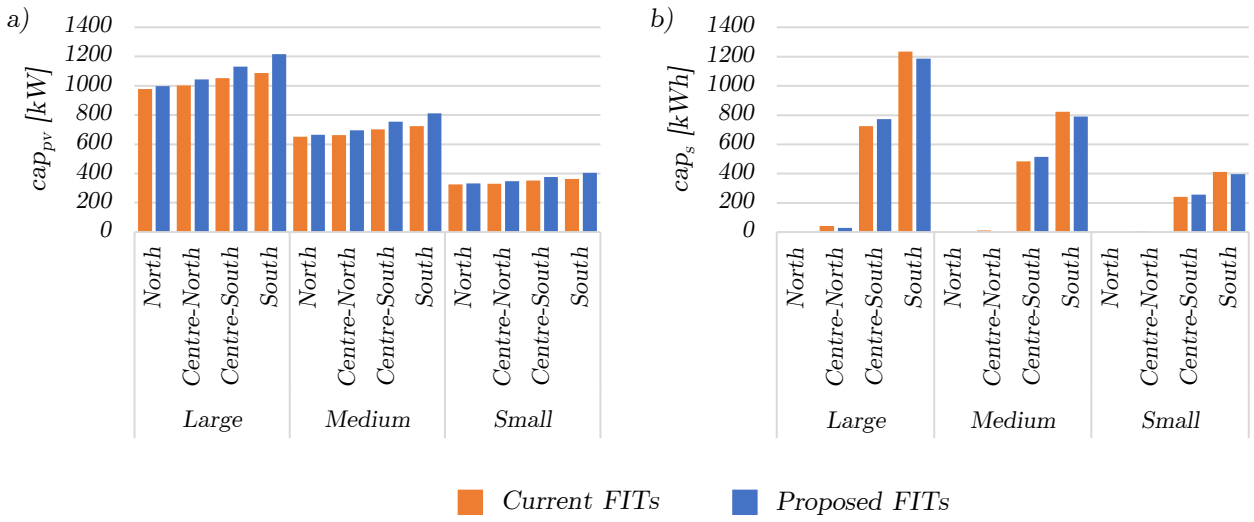

Figure 3: Representative sizes of a) the PV and b) the batteries.

or to consume its own energy production; in case a solar surplus exists, it can be injected to the grid or accumulated to be consumed or exported later.

In order to assess the effects of RECs at national level, the overall amount of electricity exported, imported and self-consumed by all communities is calculated. Differently from the situation before RECs deployment, part of the national energy demand is self-consumed by RECs and it is not supplied by the grid. Therefore the new energy mix is composed of the electricity exported to the grid by communities (RECs exports) and that injected by other producers. Part of the latter contribution is consumed by RECs (RECs imports) and part by other users not belonging to RECs (Non-RECs imports).

Figure 4 describes these results throughout an average day of the year and provides the annual value of all cumulative energy flows. The annual results show that, in case the current FITs are adopted, RECs reduce the amount of electricity on the grid by self-consuming 29.3 TWh/year and they export 4.0 TWh/year. When considering the changes brought by the proposed FITs, the further PV power installed by RECs allows to increase exports from 4.0 to 6.3 TWh/year whereas SC is slightly affected. Therefore, the amount of energy self-consumed by RECs is much bigger than the energy injection: with the proposed FITs around 83% of the electricity produced by RECs is self-consumed and only 17% is exported to the grid. Although RECs SC is relevant, 59% of RECs load is supplied by the grid and 41% through SC. These values represent a national average but results can be different depending on the installation site. Indeed, in north of Italy, SC contributes to 29% of communities load whereas in south, such percentage can reach 53% because storage is largely deployed.

The daily profile illustrated in Figure 4 provides the hourly impact of the proposed FITs. The electricity flows inside the grid are represented with different shades of yellow whereas the electricity outside the grid,

namely communities SC, is illustrated in grey. RECs decide to self-consume their own electricity from 5 AM to 10 PM and to inject power only from 7 AM to 4 PM. This finding confirms that SC is generally preferred to the injection to the grid: all RECs directly consume the PV energy they need and store the surplus in batteries (when available). All the energy accumulated is used to extend the SC time range. Therefore RECs only inject electricity to the grid when storage systems are full or not available.

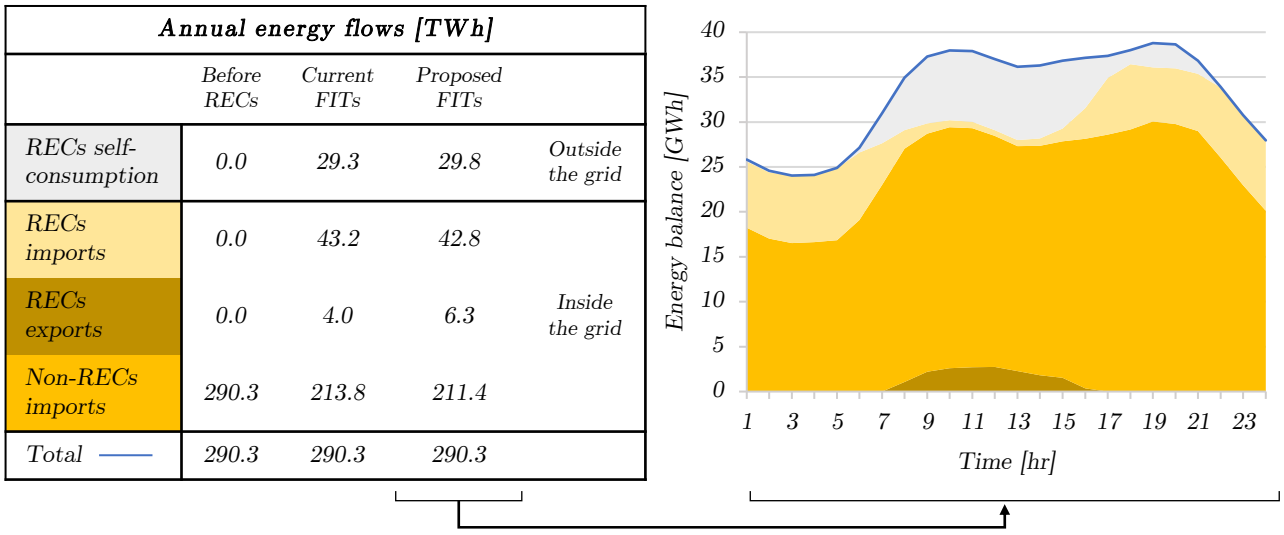

Figure 4: National energy balance during the average day of the year (evaluated using the proposed FITs) and on annual basis.

Similarly to the previous energy balance, it is possible to make the GHGs balance of the Italian energy system through evaluation of RECs environmental performances. Such GHGs balance consists on the evaluation at national level of the carbon dioxide emissions due to RECs self-consumption, imports, exports and to Non-RECs imports. Figure 5 depicts these results in terms of GHGs release over the year and throughout the average day of the year. The results obtained by applying the current FITs show that the deployment of RECs allows for a relevant mitigation of the yearly national emissions from 121.1 to 109.8 MtonCO_2eq/yr. The proposed FITs allows to further decrease this value to 108.2 MtonCO_2eq/yr; therefore the additional benefits brought by the proposed FITs is quite small compared to those provided by the current ones.

Dividing the annual GHGs emissions by the corresponding energy flow, some representative specific environmental impacts can be evaluated. Above all, the electricity produced and injected to the grid by RECs has a specific impact of 0.09 kgCO_2eq/kWh, which is very low compared to the grid one, assessed 0.40 kgCO_2eq/kWh. These results represent a national average; southern RECs have a larger productivity and the impact of their electricity is around 0.07 kgCO_2eq/kWh whereas the burden of northern communities energy production is around 0.12 kgCO_2eq/kWh. Concerning instead the energy consumption, even though RECs produce low-carbon electricity, the importation of electricity from the grid brings the specific impact of the consumed electricity to 0.29 kgCO_2eq/kWh. Nevertheless, because of the lower contribution of SC,

the impact of northern RECs load supply is 0.34 $kgCO_2eq/kWh$ whereas that related to southern RECs is 0.24 $kgCO_2eq/kWh$. Concerning the daily emissions profile during the typical day of the year, the gap between the black dotted line and the orange dashed line represents the amount of avoided emissions using the current FITs whereas the small gap between the blue and orange lines represents the additional emissions savings due to the proposed FITs. Coherently with the energy balance temporal resolution, regardless of the adopted FITs the avoided emissions are concentrated from 7 AM to 10 PM.

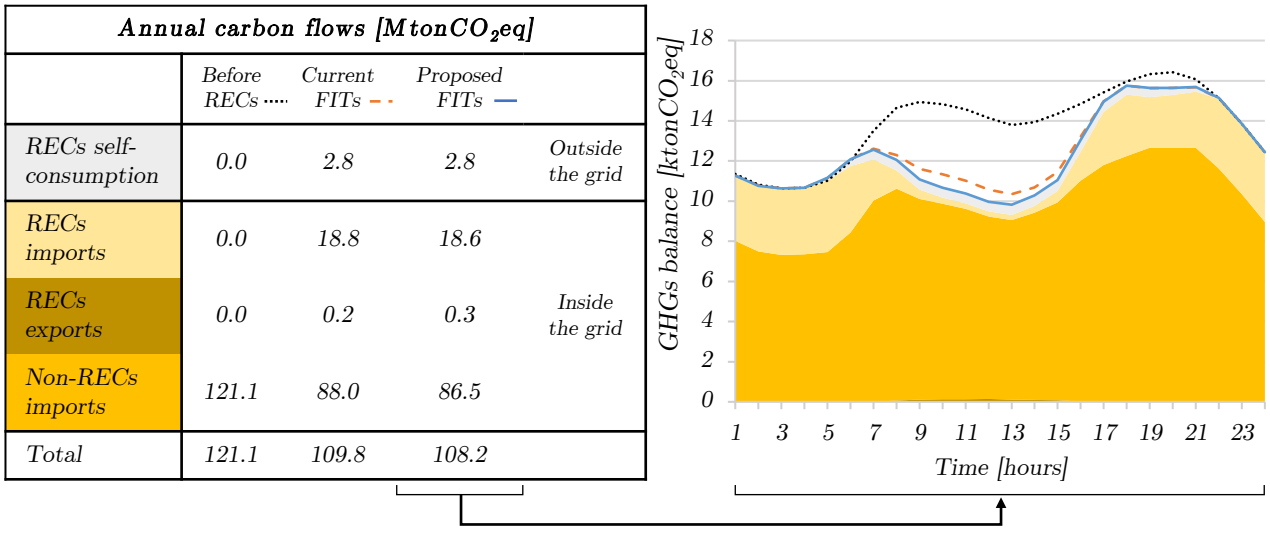

Annual carbon flows [$MtonCO_2eq$]				
	Before RECs ·····	*Current FITs* - -	*Proposed FITs* —	
RECs self-consumption	*0.0*	*2.8*	*2.8*	*Outside the grid*
RECs imports	*0.0*	*18.8*	*18.6*	
RECs exports	*0.0*	*0.2*	*0.3*	*Inside the grid*
Non-RECs imports	*121.1*	*88.0*	*86.5*	
Total	*121.1*	*109.8*	*108.2*	

Figure 5: National GHGs balance during the average day of the year (evaluated using the proposed FITs) and on annual basis.

As shown in Figure 1, the final step of the analysis is the cost allocation rewarding RECs members of their environmental advantages. The average FITs throughout the day are represented in Figure 6a: the orange one represents the current FITs whereas the blue one is evaluated through the novel methodology presented in this paper. These two profiles are very important because they, respectively, represent the starting and ending points of the overall analysis. Indeed, using the current incentives (orange profile), the algorithm designs RECs as illustrated in Figure 3 (orange columns). RECs inject electricity to the grid from 7 AM to 4 PM (Figure 4) avoiding carbon dioxide emissions within this time range (Figure 5). By the multiplication with carbon taxes, the environmental benefits are converted to economic ones increasing FITs only in those hours when some energy is exported. At the following iteration RECs decide to install more PV modules and devote them to increase the electricity injection to the grid taking advantage of FITs increments. As demonstrated by Figure 6b, iteration by iteration, FITs continue growing but the increments gradually get smaller because the energy mix is improving and RECs avoid less emissions. After some iterations the incremental incentives are unable to justify relevant further investments in PV and an equilibrium FITs condition (the blue profile) is reached.

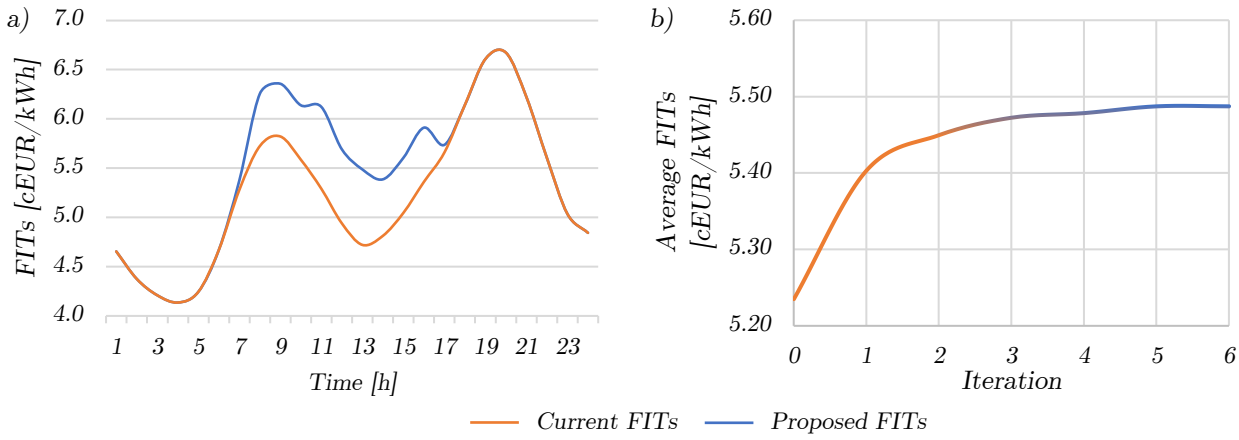

Figure 6: Average FITs a) during the representative day of the year and b) as function of iterations.

5.2. Sensitivity Analysis

The Base Case Scenario evaluation requires setting two parameters: CT and P. A sensitivity analysis for the parameter P is important because the expected number of communities on the Italian territory is uncertain; nevertheless its result does not highlight differences between the proposed and the current FITs (results are provided as Supporting Information).

Different considerations can be derived regarding the parameter CT. Although Italian carbon taxes are currently set to a specific value, the OECD [17] report underlines that some countries may increase taxes in the future to fight climate change. Therefore, in this analysis CT is gradually incremented and the corresponding results variations are assessed.

Figure 7a and Figure 7b respectively represent the average PV and the storage system sizes as function of CT and show that the former has an increasing trend whereas the latter is decreasing. The reason is that FITs increase with CT according to Eq. 8 pushing RECs to deploy larger PV systems and use them to inject more electricity to the grid. Contrarily, the size of storage systems decreases with CT because FITs promote energy injection despite of storage and SC. Notably, the components capacity variation is very fast in case CT is within the range of 17 EUR/tonCO_2eq and 20 EUR/tonCO_2eq and suddenly slows down over this range; the following results will explain this trend.

Figure 8a shows the annual energy balance of the Italian energy system, evaluated using the proposed FITs, as function of CT. This chart shows that the contribution of RECs exports to the grid rapidly rises with CT, but for a taxation higher than 20 EUR/tonCO_2eq such growth suddenly slows down. This finding can be explained by the observation of Figure 8b, representing RECs injected power as percentage of the total energy on the grid during the average day of the year. This chart shows that in case CT gets higher than 20 EUR/tonCO_2eq, the grid is saturated by RECs exports from 7 AM to 4 PM; therefore, there is no need for further electricity exports from REC within this time range. Differently, out of this time range,

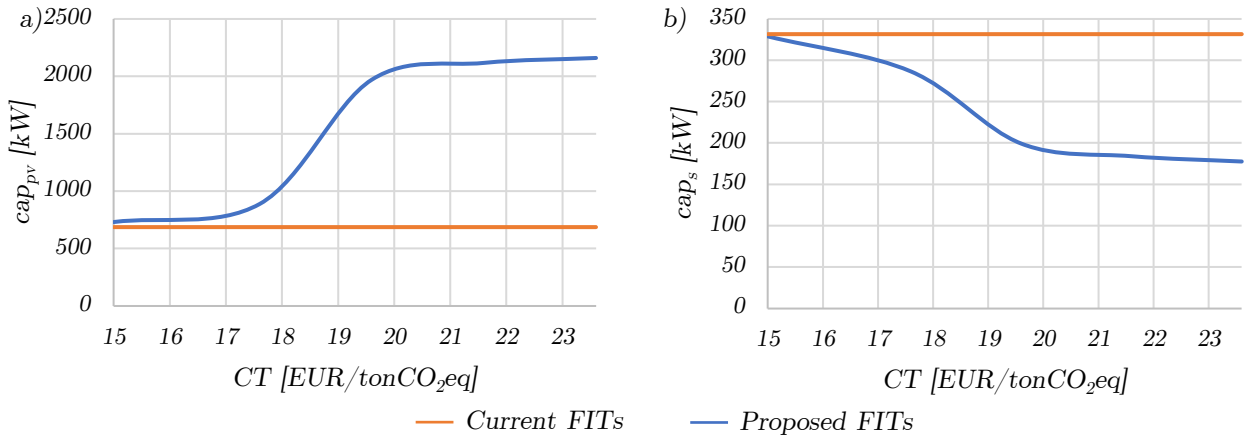

Figure 7: Optimal size of a) the PV system and b) the batteries as function of CT.

RECs exports are not affected by CT and are null for any level of carbon taxes. Indeed higher values of CT amplify additional FITs but they do not affect the energy injection time range. Due to the same reasons, the deployment of additional PV modules stops growing for CT higher than 20 EUR/tonCO$_2$eq (Figure 7).

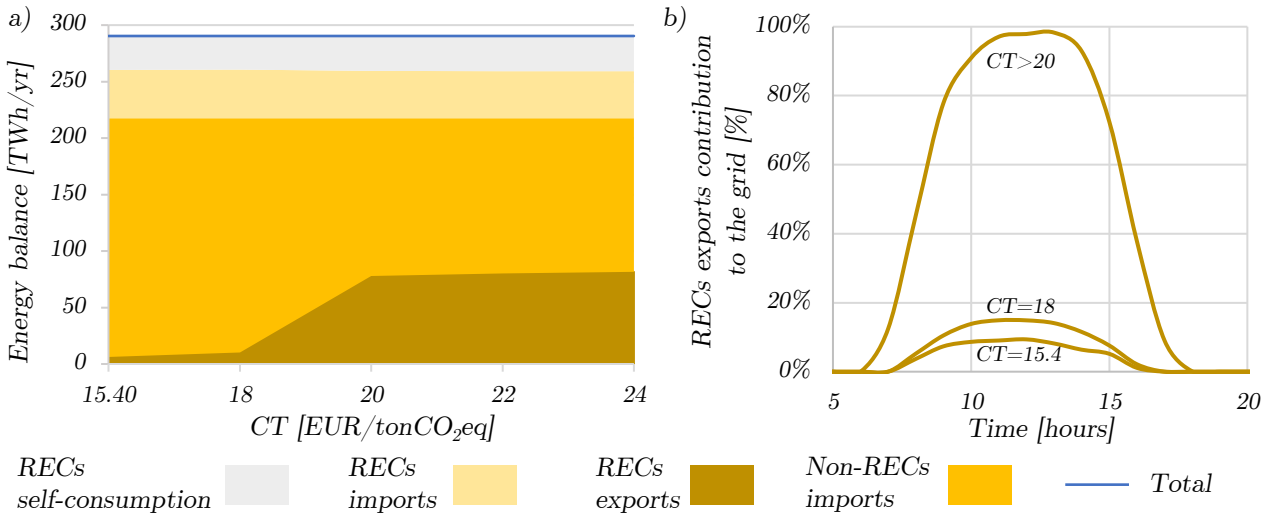

Figure 8: a) Energy balance of the grid on annual basis as function of CT; b) amount of electricity exported by RECs as percentage of the total energy on the grid during the average day of the year. Evaluated using the proposed FITs.

Figure 9 represents the annual GHGs balance of the grid calculated using the proposed FITs; contrarily to the Base Case Scenario, the proposed FITs allow to avoid a relevant amount of additional GHGs emissions compared to the current FITs. Indeed, according to the energy balance results, increasing CT allows to inject much more electricity to the grid, until CT reaches 20 EUR/tonCO$_2$eq. Above this value, RECs do not provide further environmental benefits by increasing CT due to the grid saturation mechanism illustrated

in Figure 8. This means that, in case of adoption of the proposed FITs, carbon taxes should be set to 20 EUR/tonCO_2eq because this allows to get the maximum benefits from RECs. Concerning the LCA results, the enhanced RECs exports allow to mitigate the energy mix impact from 0.40 kgCO_2eq/kWh (Base Case Scenario) to 0.31 kgCO_2eq/kWh for CT=20 EUR/tonCO_2eq. Indeed, the impact of RECs electricity exports is very low for all values of CT and it slightly varies from 0.09 kgCO_2eq/kWh (for CT=15.4 EUR/tonCO_2eq) to 0.07 kgCO_2eq/kWh (for CT=24.0 EUR/tonCO_2eq). Concerning the impact related to RECs load supply, its value is assessed around 0.29 kgCO_2eq/kWh regardless of CT. The reason is that electricity is mostly imported during the night when, according to Figure 8, RECs electricity contribution to the grid is null and the energy mix environmental impact does not change.

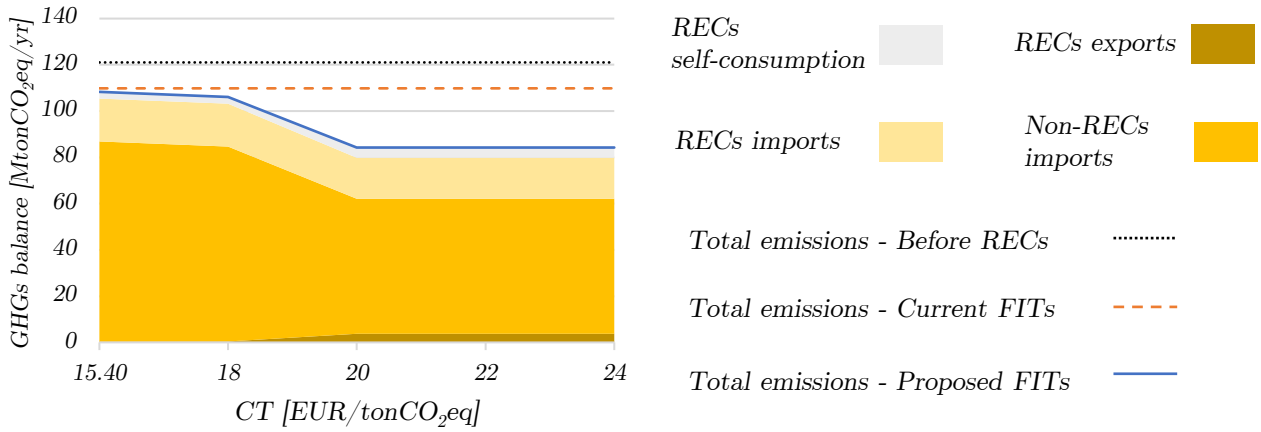

Figure 9: LCA results as function of CT.

Figure 10a depicts the average FITs as function of CT and underlines that the proposed incentives increase when carbon taxes are high; Figure 10b instead illustrates the convergence of average FITs with iterations. As described in the Base Case Scenario, for CT=15.4 EUR/tonCO_2eq, the FITs increments are so low that, after few iterations, they reach an equilibrium value where further investments in PV are not beneficial. In case CT increases to 18.0 EUR/tonCO_2eq, the economic advantages for RECs are amplified and their members continue investing in PV and accumulating additional FITs for several iterations, until incentives converge to an equilibrium value (higher than that evaluated in the Base Case Scenario). By further increasing CT, FITs get more convenient and RECs continue for many iterations deploying additional PV modules. But when taxes reach 20.0 EUR/tonCO_2eq, the curve gets flat: Figure 10b shows that, for CT=20 EUR/tonCO_2eq, after 12 iterations the growth of FITs suddenly stops. The reason is that, as demonstrated by Figure 8a, the grid is saturated by RECs injection that is unable to further improve the grid energy mix. Consequently no further emissions are avoided and converted to additional FITs. Therefore, at this taxation level, RECs get the maximum FITs allowed by this incentives design approach; indeed even for higher values of CT, the proposed FITs approximately converge to the same equilibrium value (with a lower number of

iterations).

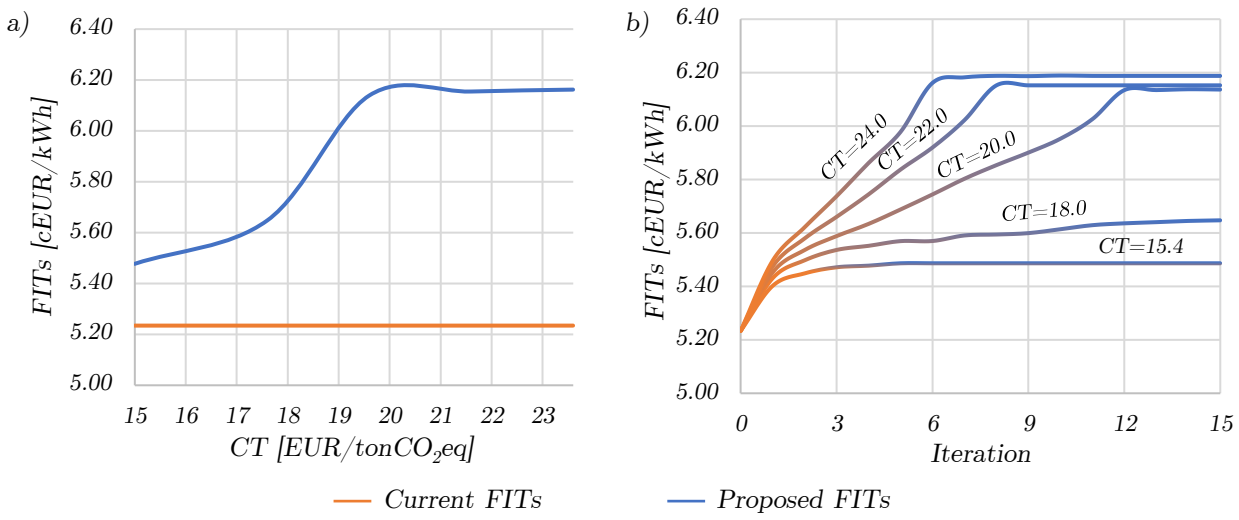

Figure 10: Average FITs a) as function of CT and b) of iterations.

6. Conclusions

This paper proposes a novel design approach for new FITs rewarding RECs members of their environmental benefits. The proposed design framework allows to consider the life cycle carbon dioxide emitted and avoided by RECs depending on time and on the changes of the energy mix. The outcomes resulting from this approach are i) the optimal RECs components size and energy management, evaluated through economic optimization; ii) the environmental performances of RECs and of the energy mix, assessed using LCA; iii) the allocation of RECs benefits on FITs. First these results are presented considering a Base Case Scenario, where carbon taxes are set to 15.4 EUR/tonCO_2eq and RECs load is 25% of the national demand; then, a sensitivity analysis is performed.

In the Base Case Scenario, first the environmental advantages provided by RECs deployment to the national energy system are assessed using the current FITs; then the additional benefits brought by the proposed FITs are calculated. Indeed, since RECs design and energy management are evaluated through economic optimization, FITs play a key role when determining the optimal portfolio of investments and the optimal energy management. Results show that RECs are effective to reduce the national GHGs emissions; indeed, in case the current incentives are adopted, the national emissions are reduced from 121.1 to 109.8 MtonCO_2eq/yr. Most of these advantages are due to SC because, according to the results, RECs prefer self-consuming energy rather than exporting it to the grid due to economic convenience. The proposed incentives instead push RECs to install further PV modules and devote them to increase the energy injection to the grid thus avoiding other GHGs emissions. Such additional advantage is actually quite small, because the injected

energy only increases from 4.0 to 6.3 TWh/yr and thus the amount of GHGs emitted at national level are mitigated by RECs to 108.2 MtonCO_2eq/yr (only 1.6 MtonCO_2eq/yr than using the current FITs). This is due to the fact that, using the proposed approach, the current value of CT in Italy (15.4 EUR/tonCO_2eq) does not determine a large FITs extension. Therefore, the adoption of this energy policy framework requires to modify carbon taxes in order to increase the effectiveness of the proposed incentives. The sensitivity analysis of the parameter CT shows that, increasing carbon taxes, the proposed FITs allow to obtain larger environmental benefits for the national energy system in terms of avoided emissions. Indeed, the PV power deployment and the energy injection to the grid grows very rapidly with CT, promoted by larger additional FITs. Notably, increasing CT from 15.4 to 20 EUR/tonCO_2eq, the energy injected to the grid rises from 6.3 TWh/yr to 78.0 TWh/yr; consequently, the national emissions are strongly reduced (from 108.2 to 84.3 MtonCO_2eq/yr). Further increasing CT does not provide relevant additional environmental advantages because, within the time range when RECs inject electricity, the grid is already saturated of RECs electricity and FITs stop growing to prevent the exportation of excessive (and impactful) electricity. Therefore, in case of adoption of these incentives, carbon taxes should be adapted and set to 20 EUR/tonCO_2eq in order to get the maximum environmental advantages from RECs.

In the future, this work can be further developed by proposing new time-based incentives more focused on the temporal aspects of RECs electricity injection, taking advantage of the dispatchable characteristics of the storage devices. Furthermore, also the SC could be promoted by proposing a novel specific incentive for RECs electricity sharing.

7. Acknowledgements

F.R.,A.S. and R.B. acknowledge MIUR Grant - Department of Excellence 2018-2022. F.R. is grateful for the Ph.D. grant within the “Progetto Pegaso” funded by Regione Toscana.

References

[1] Lowitzsch J, Hoicka CE, and Van Tulder FJ. “Renewable energy communities under the 2019 European Clean Energy Package – Governance model for the energy clusters of the future?” In: *Renewable and Sustainable Energy Reviews* 122 (2020), p. 109489. ISSN: 1364-0321. DOI: https://doi.org/10.1016/j.rser.2019.109489. URL: http://www.sciencedirect.com/science/article/pii/S1364032119306975.

[2] Caramizaru A and Uihlein A. “Energy communities: an overview of energy and social innovation”. In: (2020). URL: https://publications.jrc.ec.europa.eu/repository/bitstream/JRC119433/energy_communities_report_final.pdf (visited on 07/07/2020).

[3] Koirala BP et al. "Energetic communities for community energy: A review of key issues and trends shaping integrated community energy systems". In: *Renewable and Sustainable Energy Reviews* 56 (2016), pp. 722–744. ISSN: 1364-0321. DOI: https://doi.org/10.1016/j.rser.2015.11.080. URL: http://www.sciencedirect.com/science/article/pii/S1364032115013477.

[4] Samarakoon S. "A justice and wellbeing centered framework for analysing energy poverty in the Global South". In: *Ecological Economics* 165 (2019), p. 106385. ISSN: 0921-8009. DOI: https://doi.org/10.1016/j.ecolecon.2019.106385. URL: http://www.sciencedirect.com/science/article/pii/S0921800919300461.

[5] Betto F, Garengo P, and Lorenzoni A. "A new measure of Italian hidden energy poverty". In: *Energy Policy* 138 (2020), p. 111237. ISSN: 0301-4215. DOI: https://doi.org/10.1016/j.enpol.2019.111237. URL: http://www.sciencedirect.com/science/article/pii/S0301421519308183.

[6] Montojo M. "Crevillent – Spain's first local energy community". In: (2020). URL: https://www.oneearth.org/crevillent-spains-first-local-energy-community/ (visited on 12/12/2020).

[7] EnelX. "Renewable Energy Communities: clean energy for self-consumption". In: (2020). URL: https://www.enelx.com/it/en/resources/stories/2020/05/what-are-energy-communities (visited on 07/07/2020).

[8] Networks Italian Regulatory Authority for Energy and Environment. "Self-consumption and energy communities". In: (2020). URL: https://www.arera.it/it/inglese/index.htm (visited on 12/12/2020).

[9] GSE - Gestore dei servizi energetici. "Renewable energy - Incentive Mechanisms". In: (2020). URL: https://www.gse.it/en/what-we-do/renewable-energy#Meccanismi (visited on 01/08/2020).

[10] Sorgenia. "Servizio di scambio sul posto, come funziona". In: (2020). URL: https://www.sorgenia.it/guida-energia/mercato-libero/scambio-sul-posto-come-funziona?campaign_code=SEM-DSA&gclid=CjOKCQjwgo_5BRDuARIsADDEntTEyODyeBbpyqEVTSAYZFTMJ2V1O64x7OW9xqDJ8Yeg7bb_DttZaiQaAtqEEALw_wcB&gclsrc=aw.ds (visited on 01/08/2020).

[11] Antonelli M and Desideri U. "The doping effect of Italian feed-in tariffs on the PV market". In: *Energy Policy* 67 (2014), pp. 583–594. ISSN: 0301-4215. DOI: https://doi.org/10.1016/j.enpol.2013.12.025. URL: http://www.sciencedirect.com/science/article/pii/S030142151301269X.

[12] Energy Italian National Agency for New Technologies and Sustainable Economic Development - ENEA. "Tax deductions". In: (2018). URL: https://detrazionifiscali.enea.it/ (visited on 10/11/2020).

[13] Menanteau P, Finon D, and Lamy ML. "Prices versus quantities: choosing policies for promoting the development of renewable energy". In: *Energy Policy* 31.8 (2003), pp. 799–812. ISSN: 0301-4215. DOI: https://doi.org/10.1016/S0301-4215(02)00133-7. URL: http://www.sciencedirect.com/science/article/pii/S0301421502001337.

[14] Ringel M. "Fostering the use of renewable energies in the European Union: the race between feed-in tariffs and green certificates". In: *Renewable Energy* 31.1 (2006), pp. 1–17. ISSN: 0960-1481. DOI: https://doi.org/10.1016/j.renene.2005.03.015. URL: http://www.sciencedirect.com/science/article/pii/S0960148105000789.

[15] Fagiani R, Barquín J, and Hakvoort R. "Risk-based assessment of the cost-efficiency and the effectivity of renewable energy support schemes: Certificate markets versus feed-in tariffs". In: *Energy Policy* 55 (2013). Special section: Long Run Transitions to Sustainable Economic Structures in the European Union and Beyond, pp. 648–661. ISSN: 0301-4215. DOI: https://doi.org/10.1016/j.enpol.2012.12.066. URL: http://www.sciencedirect.com/science/article/pii/S0301421512011330.

[16] Dong CG. "Feed-in tariff vs. renewable portfolio standard: An empirical test of their relative effectiveness in promoting wind capacity development". In: *Energy Policy* 42 (2012), pp. 476–485. ISSN: 0301-4215. DOI: https://doi.org/10.1016/j.enpol.2011.12.014. URL: http://www.sciencedirect.com/science/article/pii/S0301421511010068.

[17] OECD. *Effective Carbon Rates*. 2016, p. 172. DOI: https://doi.org/https://doi.org/10.1787/9789264260115-en. URL: https://www.oecd-ilibrary.org/content/publication/9789264260115-en.

[18] Daniele Poponi, Riccardo Basosi, and Lado Kurdgelashvili. "Subsidisation cost analysis of renewable energy deployment: A case study on the Italian feed-in tariff programme for photovoltaics". In: *Energy Policy* 154 (2021), p. 112297. ISSN: 0301-4215. DOI: https://doi.org/10.1016/j.enpol.2021.112297. URL: https://www.sciencedirect.com/science/article/pii/S030142152100166X.

[19] Sayed ET et al. "A critical review on environmental impacts of renewable energy systems and mitigation strategies: Wind, hydro, biomass and geothermal". In: *Science of The Total Environment* 766 (2021), p. 144505. ISSN: 0048-9697. DOI: https://doi.org/10.1016/j.scitotenv.2020.144505. URL: http://www.sciencedirect.com/science/article/pii/S0048969720380360.

[20] Lawrence Berkeley National Laboratory (LBNL). "Distributed Energy Resources - Customer Adoption Model (DER-CAM)". In: (2019). URL: https://building-microgrid.lbl.gov/projects/der-cam (visited on 03/20/2019).

[21] Maheshwari A, Heleno M, and Ludkovski M. "The effect of rate design on power distribution reliability considering adoption of distributed energy resources". In: *Applied Energy* 268 (2020), p. 114964. ISSN: 0306-2619. DOI: https://doi.org/10.1016/j.apenergy.2020.114964. URL: https://www.sciencedirect.com/science/article/pii/S0306261920304761.

[22] Heleno M et al. "Probabilistic impact of electricity tariffs on distribution grids considering adoption of solar and storage technologies". In: *Applied Energy* 279 (2020), p. 115826. ISSN: 0306-2619. DOI: https://doi.org/10.1016/j.apenergy.2020.115826. URL: https://www.sciencedirect.com/science/article/pii/S0306261920313040.

[23] Cardoso G et al. "Battery aging in multi-energy microgrid design using mixed integer linear programming". In: *Applied Energy* 231 (2018), pp. 1059–1069. ISSN: 0306-2619. DOI: https://doi.org/10.1016/j.apenergy.2018.09.185. URL: http://www.sciencedirect.com/science/article/pii/S0306261918315058.

[24] Zubi G et al. "Lithium-ion battery-packs for solar home systems: Layout, cost and implementation perspectives". In: *Journal of Energy Storage* 32 (2020), p. 101985. ISSN: 2352-152X. DOI: https://doi.org/10.1016/j.est.2020.101985. URL: https://www.sciencedirect.com/science/article/pii/S2352152X2031820X.

[25] Rossi F et al. "Environmental and economic optima of solar home systems design: A combined LCA and LCC approach". In: *Science of The Total Environment* 744 (2020), p. 140569. ISSN: 0048-9697. DOI: https://doi.org/10.1016/j.scitotenv.2020.140569. URL: http://www.sciencedirect.com/science/article/pii/S0048969720340912.

[26] Peters JF and Weil M. "Providing a common base for life cycle assessments of Li-Ion batteries". In: *Journal of Cleaner Production* 171 (2018), pp. 704–713. ISSN: 0959-6526. DOI: https://doi.org/10.1016/j.jclepro.2017.10.016. URL: http://www.sciencedirect.com/science/article/pii/S0959652617323077.

[27] Rossi F et al. "Life Cycle Inventory datasets for nano-grid configurations". In: *Data in Brief* 28 (2020), p. 104895. ISSN: 2352-3409. DOI: https://doi.org/10.1016/j.dib.2019.104895. URL: http://www.sciencedirect.com/science/article/pii/S2352340919312508.

[28] Rossi F et al. "Life Cycle Assessment of Classic and Innovative Batteries for Solar Home Systems in Europe". In: *Energies* 13.13 (2020). ISSN: 1996-1073. DOI: 10.3390/en13133454. URL: https://www.mdpi.com/1996-1073/13/13/3454.

[29] Rossi F et al. "Environmental analysis of a nano-grid: A Life Cycle Assessment". In: *Science of The Total Environment* 700 (2020), p. 134814. ISSN: 0048-9697. DOI: https://doi.org/10.1016/j.scitotenv.2019.134814. URL: http://www.sciencedirect.com/science/article/pii/S0048969719348053.

[30] Butler L and Neuhoff K. "Comparison of feed-in tariff, quota and auction mechanisms to support wind power development". In: *Renewable Energy* 33.8 (2008), pp. 1854–1867. ISSN: 0960-1481. DOI: https://doi.org/10.1016/j.renene.2007.10.008. URL: http://www.sciencedirect.com/science/article/pii/S0960148107003242.

[31] Kitzing L. "Risk implications of renewable support instruments: Comparative analysis of feed-in tariffs and premiums using a mean–variance approach". In: *Energy* 64 (2014), pp. 495–505. ISSN: 0360-5442. DOI: https://doi.org/10.1016/j.energy.2013.10.008. URL: http://www.sciencedirect.com/science/article/pii/S0360544213008414.

[32] Falconett I and Nagasaka K. "Comparative analysis of support mechanisms for renewable energy technologies using probability distributions". In: *Renewable Energy* 35.6 (2010), pp. 1135–1144. ISSN: 0960-1481. DOI: https://doi.org/10.1016/j.renene.2009.11.019. URL: http://www.sciencedirect.com/science/article/pii/S0960148109004959.

[33] Candelise C and Ruggieri G. "Status and Evolution of the Community Energy Sector in Italy". In: *Energies* 13.8 (2020). ISSN: 1996-1073. DOI: 10.3390/en13081888. URL: https://www.mdpi.com/1996-1073/13/8/1888.

[34] Mudasser M, Yiridoe EK, and Corscadden K. "Economic feasibility of large community feed-in tariff-eligible wind energy production in Nova Scotia". In: *Energy Policy* 62 (2013), pp. 966–977. ISSN: 0301-4215. DOI: https://doi.org/10.1016/j.enpol.2013.07.108. URL: http://www.sciencedirect.com/science/article/pii/S0301421513007660.

[35] Dong S et al. "Improving the feasibility of household and community energy storage: A techno-enviro-economic study for the UK". In: *Renewable and Sustainable Energy Reviews* 131 (2020), p. 110009. ISSN: 1364-0321. DOI: https://doi.org/10.1016/j.rser.2020.110009. URL: http://www.sciencedirect.com/science/article/pii/S1364032120303002.

[36] Nolden C. "Governing community energy—Feed-in tariffs and the development of community wind energy schemes in the United Kingdom and Germany". In: *Energy Policy* 63 (2013), pp. 543–552. ISSN: 0301-4215. DOI: https://doi.org/10.1016/j.enpol.2013.08.050. URL: http://www.sciencedirect.com/science/article/pii/S0301421513008549.

[37] Kim KK and Lee CG. "Evaluation and optimization of feed-in tariffs". In: *Energy Policy* 49 (2012). Special Section: Fuel Poverty Comes of Age: Commemorating 21 Years of Research and Policy, pp. 192–203. ISSN: 0301-4215. DOI: https://doi.org/10.1016/j.enpol.2012.05.070. URL: http://www.sciencedirect.com/science/article/pii/S0301421512004831.

[38] Ayompe LM and Duffy A. "Feed-in tariff design for domestic scale grid-connected PV systems using high resolution household electricity demand data". In: *Energy Policy* 61 (2013), pp. 619–627. ISSN: 0301-4215. DOI: https://doi.org/10.1016/j.enpol.2013.06.102. URL: http://www.sciencedirect.com/science/article/pii/S0301421513006095.

[39] Mpholo M et al. "Determination of the lifeline electricity tariff for Lesotho". In: *Energy Policy* 140 (2020), p. 111381. ISSN: 0301-4215. DOI: https://doi.org/10.1016/j.enpol.2020.111381. URL: http://www.sciencedirect.com/science/article/pii/S0301421520301373.

[40] Devine MT, Farrell N, and Lee WT. "Optimising feed-in tariff design through efficient risk allocation". In: *Sustainable Energy, Grids and Networks* 9 (2017), pp. 59–74. ISSN: 2352-4677. DOI: https://doi.org/10.1016/j.segan.2016.12.003. URL: http://www.sciencedirect.com/science/article/pii/S2352467716301990.

[41] Barbosa L et al. "Feed-in tariff contract schemes and regulatory uncertainty". In: *European Journal of Operational Research* 287.1 (2020), pp. 331–347. ISSN: 0377-2217. DOI: https://doi.org/10.1016/j.ejor.2020.04.054. URL: http://www.sciencedirect.com/science/article/pii/S0377221720304070.

[42] Martin NJ and Rice JL. "Examining the use of concept analysis and mapping software for renewable energy feed-in tariff design". In: *Renewable Energy* 113 (2017), pp. 211–220. ISSN: 0960-1481. DOI: https://doi.org/10.1016/j.renene.2017.05.068. URL: http://www.sciencedirect.com/science/article/pii/S0960148117304603.

[43] Abada I, Ehrenmann A, and Lambin X. "Unintended consequences: The snowball effect of energy communities". In: *Energy Policy* 143 (2020), p. 111597. ISSN: 0301-4215. DOI: https://doi.org/10.1016/j.enpol.2020.111597. URL: http://www.sciencedirect.com/science/article/pii/S0301421520303359.

[44] International Organization for Standardization. "ISO 14040:2006 Environmental management — Life cycle assessment — Principles and framework". In: (2016). URL: https://www.iso.org/standard/37456.html (visited on 12/05/2019).

[45] International Organization for Standardization. "Environmental management — Life cycle assessment — Requirements and guidelines". In: (2016). URL: https://www.iso.org/standard/38498.html (visited on 12/05/2019).

[46] Kiss B, Kácsor E, and Szalay Z. "Environmental assessment of future electricity mix – Linking an hourly economic model with LCA". In: *Journal of Cleaner Production* 264 (2020), p. 121536. ISSN: 0959-6526. DOI: https://doi.org/10.1016/j.jclepro.2020.121536. URL: http://www.sciencedirect.com/science/article/pii/S0959652620315833.

[47] Roux C et al. "Integrating climate change and energy mix scenarios in LCA of buildings and districts". In: *Applied Energy* 184 (2016), pp. 619–629. ISSN: 0306-2619. DOI: https://doi.org/10.1016/j.apenergy.2016.10.043. URL: http://www.sciencedirect.com/science/article/pii/S0306261916314830.

[48] IBM Corporation. "IBM ILOG CPLEX Optimization Studio CPLEX User's Manual". In: (2017). URL: https://www.ibm.com/support/knowledgecenter/SSSA5P_12.8.0/ilog.odms.studio.help/pdf/usrcplex.pdf (visited on 12/12/2021).

[49] python.org. "Python user manual". In: (2019). URL: https://docs.python.org/3/download.html (visited on 03/20/2019).

[50] GreenDelta GmbH. "openLCA Comprehensive User Manual". In: (2019). URL: http://www.openlca.org/wp-content/uploads/2019/07/openLCA-1-9_User-Manual.pdf (visited on 12/05/2019).

[51] Moreno Ruiz E et al. "Ecoinvent 3.6 Report of Changes". In: (2019). URL: https://www.ecoinvent.org/database/ecoinvent-36/report-of-changes-ecoinvent-36/report-of-changes-ecoinvent-36.html (visited on 07/07/2020).

[52] Latunussa CEL et al. "Life Cycle Assessment of an innovative recycling process for crystalline silicon photovoltaic panels". In: *Solar Energy Materials and Solar Cells* 156 (2016). Life cycle, environmental, ecology and impact analysis of solar technology, pp. 101–111. ISSN: 0927-0248. DOI: https://doi.org/10.1016/j.solmat.2016.03.020. URL: http://www.sciencedirect.com/science/article/pii/S0927024816001227.

[53] Weber S et al. "Life Cycle Assessment of a Vanadium Redox Flow Battery". In: *Environmental Science & Technology* 52.18 (2018). PMID: 30132664, pp. 10864–10873. DOI: 10.1021/acs.est.8b02073. eprint: https://doi.org/10.1021/acs.est.8b02073. URL: https://doi.org/10.1021/acs.est.8b02073.

[54] European Commission. "Characterisation factors of the ILCD Recommended Life Cycle Impact Assessment methods". In: (2018). URL: https://eplca.jrc.ec.europa.eu/uploads/LCIA-characterization-factors-of-the-ILCD.pdf (visited on 07/07/2020).

[55] Joint Research Center - JRC. "Photovoltaic Geographical Information System". In: (2020). URL: https://re.jrc.ec.europa.eu/pvg_tools/it/#PVP (visited on 07/07/2020).

[56] Quoilin S et al. "Quantifying self-consumption linked to solar home battery systems: Statistical analysis and economic assessment". In: *Applied Energy* 182 (2016), pp. 58–67. ISSN: 0306-2619. DOI: https://doi.org/10.1016/j.apenergy.2016.08.077. URL: http://www.sciencedirect.com/science/article/pii/S0306261916311643.

[57] Terna S.p.a. "Terna - download Center". In: (2019). URL: https://www.terna.it/en/electric-system/transparency-report/download-center (visited on 01/08/2020).

[58] Gestore Mercati Energetici. "GME Historic Data". In: (2019). URL: https://www.mercatoelettrico.org/En/Tools/Accessodati.aspx?ReturnUrl=%5C%2fen%5C%2fdownload%5C%2fDatiStorici.aspx (visited on 01/08/2020).

[59] Notter DA et al. "Contribution of Li-Ion Batteries to the Environmental Impact of Electric Vehicles". In: *Environmental Science & Technology* 44.19 (2010), pp. 7744–7744. DOI: 10.1021/es1029156. eprint: https://doi.org/10.1021/es1029156. URL: https://doi.org/10.1021/es1029156.

5. Conclusions

Over the last years, research on sustainable energy became a fundamental hotspot in many national and international programs aiming to face huge environmental challenges like Climate Change and the depletion of the Earth natural resources. The large-scale deployment of renewable energy technologies, including PV and storage, is gradually leading the energy transition towards a decarbonized society. Nevertheless, this transformation of the current national energy systems implies many technical, economic, and environmental challenges:

- The variability of some energy sources, such as solar radiation, determines a mismatch between energy production and demand profiles. Such mismatch may lead to overload the grid during peaks of PV productivity whereas, in other moments, a massive amount of fossils fuels is consumed to compensate the lack of solar radiation. Storing the PV energy surplus allows to disconnect the production and the demand of electricity in time.
- Renewable energy and energy storage technologies should be economically competitive with traditional technologies and incentives play a key role in this perspective.
- All technologies, including PV and energy storage systems, generates environmental impacts over their life cycle affecting other indicators like metal depletion, acidification, and toxicity over the global warming potential. Therefore, an excessive and inadequate deployment of renewable energy systems could have negative consequences for the environment.

Among all the energy systems producing electricity from renewable sources, residential installations like SHSs and RECs are spreading rapidly because they guarantee benefits both to their users and to the national energy system. Among storage technologies, this thesis particularly focuses on LIBs because they currently represent the leader technology on the market but also PHS and more advanced ESSs like SSLIBs, post-LIBs, CHS, TEES and hybrid storage systems are considered.

LCA is applied as main methodology to assess SHSs and RECs environmental sustainability, but some auxiliary approaches are combined within an "Integrated LCA" analysis that includes a techno-economic evaluation. Notably, the design and modelling equations allows to compare the technical properties of different ESSs and to catch the spatial and temporal variability of solar radiation. LCC and MILP optimization are used to combine techno-economic and environmental evaluations concerning SHSs and RECs optimal design and energy management. Exergo-economic and exergo-environmental analyses instead are applied to include exergy losses when evaluating TEES sustainability.

A preliminary comparison of storage technologies involves LIBs, PHS, CHS and TEES. Among them, LIBs and TEES have the lowest environmental burdens but the costs of TEES, assessed through an exergo-economic analysis, are too high compared to the market values of electricity. Therefore, TEES operation time could be reduced and limited to the high-solar radiation months for economic reasons, which would drastically affect the environmental performances. Furthermore, the exergo-environmental analysis demonstrates that energy quality losses occurring in heat exchangers are responsible for additional burdens. For these reasons, a combination of LIBs and PV results to be the most sustainable system among the proposed solutions. Therefore, this thesis focuses on the comparison of off-grid and on-grid SHSs through a case study set in Siena (Italy); NCA, NCM, LTO,

LFP, LMO devices are compared to select the most sustainable choice for this application. This comparison is also extended to a nano-grid equipped with a hybrid storage system integrating LIBs and CHS. NCA batteries result as the most suitable choice, but NCM devices also have a very similar eco-profile. These batteries can take advantage of the best compromise between materials availability, energy density and lifespan, being the most influencing factors for the evaluation. Off-grid SHSs, although competitive with the Italian national energy mix, are strongly penalized during winter because of the impact of a diesel backup generator. Moreover, they do not have the possibility to export the PV surplus to the grid when batteries capacity is full. Hybrid nano-grids allow to go beyond this issue because CHS is designed for seasonal storage; on the other hand, the depletion of rare metals used to produce fuel cells, electrolyzers and hydrogen tanks negatively affect the eco-profile of the hybrid nano-grid. Therefore, the most sustainable configuration consists of a grid connected SHS deploying NCA batteries. An equivalent analysis is applied to an extended range of European installation sites and to a larger number of batteries including LIBs, SSLIBs and post-LIBs. This assessment shows that SHSs are competitive with the national energy mixes in southern Europe countries where they take advantage of larger solar radiation levels than in northern Europe. Among the considered batteries, NCA and NCM batteries are confirmed as the most sustainable choice in all installation sites. The entry of SSLIBs, that could occur in a mid-term scenario (2025), could provide environmental benefits thanks to an enhanced energy density. Some post-LIBs like SIBs and VRFB, that could become mature on long-term (2030), are already competitive from the environmental point of view with the most consolidated storage technologies and could become the most sustainable ones in case the research will be able to enhance their lifespan and energy density. When lithium-ion batteries costs are considered, a cross-analysis of the economic and the environmental optimal design of SHSs underlines the need of reducing batteries costs. Indeed, the environmental impact minimization allows optimize the SHSs eco-profile but provides a too expensive solution. Differently, economic optimization allows for the best combination between economic and environmental performances but, in this case, batteries are not included in the optimal configuration. Nevertheless, the costs of PV and LIBs are expected to drastically decrease in the next future; in this scenario, LTO batteries could become the most profitable choice and the economic optimum impact could be reduced thus getting much closer to the environmental optimum. Assuming a large-scale diffusion of renewable energy technologies and, particularly, of RECs on Italian territory would avoid a relevant amount of GHGs emissions. Economic incentives have a very important role in RECs members decisions in terms of energy management strategy and technologies deployment. The novel incentives proposed in this thesis are designed to reward RECs for their environmental benefits and, at the same time, to prevent an excessive production of PV systems. The magnitude of additional environmental advantages provided by the proposed feed-in tariffs depends on carbon taxes level: in case of adoption of the proposed incentives framework, carbon taxes should be adequately modified and increased from 15.4 €/tonCO_2 to 20 €/tonCO_2 to strongly amplify the amount of avoided GHGs emissions.

Bibliography

[1] Narayan N, Papakosta T, Vega-Garita V, Qin Z, Popovic-Gerber J, Bauer P, et al. Estimating battery lifetimes in Solar Home System design using a practical modelling methodology. Appl Energy 2018;228:1629–39. https://doi.org/10.1016/j.apenergy.2018.06.152.

[2] Pourakbari-Kasmaei M, Asensio M, Lehtonen M, Contreras J. Trilateral Planning Model for Integrated Community Energy Systems and PV-Based Prosumers—A Bilevel Stochastic Programming Approach. IEEE Trans Power Syst 2020;35:346–61. https://doi.org/10.1109/TPWRS.2019.2935840.

[3] International Standards Organization. EN ISO 14040:2006 - Valutazione del ciclo di vita Principi e quadro di riferimento. Environ Manage 2010;14040.

[4] International Standards Organization. UNI EN ISO 14044:2006 - Gestione ambientale - Valutazione del ciclo di vita - Requisiti e linee guida. Environ Manage 2006.

[5] International Standards Organization. UNI EN ISO 15686 Buildings and constructed assets — Service life planning — Part 5: Life-cycle costing 2017.

[6] European Commission. What is the European Green Deal ? What will we do ? 2019.

[7] International Energy Agency - iea. Data and Statistics 2020. https://www.iea.org/data-and-statistics?country=WEOAFRICA&fuel=Energy consumption&indicator=Electricity consumption (accessed August 17, 2020).

[8] Enerdata. Global Energy Statistical Yearbook 2020. https://yearbook.enerdata.net/ (accessed December 2, 2020).

[9] Hannah Ritchie. How long before we run out of fossil fuels? 2017. https://ourworldindata.org/how-long-before-we-run-out-of-fossil-fuels (accessed September 14, 2020).

[10] United Nations. Kyoto Protocol to the United Natoions framework convention on Climate Change 1998.

[11] Steffen W, Rockström J, Richardson K, Lenton TM, Folke C, Liverman D, et al. Trajectories of the Earth System in the Anthropocene. Proc Natl Acad Sci U S A 2018;115:8252–9. https://doi.org/10.1073/pnas.1810141115.

[12] United Nations. Paris Agreement 2015:1–27. https://unfccc.int/sites/default/files/english_paris_agreement.pdf (accessed August 18, 2020).

[13] Integrated Panel on Climate Changes. Charts 2020. https://www.ipcc.ch/sr15/faq/faq-chapter-1/ (accessed August 18, 2020).

[14] International Energy Agency. World Energy Outlook 2019. https://www.iea.org/reports/world-energy-outlook-2019/electricity#abstract (accessed August 18, 2020).

[15] European Commission. 2030 climate & energy framework 2020.

[16] Ministry of Economic Development. Integrated National Energy and Climate Plan 2019. https://www.mise.gov.it/images/stories/documenti/it_final_necp_main_en.pdf (accessed August 18, 2020).

[17] European Commission. European SmartGrids Technology Platform - Vision and Strategy for Europe's Electricity Networks of the Future. 2006.

[18] Campos I, Marín-gonzález E. Energy Research & Social Science People in transitions : Energy citizenship , prosumerism and social movements in Europe. Energy Res Soc Sci 2020;69:101718. https://doi.org/10.1016/j.erss.2020.101718.

[19] Nosratabadi SM, Hooshmand R, Gholipour E. A comprehensive review on microgrid and virtual power plant concepts employed for distributed energy resources scheduling in power systems. Renew Sustain Energy Rev 2017;67:341–63. https://doi.org/10.1016/j.rser.2016.09.025.

[20] Baker GH. Microgrids — A Watershed Moment. Wiley - Insight 2020:32–5. https://doi.org/10.1002/inst.12295.

[21] Nordman B. Nanogrids Evolving our electricity systems from the bottom up, 2010.

[22] Caramizaru A. Energy communities : an overview of energy and social innovation. n.d. https://doi.org/10.2760/180576.

[23] Fitzgerald G, Mandel J, Morris J, Hervé Touati. The economics of battery energy storage - How multi-use, custumer-sited batteries deliver the most services and value to costumers and the grid 2015. https://rmi.org/wp-content/uploads/2017/03/RMI-TheEconomicsOfBatteryEnergyStorage-FullReport-FINAL.pdf (accessed August 24, 2020).

[24] Manfrida G, Petela K, Rossi F. Natural circulation solar thermal system for water disinfection. Energy 2017;141:1204–14. https://doi.org/10.1016/j.energy.2017.09.132.

[25] Dainelli N, Manfrida G, Petela K, Rossi F. Exergo-economic evaluation of the cost for solar thermal depuration of water. Energies 2017;10. https://doi.org/10.3390/en10091395.

[26] Betto F, Garengo P, Lorenzoni A. A new measure of Italian hidden energy poverty. Energy Policy 2020;138:111237. https://doi.org/https://doi.org/10.1016/j.enpol.2019.111237.

[27] Piernas Muñoz MJ, Castillo Martínez E. Introduction to Batteries. SpringerBriefs Appl. Sci. Technol., 2018, p. 1–8. https://doi.org/10.1007/978-3-319-91488-6_1.

[28] Ease, EERA. European Energy Storage Technology Development 2017.

[29] U.S. Department of Energy. Hydrogen Storage 2020. https://www.energy.gov/eere/fuelcells/hydrogen-storage (accessed September 15, 2020).

[30] EASE, EERA. Energy Storage Technology Descriptions. 2017.

[31] U.S. Department of Energy. Solar Fuels 2020. https://www.energy.gov/science/doe-explainssolar-fuels (accessed December 12, 2020).

[32] Song W, Chen J. Understanding the Energy Storage Principles of Nanomaterials in Lithium-Ion Battery. In: Zhen Q, Bashir S, Liu JL, editors. Nanostructured Mater. Next-Generation Energy Storage Convers. Adv. Batter. Supercapacitors, Berlin, Heidelberg: Springer Berlin Heidelberg; 2019, p. 61–104. https://doi.org/10.1007/978-3-662-58675-4_2.

[33] Kim Y, Shin D, Lee S, Favrat D. Isothermal transcritical CO 2 cycles with TES (thermal energy storage) for electricity storage. Energy 2013;49:484–501. https://doi.org/10.1016/j.energy.2012.09.057.

[34] Buchamann I. Batteries in a Portable World. Fourth Edi. Cadex Electronics Inc.; 2016.

[35] Liu C, Neale ZG, Cao G. Understanding electrochemical potentials of cathode materials in

rechargeable batteries. Mater Today 2016;19:109–23. https://doi.org/10.1016/j.mattod.2015.10.009.

[36] US Geological Survey. Mineral Commodity Study 2018. 2018. https://doi.org/10.3133/70194932.

[37] Bobba S, Carrara S, Huisman J, Mathieux F, Pavel C. Critical Raw Materials for Strategic Technologies and Sectors in the EU - a Foresight Study. 2020. https://doi.org/10.2873/58081.

[38] Nitta N, Wu F, Lee JT, Yushin G. Li-ion battery materials: Present and future. Mater Today 2015;18:252–64. https://doi.org/10.1016/j.mattod.2014.10.040.

[39] Raugei M, Winfield P. Prospective LCA of the production and EoL recycling of a novel type of Li-ion battery for electric vehicles. J Clean Prod 2019;213:926–32. https://doi.org/10.1016/j.jclepro.2018.12.237.

[40] Cusenza MA, Bobba S, Ardente F, Cellura M, Di Persio F. Energy and environmental assessment of a traction lithium-ion battery pack for plug-in hybrid electric vehicles. J Clean Prod 2019;215:634–49. https://doi.org/10.1016/j.jclepro.2019.01.056.

[41] Deng Y, Li J, Li T, Zhang J, Yang F, Yuan C. Life cycle assessment of high capacity molybdenum disulfide lithium-ion battery for electric vehicles. Energy 2017;123:77–88. https://doi.org/10.1016/j.energy.2017.01.096.

[42] Barré A, Deguilhem B, Grolleau S, Gérard M, Suard F, Riu D. A review on lithium-ion battery ageing mechanisms and estimations for automotive applications. J. Power Sources, vol. 241, Elsevier B.V; 2013, p. 680–9. https://doi.org/10.1016/j.jpowsour.2013.05.040.

[43] Leng F, Tan CM, Pecht M. Effect of Temperature on the Aging rate of Li Ion Battery Operating above Room Temperature. Sci Rep 2015;5:1–12. https://doi.org/10.1038/srep12967.

[44] Koleti UR, Rajan A, Tan C, Moharana S, Dinh TQ, Marco J. A Study on the Influence of Lithium Plating on Battery Degradation 2020.

[45] Feng X, Ouyang M, Liu X, Lu L, Xia Y, He X. Thermal runaway mechanism of lithium ion battery for electric vehicles : A review. Energy Storage Mater 2018;10:246–67. https://doi.org/10.1016/j.ensm.2017.05.013.

[46] Lastoskie CM, Dai Q. Comparative life cycle assessment of laminated and vacuum vapor-deposited thin fi lm solid-state batteries. J Clean Prod 2015;91:158–69. https://doi.org/10.1016/j.jclepro.2014.12.003.

[47] Fan L, Deng N, Yan J, Li Z, Kang W, Cheng B. The recent research status quo and the prospect of electrolytes for lithium sulfur batteries. Chem Eng J 2019;369:874–97. https://doi.org/10.1016/j.cej.2019.03.145.

[48] Zackrisson M, Fransson K, Hildenbrand J, Lampic G, O'Dwyer C. Life cycle assessment of lithium-air battery cells. J Clean Prod 2016;135:299–311. https://doi.org/10.1016/j.jclepro.2016.06.104.

[49] Wang H, Xu Q. Materials Design for Rechargeable Metal-Air Batteries. Matter 2019;1:565–95. https://doi.org/10.1016/j.matt.2019.05.008.

[50] Monge M, Gil-alana LA. Automobile components : Lithium and cobalt . Evidence of persistence. Energy 2019;169:489–95. https://doi.org/10.1016/j.energy.2018.12.068.

[51] Hwang JY, Myung ST, Sun YK. Sodium-ion batteries: Present and future. Chem Soc Rev

2017;46:3529–614. https://doi.org/10.1039/c6cs00776g.

[52] Chen Y, Zhuo S, Li Z, Wang C. Redox polymers for rechargeable metal-ion batteries. EnergyChem 2020;100030:100030. https://doi.org/10.1016/j.enchem.2020.100030.

[53] Yusoff NFM, Idris NH, Din MFM, Majid SR, Harun NA, Rahman MM. Investigation on the Electrochemical Performances of Mn2O3 as a Potential Anode for Na- Ion Batteries 2020:1–10. https://doi.org/10.1038/s41598-020-66148-w.

[54] Longo S, Antonucci V, Cellura M, Ferraro M. Life cycle assessment of storage systems: The case study of a sodium/nickel chloride battery. J Clean Prod 2014;85:337–46. https://doi.org/10.1016/j.jclepro.2013.10.004.

[55] Salama M, Attias R, Yemini R, Gofer Y, Aurbach D, Noked M. Metal − Sulfur Batteries: Overview and Research Methods 2019. https://doi.org/10.1021/acsenergylett.8b02212.

[56] Choi C, Kim S, Kim R, Choi Y, Kim S, Jung H. A review of vanadium electrolytes for vanadium redox fl ow batteries. Renew Sustain Energy Rev 2017;69:263–74. https://doi.org/10.1016/j.rser.2016.11.188.

[57] Gubler L. Membranes and separators for redox flow batteries. Curr Opin Electrochem 2019;18:31–6. https://doi.org/10.1016/j.coelec.2019.08.007.

[58] Sanson A, Giuffrida LG. Decarbonizzazione dell'economia italiana. ENEA; 2017.

[59] Huang B. Recycling of lithium-ion batteries : Recent advances and perspectives. J Power Sources 2018;399:274–86. https://doi.org/10.1016/j.jpowsour.2018.07.116.

[60] SET-Plan - European Commission. Implementation Plan - Become competitive in the global battery sector to drive e- mobility and stationary storage forward. 2016.

[61] European Commissio. European Battery Alliance 2017. https://ec.europa.eu/growth/industry/policy/european-battery-alliance_en (accessed September 18, 2020).

[62] Pettit C. PEFCR - Product Environmental Footprint Category Rules for High Specific Energy Rechargeable Batteries for Mobile Applications Version : H Time of validity : 31 December 2020 2020:1–98.

[63] Peters JF, Baumann M, Zimmermann B, Braun J, Weil M. The environmental impact of Li-Ion batteries and the role of key parameters – A review. Renew Sustain Energy Rev 2017;67:491–506. https://doi.org/10.1016/j.rser.2016.08.039.

[64] Peters JF, Weil M. Providing a common base for life cycle assessments of Li-Ion batteries. J Clean Prod 2018;171:704–13. https://doi.org/10.1016/j.jclepro.2017.10.016.

[65] Greendelta GmbH. openLCA software 2019.

[66] Ellingsen LA, Majeau-bettez G, Singh B, Srivastava AK, Valøen LO, Strømman AH. Life Cycle Assessment of a Lithium-Ion Battery Vehicle Pack 2013;18:113–24. https://doi.org/10.1111/jiec.12072.

[67] Majeau-bettez G, Hawkins TR, Strømman AH. Life Cycle Environmental Assessment of Lithium-Ion and Nickel Metal Hydride Batteries for Plug-In Hybrid and Battery Electric Vehicles 2011:4548–54. https://doi.org/10.1021/es103607c.

[68] Notter DA, Gauch M, Widmer R, Patrick WA, Stamp A, Zah R, et al. Contribution of Li-Ion Batteries to the Environmental Impact of Electric Vehicles. Environ Sci Technol

2010;44:6550–6. https://doi.org/10.1021/es903729a.

[69] Zackrisson M, Avellán L, Orlenius J. Life cycle assessment of lithium-ion batteries for plug-in hybrid electric vehicles e Critical issues. J Clean Prod 2010;18:1519–29. https://doi.org/10.1016/j.jclepro.2010.06.004.

[70] Bauer C. Okobilanz von Lithium-Ionen Batterien 2010.

[71] Pellow MA, Ambrose H, Mulvaney D, Betita R, Shaw S. Research gaps in environmental life cycle assessments of lithium ion batteries for grid-scale stationary energy storage systems: End-of-life options and other issues. Sustain Mater Technol 2020;23:e00120. https://doi.org/10.1016/j.susmat.2019.e00120.

[72] Dunn JB, Gaines L, Kelly JC, James C, Gallagher KG. Environmental Science vehicle life-cycle energy and emissions and 2015:158–68. https://doi.org/10.1039/c4ee03029j.

[73] Ambrose H, Kendall A. Effects of battery chemistry and performance on the life cycle greenhouse gas intensity of electric mobility. Transp Res Part D Transp Environ 2016;47:182–94. https://doi.org/10.1016/j.trd.2016.05.009.

[74] Mcmanus MC. Environmental consequences of the use of batteries in low carbon systems : The impact of battery production. Appl Energy 2012;93:288–95. https://doi.org/10.1016/j.apenergy.2011.12.062.

[75] Hammond GP, Hazeldine T. Indicative energy technology assessment of advanced rechargeable batteries Intergovernmental Panel on Climate Change. Appl Energy 2015;138:559–71. https://doi.org/10.1016/j.apenergy.2014.10.037.

[76] Hiremath M, Derendorf K, Vogt T. Comparative Life Cycle Assessment of Battery Storage Systems for Stationary Applications 2015. https://doi.org/10.1021/es504572q.

[77] Troy S, Schreiber A, Reppert T, Gehrke HG, Finsterbusch M, Uhlenbruck S, et al. Life Cycle Assessment and resource analysis of all-solid-state batteries. Appl Energy 2016;169:757–67. https://doi.org/10.1016/j.apenergy.2016.02.064.

[78] Richa K, Babbitt CW, Nenadic NG, Gaustad G. Environmental trade-offs across cascading lithium-ion battery life cycles. Int J Life Cycle Assess 2017;22:66–81. https://doi.org/10.1007/s11367-015-0942-3.

[79] Peters J, Buchholz D, Weil M. Environmental Science 2016:1744–51. https://doi.org/10.1039/c6ee00640j.

[80] Kim HC, Wallington TJ, Arsenault R, Bae C, Ahn S, Lee J. Cradle-to-Gate Emissions from a Commercial Electric Vehicle Li-Ion Battery: A Comparative Analysis. Environ Sci Technol 2016;50:7715–22. https://doi.org/10.1021/acs.est.6b00830.

[81] Faria R, Marques P, Garcia R, Moura P, Freire F, Delgado J, et al. Primary and secondary use of electric mobility batteries from a life cycle perspective. J Power Sources 2014;262:169–77. https://doi.org/10.1016/j.jpowsour.2014.03.092.

[82] Delgado MAS, Usai L, Ellingsen LAW, Pan Q, Strømman AH. Correction: Comparative Life Cycle Assessment of a Novel Al-Ion and a Li-Ion Battery for Stationary Applications. [Materials., 12, (2019) (3270)] DOI: 10.3390/ma12193270. Materials (Basel) 2019;12:1–14. https://doi.org/10.3390/MA12233893.

[83] Larcher D, Tarascon JM. Towards greener and more sustainable batteries for electrical energy storage. Nat Chem 2015;7:19–29. https://doi.org/10.1038/nchem.2085.

[84] Santos F, Urbina A, Abad J, López R, Toledo C, Fernández Romero AJ. Environmental and economical assessment for a sustainable Zn/air battery. Chemosphere 2020;250. https://doi.org/10.1016/j.chemosphere.2020.126273.

[85] Weber S, Peters JF, Baumann M, Weil M. Life Cycle Assessment of a Vanadium Redox Flow Battery. Environ Sci Technol 2018;52:10864–73. https://doi.org/10.1021/acs.est.8b02073.

[86] International Energy Agency - Photovoltaic Power Systems Programme. Environmental Life Cycle Assessment of Residential PV and Battery Storage Systems. 2020.

[87] Kabakian V, Mcmanus MC, Harajli H. Attributional life cycle assessment of mounted 1 . 8 kWp monocrystalline photovoltaic system with batteries and comparison with fossil energy production system. Appl Energy 2015;154:428–37. https://doi.org/10.1016/j.apenergy.2015.04.125.

[88] Stolz P, Frischknecht R, Kessler T, Züger Y. Life cycle assessment of PV-battery systems for a cloakroom and club building in Zurich. Prog Photovoltaics Res Appl 2019;27:926–33. https://doi.org/10.1002/pip.3089.

[89] Dufo-López R, Bernal-Agustín JL, Yusta-Loyo JM, Domínguez-Navarro JA, Ramírez-Rosado IJ, Lujano J, et al. Multi-objective optimization minimizing cost and life cycle emissions of stand-alone PV-wind-diesel systems with batteries storage. Appl Energy 2011;88:4033–41. https://doi.org/10.1016/j.apenergy.2011.04.019.

[90] Belmonte N, Girgenti V, Florian P, Peano C, Luetto C, Rizzi P, et al. A comparison of energy storage from renewable sources through batteries and fuel cells: A case study in Turin, Italy. Int J Hydrogen Energy 2016;41:21427–38. https://doi.org/10.1016/j.ijhydene.2016.07.260.

[91] Jones C, Peshev V, Gilbert P, Mander S. Battery storage for post-incentive PV uptake? A financial and life cycle carbon assessment of a non-domestic building. J Clean Prod 2017;167:447–58. https://doi.org/10.1016/j.jclepro.2017.08.191.

[92] Hunt RG, Sellers JD, Franklin WE. Resource and environmental profile analysis: A life cycle environmental assessment for products and procedures. Environ Impact Assess Rev 1992;12:245–69. https://doi.org/https://doi.org/10.1016/0195-9255(92)90020-X.

[93] Klöpffer W. Life Cycle Assessment: From the beginning to the current state. Environ Sci Pollut Res 1997;4:223–8. https://doi.org/10.1007/BF02986351.

[94] Guinée JB, Heijungs R, Huppes G, Zamagni A, Masoni P, Buonamici R, et al. Life cycle assessment: Past, present, and future. Environ Sci Technol 2011;45:90–6. https://doi.org/10.1021/es101316v.

[95] Ecoinvent. Ecoinvent databases 2020. https://www.ecoinvent.org/database/database.html (accessed October 13, 2020).

[96] IBM. IBM ILOG CPLEX Optimization Studio CPLEX User's Manual 2017. https://www.ibm.com/support/knowledgecenter/SSSA5P_12.8.0/ilog.odms.studio.help/pdf/usrcplex.pdf (accessed October 14, 2020).

[97] Bonforte G, Buchgeister J, Manfrida G, Petela K. Exergoeconomic and exergoenvironmental analysis of an integrated solar gas turbine / combined cycle power plant. Energy 2018;156:352–9. https://doi.org/10.1016/j.energy.2018.05.080.

[98] Mathworks. Matlab/Simulink 2019b software 2018. https://it.mathworks.com/ (accessed

March 20, 2019).

[99] The University of Wisconsin Madison. TRaNsient SYstems Simulation Program-TRNSYS16 2006.

[100] F-Chart Software. Engineering Equation Solver user manual n.d. http://www.fchart.com/assets/downloads/ees_manual.pdf (accessed December 14, 2020).

[101] Pranskevichus E. What's New In Python 3.7 2018. https://docs.python.org/3.7/whatsnew/3.7.html (accessed October 14, 2020).

[102] Rossi F, Parisi ML, Maranghi S, Basosi R, Sinicropi A. Environmental analysis of a nano-grid: A Life Cycle Assessment. Sci Total Environ 2020;700. https://doi.org/10.1016/j.scitotenv.2019.134814.

[103] Rossi F, Parisi ML, Maranghi S, Basosi R, Sinicropi A. Life Cycle Inventory datasets for nano-grid configurations. Data Br 2020;28:104895. https://doi.org/10.1016/j.dib.2019.104895.

[104] Rossi F, Parisi ML, Greven S, Basosi R, Sinicropi A. Life Cycle Assessment of Classic and Innovative Batteries for Solar Home Systems in Europe. Energies 2020;13:3454. https://doi.org/10.3390/en13133454.

[105] Fiaschi D, Manfrida G, Petela K, Rossi F, Sinicropi A, Talluri L. Exergo-Economic and Environmental Analysis of a Solar Integrated Thermo-Electric Storage. Energies 2020;13:3484. https://doi.org/10.3390/en13133484.

[106] Rossi F, Heleno M, Basosi R, Sinicropi A. Environmental and economic optima of solar home systems design: A combined LCA and LCC approach. Sci Total Environ 2020;744. https://doi.org/10.1016/j.scitotenv.2020.140569.

[107] Rossi F, Parisi ML, Maranghi S, Manfrida G, Basosi R, Sinicropi A. Environmental impact analysis applied to solar pasteurization systems. J Clean Prod 2019;212. https://doi.org/10.1016/j.jclepro.2018.12.020.

Appendix A

Appendix A contains an additional paper published in *Journal of Cleaner Production* that concerns the environmental assessment of a water disinfection system based on solar energy. This paper addresses the LCA and the exergo-environmental analysis of a Solar Pasteurization system, namely a simple installation to produce safe drinking water by thermal way. Indeed, in case water temperature reaches 80°C, it is disinfected from dangerous bacteria like Escherichia Coli. Such temperature can be easily reached by solar collectors and can be maintained using a sensible heat storage tank. As stressed by this paper, Solar Pasteurization is particularly suitable to face energy poverty in developed and underdeveloped countries. As underlined in Section 2 of this thesis such a relevant issue is also addressed by SHSs and RECs; therefore, these systems could be fruitfully combined with Solar Pasteurization to supply primary needs like water and energy to remote communities. The main outcomes of the paper are:

- The comparison between two different types of Solar Pasteurization Systems in terms of midpoint and endpoint environmental indicators.
- The assessment of the environmental impact due to exergy losses.
- An estimation of the humanitarian benefits provided by Pasteurization systems using the human health damage category in different contexts.

The Ph.D. is the first author of the paper and contributed to the conceptualization, the development of the methodology, the results evaluation, and the writing of the paper.

Journal of Cleaner Production 212 (2019) 1368–1380

Contents lists available at ScienceDirect

Journal of Cleaner Production

journal homepage: www.elsevier.com/locate/jclepro

Environmental impact analysis applied to solar pasteurization systems

Federico Rossi [a, b], Maria Laura Parisi [a, c, *], Simone Maranghi [a, c], Giampaolo Manfrida [b], Riccardo Basosi [a, c, d], Adalgisa Sinicropi [a, c, d, *]

[a] University of Siena, Department of Biotechnology, Chemistry and Pharmacy, Via A. Moro 2, Siena, Italy
[b] University of Florence, Department of Industrial Engineering, Via Santa Marta 3, Florence, Italy
[c] CSGI, Center for Colloid and Surface Science, Via della Lastruccia 3, 50019, Sesto Fiorentino, Italy
[d] Institute of Chemistry of Organometallic Compounds (CNR-ICCOM), Via Madonna del Piano 10, 50019, Sesto Fiorentino, Italy

ARTICLE INFO

Article history:
Received 21 August 2018
Received in revised form
15 November 2018
Accepted 3 December 2018
Available online 7 December 2018

Keywords:
Solar pasteurization
Solar energy
Life cycle assessment
Exergo-environmental analysis
Water treatment
Water disinfection

ABSTRACT

In many under-developed regions of the world, most people live in rural villages, where the electrical grid is often not available and traditional potabilization systems would be too expensive and technologically too complex to be implemented. Thus every year, millions of people in the world die due to diseases related to water contamination. Solar Pasteurization Systems represents a promising alternative to address such problems, as they can thermally disinfect water employing solar energy alone, without using fossil fuels or electrical grid connection. Evaluating the cradle-to-grave environmental footprint of Solar Pasteurization Systems, and in general of technologies aimed at producing safe drinking water, represents an issue of major importance. This is relevant because an effective solution has to be, at the same time, environmentally and locally sustainable for a given geographical context. In this work, a complete Life Cycle Assessment and Exergo-environmental analysis are performed in order to calculate and compare the eco-profiles of two Solar Pasteurization technologies: a Natural Circulation and a Thermostatic Valve System. Results show that Natural Circulations Systems are generally more environmentally sustainable (0.30 mPt/l) than the Thermostatic Valve System (0.83 mPt/l) thanks to the higher productivity of treated water. A sensitivity analysis is performed to investigate the dependency of the model systems from different operational and environmental conditions, at different installation sites, i.e. Somalia, Brazil and Italy. The main difference is represented by the productivity of the systems. In all cases the solar collector array is the main item responsible for environmental burdens, impacting for almost 45% of the total score. The analysis also shows that the use of solar energy in Pasteurization is important to avoid direct emissions and to lower the global environmental impact connected with thermal energy production compared to the eco-profiles of other widely diffused pasteurization technologies based on the combustion of fossil fuels or biomass that can be used to provide the same function (in general higher than 1.2 mPt/l). Moreover, with the aim of qualitatively assessing the benefit associated with the potential implementation of solar pasteurization systems, an improvement of the sanitary conditions is envisioned, especially in under-developed countries where, definitively, a large scale diffusion would be recommended.

1. Introduction

According to UNICEF and World Health Organization (UNICEF and WHO, 2009) diarrhoeal diseases are the second major reason of mortality of children under five years old, killing around 1.5 million of them every year. This situation is extremely aggravated in Africa, where the mortality rate due to unsafe water, hygiene and sanitation services is triple that of the global rate; e.g., in Somalia, more than 60,000 cases of suspected cholera have been reported between January and August 2017 and more than 800 people have died (World Health Organization (WHO) (accessed on 05/04/2018)). Indeed, Somalia is one of the most affected countries by such sanitary disaster related to unsafe water, probably the main vector of cholera's pathogens and many other diseases.

Among technologies that can be applied (Shannon et al., 2008)

* Corresponding authors. University of Siena, Department of Biotechnology, Chemistry and Pharmacy, Via A. Moro 2, Siena, Italy.
E-mail addresses: marialaura.parisi@unisi.it (M.L. Parisi), adalgisa.sinicropi@unisi.it (A. Sinicropi).

https://doi.org/10.1016/j.jclepro.2018.12.020
0959-6526/

Nomenclature

$\dot{Ex}$	Exergy rate, J/s
$\dot{m}$	Mass flow rate, kg/s
h	Specific enthalpy, J/kg
T	Temperature, K
s	Specific entropy, J/(kg × K)
$\dot{B}$	Environmental impact rate of an energy stream, points/s (ReCiPe 2008)
B	Environmental impact of an energy stream, points/d (ReCiPe 2008)
b	Specific environmental impact, points/J (ReCiPe 2008)
$\dot{Y}$	Component-related environmental impact rate associated with the life cycle of the component, points/s (ReCiPe 2008)
Y	Component-related environmental impact associated with the life cycle of the component, points/d (ReCiPe 2008)
f	Exergo-environmental factor, non-dimensional
A	Surface of the solar collector, m^2
ab	Inhabitants
d	Days
h	Hours
NCS	Natural Circulation System
NCS_80	Natural Circulation System with a productivity of the 80%
NCS_eq	Natural Circulation System with an equivalent productivity to the Thermostatic Valve System
NCS_Italy	Natural Circulation System installed in Italy
NCS_Brazil	Natural Circulation System installed in Brazil
NCS_Somalia	Natural Circulation System installed in Somalia
TVS	Thermostatic Valve System
TVS_Italy	Thermostatic Valve System installed in Italy
TVS_Brazil	Thermostatic Valve System installed in Brazil
TVS_Somalia	Thermostatic Valve System installed in Somalia
PTC	Parabolic Trough Concentrator
SC	Solar Collector
CT	Compensation Tank
PV	Photovoltaic
HE	Heat Exchanger
TV	Thermostatic Valve
WT	Water Tank

Subscripts

0	Relative to the environment
j	Relative to the j-th flow
k	Relative to the k-th component
D	Destructions
F	Exergetic fuel
P	Exergetic product
in	Relative to an inlet flow in a component
out	Relative to an outlet flow from a component
TOT	Relative to a total amount
80	Referred to the 80% of ideal productivity
eq	Referred to an equivalent productivity of both systems
Italy	Referred to the case of Italy as installation site
Brazil	Referred to the case of Brazil as installation site
Somalia	Referred to the case of Somalia as installation site

Superscripts

CO	Relative to the construction phase of a component
OM	Relative to the operation and maintenance phase of a component
DI	Relative to the disposal phase of a component

Greek symbols

Δ	Variation

to avoid or limit drinking water contamination, Solar Pasteurization Systems are rather cheap and simple plants able to disinfect water by employing solar energy. Two different Solar Pasteurization Systems are available: The Natural circulation systems (NCSs) and Thermostatic valve systems (TVSs).

The first NCS system was proposed by Boettcher et al. (1983) in which the only driving force of the fluid is the variation of its density induced by solar energy. The volumetric expansion is used to separate treated and untreated water thanks to a well-dimensioned system of pipes. Then Bansal et al. (1988) built and tested a density driven system with an evacuated tubes SC in order to estimate its energetic performances. Ten years later, Cobb (1998) investigated a simple Pasteurization System composed of two concentric copper pipes with a productivity of 7.5 l/h-m^2.

With the aim of improving the NCS's performance, several implementations have been proposed. Duff and Hodgson (2001) built and tested a simple NCS prototype composed of a collector tube and a riser tube. The water in the riser tube is not warmed by the solar radiation and even if the fluid inside the collector tube reaches the required temperature, it impedes the natural circulation and the water inside the collector continues warming up until it boils. To avoid such problem, they introduced an internal loop ensuring that the temperature of the water in the riser tube is always close to the temperature inside the collector (Duff and Hodgson, 2002). Taking inspiration from Duff and Hodgson's idea, Dainelli et al. (2017) and Manfrida et al. (2017) studied a new NCS system (Fig. 1) working as follows: untreated water flows through the makeup pipe from the supply water tank to a regenerative heat

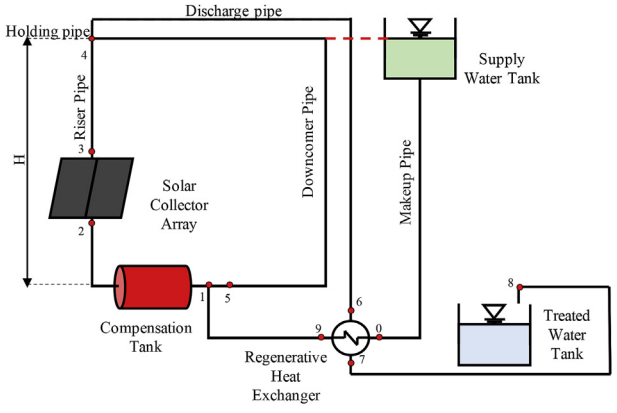

Fig. 1. NCS technical configuration and representative points of the plant (adapted from Manfrida et al., 2017). (0 = inlet cold water flow inside HE; 1 = inlet flow inside the circuit; 2 = inlet water inside the SCs; 3 = outlet water inside the SCs; 4 = outlet water from riser pipe; 5 = end of the circuit; 6 = inlet hot water flow inside the HE; 7 = outlet hot water flow from the HE; 8 = Inlet water to treated WT; 9 = outlet cold water from HE).

exchanger (HE) where it is preheated by the outlet water. Afterwards, inside the circuit, the inlet water flows across a compensation tank (CT) and enters a solar collectors (SCs) array where it is warmed by solar radiation. The concomitant volume increase ensures that the water flows across the riser pipe and, thanks to the difference of volume, enters the holding pipe where, only if the temperature is $\geq 85°$ (enough to kill or inactivate pathogens almost instantly (Burch and Thomas, 1998)), the thermal expansion is sufficient to allow water reaching the treated water tank through the discharge pipe. In that case, the outlet flux is replaced by the same mass of raw water because of the communicating vessels principle. The down-comer pipe brings in the non-overtopped water to close the loop. The mixture of inflow and circulating water goes around the pipes system until a low level of solar radiation causes the flow to stop.

The NCS developed by Manfrida et al. (2017) is sized to warm water up to 85 °C and its productivity is estimated using a mathematical model of the thermo-hydraulics of the system in off-design conditions. Based on the same mathematical model for the estimation of system performances, Dainelli and co-workers performed an exergy analysis and the results were applied for an exergo-economic study of the system (Dainelli et al., 2017).

Duff and Hodgson (Duff and Hodgson, 2005) also reviewed the studies related to the TVSs. In a TVS, the presence of an electronic control device, composed of thermostatic valves and time and temperature sensors, allows the setting of the disinfection conditions for treated water. Thus, contrarily to NCSs, TVSs face the problem of obsolescence and malfunctioning of the thermostatic valves (Duff and Hodgson, 2005) that, as every electronic device, can be damaged. The TVS simplest scheme consists of a flat plate SC between two reservoirs with a thermostatic valve (TV) to regulate the flow of water (Jorgensen, A.J., Nohr, K., Sorensen, H., Boisen, 1998), its productivity was estimated to 50 l/m^2-d. The introduction of a HE to preheat the inlet raw water, improved this value obtaining up to 55 l/h-m^2 as described in the study of Stevens et al. (1998) and up to 205 l/h-m^2 as estimated by Safe Water Systems (2002). A Solar Pasteurization System with a parabolic trough concentrator (PTC), which is estimated to produce 89.3 l/m^2-day of drinking water, has been used by Anderson (1996); after several years Bigoni et al. (2014) tested a very similar PTC Pasteurization plant in order to analyse the efficiency of water disinfection. A prototype of an automated Pasteurization System regulated by TVs has been built, tested and optimised by Carielo da Silva et al. (2016) and Carielo et al. (2017). The layout of the system shown in Fig. 2 is composed of a flat plate SC, a HE, two water tanks (WTs) and a 10 W photovoltaic (PV) panel to provide energy to the electric parts. The system was made operative from 7:00 a.m. to 4:00 p.m. and a control algorithm was implemented so that five set-point conditions are defined: 55 °C/3600 s, 60 °C/2700 s, 65 °C/1800 s, 75 °C/900 s and 85 °C/15 s.

A linear regression (Fig. 3) correlated its productivity, expressed as number of refilled batches (vessels with 2 L of capacity), with solar irradiation in order to estimate the performances of the system in each moment of the year and all over the world (Carielo et al., 2017).

Although a complete potabilization would require the removal of suspended and dissolved contaminants by physical or biological treatments, the NCSs and TVSs can be still used to disinfect water in rural villages where pathogens are the most relevant problem. Indeed, they are responsible for so many victims and their elimination represents the most critical issue for sanitation. Furthermore, physical and biological plants would require a massive consumption of electricity, the employment of expensive chemicals and onerous maintenance.

Thus, taking into account that rural areas are often very poor and unachievable by the electrical grid and transports, these technologies cannot be reliable and a Solar Pasteurization System can represent a suitable and affordable solution in that particular context.

As clarified in the introduction, the performances of the NCSs and the TVSs have been already discussed in several literature papers but none of them encompasses the whole life cycle of the system with an environmental, resource or energy consumption perspective approach. Evaluating the eco-profile of Solar Pasteurization Systems, and in general of technologies aimed at producing safe drinking water, represents an issue of major importance. This is relevant because an effective solution must be, at the same time, environmentally and locally sustainable for a given geographical context. The latter issue is particularly important to contribute to an integrated assessment envisioning the environmental, social and economic dimensions on topics related to water's sanitation and hygiene (Tilley et al., 2014) (Murphy et al., 2009). Such a comprehensive approach is well within the directives of the United Nations (UN) collected in the Agenda for Sustainable Development (United Nations, 2015) (United Nations, 2016) (United Nations, 2017). Indeed, among the 17 Sustainable Development Goals (SDGs), the mission of Goal 6 is precisely to “Ensure availability and sustainable management of water and sanitation for all”. In this context, water research and development is strongly encouraged (United Nations, 2016). However, the present study could also contribute to reach the objectives of other SDGs concerning poverty, food and energy matters (e.g., SDG 7: “Ensure access to affordable, reliable, sustainable and modern energy for all”).

The aim of this study is to apply the Life Cycle Assessment (LCA)

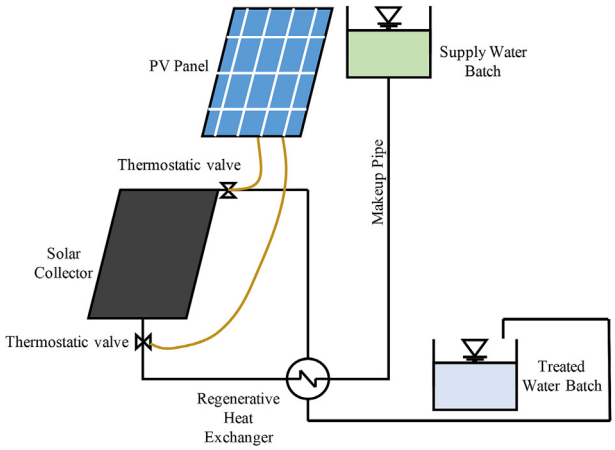

Fig. 2. TVS technical configuration (adapted from Carielo et al., 2017).

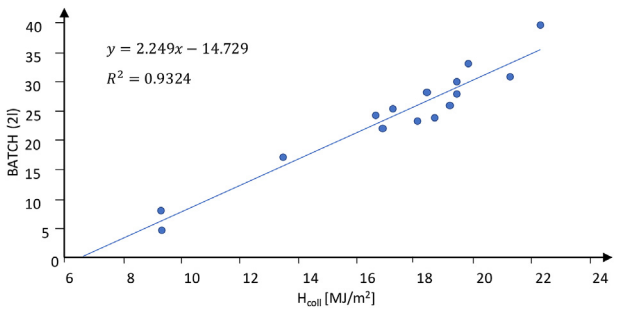

Fig. 3. TVS productivity (refilled batches, i.e. 2 L vessels) as function of the solar irradiance (adapted from Carielo et al., 2017).

and exergo-environmental methodology to estimate the potential environmental advantages connected with the use of Solar Pasteurization. The LCA is a powerful methodology to assess the potential environmental impacts connected with a product system embracing all raw materials and energy flows involved in its life cycle from a quantitative point of view (Bravi et al., 2010; Parisi et al., 2013). The exergo-environmental analysis is a very useful tool integrating the quantitative approach of LCA with qualitative aspects. Exergy is defined as the maximum useful work possible during a process that brings the system into equilibrium with a heat reservoir (Perrot, 1998) and for such reason it is considered as an indicator of the quality of energy.

Indeed, the quality of the energy flows, represented by the exergy content of water, decreases because of the thermodynamic irreversibility. Thus, the goal of the exergo-environmental analysis is to assess how this unavoidable problem affects the environmental performance of systems which mainly work with thermal energy The LCA approach has already been successfully applied to compare conventional and alternative non-solar Pasteurization Systems of tomato and watermelon juice (Aganovic et al., 2017). An exergy analysis has been performed on a milk processing plant, that also includes a pasteurization system, but no exergo-environmental analysis was implemented as a further investigation (Mojarab Soufiyan et al., 2016). Thus, the application of exergo-environmental analysis to pasteurization system represents an innovative approach. In this study the environmental footprint of the NCS system described by Dainelli et al. (2017) and Manfrida et al. (2017) is calculated and compared to that of the TVS system reported in Carielo da Silva et al. (2016) and Carielo et al. (2017). The evaluation of the dependency of the NCS and TVS eco-profiles on geographical boundaries have been performed through a sensitivity analysis considering different installation sites. Moreover, as both NCS and TVS are powered by solar energy only, to evaluate the environmental benefit associated with a renewable source of energy, a comparison is performed with other technologies based on the combustion of fossil fuels or biomass employed to provide the same amount of thermal energy to heat water. Indeed, the literature provides several examples about how the use of a non renewable source of energy in traditional plants determines high environmental footprints for traditional pasteurization systems (Pardo and Zufía, 2012), especially concerning the global warming and energy depletion categories (Li et al., 2018). Finally, to further investigate the potential of Solar Pasteurization, we perform a qualitative assessment of the potential benefits concerning the human health issue that could be achieved with the implementation of solar pasteurization systems in under-developed countries.

Such results would allow for improved knowledge about available solutions to guarantee potable water supply and thus could contribute to inform and support in choosing the best options for a specific geographical context.

2. Methodological approach

Life Cycle Assessment (LCA) is a very useful methodology to investigate and quantify the environmental impacts connected to a product, process or service system. In this work, an LCA study is presented according to the ISO 14040 (International Standards Organization, 2010) and ISO 14044 (The International Standards Organisation, 2006), regulations that standardize the method that is composed of four phases:

- *Definition of the goal and scope of the system*: includes the description of the model system and its borders, along with the methodological framework;
- *Life Cycle Inventory, LCI*: lists and quantifies all the inlet and outlet flows of energy and materials and releases to the environment;
- *Life Cycle Impact Assessment, LCIA*: impacts generated by the system are assessed through the application of an impact calculation method that translate emissions, resources and energy use into a limited number of environmental indicators;
- *Life Cycle Interpretation*: technical findings and critical points identified through the analysis are employed to outline recommendations and conclusions to improve the sustainability of the system and choosing the best available alternative.

Calculations have been performed with the open source software OpenLCA version 1.7 (developed by Greendelta,). As no prototypes for the NCS and TVS are available and, thus, no primary data could be collected, their analytical models were built considering the configurations described in Dainelli et al. (2017), Manfrida et al. (2017) and Carielo da Silva et al. (2016), Carielo et al. (2017), respectively. Secondary data are taken from the database Ecoinvent 3.4, customized when necessary.

2.1. Definition of the goal and scope of the system

The boundaries of the systems are defined according to a cradle-to-grave approach, including production, operation and disposal phases as represented in Fig. 4:

As already stated in the introduction, the goal of the present analysis is to evaluate and compare the environmental performances of the NCS and TVS systems. The functional unit is defined as 1 L of treated water. In more detail, the study aims to: (i) compare the environmental footprints of solar pasteurization systems in three different locations and to point out the most sustainable solution; (ii) point out the most impactful components and processes involved in the systems; and (iii) evaluate the potential advantages connected with the implementation of Solar Pasteurization Systems respect to the effect of diseases connected with the consumption of unsafe water in the three different geographical context. Concerning these last, the following installation sites have been considered:

- Somalia: a country most affected by diarrhoeal diseases, as highlighted in the introduction;
- Brazil: the country where Carielo da Silva et al. (2016) and Carielo et al. (2017) built and tested the system;

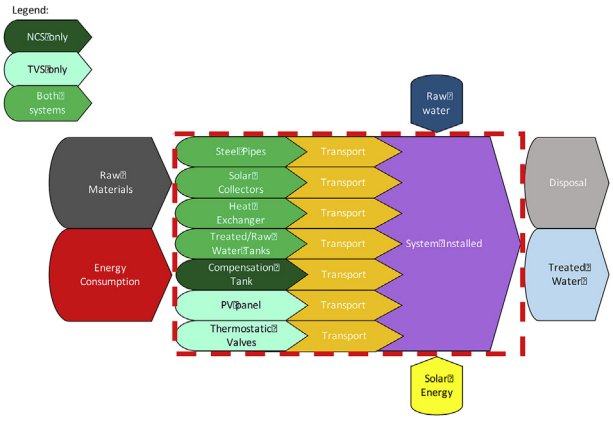

Fig. 4. System boundaries of the solar pasteurization systems considered in this study. Green boxes are referred to common systems components, dark green box refers to the NCS and light green to TVS only. (For interpretation of the references to colour in this figure legend, the reader is referred to the Web version of this article.)

- Italy: one of the countries where Dainelli et al. (2017) and Manfrida et al. (2017) simulated their Solar Pasteurization System.

2.2. LCI

In the framework of LCI, all processes included within the system boundaries are modelled as operational units: for each one of these inlet and outlet flows of matter and energy, environmental releases to the atmosphere, ground and water compartments are accounted. Detailed LCIs for the systems investigated in this study are provided in the supporting information. (SI, section 1). Data collected for the LCI analysis of the components are reported in Table 1.

2.2.1. Transportation

The transportation of the components of the plant can be at the origin of a substantial impact. Jorgensen and Ywema (Jorgensen and Ywema, 1996) focus on the relevance but also on the variability of transportation contribution to the LCA of a product, underlining that is noteworthy to estimate how influencing the transportation parameters (mass of the products, which is set by the physical properties of the components, distances and modes of transport, which vary depending on the starting and arriving points, etc) can affect the results of the analysis. As a definite fabrication site does not exist for the NCS and TVS in this study, an average of all the production and transportation processes connected with the same reference flow characterizing the various components is considered. To take into account the sensitivity of the results to transportation distances and modes, a common starting point is set in Milan and the installation sites are supposed to be rural villages 130 km distant from the nearest city centre and, in particular:

- for Somalia, the components are transported to Ancona port by an EURO6 lorry (about 400 km), to Mogadishu by boat (about 9800 km) and finally to the installation site by an EURO3 lorry (130 km);
- for Brazil, the components are transported to Lisbon by rail (about 2100 km), to Recife by boat (about 5800 km) and finally to the installation site by an EURO3 lorry (130 km);
- for Italy, the components are transported to the installation site near Brindisi by an EURO6 lorry (about 1100 km).

Such a transportation system is schematically represented in Fig. 5.

2.2.2. Installation and maintenance

The installation and maintenance phases of the investigated systems do not require complex procedures nor material nor energy consuming processes (Dainelli et al., 2017) thus their contribution to the analysis has been neglected. The same assumption applies for human labour because, considering the use of plug-and-play components allowing for an easy set-up of the NCS and TVS without the need for qualified operators, its contribution to the total environmental impact would be quite low. On the other hand, the direct occupation and transformation of land connected with systems' installation have been taken into account and evaluated according to an estimation of the area occupied by the plants (Table 2).

For each installation site, the types of landscape considered are:

- Somalia: pasture and meadow as it covers most of the Somalian territory (Hadden and Lee, 2007);
- Brazil (Pernambuco): equatorial forest;
- Italy (Puglia): agricultural landscape.

2.2.3. Operative phase

The operative life of the two systems, defined as the period of time during which they work to produce drinking water, is considered to be fifteen years (Dainelli et al., 2017). The thermostatic valves included in TVSs have a shorter service life, assumed about six years, thus it is necessary to consider their replacement for at least three times during the whole TVS life cycle, for a total of six valves employed.

Concerning the production of drinking water, for the NCS case, the volume produced is estimated using the numerical model developed by Dainelli et al. (2017) and Manfrida et al. (2017); the performances of the TVS are evaluated using the linear regression relation defined by Carielo et al. (2017). The meteorological data are provided by the Meteonorm libraries (Meteonorm Information (accessed on 05/04/2018)) and simulated using the software

Fig. 5. Sketch of the transportation routes and modes.

Table 1
LCI of the systems.

Components	NCS		TVS	
	n° of items	Description	n° of items	Description
Solar collectors (SCs)	2	flat plate evacuated tube SCs with a surface of 1.95 m^2 (VPsolar (accessed on 05/04/2018)).	2	Flat plate SC with a copper absorber and a surface of 1.34 m^2 (Heliotek Bosch Group (accessed on 05/04/2018)).
Compensation Tank (CT)	1	expansion vessel with volume 80 l.	–	
Heat Exchangers (HEs)	1	pipe-in-pipe Heat Exchanger composed of steel pipes and rockwool thermal insulation.	1	Heat exchanger composed of a copper conductive part, rockwool insulation and an external iron box (Carielo da Silva et al., 2016), (Carielo et al., 2017).
Water Tanks (WTs)	2	Polyethylene tanks for inlet and outlet water.	2	Polyethylene tanks for inlet and outlet water.
Photovoltaic (PV) panels	–		1	PV panel with nominal rated power equal to 10 W (Carielo da Silva et al., 2016), (Carielo et al., 2017)
Thermostatic valves (TVs)	–		6	Electronic control devices with 6 years operative life.
Wires	–		–	bipolar copper wire with a length of 7 m (estimated from the arrangement in. Carielo et al., 2017).

Table 2
LCI of the system's installation.

Components	Representative Dimension	NCS	TVS
Direct Land Occupation [m^2·a]	Surface Time	210	163.8
Direct Land Transformation [m^2]	Surface	17.8	10.92

TRNSYS16 (developed by The University of Wisconsin Madison).

The volume of drinking water produced by the NCS and TVS is reported in Table 3. The productivity of the NCS is provided by a mathematical model and has not been validated by experimental tests. The model is based on thermodynamics equations and does not consider that, in real operative conditions, many unpredictable factors could lower the productivity (for instance the growth of seaweeds or the sedimentation of solids inside the pipes). Thus, values reported in Table 3 represent the maximum productivity of the system in ideal conditions. To further investigate the environmental performance of the Solar Pasteurization Systems, two more uncertainty scenarios are analysed: in the first one, a load loss of 20% is assumed (NCS_80) and in the latter the two systems are considered to have the same yearly productivity (NCS_eq).

2.2.4. End-of-Life-phase

Concerning the end-of-life phase, it should be noticed that waste management strategies are very different depending on the countries where the installation sites are set and characterized by variable average recycling rates. In particular:

- Somalia: in under-developed countries waste management options are basically reduced to waste collection without any further treatment, thus no recycling or recovering processes have been taken into account and all the components are supposed to be landfilled;
- Brazil: an average recycling percentage has been set according to Waste TM (accessed on 05/04/2018); the remaining part is supposed to be landfilled;
- Italy: an average recycling percentage has been set according to Eurostat-waste (accessed on 05/04/2018), the remaining part is supposed to be landfilled.

According to these considerations, the recycling rates reported in Table 4 have been implemented in the model:

2.3. LCIA

After having collected all the energy and raw materials flows which enter and exit the system, the LCIA phase allows the calculation of the eco-profile of the systems according to several environmental impact categories. To this aim, various calculation methods are available.

In this study the *ReCiPe 2008, Endpoint (H) [v1.11, December 2014]* method, composed by 17 impact categories, is applied to perform the analysis. As the purpose of this paper is to provide results as general as possible, a hierarchist approach is selected. Endpoint results estimate the damages to the environment of a process or a product grouping them into issues of concern (damage-oriented approach) while midpoint ones express a measurement of effect before damage occurs (problem-oriented approach).

Table 3
Drinking water productivity for one year of the system.

Location	Production [l/year]	
	NCS	TVS
Somalia	75,718	20,562
Brazil	87,935	23,011
Italy	28,342	16,783

Table 4
Recycling rate by installation site.

Location	Somalia	Brazil	Italy
Recycling Rate	0.00%	1.00%	45.1%

The classification of Endpoint results considers three damage categories:

- *Ecosystem*: damage to ecosystems is expressed as number of natural species lost per year (*species/year*);
- *Human Health*: damage to humans is expressed as *disability-adjusted life year* (*DALY*);
- *Resources*: damage to natural resources is expressed as the economic value in dollars of exploitation ($).

Normalisation and weighting are applied *(World ReCiPe H/A [person/year])* in order to express the impact into points allowing for a global comparison among different systems.

2.4. Energy and exergo-environmental analysis

The comparison among NCS and TVS and conventional pasteurization systems is performed to assess the advantages associated with the use of solar energy for water heating. The environmental burden related to the conventional technologies (boilers burning oil, gas, or wood) has been estimated using secondary data from the database Ecoinvent 3.4, ("Ecoinvent," https://www.ecoinvent.org/). Oil is burned in a traditional 10 kW boiler for residential applications; all energy and material flows involved during its life cycle are provided directly by the producers. The same technology is applied to the natural gas combustion as Ecoinvent assumes that the same material and energy flows are involved in the production of oil boilers with similar size. Mixed logs are burned in a furnace developed in Switzerland and considered by Ecoinvent as the average technology for domestic applications. These processes are also inclusive of all the required ancillary technologies, such as fuel storage systems and electronic control devices.

In Solar Pasteurization Systems, water is warmed up to 85 °C and has a sensible energy and exergy content that allows it to be considered as an energy carrier. In the analysed system, the exergy content of water is different in each point of the plant. For such reason the following equations are evaluated at representative points of the plant (Fig. 1) indicated by the subscript "j". Considering the environmental conditions as the reference and water as a non-reactive species, the exergy rate of the j-flow $\dot{E}x_j$ (J/s) can be evaluated by Eq. (1):

$$\dot{E}x_j = \dot{m}_j\left[(h_j - h_0) - T_0(s_j - s_0)\right] \quad (1)$$

Where $\dot{m}_j$, h_j and s_j are respectively the water mass flow rate (kg/s), the specific enthalpy (J/kg) and the specific entropy (J/(kg × K)) related to the j-th flow; h_0, T_0 and s_0 are the specific enthalpy (J/kg), the temperature (K) and the specific entropy (J/(kg × K)) of the environment.

We see that temperature rise of water inside the SCs represents an increase of exergy, and thus a quality improvement but it has a cost in terms of environmental impact.

Thus, a damage can be allocated to the exergy content of water applying the definition of specific impact rate (Buchgeister, 2010) b_j

(points/J):

$$b_j = \frac{\dot{B}}{\dot{E}x_j} \tag{2}$$

Where $\dot{B}_j$ is the environmental impact rate of j-th flow (points/s).

On the other hand, the environmental impact rate related to the construction, operation and maintenance and the disposal of the k-component of a system is evaluated by Eq. (3) (Buchgeister, 2010):

$$\dot{Y}_k = \dot{Y}_k^{CO} + \dot{Y}_k^{OM} + \dot{Y}_k^{DI} \tag{3}$$

Where $\dot{Y}_k$ is the total environmental impact rate associated with the life cycle of the k-th component (points/s) while $\dot{Y}_k^{CO}$, $\dot{Y}_k^{OM}$ and $\dot{Y}_k^{DI}$ are the contributions of the construction, the operation and maintenance and disposal phase (points/s).

The Exergo-environmental analysis is based on the impact balances for each entering and exiting *j*-flow related to each *k*-component (Buchgeister, 2010):

$$\sum \dot{B}_{j,k,in} + \dot{Y}_k = \sum \dot{B}_{j,k,out} \tag{4}$$

Where $\dot{B}_{k,in}$ are the environmental impact rates related to all the flows entering the k-th component (points/s) and $\dot{B}_{k,out}$ are the environmental impact rates related to all the flows exiting from the k-th component (points/s).

An exergy analysis of a NCS has been performed by Manfrida et al. (2017) estimating the exergy content of water in each point of the plant, and $\dot{Y}_k$ is provided by the LCA analysis (a mass based allocation approach has been used for the calculation of the environmental impacts of transports, packaging and direct land occupation for all the system components). These inputs permit us to solve the system of equations in integral form referring to the average day of each month.

Furthermore, inside each component, several exergy destructions occur: they are due to different forms of irreversibility such as non-ideal mixing of fluids, heat exchanges with finite difference of temperature and frictions across the pipes. An environmental impact $\dot{B}_{D,k}$ (points/s) can be associated to them because they vanquish part of such costly increasing exergy and it is calculated by Eq. (5) (Buchgeister, 2010; Buchgeister et al., 2009):

$$\dot{B}_{D,k} = b_{F,k} \cdot \dot{E}x_{D,k} \tag{5}$$

Where $b_{F,k}$ is the specific environmental impact related to the exergetic fuel (Lazzaretto and Tsatsaronis, 2006) of the k-th component.

So, the total environmental impact for each k-component $\dot{B}_{TOT,k}$ is obtained by Eq. (6) while the contribution of $\dot{Y}_k$ respect to $\dot{B}_{TOT,k}$ is named exergo-environmental factor ($f_{d,k}$) and is defined by Eq. (7). The relative environmental impact difference $r_{d,k}$ is another parameter expressing, as percentage, how much the environmental cost of a water stream is increased by flowing across each component and it is defined by Eq. (8) (Buchgeister, 2010; Buchgeister et al., 2009).

$$\dot{B}_{TOT,k} = \dot{B}_{D,k} + \dot{Y}_k \tag{6}$$

$$f_{d,k} = \frac{\dot{Y}_k}{\dot{B}_{D,k} + \dot{Y}_k} \tag{7}$$

$$r_{d,k} = \frac{b_{p,k} - b_{F,k}}{b_{F,k}} \tag{8}$$

3. Results and discussions

In this paragraph, the description of results is organized as follows:

- In Section 3.1, the endpoint results and contribution analysis of both NCS and TVS for Somalia, (i.e., the country with the most critical sanitary situation related to diarrhoeal diseases among the three investigated installation sites) are reported;
- In Section 3.2, the total environmental impact profiles for Somalia and, for comparison, for Brazil and Italy are reported;
- In Section 3.3 and 3.4, the energy, exergo-environmental results and sensitivity analysis outcomes for Somalia are reported.

3.1. Endpoint results and contribution analysis - Somalia

Fig. 6 shows the endpoint results for the NCS, NCS_80, NCS_eq and TVS in Somalia. The NCS system turns out to be the most sustainable solution for each category thanks to its higher productivity of treated water, even if a higher amount of materials is required. Furthermore, for each damage category, some major environmental burden can be identified. More in details, the *Agricultural land occupation and Climate Change* impact categories represent together about 70% of the contribution to the *Ecosystem*; the *Climate Change, Human Toxicity and Particulate matter formation* impact categories represent together more than 99% of the contribution to the *Human Health*; and finally the *Metal depletion impact category* represents about 60% of the contribution to the *Resources*.

Fig. 6 also shows that the productivity is a pivotal parameter for the NCS: if it is decreased of 20% with respect to ideal conditions (NCS_80) the environmental burden on all the damage categories increases but it is still lower than the TVS profile, while in the case of equivalent productivity of the two plants (NCS_eq), the resulting NCS environmental burden would turn out to be higher than TVS. This last outcome clearly depends on the larger amount of materials required for the NCS's construction but it cannot be considered as a drawback for the NCS as this equal productivity limiting case represents the worst scenario for NCS and it has been simulated to understand the sensitivity of the model (NCS productivity has been assessed through a mathematical model and the productivity of the TSV has been measured experimentally).

Observing the contribution analysis results reported in Table 5, another major output is that the SCs are largely the most impactful components among the most relevant categories.

The contribution analysis allows us to highlight that all the calculated impacts are mainly due to the manufacturing of the SCs except for the *Agricultural land occupation,* for which the surface physically occupied by the plant is the most important contributing factor. Moreover, the toxic emissions of arsenic and manganese in the life cycle of the SCs and the HEs are the main factors responsible for the impact on the *Human Toxicity* category, whereas for the *Metal and fossil depletion* category the major impacts are associated with the consumption of natural resources, especially metals (iron and copper) and fossil fuels (coal, gas and oil).

From the perspective of a possible beneficial contribution of solar pasteurization systems to the sanitary problem, a significant observation could be made by comparing, on a qualitative basis, the obtained LCA results with data regarding impact of diseases and life

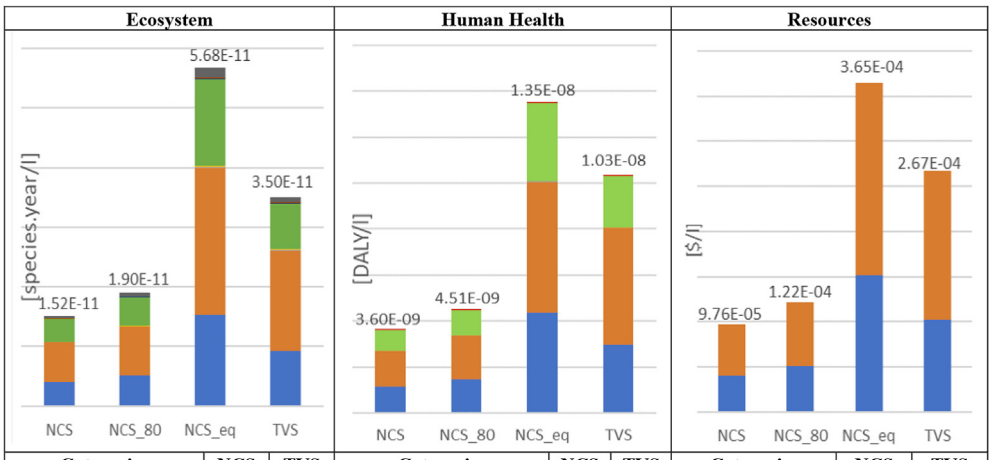

Categories	NCS	TVS
Agricultural land occupation	26.87%	26.33%
Climate Change	44.41%	47.98%
Freshwater ecotoxicity	0.30%	0.37%
Freshwater eutrophication	0.32%	0.46%
Marine ecotoxicity	0.06%	0.08%
Natural land transformation	24.41%	21.57%
Terrestrial acidification	0.28%	0.35%
Terrestrial ecotoxicity	0.35%	0.39%
Urban land occupation	2.99%	2.48%

Categories	NCS	TVS
Climate Change	32.29%	28.79%
Human Toxicity	42.34%	49.23%
Ionising Radiation	0.03%	0.03%
Ozone Depletion	0.01%	0.01%
Particulate matter formation	25.33%	21.95%
Photochemical oxidant formation	0.00%	0.00%

Categories	NCS	TVS
Fossil Depletion	41.69%	38.34%
Metal Depletion	58.31%	61.66%

Fig. 6. Weighting results at the endpoint level for the NCS, NCS_80, NCS_eq and TVS installed in Somalia. For each damage category, the contribution analysis of the impact categories affecting the total environmental burden score is shown at the bottom of the figure.

Table 5
Contribution analysis of the most relevant categories (>25% of the global impact on each damage category as shown in Fig. 6).

Components	Agricultural land occupation		Climate change		Particulate matter formation		Human toxicity		Metal depletion		Fossil depletion	
	NCS	TVS	NCS	TVS	NCS	TVS	NCS	TVS	NCS	TVS	NCS	TVS
Solar Collectors	15.02%	11.29%	46.00%	47.69%	57.65%	52.66%	91.33%	53.52%	59.93%	62.28%	42.03%	39.47%
Compensation Tank	1.10%	0.00%	5.81%	0.00%	3.84%	0.00%	1.73%	0.00%	3.52%	0.00%	4.92%	0.00%
Water Tanks	0.96%	1.43%	10.26%	13.44%	4.04%	5.46%	1.34%	1.34%	0.58%	0.66%	17.40%	23.12%
Heat Exchanger	1.28%	3.48%	9.01%	9.49%	10.24%	18.18%	1.84%	32.87%	15.65%	19.02%	6.89%	8.60%
Pipes	1.56%	1.24%	10.99%	7.81%	12.63%	9.17%	2.26%	1.23%	19.54%	12.16%	8.38%	6.04%
PV Panel and connections	0.00%	0.39%	0.00%	2.10%	0.00%	1.21%	0.00%	0.52%	0.00%	0.27%	0.00%	1.94%
Thermostatic Valve	0.00%	1.25%	0.00%	6.75%	0.00%	4.86%	0.00%	9.70%	0.00%	5.11%	0.00%	6.17%
Transports	0.44%	0.38%	16.77%	11.89%	11.01%	8.03%	1.34%	0.72%	0.73%	0.47%	19.31%	13.87%
Direct Land Occupation and transformation	78.37%	79.51%	0.00%	−0.02%	0.00%	−0.01%	0.03%	0.03%	0.03%	0.02%	−0.02%	−0.01%
Packaging	1.27%	1.03%	1.16%	0.85%	0.59%	0.44%	0.13%	0.07%	0.02%	0.01%	1.09%	0.80%
Recycling	0.00%	0.00%	0.00%	0.00%	0.00%	0.00%	0.00%	0.00%	0.00%	0.00%	0.00%	0.00%

expectancy related with unsafe water and sanitation issues. Indeed, the WHO provides comprehensive useful data for the estimation of the sanitary conditions by countries and regions expressed in DALYs; for Somalia the reference value is estimated to be 4465 *DALYs*/100,000 ab (World Health Organization (WHO) (accessed on 05/04/2018), 2012). To compare with the results obtained for the *Human Health* category within the LCA analysis, this value has been normalized to the same functional unit (*DALYs*/l). To do this, it has been multiplied by the inhabitants (ab) of Somalia (considering a population of 15,181.925 ab (World Health Organization (WHO) (accessed on 05/04/2018)) and divided by water consumption data (the Food and Agriculture Organization of the United Nations (FAO) estimates a water withdrawal for municipal use of $0.15 \cdot 10^9$ m^3/year ($0.15 \cdot 10^{12}$ l/year) (Food and Agriculture Organization (FAO) (accessed on 05/04/2018), 2003).

Inspection of Fig. 7 allows the observation that the implementation of NCS and TVS could allow a decrease in the burden of diarrhoeal diseases that is several orders of magnitude higher for the actual scenario in Somalia. Moreover, considering the above-mentioned water consumption data, a NCS would be able to satisfy the needs of about 77 people whose life expectancy is estimated to increase by 2.5 years compared to the average, that actually ranges between 54 and 57 years (World Health Organization (WHO) (accessed on 05/04/2018)). This qualitative assessment shows that in general the NCS and TVS systems could offer an effective contribution, at a limited environmental cost, to face the sanitary problems linked to unsafe water consumption.

3.2. Total environmental impact

In order to make a global evaluation of the systems based on a single score metric, weighted results are calculated referring to Somalia and are illustrated in Fig. 8:

The NCS is confirmed to be the most sustainable solution in ideal conditions but also in this case the conclusion strongly depends on the real productivity of the systems. The impact to the Resources

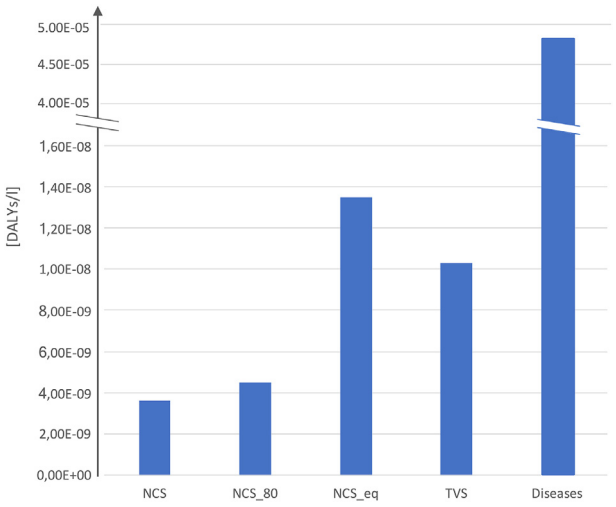

Fig. 7. Human Health damage category results at the endpoint level comparing the whole life cycle NCS and TVS impacts with that connected with unsafe water consumption impact value calculated according to the WHO and FAO estimation in Somalia.

category represents the main contribution to the total single score, followed by the impact on the Human Health category, while the impact to the Ecosystem category only accounts for a very low percentage. The SCs is still the most impactful component of the systems. As NCS, NCS_80 and NCS_eq scenarios only differ for the water output productivity, the damage categories percentage weights along the environmental profiles shown in Fig. 8 do not change. In Table 6 the contribution analysis implemented for the total environmental impact allows the investigation of the system in more detail.

Fig. 9 shows the variations of the previous results as a function of different installation sites, according to the methodological setting described in Fig. 8. As a matter of fact, the types of land, the installation site, distances between the installation and production site, transport modalities, water productivity and recycling rate are parameters that strongly affect the eco-profiles of the two systems.

On the basis of results shown in Fig. 9 and details given by the

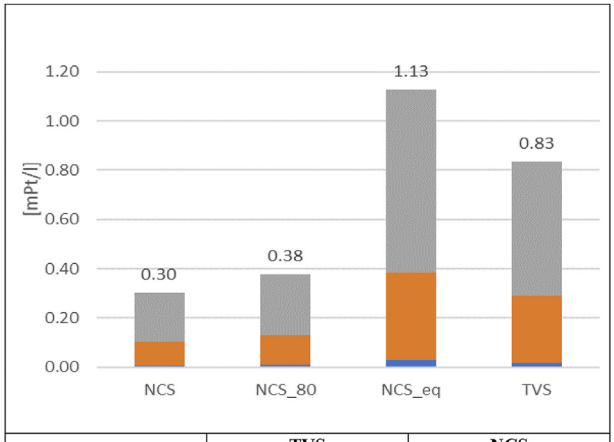

	TVS	NCS
Ecosystem ■	2.5%	2.1%
Human Health ■	31.6%	32.7%
Resources ■	65.9%	65.2%

Fig. 8. Single scores of the total environmental impact (mPt/l) for the TVS and NCS (and relative operational scenarios) installed in Somalia.

Table 6
Contribution analysis of the global environmental impacts shown in Fig.8 connected to NCS and TVS components.

Components	NCS	TVS
Solar Collectors	49.32%	47.93%
Compensation Tank	4.04%	0.00%
Water Tanks	7.12%	9.19%
Heat Exchanger	10.01%	13.09%
Pipes	12.38%	8.43%
Photovoltaic Panel and connections	0.00%	1.10%
Electronics	0.00%	5.86%
Transports	8.66%	6.10%
Direct Land Occupation and transformation	7.17%	7.26%
Packaging	1.30%	1.02%
Recycling	0.00%	0.00%

contribution analysis reported in Table 7, some major conclusions can be drawn as follows:

- the NCSs are less impactful than the TVSs at any installation site;
- comparing these results with the productivity data from Table 3, it is evident that in sites with higher productivity, such as Brazil, the environmental impact is lower for both NCS and TVS; on the other hand, when the productivities are more similar, like for the Italian installation site, it can be noted that differences between the eco-profiles of NCS and TVS are quite smaller; thus confirming that the productivity of any technological solution is crucial for the environmental assessment;
- an environmental benefit (i.e. a positive impact) from recycling option is appreciable only in Italy, even if it can counter-balance the lower productivity of the systems only in a somewhat limited way;
- the contribution of direct land occupation and transformation is always quite low, except for Brazil where the calculation methods associate a high impact factor to the transformation of forest, considered as natural land;
- the percentage impact of transportations is always low and ranges between 2.64% and 12.45% of the total, that is a quite limited contribution considering the variability of distances and modes of transports assumed in this study. The main reason is that the impact of transports also depends on the weight of the transported goods, that in this case is represented by systems designed to be not massive. Furthermore, we can observe that, despite the shorter distances, transportation in Italy gives a higher contribution with respect to the other countries because transport by road is the most impactful mode according to the impact weighting factors employed by the calculation method;

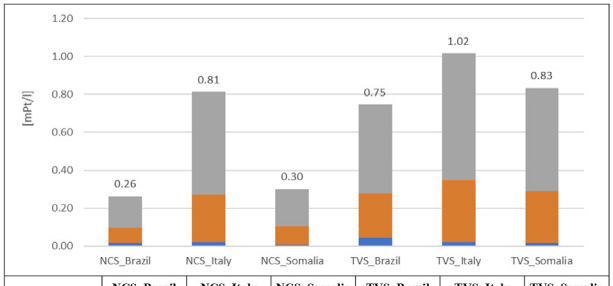

	NCS_Brazil	NCS_Italy	NCS_Somalia	TVS_Brazil	TVS_Italy	TVS_Somalia
Ecosystem ■	7.1%	2.6%	2.5%	5.9%	2.2%	2.1%
Human Health ■	30.2%	30.8%	31.6%	31.5%	32.2%	32.7%
Resources ■	62.6%	66.6%	65.9%	62.6%	65.6%	65.2%

Fig. 9. Single scores of the total environmental impact (mPt/l) for the TVS and NCS installed in Brazil, Italy and Somalia.

Table 7
Contribution analysis of the global environmental impacts shown in Fig. 9 connected to NCS and TVS components for different installation sites.

Components	NCS_Brazil	NCS_Italy	NCS_Somalia	TVS_Brazil	TVS_Italy	TVS_Somalia
Solar Collectors	39.53%	48.17%	49.32%	38.94%	46.80%	47.93%
Compensation Tank	3.16%	3.95%	4.04%	0.00%	0.00%	0.00%
Water Tanks	5.72%	6.95%	7.12%	7.08%	8.95%	9.19%
Heat Exchanger	8.55%	9.81%	10.01%	10.80%	12.79%	13.09%
Pipes	10.60%	12.13%	12.38%	7.00%	8.26%	8.43%
Photovoltaic Panel and connections	0.00%	0.00%	0.00%	0.77%	1.08%	1.10%
Electronics	0.00%	0.00%	0.00%	4.36%	5.70%	5.86%
Transports	3.89%	12.45%	8.66%	2.64%	8.75%	6.10%
Direct Land Occupation and transformation	27.96%	11.09%	7.17%	27.92%	9.93%	7.26%
Packaging	0.68%	1.25%	1.30%	0.51%	0.98%	1.02%
Recycling	−0.04%	−2.90%	0.00%	−0.02%	−1.62%	0.00%

- SCs represent the most impactful components in every country.

To perform a qualitative assessment aiming at understanding the advantages or limitations connected with the implementation of solar pasteurization systems and, consequently, to evaluate our analytic model, we compare the cradle-to-gate eco-profiles of NCS and TVS virtually functioning in Somalia, Brazil and Italy with the impact single score values of unsafe water related diseases in the different geographical contexts.

The environmental impact of diseases connected with unsafe water consumption in Brazil and Somalia has been estimated using the same approach described for the Somalian case (paragraph 3.1) and a single score has been obtained considering the burden to the *Human Health* damage category as the only relevant impact, neglecting the effect of the diseases on the *Ecosystems* and *Resources* damage categories (Fig. 10).

Fig. 10 is useful to understand the order of magnitude and the diffusion of the sanitary problem in the analysed situations giving an idea of how and to which extent a NCS or a TVS could be effective in a particular geographical context. In Brazil and in Italy, the impact of the unsafe water consumption is lower than the impact of Pasteurization systems, so a Pasteurization system would be convenient only in few specific emergency situations. Indeed. these results are estimated using data on a national scale. Different conclusions would be reached if data from more specific regional case studies (not available) would have been used. For instance, some of Brazilian regions still have sanitary problems connected to water consumption (Marques et al., 2013) thus the use of solar pasteurization systems could be very advantageous for these sites. In Somalia, however, since the burden of sanitary problems related to unsafe water consumption is significantly higher, the installation of solar pasteurization systems would be extremely beneficial.

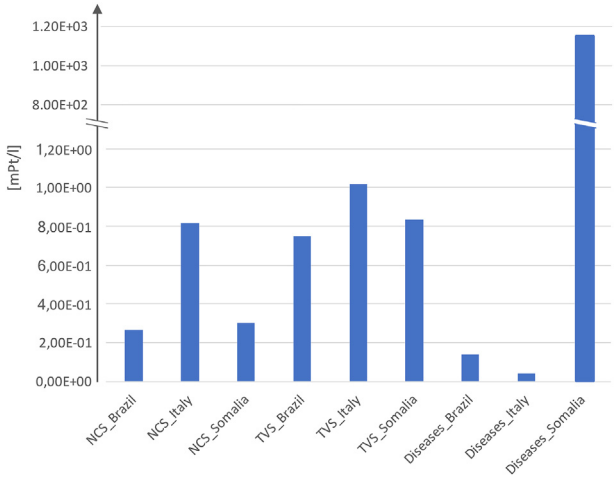

Fig. 10. Single score values of the total environmental impact comparing the whole life cycle of NCS and TVS burdens with that connected with unsafe water consumption impact value calculated according to the WHO and FAO estimation in Brazil, Italy and Somalia.

From a general methodological point of view, the outcomes of such assessment allowed us to prove the robustness of our product system model finding out that it responses rather well to the water's sanitary conditions context. In the perspective of providing an assessment procedure to support the political decision making, this model would allow to perform ex-ante qualitative assessment to investigate the environmental advantages and costs of several technological solutions and to recommend the best option for a given geographical context.

3.3. Energy and exergo-environmental analysis

In this section a comparison between Solar Pasteurization systems and other technologies for which the SCs are hypothetically replaced with fossil fuels combustion systems is presented. This estimation is made replacing the SCs with a boiler in the model system and considering that boilers useful life is longer and that they could be re-used after 15 years.

Based on the previous results according to which the most environmentally sustainable solution is the NCS, the following analysis is focused on this system installed in Somalia, as it is the country experiencing the highest need for water sanitation intervention among those considered in this study. The amount of heat required by a NCS in Somalia is estimated by the mathematical model described by Dainelli et al. (2017) and Manfrida et al. (2017).

Inspection of Fig. 11 reveals that, as expected, the use of solar energy is responsible for a lower environmental impact than the other analysed options, even if the SCs result to be a very impactful components, as shown in the contribution analysis in Table 7. Indeed, if boilers burning oil, gas or wood (some of the fuels mainly used in rural areas of Somalia (UNEP, 2015)) were used, the generated environmental impact would be at least four times higher.

The exergo-environmental analysis can provide a further insight: the environmental impact associated to the exergy content of treated water is equal to zero because solar energy is used and only the results calculated through the LCA study give a relevant contribution to the analysis. On the other hand, the exergy destructions inside the components occur anyway; they are due to the thermodynamic irreversibility such as the friction and the mixing of different flows of water inside the pipes and in the CT and the finite temperature heat exchange inside the SCs.

The exergo-environmental analysis results are averaged over each year and collected in Table 8 showing that the exergy destructions due to the irreversibility of water's warming inside the

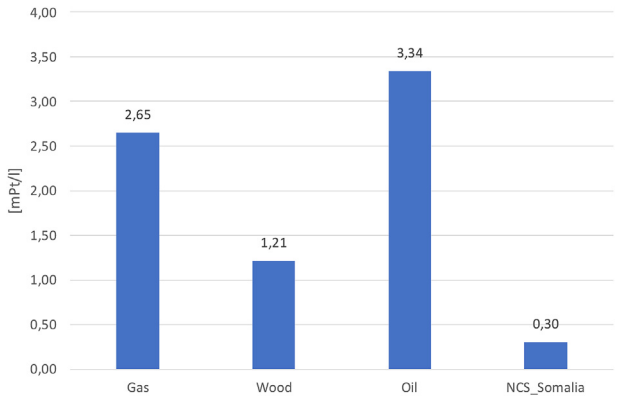

Fig. 11. Single score values of the total environmental impact calculated for different pasteurization systems. The comparison is performed based on an equivalent heat amount provided by solar energy, biomass and fossil fuels.

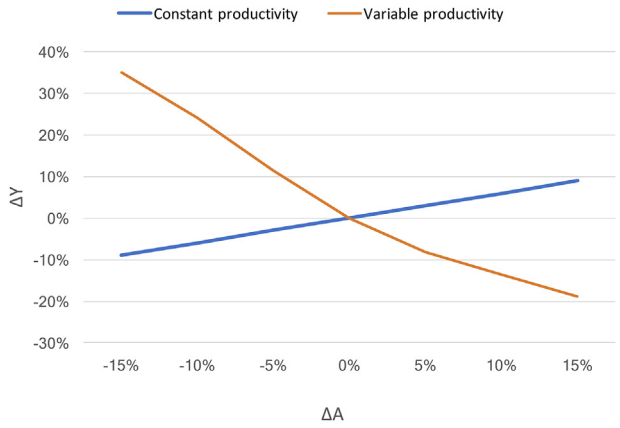

Fig. 12. Sensitivity analysis of the environmental impact (ΔY) respect to the surface of the SC (ΔA) with constant and variable productivity.

SCs determine a sizeable environmental impact (B_D) compared to the one related to the SCs' construction, maintenance and disposal (Y). The reason is that a source of energy at very high temperature (Sun) is used to heat water up to a temperature lower that 100 °C. This observation is coherent with the results obtained by Dainelli et al. (2017) and Manfrida et al. (2017) showing that the exergy losses and destructions of the SCs are much higher than those of other components of the plant. So, in the SC case, the exergo-environmental factor f_d (which represents the contribution of Y to B_{TOT}), accounts for a very small percentage value. Despite the damage of exergy destructions, the relative environmental impact difference (r_d) across the SCs is negative; this happens because the direct input of renewable solar energy, which improves the exergy content of the fluid, takes place at zero environmental cost.

The second most impactful component in terms of total environmental impact (B_{TOT}) is the CT; the main reason is the exergy destructions burden (B_D) due to the time-variable exergy content of stored water and to the mixing with the inlet stream. The effect of this irreversibility is an increase of the specific environmental cost (r_d) of the outlet flow from the CT. For such reason the cradle to grave LCA result (Y) accounts for a very low percentage (f_d) of the total damage.

The third largest contribution in absolute terms (B_{TOT}) is given by the HE; among the other components, only the HE determines a very relevant increase of the environmental cost of exergy (r_d). In this case the contribution of exergy destructions (B_D) is high, as demonstrated by the low exergo-environmental factor (f_d). However the performance cannot be improved by simply using a larger heat exchange surface because the ratio of recirculating and supply flows is limited by the natural circulation mechanism and the system should be operative – after the warm-up – at temperatures between 85 and 100 °C (Dainelli et al., 2017; Manfrida et al., 2017).

Table 8
Exergo-environmental analysis results of the NCS system concerning the impact of the irreversibility (B_D), the cradle to grave LCA result (Y), the global environmental impact (B_{TOT}), the exergo-environmental factor (f_d) and the relative environmental impact difference (r_d).

Components	B_D	Y	B_{TOT}	f_d	r_d
	[mPt/l]	[mPt/l]	[mPt/l]	[%]	[%]
Solar Collectors	19.69	0.16	19.85	0.81%	−13.68%
Compensation Tank	1.03	0.02	1.05	1.90%	6.01%
Heat Exchanger	0.70	0.04	0.74	5.41%	124.50%
Pipes	0.20	0.05	0.25	20.00%	18.71%
Water Tanks	0.00	0.03	0.03	100.00%	0.00%

The total environmental impact (B_{TOT}) of pipes is quite low and a significant contribution is represented by the exergy destructions burden (B_D) due to the frictions and the mixing of the supply and the recirculating flows.

The WTs are at the borders of the system, so no exergy balance is possible for them and thus their exergy destructions have been neglected (Dainelli et al., 2017; Manfrida et al., 2017).

3.4. Sensitivity analysis

The sensitivity analysis is a significant tool for studying the robustness of LCA outputs and their sensitivity to uncertainty factors, thus enhancing the interpretation of results. (Saltelli, 2002). In previous sections, to investigate the dependency of the model system on operational and geographical factors, the variation of the productivity and of the installation sites have already been considered. Nevertheless, considering the significant impact of the SCs on the environmental impact assessment, a sensibility analysis of the SCs' dimension will be performed here.

The installation site of the NCS is set in Somalia; the surface occupied by the SC is supposed to vary in the range ±15%. As a preliminary speculation, the productivity of the system is set to be constant and so the environmental impact increases linearly with the SC's area in a range of ±10% (Fig. 12).

Applying the perturbation of the SC's area to the mathematical model described by Dainelli et al. (2017) and Manfrida et al. (2017), the corresponding variation of productivity can be evaluated. In this case the results show a contrary non-linear trend because environmental impacts decrease sensibly with an increasing of the SC's area and vice versa; variations are assessed between −20% and +35%.

4. Conclusions

Many regions of the world are affected by serious sanitary conditions due to the consumption of contaminated water. The role of this primary element as a vector of several kinds of diseases, especially diarrhoeal, has been investigated from a humanitarian and sanitary point of view, but a comprehensive approach to this problem cannot overlook also the strictly connected environmental and energetic issues in order to propose an integrated solution. In this context, the choice of the best technical solution to purify water from pathogens should be based on criteria that take into consideration these aspects to individuate simple, reliable and sustainable technologies. This is particularly relevant to address the

objectives of SDGs of the Agenda adopted by the General Assembly of the United Nations, in particular those of Goal 6 which focuses on "Ensure availability and sustainable management of water and sanitation for all". In this study, an LCA and an exergo-environmental analysis have been integrated to propose a methodological framework useful for environmental sustainability assessment to support the political decision making for the choice of the best technically and environmentally solution for a specific geographical context.

The assessment of Solar Pasteurization Systems performances has been carried out in different conditions. First, these plants are supposed to be installed in Somalia where sanitary problems connected with unsafe water consumption are very critical. Indeed, we can conclude that a NCS would be more sustainable than a TVS thanks to its higher productivity: under ideal conditions the total environmental impact of the analysed NCS is calculated to be 0.3 mPt/l, versus 0.83 mPt/l of the TVS. A significative output of the analysis is represented by the eco-profiles calculated for both plants that show a substantial total environmental impact reduction compared to the actual sanitary scenario. It is estimated that the human life expectancy could be at least two years longer thanks to the application of a disinfection device. Different installation sites (Somalia, Brazil and Italy) have been considered and in all cases the NCS results more sustainable than the TVS: in Brazil very similar results to Somalia are evaluated and they are respectively 0.26 mPt/l for the NCS and 0.75 mPt for the TVS; in Italy the impact is higher because of a lower water productivity and thus the difference between the two systems eco-profiles decreases (0.81 mPt/l for the NCS and 1.02 mPt/l for TVS). The results show that the best installation site, from an environmental point of view, is in Brazil but considering the burden related to the consumption of unsafe water, Somalia represents the most critical situation and it would be very advantageous to employ these systems on a large scale; in Brazil and in Italy the installation could be beneficial only in specific situations because, in general, the impact of unsafe water related diseases is lower than the whole systems eco-profiles. From the energetic point of view, the saving of fossil resources due to the use of solar energy represents an environmental benefit respect to the installation of boilers burning gas, wood or oil to produce an equivalent amount of heat because their environmental impacts are higher (respectively 2.65 mPt/l, 1.21 mPt/l, 3.32 mPt/l). The exergo-environmental analysis shows that no direct environmental damages occur during the operative phase but considering the contribution of exergy destructions, the SCs resulted to be the most impactful component. This conclusion is confirmed also by the LCA that estimates their contribution to the global environmental impact in the range 39–49%. A sensitivity analysis performed for the NCS shows that the surface of the collector is a very crucial parameter because variations from −15% to +15% of the surface determine an increasing of the impact that varies between −10% and +10%, but the model is also very dependent on the productivity because the increasing of treated water due to a higher thermal exchange surface would balance it and make the environmental impact sensibly lower; the variations are assessed between +40% and −20%.

Declarations of interest

None.

Funding

This research did not receive any specific grant from funding agencies in the public, commercial, or not-for-profit sectors.

Author contributions

F.R. and A.S. designed research; F.R. and S.M. performed LCA analysis; all authors participated in the interpretation and discussion of results; F.R., M.L.P, and A.S. wrote the paper.

Notes

The authors declare no conflict of interest.

Acknowledgments

F.R., M.L.P., S.M., R.B. and A.S. acknowledge MIUR Grant - Department of Excellence 2018–2022. FR is grateful for the Ph.D. grant within the "Progetto Pegaso" funded by Regione Toscana.

Careful reading and revising of the manuscript by Professor Emeritus Michael Rodgers, Bowling Green State University, is gratefully acknowledged.

Appendix A. Supplementary data

Supplementary data to this article can be found online at https://doi.org/10.1016/j.jclepro.2018.12.020.

References

Aganovic, K., Smetana, S., Grauwet, T., Toepfl, S., Mathys, A., Van Loey, A., Heinz, V., 2017. Pilot scale thermal and alternative pasteurization of tomato and watermelon juice: An energy comparison and life cycle assessment. J. Clean. Prod. 141, 514–525. https://doi.org/10.1016/j.jclepro.2016.09.015.

Anderson, R., 1996. Solar Water Disinfection. In: Annual Conference of the American Solar Energy Society.

Bansal, N.K., Sawhney, R.L., Misra, A., Boettcher, A., 1988. Solar sterilization of water. Sol. Energy 40, 35–39.

Bigoni, R., Kötzsch, S., Sorlini, S., Egli, T., 2014. Solar water disinfection by a Parabolic Trough Concentrator (PTC): Flow-cytometric analysis of bacterial inactivation. J. Clean. Prod. 67, 62–71. https://doi.org/10.1016/j.jclepro.2013.12.014.

Boettcher, A., Heybutzki, H., Krug, W., 1983. Self-regulating solar water heaters with very short start-up phase. In: Eighth Biennial Congress of the International Solar Energy Society, pp. 1170–1173.

Bravi, M., Laura, M., Tiezzi, E., Basosi, R., 2011. Life cycle assessment of a micromorph photovoltaic system. Energy 36, 4297–4306. https://doi.org/10.1016/j.energy.2011.04.012.

Buchgeister, J., 2010. Comparison of exergoenvironmental analysis using three different environmental impact assessment methods in a case of a process of electricity production. In: Proc. 23rd Int. Conf. Effic. Cost, Optim. Simulation, Environ. Impact Energy Syst. ECOS 2010 1.

Buchgeister, J., Meyer, L., Castillo, R., Tsatsaronis, G., 2009. Exergoeconomic and exergoenvironmental analysis of different optimisation options for electricity production using SOFC with integrated allothermal biomass gasification. In: ECOS 2009 - 22nd Int. Conf. Effic. Cost, Optim. Simul. Environ. Impact Energy Syst, pp. 923–932.

Burch, J.D., Thomas, K.E., 1998. Water disinfection for developing countries and potential for solar thermal pasteurization. Sol. Energy 64, 87–97. https://doi.org/10.1016/S0038-092X(98)00036-X.

Carielo, G., Calazans, G., Lima, G., Tiba, C., 2017. Solar water pasteurizer: Productivity and treatment efficiency in microbial decontamination. Renew. Energy 105, 257–269. https://doi.org/10.1016/j.renene.2016.12.042.

Carielo da Silva, G., Tiba, C., Calazans, G.M.T., 2016. Solar pasteurizer for the microbiological decontamination of water. Renew. Energy 87, 711–719. https://doi.org/10.1016/j.renene.2015.11.012.

Cobb, J.C., 1998. Simple self-regulating solar pasteurizer for contaminated water. In: International Solar Energy Conference, pp. 323–326.

Dainelli, N., Manfrida, G., Petela, K., Rossi, F., 2017. Exergo-Economic Evaluation of the Cost for Solar Thermal Depuration of Water. Energies 1–19. https://doi.org/10.3390/en10091395.

Duff, W.S., Hodgson, D., 2001. A passive solar water pasteurization system without valves. In: Annual Conference of the American Solar Energy Society.

Duff, W.S., Hodgson, D., 2002. A simple high efficiency solar water purification system. In: Annual Conference of the American Solar Energy Society, pp. 15–20.

Duff, W.S., Hodgson, D.A., 2005. A simple high efficiency solar water purification system. Sol. Energy 79, 25–32. https://doi.org/10.1016/j.solener.2004.10.005.

Ecoinvent Database 3.4, 2017. Available on https://www.ecoinvent.org/database/older-versions/ecoinvent-34/report-of-changes-ecoinvent-34/report-of-changes-ecoinvent-34.html (Accessed on 05/04/2018).

Eurostat-waste. Available on http://ec.europa.eu/eurostat/web/environment/waste/database (Accessed on 05/04/2018).

Food and Agriculture Organization (FAO), 2003. AQUASTAT, Municipal water withdrawal, Somalia. Available on http://www.fao.org/nr/water/aquastat/data/query/results.html (Accessed on 05/04/2018).
Greendelta, openLCA. Available on http://www.openlca.org/(Accessed on 26/10/2018).
Hadden, B.R.L., Lee, R., 2007. The Geology of Somalia : a Selected Bibliography of Somalian Geology. Geography and Earth Science US Army Co.
Heliotek Bosch Group. MC Evolution, MC Evolution Pro. Available on. http://www.heliotek.com.br/. (Accessed 5 April 2018).
International Standards Organization, 2010. EN ISO 14040:2006 - Valutazione del ciclo di vita Principi e quadro di riferimento. Environ. Manag. 14040.
Jorgensen, A.M., Ywema, I.E., 1996. Transportation in LCA A Comparative Evaluation of the Importance of Transport in Four LCAs, vol. 1, pp. 218–220.
Jorgensen, A.J., Nohr, K., Sorensen, H., Boisen, F., 1998. Decontamination of drinking water by direct heating in solar panels. J. Appl. Microbiol. 85, 441–447. https://doi.org/10.1046/j.1365-2672.1998.853497.x.
Lazzaretto, A., Tsatsaronis, G., 2006. SPECO: A systematic and general methodology for calculating efficiencies and costs in thermal systems. Energy 31, 1257–1289. https://doi.org/10.1016/j.energy.2005.03.011.
Li, S., Kinser, C., Ziara, R.M.M., Dvorak, B., Subbiah, J., 2018. Environmental and economic implications of food safety interventions: Life cycle and operating cost assessment of antimicrobial systems in U.S. beef packing industry. J. Clean. Prod. 198, 541–550. https://doi.org/10.1016/j.jclepro.2018.07.020.
Manfrida, G., Petela, K., Rossi, F., 2017. Natural circulation solar thermal system for water disinfection. Energy 141, 1204–1214. https://doi.org/10.1016/j.energy.2017.09.132.
Marques, A.R., Gomes, F. de C.O., Fonseca, M.P.P., Parreira, J.S., Santos, V.P., 2013. Efficiency of PET reactors in solar water disinfection for use in southeastern Brazil. Sol. Energy 87, 158–167. https://doi.org/10.1016/j.solener.2012.10.016.
Meteonorm Information. Available on http://www.meteonorm.com/(Accessed on 05/04/2017).
Mojarab Soufiyan, M., Aghbashlo, M., Mobli, H., 2016. Exergetic performance assessment of a long-life milk processing plant: A comprehensive survey. J. Clean. Prod. 30, 1–18. https://doi.org/10.1016/j.jclepro.2015.11.066.
Murphy, H.M., McBean, E.A., Farahbakhsh, K., 2009. Appropriate technology - A comprehensive approach for water and sanitation in the developing world. Technol. Soc. 31, 158–167. https://doi.org/10.1016/j.techsoc.2009.03.010.
Pardo, G., Zufía, J., 2012. Life cycle assessment of food-preservation technologies. J. Clean. Prod. 28, 198–207. https://doi.org/10.1016/j.jclepro.2011.10.016.
Parisi, M.L., Maranghi, S., Sinicropi, A., Basosi, R., 2013. Development of dye sensitized solar cells: a life cycle perspective for the environmental and market potential assessment of a renewable energy production technology. Int. J. Heat Tech. 31 (2). ISSN: 03928764.
Perrot, P., 1998. A to Z thermodinamics. Oxford University Press.
Safe Water Systems, 2002. Sol*Saver Product Information Sheet. Available on. www.safewatersystems.com. (Accessed 5 April 2018).
Saltelli, A., 2002. Sensitivity Analysis for Importance Assessment 22. https://doi.org/10.1111/0272-4332.00040.
Shannon, M.A., Bohn, P.W., Elimelech, M., Georgiadis, J.G., Marõas, B.J., Mayes, A.M., 2008. Science and technology for water purification in the coming decades. Nature 452, 301–310. https://doi.org/10.1038/nature06599.
Stevens, R.J., Johnson, R., Eckerlin, H., 1998. An investigation of a solar pasteurizer with in integral heat exchanger (SPIHX). In: Annual Conference of the American Solar Energy Society.
The International Standards Organisation, 2006. INTERNATIONAL STANDARD assessment — Requirements and guilelines. Int. J. Life Cycle Assess. 652–668, 2006. https://doi.org/10.1007/s11367-011-0297-3.
The University of Wisconsin Madison, n.d. Trnsys: TRaNsient SYstems Simulation Program.
Tilley, E., Strande, L., Lüthi, C., Mosler, H.-J., Udert, K.M., Gebauer, H., Hering, J.G., 2014. Looking beyond Technology: An Integrated Approach to Water, Sanitation and Hygiene in Low Income Countries. Environ. Sci. Technol. 48, 9965–9970. https://doi.org/10.1021/es501645d.
UNEP, 2015. Somalia Energy Profile.
UNICEF, WHO, 2009. Diarrhoea: Why children are still dying and what can be done. WHO Libr, Cat.
United Nations, 2015. Transforming our world: the 2030 Agenda for Sustainable Development. Gen. Assem 16301, 1–35, 70 Sess. https://doi.org/10.1007/s13398-014-0173-7.2.
United Nations, 2016. Clean Water and Sanitation: Why It Matters. Sustain. Dev. Goals Briefs 2.
United Nations, 2017. The Sustainable Development Goals Report. United Nations Publ, pp. 1–56. https://doi.org/10.18356/3405d09f-en.
VPsolar. Lt-power flat plate collectors technical data sheet. Available on http://www.tvpsolar.com./. (Accessed 5 April 2018).
Waste TM, Waste Atlas. Available on http://www.atlas.d-waste.com/(Accessed on 05/04/2018).
World Health Organization (WHO), Home Page. Available on http://www.who.int/countries/som/en/(Accessed on 05/04/2018).
World Health Organization (WHO), 2012. Interactive charts: Public Health and Environment: water, sanitation and hygene attributable burden of disease (low- and middle-income countries)- Inadequate water: DALYs (per 100 000 population, all ages). Available on http://gamapserver.who.int/gho/interactive_charts/phe/wsh_mbd/atlas.html (Accessed on 05/04/2018).

Appendix B

Appendix B contains the Supporting Information files of:

- Paper 2.
- Paper 3.
- Paper 4.
- Paper 5.
- Appendix A.

These documents contain full Life Cycle Inventory tables and additional results like midpoint indicators and sensitivity analyses.

Data in brief 28 (2020) 104895

Contents lists available at ScienceDirect

Data in brief

journal homepage: www.elsevier.com/locate/dib

Data Article

Life Cycle Inventory datasets for nano-grid configurations

Federico Rossi [a, b], Maria Laura Parisi [a, c, d], Simone Maranghi [a, c], Riccardo Basosi [a, c, d], Adalgisa Sinicropi [a, c, d, *]

[a] University of Siena, R²ES Lab, Department of Biotechnology, Chemistry and Pharmacy, Via A. Moro,2, Siena, Italy
[b] University of Florence, Department of Industrial Engineering, Via Santa Marta,3, Florence, Italy
[c] CSGI, Center for Colloid and Surface Science, Via Della Lastruccia 3, 50019, Sesto Fiorentino, Italy
[d] National Research Council, Institute of Chemistry of Organometallic Compounds (CNR-ICCOM), Via Madonna Del Piano 10, 50019 Sesto Fiorentino, Italy

ARTICLE INFO

Article history:
Received 11 October 2019
Received in revised form 19 November 2019
Accepted 20 November 2019
Available online 28 November 2019

Keywords:
Storage
Photovoltaics
Smart grids
Life cycle assessment
Batteries
Solar energy

ABSTRACT

Datasets concerning some user-scale Smart Grids, named Nano-grids, are reported in this paper. First several Solar Home Systems composed of a photovoltaic plant, a backup generator and different types of lithium-ion batteries are provided. Then, the inventory analysis of hybrid Nano-grids integrating batteries and hydrogen storage is outlined according to different scenarios. These data inventory could be useful for any academic or stakeholder interested in reproducing this analysis and/or developing environmental sustainability assessment in the field of Smart Grids. For more insight, please see "Environmental analysis of a Nano-Grid: a Life Cycle Assessment" by Rossi F, Parisi M.L., Maranghi S., Basosi R., Sinicropi A. [1].

DOI of original article: https://doi.org/10.1016/j.scitotenv.2019.134814.
* Corresponding author. University of Siena, R²ES Lab, Department of Biotechnology, Chemistry and Pharmacy, Via A. Moro,2, Siena, Italy.
E-mail address: adalgisa.sinicropi@unisi.it (A. Sinicropi).

https://doi.org/10.1016/j.dib.2019.104895

Specifications Table

Subject	Renewable Energy, Sustainability and the Environment
Specific subject area	Life Cycle Assessment
Type of data	Tables
How data were acquired	Ecoinvent 3.2 database and scientific literature
Data format	Raw Analyzed
Parameters for data collection	Technological, temporal and geographical representativeness of data are described in Ecoinvent 3.2 reports.
Description of data collection	Data collection is performed employing the Ecoinvent 3.2 database. When the required information is not available from the Ecoinvent database, secondary data are acquired from literature.
Data source location	Institution: Ecoinvent City/Town/Region: Zurich Country: Switzerland
Data accessibility	The Life Cycle Inventories are reported with this article
Related research article	Federico Rossi, Maria Laura Parisi, Simone Maranghi, Riccardo Basosi, Adalgisa Sinicropi "Environmental analysis of a Nano-Grid: a Life Cycle Assessment" (https://doi.org/10.1016/j.scitotenv.2019.134814)

Value of the Data

- Life Cycle Inventories for nano-grids components and manufacturing processes concerning raw materials and energy input-output flows are provided.
- Data are useful for any academics studying smart grids value chain and for any stakeholders interested in the environmental sustainability of energy systems network.
- These comprehensive life cycle inventories can be employed for direct use or as data-proxies to be further customized and adapted for the development of environmental Life Cycle Assessment studies in the field of Smart Grids.
- Up-to-date datasets are built from technical data presented in scientific reports and papers and modelled according to the Ecoinvent 3.2 database for easy employment and reproducibility

1. Data

Datasets concerning some user-scale Smart Grids (Nano-grids) components and manufacturing processes are presented. Several Solar Home Systems composed of a photovoltaic plant, a backup generator and different types of lithium-ion batteries are described. Then, the inventory analysis of hybrid Nano-grids integrating batteries and hydrogen storage is outlined according to different scenarios [1]. The inventory analysis presented in this paper corresponds to the Life Cycle Inventory (LCI) phase that is a mandatory phase of the Life Cycle Assessment methodology, ISO 14040 standardized procedure for the environmental impact analysis of a product or a system. The LCI consists of a comprehensive dataset containing quantitative information about all the energy and matter flows involved in the life cycle of a product, process or system. The inventory analysis is performed using openLCA and is based on the Ecoinvent 3.2 database. In case some of the components of the Nano-grids are not present in the database, secondary data must be recovered from the literature, in order to create a representative Life Cycle Inventory for the missing components [2–4]. Table 1,2 describe the LCI of two different types of Hydrogen Storage Tanks during the production phase. Tables from Tables 3–9 summarize the LCI of the Solar Home Systems whereas tables from Tables 10–13 describe the LCIs of hybrid Nano-grids with four different scenarios [1]. Concerning tables from Tables 14–19, they represent the inventories dealing with the end of life of lithium-ion batteries, photovoltaic panels,

Table 1
Life Cycle Inventory of Type III Hydrogen Storage Tank production [6].

Component	Amount	Unit	Process	Comments and Sources
Input				
carbon fibre	21.2	kg	market for ammonia, liquid | ammonia, liquid | APOS, U - RER	Carbon fibre production [7]
	404.9	MJ	market for electricity, low voltage | electricity, low voltage | APOS, U - IT	Carbon fibre production [7]
	53.0	kg	market for propylene | propylene | APOS, U - GLO	Carbon fibre production [7]
chromium steel pipe	4.0	kg	chromium steel pipe production | chromium steel pipe | APOS, U - GLO	Ecoinvent 3.2 [8]
glass fibre reinforced plastic, polyester resin, hand lay-up	6.1	kg	market for glass fibre reinforced plastic, polyester resin, hand lay-up| glass fibre reinforced plastic, polyester resin, hand lay-up | APOS, U - GLO	Ecoinvent 3.2 [8]
polyethylene, high density, granulate	11.4	kg	market for polyethylene, high density, granulate | polyethylene, high density, granulate | APOS, U - GLO	Ecoinvent 3.2 [8] provides HDPE at granulate grade.
polymer foaming	5.2	kg	market for polymer foaming | polymer foaming | APOS, U - GLO	Ecoinvent 3.2 [8]
silicon, electronics grade	1.0	kg	market for silicon, electronics grade | silicon, electronics grade | APOS, U - GLO	Ecoinvent 3.2 [8]
steel, low-alloyed	14.5	kg	market for steel, low-alloyed | steel, low-alloyed | APOS, U - GLO	It contains all the steel-based parts [8].
Output				
Type III Hydrogen storage tank	258.0	l	Hydrogen storage tank production 350 bar	Reference output

Table 2
Life Cycle Inventory of Type IV Hydrogen Storage Tank production [6].

Component	Amount	Unit	Process	Comments and Sources
Input				
carbon fibre	27.0	kg	market for ammonia, liquid | ammonia, liquid | APOS, U - RER	Carbon fibre production [7]
	514.9	kg	market for electricity, low voltage | electricity, low voltage | APOS, U - IT	Carbon fibre production [7]
	67.4	kg	market for propylene | propylene | APOS, U - GLO	Carbon fibre production [7]
chromium steel pipe	4	kg	chromium steel pipe production | chromium steel pipe | APOS, U - GLO	Ecoinvent 3.2 [8]
glass fibre reinforced plastic, polyester resin, hand lay-up	4.6	kg	market for glass fibre reinforced plastic, polyester resin, hand lay-up| glass fibre reinforced plastic, polyester resin, hand lay-up | APOS, U - GLO	Ecoinvent 3.2 [8]
polyethylene, high density, granulate	8.0	kg	market for polyethylene, high density, granulate | polyethylene, high density, granulate | APOS, U - GLO	Ecoinvent 3.2 [8] provides HDPE at granulate grade.
polymer foaming	4.0	kg	market for polymer foaming | polymer foaming | APOS, U - GLO	Ecoinvent 3.2 [8]
silicon, electronics grade	1.0	kg	market for silicon, electronics grade | silicon, electronics grade | APOS, U - GLO	Ecoinvent 3.2 [8]
steel, low-alloyed	13.7	kg	market for steel, low-alloyed | steel, low-alloyed | APOS, U - GLO	It contains all the steel-based parts [8].
Output				
Type IV Hydrogen storage tank	149.0	l	Hydrogen storage tank production 700 bar	Reference output

Table 3
Life Cycle Inventory of a SHS equipped with M-B (LFP) LIBs.

Component	Amount	Unit	Process	Comments and Sources
Input				
PV panels	34.9	m^2	market for photovoltaic panel, single-Si wafer | photovoltaic panel, single-Si wafer | APOS, U - GLO	Ecoinvent 3.2 [8]
Is	2.5	Items	market for inverter, 2.5kW | inverter, 2.5kW | APOS, U - GLO	Ecoinvent 3.2 [8]
CCs	27.5	kg	charger production, for electric passenger car | charger, electric passenger car | APOS, U - GLO	Ecoinvent 3.2 [8]
Wiring	3.5	kg	cable production, unspecified | cable, unspecified | APOS, U - GLO	Evaluation based on [11]
	2.1	kg	tube insulation production, elastomere | tube insulation, elastomere | APOS, U - DE	Evaluation based on [11]
Backup Energy	15.1	MWh	market for diesel, burned in diesel-electric generating set, 18.5kW | diesel, burned in diesel-electric generating set, 18.5kW | APOS, U - GLO	Ecoinvent 3.2 [8]
M-B (LFP) LIBs	438.2	kg	Li-Ion battery pack production, LFP-C, modular, at plant (NTNU)	Database imported from Ref. [10]
Output				
Electricity	100.4	MWh		Reference output

Table 4
Life Cycle Inventory of a SHS equipped with Zack (LFP) LIBs.

Component	Amount	Unit	Process	Comments and Sources
Input				
PV panels	34.9	m^2	market for photovoltaic panel, single-Si wafer | photovoltaic panel, single-Si wafer | APOS, U - GLO	Ecoinvent 3.2 [8]
Is	2.5	Items	market for inverter, 2.5kW | inverter, 2.5kW | APOS, U - GLO	Ecoinvent 3.2 [8]
CCs	27.5	kg	charger production, for electric passenger car | charger, electric passenger car | APOS, U - GLO	Ecoinvent 3.2 [8]
Wiring	3.5	kg	cable production, unspecified | cable, unspecified | APOS, U - GLO	Evaluation based on [11]
	2.1	kg	tube insulation production, elastomere | tube insulation, elastomere | APOS, U - DE	Evaluation based on [11]
Backup Energy	15.5	MWh	market for diesel, burned in diesel-electric generating set, 18.5kW | diesel, burned in diesel-electric generating set, 18.5kW | APOS, U - GLO	Ecoinvent 3.2 [8]
Zack (LFP) LIBs	753.9	kg	LFP-C type Li-Ion Battery, modular, at plant (Zackrisson, org.)	Database imported from Ref. [10]
Output				
Electricity	100.4	MWh		Reference output

Table 5
Life Cycle Inventory of a SHS equipped with Bauer (LTO) LIBs.

Component	Amount	Unit	Process	Comments and Sources
Input				
PV panels	34.9	m^2	market for photovoltaic panel, single-Si wafer | photovoltaic panel, single-Si wafer | APOS, U - GLO	Ecoinvent 3.2 [8]
Is	2.5	Items	market for inverter, 2.5kW | inverter, 2.5kW | APOS, U - GLO	Ecoinvent 3.2 [8]
CCs	27.5	kg	charger production, for electric passenger car | charger, electric passenger car | APOS, U - GLO	Ecoinvent 3.2 [8]
Wiring	3.5	kg	cable production, unspecified | cable, unspecified | APOS, U - GLO	Evaluation based on [11]
	2.1	kg	tube insulation production, elastomere | tube insulation, elastomere | APOS, U - DE	Evaluation based on [11]
Backup Energy	14.9		market for diesel, burned in diesel-electric generating set, 18.5kW | diesel, burned in diesel-electric generating set, 18.5kW | APOS, U - GLO	Ecoinvent 3.2 [8]
Bauer (LTO) LIBs	734.7	kg	Li-Ion Battery Pack production, LFP-TiO, modular (Bauer)	Database imported from Ref. [10]
Output				
Electricity	100.4	MWh		Reference output

Table 6
Life Cycle Inventory of a SHS equipped with Notter (LMO) LIBs.

Component	Amount	Unit	Process	Comments and Sources
Input				
PV panels	34.9	m^2	market for photovoltaic panel, single-Si wafer | photovoltaic panel, single-Si wafer | APOS, U - GLO	Ecoinvent 3.2 [8]
Is	2.5	Items	market for inverter, 2.5kW | inverter, 2.5kW | APOS, U - GLO	Ecoinvent 3.2 [8]
CCs	27.5	kg	charger production, for electric passenger car | charger, electric passenger car | APOS, U - GLO	Ecoinvent 3.2 [8]
Wiring	3.5	kg	cable production, unspecified | cable, unspecified | APOS, U - GLO	Evaluation based on [11]
	2.1	kg	tube insulation production, elastomere | tube insulation, elastomere | APOS, U - DE	Evaluation based on [11]
Backup Energy	13.9	MWh	market for diesel, burned in diesel-electric generating set, 18.5kW | diesel, burned in diesel-electric generating set, 18.5kW | APOS, U - GLO	Ecoinvent 3.2 [8]
Notter (LMO) LIBs	764.9	kg	Li-ion battery, LMO-C, modular | cut-off, U (Notter/ecoinvent) - GLO	Database imported from Ref. [10]
Output				
Electricity	100.4	MWh		Reference output

Table 7
Life Cycle Inventory of a SHS equipped with Bauer (NCA) LIBs.

Component	Amount	Unit	Process	Comments and Sources
Input				
PV panels	34.9	m^2	market for photovoltaic panel, single-Si wafer | photovoltaic panel, single-Si wafer | APOS, U - GLO	Ecoinvent 3.2 [8]
Is	2.5	Items	market for inverter, 2.5kW | inverter, 2.5kW | APOS, U - GLO	Ecoinvent 3.2 [8]
CCs	27.5	kg	charger production, for electric passenger car | charger, electric passenger car | APOS, U - GLO	Ecoinvent 3.2 [8]
Wiring	3.5	kg	cable production, unspecified | cable, unspecified | APOS, U - GLO	Evaluation based on [11]
	2.1	kg	tube insulation production, elastomere | tube insulation, elastomere | APOS, U - DE	Evaluation based on [11]
Backup Energy	13.9	MWh	market for diesel, burned in diesel-electric generating set, 18.5kW | diesel, burned in diesel-electric generating set, 18.5kW | APOS, U - GLO	Ecoinvent 3.2 [8]
Bauer (NCA) LIBs	259.2	kg	Li-Ion Battery Pack production, NCA-C, modular (Bauer)	Database imported from Ref. [10]
Output				
Electricity	100.4	MWh		Reference output

Table 8
Life Cycle Inventory of a SHS equipped with Ell (NCM) LIBs.

Component	Amount	Unit	Process	Comments and Sources
Input				
PV panels	34.9	m^2	market for photovoltaic panel, single-Si wafer | photovoltaic panel, single-Si wafer | APOS, U - GLO	Ecoinvent 3.2 [8]
Is	2.5	Items	market for inverter, 2.5kW | inverter, 2.5kW | APOS, U - GLO	Ecoinvent 3.2 [8]
CCs	27.5	kg	charger production, for electric passenger car | charger, electric passenger car | APOS, U - GLO	Ecoinvent 3.2 [8]
Wiring	3.5	kg	cable production, unspecified | cable, unspecified | APOS, U - GLO	Evaluation based on [11]
	2.1	kg	tube insulation production, elastomere | tube insulation, elastomere | APOS, U - DE	Evaluation based on [11]
Backup Energy	13.2	MWh	market for diesel, burned in diesel-electric generating set, 18.5kW | diesel, burned in diesel-electric generating set, 18.5kW | APOS, U - GLO	Ecoinvent 3.2 [8]
Ell (NCM) LIBs	376.8	kg	Li-Ion battery pack production, NCM-C, modular (Ellingsen)	Database imported from Ref. [10]
Output				
Electricity	100.4	MWh		Reference output

Table 9
Life Cycle Inventory of a SHS equipped with M-B (NCM) LIBs.

Component	Amount	Unit	Process	Comments and Sources
Input				
PV panels	34.9	m^2	market for photovoltaic panel, single-Si wafer | photovoltaic panel, single-Si wafer | APOS, U - GLO	Ecoinvent 3.2 [8]
Is	2.5	Items	market for inverter, 2.5kW | inverter, 2.5kW | APOS, U - GLO	Ecoinvent 3.2 [8]
CCs	27.5	kg	charger production, for electric passenger car | charger, electric passenger car | APOS, U - GLO	Ecoinvent 3.2 [8]
Wiring	3.5	kg	cable production, unspecified | cable, unspecified | APOS, U - GLO	Evaluation based on [11]
	2.1	kg	tube insulation production, elastomere | tube insulation, elastomere | APOS, U - DE	Evaluation based on [11]
Backup Energy	13.9	MWh	market for diesel, burned in diesel-electric generating set, 18.5kW | diesel, burned in diesel-electric generating set, 18.5kW | APOS, U - GLO	Ecoinvent 3.2 [8]
M-B (NCM) LIBs	268.9	kg	Li-Ion battery pack production, NCM-C, modular, at plant (NTNU)	Database imported from Ref. [10]
Output				
Electricity	100.4	MWh		Reference output

Table 10
Life cycle inventory of a HNG-A.

Component	Amount	Unit	Process	Comments and Sources
Input				
PV panels	34.9	m^2	market for photovoltaic panel, single-Si wafer | photovoltaic panel, single-Si wafer | APOS, U - GLO	Ecoinvent 3.2 [8]
Is	2.5	Items	market for inverter, 2.5kW | inverter, 2.5kW | APOS, U - GLO	Ecoinvent 3.2 [8]
CCs	27.5	kg	charger production, for electric passenger car | charger, electric passenger car | APOS, U - GLO	Ecoinvent 3.2 [8]
Wiring	3.5	kg	cable production, unspecified | cable, unspecified | APOS, U - GLO	Evaluation based on [11]
	2.1	kg	tube insulation production, elastomere | tube insulation, elastomere | APOS, U - DE	Evaluation based on [11]
Backup Energy	0.4	MWh	market for diesel, burned in diesel-electric generating set, 18.5kW | diesel, burned in diesel-electric generating set, 18.5kW | APOS, U - GLO	Ecoinvent 3.2 [8]
Bauer (NCA) LIBs	259.2	kg	Li-Ion Battery Pack production, NCA-C, modular (Bauer)	Database imported from Ref. [10]
Type III Hydrogen storage tank	8.8	m^3	Hydrogen storage tank production 350 bar	Table 1
Compressor	0.4	Items	air compressor production, screw-type compressor, 4kW | air compressor, screw-type compressor, 4kW | APOS, U - RER	Ecoinvent 3.2 [8]
PEMFCs	2.5	Items	fuel cell production, polymer electrolyte membrane, 2kW electrical, future | fuel cell, polymer electrolyte membrane, 2kW electrical, future | APOS, U - CH	Ecoinvent 3.2 [8]
PEMEs	2.8	Items	fuel cell production, polymer electrolyte membrane, 2kW electrical, future | fuel cell, polymer electrolyte membrane, 2kW electrical, future | APOS, U - CH	Ecoinvent 3.2 [8]
Water	10.8	m^3	water production, deionised, from tap water, at user | water, deionised, from tap water, at user | APOS, U - CH	Ecoinvent 3.2 [8]
Output				
Electricity	100.4	MWh		Reference output
Compressed hydrogen	507.8	kg		By-product

Table 11
Life cycle inventory of a HNG-B.

Component	Amount	Unit	Process	Comments and Sources
Input				
PV panels	34.9	m^2	market for photovoltaic panel, single-Si wafer | photovoltaic panel, single-Si wafer | APOS, U - GLO	Ecoinvent 3.2 [8]
Is	2.5	Items	market for inverter, 2.5kW | inverter, 2.5kW | APOS, U - GLO	Ecoinvent 3.2 [8]
CCs	27.5	kg	charger production, for electric passenger car | charger, electric passenger car | APOS, U - GLO	Ecoinvent 3.2 [8]
Wiring	3.5	kg	cable production, unspecified | cable, unspecified | APOS, U - GLO	Evaluation based on [11]
	2.1	kg	tube insulation production, elastomere | tube insulation, elastomere | APOS, U - DE	Evaluation based on [11]
Backup Energy	0.5	MWh	market for diesel, burned in diesel-electric generating set, 18.5kW | diesel, burned in diesel-electric generating set, 18.5kW | APOS, U - GLO	Ecoinvent 3.2 [8]
Bauer (NCA) LIBs	259.2	kg	Li-Ion Battery Pack production, NCA-C, modular (Bauer)	Database imported from Ref. [10]
Type IV Hydrogen storage tank	4.5	m^3	Hydrogen storage tank production 700 bar	Table 2
Compressor	0.6	Items	air compressor production, screw-type compressor, 4kW | air compressor, screw-type compressor, 4kW | APOS, U - RER	Ecoinvent 3.2 [8]
PEMFCs	2.5	Items	fuel cell production, polymer electrolyte membrane, 2kW electrical, future | fuel cell, polymer electrolyte membrane, 2kW electrical, future | APOS, U - CH	Ecoinvent 3.2 [8]
PEMEs	2.8	Items	fuel cell production, polymer electrolyte membrane, 2kW electrical, future | fuel cell, polymer electrolyte membrane, 2kW electrical, future | APOS, U - CH	Ecoinvent 3.2 [8]
Water	10.8	m^3	water production, deionised, from tap water, at user | water, deionised, from tap water, at user | APOS, U - CH	Ecoinvent 3.2 [8]
Output				
Electricity	100.4	MWh		Reference output
Compressed hydrogen	470.6	kg		By-product

Table 12
Life cycle inventory of a HNG-C.

Component	Amount	Unit	Process	Comments and Sources
Input				
PV panels	34.9	m^2	market for photovoltaic panel, single-Si wafer | photovoltaic panel, single-Si wafer | APOS, U - GLO	Ecoinvent 3.2 [8]
Is	2.5	Items	market for inverter, 2.5kW | inverter, 2.5kW | APOS, U - GLO	Ecoinvent 3.2 [8]
CCs	27.5	kg	charger production, for electric passenger car | charger, electric passenger car | APOS, U - GLO	Ecoinvent 3.2 [8]
Wiring	3.5	kg	cable production, unspecified | cable, unspecified | APOS, U - GLO	Evaluation based on [11]
	2.1	kg	tube insulation production, elastomere | tube insulation, elastomere | APOS, U - DE	Evaluation based on [11]
Backup Energy	0.4	MWh	market for diesel, burned in diesel-electric generating set, 18.5kW | diesel, burned in diesel-electric generating set, 18.5kW | APOS, U - GLO	Ecoinvent 3.2 [8]
Bauer (NCA) LIBs	259.2	kg	Li-Ion Battery Pack production, NCA-C, modular (Bauer)	Database imported from Ref. [10]
Type III Hydrogen storage tank	8.8	m^3	Hydrogen storage tank production 350 bar	Table 1
Compressor	0.4	Items	air compressor production, screw-type compressor, 4kW | air compressor, screw-type compressor, 4kW | APOS, U - RER	Ecoinvent 3.2 [8]

(*continued on next page*)

Table 12 (*continued*)

Component	Amount	Unit	Process	Comments and Sources
PEMFCs	0.5	Items	fuel cell production, polymer electrolyte membrane, 2kW electrical, future | fuel cell, polymer electrolyte membrane, 2kW electrical, future | APOS, U - CH	Ecoinvent 3.2 [8]
PEMEs	0.6	Items	fuel cell production, polymer electrolyte membrane, 2kW electrical, future | fuel cell, polymer electrolyte membrane, 2kW electrical, future | APOS, U - CH	Ecoinvent 3.2 [8]
Water	10.8	m^3	water production, deionised, from tap water, at user | water, deionised, from tap water, at user | APOS, U - CH	Ecoinvent 3.2 [8]
Output				
Electricity	100.4	MWh		Reference output
Compressed hydrogen	507.8	kg		By-product

Table 13
Life cycle inventory of a HNG-D.

Component	Amount	Unit	Process	Comments and Sources
Input				
PV panels	34.9	m^2	market for photovoltaic panel, single-Si wafer | photovoltaic panel, single-Si wafer | APOS, U - GLO	Ecoinvent 3.2 [8]
Is	2.5	Items	market for inverter, 2.5kW | inverter, 2.5kW | APOS, U - GLO	Ecoinvent 3.2 [8]
CCs	27.5	kg	charger production, for electric passenger car | charger, electric passenger car | APOS, U - GLO	Ecoinvent 3.2 [8]
Wiring	3.5	kg	cable production, unspecified | cable, unspecified | APOS, U - GLO	Evaluation based on [11]
	2.1	kg	tube insulation production, elastomere | tube insulation, elastomere | APOS, U - DE	Evaluation based on [11]
Backup Energy	0.5	MWh	market for diesel, burned in diesel-electric generating set, 18.5kW | diesel, burned in diesel-electric generating set, 18.5kW | APOS, U - GLO	Ecoinvent 3.2 [8]
Bauer (NCA) LIBs	259.2	kg	Li-Ion Battery Pack production, NCA-C, modular (Bauer)	Database imported from Ref. [10]
Type IV Hydrogen storage tank	4.5	m^3	Hydrogen storage tank production 700 bar	Table 2
Compressor	0.6	Items	air compressor production, screw-type compressor, 4kW | air compressor, screw-type compressor, 4kW | APOS, U - RER	Ecoinvent 3.2 [8]
PEMFCs	0.5	Items	fuel cell production, polymer electrolyte membrane, 2kW electrical, future | fuel cell, polymer electrolyte membrane, 2kW electrical, future | APOS, U - CH	Ecoinvent 3.2 [8]
PEMEs	0.6	Items	fuel cell production, polymer electrolyte membrane, 2kW electrical, future | fuel cell, polymer electrolyte membrane, 2kW electrical, future | APOS, U - CH	Ecoinvent 3.2 [8]
Water	10.8	m^3	water production, deionised, from tap water, at user | water, deionised, from tap water, at user | APOS, U - CH	Ecoinvent 3.2 [8]
Output				
Electricity	100.4	MWh		Reference output
Compressed hydrogen	470.6	kg		By-product

electricity converters, proton exchange membrane fuel cells and electrolysers and hydrogen storage tanks.

2. Experimental design, materials, and methods

Data are represented in Tables divided in two sections: Inputs and Outputs.

- The first column collects the Ecoinvent 3.2 reference flows;

Table 14
Life Cycle Inventory of a LIBs end of life based on Ecoinvent 3.2 [8] and Weber et al. [16].

Component	Amount	Unit	Process	Comments and Sources
Input				
diesel, burned in building machine	0.1	MJ	diesel, burned in building machine | diesel, burned in building machine | APOS, U - GLO	Ecoinvent 3.2 [8]
electricity, medium voltage	10	Wh	electricity voltage transformation from high to medium voltage | electricity, medium voltage | APOS, U - IT	Ecoinvent 3.2 [8]
Iron scrap, sorted, pressed	0.3	kg	market for iron scrap, sorted, pressed | iron scrap, sorted, pressed | APOS, U - GLO	Ecoinvent 3.2 [8]
Used cable	−70.5	g	market for used cable | used cable | APOS, U - GLO	Ecoinvent 3.2 [8]
treatment of used Li-ion battery, hydrometallurgical treatment	−340.0	g	treatment of used Li-ion battery, hydrometallurgical treatment | used Li-ion battery | APOS, U - GLO	Ecoinvent 3.2 [8]
treatment of used Li-ion battery, pyrometallurgical treatment	−340.0	g	treatment of used Li-ion battery, pyrometallurgical treatment | used Li-ion battery | APOS, U - GLO	Ecoinvent 3.2 [8]
waste electric and electronic equipment	−31.0	g	treatment of waste electric and electronic equipment, shredding | waste electric and electronic equipment | APOS, U - GLO	Ecoinvent 3.2 [8]
waste plastic, consumer electronics	−41.0	g	treatment of waste plastic, consumer electronics, municipal incineration | waste plastic, consumer electronics | APOS, U - CH	Ecoinvent 3.2 [8]
used battery	1.0	kg		Reference input
Output				
Cable, unspecified	7.1	g	market for cable, unspecified | cable, unspecified | APOS, U - GLO	Avoided product Ecoinvent 3.2 [8]
Electronic scrap	31.0	g	market for electronics scrap | electronics scrap | APOS, U - GLO	Avoided product Ecoinvent 3.2 [8]
Iron scrap, sorted, pressed	26.0	g	gold-silver-zinc-lead-copper mining and beneficiation | iron scrap, sorted, pressed | APOS, U - CA-QC	Avoided product Ecoinvent 3.2 [8]

Table 15
Life Cycle Inventory of a PV end of life [17].

Component	Amount	Unit	Process	Comments and Sources
Input				
aluminium scrap, post-consumer	−182.7	kg	market for aluminium scrap, post-consumer | aluminium scrap, post-consumer | APOS, U - GLO	Ecoinvent 3.2 [8]
average incineration residue	−2.0	kg	treatment of average incineration residue, residual material landfill | average incineration residue | APOS, U - CH	Ecoinvent 3.2 [8]
Copper	4.4	kg	treatment of used cable | copper | APOS, U - GLO	Ecoinvent 3.2 [8]
diesel, burned in building machine	41.0	MJ	diesel, burned in building machine | diesel, burned in building machine | APOS, U - GLO	Ecoinvent 3.2 [8]
electricity, medium voltage	113.6	kWh	market for electricity, medium voltage | electricity, medium voltage | APOS, U - IT	Ecoinvent 3.2 [8]
glass cullet, sorted	686.0	kg	market for glass cullet, sorted | glass cullet, sorted | APOS, U - GLO	Ecoinvent 3.2 [8]
lime, hydrated, loose weight	36.5	kg	lime production, hydrated, loose weight | lime, hydrated, loose weight | APOS, U - CH	Ecoinvent 3.2 [8]
limestone residue	−306.1	kg	treatment of limestone residue, inert material landfill | limestone residue | APOS, U - CH	Ecoinvent 3.2 [8]
	7.1	kg		Ecoinvent 3.2 [8]

(*continued on next page*)

Table 15 (*continued*)

Component	Amount	Unit	Process	Comments and Sources
nitric acid, without water, in 50% solution state			nitric acid production, product in 50% solution state | nitric acid, without water, in 50% solution state | APOS, U - RER	
silicon carbide	34.7	kg	treatment of spent sawing slurry from Si-wafer cutting | silicon carbide | APOS, U - RER	Ecoinvent 3.2 [8]
sludge, pig iron production	−50.3	kg	treatment of sludge, pig iron production, residual material landfill | sludge, pig iron production | APOS, U - CH	Ecoinvent 3.2 [8]
waste electric wiring	−0.6	kg	treatment of waste electric wiring, collection for final disposal | waste electric wiring | APOS, U - RoW	Ecoinvent 3.2 [8]
waste glass	−14.0	kg	treatment of waste glass, inert material landfill | waste glass | APOS, U - CH	Ecoinvent 3.2 [8]
waste plastic, mixture	−51.0	kg	treatment of waste plastic, mixture, municipal incineration | waste plastic, mixture | APOS, U - CH	Ecoinvent 3.2 [8]
waste polyvinylfluoride	−15.0	kg	treatment of waste polyvinylfluoride, municipal incineration | waste polyvinylfluoride | APOS, U - CH	Ecoinvent 3.2 [8]
Waste treatment PV	1000.0	kg		Reference input
waste wire plastic, municipal incineration	−5.0	kg	treatment of waste wire plastic, municipal incineration | waste wire plastic | APOS, U - CH	Ecoinvent 3.2 [8]
water, completely softened, from decarbonised water, at user |	309.7	kg	water production, completely softened, from decarbonised water, at user | water, completely softened, from decarbonised water, at user | APOS, U - RER	Ecoinvent 3.2 [8]
Output				
Nitrogen oxides	2.0	kg		
aluminium scrap, new	182.7	kg	market for aluminium scrap, new | aluminium scrap, new | APOS, U - RER	Avoided product Ecoinvent 3.2 [8]
copper scrap, sorted, pressed	4.4	kg	market for copper scrap, sorted, pressed | copper scrap, sorted, pressed | APOS, U - GLO	Avoided product Ecoinvent 3.2 [8]
electricity, medium voltage	248.8	MJ	electricity voltage transformation from high to medium voltage | electricity, medium voltage | APOS, U - IT	Avoided product Ecoinvent 3.2 [8]
glass cullet	686.0	kg	market for glass cullet, for Saint-Gobain ISOVER SA | glass cullet, for Saint-Gobain ISOVER SA | APOS, U - GLO	Avoided product Ecoinvent 3.2 [8]
heat, district or industrial, natural gas	502.8	MJ	heat production, natural gas, at industrial furnace >100kW | heat, district or industrial, natural gas | APOS, U - Europe without Switzerland	Avoided product Ecoinvent 3.2 [8]
silicon, metallurgical grade	34.7	kg	market for silicon, metallurgical grade | silicon, metallurgical grade | APOS, U - GLO	Avoided product Ecoinvent 3.2 [8]

- The second column contains the amount of energy or material whose evaluation is based on the Nano-grid design and modelling as described in Ref. [1]. A negative number must be used in end of life processes because of the logic used by Ecoinvent in building these processes;
- The third column contains the unit of measurement of inputs and outputs;
- The fourth column contains the provider process for the flows;
- The fifth column contains sources and comments. The whole inventory is based on Ecoinvent 3.2 but when a component is not available in the database, information has been gathered from scientific papers in the literature. Based on literature data, the inventory of the missing components has been built using Ecoinvent 3.2 [5]. Other comments specify if the flow represents a reference flow, which means that the provider is the process described it the table itself, or an avoided product to estimate the environmental benefits of recycling processes.

Table 1 represents the inventory for the manufacturing of a tank storing gaseous hydrogen at 350 bar (Type III).

Table 16
Life Cycle Inventory of Inverters and a Charge Controllers (adapted from Inverter) end of life [18].

Component	Amount	Unit	Process	Comments and Sources
Output				
aluminium scrap, post-consumer	−5.0	kg	treatment of aluminium scrap, post-consumer, by collecting, sorting, cleaning, pressing | aluminium scrap, post-consumer | APOS, U - RER	Ecoinvent 3.2 [8]
Copper	1.9	kg	treatment of used cable | copper | APOS, U - GLO	Ecoinvent 3.2 [8]
electronics scrap from control unit	−0.9	kg	treatment of electronics scrap from control units | electronics scrap from control units | APOS, U - RER	Ecoinvent 3.2 [8]
Inverter/charge controller	1.0	Items		Reference input
hazardous waste, for incineration	−12.8	Wh	treatment of hazardous waste, hazardous waste incineration | hazardous waste, for incineration | APOS, U - CH	Ecoinvent 3.2 [8]
iron scrap, sorted, pressed	0.9	kg	sorting and pressing of iron scrap | iron scrap, sorted, pressed | APOS, U - RER	Ecoinvent 3.2 [8]
municipal solid waste	−0.2	kg	treatment of municipal solid waste, municipal incineration with fly ash extraction | municipal solid waste | APOS, U - CH	Ecoinvent 3.2 [8]
used printed wiring boards	−1.2	kg	market for used printed wiring boards | used printed wiring boards | APOS, U - GLO	Ecoinvent 3.2 [8]
waste paperboard	−1.8	kg	treatment of waste paperboard, municipal incineration | waste paperboard | APOS, U - CH	Ecoinvent 3.2 [8]
waste polyethylene	−11.5	g	treatment of waste polyethylene, municipal incineration | waste polyethylene | APOS, U - CH	Ecoinvent 3.2 [8]
wastewater, unpolluted	−19.9	l	treatment of wastewater, unpolluted, capacity 5E9l/ year | wastewater, unpolluted | APOS, U - CH	Ecoinvent 3.2 [8]
Output				
aluminium, cast alloy	5.0	kg	market for aluminium, cast alloy | aluminium, cast alloy | APOS, U - GLO	Avoided product Ecoinvent 3.2 [8]
Copper	1.9	kg	market for copper | copper | APOS, U - GLO	Avoided product Ecoinvent 3.2 [8]
iron ore, crude ore, 46% Fe	0.9	kg	market for iron ore, crude ore, 46% Fe | iron ore, crude ore, 46% Fe | APOS, U - GLO	Avoided product Ecoinvent 3.2 [8]

Table 17
Life Cycle Inventory of a PEMFCs and PEMEs end of life [19].

Component	Amount	Unit	Process	Comments and Sources
Input				
aluminium scrap, post-consumer	−57.5	kg	market for aluminium scrap, post-consumer | aluminium scrap, post-consumer | APOS, U - GLO	Ecoinvent 3.2 [8]
copper	−9.5	kg	treatment of used cable | copper | APOS, U - GLO	Ecoinvent 3.2 [8]
hazardous waste, for incineration	−5.6	kg	treatment of hazardous waste, hazardous waste incineration | hazardous waste, for incineration | APOS, U - CH	Ecoinvent 3.2 [8]
inert waste, for final disposal	−9.8	kg	market for inert waste, for final disposal | inert waste, for final disposal | APOS, U - GLO	Ecoinvent 3.2 [8]
scrap copper	−2.5	kg	market for scrap copper | scrap copper | APOS, U - GLO	Ecoinvent 3.2 [8]
scrap steel	−23.1	kg	treatment of scrap steel, inert material landfill | scrap steel | APOS, U - CH	Ecoinvent 3.2 [8]
slag from metallurgical grade silicon production	−0.2	kg	treatment of slag from metallurgical grade silicon production, inert material landfill | slag from metallurgical grade silicon production | APOS, U - CH	Ecoinvent 3.2 [8]

(*continued on next page*)

Table 17 (*continued*)

Component	Amount	Unit	Process	Comments and Sources
waste aluminium	−50.0	g	treatment of waste aluminium, sanitary landfill | waste aluminium | APOS, U - CH	Ecoinvent 3.2 [8]
Waste management 3kW FC	1	Items		Reference input
waste plastic, industrial electronics	−22.4	kg	market for waste plastic, industrial electronics | waste plastic, industrial electronics | APOS, U - GLO	Ecoinvent 3.2 [8]
Output				
aluminium, cast alloy	58.6	kg	market for aluminium, cast alloy | aluminium, cast alloy | APOS, U - GLO	Avoided product Ecoinvent 3.2 [8]
steel, unalloyed	140.2	kg	market for steel, unalloyed | steel, unalloyed | APOS, U - GLO	Avoided product Ecoinvent 3.2 [8]

Table 18
Life Cycle Inventory of platinum recovery process [20] from PEMFCs and PEMEs membranes.

Component	Amount	Unit	Process	Comments and Sources
Input				
1-pentanol	620.0	kg	hydroformylation of butene | 1-pentanol | APOS, U - RER	Ecoinvent 3.2 [8]
ammonium chloride	26.6	kg	market for ammonium chloride | ammonium chloride | APOS, U - GLO	Ecoinvent 3.2 [8]
Phosphoryl chloride	36.6	kg	phosphoryl chloride production | phosphoryl chloride | APOS, U - RER	Cyanex production [20]
Solvent, organic	80.4	kg	market for solvent, organic | solvent, organic | APOS, U - GLO	Cyanex production [20]
hazardous waste	−1.4	kg	treatment of hazardous waste, hazardous waste incineration | hazardous waste, for incineration | APOS, U - CH	Ecoinvent 3.2 [8]
hydrochloric acid, without water, in 30% solution state	284.0	kg	tetrafluoroethane production | hydrochloric acid, without water, in 30% solution state | APOS, U - GLO	Ecoinvent 3.2 [8]
hydrogen peroxide, without water, in 50% solution state	5.0	kg	hydrogen peroxide production, product in 50% solution state | hydrogen peroxide, without water, in 50% solution state | APOS, U - RER	Ecoinvent 3.2 [8]
sodium hydroxide, without water, in 50% solution state	74.0	kg	market for sodium hydroxide, without water, in 50% solution state | sodium hydroxide, without water, in 50% solution state | APOS, U - GLO	Ecoinvent 3.2 [8]
spent solvent mixture	737.0	kg	clinker production | spent solvent mixture | APOS, U - CH	Ecoinvent 3.2 [8]
Waste Pt	1.0	kg		Reference input
wastewater, average	−1.9	m^3	treatment of wastewater, average, capacity 4.7E10l/year | wastewater, average | APOS, U - CH	Ecoinvent 3.2 [8]
water, deionised, from tap water, at user	1900.0	kg	water production, deionised, from tap water, at user | water, deionised, from tap water, at user | APOS, U - CH	Ecoinvent 3.2 [8]
Output				
Platinum	0.7	kg	market for platinum | platinum | APOS, U - GLO	Avoided product Ecoinvent 3.2 [8]

Table 19
Life Cycle Inventory of carbon fibre recovery process [20] from Hydrogen Storage Tanks.

Component	Amount	Unit	Process	Comments and Sources
Input				
acetic acid, without water, in 98% solution state	250.0	g	market for acetic acid, without water, in 98% solution state | acetic acid, without water, in 98% solution state | APOS, U - GLO	Ecoinvent 3.2 [8]
electricity, low voltage	1.0	kWh	market for electricity, low voltage | electricity, low voltage | APOS, U - IT	Ecoinvent 3.2 [8]
polymer foaming	200.0	g	market for polymer foaming | polymer foaming | APOS, U - GLO	Ecoinvent 3.2 [8]
waste carbon fibre	556.0	g		Reference input
sodium hydroxide, without water, in 50% solution state	20.0	g	market for sodium hydroxide, without water, in 50% solution state | sodium hydroxide, without water, in 50% solution state | APOS, U - GLO	Ecoinvent 3.2 [8]
water, deionised, from tap water at user	750.0	g	market for water, deionised, from tap water, at user | water, deionised, from tap water, at user | APOS, U - GLO	Ecoinvent 3.2 [8]
Output				
carbon fibre	300.0	g		Avoided product Carbon fibre production [7]

Table 2 represents the inventory for the manufacturing of a tank storing gaseous hydrogen at 700 bar (Type IV).

Table 3 represents the inventory for a Solar Home System equipped with the lithium iron phosphates (LFP) batteries studied by Majeau-Bettez et al. [9] (M-B) whose inventory is provided by Peters and Weil [10].

Table 4 represents the inventory for a Solar Home System equipped with the lithium iron phosphates (LFP) batteries studied by Zackrisson et al. [12] (Zack) whose inventory is provided by Peters and Weil [10].

Table 5 represents the inventory for a Solar Home System equipped with the lithium titanate (LTO) batteries studied by Bauer [13] whose inventory is provided by Peters and Weil [10].

Table 6 represents the inventory for a Solar Home System equipped with the lithium manganese oxide (LMO) batteries studied by Notter et al. [14] whose inventory is provided by Peters and Weil [10].

Table 7 represents the inventory for a Solar Home System equipped with the lithium nickel cobalt aluminium (NCA) oxide batteries studied by Bauer [13] whose inventory is provided by Peters and Weil [10].

Table 8 represents the inventory for a Solar Home System equipped with the lithium nickel cobalt manganese oxide (NCM) batteries studied by Ellingsen et al. [15] (Ell) whose inventory is provided by Peters and Weil [10].

Table 9 represents the inventory for a Solar Home System equipped with the lithium nickel cobalt manganese (NCM) oxide batteries studied by Majeau-Bettez et al. [9] (M-B) whose inventory is provided by Peters and Weil [10].

Table 10 represents the inventory for a hybrid Nano-grid (HNG) equipped with the lithium nickel cobalt aluminium oxide (NCA) batteries studied by Bauer [13] whose inventory is provided by Peters and Weil [10] and with hydrogen storage. In this scenario (A) hydrogen is stored at 350 bar, produced by electrolysers powered by photovoltaics and converted to electricity by fuel cells whose lifespan is supposed to be 12.000 hours.

Table 11 represents the inventory for a hybrid Nano-grid (HNG) equipped with the lithium nickel cobalt aluminium (NCA) oxide batteries studied by Bauer [13] whose inventory is provided by Peters and Weil [10] and with hydrogen storage. In this scenario (B) hydrogen is stored at 700 bar, produced by electrolysers powered by photovoltaics and converted to electricity by fuel cells whose lifespan is supposed to be 12.000 hours.

Table 12 represents the inventory for a hybrid Nano-grid (HNG) equipped with the lithium nickel cobalt aluminium oxide (NCA) batteries studied by Bauer [13] whose inventory is provided by Peters

and Weil [10] and with hydrogen storage. In this scenario (C) hydrogen is stored at 350 bar, produced by electrolysers powered by photovoltaics and converted to electricity by fuel cells whose lifespan is supposed to be 60.000 hours.

Table 13 represents the inventory for a hybrid Nano-grid (HNG) equipped with the lithium nickel cobalt aluminium oxide (NCA) batteries studied by Bauer [13] whose inventory is provided by Peters and Weil [10] and with hydrogen storage. In this scenario (B) hydrogen is stored at 700 bar, produced by electrolysers powered by photovoltaics and converted to electricity by fuel cells whose lifespan is supposed to be 60.000 hours.

Table 14 represents the inventory for a generic lithium-ion battery end of life management, where part of the materials is recovered [16].

Table 15 represents the inventory for a crystalline photovoltaic (PV) panel end of life management where part of the materials is recovered [17].

Table 16 represents the inventory for an inverter end of life management where part of the materials is recovered [18]. As no inventory for charge controllers end of life management is available in the literature, this component has been approximated to an inverter as both are electric converters composed of many other small electronic sub-components.

Table 17 represents the inventory for proton exchange membrane electrolysers (PEMEs) and fuel cells (PEMFCs) end of life management, electrochemical devices composed of the same materials that are partially recovered [19].

Table 18 represents the inventory for platinum recovery from PEMEs and PEMFCs membranes as, even if the use of this rare material could be impactful for the environment, it was not considered in Ref. [19].

Table 19: as no inventory exists for hydrogen storage tanks end of life management, a recovering process has been considered for carbon fibre, representing the most weighting material of the tanks.

Funding

This research did not receive any specific grant from funding agencies in the public, commercial, or not-for-profit sectors.

Acknowledgments

Authors acknowledge MIUR Grant - Department of Excellence 2018−2022. FR is grateful for the Ph.D. grant within the “Progetto Pegaso” funded by Regione Toscana.

Conflict of Interest

The authors declare that they have no known competing financial interests or personal relationships that could have appeared to influence the work reported in this paper.

References

[1] F. Rossi, M.L. Parisi, S. Maranghi, R. Basosi, A. Sinicropi, Environmental analysis of a nano-grid: a life cycle assessment,, Sci. Total Environ. 700 (2019) 134814, https://doi.org/10.1016/j.scitotenv.2019.134814.
[2] M. Bravi, M.L. Parisi, E. Tiezzi, R. Basosi, Life cycle assessment of advanced technologies for photovoltaic panels production, Int. J.Heat Technol. 28 (2010) 129−135.
[3] M.L. Parisi, S. Maranghi, A. Sinicropi, R. Basosi, Development of dye sensitized solar cells: a life cycle perspective for the environmental and market potential assessment of a renewable energy technology, Int. J.Heat Technol. 31 (2013).
[4] S. Maranghi, M.L. Parisi, R. Basosi, A. Sinicropi, Environmental profile of the manufacturing process of perovskite photovoltaics: harmonization of life cycle assessment studies, Energies 12 (2019) 3746, https://doi.org/10.3390/en12193746.
[5] M.L. Parisi, N. Ferrara, L. Torsello, R. Basosi, Life cycle assessment of atmospheric emission profiles of the Italian geothermal power plants, J. Clean. Prod. 234 (2019) 881−894, https://doi.org/10.1016/j.jclepro.2019.06.222.
[6] A. Elgowainy, K. Reddi, M. Wang, Life-cycle analysis of hydrogen on-board storage options, in: 2013 DOE Fuel Cell Technol. Progr. Annu. Merit Rev, Peer Eval. Meet., Arlington, VA, 2012.
[7] O.M. De Vegt, W.G. Haije, Comparative Environmental Life Cycle Assessment of Composite Materials, 1997.
[8] E. Moreno Ruiz, T. Lévová, G. Bourgault, G. Wernet, Documentation of Changes Implemented in Ecoinvent Database 3 vol. 2, 2015, p. 2.

[9] G. Majeau-bettez, T.R. Hawkins, A.H. Strømman, Life Cycle Environmental Assessment of Lithium-Ion and Nickel Metal Hydride Batteries for Plug-In Hybrid and Battery Electric Vehicles, 2011, pp. 4548–4554, https://doi.org/10.1021/es103607c.
[10] J.F. Peters, M. Weil, Providing a common base for life cycle assessments of Li-Ion batteries, J. Clean. Prod. 171 (2018) 704–713, https://doi.org/10.1016/j.jclepro.2017.10.016.
[11] K. Bekkelund, A Comparative Life Cycle Assessment of PV Solar Systems, Master Thesis in Energy and Environmental Engineering, Norwegian University of Science and Technology (NTNU), Department of Energy and Process Engineering, 2013, p. 243.
[12] M. Zackrisson, L. Avellán, J. Orlenius, Life cycle assessment of lithium-ion batteries for plug-in hybrid electric vehicles e Critical issues, J. Clean. Prod. 18 (2010) 1519–1529, https://doi.org/10.1016/j.jclepro.2010.06.004.
[13] C. Bauer, Okobilanz von Lithium-Ionen Batterien, 2010.
[14] D.A. Notter, M. Gauch, R. Widmer, W.A. Patrick, A. Stamp, R. Zah, R.G. Althaus, Contribution of Li-Ion Batteries to the Environmental Impact of Electric Vehicles vol.44, 2010, pp. 6550–6556.
[15] L.A. Ellingsen, G. Majeau-Bettez, B. Singh, A.K. Srivastava, L.O. Valøen, A.H. Strømman, Life cycle assessment of a lithium-ion battery vehicle pack, J. Ind. Ecol. 18 (2014) 113–124, https://doi.org/10.1111/jiec.12072.
[16] S. Weber, J.F. Peters, M. Baumann, M. Weil, Life cycle assessment of a vanadium redox flow battery, Environ. Sci. Technol. 52 (2018) 10864–10873, https://doi.org/10.1021/acs.est.8b02073.
[17] C.E.L. Latunussa, F. Ardente, G.A. Blengini, L. Mancini, Life Cycle Assessment of an innovative recycling process for crystalline silicon photovoltaic panels, Sol. Energy Mater. Sol. Cells 156 (2016) 101–111, https://doi.org/10.1016/j.solmat.2016.03.020.
[18] L. Tschümperlin, P. Stolz, R. Frischknecht, Life cycle assessment of low pow- er solar inverters (2.5 to 20 kW) 3, Swiss Federal Office of Energy SFOE, 2016.
[19] R. Stropnik, M. Sekavčnik, A.M. Ferriz, M. Mori, Reducing environmental impacts of the ups system based on PEM fuel cell with circular economy, Energy 165 (2018) 824–835, https://doi.org/10.1016/j.energy.2018.09.201.
[20] L. Duclos, M. Lupsea, G. Mandil, L. Svecova, P.-X. Thivel, V. Laforest, Environmental assessment of proton exchange membrane fuel cell platinum catalyst recycling, J. Clean. Prod. 142 (2017) 2618–2628, https://doi.org/10.1016/j.jclepro.2016.10.197.

energies

MDPI

Article

Life Cycle Assessment of classic and innovative batteries for Solar Home Systems in Europe – Supporting Information

Federico Rossi[1] Maria Laura Parisi[2], Sarah Greven[3], Riccardo Basosi[4], Adalgisa Sinicropi[5]

[1] University of Siena, R2ES Lab, Department of Biotechnology, Chemistry and Pharmacy, Via A. Moro,2, Siena, Italy. University of Florence, Department of Industrial Engineering, Via Santa Marta,3, Florence, Italy,

[2] University of Siena, R2ES Lab, Department of Biotechnology, Chemistry and Pharmacy, Via A. Moro,2, Siena, Italy. CSGI, Center for colloid and surface science, via della Lastruccia 3, 50019, Sesto Fiorentino, Italy. Institute of Chemistry of Organometallic Compounds (CNR-ICCOM), Via Madonna del Piano 10, 50019 Sesto Fiorentino, Italy.

[3] ENSICAEN, Chimie Materiaux, 6 bd Maréchal Juin – CS 45053, F-14050 CAEN Cedex 4- France

[4] University of Siena, R2ES Lab, Department of Biotechnology, Chemistry and Pharmacy, Via A. Moro,2, Siena, Italy. CSGI, Center for colloid and surface science, via della Lastruccia 3, 50019, Sesto Fiorentino, Italy. Institute of Chemistry of Organometallic Compounds (CNR-ICCOM), Via Madonna del Piano 10, 50019 Sesto Fiorentino, Italy.

[5] University of Siena, R2ES Lab, Department of Biotechnology, Chemistry and Pharmacy, Via A. Moro,2, Siena, Italy. CSGI, Center for colloid and surface science, via della Lastruccia 3, 50019, Sesto Fiorentino, Italy. Institute of Chemistry of Organometallic Compounds (CNR-ICCOM), Via Madonna del Piano 10, 50019 Sesto Fiorentino, Italy.

* Correspondence: adalgisa.sinicropi@unisi.it

energies

MDPI

1. Results of the modelling phase

In this section, all the results obtained by the simulation of Solar Home Systems (SHSs) performances are collected in Table S1. Particularly, the battery energy storage system lifespan (L_{BESS}) the missing amount of energy (E_{miss}) and th exceeding one (E_{exc}) are collected for all the installation sites: Denmark (DK), Spain (ES), France (FR), Greece (GR), Hungary (HU), Italy (IT), Portugal (PT) and Romania (RO).

Table S1: Complete results of the SHS modelling phase.

	Bauer (LTO, SSLTO)	Bauer (NCA, SSNCA)	Ell (NCM, SSNCM)	M-B (LFP, SSLFP)	M-B (NCM, SSNCM)	Notter (LMO, SSLMO)	Zack (LFP, SSLFP)	Peters (SIB)	Deng (LiSB)	Eco. (ZEBRA)	Weber (VRFB)	
DK												
L_{BESS}	8.04	6.81	4.63	7.13	5.63	3.31	5.63	4.81	1.63	8.31	20.00	yr
E_{miss}	11.85	11.44	11.31	11.78	11.77	11.75	11.77	11.33	12.80	11.40	13.93	MWh
E_{exc}	354.83	360.22	355.22	352.56	351.75	361.58	351.50	361.76	337.73	359.50	347.26	MWh
ES												
L_{BESS}	8.21	7.05	5.00	7.38	5.98	3.58	5.98	5.07	1.89	8.95	20.00	yr
E_{miss}	8.22	8.30	7.30	8.03	8.09	9.29	8.09	8.38	13.02	8.03	11.50	MWh
E_{exc}	11.00	11.06	12.59	11.31	11.18	9.47	11.18	10.99	19.28	11.20	7.52	MWh
FR												
L_{BESS}	7.79	6.57	4.48	6.85	5.35	3.11	5.35	4.48	1.60	8.13	20.00	yr

E_{miss}	9.28	9.43	8.30	9.22	9.12	11.67	9.12	9.12	10.48	9.29	11.35	MWh
E_{exc}	100.11	98.96	103.48	101.10	101.44	66.55	101.44	100.19	89.64	98.91	86.95	MWh
GR												
L_{BESS}	8.21	6.99	4.99	7.36	5.96	3.51	5.96	5.00	1.86	8.86	20.00	yr
E_{miss}	10.90	10.85	10.16	10.65	10.83	12.18	10.83	10.84	10.91	10.67	13.54	MWh
E_{exc}	33.58	33.56	36.24	34.00	33.75	30.97	33.75	33.50	32.94	33.93	26.74	MWh
HU												
L_{BESS}	8.02	6.79	4.79	7.12	5.72	3.31	5.72	4.79	1.72	8.52	20.00	yr
E_{miss}	4.02	3.89	3.64	4.00	3.92	3.98	3.92	3.85	4.11	3.98	4.90	MWh
E_{exc}	71.59	72.29	75.35	70.99	71.57	71.03	71.57	72.56	68.52	71.73	62.16	MWh
IT												
L_{BESS}	8.29	7.13	5.13	7.48	6.06	3.63	6.06	5.13	1.97	9.06	20.00	yr
E_{miss}	6.19	6.24	5.75	6.20	6.23	6.90	6.23	6.21	6.59	6.24	8.31	MWh
E_{exc}	12.92	12.62	13.64	12.80	12.70	11.54	12.70	12.58	12.04	12.73	9.60	MWh
PT												
L_{BESS}	8.02	6.79	7.14	4.77	5.69	3.29	5.69	4.79	1.71	8.52	20.00	yr
E_{miss}	4.86	4.81	4.91	4.45	4.89	5.17	4.89	4.81	5.44	4.84	6.30	MWh
E_{exc}	15.49	15.60	15.36	16.57	15.35	14.62	15.35	15.64	14.07	15.48	11.23	MWh
RO												
L_{BESS}	8.23	7.04	5.04	7.36	5.96	3.54	5.96	5.04	1.86	8.88	20.00	yr
E_{miss}	3.00	3.05	2.94	2.94	2.99	3.26	2.99	3.06	2.93	2.93	3.67	MWh
E_{exc}	33.06	33.04	34.15	33.63	33.40	31.92	33.40	32.99	33.84	33.58	29.86	MWh

2. Life Cycle Inventory

In this section, the full version of the SHSs life cycle inventory (LCI) is proposed for every installation site (Table S2 to Table S9).

Table S2: Complete Life Cycle Inventory of SHSs in Denmark.

Process	Bauer (LTO, SSLTO)	Bauer (NCA, SSNCA)	Ell (NCM, SSNCM)	M-B (LFP, SSLFP)	M-B (NCM, SSNCM)	Notter (LMO, SSLMO)	Zack (LFP, SSLFP)	Peters (SIB)	Deng (LiSB)	Eco. (ZEBRA)	Weber (VRFB)	Unit
Inputs												
market for photovoltaic slanted-roof installation, 3kWp, single-Si, panel, mounted, on roof – GLO (inverter considered separately)	10.68	10.68	10.68	10.68	10.68	10.68	10.68	10.68	10.68	10.68	10.68	items
market for cable, unspecified ǀ cable, unspecified ǀ - GLO	47.10	47.10	47.10	47.10	47.10	47.10	47.10	47.10	47.10	47.10	47.10	kg
market for tube insulation, elastomere - GLO	28.26	28.26	28.26	28.26	28.26	28.26	28.26	28.26	28.26	28.26	28.26	kg
market for inverter, 2.5kW - GLO	4.53	4.53	4.53	4.53	4.53	4.53	4.53	4.53	4.53	4.53	4.53	items
market for charger, electric passenger car - GLO	122.51	122.51	122.51	122.51	122.51	122.51	122.51	122.51	122.51	122.51	122.51	kg
BESS	57.65	68.02	100.03	64.97	82.27	139.92	82.27	96.30	267.21	55.75	19.51	kWh
VRFB stack	0.00	0.00	0.00	0.00	0.00	0.00	0.00	0.00	0.00	0.00	390.98	kg
VRFB periphery	0.00	0.00	0.00	0.00	0.00	0.00	0.00	0.00	0.00	0.00	200.17	kg

MDPI

market for electricity, low voltage (off-grid)		36.86	42.00	61.04	41.28	52.26	88.72	52.26	58.86	196.04	34.27	17.42	MWh
market for diesel, burned in diesel-electric generating set, 18.5kW – GLO (off-grid)		36.86	42.00	61.04	41.28	52.26	88.72	52.26	58.86	196.04	34.27	17.42	MWh
market for waste electric wiring - GLO		-4.71	-4.71	-4.71	-4.71	-4.71	-4.71	-4.71	-4.71	-4.71	-4.71	-4.71	kg
market for used cable - GLO		-42.39	-42.39	-42.39	-42.39	-42.39	-42.39	-42.39	-42.39	-42.39	-42.39	-42.39	kg
market for waste wire plastic - GLO		-28.26	-28.26	-28.26	-28.26	-28.26	-28.26	-28.26	-28.26	-28.26	-28.26	-28.26	kg
market for waste electric and electronic equipment - GLO		-122.51	-122.51	-122.51	-122.51	-122.51	-122.51	-122.51	-122.51	-122.51	-122.51	-122.51	kg
market for waste electric and electronic equipment - GLO		-49.48	-49.48	-49.48	-49.48	-49.48	-49.48	-49.48	-49.48	-49.48	-49.48	-49.48	kg
market for auxiliary heating unit, electric, 5kW– GLO		0.00	0.00	0.00	0.00	0.00	0.00	0.00	0.00	0.00	0.06	0.00	items
Outputs													
Electricity (RF)	**On-grid**	152.45	181.86	264.74	171.01	216.20	375.10	216.08	258.26	724.59	148.83	60.32	MWh
	Off-grid	42.08	49.66	73.02	47.43	60.06	102.14	60.06	70.30	207.25	40.70	16.91	MWh
Exhausted BESS, waste treatment		57.65	68.02	100.03	64.97	82.27	139.92	82.27	96.30	267.21	55.75	19.51	kWh
Exhausted VRFB stack, waste management		0.00	0.00	0.00	0.00	0.00	0.00	0.00	0.00	0.00	0.00	390.98	kg
Exhausted VRFB periphery, waste management		0.00	0.00	0.00	0.00	0.00	0.00	0.00	0.00	0.00	0.00	200.17	kg
Exhausted PV, waste treatment		137.41	137.41	137.41	137.41	137.41	137.41	137.41	137.41	137.41	137.41	137.41	kg
Market for cable, unspecified – GLO (Avoided Product)		42.39	42.39	42.39	42.39	42.39	42.39	42.39	42.39	42.39	42.39	42.39	kg

energies

MDPI

Table S3: Complete Life Cycle Inventory of SHSs in Spain.

Process	Bauer (LTO, SSLTO)	Bauer (NCA, SSNCA)	Ell (NCM, SSNCM)	M-B (LFP, SSLFP)	M-B (NCM, SSNCM)	Notter (LMO, SSLMO)	Zack (LFP, SSLFP)	Peters (SIB)	Deng (LiSB)	Eco. (ZEBRA)	Weber (VRFB)	Unit
Inputs												
market for photovoltaic slanted-roof installation, 3kWp, single-Si, panel, mounted, on roof – GLO (inverter considered separately)	1.44	1.44	1.44	1.44	1.44	1.44	1.44	1.44	1.44	1.44	1.44	items
market for cable, unspecified | cable, unspecified | - GLO	6.37	6.37	6.37	6.37	6.37	6.37	6.37	6.37	6.37	6.37	6.37	kg
market for tube insulation, elastomere - GLO	3.82	3.82	3.82	3.82	3.82	3.82	3.82	3.82	3.82	3.82	3.82	kg
market for inverter, 2.5kW - GLO	2.55	2.55	2.55	2.55	2.55	2.55	2.55	2.55	2.55	2.55	2.55	items
market for charger, electric passenger car - GLO	16.56	16.56	16.56	16.56	16.56	16.56	16.56	16.56	16.56	16.56	16.56	kg
BESS	46.93	54.66	77.03	52.21	64.41	107.64	64.41	76.05	192.27	43.04	16.22	kWh
VRFB stack	0.00	0.00	0.00	0.00	0.00	0.00	0.00	0.00	0.00	0.00	325.03	kg
VRFB periphery	0.00	0.00	0.00	0.00	0.00	0.00	0.00	0.00	0.00	0.00	166.41	kg
market for electricity, low voltage (on-grid)	25.04	29.43	36.51	27.21	33.81	64.91	33.81	41.35	172.62	22.44	14.37	MWh
market for diesel, burned in diesel-electric generating set, 18.5kW – GLO (off-grid)	25.04	29.43	36.51	27.21	33.81	64.91	33.81	41.35	172.62	22.44	14.37	MWh
market for waste electric wiring - GLO	-0.64	-0.64	-0.64	-0.64	-0.64	-0.64	-0.64	-0.64	-0.64	-0.64	-0.64	kg

market for used cable - GLO		-5.73	-5.73	-5.73	-5.73	-5.73	-5.73	-5.73	-5.73	-5.73	-5.73	-5.73	kg
market for waste wire plastic - GLO		-3.82	-3.82	-3.82	-3.82	-3.82	-3.82	-3.82	-3.82	-3.82	-3.82	-3.82	kg
market for waste electric and electronic equipment - GLO		-16.56	-16.56	-16.56	-16.56	-16.56	-16.56	-16.56	-16.56	-16.56	-16.56	-16.56	kg
market for waste electric and electronic equipment - GLO		-27.90	-27.90	-27.90	-27.90	-27.90	-27.90	-27.90	-27.90	-27.90	-27.90	-27.90	kg
market for auxiliary heating unit, electric, 5kW– GLO		0.00	0.00	0.00	0.00	0.00	0.00	0.00	0.00	0.00	0.04	0.00	items
Outputs													
Electricity (RF)	**On-grid**	37.61	43.83	62.53	41.95	51.69	85.19	51.69	60.94	174.69	34.55	15.00	MWh
	Off-grid	34.26	39.90	56.23	38.12	47.02	78.57	47.02	55.52	149.13	31.42	14.06	MWh
Exhausted BESS, waste treatment		46.93	54.66	77.03	52.21	64.41	107.64	64.41	76.05	192.27	43.04	16.22	kWh
Exhausted VRFB stack, waste management		0.00	0.00	0.00	0.00	0.00	0.00	0.00	0.00	0.00	0.00	325.03	kg
Exhausted VRFB periphery, waste management		0.00	0.00	0.00	0.00	0.00	0.00	0.00	0.00	0.00	0.00	166.41	kg
Exhausted PV, waste treatment		18.58	18.58	18.58	18.58	18.58	18.58	18.58	18.58	18.58	18.58	18.58	kg
Market for cable, unspecified – GLO (Avoided Product)		5.73	5.73	5.73	5.73	5.73	5.73	5.73	5.73	5.73	5.73	5.73	kg

energies

MDPI

Table S4: Complete Life Cycle Inventory of SHSs in France.

Process	Bauer (LTO, SSLTO)	Bauer (NCA, SSNCA)	Ell (NCM, SSNCM)	M-B (LFP, SSLFP)	M-B (NCM, SSNCM)	Notter (LMO, SSLMO)	Zack (LFP, SSLFP)	Peters (SIB)	Deng (LiSB)	Eco. (ZEBRA)	Weber (VRFB)	Unit
Inputs												
market for photovoltaic slanted-roof installation, 3kWp, single-Si, panel, mounted, on roof – GLO (inverter considered separately)	5.62	5.62	5.62	5.62	5.62	5.62	5.62	5.62	5.62	5.62	5.62	items
market for cable, unspecified ǀ cable, unspecified ǀ - GLO	24.79	24.79	24.79	24.79	24.79	24.79	24.79	24.79	24.79	24.79	24.79	kg
market for tube insulation, elastomere - GLO	14.88	14.88	14.88	14.88	14.88	14.88	14.88	14.88	14.88	14.88	14.88	kg
market for inverter, 2.5kW - GLO	17.44	17.44	17.44	17.44	17.44	17.44	17.44	17.44	17.44	17.44	17.44	items
market for charger, electric passenger car - GLO	64.49	64.49	64.49	64.49	64.49	64.49	64.49	64.49	64.49	64.49	64.49	kg
BESS	78.80	93.41	137.05	89.61	114.76	197.50	114.76	137.05	361.98	75.48	25.83	kWh
VRFB stack	0.00	0.00	0.00	0.00	0.00	0.00	0.00	0.00	0.00	0.00	517.69	kg
VRFB periphery	0.00	0.00	0.00	0.00	0.00	0.00	0.00	0.00	0.00	0.00	265.04	kg
market for electricity, low voltage (on-grid)	29.80	35.89	46.36	33.66	42.64	93.92	42.64	50.91	164.17	28.56	14.19	MWh

market for diesel, burned in diesel-electric generating set, 18.5kW – GLO (off-grid)		29.80	35.89	46.36	33.66	42.64	93.92	42.64	50.91	164.17	28.56	14.19	MWh
market for waste electric wiring - GLO		-2.48	-2.48	-2.48	-2.48	-2.48	-2.48	-2.48	-2.48	-2.48	-2.48	-2.48	kg
market for used cable - GLO		-22.31	-22.31	-22.31	-22.31	-22.31	-22.31	-22.31	-22.31	-22.31	-22.31	-22.31	kg
market for waste wire plastic - GLO		-14.88	-14.88	-14.88	-14.88	-14.88	-14.88	-14.88	-14.88	-14.88	-14.88	-14.88	kg
market for waste electric and electronic equipment - GLO		-64.49	-64.49	-64.49	-64.49	-64.49	-64.49	-64.49	-64.49	-64.49	-64.49	-64.49	kg
market for waste electric and electronic equipment - GLO		-190.55	-190.55	-190.55	-190.55	-190.55	-190.55	-190.55	-190.55	-190.55	-190.55	-190.55	kg
market for auxiliary heating unit, electric, 5kW– GLO		0.00	0.00	0.00	0.00	0.00	0.00	0.00	0.00	0.00	0.08	0.00	items
Outputs													
Electricity (RF)	**On-grid**	89.67	105.86	157.84	102.34	131.21	197.74	131.21	156.01	421.24	85.52	33.26	MWh
	Off-grid	57.52	68.19	100.05	65.42	83.77	144.18	83.77	100.05	280.76	55.10	22.39	MWh
Exhausted BESS, waste treatment		78.80	93.41	137.05	89.61	114.76	197.50	114.76	137.05	361.98	75.48	25.83	kWh
Exhausted VRFB stack, waste management		0.00	0.00	0.00	0.00	0.00	0.00	0.00	0.00	0.00	0.00	517.69	kg
Exhausted VRFB periphery, waste management		0.00	0.00	0.00	0.00	0.00	0.00	0.00	0.00	0.00	0.00	265.04	kg
Exhausted PV, waste treatment		72.33	72.33	72.33	72.33	72.33	72.33	72.33	72.33	72.33	72.33	72.33	kg
Market for cable, unspecified – GLO (Avoided Product)		22.31	22.31	22.31	22.31	22.31	22.31	22.31	22.31	22.31	22.31	22.31	kg

energies

MDPI

Table S5: Complete Life Cycle Inventory of SHSs in Greece.

Process	Bauer (LTO, SSLTO)	Bauer (NCA, SSNCA)	Ell (NCM, SSNCM)	M-B (LFP, SSLFP)	M-B (NCM, SSNCM)	Notter (LMO, SSLMO)	Zack (LFP, SSLFP)	Peters (SIB)	Deng (LiSB)	Eco. (ZEBRA)	Weber (VRFB)	Unit
Inputs												
market for photovoltaic slanted-roof installation, 3kWp, single-Si, panel, mounted, on roof – GLO (inverter considered separately)	2.17	2.17	2.17	2.17	2.17	2.17	2.17	2.17	2.17	2.17	2.17	items
market for cable, unspecified ǀ cable, unspecified ǀ - GLO	9.59	9.59	9.59	9.59	9.59	9.59	9.59	9.59	9.59	9.59	9.59	kg
market for tube insulation, elastomere - GLO	5.75	5.75	5.75	5.75	5.75	5.75	5.75	5.75	5.75	5.75	5.75	kg
market for inverter, 2.5kW - GLO	5.64	5.64	5.64	5.64	5.64	5.64	5.64	5.64	5.64	5.64	5.64	items
market for charger, electric passenger car - GLO	24.94	24.94	24.94	24.94	24.94	24.94	24.94	24.94	24.94	24.94	24.94	kg
BESS	58.02	68.13	95.44	64.67	79.94	135.74	79.94	95.22	240.41	53.73	20.05	kWh
VRFB stack	0.00	0.00	0.00	0.00	0.00	0.00	0.00	0.00	0.00	0.00	401.89	kg
VRFB periphery	0.00	0.00	0.00	0.00	0.00	0.00	0.00	0.00	0.00	0.00	205.76	kg
market for electricity, low voltage (on-grid)	33.20	38.82	50.87	36.17	45.46	86.76	45.46	54.16	146.22	30.09	16.92	MWh

market for diesel, burned in diesel-electric generating set, 18.5kW – GLO (off-grid)		33.20	38.82	50.87	36.17	45.46	86.76	45.46	54.16	146.22	30.09	16.92	MWh
market for waste electric wiring - GLO		-0.96	-0.96	-0.96	-0.96	-0.96	-0.96	-0.96	-0.96	-0.96	-0.96	-0.96	kg
market for used cable - GLO		-8.63	-8.63	-8.63	-8.63	-8.63	-8.63	-8.63	-8.63	-8.63	-8.63	-8.63	kg
market for waste wire plastic - GLO		-5.75	-5.75	-5.75	-5.75	-5.75	-5.75	-5.75	-5.75	-5.75	-5.75	-5.75	kg
market for waste electric and electronic equipment - GLO		-24.94	-24.94	-24.94	-24.94	-24.94	-24.94	-24.94	-24.94	-24.94	-24.94	-24.94	kg
market for waste electric and electronic equipment - GLO		-61.60	-61.60	-61.60	-61.60	-61.60	-61.60	-61.60	-61.60	-61.60	-61.60	-61.60	kg
market for auxiliary heating unit, electric, 5kW– GLO		0.00	0.00	0.00	0.00	0.00	0.00	0.00	0.00	0.00	0.05	0.00	items
Outputs													
Electricity (RF)	**On-grid**	52.58	61.74	87.83	58.75	72.52	121.15	72.52	86.25	230.63	48.79	20.73	MWh
	Off-grid	42.36	49.74	69.67	47.21	58.36	99.09	58.36	69.51	186.47	39.22	17.38	MWh
Exhausted BESS, waste treatment		58.02	68.13	95.44	64.67	79.94	135.74	79.94	95.22	240.41	53.73	20.05	kWh
Exhausted VRFB stack, waste management		0.00	0.00	0.00	0.00	0.00	0.00	0.00	0.00	0.00	0.00	401.89	kg
Exhausted VRFB periphery, waste management		0.00	0.00	0.00	0.00	0.00	0.00	0.00	0.00	0.00	0.00	205.76	kg
Exhausted PV, waste treatment		27.97	27.97	27.97	27.97	27.97	27.97	27.97	27.97	27.97	27.97	27.97	kg
Market for cable, unspecified – GLO (Avoided Product)		8.63	8.63	8.63	8.63	8.63	8.63	8.63	8.63	8.63	8.63	8.63	kg

Table S6: Complete Life Cycle Inventory of SHSs in Hungary.

Process	Bauer (LTO, SSLTO)	Bauer (NCA, SSNCA)	Ell (NCM, SSNCM)	M-B (LFP, SSLFP)	M-B (NCM, SSNCM)	Notter (LMO, SSLMO)	Zack (LFP, SSLFP)	Peters (SIB)	Deng (LiSB)	Eco. (ZEBRA)	Weber (VRFB)	Unit
Inputs												
market for photovoltaic slanted-roof installation, 3kWp, single-Si, panel, mounted, on roof – GLO (inverter considered separately)	2.74	2.74	2.74	2.74	2.74	2.74	2.74	2.74	2.74	2.74	2.74	items
market for cable, unspecified ǀ cable, unspecified ǀ - GLO	12.09	12.09	12.09	12.09	12.09	12.09	12.09	12.09	12.09	12.09	12.09	kg
market for tube insulation, elastomere - GLO	7.25	7.25	7.25	7.25	7.25	7.25	7.25	7.25	7.25	7.25	7.25	kg
market for inverter, 2.5kW - GLO	2.21	2.21	2.21	2.21	2.21	2.21	2.21	2.21	2.21	2.21	2.21	items
market for charger, electric passenger car - GLO	31.44	31.44	31.44	31.44	31.44	31.44	31.44	31.44	31.44	31.44	31.44	kg
BESS	35.67	42.16	59.79	40.18	50.00	86.35	50.00	59.77	156.26	33.58	12.05	kWh
VRFB stack	0.00	0.00	0.00	0.00	0.00	0.00	0.00	0.00	0.00	0.00	241.50	kg
VRFB periphery	0.00	0.00	0.00	0.00	0.00	0.00	0.00	0.00	0.00	0.00	123.64	kg
market for electricity, low voltage (on-grid)	12.52	14.31	19.02	14.03	17.11	30.02	17.11	20.10	59.63	11.68	6.12	MWh

market for diesel, burned in diesel-electric generating set, 18.5kW – GLO (off-grid)		12.52	14.31	19.02	14.03	17.11	30.02	17.11	20.10	59.63	11.68	6.12	MWh
market for waste electric wiring - GLO		-1.21	-1.21	-1.21	-1.21	-1.21	-1.21	-1.21	-1.21	-1.21	-1.21	-1.21	kg
market for used cable - GLO		-10.88	-10.88	-10.88	-10.88	-10.88	-10.88	-10.88	-10.88	-10.88	-10.88	-10.88	kg
market for waste wire plastic - GLO		-7.25	-7.25	-7.25	-7.25	-7.25	-7.25	-7.25	-7.25	-7.25	-7.25	-7.25	kg
market for waste electric and electronic equipment - GLO		-31.44	-31.44	-31.44	-31.44	-31.44	-31.44	-31.44	-31.44	-31.44	-31.44	-31.44	kg
market for waste electric and electronic equipment - GLO		-24.13	-24.13	-24.13	-24.13	-24.13	-24.13	-24.13	-24.13	-24.13	-24.13	-24.13	kg
market for auxiliary heating unit, electric, 5kW– GLO		0.00	0.00	0.00	0.00	0.00	0.00	0.00	0.00	0.00	0.03	0.00	items
Outputs													
Electricity (RF)	**On-grid**	48.34	57.40	83.00	54.25	67.76	116.61	67.76	81.52	220.57	45.55	18.22	MWh
	Off-grid	26.04	30.78	43.65	29.33	36.50	63.04	36.50	43.63	121.20	24.51	10.45	MWh
Exhausted BESS, waste treatment		35.67	42.16	59.79	40.18	50.00	86.35	50.00	59.77	156.26	33.58	12.05	kWh
Exhausted VRFB stack, waste management		0.00	0.00	0.00	0.00	0.00	0.00	0.00	0.00	0.00	0.00	241.50	kg
Exhausted VRFB periphery, waste management		0.00	0.00	0.00	0.00	0.00	0.00	0.00	0.00	0.00	0.00	123.64	kg
Exhausted PV, waste treatment		35.26	35.26	35.26	35.26	35.26	35.26	35.26	35.26	35.26	35.26	35.26	kg
Market for cable, unspecified – GLO (Avoided Product)		10.88	10.88	10.88	10.88	10.88	10.88	10.88	10.88	10.88	10.88	10.88	kg

energies

MDPI

Table S7: Complete Life Cycle Inventory of SHSs in Italy.

Process	Bauer (LTO, SSLTO)	Bauer (NCA, SSNCA)	Ell (NCM, SSNCM)	M-B (LFP, SSLFP)	M-B (NCM, SSNCM)	Notter (LMO, SSLMO)	Zack (LFP, SSLFP)	Peters (SIB)	Deng (LiSB)	Eco. (ZEBRA)	Weber (VRFB)	Unit
Inputs												
market for photovoltaic slanted-roof installation, 3kWp, single-Si, panel, mounted, on roof – GLO (inverter considered separately)	1.27	1.27	1.27	1.27	1.27	1.27	1.27	1.27	1.27	1.27	1.27	items
market for cable, unspecified | cable, unspecified | - GLO	5.62	5.62	5.62	5.62	5.62	5.62	5.62	5.62	5.62	5.62	5.62	kg
market for tube insulation, elastomere - GLO	3.37	3.37	3.37	3.37	3.37	3.37	3.37	3.37	3.37	3.37	3.37	kg
market for inverter, 2.5kW - GLO	3.56	3.56	3.56	3.56	3.56	3.56	3.56	3.56	3.56	3.56	3.56	items
market for charger, electric passenger car - GLO	14.61	14.61	14.61	14.61	14.61	14.61	14.61	14.61	14.61	14.61	14.61	kg
BESS	32.86	38.19	53.09	36.42	44.96	75.03	44.96	53.09	130.31	30.07	11.46	kWh
VRFB stack	0.00	0.00	0.00	0.00	0.00	0.00	0.00	0.00	0.00	0.00	229.73	kg
VRFB periphery	0.00	0.00	0.00	0.00	0.00	0.00	0.00	0.00	0.00	0.00	117.61	kg
market for electricity, low voltage (on-grid)	18.68	21.90	28.01	20.74	25.71	47.55	25.71	30.25	83.81	17.23	10.39	MWh

market for diesel, burned in diesel-electric generating set, 18.5kW – GLO (off-grid)		18.68	21.90	28.01	20.74	25.71	47.55	25.71	30.25	83.81	17.23	10.39	MWh
market for waste electric wiring - GLO		-0.56	-0.56	-0.56	-0.56	-0.56	-0.56	-0.56	-0.56	-0.56	-0.56	-0.56	kg
market for used cable - GLO		-5.06	-5.06	-5.06	-5.06	-5.06	-5.06	-5.06	-5.06	-5.06	-5.06	-5.06	kg
market for waste wire plastic - GLO		-3.37	-3.37	-3.37	-3.37	-3.37	-3.37	-3.37	-3.37	-3.37	-3.37	-3.37	kg
market for waste electric and electronic equipment - GLO		-14.61	-14.61	-14.61	-14.61	-14.61	-14.61	-14.61	-14.61	-14.61	-14.61	-14.61	kg
market for waste electric and electronic equipment - GLO		-38.91	-38.91	-38.91	-38.91	-38.91	-38.91	-38.91	-38.91	-38.91	-38.91	-38.91	kg
market for auxiliary heating unit, electric, 5kW– GLO		0.00	0.00	0.00	0.00	0.00	0.00	0.00	0.00	0.00	0.03	0.00	items
Outputs													
Electricity (RF)	**On-grid**	27.88	32.31	45.41	30.87	38.06	62.73	38.06	44.89	116.38	25.46	11.14	MWh
	Off-grid	23.99	27.88	38.75	26.59	32.82	54.77	32.82	38.75	101.07	21.95	9.94	MWh
Exhausted BESS, waste treatment		32.86	38.19	53.09	36.42	44.96	75.03	44.96	53.09	130.31	30.07	11.46	kWh
Exhausted VRFB stack, waste management		0.00	0.00	0.00	0.00	0.00	0.00	0.00	0.00	0.00	0.00	229.73	kg
Exhausted VRFB periphery, waste management		0.00	0.00	0.00	0.00	0.00	0.00	0.00	0.00	0.00	0.00	117.61	kg
Exhausted PV, waste treatment		16.39	16.39	16.39	16.39	16.39	16.39	16.39	16.39	16.39	16.39	16.39	kg
Market for cable, unspecified – GLO (Avoided Product)		5.06	5.06	5.06	5.06	5.06	5.06	5.06	5.06	5.06	5.06	5.06	kg

Table S8: Complete Life Cycle Inventory of SHSs in Portugal.

Process	Bauer (LTO, SSLTO)	Bauer (NCA, SSNCA)	Ell (NCM, SSNCM)	M-B (LFP, SSLFP)	M-B (NCM, SSNCM)	Notter (LMO, SSLMO)	Zack (LFP, SSLFP)	Peters (SIB)	Deng (LiSB)	Eco. (ZEBRA)	Weber (VRFB)	Unit
Inputs												
market for photovoltaic slanted-roof installation, 3kWp, single-Si, panel, mounted, on roof – GLO (inverter considered separately)	1.42	1.42	1.42	1.42	1.42	1.42	1.42	1.42	1.42	1.42	1.42	items
market for cable, unspecified | cable, unspecified | - GLO	6.28	6.28	6.28	6.28	6.28	6.28	6.28	6.28	6.28	6.28	6.28	kg
market for tube insulation, elastomere - GLO	3.77	3.77	3.77	3.77	3.77	3.77	3.77	3.77	3.77	3.77	3.77	kg
market for inverter, 2.5kW - GLO	4.44	4.44	4.44	4.44	4.44	4.44	4.44	4.44	4.44	4.44	4.44	items
market for charger, electric passenger car - GLO	16.33	16.33	16.33	16.33	16.33	16.33	16.33	16.33	16.33	16.33	16.33	kg
BESS	40.53	47.89	45.51	68.13	57.10	98.84	57.10	67.93	178.62	38.15	13.69	kWh
VRFB stack	0.00	0.00	0.00	0.00	0.00	0.00	0.00	0.00	0.00	0.00	274.33	kg
VRFB periphery	0.00	0.00	0.00	0.00	0.00	0.00	0.00	0.00	0.00	0.00	140.45	kg
market for electricity, low voltage (on-grid)	15.15	17.71	17.19	23.29	21.47	39.32	21.47	25.12	79.43	14.21	7.88	MWh

market for diesel, burned in diesel-electric generating set, 18.5kW – GLO (off-grid)		15.15	17.71	17.19	23.29	21.47	39.32	21.47	25.12	79.43	14.21	7.88	MWh
market for waste electric wiring - GLO		-0.63	-0.63	-0.63	-0.63	-0.63	-0.63	-0.63	-0.63	-0.63	-0.63	-0.63	kg
market for used cable - GLO		-5.65	-5.65	-5.65	-5.65	-5.65	-5.65	-5.65	-5.65	-5.65	-5.65	-5.65	kg
market for waste wire plastic - GLO		-3.77	-3.77	-3.77	-3.77	-3.77	-3.77	-3.77	-3.77	-3.77	-3.77	-3.77	kg
market for waste electric and electronic equipment - GLO		-16.33	-16.33	-16.33	-16.33	-16.33	-16.33	-16.33	-16.33	-16.33	-16.33	-16.33	kg
market for waste electric and electronic equipment - GLO		-48.45	-48.45	-48.45	-48.45	-48.45	-48.45	-48.45	-48.45	-48.45	-48.45	-48.45	kg
market for auxiliary heating unit, electric, 5kW– GLO		0.00	0.00	0.00	0.00	0.00	0.00	0.00	0.00	0.00	0.04	0.00	items
Outputs													
Electricity (RF)	**On-grid**	34.41	40.70	38.59	58.42	48.42	83.26	48.42	57.75	159.07	32.39	13.27	MWh
	Off-grid	29.58	34.96	33.22	49.73	41.68	72.15	41.68	49.59	138.54	27.85	11.87	MWh
Exhausted BESS, waste treatment		40.53	47.89	45.51	68.13	57.10	98.84	57.10	67.93	178.62	38.15	13.69	kWh
Exhausted VRFB stack, waste management		0.00	0.00	0.00	0.00	0.00	0.00	0.00	0.00	0.00	0.00	274.33	kg
Exhausted VRFB periphery, waste management		0.00	0.00	0.00	0.00	0.00	0.00	0.00	0.00	0.00	0.00	140.45	kg
Exhausted PV, waste treatment		18.32	18.32	18.32	18.32	18.32	18.32	18.32	18.32	18.32	18.32	18.32	kg
Market for cable, unspecified – GLO (Avoided Product)		5.65	5.65	5.65	5.65	5.65	5.65	5.65	5.65	5.65	5.65	5.65	kg

energies

MDPI

Table S9: Complete Life Cycle Inventory of SHSs in Romania.

Process	Bauer (LTO, SSLTO)	Bauer (NCA, SSNCA)	Ell (NCM, SSNCM)	M-B (LFP, SSLFP)	M-B (NCM, SSNCM)	Notter (LMO, SSLMO)	Zack (LFP, SSLFP)	Peters (SIB)	Deng (LiSB)	Eco. (ZEBRA)	Weber (VRFB)	Unit
Inputs												
market for photovoltaic slanted-roof installation, 3kWp, single-Si, panel, mounted, on roof – GLO (inverter considered separately)	1.34	1.34	1.34	1.34	1.34	1.34	1.34	1.34	1.34	1.34	1.34	items
market for cable, unspecified ǀ cable, unspecified ǀ - GLO	5.90	5.90	5.90	5.90	5.90	5.90	5.90	5.90	5.90	5.90	5.90	kg
market for tube insulation, elastomere - GLO	3.54	3.54	3.54	3.54	3.54	3.54	3.54	3.54	3.54	3.54	3.54	kg
market for inverter, 2.5kW - GLO	1.56	1.56	1.56	1.56	1.56	1.56	1.56	1.56	1.56	1.56	1.56	items
market for charger, electric passenger car - GLO	15.34	15.34	15.34	15.34	15.34	15.34	15.34	15.34	15.34	15.34	15.34	kg
BESS	19.07	22.27	31.10	21.30	26.33	44.27	26.33	31.10	70.93	17.67	7.38	kWh
VRFB stack	0.00	0.00	0.00	0.00	0.00	0.00	0.00	0.00	0.00	0.00	147.92	kg
VRFB periphery	0.00	0.00	0.00	0.00	0.00	0.00	0.00	0.00	0.00	0.00	75.73	kg
market for electricity, low voltage (on-grid)	9.12	10.82	14.58	9.99	12.55	22.97	12.55	15.18	39.36	8.26	4.58	MWh

market for diesel, burned in diesel-electric generating set, 18.5kW – GLO (off-grid)		9.12	10.82	14.58	9.99	12.55	22.97	12.55	15.18	39.36	8.26	4.58	MWh
market for waste electric wiring - GLO		-0.59	-0.59	-0.59	-0.59	-0.59	-0.59	-0.59	-0.59	-0.59	-0.59	-0.59	kg
market for used cable - GLO		-5.31	-5.31	-5.31	-5.31	-5.31	-5.31	-5.31	-5.31	-5.31	-5.31	-5.31	kg
market for waste wire plastic - GLO		-3.54	-3.54	-3.54	-3.54	-3.54	-3.54	-3.54	-3.54	-3.54	-3.54	-3.54	kg
market for waste electric and electronic equipment - GLO		-15.34	-15.34	-15.34	-15.34	-15.34	-15.34	-15.34	-15.34	-15.34	-15.34	-15.34	kg
market for waste electric and electronic equipment - GLO		-17.02	-17.02	-17.02	-17.02	-17.02	-17.02	-17.02	-17.02	-17.02	-17.02	-17.02	kg
market for auxiliary heating unit, electric, 5kW– GLO		0.00	0.00	0.00	0.00	0.00	0.00	0.00	0.00	0.00	0.02	0.00	items
Outputs													
Electricity (RF)	**On-grid**	23.97	27.99	39.63	26.97	33.23	54.84	33.23	39.06	106.92	22.35	9.46	MWh
	Off-grid	13.92	16.26	22.70	15.55	19.22	32.32	19.22	22.70	61.49	12.90	5.73	MWh
Exhausted BESS, waste treatment		19.07	22.27	31.10	21.30	26.33	44.27	26.33	31.10	70.93	17.67	7.38	kWh
Exhausted VRFB stack, waste management		0.00	0.00	0.00	0.00	0.00	0.00	0.00	0.00	0.00	0.00	147.92	kg
Exhausted VRFB periphery, waste management		0.00	0.00	0.00	0.00	0.00	0.00	0.00	0.00	0.00	0.00	75.73	kg
Exhausted PV, waste treatment		17.20	17.20	17.20	17.20	17.20	17.20	17.20	17.20	17.20	17.20	17.20	kg
Market for cable, unspecified – GLO (Avoided Product)		5.31	5.31	5.31	5.31	5.31	5.31	5.31	5.31	5.31	5.31	5.31	kg

3. Life Cycle Impact Assessment

In this section, the results concerning the midpoint environmental impact indicators are collected and illustrated with histograms for all the batteries and installation sites (excluding IT that is available in the main manuscript). Particularly, three impact categories have been considered because they represent the highest contribution to the overall SHS eco-profile: Climate Change, Human Toxicity, Fossil Depletion. These results have been collected from Figure S1 to Figure S21.

Figure S1: Climate change SHSs environmental impact indicator in Denmark.

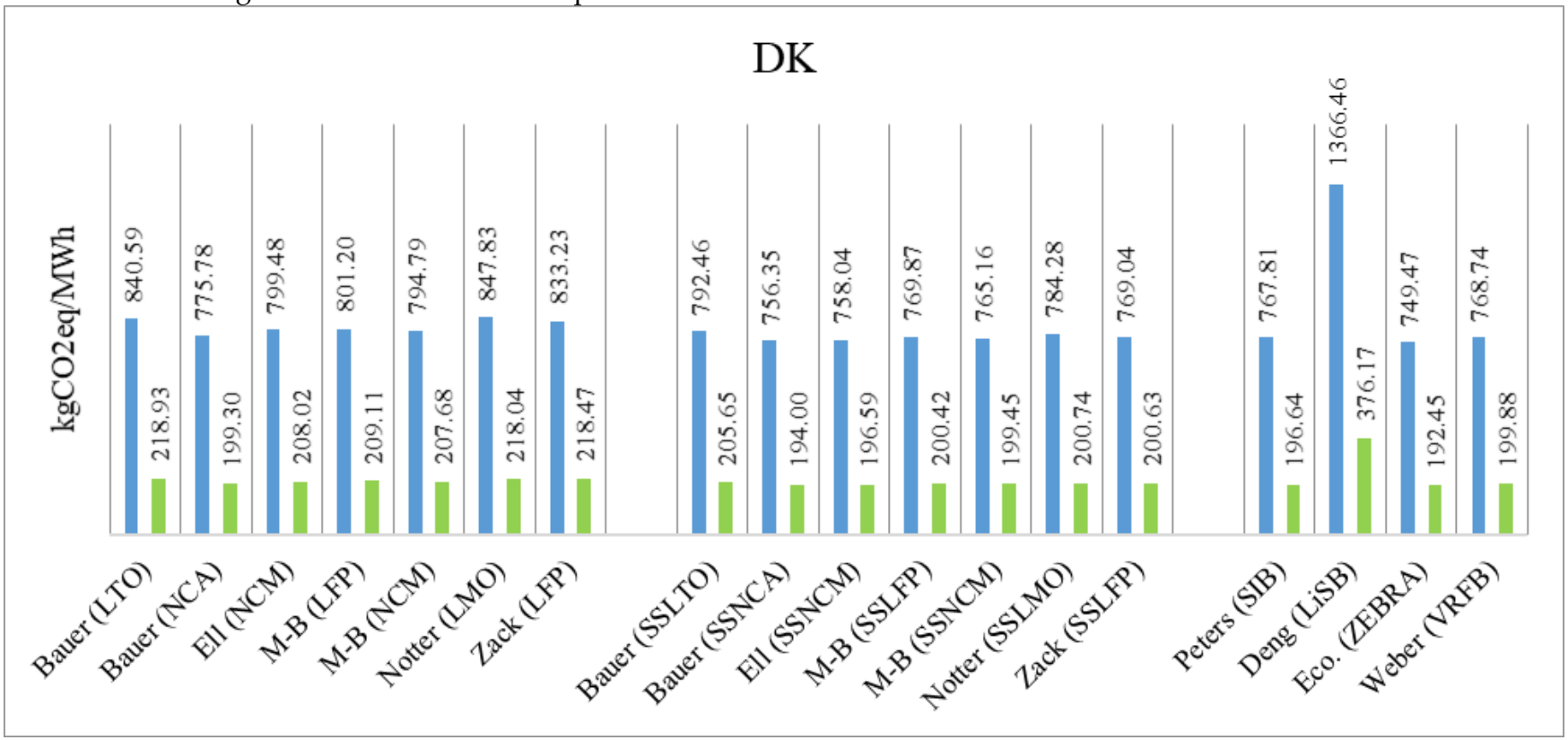

MDPI

Figure S2: Climate change SHSs environmental impact indicator in Spain.

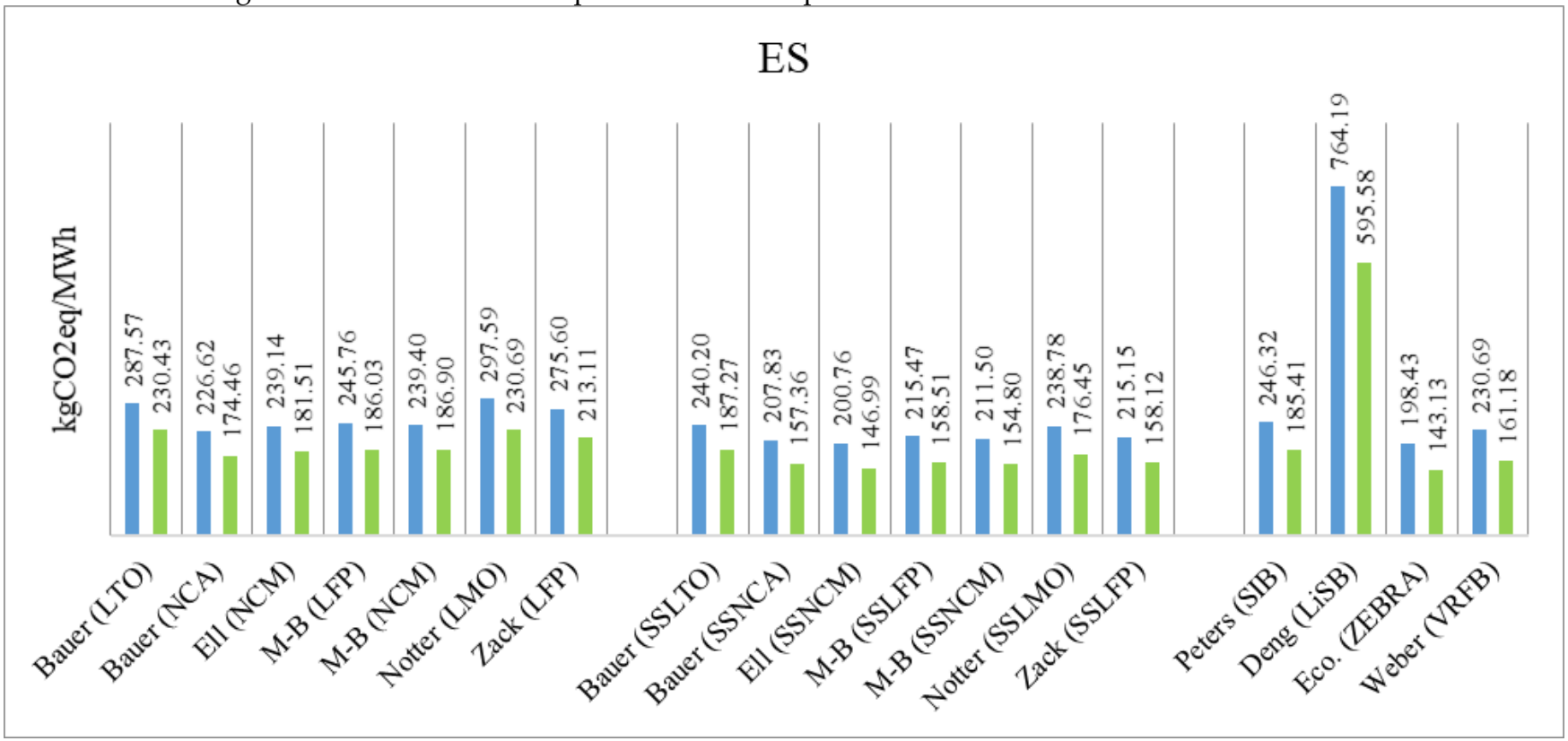

Figure S3: Climate change SHSs environmental impact indicator in France.

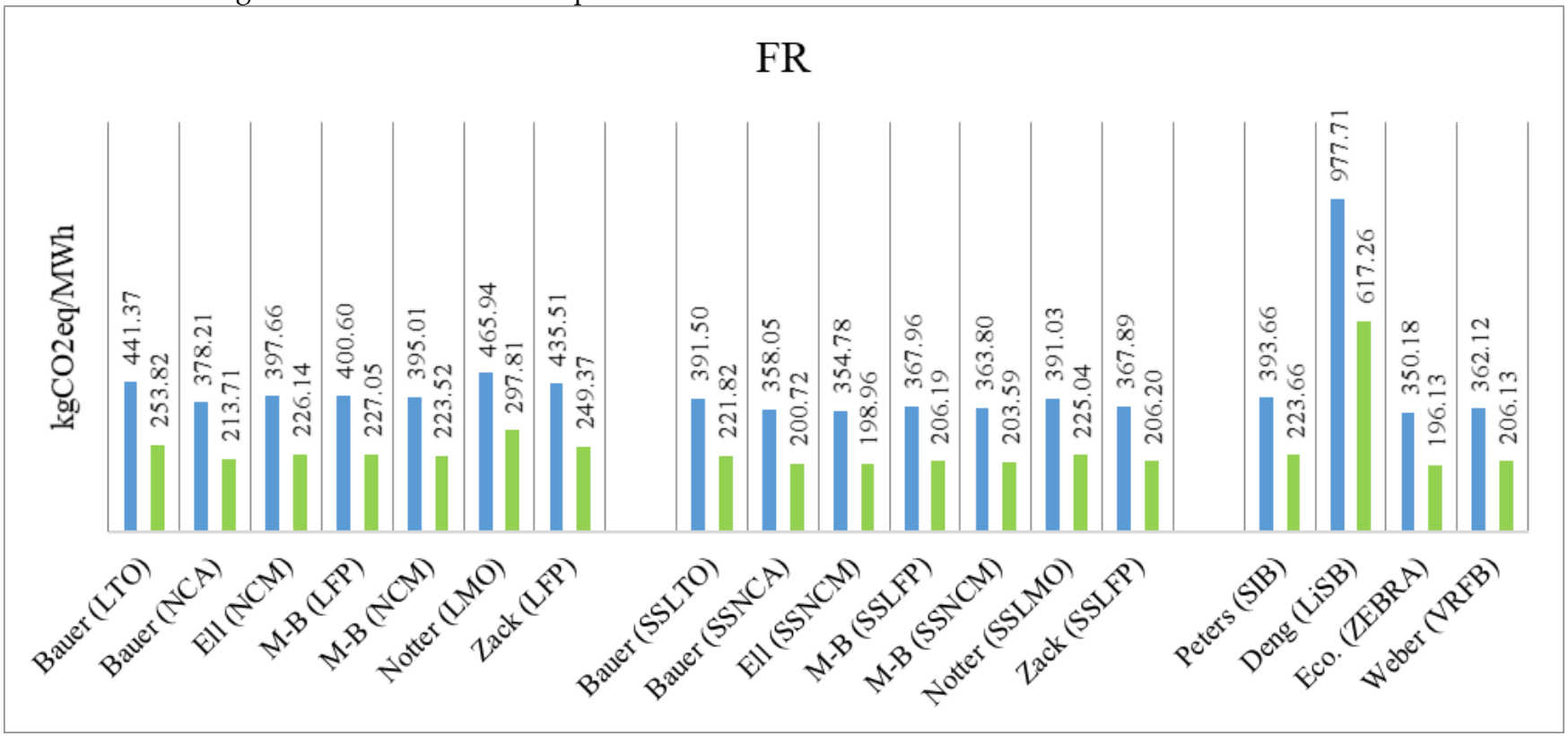

Figure S4: Climate change SHSs environmental impact indicator in Greece.

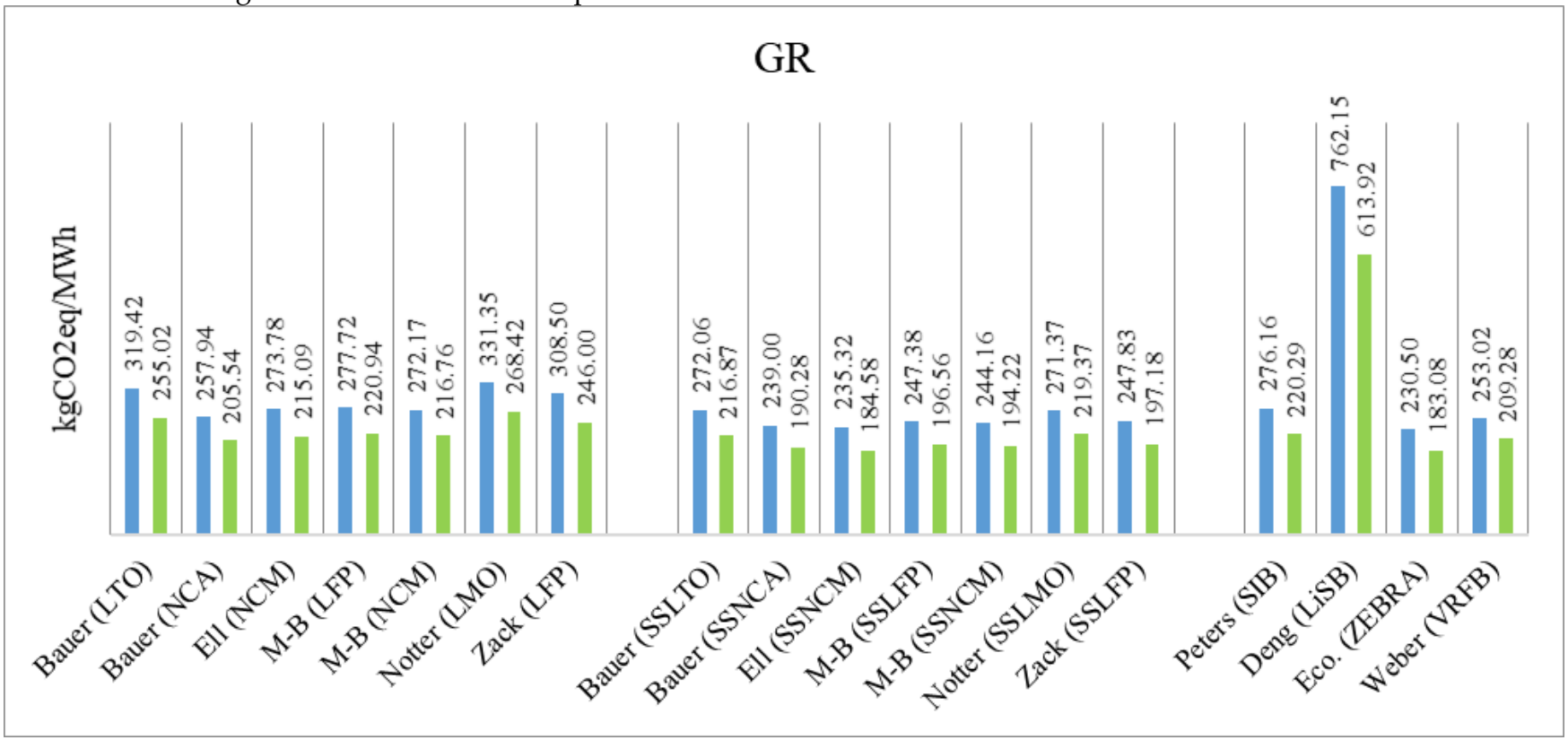

Figure S5: Climate change SHSs environmental impact indicator in Hungary.

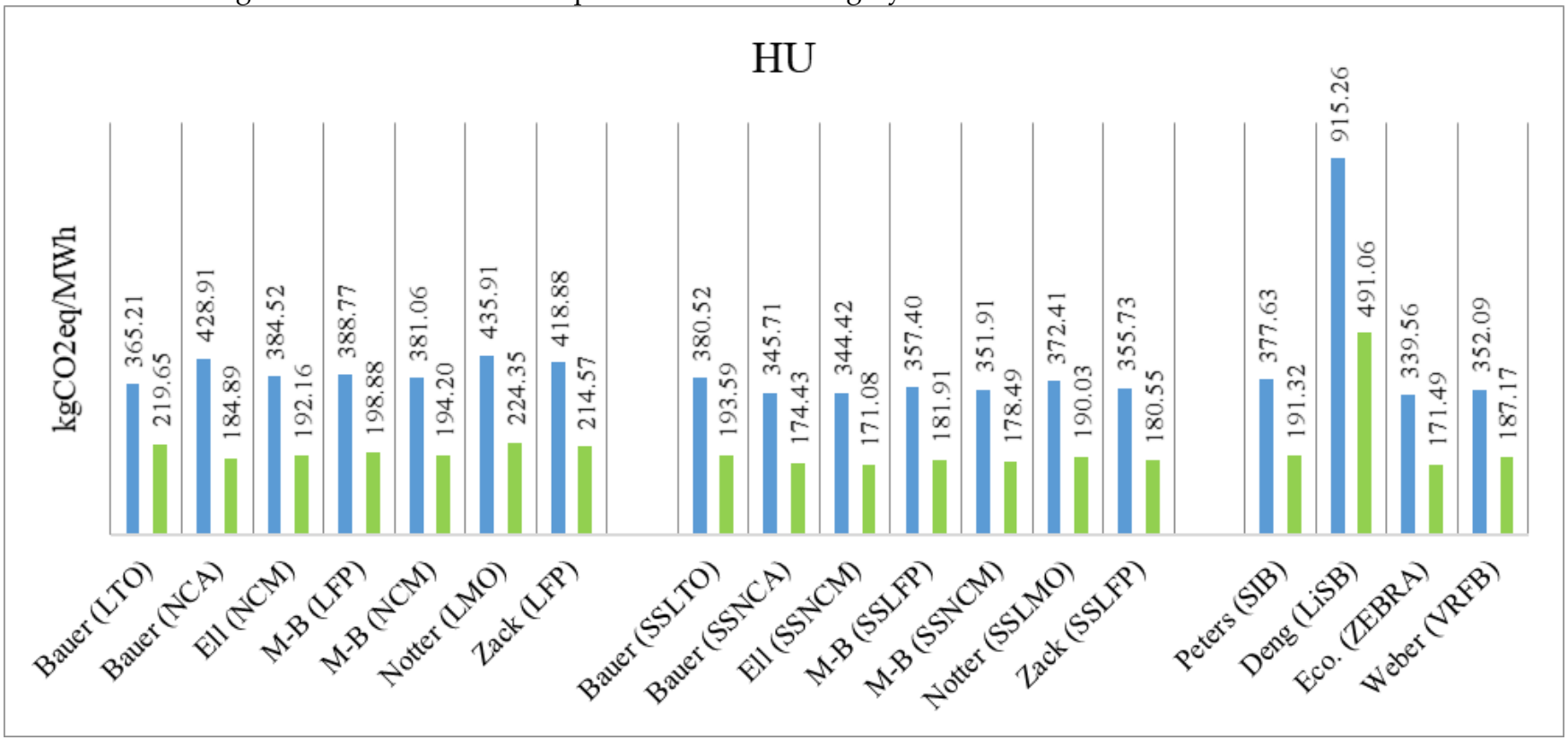

Figure S6: Climate change SHSs environmental impact indicator in Portugal.

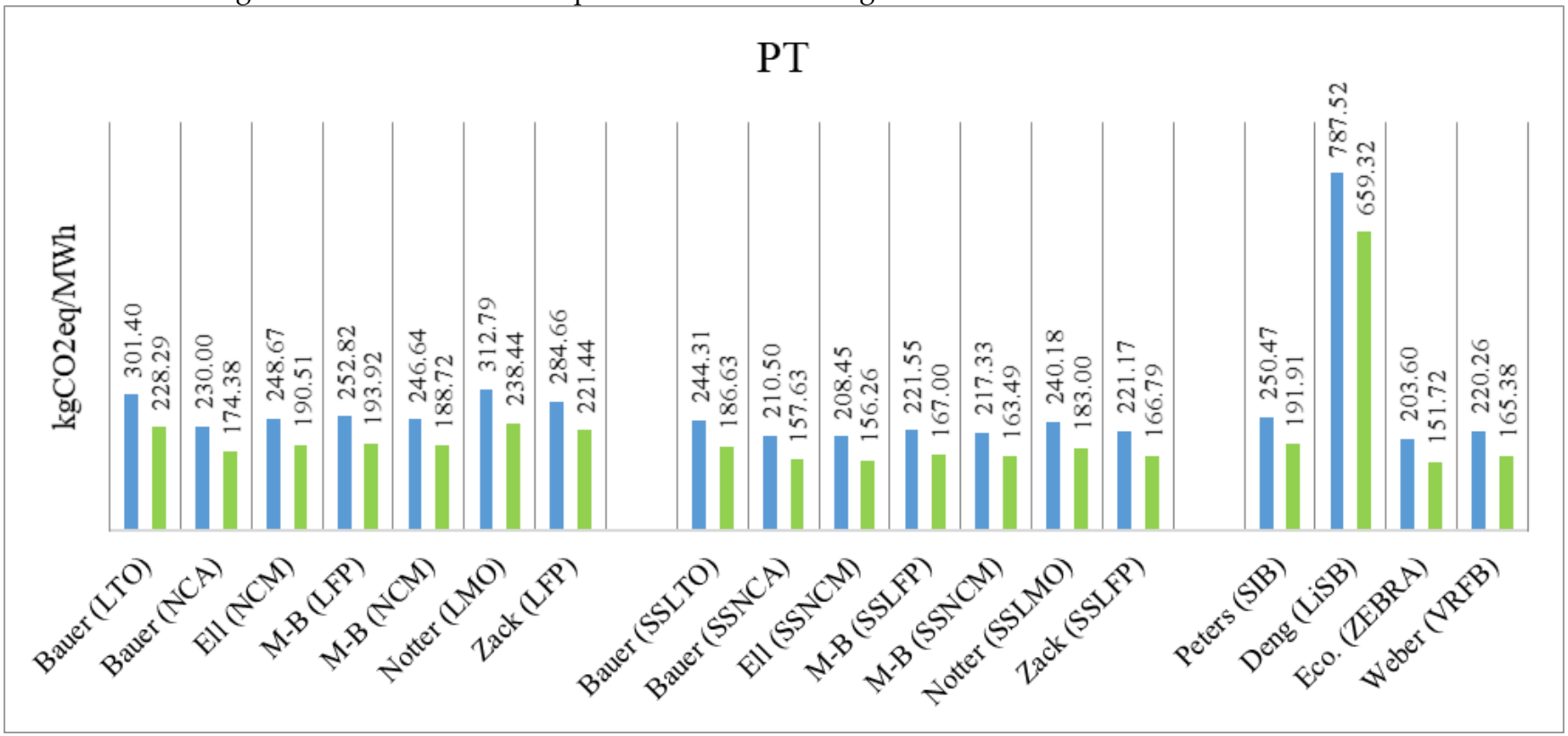

Figure S7: Climate change SHSs environmental impact indicator in Romania.

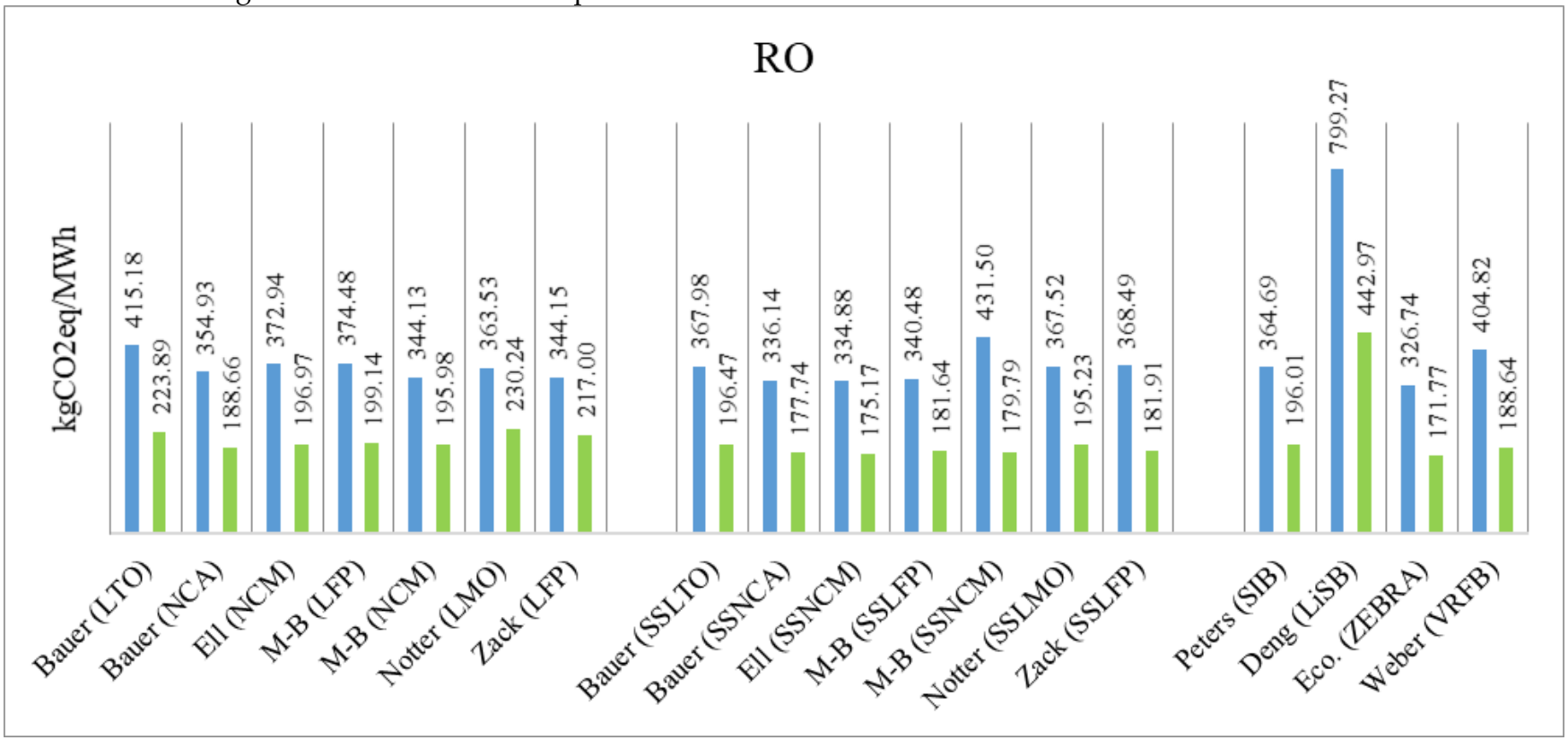

Figure S8: Human Toxicity SHSs environmental impact indicator in Denmark.

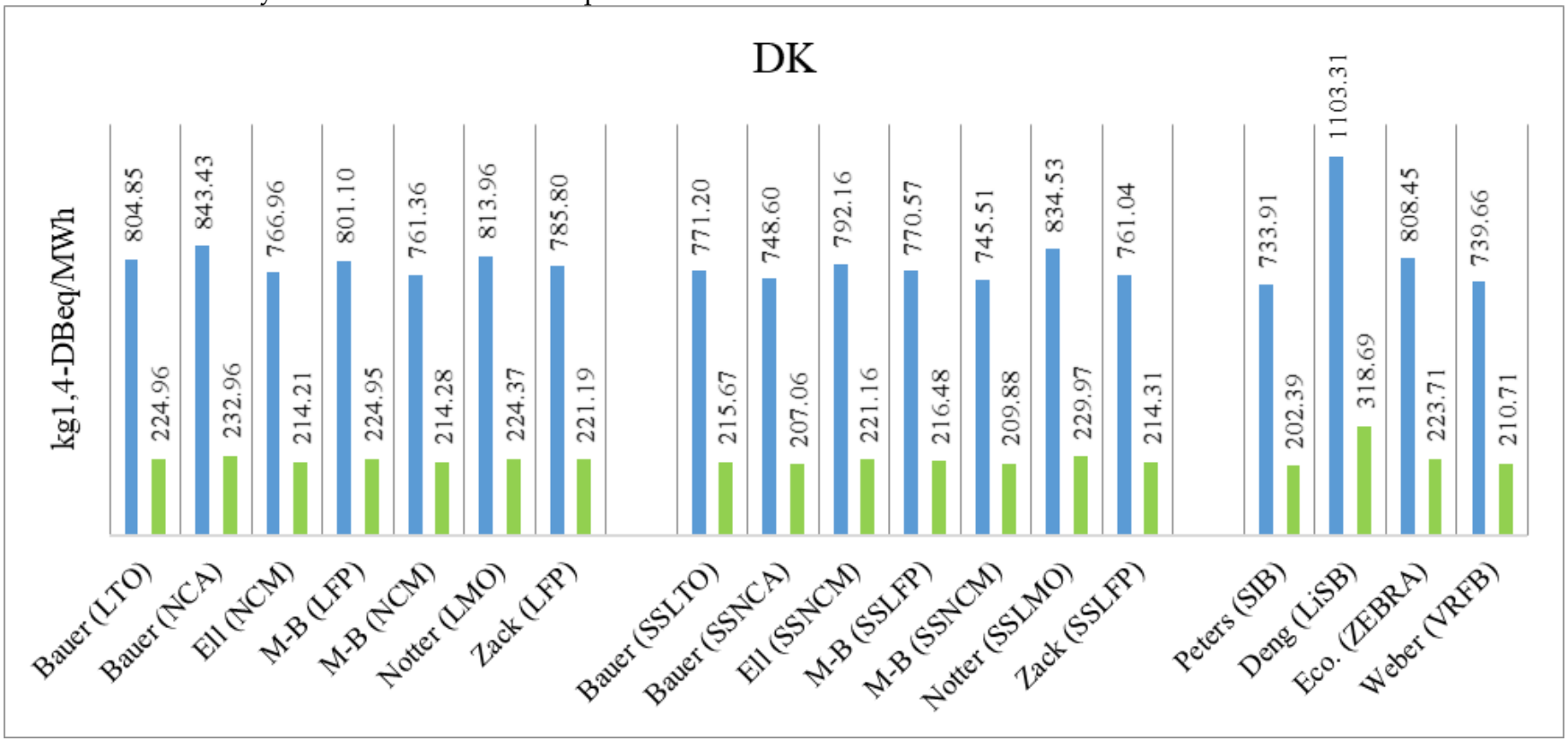

Figure S9: Human Toxicity SHSs environmental impact indicator in Spain.

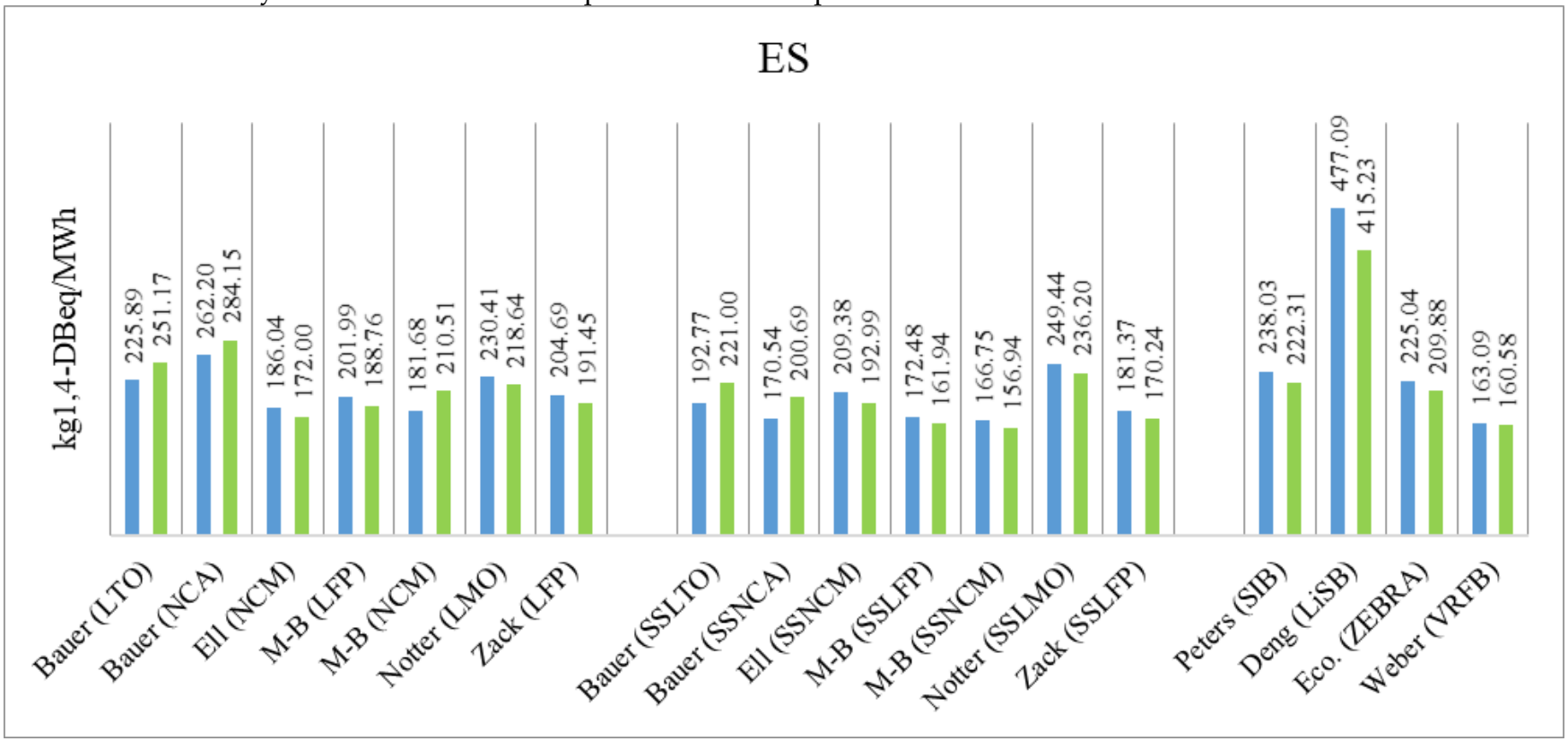

Figure S10: Human Toxicity SHSs environmental impact indicator in France.

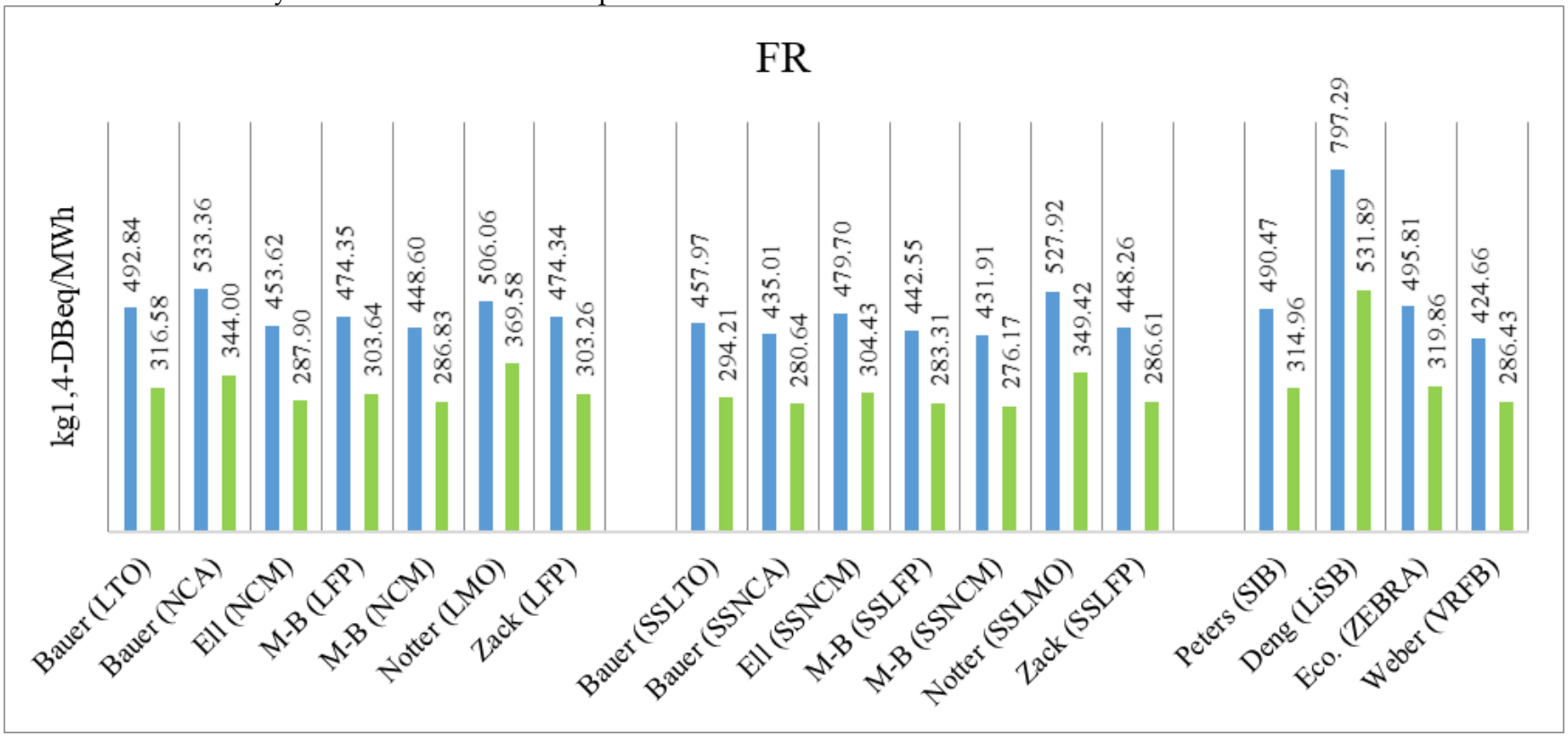

Figure S11: Human Toxicity SHSs environmental impact indicator in Greece.

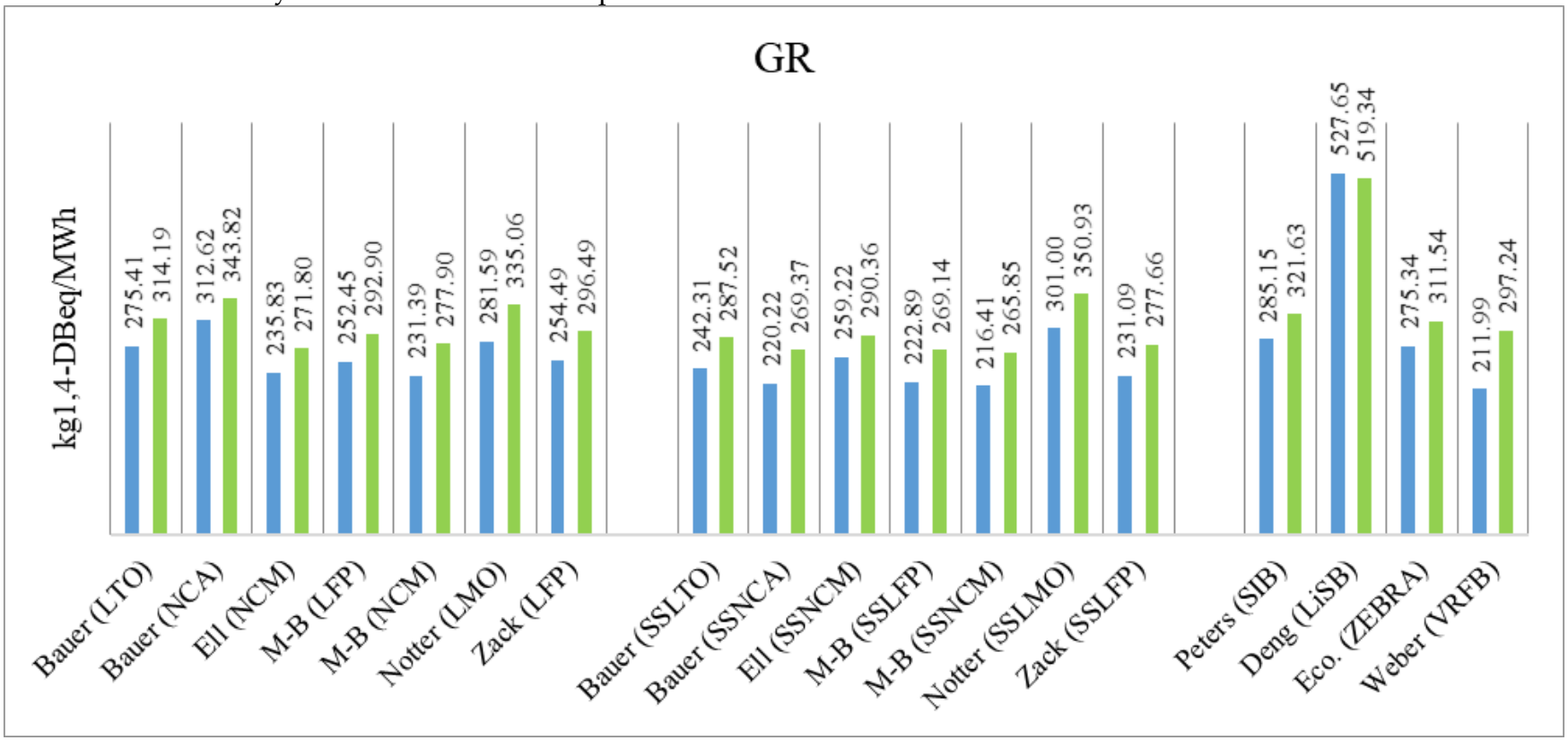

Figure S12: Human Toxicity SHSs environmental impact indicator in Hungary.

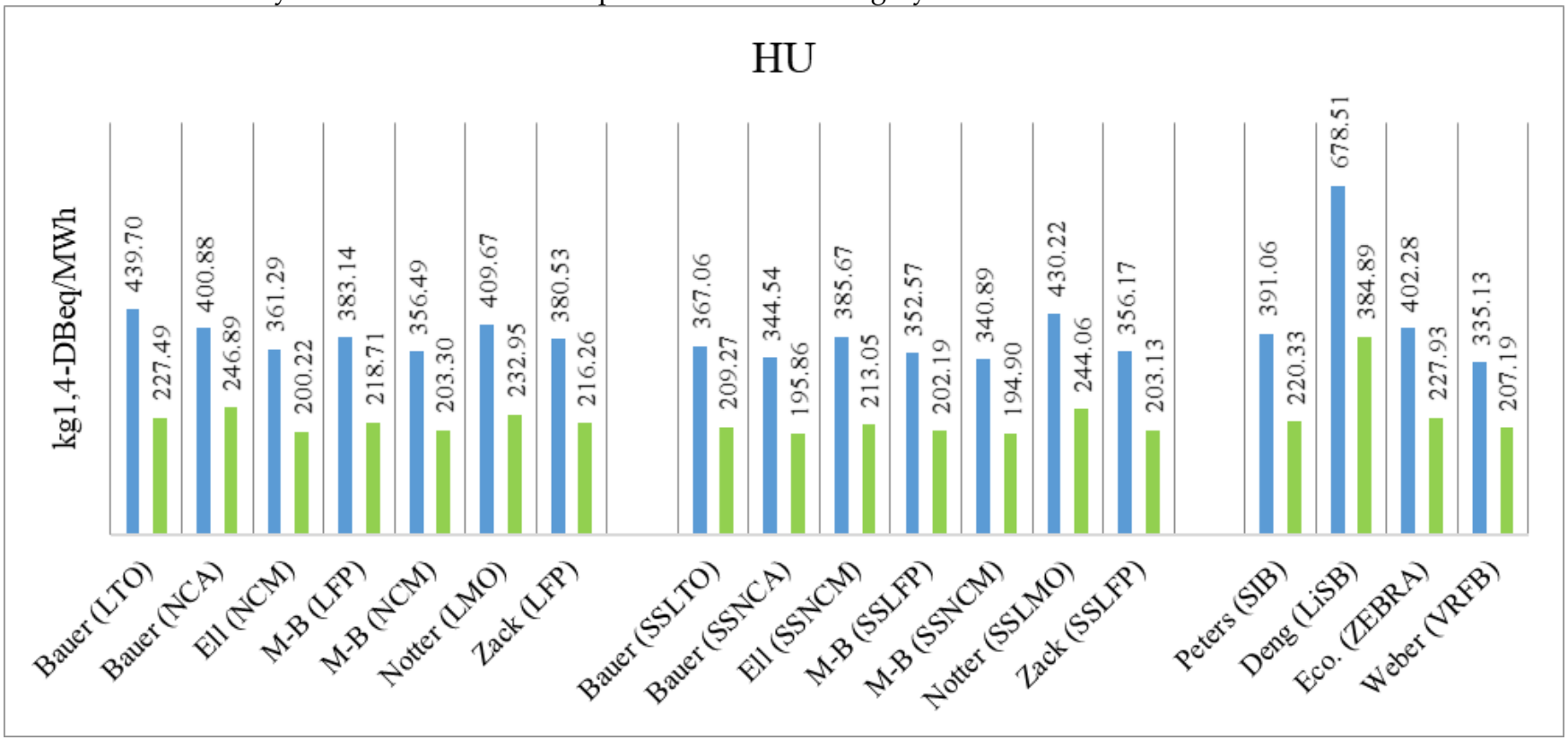

Figure S13: Human Toxicity SHSs environmental impact indicator in Portugal.

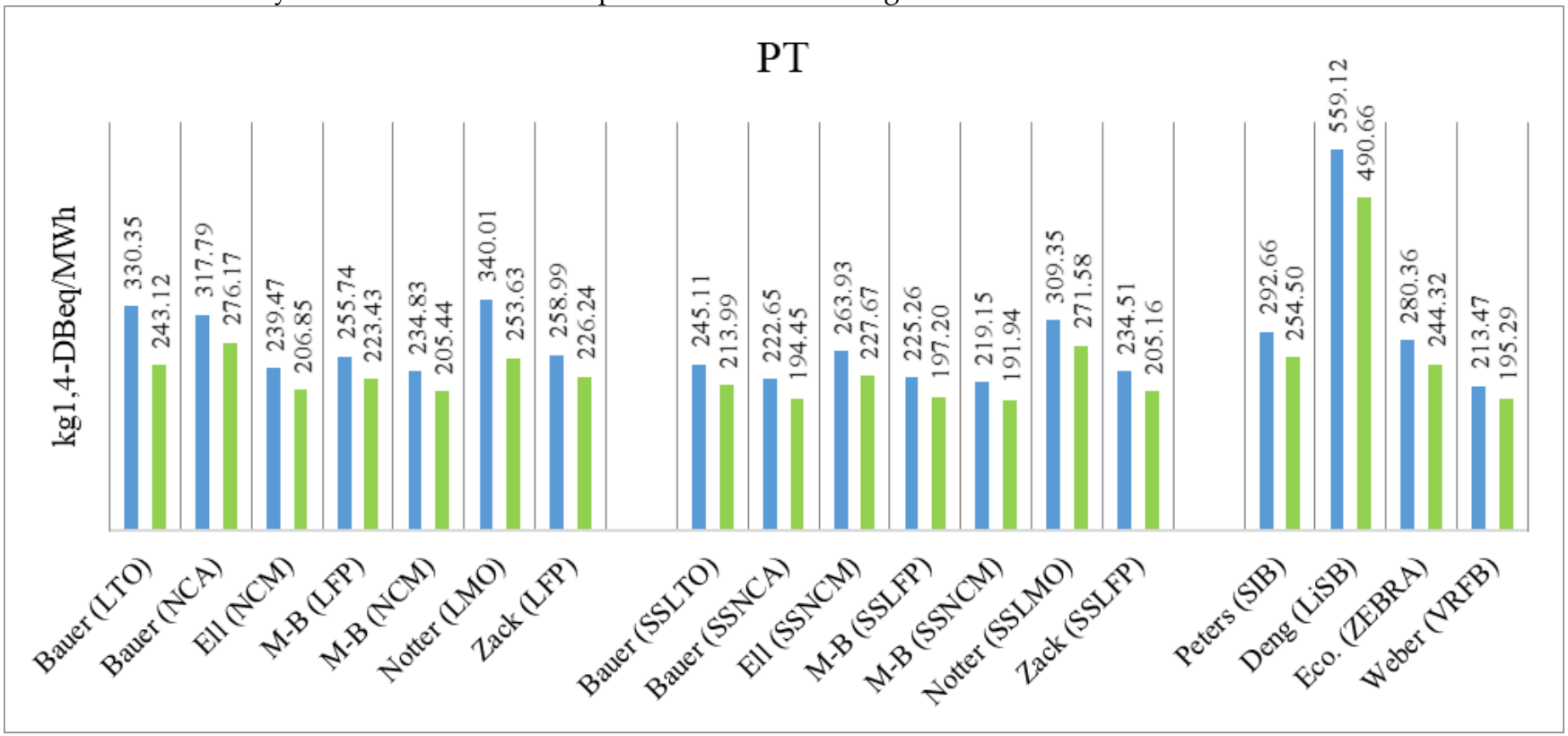

Figure S14: Human Toxicity SHSs environmental impact indicator in Romania.

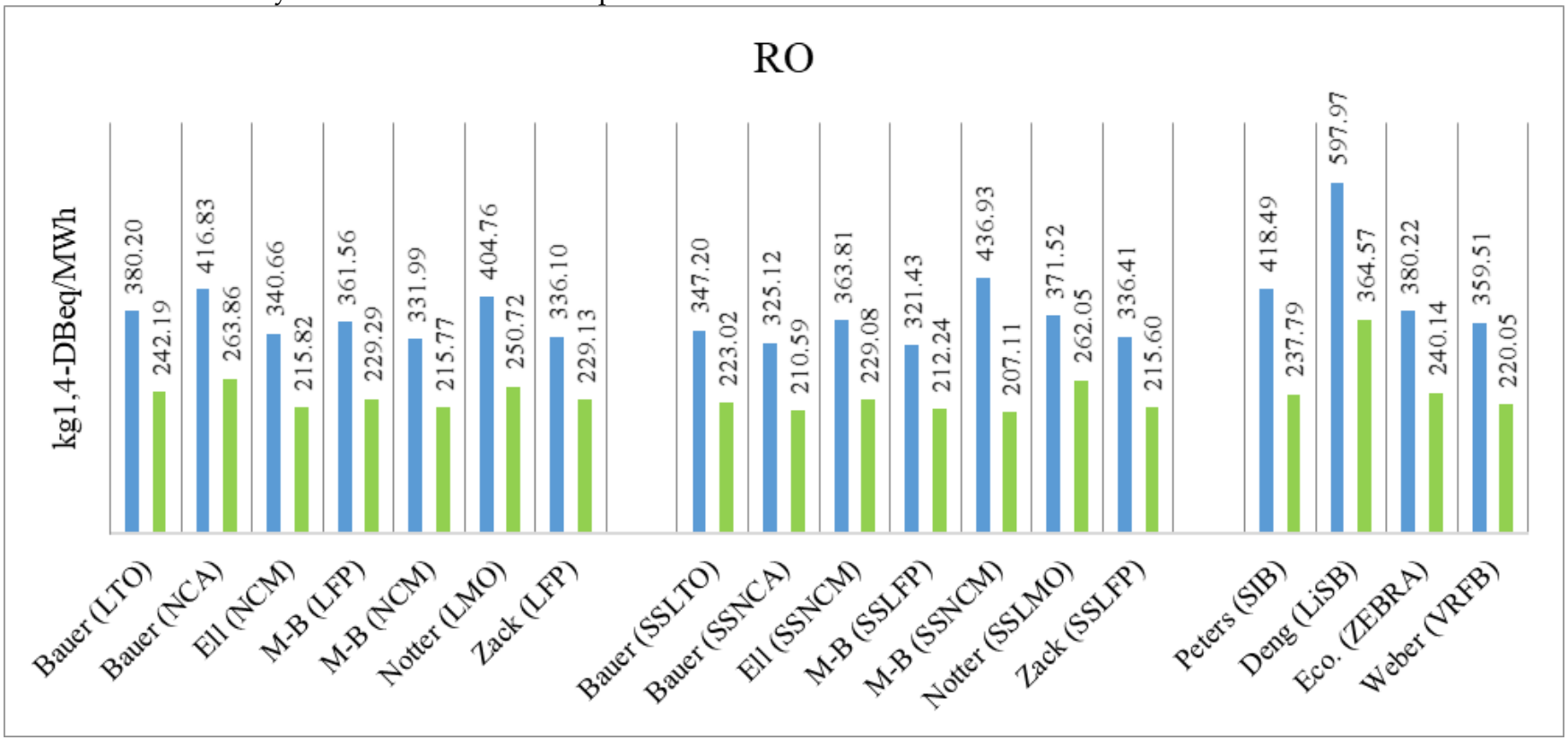

Figure S15: Fossil Depletion SHSs environmental impact indicator in Denmark.

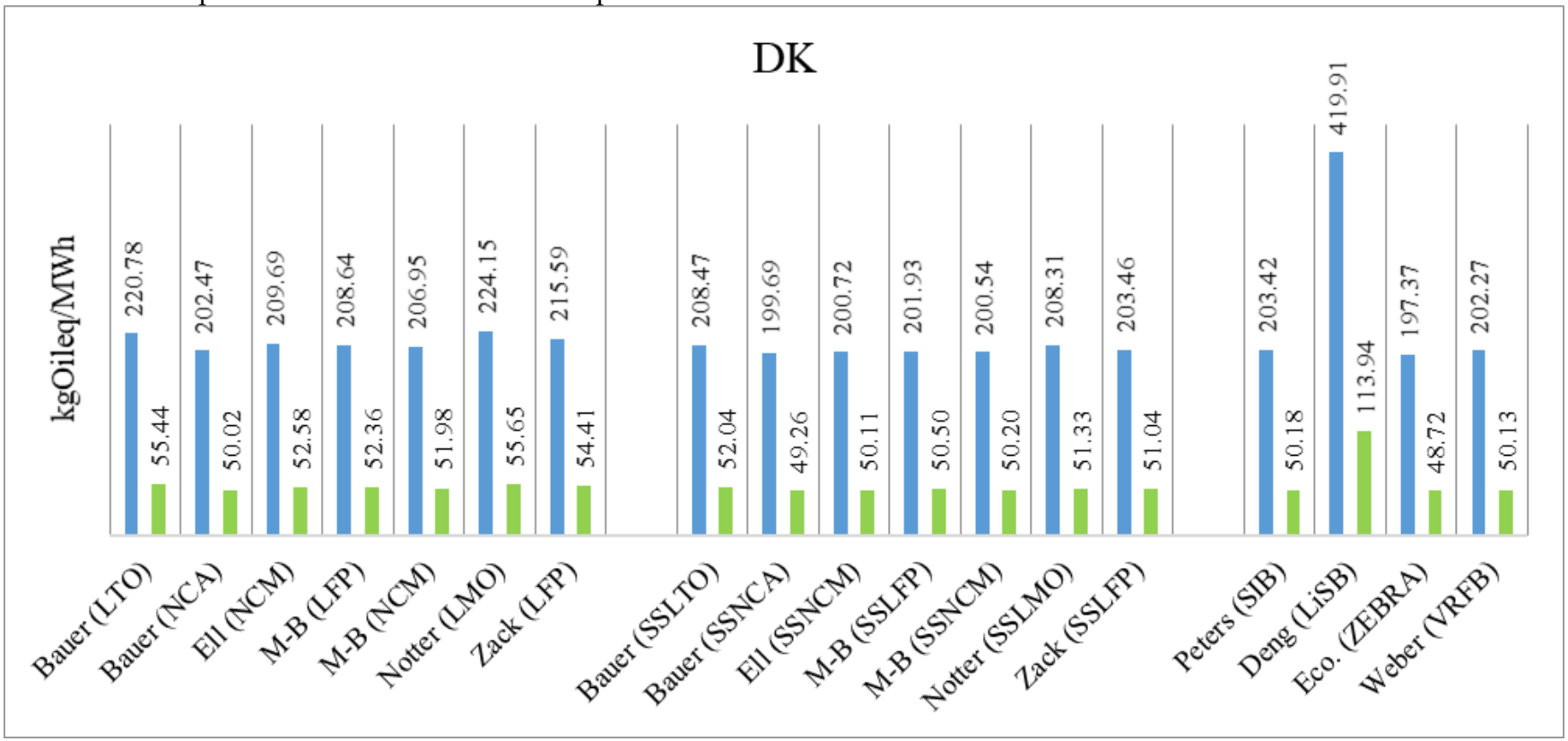

Figure S16: Fossil Depletion SHSs environmental impact indicator in Spain.

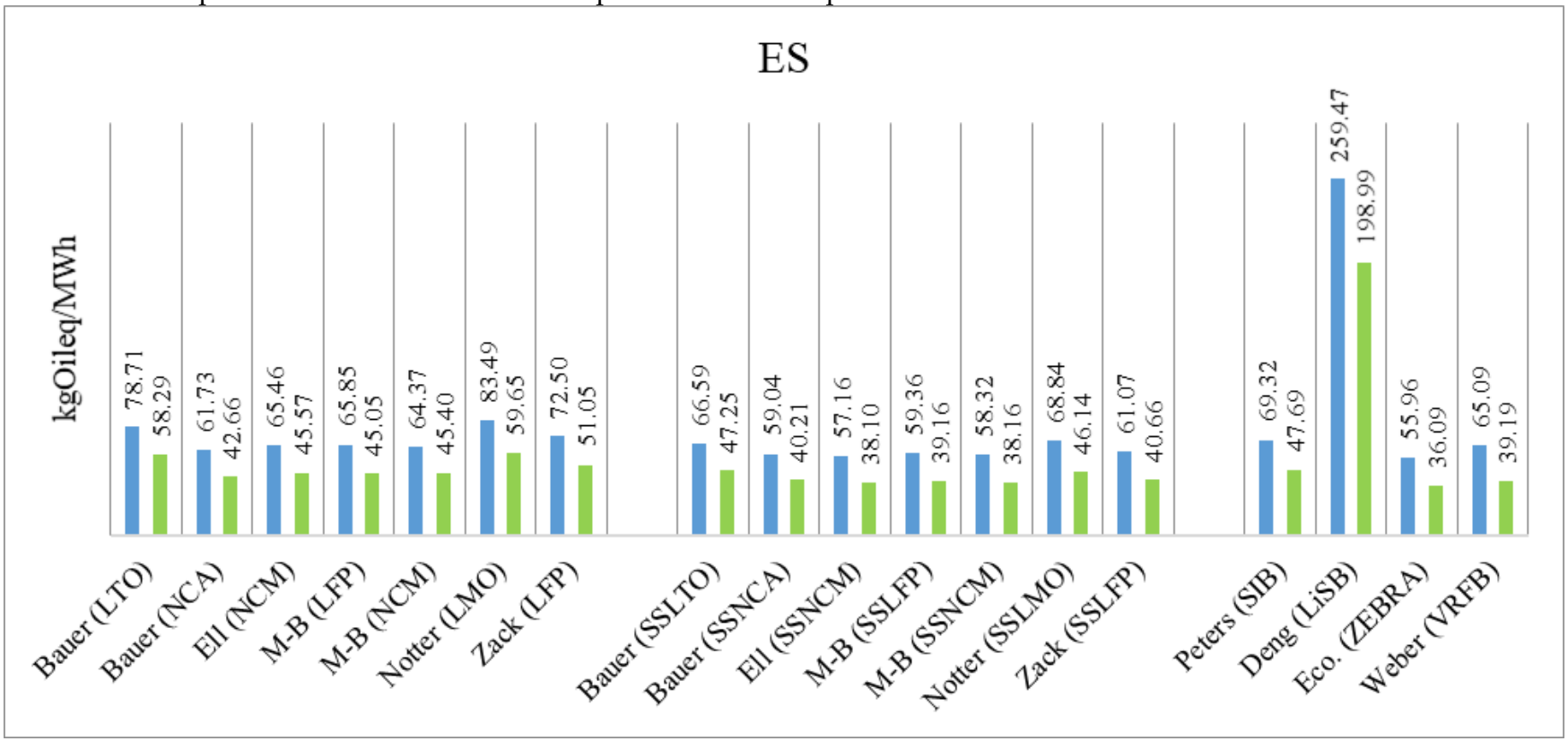

Figure S17: Fossil Depletion SHSs environmental impact indicator in France.

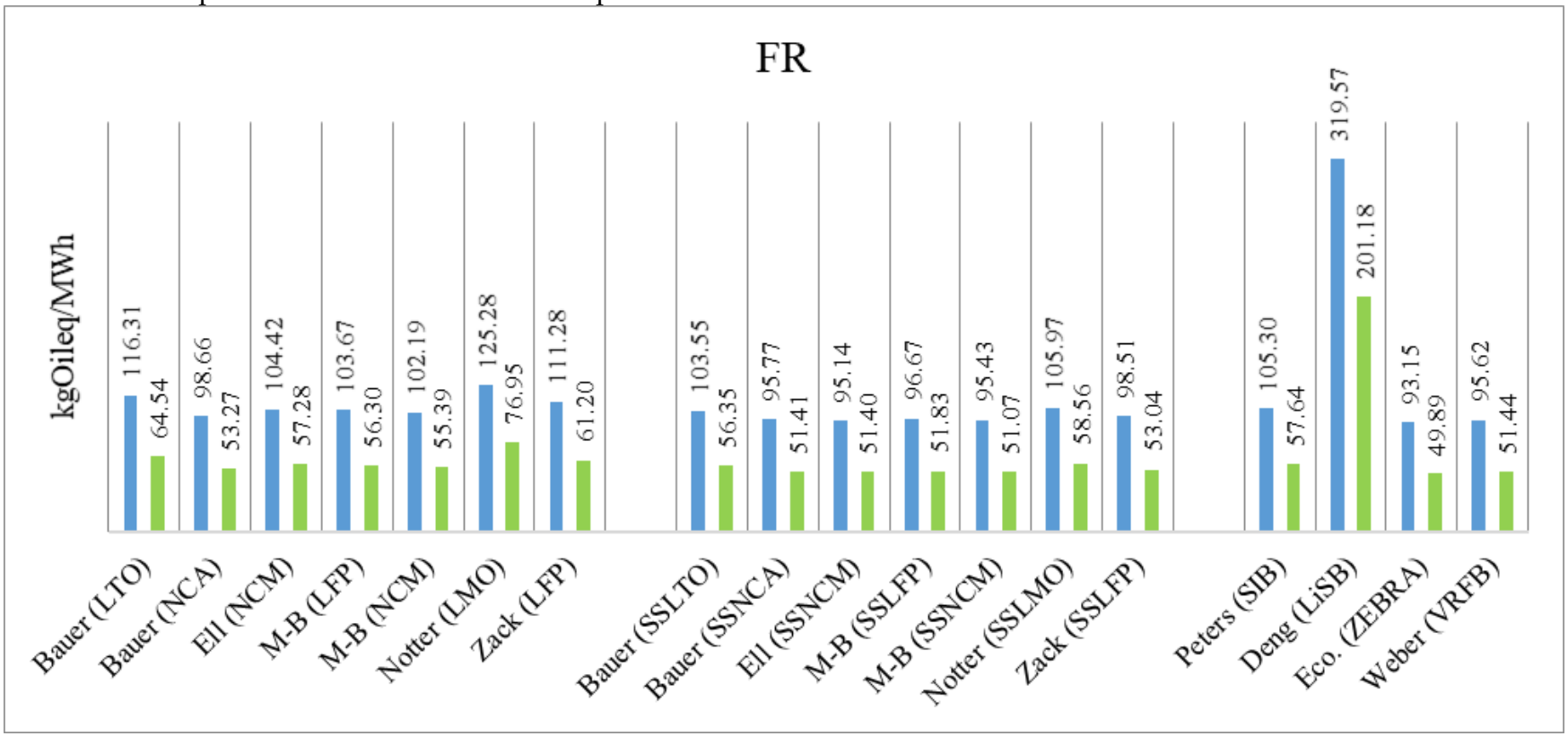

Figure S18: Fossil Depletion SHSs environmental impact indicator in Greece.

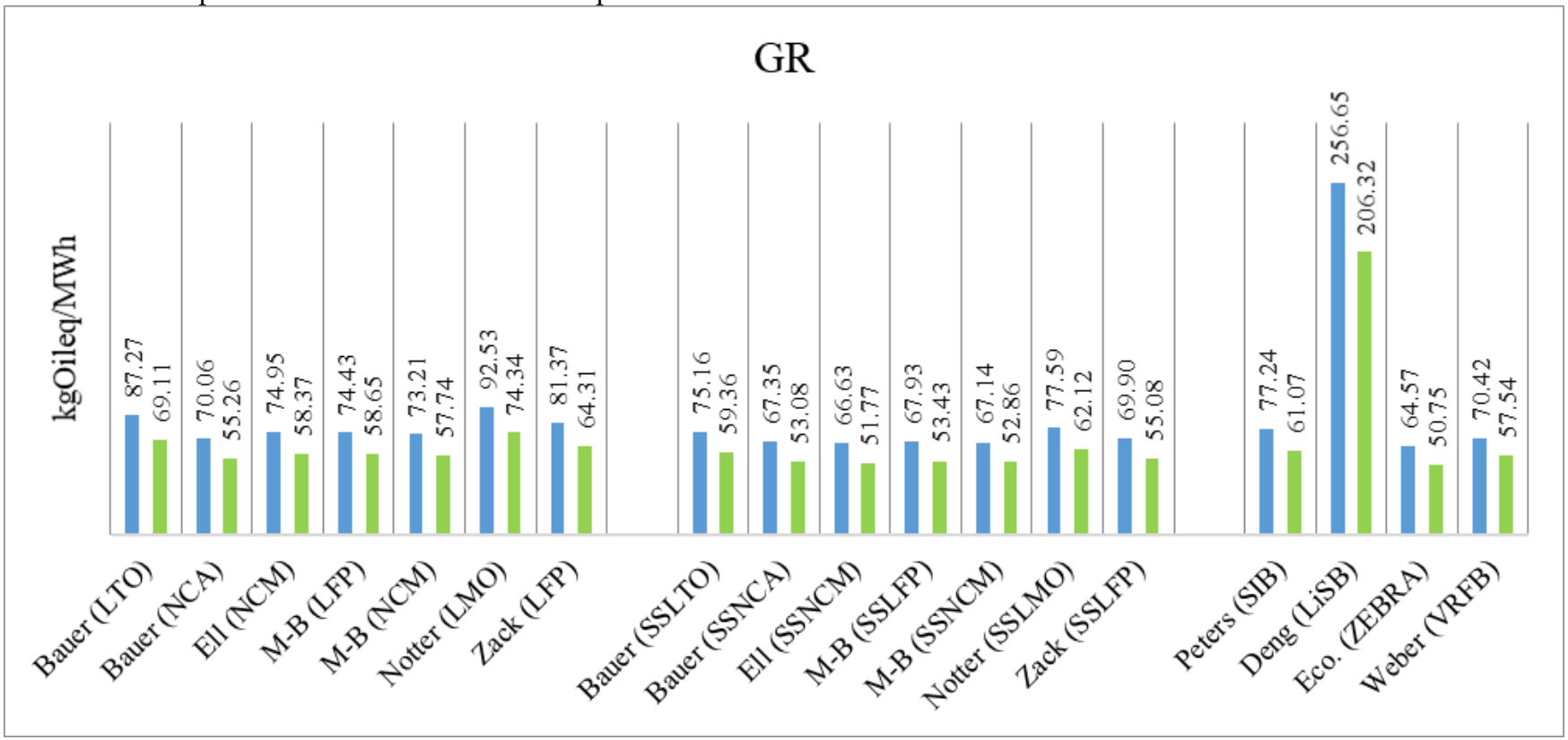

Figure S19: Fossil Depletion SHSs environmental impact indicator in Hungary.

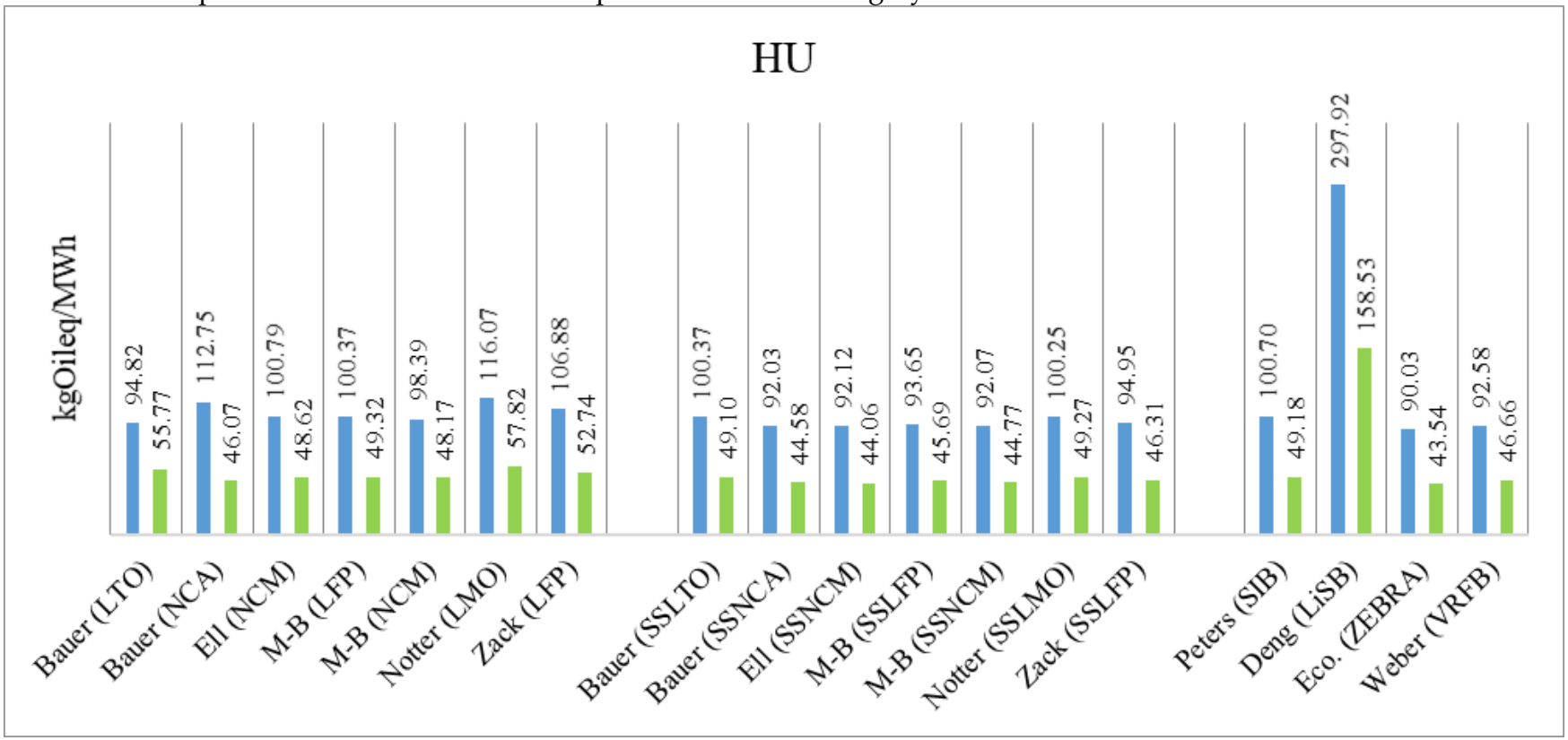

Figure S20: Fossil Depletion SHSs environmental impact indicator in Portugal.

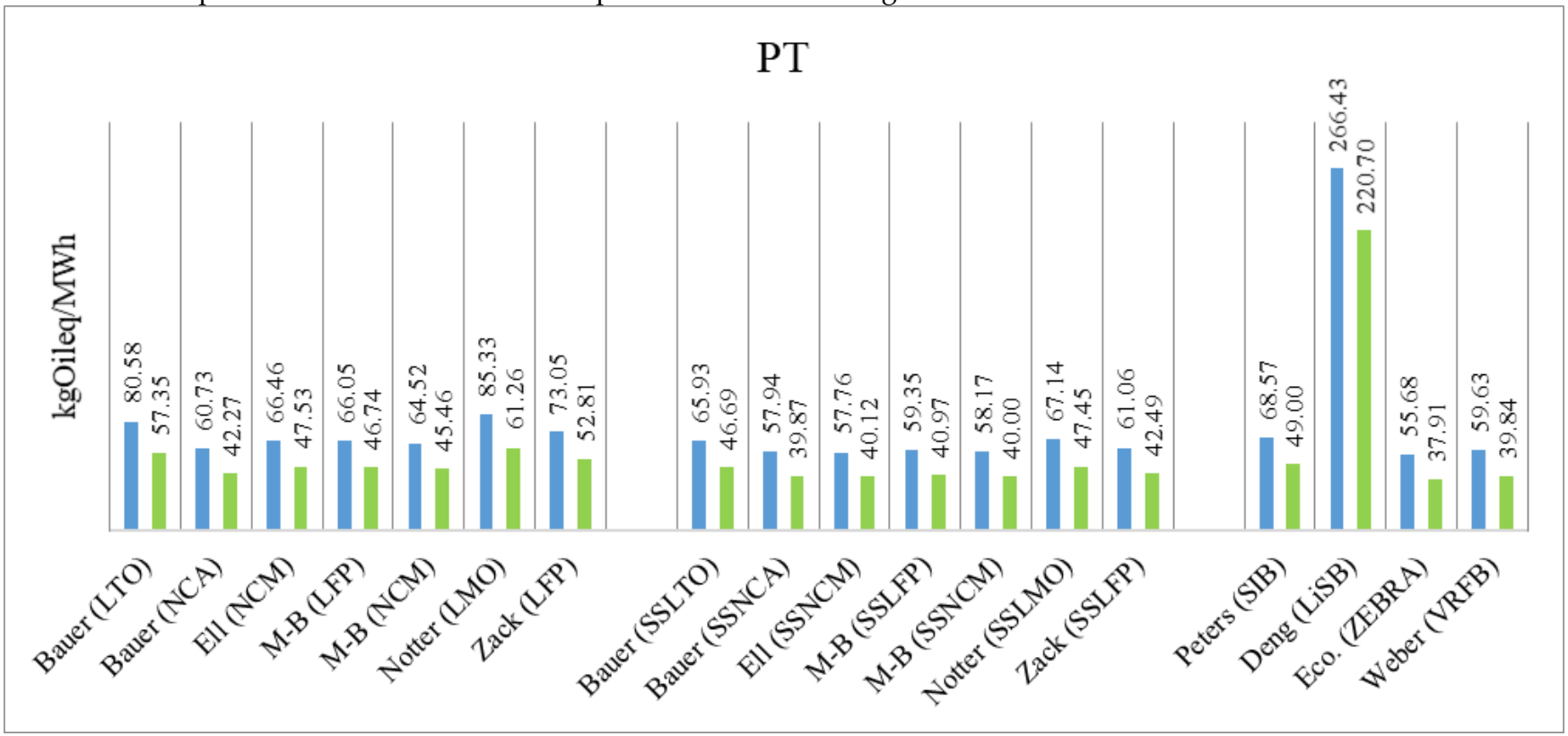

Figure S21: Fossil Depletion SHSs environmental impact indicator in Romania.

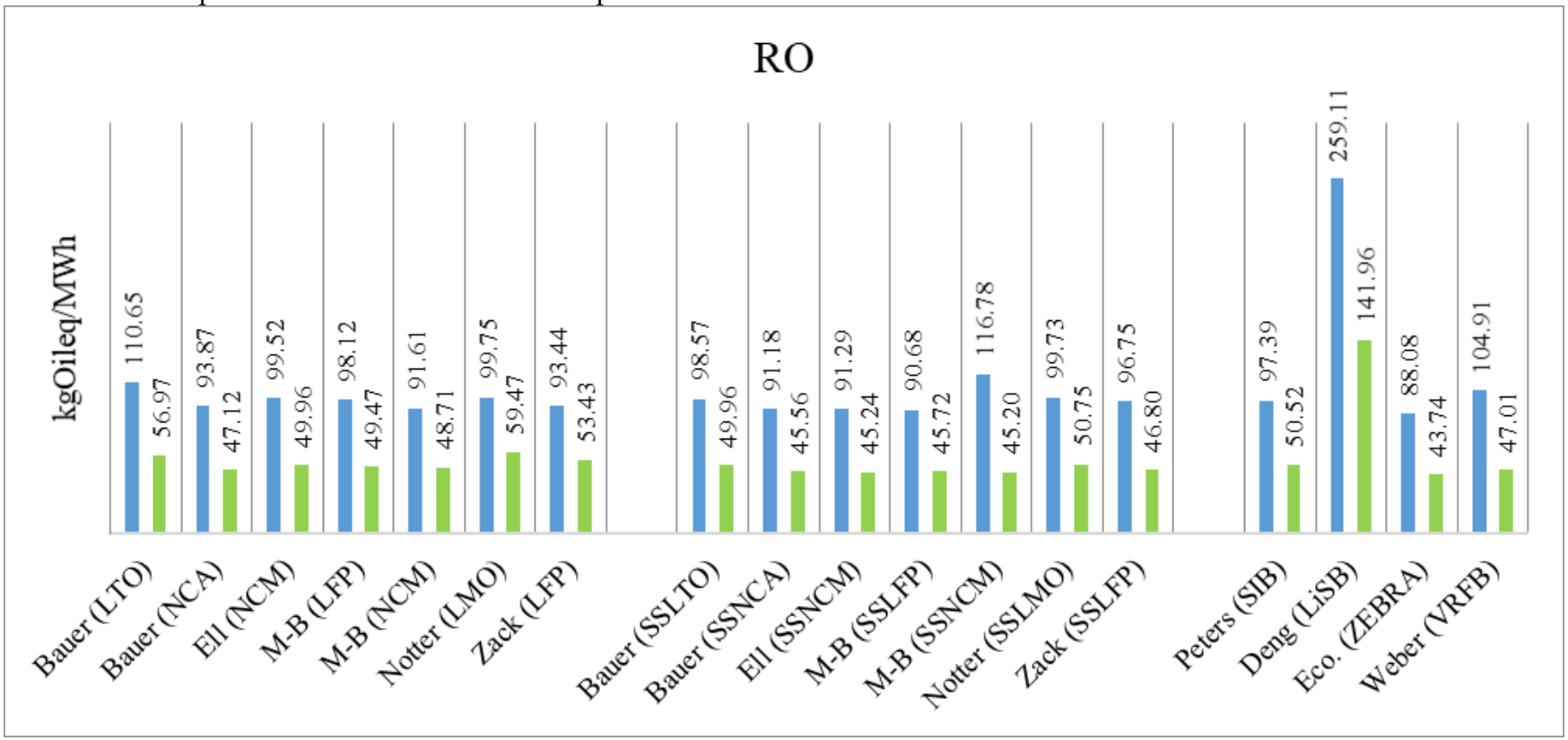

Environmental and Economic Optima of Solar Home Systems Design: a combined LCA and LCC approach - Supporting Information

Federico Rossi[a,b,*], Miguel Heleno[c], Riccardo Basosi[b,d,e], Adalgisa Sinicropi[b,d,e]

[a] *University of Florence, Department of Industrial Engineering, Via Santa Marta,3, Florence, Italy.*
[b] *University of Siena, R^2ES lab, Department of Biotechnology, Chemistry and Pharmacy, Via A. Moro,2, Siena, Italy.*
[c] *Grid Integration Group, Lawrence Berkeley National Laboratory, Berkeley, Cyclotron Road, 1, CA 94720, USA.*
[d] *CSGI, Center for colloid and surface science, via della Lastruccia 3, 50019, Sesto Fiorentino, Italy.*
[e] *Institute of Chemistry of Organometallic Compounds (CNR-ICCOM), Via Madonna del Piano 10, 50019 Sesto Fiorentino, Italy.*

Nomenclature

Abbreviations

BESS Battery Energy Storage System.

CC Charge Controller.

CHP Combined Heat and Power.

CO Construction.

DER Distributed Energy Resources.

EE Exported Energy.

EoL End of Life.

ESS Energy Storage System.

FU Functional Unit.

IE Imported Energy.

In Inverter.

ISO International Organization for Standardization.

LCA Life Cycle Assessment.

LCC Life Cycle Costing.

LCI Life Cycle Inventory.

*Corresponding author
Email address: fe.rossi@unifi.it (Federico Rossi)

LCIA Life Cycle Impact Assessment.

LFP Lithium Iron Phosphates.

LIB Lithium-ion battery.

LMO Lithium Manganese Oxide.

LTO Lithium Iron Titanate.

MILP Mixed Integer Linear Programming.

MINLP Mixed Integer Non Linear Programming.

NCA Nickel Cobalt Aluminium.

NCM Nickel Cobalt Manganese.

NREL National Renewable Energy Laboratory.

OP Operation.

PV Photovoltaic.

RF Reference Flow.

SHS Solar Home System.

Variabes and parameters

Ann_k Ann. interest rate for investments in tech. k.

C Life Cycle cost of the SHS (EUR/MWh).

cap_k Installed capacity of technology k (kW or kWh).

cap_s^r Reference battery capacity (kWh).

$CFix_k$ Fixed cost of technology k (EUR).

ch_t Battery charge at time t (kW).

$ch_{t,j}$ Battery charge of battery j at time t (kW).

$CVar_k$ Variable cost of technology k (EUR/kW or EUR/kWh).

dch_t Battery discharge at time t (kW).

$dch_{t,j}$ Battery discharge of battery j at time t (kW).

E_a Activation Energy (Jmol^{-1}).

$EAnn_k$ Environmental annualisation factor of tech. k.

EC_t Energy cost at time t (EUR/kWh).

EI_t Energy environmental impact at time t (Pts/kWh).

EFI_t Environmental Feed-in remuneration at time t (Pts/kWh).

FI_t Feed-in remuneration at time t (EUR/kWh).

I Life Cycle impact of the SHS (Pts/MWh).

i_k Investment decision for tech. k (binary).

$IFix_k$ Fixed environmental impact of technology k (Pts).

ir Interest rate (%).

$IVar_k$ Variable environmental impact of technology k (Pts/kW or Pts/kWh).

k_j Calendar ageing correction factor of battery j (-).

K Cells temperature (K).

L_k Expected lifespan of technology k (yrs).

Ld_t Consumer load at time t (kW).

$MiSoc$ Minimum battery state-of-charge ($[0, 1]$).

n Number of battery types considered in the analysis.

N^0 Maximum number of cycles of the batteries per year (-).

N_j^0 Maximum number of cycles of the battery j per year (-).

P_1 Representative point of the Environmental Optimum on the impact-costs diagram.

P_2 Representative point of the Economic Optimum on the impact-costs diagram.

P_g Representative point of the grid on the impact-costs diagram.

PCr Battery maximum power/capacity ratio h^{-1}.

pv_t PV power at time t (kW).

$\bar{Q}$ Maximum accepted degradation level (%).

R Gas constant ($\mathrm{Jmol}^{-1}K^{-1}$).

RF Reference Flow (MWh/yr).

soc_t Battery state of charge at time t (kWh).

SR_t Normalized solar gen. at t (kWh/kW installed).

ui_t Import from utility at time t (kW).

ue_t Electricity export to utility at time t (kW).

V Reference battery voltage (V).

α Charging/discharging aux. variable (binary).

α_s Cyclic ageing parameter ($\mathrm{Ah}^{-1}\mathrm{K}^{-2}$).

β_s Cyclic ageing parameter($\mathrm{Ah}^{-1}\mathrm{K}^{-1}$).

γ_s Cyclic ageing parameter (Ah^{-1}).

δ_s Cyclic ageing parameter ($\mathrm{h} \cdot \mathrm{K}^{-1}$).

ϵ_s Cyclic ageing parameter (h).

η_{cc} Efficiency of the Charge Controller ([0, 1]).

η_{in} Efficiency of the Inverter ([0, 1]).

$\eta_{s,c}$ Charging efficiency of the battery ([0, 1]).

$\eta_{s,d}$ Discharging efficiency of the battery ([0, 1]).

θ_s Calendar ageing parameter (yr^{-1}).

Subscripts

cc Related to of Charge Controllers.

g Related to the grid.

in Related to of Inverters.

j Battery type index.

k Variable withe technology.

s Related to generic energy storage.

$s, 1$ M-B (LFP).

$s, 2$ Zack (LFP).

$s, 3$ Bauer (LTO).

$s, 4$ Notter (LMO).

$s, 5$ Bauer (NCA).

$s, 6$ Ell (NCM).

$s, 7$ M-B (NCM).

pv Related to photovoltaic technologies.

SHS Related to of all the components included by the system.

t Variable with time.

τ_{yr} Set of hourly time points over a year.

LCA driven solar compensation mechanism for Renewable Energy Communities: the Italian case - Supporting Material

Federico Rossi[a,c,d,*], Miguel Heleno[b], Riccardo Basosi[a,c,e], Adalgisa Sinicropi[a,c,e]

[a] *University of Siena, R²ES lab, Department of Biotechnology, Chemistry and Pharmacy, Via A. Moro,2, Siena, Italy.*
[b] *Grid Integration Group, Lawrence Berkeley National Laboratory, Berkeley, Cyclotron Road, 1, CA 94720, USA.*
[c] *CSGI, Center for colloid and surface science, via della Lastruccia 3, 50019, Sesto Fiorentino, Italy.*
[d] *University of Florence, Department of Industrial Engineering, Via Santa Marta,3, Florence, Italy.*
[e] *Institute of Chemistry of Organometallic Compounds (CNR-ICCOM), Via Madonna del Piano 10, 50019 Sesto Fiorentino, Italy.*

Keywords: Renewable Energy Communities, Photovoltaic Systems, Batteries, Life Cycle Assessment, Incentives.

Nomenclature

Abbreviations

BESS Battery Energy Storage System.

CC Charge Controller.

DER-CAM Distributed Energy Resources Customer Adoption Model.

GHG Greenhouse Gas.

GWP Global Warming Potential.

ILCD International Reference Life Cycle Data System.

In Inverter.

ISO International Organization for Standardization.

LCA Life Cycle Assessment.

LCI Life Cycle Inventory.

LCIA Life Cycle Impact Assessment.

LMO Lithium Manganese Oxide.

OECD Organisation for Economic Co-operation and Development.

PV Photovoltaic.

PV-GIS Photovoltaic Geographical Information System.

*Corresponding author
Email address: federico.rossi3@unisi.it (Federico Rossi)

SC Self Consumption.

REC Renewable Energy Community.

RED Renewable Energy Directive.

Variables

Ann Annualization factor (-).

C Cost of communities (EUR).

cap capacity of a component (kW or kWh).

$CFix$ Fixed Cost (EUR).

$\bar{CL}$ Average communities demand (kW).

CT Carbon Tax (EUR/tonCO_2eq).

$CVar$ Variable Cost (EUR/kW or EUR/kWh).

D National electricity demand (kWh).

$EAnn$ Emissions annualization factor (-).

EC Energy Cost (EUR/kWh or cEUR/kWh).

$Eload$ Emissions for load supply (-).

Esc Hourly emissions for self-consumption (kgCO_2eq/h).

Eue Hourly emissions from imported energy (kgCO_2eq/h).

$FITs$ Feed-in Tariffs (EUR/kWh or cEUR/kWh).

i Binary decision variable (-).

$Imix$ Impact of the energy mix (kgCO_2eq/kWh).

ir Discount rate (%).

L Lifespan (yr).

$load$ Communities load (kWh).

Nc Number of installations by community type (-).

Nk Number of components (-).

$\bar{NL}$ Average national demand (kW).

Nt Number of community types (-).

OT Operative Time (hr).

P Penetration of communities (%).

sc Self Consumption (kWh).

ue Electricity exported (kWh).

ui Electricity imported (kWh).

Subscripts

cc Related to the charge controller.

i Variable which depends on the iteration number.

in Related to the inverter.

j Variable which depends on the community type.

j Related to the k-component.

pv Related to the photovoltaic system.

$s1$ Related to the 1st battery type.

$s2$ Related to the 2nd battery type.

$s3$ Related to the 3rd battery type.

$s4$ Related to the 4th battery type.

$s5$ Related to the 5th battery type.

$s6$ Related to the 6th battery type.

$s7$ Related to the 7th battery type.

t Variable which depends on time.

1. Sensitivity Analysis - Penetration of Renewable Energy Communities

In the previous subsection, the results are presented considering a Base Case Scenario where Renewable Energy Communities (RECs) penetration (P) is set to 25 % whereas the carbon taxes (CT) are 15.4 EUR/tonCO_2eq. In order to address the uncertainty of these parameters, a sensitivity analysis is performed by keeping the same CT as in the Base Case Scenario and varying P from 10% to 50%. Figure S1a represents the average photovoltaic (PV) system size as function of P, whereas Figure S1b concerns the storage system capacity. Both charts highlight that P does not sensibly affect the optimal size of components because the results variation is very small. Nevertheless, it can be observed that the PV system size has a slightly decreasing trend. The reason is that, by increasing RECs number on the territory, the environmental benefit provided to the grid by single communities is lower and thus the feed-in tariffs FITs increments are smaller as well. This explanation can be demonstrated by discussing the cost allocation results. This pushes single RECs members to reduce the investments in PV and to deploy more batteries because, if FITs get lower, extending SC with storage gets economically more convenient. This is the reason for the increase in storage capacity with the proposed FITs.

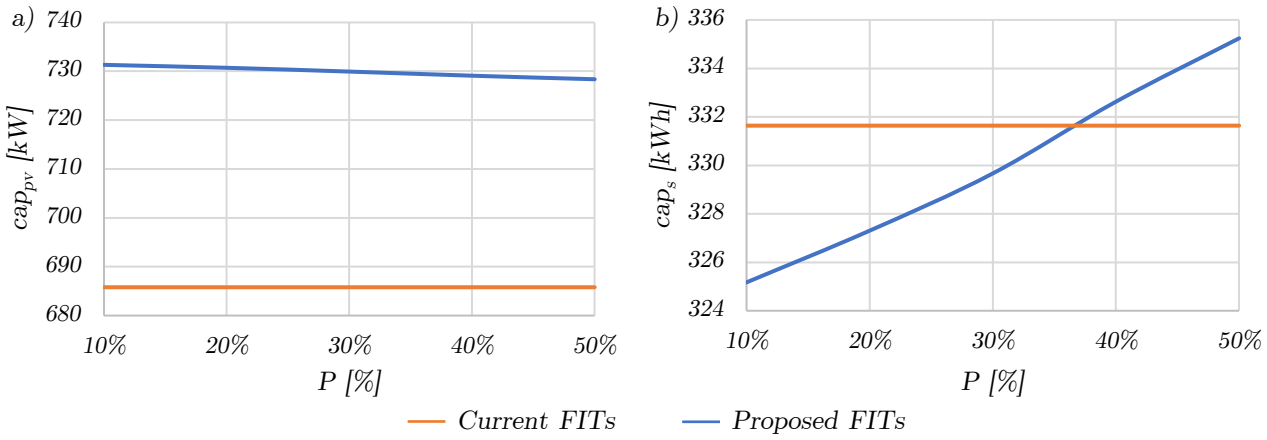

Figure S1: Optimal size of a) the PV system and b) the batteries as function of P.

Figure S2a represents the variations of the annual energy balance of the grid as function of P, resulting from the adoption of the proposed FITs. Although the PV power deployed by RECs slowly decreases with P, the overall amount of energy injected to the grid at national level linearly increases as consequence of the higher number of communities. Nevertheless the overall RECs electricity on the grid represents a small percentage of the total even for high values of P. An explanation for that can be derived by discussing Figure S2b. This chart represents the share of RECs electricity on the grid during the average day of the year. Similarly to the Base Case Scenario, RECs only inject electricity to the grid from 7 AM to 4 PM: indeed changing the number of communities on the territory, the energy management of single RECs is not affected. Even though the share of RECs electricity can achieve a relevant percentage during the day, the

narrowness of the energy exportation time range is the reason for RECs limited contribution to the grid on annual basis. Also the SC increases proportionally with P and, similarly to the Base Case Scenario, it is generally preferred to the energy injection. In other words, extending the number of communities on the territory does not entail remarkable changes for single communities but allows for a proportional scaling of their contribution in the national energy balance.

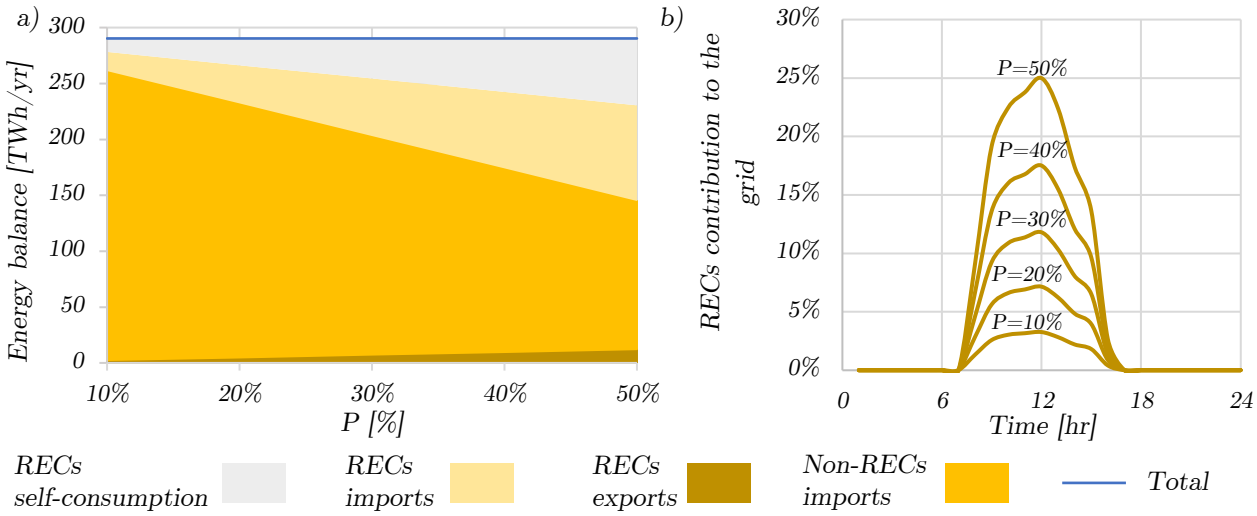

Figure S2: a) Energy balance of the grid on annual basis as function of P; b) amount of electricity exported by RECs as percentage of the total energy on the grid during the average day of the year. Evaluated using the proposed FITs.

Figure S3a represents the variation of the annual carbon dioxide emissions balance. Similarly to the energy flows, also the life cycle emissions proportionally increase with P. Indeed, as communities design is not significantly affected by penetration, RECs electricity environmental impact is about constant with their number (0.09 $kgCO_2eq/kWh$). The energy mix environmental impact instead could, in principle, vary due to the higher RECs electricity overall throughput at national level. Nevertheless, as RECs electricity annual contribution to the grid is quite limited even for high penetration levels, the energy mix specific impact just decreases from 0.41 $kgCO_2eq/kWh$ (for P=10%) to 0.39 $kgCO_2eq/kWh$ (for P=50%). Consequently, also the environmental impact related to RECs load is not relevantly affected by P and is equal to 0.29 $kgCO_2eq/kWh$. Therefore, compared to the situation before RECs deployment, the main environmental advantage obtained by increasing the number of communities is provided by SC which, increasing proportionally with P, allows to remarkably mitigate the national emissions. The increasing gap between the blue and the red lines shows the national greenhouse gases (GHGs) mitigation with P compared to the situation before RECs deployment. Concerning the comparison between the current and the proposed FITs, the gap between the orange and the blue lines is not affected by P. The reason is that the above-mentioned environmental benefits are just due to a scaling of RECs effects and not to a relevant difference in terms of FITs, as clearly demonstrated by the following cost allocation results.

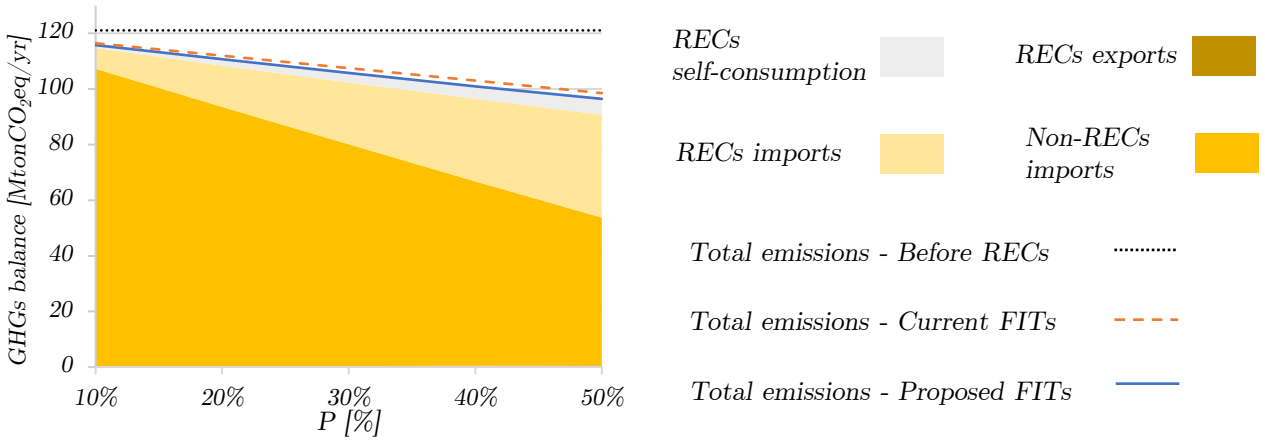

Figure S3: National GHGs balance on annual basis as function of P. Evaluated using the proposed FITs.

Figure S4a illustrates the annual variation of the average FITs, assessed through the adoption of the proposed FITs, as function of P whereas Figure S4b depicts the convergence of FITs with iterations. It is possible to appreciate that the average FITs converge to a slightly different equilibrium value depending on RECs penetration. At every iteration, all RECs in the country inject some electricity to the grid and allow to save some GHGs emissions thus mitigating the grid environmental impact. If there are more communities, the energy mix impact calculated at first iteration is lower; for such reason at the second iteration, single RECs can avoid less emissions. A lower amount of avoided GHGs emissions implies that the additional incentives accumulated with the iterations are lower and the FITs gradually converge to a lower equilibrium value. This mechanism also explains the PV and the storage capacity trends illustrated in Figure S1a and Figure S1b.

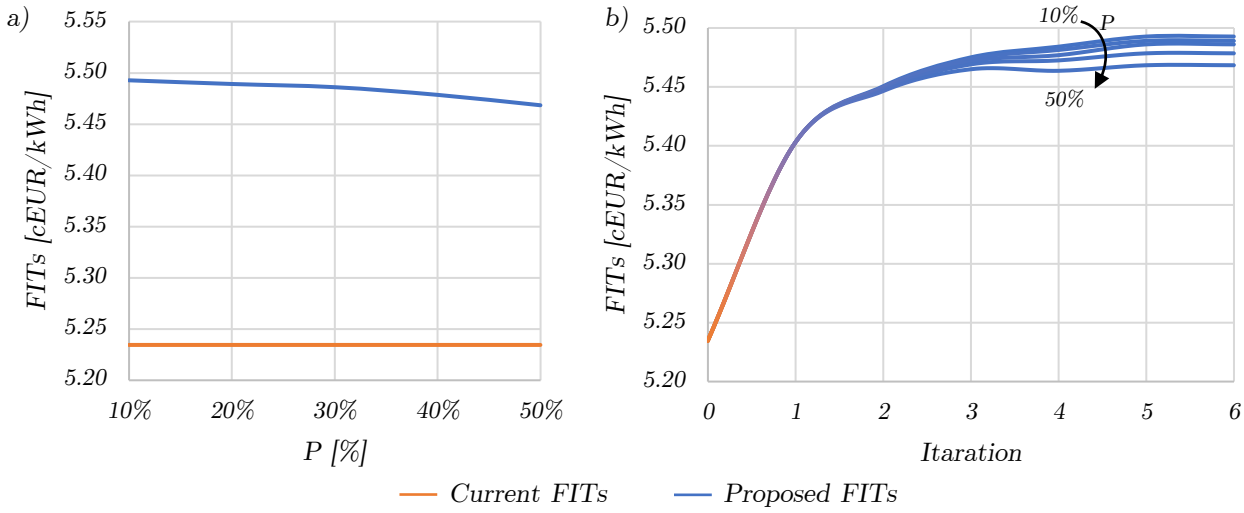

Figure S4: Average FITs a) as function of P and b) of iterations.

Environmental impact analysis applied to Solar Pasteurization Systems: Supporting information

Federico Rossi[a,b] Maria Laura Parisi*[,a,c], Simone Maranghi[a,c], Giampaolo Manfrida[b], Riccardo Basosi[a,c,d], Adalgisa Sinicropi*[,a,c,d]

[a]University of Siena, Department of Biotechnology, Chemistry and Pharmacy, Via A. Moro,2, Siena, Italy. [b]University of Florence, Department of Industrial Engineering, Via Santa Marta,3, Florence, Italy, [c]CSGI, Center for colloid and surface science, via della Lastruccia 3, 50019, Sesto Fiorentino, Italy, [d]Institute of Chemistry of Organometallic Compounds (CNR-ICCOM), Via Madonna del Piano 10, 50019 Sesto Fiorentino, Italy

Corresponding authors: Adalgisa Sinicropi, Maria Laura Parisi

e-mail: adalgisa.sinicropi@unisi.it, marialaura.parisi@unisi.it

Table of contents

1. LCI

The original configurations of the NCS (Dainelli et al., 2017; Manfrida et al., 2017) and of the TVS (Carielo da Silva et al., 2016; Carielo et al., 2017) have been maintained faithfully. For such reason the number, the mass, the building materials and the productivity of NCS and TVS can be different. LCA analysis takes into account these differences setting the LCI.

1.1. NCS

1.1.1. Components

Table S1

LCI: Solar collector				
Component	**Quantity**	**Unit**	**Ecoinvent Process**	**Ecoinvent Category**
Input				
Solar collector	1.95	m^2	market for evacuated tube collector | evacuated tube collector | APOS, S - GLO	Manufacture of permanent mount non-electric household heating equipment
Packaging	5.3	kg	market for carton board box production, with offset printing | carton board box production, with offset printing | APOS, S - GLO	Manufacture of corrugated paper and paperboard and of containers of paper
Transport to Somalia	7.6	t*km	transport, freight, lorry 3.5-7.5 metric ton, EURO3 | transport, freight, lorry 3.5-7.5 metric ton, EURO3 | APOS, S - RoW	Freight transport by road
	25.1	t*km	transport, freight, lorry 3.5-7.5 metric ton, EURO6 | transport, freight, lorry 3.5-7.5 metric ton, EURO6 | APOS, S - RER	Freight transport by road
	572.2	t*km	market for transport, freight, sea, transoceanic ship | transport, freight, sea, transoceanic ship | APOS, S - GLO	Sea and coastal freight water transport
Transport to Brazil	124.1	t*km	market for transport, freight train | transport, freight train | APOS, S - Europe without Switzerland	Freight rail transport
	7.6	t*km	transport, freight, lorry 3.5-7.5 metric ton, EURO3 | transport, freight, lorry 3.5-7.5 metric ton, EURO3 | APOS, S - RoW	Freight transport by road
	349.8	t*km	market for transport, freight, sea, transoceanic ship | transport, freight, sea, transoceanic ship | APOS, S - GLO	Sea and coastal freight water transport
Transport to Italy	65.8	t*km	transport, freight, lorry 3.5-7.5 metric ton, EURO6 | transport, freight, lorry 3.5-7.5 metric ton, EURO6 | APOS, S - RER	Freight transport by road
Output				
Solar Collector transported	1	Items		

Table S2

LCI: Compensation Tank				
Component	**Quantity**	**Unit**	**Ecoinvent Process**	**Ecoinvent Category**
Input				
Compensation Tank	1.0	Item	market for expansion vessel, 80l | expansion vessel, 80l | APOS, S - GLO	Manufacture of tanks, reservoirs and containers of metal
Packaging	0.8	kg	market for carton board box production, with offset printing | carton board box production, with offset printing | APOS, S - GLO	Manufacture of corrugated paper and paperboard and of containers of paper
Transport to Somalia	1.1	t*km	transport, freight, lorry 3.5-7.5 metric ton, EURO3 | transport, freight, lorry 3.5-7.5 metric ton, EURO3 | APOS, S - RoW	Freight transport by road
	3.4	t*km	transport, freight, lorry 3.5-7.5 metric ton, EURO6 | transport, freight, lorry 3.5-7.5 metric ton, EURO6 | APOS, S - RER	Freight transport by road
	78.5	t*km	market for transport, freight, sea, transoceanic ship | transport, freight, sea, transoceanic ship | APOS, S - GLO	Sea and coastal freight water transport
Transport to Brazil	17.1	t*km	market for transport, freight train | transport, freight train | APOS, S - Europe without Switzerland	Freight rail transport
	1.04	t*km	transport, freight, lorry 3.5-7.5 metric ton, EURO3 | transport, freight, lorry 3.5-7.5 metric ton, EURO3 | APOS, S - RoW	Freight transport by road
	48	t*km	market for transport, freight, sea, transoceanic ship | transport, freight, sea, transoceanic ship | APOS, S - GLO	Sea and coastal freight water transport
Transport to Italy	9.02	t*km	transport, freight, lorry 3.5-7.5 metric ton, EURO6 | transport, freight, lorry 3.5-7.5 metric ton, EURO6 | APOS, S - RER	Freight transport by road
Output				
Compensation Tank Transported	1	items		

Table S3

LCI: Heat Exchanger				
Component	**Quantity**	**Unit**	**Ecoinvent Process**	**Ecoinvent Category**
Input				
Heat exchanger pipes	15.8	kg	market for chromium steel pipe | chromium steel pipe | APOS, S - GLO	Manufacture of basic iron and steel
Thermal insulation	1.7	kg	market for stone wool | stone wool | APOS, S - GLO	Manufacture of other non-metallic mineral product
Packaging	1.8	kg	market for carton board box production, with offset printing | carton board box production, with offset printing | APOS, S - GLO	Manufacture of corrugated paper and paperboard and of containers of paper
Transport to Somalia	2.5	t*km	transport, freight, lorry 3.5-7.5 metric ton, EURO3 | transport, freight, lorry 3.5-7.5 metric ton, EURO3 | APOS, S - RoW	Freight transport by road
	8.3	t*km	transport, freight, lorry 3.5-7.5 metric ton, EURO6 | transport, freight, lorry 3.5-7.5 metric ton, EURO6 | APOS, S - RER	Freight transport by road
	189.2	t*km	market for transport, freight, sea, transoceanic ship | transport, freight, sea, transoceanic ship | APOS, S - GLO	Sea and coastal freight water transport
Transport to Brazil	41.1	t*km	market for transport, freight train | transport, freight train | APOS, S - Europe without Switzerland	Freight rail transport
	2.5	t*km	transport, freight, lorry 3.5-7.5 metric ton, EURO3 | transport, freight, lorry 3.5-7.5 metric ton, EURO3 | APOS, S - RoW	Freight transport by road
	115.7	t*km	market for transport, freight, sea, transoceanic ship | transport, freight, sea, transoceanic ship | APOS, S - GLO	Sea and coastal freight water transport
Transport to Italy	21.7	t*km	transport, freight, lorry 3.5-7.5 metric ton, EURO6 | transport, freight, lorry 3.5-7.5 metric ton, EURO6 | APOS, S - RER	Freight transport by road
Output				
Heat Exchanger transported	1	Items		

Table S4

LCI: Supply and Treated Water Tanks				
Component	**Quantity**	**Unit**	**Ecoinvent Process**	**Ecoinvent Category**
Input				
Water Tank	14.3	kg	market for polyethylene terephthalate, granulate, bottle grade | polyethylene terephthalate, granulate, bottle grade | APOS, S - GLO	Manufacture of plastics and synthetic rubber in primary forms
Packaging	1.4	kg	market for carton board box production, with offset printing | carton board box production, with offset printing | APOS, S - GLO	Manufacture of corrugated paper and paperboard and of containers of paper
Transport to Somalia	2.04	t*km	transport, freight, lorry 3.5-7.5 metric ton, EURO3 | transport, freight, lorry 3.5-7.5 metric ton, EURO3 | APOS, S - RoW	Freight transport by road
	6.8	t*km	transport, freight, lorry 3.5-7.5 metric ton, EURO6 | transport, freight, lorry 3.5-7.5 metric ton, EURO6 | APOS, S - RER	Freight transport by road
	154.6	t*km	market for transport, freight, sea, transoceanic ship | transport, freight, sea, transoceanic ship | APOS, S - GLO	Sea and coastal freight water transport
Transport to Brazil	33.6	t*km	market for transport, freight train | transport, freight train | APOS, S - Europe without Switzerland	Freight rail transport
	2.05	t*km	transport, freight, lorry 3.5-7.5 metric ton, EURO3 | transport, freight, lorry 3.5-7.5 metric ton, EURO3 | APOS, S - RoW	Freight transport by road
	94.5	t*km	market for transport, freight, sea, transoceanic ship | transport, freight, sea, transoceanic ship | APOS, S - GLO	Sea and coastal freight water transport
Transport to Italy	17.8	t*km	transport, freight, lorry 3.5-7.5 metric ton, EURO6 | transport, freight, lorry 3.5-7.5 metric ton, EURO6 | APOS, S - RER	Freight transport by road
Output				
Water Tank transported	1	Items		

Table S5

LCI: Pipes				
Component	**Quantity**	**Unit**	**Ecoinvent Process**	**Ecoinvent Category**
Input				
Pipes	1.23	kg	market for chromium steel pipe | chromium steel pipe | APOS, S - GLO	Manufacture of basic iron and steel
Thermal insulation	0.01	kg	market for stone wool | stone wool | APOS, S - GLO	Manufacture of other non-metallic mineral product
Packaging	0.13	kg	market for carton board box production, with offset printing | carton board box production, with offset printing | APOS, S - GLO	Manufacture of corrugated paper and paperboard and of containers of paper
Transport to Somalia	1.8	t*km	transport, freight, lorry 3.5-7.5 metric ton, EURO3 | transport, freight, lorry 3.5-7.5 metric ton, EURO3 | APOS, S - RoW	Freight transport by road
	5.9	t*km	transport, freight, lorry 3.5-7.5 metric ton, EURO6 | transport, freight, lorry 3.5-7.5 metric ton, EURO6 | APOS, S - RER	Freight transport by road
	134	t*km	market for transport, freight, sea, transoceanic ship | transport, freight, sea, transoceanic ship | APOS, S - GLO	Sea and coastal freight water transport
Transport to Brazil	29.2	t*km	market for transport, freight train | transport, freight train | APOS, S - Europe without Switzerland	Freight rail transport
	1.78	t*km	transport, freight, lorry 3.5-7.5 metric ton, EURO3 | transport, freight, lorry 3.5-7.5 metric ton, EURO3 | APOS, S - RoW	Freight transport by road
	82.2	t*km	market for transport, freight, sea, transoceanic ship | transport, freight, sea, transoceanic ship | APOS, S - GLO	Sea and coastal freight water transport
Transport to Italy	15.5	t*km	transport, freight, lorry 3.5-7.5 metric ton, EURO6 | transport, freight, lorry 3.5-7.5 metric ton, EURO6 | APOS, S - RER	Freight transport by road
Output				
Pipes transported	1	m		

1.1.2. Installation

Table S6

LCI: System installed				
Component	**Quantity**	**Unit**	**Ecoinvent Process**	**Ecoinvent Category**
Input				
Compensation Tank Transported	1	Items		
Water Tank transported	2	Items		
Heat Exchanger transported	1	Items		
Pipes, transported	16	m		
Solar Collector transported	2	Items		
Heat from natural gas	2.28+E5	MJ	heat production, natural gas, at boiler modulating <100kW | heat, central or small-scale, natural gas | APOS, S - RoW	Steam and air conditioning supply
Heat from mixed logs	2.28+E5	MJ	heat production, mixed logs, at wood heater 6kW | heat, central or small-scale, other than natural gas | APOS, S - RoW	Steam and air conditioning supply
Heat from fuels	2.28+E5	MJ	heat production, light fuel oil, at boiler 10kW, non-modulating | heat, central or small-scale, other than natural gas | APOS, S - RoW	Steam and air conditioning supply
Land occupation Somalia	267	m^2*years	Occupation, pasture, man made, extensive	Resource/Land
Land Transformation Somalia	17.8	m^2	Transformation, from pasture, man made, extensive	Resource/Land
Land occupation Brazil	267	m^2*years	Occupation, forest	Resource/Land
Land Transformation Brazil	17.8	m^2	Transformation, from forest	Resource/Land
Land occupation Italy	267	m^2*years	Occupation, permanent crop, irrigated	Resource/Land
Land Transformation Italy	17.8	m^2	Transformation, from permanent crop, irrigated	Resource/Land
Output				
NCS Pasteurization System installed	1	Items		

1.1.3. Operative phase

Table S7

LCI: Operative phase				
Component	**Quantity**	**Unit**	**Ecoinvent Process**	**Ecoinvent Category**
Input				
NCS Pasteurization System installed	1	Items		
Raw Water Somalia	1,135,770	l	Water, ground	Resource, in water
Raw Water Brazil	1,319,025	l	Water, ground	Resource, in water
Raw Water Italy	425,130	l	Water, ground	Resource, in water
Output				
Treated Water Somalia	1,135,770	l		
Treated Water Brazil	1,319,025	l		
Treated Water Italy	425,130	l		

1.1.4. End of Life

Table S8

LCI: End-of-Life phase					
Component		**Quantity**	**Unit**	**Ecoinvent Process**	**Ecoinvent Category**
Input					
Recycling non-ferrous metals		72.71*R	kg	market for aluminium scrap, post-consumer | aluminium scrap, post-consumer | APOS, S	Materials Recovery
Output					
Recycled non ferrous metals		72.71*R			
Input					
Recycling ferrous metals		58.78*R	kg	market for iron scrap, sorted, pressed | iron scrap, sorted, pressed | APOS, S	Materials Recovery
Output					
Recycled ferrous metals		58.78*R	kg		
Input					
Recycling Glass		20.28*R	kg	market for glass cullet, sorted | glass cullet, sorted | APOS, S	Materials Recovery
Output					
Recycled Glass		20.28*R			
Input					
Recycling Plastic Tanks		28.6*R	kg	market for polyethylene terephthalate, granulate, bottle grade, recycled | polyethylene terephthalate, granulate, bottle grade, recycled | APOS, S	Materials Recovery
Output					
Recycled Plastic		28.6*R			
Input					
Recycling paperboard		18.08*R	kg	market for waste paperboard, sorted | waste paperboard, sorted | APOS, S	Materials Recovery
Output					
Recycled paperboard		18.08*R			
Input					
Recycling Mineral Wool		1.86*R	kg	treatment of waste mineral wool, recycling | waste mineral wool | APOS, S	Materials Recovery
Output					
Recycled mineral wool		1.86*R			
R	Somalia	0.00%			
	Brazil	1.00%			
	Italy	45.1%			

1.2. TVS

1.2.1. Components

Table S9

LCI: Solar collector				
Component	**Quantity**	**Unit**	**Ecoinvent Process**	**Ecoinvent Category**
Input				
Solar collector	2	m^2	market for flat plate solar collector, Cu absorber | flat plate solar collector, Cu absorber | APOS, S - GLO	Manufacture of permanent mount non-electric household heating equipment
Packaging	5.3	kg	market for carton board box production, with offset printing | carton board box production, with offset printing | APOS, S - GLO	Manufacture of corrugated paper and paperboard and of containers of paper
Transport to Somalia	3.8	t*km	transport, freight, lorry 3.5-7.5 metric ton, EURO3 | transport, freight, lorry 3.5-7.5 metric ton, EURO3 | APOS, S - RoW	Freight transport by road
	12.8	t*km	transport, freight, lorry 3.5-7.5 metric ton, EURO6 | transport, freight, lorry 3.5-7.5 metric ton, EURO6 | APOS, S - RER	Freight transport by road
	291.5	t*km	market for transport, freight, sea, transoceanic ship | transport, freight, sea, transoceanic ship | APOS, S - GLO	Sea and coastal freight water transport
Transport to Brazil	63.4	t*km	market for transport, freight train | transport, freight train | APOS, S - Europe without Switzerland	Freight rail transport
	3.86	t*km	transport, freight, lorry 3.5-7.5 metric ton, EURO3 | transport, freight, lorry 3.5-7.5 metric ton, EURO3 | APOS, S - RoW	Freight transport by road
	178.2	t*km	market for transport, freight, sea, transoceanic ship | transport, freight, sea, transoceanic ship | APOS, S - GLO	Sea and coastal freight water transport
Transport to Italy	33,5	t*km	transport, freight, lorry 3.5-7.5 metric ton, EURO6 | transport, freight, lorry 3.5-7.5 metric ton, EURO6 | APOS, S - RER	Freight transport by road
Output				
Solar Collector transported	1	Items		

Table S10

LCI: Supply Water Tank				
Component	**Quantity**	**Unit**	**Ecoinvent Process**	**Ecoinvent Category**
Input				
Supply Water Tank	14.3	kg	market for polyethylene terephthalate, granulate, bottle grade | polyethylene terephthalate, granulate, bottle grade | APOS, S - GLO	Manufacture of plastics and synthetic rubber in primary forms
Packaging	1.4	kg	market for carton board box production, with offset printing | carton board box production, with offset printing | APOS, S - GLO	Manufacture of corrugated paper and paperboard and of containers of paper
Transport to Somalia	2.04	t*km	transport, freight, lorry 3.5-7.5 metric ton, EURO3 | transport, freight, lorry 3.5-7.5 metric ton, EURO3 | APOS, S - RoW	Freight transport by road
	6.8	t*km	transport, freight, lorry 3.5-7.5 metric ton, EURO6 | transport, freight, lorry 3.5-7.5 metric ton, EURO6 | APOS, S - RER	Freight transport by road
	154.6	t*km	market for transport, freight, sea, transoceanic ship | transport, freight, sea, transoceanic ship | APOS, S - GLO	Sea and coastal freight water transport
Transport to Brazil	33.5	t*km	market for transport, freight train | transport, freight train | APOS, S - Europe without Switzerland	Freight rail transport
	2.04	t*km	transport, freight, lorry 3.5-7.5 metric ton, EURO3 | transport, freight, lorry 3.5-7.5 metric ton, EURO3 | APOS, S - RoW	Freight transport by road
	94.3	t*km	market for transport, freight, sea, transoceanic ship | transport, freight, sea, transoceanic ship | APOS, S - GLO	Sea and coastal freight water transport
Transport to Italy	17.7	t*km	transport, freight, lorry 3.5-7.5 metric ton, EURO6 | transport, freight, lorry 3.5-7.5 metric ton, EURO6 | APOS, S - RER	Freight transport by road
Output				
Water Tank transported	1	Items		

Table S11

LCI: Heat Exchanger				
Component	**Quantity**	**Unit**	**Ecoinvent Process**	**Ecoinvent Category**
Input				
Heat exchanger copper internal part	17.1	kg	market for metal working, average for copper product manufacturing | metal working, average for copper product manufacturing | APOS, S - GLO	Manufacture of other fabricated metal products; metalworking service activity
Heat exchanger steel external part	1.23	m^2	market for selective coat, stainless steel sheet, black chrome | selective coat, stainless steel sheet, black chrome | APOS, S - GLO	Treatment and coating of metals; machining
Thermal insulation	0.33	kg	market for stone wool | stone wool | APOS, S - GLO	Manufacture of other non-metallic mineral product
Packaging	1.75	kg	market for carton board box production, with offset printing | carton board box production, with offset printing | APOS, S - GLO	Manufacture of corrugated paper and paperboard and of containers of paper
Transport to Somalia	3.3	t*km	transport, freight, lorry 3.5-7.5 metric ton, EURO3 | transport, freight, lorry 3.5-7.5 metric ton, EURO3 | APOS, S - RoW	Freight transport by road
	11.0	t*km	transport, freight, lorry 3.5-7.5 metric ton, EURO6 | transport, freight, lorry 3.5-7.5 metric ton, EURO6 | APOS, S - RER	Freight transport by road
	249.5	t*km	market for transport, freight, sea, transoceanic ship | transport, freight, sea, transoceanic ship | APOS, S - GLO	Sea and coastal freight water transport
Transport to Brazil	54.2	t*km	market for transport, freight train | transport, freight train | APOS, S - Europe without Switzerland	Freight rail transport
	3.30	t*km	transport, freight, lorry 3.5-7.5 metric ton, EURO3 | transport, freight, lorry 3.5-7.5 metric ton, EURO3 | APOS, S - RoW	Freight transport by road
	152.5	t*km	market for transport, freight, sea, transoceanic ship | transport, freight, sea, transoceanic ship | APOS, S - GLO	Sea and coastal freight water transport
Transport to Italy	28.7	t*km	transport, freight, lorry 3.5-7.5 metric ton, EURO6 | transport, freight, lorry 3.5-7.5 metric ton, EURO6 | APOS, S - RER	Freight transport by road
Output				
Heat Exchanger transported	1	Items		

Table S12

LCI: Treated Water Tank				
Component	**Quantity**	**Unit**	**Ecoinvent Process**	**Ecoinvent Category**
Input				
Treated Water Tank	11.28	kg	market for polyethylene terephthalate, granulate, bottle grade | polyethylene terephthalate, granulate, bottle grade | APOS, S - GLO	Manufacture of plastics and synthetic rubber in primary forms
Packaging	1.12	kg	market for carton board box production, with offset printing | carton board box production, with offset printing | APOS, S - GLO	Manufacture of corrugated paper and paperboard and of containers of paper
Transport to Somalia	1.16	t*km	transport, freight, lorry 3.5-7.5 metric ton, EURO3 | transport, freight, lorry 3.5-7.5 metric ton, EURO3 | APOS, S - RoW	Freight transport by road
	5.35	t*km	transport, freight, lorry 3.5-7.5 metric ton, EURO6 | transport, freight, lorry 3.5-7.5 metric ton, EURO6 | APOS, S - RER	Freight transport by road
	121.8	t*km	market for transport, freight, sea, transoceanic ship | transport, freight, sea, transoceanic ship | APOS, S - GLO	Sea and coastal freight water transport
Transport to Brazil	26.5	t*km	market for transport, freight train | transport, freight train | APOS, S - Europe without Switzerland	Freight rail transport
	1.6	t*km	transport, freight, lorry 3.5-7.5 metric ton, EURO3 | transport, freight, lorry 3.5-7.5 metric ton, EURO3 | APOS, S - RoW	Freight transport by road
	74.4	t*km	market for transport, freight, sea, transoceanic ship | transport, freight, sea, transoceanic ship | APOS, S - GLO	Sea and coastal freight water transport
Transport to Italy	13.99	t*km	transport, freight, lorry 3.5-7.5 metric ton, EURO6 | transport, freight, lorry 3.5-7.5 metric ton, EURO6 | APOS, S - RER	Freight transport by road
Output				
Water Tank transported	1	Items		

Table S13

LCI: Pipes				
Component	**Quantity**	**Unit**	**Ecoinvent Process**	**Ecoinvent Category**
Input				
Pipes	1.23	kg	market for chromium steel pipe | chromium steel pipe | APOS, S - GLO	Manufacture of basic iron and steel
Thermal insulation	0.01	kg	market for stone wool | stone wool | APOS, S - GLO	Manufacture of other non-metallic mineral product
Packaging	0.13	kg	market for carton board box production, with offset printing | carton board box production, with offset printing | APOS, S - GLO	Manufacture of corrugated paper and paperboard and of containers of paper
Transport to Somalia	1.8	t*km	transport, freight, lorry 3.5-7.5 metric ton, EURO3 | transport, freight, lorry 3.5-7.5 metric ton, EURO3 | APOS, S - RoW	Freight transport by road
	5.9	t*km	transport, freight, lorry 3.5-7.5 metric ton, EURO6 | transport, freight, lorry 3.5-7.5 metric ton, EURO6 | APOS, S - RER	Freight transport by road
	134	t*km	market for transport, freight, sea, transoceanic ship | transport, freight, sea, transoceanic ship | APOS, S - GLO	Sea and coastal freight water transport
Transport to Brazil	29.2	t*km	market for transport, freight train | transport, freight train | APOS, S - Europe without Switzerland	Freight rail transport
	1.78	t*km	transport, freight, lorry 3.5-7.5 metric ton, EURO3 | transport, freight, lorry 3.5-7.5 metric ton, EURO3 | APOS, S - RoW	Freight transport by road
	82.2	t*km	market for transport, freight, sea, transoceanic ship | transport, freight, sea, transoceanic ship | APOS, S - GLO	Sea and coastal freight water transport
Transport to Italy	15.5	t*km	transport, freight, lorry 3.5-7.5 metric ton, EURO6 | transport, freight, lorry 3.5-7.5 metric ton, EURO6 | APOS, S - RER	Freight transport by road
Output				
Pipes transported	1	m		

Table S14

LCI: Photovoltaics				
Component	**Quantity**	**Unit**	**Ecoinvent Process**	**Ecoinvent Category**
Input				
Photovoltaic panel	0.06	m^2	market for photovoltaic panel, multi-Si wafer | photovoltaic panel, multi-Si wafer | APOS, S - GLO	Manufacture of electronic components and boards
Wires	0.13	kg	market for wire drawing, copper | wire drawing, copper | APOS, S - GLO	Manufacture of basic precious and other non-ferrous metals
Packaging	1.04	kg	market for carton board box production, with offset printing | carton board box production, with offset printing | APOS, S - GLO	Manufacture of corrugated paper and paperboard and of containers of paper
Transport to Somalia	0.24	t*km	transport, freight, lorry 3.5-7.5 metric ton, EURO3 | transport, freight, lorry 3.5-7.5 metric ton, EURO3 | APOS, S - RoW	Freight transport by road
	0.78	t*km	transport, freight, lorry 3.5-7.5 metric ton, EURO6 | transport, freight, lorry 3.5-7.5 metric ton, EURO6 | APOS, S - RER	Freight transport by road
	17.89	t*km	market for transport, freight, sea, transoceanic ship | transport, freight, sea, transoceanic ship | APOS, S - GLO	Sea and coastal freight water transport
Transport to Brazil	3.9	t*km	market for transport, freight train | transport, freight train | APOS, S - Europe without Switzerland	Freight rail transport
	0.24	t*km	transport, freight, lorry 3.5-7.5 metric ton, EURO3 | transport, freight, lorry 3.5-7.5 metric ton, EURO3 | APOS, S - RoW	Freight transport by road
	10.9	t*km	market for transport, freight, sea, transoceanic ship | transport, freight, sea, transoceanic ship | APOS, S - GLO	Sea and coastal freight water transport
Transport to Italy	2.05	t*km	transport, freight, lorry 3.5-7.5 metric ton, EURO6 | transport, freight, lorry 3.5-7.5 metric ton, EURO6 | APOS, S - RER	Freight transport by road
Output				
Photovoltaic panel transported	1	Items		

Table S15

LCI: Thermostatic Valve				
Component	**Quantity**	**Unit**	**Ecoinvent Process**	**Ecoinvent Category**
Input				
Thermostatic valves	0.2	kg	market for electronics, for control units | electronics, for control units | APOS, S - GLO	Manufacture of measuring, testing, navigating and control equipment
Packaging	0.0	kg	market for carton board box production, with offset printing | carton board box production, with offset printing | APOS, S - GLO	Manufacture of corrugated paper and paperboard and of containers of paper
Transport to Somalia	0.00	t*km	transport, freight, lorry 3.5-7.5 metric ton, EURO3 | transport, freight, lorry 3.5-7.5 metric ton, EURO3 | APOS, S - RoW	Freight transport by road
	0.08	t*km	transport, freight, lorry 3.5-7.5 metric ton, EURO6 | transport, freight, lorry 3.5-7.5 metric ton, EURO6 | APOS, S - RER	Freight transport by road
	1.9	t*km	market for transport, freight, sea, transoceanic ship | transport, freight, sea, transoceanic ship | APOS, S - GLO	Sea and coastal freight water transport
Transport to Brazil	0.4	t*km	market for transport, freight train | transport, freight train | APOS, S - Europe without Switzerland	Freight rail transport
	0.02	t*km	transport, freight, lorry 3.5-7.5 metric ton, EURO3 | transport, freight, lorry 3.5-7.5 metric ton, EURO3 | APOS, S - RoW	Freight transport by road
	1.2	t*km	market for transport, freight, sea, transoceanic ship | transport, freight, sea, transoceanic ship | APOS, S - GLO	Sea and coastal freight water transport
Transport to Italy	0.23	t*km	transport, freight, lorry 3.5-7.5 metric ton, EURO6 | transport, freight, lorry 3.5-7.5 metric ton, EURO6 | APOS, S - RER	Freight transport by road
Output				
Thermostatic valve transported	1	Items		

1.2.2. Installation

Table S16

LCI: System installed				
Component	**Quantity**	**Unit**	**Ecoinvent Process**	**Ecoinvent Category**
Input				
Supply Water Tank transported	1	Items		
Treated Water Tank transported	1	Items		
Heat Exchanger transported	1	Items		
Photovoltaic panel transported	1	Items		
Thermostatic valve transported	6	Items		
Pipes, transported	7.7	m		
Solar collector, transported	1	Items		
Land occupation Somalia	163.8	m^2*years	Occupation, pasture, man made, extensive	Resource/Land
Land Transformation Somalia	10.92	m^2	Transformation, to pasture, man made extensive	Resource/Land
Land occupation Brazil	163.8	m^2*years	Occupation, forest	Resource/Land
Land Transformation Brazil	10.92	m^2	Transformation, from forest	Resource/Land
Land occupation Italy	163.8	m^2*years	Occupation, permanent crop, irrigated	Resource/Land
Land Transformation Italy	10.92	m^2	Transformation, from permanent crop, irrigated	Resource/Land
Output				
TVS Pasteurization System installed	1	Items		

1.2.3. Operative phase

Table S17

LCI: Operative phase				
Component	**Quantity**	**Unit**	**Ecoinvent Process**	**Ecoinvent Category**
Input				
TVS Pasteurization System installed	1	Items		
Raw Water Somalia	308,430	l	Water, ground	Resource, in water
Raw Water Brazil	345,165	l	Water, ground	Resource, in water
Raw Water Italy	251,745	l	Water, ground	Resource, in water
Output				
Treated Water Somalia	308,430	l		
Treated Water Brazil	345,165	l		
Treated Water Italy	251,745	l		

1.2.4. End of life

Table S18

LCI: End-of-Life phase				
Component	**Quantity**	**Unit**	**Ecoinvent Process**	**Ecoinvent Category**
Input				
Recycling non-ferrous metals	31.16*R	kg	market for aluminium scrap, post-consumer | aluminium scrap, post-consumer | APOS, S	Materials Recovery
Output				
Recycled non ferrous metals	31.16*R			
Input				
Recycling ferrous metals	28.531*R	kg	market for iron scrap, sorted, pressed | iron scrap, sorted, pressed | APOS, S	Materials Recovery
Output				
Recycled ferrous metals	28.531*R	kg		
Input				
Recycling Glass	10.2*R	kg	market for glass cullet, sorted | glass cullet, sorted | APOS, S	Materials Recovery
Output				
Recycled Glass	10.2*R			
Input				
Recycling Plastic Tanks	25.58*R	kg	market for polyethylene terephthalate, granulate, bottle grade, recycled | polyethylene terephthalate, granulate, bottle grade, recycled | APOS, S	Materials Recovery
Output				
Recycled Plastic	25.58*R			
Input				
Recycling paperboard	11.6*R	kg	market for waste paperboard, sorted | waste paperboard, sorted | APOS, S	Materials Recovery
Output				
Recycled paperboard	11.6*R			
Input				
Recycling Mineral Wool	0.4*R	kg	treatment of waste mineral wool, recycling | waste mineral wool | APOS, S	Materials Recovery
Output				
Recycled mineral wool	0.4*R			
Input				
Recycling PV and Thermostatic Valve	0.75*R	kg	market for electronics scrap from control units | electronics scrap from control units | APOS, S	Materials Recovery
Output				
Recycled PV and Thermostatic Valve	0.75*R	kg		

2. Estimation of Direct Land Occupation and transformation.

2.1.NCS plant

The previous papers (Dainelli et al., 2017; Manfrida et al., 2017) don't provide any detailed information about the disposition of the components of the plant during the installation. In order to estimate its contribution to the environmental impact of the NCS, a realistic plan view of the system has been represented in **Fig. S1:**

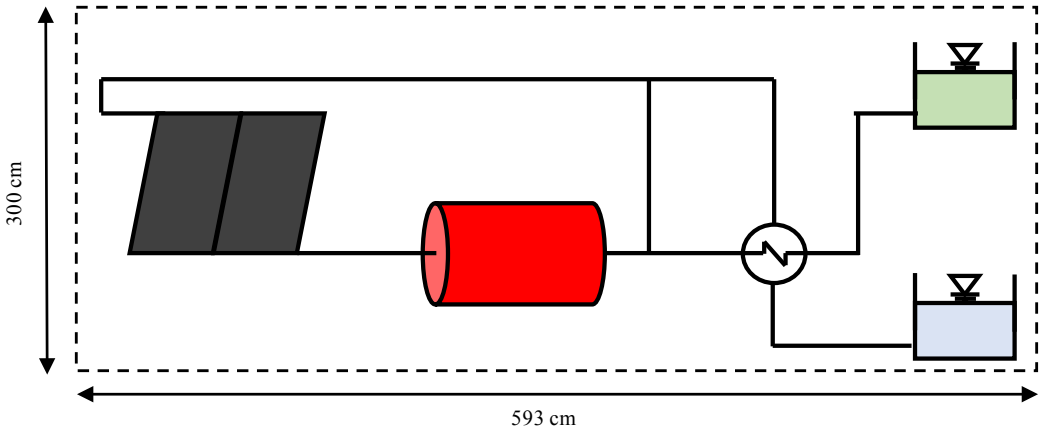

Fig. S1: NCS plan view (adapted from (Manfrida et al., 2017)).

The Life Cycle Inventory of the installation of NCS is described by **Table S6**.

2.2.TVS Plant

The previous papers (Carielo et al., 2017) provide a frontal and a lateral view of the system with some measurements from which the occupied surface can be estimated; the plan view is represented in **Fig. S2:**

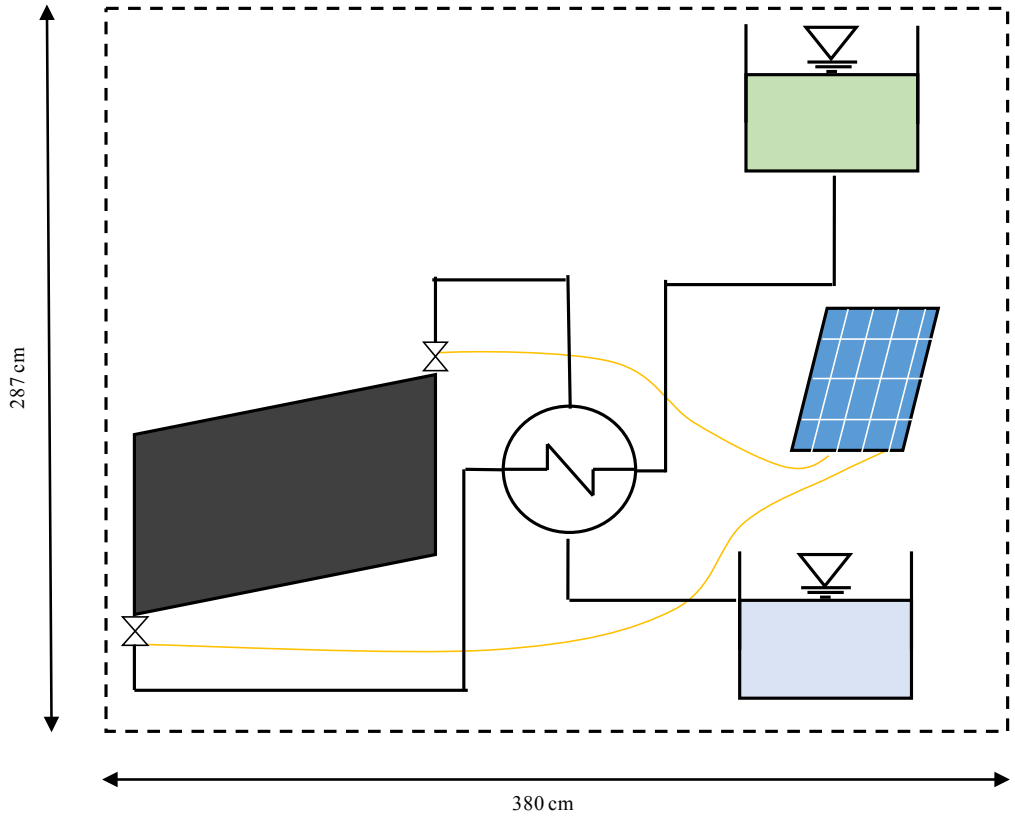

Fig. S2: NCS plan view (adapted from (Carielo et al., 2017)).

The Life Cycle Inventory of the installation of NCS is described by **Table S12**.

3. Thermo-fluid dynamic model of NCS

In this work the environmental impacts of a NCS have been evaluated performing a Life Cycle Assessment (LCA) and an exergo-environmental analysis. This article stresses the importance of treated water productivity as the most influencing parameter for the results. For such reason, its value should be estimated as carefully as possible depending on the climatic conditions of the installation sites. For such reason, further information about the model used to estimate this parameter are provided.

The analysed Natural Circulation System (NCS) has been designed for standard environmental conditions in previous papers (Dainelli et al., 2017; Manfrida et al., 2017). In these articles, after the design of the systems, a thermo-fluid dynamic model was developed to estimate the performances of the system in several locations.

Weather data can be obtained using the meteorological model of TRNSYS (developed by The University of Wisconsin Madison, http://www.trnsys.com/). This program contains the Meteonorm library (Meteonorm Information (05/04/2017), https://www.meteonorm.com/) which provides data

measured from over 8000 stations and five geostationary satellites. The discrete values are interpolated to estimate the typical yearly trend of ambient conditions in many locations worldwide.

The mathematics of the model has been described using EES (developed by F-chart, http://www.fchart.com/ees/), an equation solver software containing a detailed library for a wide range of physical phenomena. EES also allows the user to create lookup tables whose data can be addressed inside the equations.

The output data of the TRNSYS meteorological model has been processed to create EES lookup tables containing the hourly values of the ambient temperature and of the solar radiation in the typical day of each months. A continuous function describing these environmental conditions is obtained by the interpolation of these values.

To perform a dynamic simulation, a time-space discretization is required: the properties of the fluid in the main points of the plants (indicated in **Figure 1** of the manuscript) are evaluated for each lap of the circuit.

This methodological choice is interesting because the time step (τ) is variable and calculated as the ratio between the length of the circuit (L) and the average velocity of water ($V_{av,i}$) (1):

$$\tau_i = \frac{L}{V_{av,i}} \tag{S1}$$

As described in the paper, the solar radiation gradually warms the fluid inside the Solar Collectors (SCs) with surface area (A) and efficiency (η_{SC}) evaluated by the Bliss Equation (2):

$$\eta_{SC} = C_0 - C_1 \frac{\Delta T_m}{G} - C_2 \frac{{\Delta T_m}^2}{G} \tag{S2}$$

Where C_0, C_1 (W/(m^2*k)) and C_2 (W/m^2*K^2) are provided by the producer, G is the solar radiation (W/m^2) and ΔT_m is the difference between the average temperature inside the collector T_{av_23} and the ambient temperature T_{amb}:

$$\Delta T_m = T_{av\_23} - T_{amb} \tag{S3}$$

The heat transfer to the water mass flow rate $\dot{m}$ determines and increasing of temperature from T_2 to T_3:

$$\eta_{SC}\, G\, A = \dot{m}\, c_P (T_3 - T_2) \tag{S4}$$

Where c_P is the specific heat of water (J/(kg*K)).

According to the thermophysical properties of water, the value of the fluid density decreases from ρ_2 to ρ_3 inducing an over-pressure Δp, which also depends on the geodetic difference H defined by the geometry of the circuit (**Figure 1** of the manuscript):

$$\Delta p = gH(\rho_2 - \rho_3) \tag{S5}$$

This buoyancy-induced pressure is the driving force of the fluid and is contrasted by the mechanical resistance inside the pipes which is evaluated by Eq. (6):

$$\Delta p = k\, \dot{m}^2 \tag{S6}$$

Where k is a coefficient accounting for all the friction losses around the circuit (Pa*s^2/kg^2).

The previously set equations allow the evaluation of the thermal dilatation of water for each *i*-step (7) respect to its refence value at 85°C (8):

$$\Delta V_i = m\left(\frac{1}{\rho_{3,i}} - \frac{1}{\rho_{20°}}\right) \tag{S7}$$

$$\Delta V_{85°} = m\left(\frac{1}{\rho_{85°}} - \frac{1}{\rho_{20°}}\right) \tag{S8}$$

Where m is the mass of water contained inside the circuit (9):

$$m = V\ \rho_{20°} \tag{S9}$$

From the moment when the fluid reaches the temperature required for pasteurization, ΔV becomes higher than $\Delta V_{85°}$ and the mass rate $\dot{m}_{MU}$ of treated water overcoming the holding pipe is evaluated (10):

$$\dot{m}_{MU} = \frac{\Delta V_i - \Delta V_{85°}}{\rho_{20°}\tau} \tag{S10}$$

The relatively high temperature of treated water suggests a heat recovery for the incoming flow as modelled by Eq. (11):

$$\dot{m}_{MU} c_p (T_9 - T_0) = \dot{m}_{MU} c_p (T_6 - T_7) \tag{S11}$$

Thanks to the knowledge of the thermodynamic properties of water, the model also allows the evaluation of the exergy rate of each *j*-stream (12):

$$\dot{E}x_j = \dot{m}_j[(h_j - h_0) - T_0(s_j - s_0)] \tag{S12}$$

This system of equations is solved by the software step by step, for each typical day of the month; an estimation of the yearly values of productivity ($m_{MU,yr}$) and of the daily values of exergy ($Ex_{day,j}$) is possible integrating the results over time (13,14):

$$m_{MU,yr} = \sum_{months}\left(N_{month} \cdot \int_{day} \dot{m}_{MU}\, dt\right) \tag{S13}$$

$$Ex_{day,j} = \int_{day} \dot{E}x_j\, dt \tag{S14}$$

Where N_{month} is the number of days per month.

In this article the described model is applied using an input-output approach: the climatic conditions related to Mogadishu (Somalia), Recife (Brazil) and Brindisi (Italy) are provided from TRNSYS simulation as an input, while the yearly productivity and the daily exergy flows are the output. The output results of the model also represent the input for the LCA and exergo-environmental analysis, subjects of this article.

This procedure can be applied for all the locations of the world because a physical-based model is applied: all the above-mentioned equations come directly from the thermodynamics; for such reason their validity is independent from the climatic conditions. Furthermore, the design of the system (Dainelli et al., 2017; Manfrida et al., 2017) is not affected by environmental conditions because standard values are applied for ambient temperature and solar radiation during the sizing.

[dataset] Meteonorm Information. Available on http://www.meteonorm.com/ (Accessed on 05/04/2017)

Carielo, G., Calazans, G., Lima, G., Tiba, C., 2017. Solar water pasteurizer: Productivity and treatment efficiency in microbial decontamination. Renew. Energy 105, 257–269. https://doi.org/10.1016/j.renene.2016.12.042

Dainelli, N., Manfrida, G., Petela, K., Rossi, F., 2017. Exergo-Economic Evaluation of the Cost for Solar Thermal Depuration of Water. Energies 1–19. https://doi.org/10.3390/en10091395

F-chart, Engineering Equation Solver. http://www.fchart.com/ (Accessed on 05/04/2017)

Manfrida, G., Petela, K., Rossi, F., 2017. Natural circulation solar thermal system for water disinfection. Energy 141, 1204–1214. https://doi.org/10.1016/j.energy.2017.09.132

The University of Wisconsin Madison, Trnsys: TRaNsient SYstems Simulation Program. http://www.trnsys.com/ (Accessed on 05/04/2017)